TECHNISCHE
UNIVERSITÄT
DARMSTADT

Mitteilungen des Institutes und der Versuchsanstalt für Geotechnik der Technischen Universität Darmstadt

Herausgegeben von Prof. Dr.-Ing. Rolf Katzenbach

Stiffness and strength of Dubai sedimentary rock

Dr.-Ing. Marwan Alzaylaie

Heft 102 · Darmstadt · Dezember 2017

Vom Fachbereich Bau- und Umweltingenieurwissenschaften
der Technischen Universität Darmstadt
zur Erlangung des akademischen Grades eines
Doktor-Ingenieurs (Dr.-Ing.) genehmigte

Dissertation

von

Marwan Alzaylaie

aus Dubai, Vereinigten Arabischen Emirate

D17

Darmstadt 2017

Referent:	Prof. Dr.-Ing. Rolf Katzenbach Institut und Versuchsanstalt für Geotechnik Technische Universität Darmstadt
Korreferent:	Prof. Dr.-Ing. Carl-Alexander Graubner Institut für Massivbau Technische Universität Darmstadt

Tag der Einreichung: 17.10.2017
Tag der mündlichen Prüfung: 13.12.2017

Impressum

Herausgeber:
Prof. Dr.-Ing. Rolf Katzenbach
Institut und Versuchsanstalt für Geotechnik
der Technischen Universität Darmstadt
Franziska-Braun-Straße 7
D - 64287 Darmstadt
Telefon +49 (0) 6151/16-22810
Telefax +49 (0) 6151/16-22813
E-Mail: katzenbach@geotechnik.tu-darmstadt.de

ISBN 978-3-942068-22-2
ISSN 1436-6320

Die Herstellung dieses Heftes erfolgte dankenswerter Weise auch mit Unterstützung des Fördervereins der Freunde des Institutes für Geotechnik an der Technischen Universität Darmstadt e.V.

Editor's Foreword

The publication no. 102 of the Institute and the Laboratory of Geotechnics of Technische Universität Darmstadt presents the research works conducted by Dr.-Ing. Marwan Alzaylaie, who dealt with the stiffness and strength of Dubai sedimentary rock. Dr. Alzaylaie employed the two-dimensional numerical simulation to back-calculate the modulus of elasticity of Dubai sedimentary rock. The geotechnical data used in this study is collected from geotechnical investigation reports (195 boreholes) and static load test (116 piles) from more than 45 towers in Business Bay and Downtown Dubai areas as well as a case study evaluating one project located in Business Bay.

A comprehensive study has been conducted by Dr. Alzaylaie to identify the influence of soil parameters, back calculating the elastic modulus of Dubai sedimentary rock on the predicted load settlement behaviour of pile by simulating the static load test using finite element analysis. The results of 116 static load tests conducted on the pile relating to high-rise buildings in the Business Bay and Downtown Dubai areas has been considered for the analysis. The results obtained through conventional methods (empirical and analytical equations), numerical method (finite element method, FEM models) and experimental methods (static load pile testing) has primarily been adopted for the analysis.

Based on the research finding from numerical analyses, Dr. Alzaylaie found that it can be interpreted that the design of pile foundation based on the modulus of elasticity from the soil investigation report relying on the conventional methods will lead to uneconomical over-design of the pile foundation. It is evident that the 116 static load test results used for the analysis were preliminarily designed based on the geotechnical parameters from the geotechnical soil report, which leads to additional over-design of the pile dimensions than as per the required standards, resulting in additional material and labour having to be used, and increased costs for equipment. This research outcome is expected to offer a useful guideline to engineers in designing and analysing the piles in Dubai sedimentary rock and lead to green construction.

Darmstadt, in December 2017

Rolf Katzenbach

Acknowledgments

Firstly, I would like to express my sincere gratitude to my advisor Prof. Dr.-Ing. Rolf Katzenbach for the continuous support of my PhD study and related research, for his patience, motivation, and immense knowledge. His guidance helped me in all the time of research and writing of this dissertation

I would also like to acknowledge Prof. Dr.-Ing. Carl-Alexander Graubner of the as the second reader of this thesis, and I am gratefully indebted to very valuable comments on this thesis which improved my thesis.

Besides my advisor, I would like to thank my co-supervisor Prof. Alaa Ashmawy from American university in Dubai for for his support during my study, also I would like to thank the rest of my thesis committee: Prof. Dr.-Ing. Andreas Eichhorn, Prof. Dr.-Ing. Christoph Motzko and Prof. Dipl.-Ing. Stefan Schäfer, for their insightful comments, encouragement and valuable question which incented me to widen my research from various perspectives.

In addition, I would like to sincerely thank all scientific and supported staffs of the institute who kindly help and cordially collaborate. Many thanks are gratefully sent forward to Dr.-Ing. Steffen Leppla, Dipl.-Ing. Solenne Rochée, Dipl.-Ing. Sebastian Fischer, Dipl.-Ing. Hendrik Ramm, Dr.-Ing. Jörg Gutwald, Dipl.-Ing. Jörg Kreuzer, Joachim Schneider Dipl.-Ing. Alexandra Weidle, Dipl.-Ing. Jie Zheng and Dr.-Ing. Thomas Waberseck who always provided helpful assistance and guidance to the author.

Also I would like to thank Dubai Creative Clusters Authority for their support during my study and providing me with all data used in the research. Specially I would like to thank Eng. Mohamed Al Bahri, Eng. Ali Buruhaima and Eng. Badr AlGargawi.

Finally, I must express my very profound gratitude to my mother, father, wife and my siblings for providing me with unfailing support and continuous encouragement throughout my years of study and through the process of researching and writing this thesis. This accomplishment would not have been possible without them. Thank you.

Darmstadt, in December 2017

Dr.-Ing. Marwan Alzaylaie

Table of contents

On enclosed CD:

List of Symbols and Abbreviations

Symbols

A_o	Initial area of specimen
A_b	Area of pile base
A_p	Average area of cross section of pile
A_s	Surface area of pile shaft
A	Area of specimen corresponding to P
C_d	Shape and rigidity factor
C_p	Empirical coefficient
c_u/C	Cohesion of soil
c’	Effective cohesion
D	Diameter of Pile
[D]	Matrix of the soil characteristics
ER_M	Energy ratio
E_s	Secant elastic modulus
E_t	Tangent elastic modulus
E	Modulus of elasticity
E_i	Initial tangent elastic modulus
E_p	Modulus of elasticity of Pile
e	Void ratio
E_b	Elastic modulus of soil beneath the pile tip
E_s	Elastic modulus of soil surrounding the pile shaft
{F}	Vector representing the applied nodal loads
F_1	Reduction factor
G_s	Specific gravity
I_F	Embedment Factor by Fox
I_b	Influence factor
I_s	Influence factor
j	Rock Mass Factor
[K]	Global stiffness matrix

l_o	Initial length of the specimen
Δl	Change in length
L	Pile length
mI_s	Shape Factor
M_r	Modulus ratio
[N]	Shape function
N_{60}	Corrected value of N
N_M	Observed value of N
N_c, N_q, N_γ, N_Φ	Bearing capacity factors
N	Standard penetration number
n	Porosity
p	Perimeter of pile
P	Applied Load
Q_a	Allowable/safe working load capacity of pile
Q_a	Allowable load / working load of pile
Q_b	Load carried by base resistance
Q_s	Load carried by skin friction
Q_t	Total axial force acting on the pile
Q_u	Ultimate load capacity of single pile
q_s	Unit frictional resistance
q_b	Unit base resistance
q_c	Cone penetration tip resistance
q_{uc}	Unconfined compressive strength
q_p	Load acting at pile base per unit area
r_o	Initial radius of specimen
Δr	Change in radius
S	Degree of saturation
s/s_t	Total pile head settlement
s_b	Pile settlement due to the load at the pile tip
s_e	The elastic settlement of pile
s_f	Pile settlement due to load transfer along the pile shaft

{U}	Vector representing the unknown nodal variable
V_v	Volume of the void
V_a	Volume of air
V_s	Volume of solid/soil
V_w	Volume of water
W	Weight of pile
w	Water content
W_a	Weight of air
W_s	Weight of solid
W_w	Weight of water
W_{sub}	Submerged weight of the soil
γ'	Submerged unit weight
γ_d	Dry unit weight
γ_s	Saturated unit weight
ε_i	Strain
ε_r	Radial strain
ε_z	Vertical strain
σ_1	Major principle stress at failure
σ_3	Minor principle stress at failure
σ_n	Normal stress at failure
σ_z	Vertical stress
τ_f	Shear strength or shear stress at failure
Φ	Angle of internal friction
Φ'	Effective angle of internal friction
α	Failure angle with major principle plane
α	Reduction factor depending on q_{uc}
β	Correlation factor for rock mass discontinuity
γ	Bulk unit weight
μ	Poisson's ratio
ξ	Skin friction distribution factor
τ	Shear strength of soil

Abbreviations

ASTM	American Society for Testing and Materials
BS	British Standards
CPT	Cone Penetration Test
CRP	Constant Rate of Penetration
DMD	Dubai Municipality Datum
FEM	Finite Element Method
ICE	Institute of Civil Engineers
ML	Maintained Load
N	Standard Penetration Number
RF	Reduction Factor
RQD	Rock Quality Designation
SCR	Solid Core Recovery
SPT	Soil Penetration Test
SLT	Static Load Test
TCR	Total Core Recovery
UCS	Unconfined Compressive Strength

1 Introduction

1.1 General

The United Arab Emirates (UAE) is located in the Middle East, bordering the Gulf of Oman, the Arabian Gulf, Oman and Saudi Arabia. As shown in the figure below, the UAE is a federation of seven emirates. One of these emirates, Dubai, has witnessed an unparalleled boom in construction over the last decade, the view of the city's skyline now being dominated by numerous high-rise buildings, multi-storey towers and landmark skyscrapers.

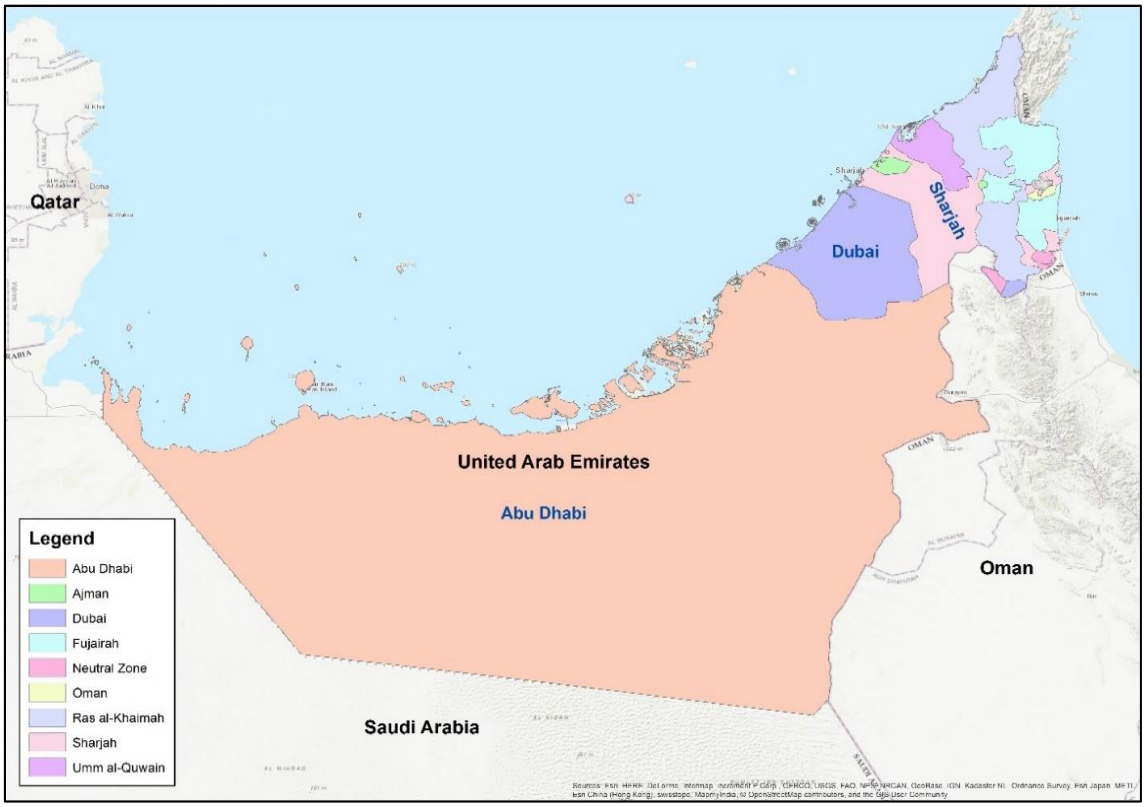

Fig. 1.1 Location of Dubai in the UAE

The Business Bay and Downtown Dubai areas are adjoining developments located in Dubai's central business district. When these developments are complete, the areas combined will feature more than 500 high rise commercial and residential buildings, all of which will be supported by complex infrastructure. Upon completion, these areas are anticipated to become the new business capital of Dubai.

The geotechnical properties of the Business Bay and Downtown Dubai areas normally feature loose to dense sand for the top six meters, which overlies weak sedimentary rock for depth more than 60 m. High-rise buildings usually have pile foundations resting on weak rock. The data for this research study is obtained from actual construction

projects. The single piles data consists of 116 piles load static tests collected from more than 45 towers contracted in the Business Bay and Downtown Dubai areas. In addition, the research includes 195 boreholes from 40 plots, as well as a case study evaluating one project located in Business Bay.

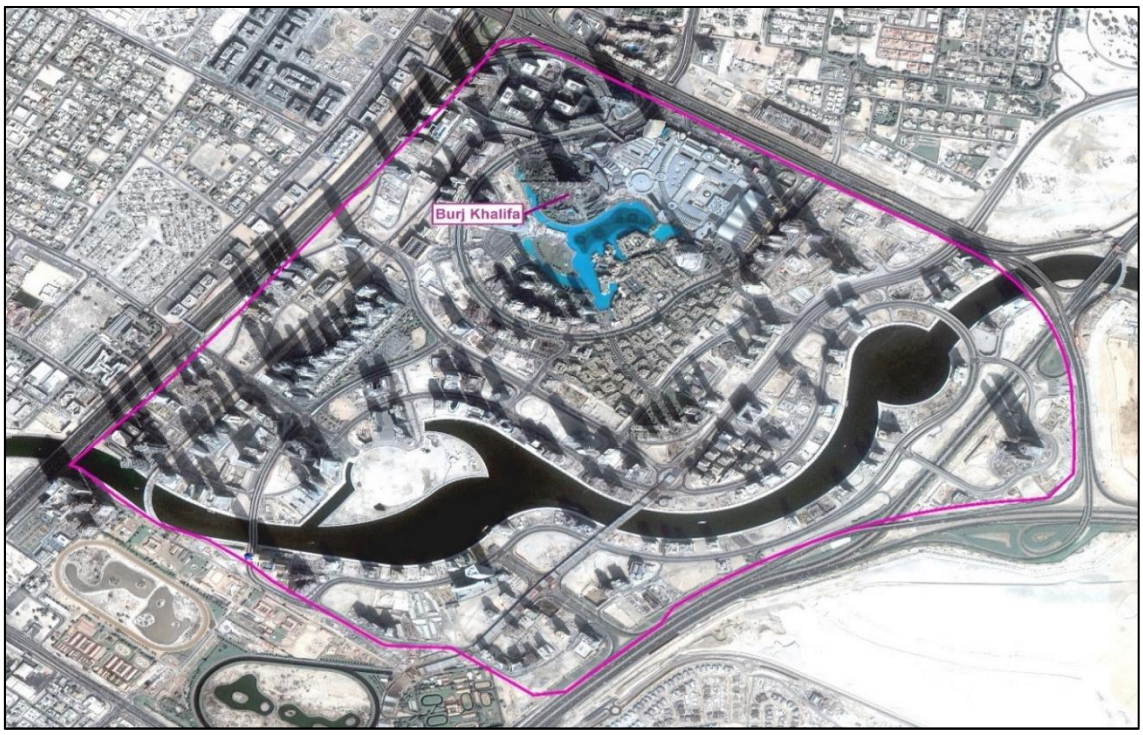

Fig. 1.2 Location of Business Bay and Downtown Dubai

1.2 Objectives of the study

- To evaluate the soil properties from the geotechnical investigation reports of numerous projects.
- To perform a comparative analysis between the calculated settlement from conventional methods (empirical & analytical equations), settlement from numerical model FEM and the actual settlement from static load test.
- To investigate the performance of single pile on the weak rock and evaluate the Young's modulus of soil.
- To develop a comprehensive methodology for the analysis and design of single piles resting on weak rock.
- To provide a contribution to the field of the geotechnical engineering, particularly related to the design of economical foundations and green construction.

1.3 Research scope

At present, research is devoted to analysis of the settlement of single piles through comparison of the load-deformation characteristics, as per the following.

- Actual settlement (Static Load Test)
- Numerically Computed settlement (finite Element)
- Empirical and Analytical Calculations (Equations)

Based on the outcome of this part of the research, a comparative study will be performed between the actual settlement from static load test, numerically computed settlement and settlements calculated using conventional methods empirical and analytical equations. The results will be used to validate or calibrate the rock properties of Dubai sedimentary rock, as used in the projects' design in Dubai. The ultimate objective is to achieve a robust recommendation for the optimum design parameters for Dubai sedimentary rock.

1.4 Study approach and methodology

The data used in this study is collected from geotechnical investigation reports (195 boreholes) and static load test (116 piles) from actual projects. The main emphasis of the study will be on the behaviour and performance of pile foundations. The study methodology can be summarised as per the below:

- Comparisons between the existing approach and practice, as applicable to pile design: all the current codal regulations and requirements of the Eurocode and the International Building code has been studied as applicable to the settlement of piles.
- Field data collection: collection of the entire static load test results as conducted on project construction sites in the Business Bay and Downtown Dubai areas.
- Soil laboratory data: all the soil parameter data from the geotechnical investigation report will be used to predict settlement behaviour in piles.
- Develop Finite Element Model for single pile.
- Comparison between the calculated settlement based on conventional methods for empirical and analytical equations, settlement calculated based on finite element model analysis (PLAXIS) and the actual settlement from static load test.
- Estimate an appropriate value for modulus of elasticity of Dubai sedimentary rock by back calculating the modulus of elasticity using FEM, and match the settlements observed in static load tests.

1.5 Research information and details

As defined in Section 1.1, the projects located in Business Bay and Downtown Dubai, alongside the applicable research output, includes the following key data:

- Projects: 28 constructed projects
- Building plots: 28 plots
- Towers: more than 45 towers
- Piles tests: 116 static load tests
- Geotechnical investigation: 195 boreholes, 28 geotechnical soil reports

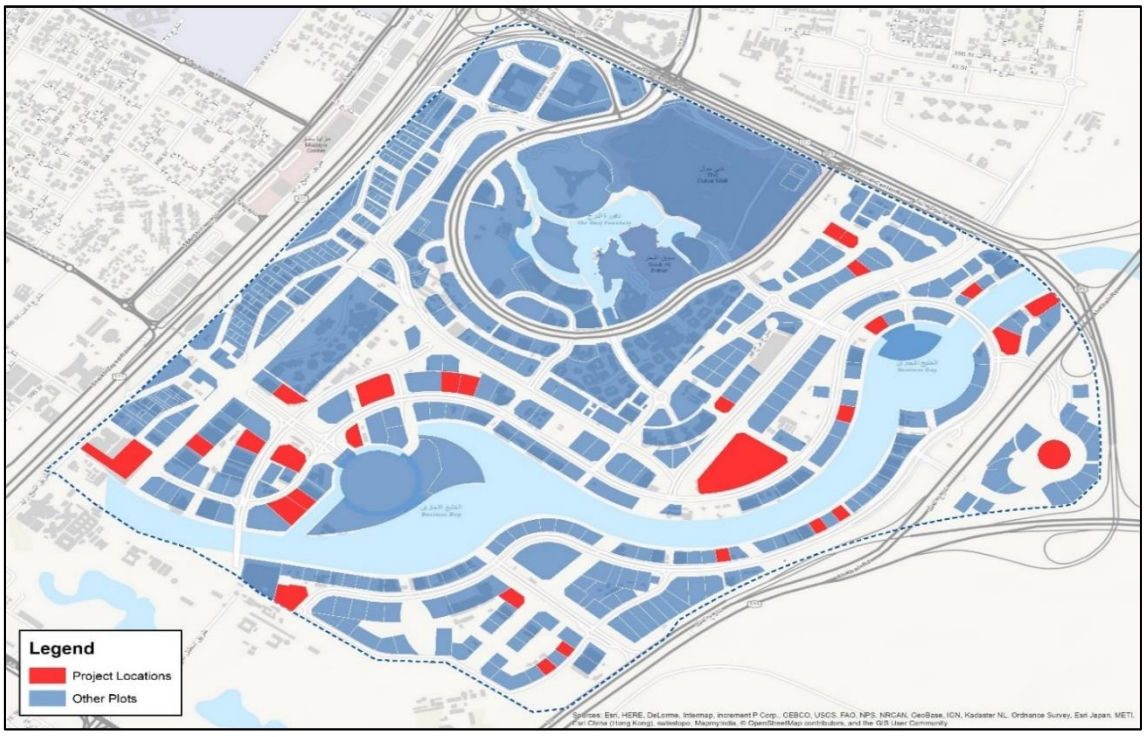

Fig. 1.3 Projects locations covered by the study

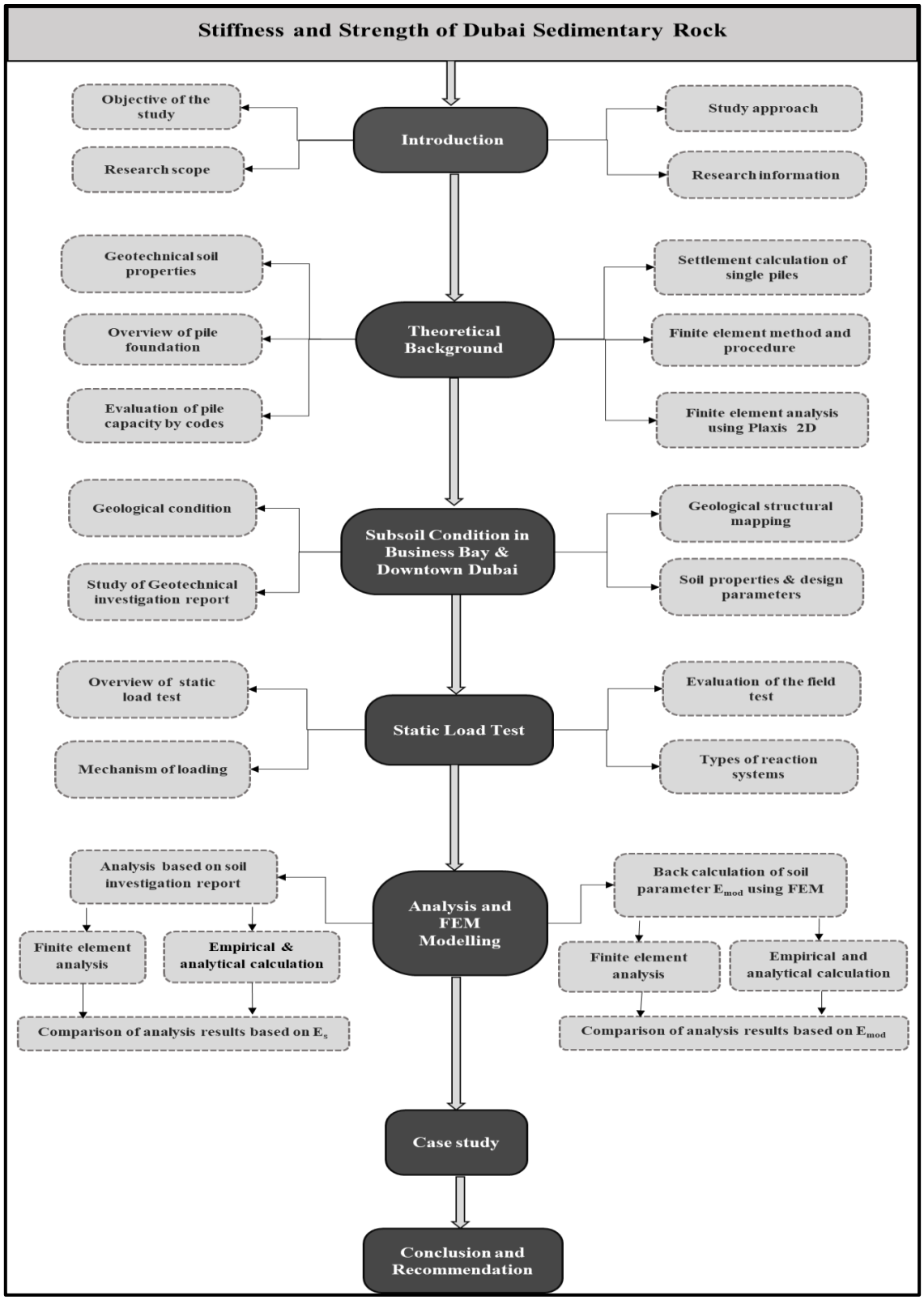

Fig. 1.4 Organisation of thesis

2 Theoretical background

2.1 General

Pile foundation is currently one of the most popular and widely used foundation methods applied to support various structures in different geotechnical or geologic conditions. Due to the essential role they have to play in supporting structures, substantial effort and cost needs to be expended in the construction process to ensure that this support is adequate in order to minimise the potentially disastrous consequence of their failure. Thus, there has always been both a desire and a strong need to evaluate and study behaviour of pile load in order to enhance contemporary state-of-the-art knowledge.

2.2 Geotechnical soil properties

The following information details the key properties of soil, as determined in the laboratory, that are relevant for estimating the mechanical, strength and stiffness properties.

2.2.1 Unit weight γ

The bulk unit weight is defined as the ratio of total weight of the soil to the total volume of soil. In simple terms, this represents the weight of the soil per unit volume. The general equation is represented below

$$\gamma_{bulk} = \frac{W}{V} \qquad \text{(Eq. 2.1)}$$

where W is the weight of soil, and V is the volume of soil.

When all the voids inside the soil mass are filled with water, it will attain a fully saturated condition and the bulk unit weight will become equivalent to saturated unit weight, γ_{sat}.

Similarly, when all the voids inside the soil mass are filled with air, the bulk unit weight will become equivalent to dry unit weight, γ_{dry}. In general, when discussing soil properties under saturated conditions, it is common practise to discuss the dry unit weight of the soil due to its correlation with the void ratio. The unit weight of the soil under submerged conditions is occasionally used when the soil is fully saturated and is computed using the equation below:

$$\gamma' = \gamma_{sat} - \gamma_w \qquad \text{(Eq. 2.2)}$$

Two main studies (Bowles 1996) and (Naval Facilities Engineering Command 1986b) have been carried out to develop ranges for the unit weight of soil. Those pertaining to granular soil are discussed herein (Punmia and Jain 2005).

SPT Penetration N-Value (blows/ foot)	γ (lb/ft^3)	γ (t/m^3)
0 - 4	70 - 100	1.1 - 1.6
4 – 10	90 - 115	1.4 - 1.8
10 - 30	110 - 130	1.7 - 1.9
30 - 50	110 - 140	1.7 - 2.2
>50	130 - 150	1.9 - 2.4

Table 2.1 Unit weight (Bowles 1996)

Soil Type	γ (lb/ft^3)	γ (lb/ft^3)	γ (t/m^3)	γ (t/m^3)
Sand, loose and uniform	90	118	1.4	1.9
Sand, dense and uniform	109	130	1.7	2.1
Sand, loose and well graded	99	124	1.6	2
Sand, dense and well graded	116	135	1.8	2.2

Table 2.2 Unit weight (Naval Facilities Engineering Command 1986b)

2.2.2 Shear strength

Mohr (1990) presented a theory for rupture in materials which occur at the critical combination of normal stresses and shear stresses. The fundamental relationship between normal stress and shear stress on a failure plane can be expressed by the following relationship:

$$\tau_f = c + \sigma \tan \varphi \qquad \text{(Eq. 2.3)}$$

where

c = Cohesion
φ = Angle of internal friction
σ = Normal stress on the failure plane
τ_f = Shear strength

The above equation is the Mohr- Coulomb failure criterion. In saturated soil, the total normal stress at a point is the sum of the effective stress (σ') and pore water pressure (u) (Reddy 1999).

$$\sigma = \sigma' + u \qquad \text{(Eq. 2.4)}$$

2.2.3 Angle of Internal Friction

Soil friction angle is the shear strength parameter of soils. Its definition is derived from the Mohr-Coulomb failure criterion and is used to describe the friction shear resistance of soils together with the normal effective stress. In the stress plane of shear stress-effective normal stress, the soil friction angle is the angle of inclination with respect to the horizontal axis of the Mohr-Coulomb shear resistance line (Reddy 1999). Many studies have been carried out to investigate this relationship (Bowles 1996), (Peck et al. 1974) and (Meyerhof 1976).

Type of Soil	**SPT, N**	**Relative Density, D_r**	**Angle of Internal Friction, ϕ**	
			Peck et al. (1974)	**Meyerhof (1956)**
Very loose sand	< 4	< 0.2	< 29	< 30
Loose sand	4 – 10	0.2 – 0.4	29 – 30	30 – 35
Medium sand	10 – 30	0.4 – 0.6	30 – 36	35 – 40
Dense sand	30 –50	0.6 – 0.8	36 – 41	40 – 45
Very dense sand	> 50	> 0.8	> 41	> 45

Table 2.3 Angle of internal friction (Fang 1991)

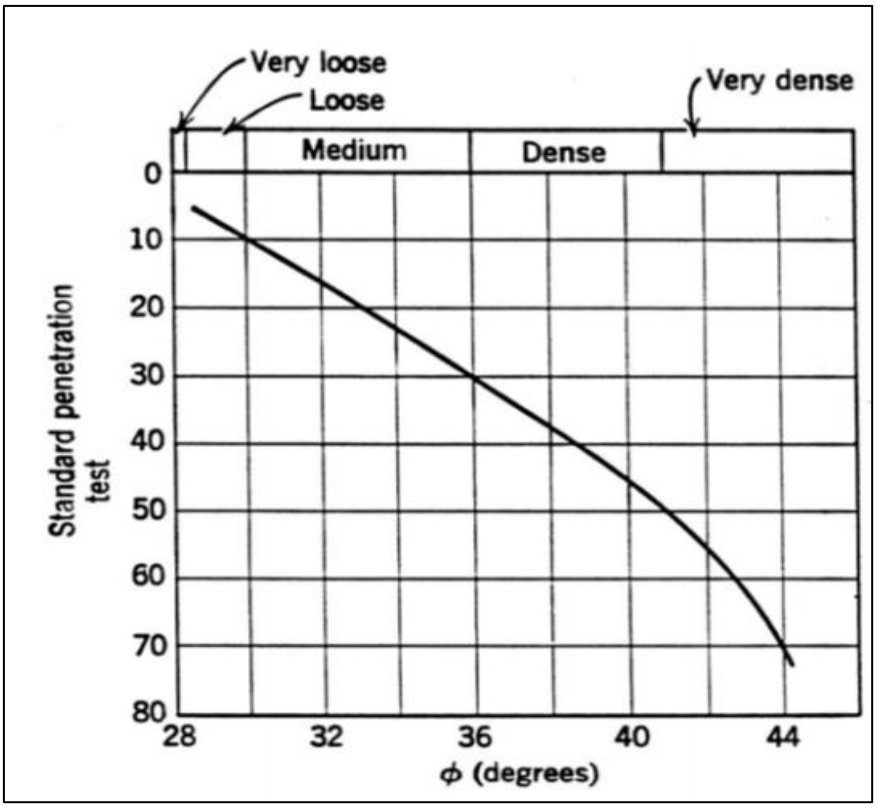

Fig. 2.1 Angle of internal friction (Pack et al. 1974)

2.2.4 Cohesion

The cohesion is used to characterise the shear strength of soil. It is defined based on the Mohr-Coulomb failure criterion and used to describe the non-frictional part of the shear resistance, independent from the normal stress. In the plane of shear stress and effective normal stress, the soil cohesion is determined as the intercept of Mohr-Coulomb shear resistance line on the shear axis. Evaluation of the cohesion for soil based on the standard penetration test (SPT) is as per the following table:

SPT Penetration	Estimated Consistency	S_{uc} (t/ft^2)
<2	Very Soft	<0.25
02-04	Soft	0.25 - 0.50
04-10	Medium	0.50 - 1.0
10-15	Stiff	1.0 - 2.0
15 - 30	Very Stiff	2.0 - 4.0
>30	Hard	>4

Table 2.4 Cohesion (Naval Facilities Engineering Command 1986b)

As per ASTM, the cohesion is electrostatic bond forces between the soil particles. It is the resistance to tangential motion rising from mutual attractive forces between soil particles and the resistance to shearing performing from cohesion. The normal stress σ_n applied to the soil will not have any influence in the resistance (ASTM 1960).

The cohesion can also be expressed as the component of the shear strength in rocks and dense soil, which is independent of the inter-particle frictional forces. Depending on the contributing factors, cohesion can be further classified into two types of cohesion, either apparent or true cohesion. In apparent cohesion, the soil particles are held to each other due to the inter-capillary forces and the interlocking between the soil particles of rough surfaces: due to this the soil mass can afford the deformation without falling in the soil, but these types of deformations cannot be considered or described as plastic deformations because failure could accrue when the soil mass is dry. In true cohesion, the soil particles are held together due to the electrostatic and electromagnetic forces of attraction and the presence of cementing agents; true cohesion is responsible for the plastic nature of soil (Lal 2006).

Generally, to evaluate the cohesion of rock and, specifically, for weak rock, there are several methods used to calculate cohesion based on unconfined compressive strength values (UCS). These methods are summarised as follows:

Method 1: By Z.T Bieniawski 1989 & ASTM D5878

In this method, the values of RMR, GSI, angle of internal friction and UCS are used to evaluate the cohesion of sandstone Rock Mass Rating RMR, calculated by using the six factors:

$$\mathrm{RMR} = \mathrm{Ja1} + \mathrm{Ja2} + \mathrm{Ja3} + \mathrm{Ja4} + \mathrm{Ja5} + \mathrm{JB} \qquad \text{(Eq. 2.5)}$$

$$\mathrm{GSI} = \mathrm{RMR} + 10 \qquad \text{(Eq. 2.6)}$$

The angle of internal friction φ and UCS are obtained from soil report and tests. A normalised cohesion strength/ uniaxial strength value is found as per the chart below. Cohesion is calculated as c = UCS x ratio of cohesion strength/ uniaxial strength.

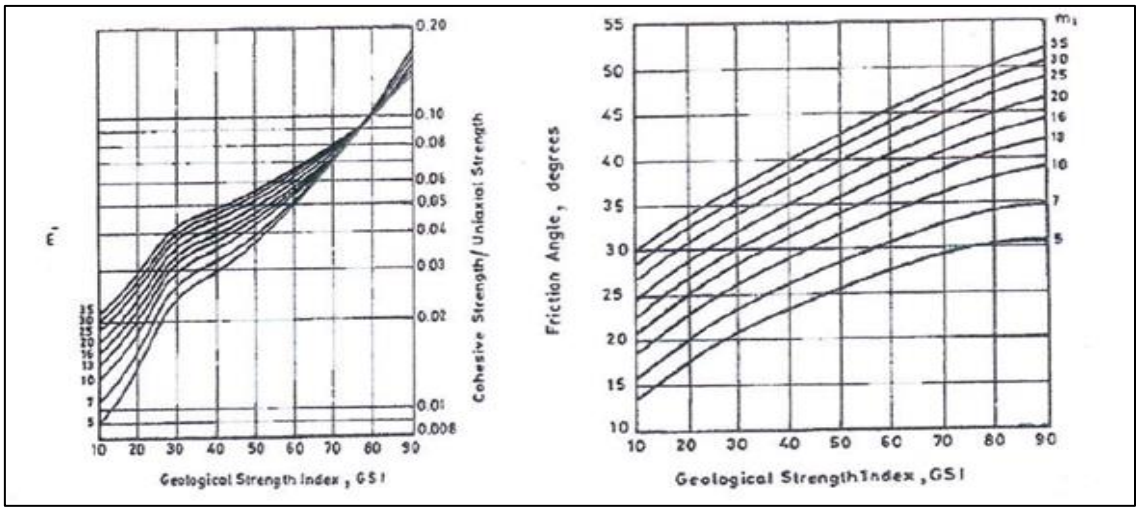

Fig. 2.2 Chart to obtain cohesion from GSI (After Hoek &Brown 1997)- Chang

Method 2: By Schroeder & Dickenson 1996 & Terzaghi et al. 1996

To determine undrained shear strength or undrained cohesion (c_u) using unconfined compressive strength then the undrained cohesion at failure is 1/2 of the UCS and cohesion is calculated as follows:

$$c_u = \frac{UCS}{2} \qquad \text{(Eq. 2.7)}$$

Method 3:

Calculation of cohesion c is made by using unconfined compressive strength and angle of internal Friction φ. In this method c is calculated as follows:

$$\text{Cohesion} = UCS_{design} \times (1 - \sin\phi'/2)/(2 \times \cos\phi') \qquad \text{(Eq. 2.8)}$$

$$UCS_{design} = 0.25 \times UCS \qquad \text{(Eq. 2.9)}$$

2.2.5 Unconfined compressive strength (UCS)

The unconfined compressive strength (UCS) of the rock is the uniaxial load acting per unit area of a cylindrical rock specimen of standard dimension, at which the failure of the specimen occurs in a compression test. The UCS is one of the important rock properties and so is used for defining the rock strength.

The uniaxial compression test or unconfined compressive strength test is one of the most popular tests used for determining the strength of the rock. However, the UCS test conducted is based on ASTM standers [ASTM D 2938 (95); preparation (ASTM D 4543)] is used to determine the value of unconfined compressive strength.

The classification that mainly emerged in the 1960, (Deere, Miller 1966) was developed for and primarily applied to the tunnelling and mining industries.

Rock Classification	UCS (MPa)
Very weak rock	1-2.5
Weak rock	2.5-5.0
Moderately weak rock	5.0-10.0
Hard rock	10.0-20.0
Very hard rock	>20.0

Table 2.5 Unconfined compressive strength UCS (Deere, Miller 1966)

Rock Classification	UCS (MPa)
Very weak rock	< 1.25
Weak rock	1.25 – 5
Moderately weak rock	5 – 12.5
Moderately strong	12.5 – 50
Strong	50 - 100
Very strong	100 – 200
Extremely strong	> 200

Table 2.6 Unconfined compressive strength (UCS) (Standard)

Rock/Soil Description	UCS (MPa)	Field Properties
Very strong rock	> 100	Firm hammering to break
Strong rock	50 to 100	Break by hammer in hand
Moderately strong rock	12.5 to 50	Dent with hammer pick
Moderately weak rock	5 to 12.5	Cannot be cut by hand
Weak rock	1.5 to 5	Crumbles under pick blows
Very weak rock	0.6 to 1.5	Break by hand
Very stiff soil	0.3 to 0.6	Indent by finger nail
Stiff soil	0.15 to 0.3	Cannot mould in fingers
Firm soil	0.08 to 0.15	Mould by fingers
Soft soil	0.04 to 0.08	Moulds easily in fingers
Very soft soil	< 0.04	Exudes between fingers

Table 2.7 Rock Strength (From Waltham 2009)

2.2.6 Rock quality designation (RQD)

The rock quality designation (RQD) is an estimate of the extent of jointing or fracturing that which occurs in the rock mass. It is indicated in terms of percentage in relation to the drill core running to the core pieces obtained with a length greater than 10 cm or more.

In 1964, the most widely used definition was developed by D. U. Deere. In accordance, the rock quality designation is defined as being the percentage of borehole core recovery considering only pieces of core greater than 100 mm in length measured through the centre of the core. RQD is a basic factor in many of the rock mass classification systems, including the: rock mass rating system (RMR) and Q-system. RQD is calculated based on the following equation:

$$\mathrm{RQD} = \frac{(\mathrm{l}_{\mathrm{sum\ of\ 100}})}{\mathrm{l}_{\mathrm{tot\ core\ run}}}\ \mathrm{X}\ 100\ (\%) \qquad \text{(Eq.2.10)}$$

$l_{sum\ of\ 100}$= Sum of the length of core sticks greater than 100 mm estimated along the centre of the core $l_{tot\ core\ run}$= Total length of core run (Deere 1988) classified the Rock Quality designation based on its use and adequacy for engineering purpose. Although the studies were oriented toward the tunnelling industry, they slowly became an integral part of everyday civil engineering and solving geotechnical problems (Bell 2004).

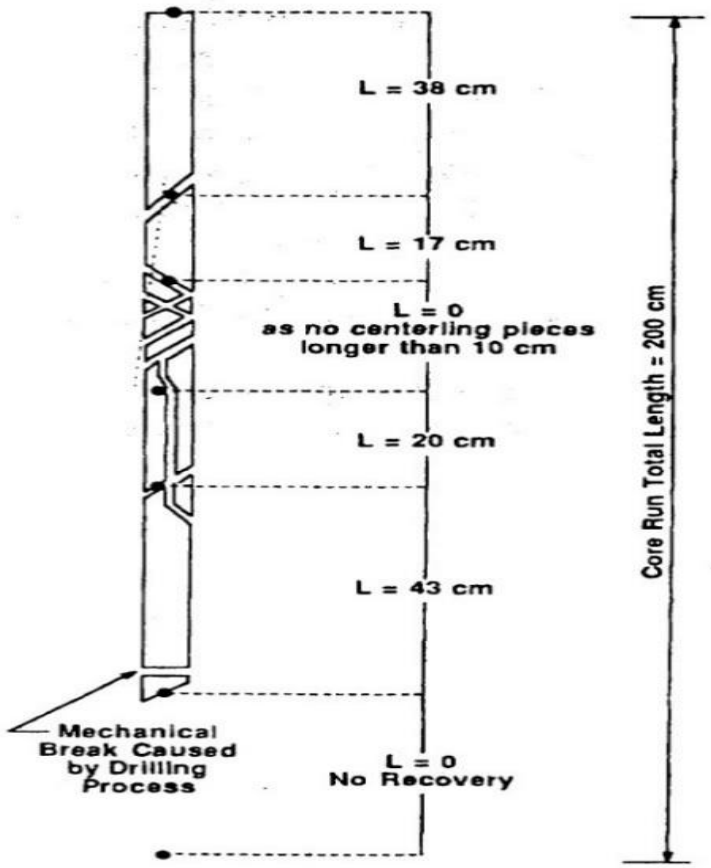

Fig. 2.3 Rock quality designation (RQD) Calculation

RQD	Rock Quality description
0 – 25	Very Poor
25 – 50	Poor
50 – 75	Fair
75 - 90	Good
90 - 100	Excellent

Table 2.8 Classification of rock quality (Deere 1988)

With the advancement of geotechnical engineering - especially in the civil engineering domain - the need arose for new strength boundaries as deemed mandatory. This was especially the case for rocks in the very weak zone, as they expand over a large range in the near sub-surface. These categories were revised to make them more applicable for civil engineering problems (Terzaghi et al. 1996).

The disadvantage of the RQD factor is that it does not account for the deformability present in the rock due to joint openings and other conditions. In order to combat this omission, the concept of rock mass factor (j) was proposed by Hobbs (1975). This factor quantifies the effect of discontinuities on the proposed performance of the rock mass. It can be defined as the ratio of the deformability present within any readily identifiable lithological and structural component to that of the deformability of the intact rock mass comprising the component. Due to this deformability of the rock mass, fractures will be created causing the elastic deformation of the rock mass, due to which the strength of the rock may be reduced by five to ten times the strength of the intact rock. The plate loading test and the seismic velocity measurement methods are also used to determine the mass factor (j). The following relationship based on the RQD and discontinuity spacing has been proposed by Hobbs (1965) to estimate the mass factor (Bell 2004).

Quality Classification	RQD (%)	Fracture Frequency per meter	Mass Factor (j)	Velocity Ratio
Very poor	0-25	Over 15	Less than 0.2	0-0.2
Poor	25-50	15-8		0.2-0.4
Fair	50-75	8-5	0.2-0.5	0.4-0.6
Good	75-90	5-1	0.5-0.8	0.6-0.8
Excellent	90-100	Less than 1	0.8-1.0	0.8-1

Table 2.9 Rock quality classification based on discontinuities (Waltham 2009)

When satisfactory rock samples cannot be obtained for the determining the angle of friction ϕ and cohesion c to establish the relationship of these parameters with the unconfined compressive strength UCS, the following correlation has been suggested based on the RQD (%).

RQD (%)	UCS	c	ϕ^0
0-70	0.33 UCS	0.1 UCS	30
70-100	0.33-0.8 UCS	0.1 UCS	30-60

Table 2.10 Correlation to RQD (Tomlinson and Woodward 2007)

2.2.7 Modulus of elasticity

Soil Young's modulus (E or Es), commonly referred to as soil elastic modulus, is an elastic soil parameter for measuring the soil stiffness, defined as the ratio of incremental stress to the corresponding incremental strain along that axis within the limit of elastic behaviour. The elastic modulus is used for estimation of soil settlement and to perform elastic deformation analysis.

Several methods have been used to calculate the modulus of elasticity, which is referred to as E, Es or Em by several authors. The methodologies of evaluation vary largely due to the parameters considered. The following methods have been outlined in several research papers/ references and are widely used in applications in geotechnical design (Budhu 2010). In most of cases, the immediate settlement of the foundation is calculated using the relationships established based on the theory of elasticity. The modulus of elasticity E and Poisson's ratio μ are the two parameters used for these relationships. For elastic materials, the uniaxial load test is conducted to obtain these parameters. However, soil cannot be considered as a fully elastic material. Thus, for soil particles, the triaxial compression test is conducted to determine these parameters (Das 2007).

Consider a deformable cylinder of initial length l_o, cross sectional area A and radius r_o subjected to a uniaxial loading during the triaxial compression test. Let the increment load ΔP applied to the cylinder, compress the cylinder by Δl and increase the radius by Δr, as shown in the figure below. Then the change in stress $\Delta\sigma_z$ can be calculated by using the following equation:

$$\sigma_z = \frac{\Delta P}{A} \qquad \text{(Eq. 2.11)}$$

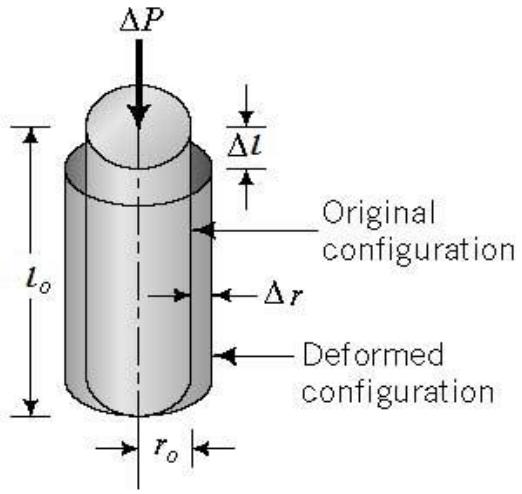

Fig. 2.4 Forces and corresponding deformations in the cylinder

The corresponding vertical strain $\Delta\varepsilon_z$ and radial strain $\Delta\varepsilon_r$ are:

$$\Delta\varepsilon_z = \frac{\Delta l}{l_o} \qquad \text{(Eq. 2.12)}$$

$$\Delta\varepsilon_r = \frac{\Delta r}{r_o} \qquad \text{(Eq. 2.13)}$$

In the Eq. 2.12 and 2.13, a (-) sign should be considered for expansion and a (+) sign for compression. As the cylinder undergoes radial expansion, so the Eq.2.11 should be modified accordingly (Budhu 2010).

Method 1: (Tomlinson)

In this method, E_m depends on Mass factor j, Modulus ratio M_R and unconfined compressive strength quc of rock. Modulus of elasticity

$$E_m = j \times M_R \times q_{uc} \qquad \text{(Eq. 2.14)}$$

The mass factor is defined as per the table provided below.

Mass Factor Values				
Quality Classification	**RQD (%)**	**Fracture Frequency/m**	**Velocity Index $(V_f/V_L)^2$**	**Mass factor j**
Very poor	0-25	15	0-0.2	0.2
Poor	25-50	15-8	0.2-0.4	0.2
Fair	50-75	8-5	0.4-0.6	0.2-0.5
Good	75-90	5-1	0.6-0.8	0.5-0.8
Excellent	90-100	1	0.8-1.0	0.8-1.0

Table 2.11 Mass Factor (j) values

Group	Type of rock	Modulus ratio (M_R)
1	Pure limestones and dolomites	600
	Carbonate sandstones of low porosity	
2	Igneous	300
	Oolitic and and marly limestones	
	Well cemented sandstones	
	Indurated carbonate mudstones	
	Metamorphic rocks	
	Slates and schists (flat cleavage/foliation)	
3	Very marly limestones	150
	Poorly cemented sandstones	
	Cemented mudstones and shales	
	Slates and schists (steep cleavage/foliation)	
4	Uncemented mudstone and shales	75

Table 2.12 Modulus ratio (M_R) values

Method 2: (Rowe & Armitage Method)

In this method, the modulus of elasticity E_m depends solely on the unconfined compressive strength q_{uc} of rock.

$$E_m = 215 \times \sqrt{q_{uc}} \qquad \text{(Eq. 2.15)}$$

Method 3: (Bowles)

In this method, a range of values have been recommended for the static stress-strain modulus E_s for several soils. In the table below, it is seen that the range of values for E_s corresponds to weak rock. The values are tabulated as per the table below:

Typical range of values for the static stress-strain modulus E_s for selected soils	
Soil- Glacial till	**E_S Mpa**
Loose	10-150
Dense	150-270
Very Dense	500-1440
Sand-Silty	5-20
Sand-Loose	10-25
Sand-Dense	50-81
Sand and Gravel (Loose)	50-150
Sand and Gravel (Dense)	100-200
Shale	150-5000
Silt	2-30

Table 2.13 Typical Range of Values for the static stress-strain Modulus E_s

Method 4: Evaluation of E_{rm} based on Rock Mass Rating (RMR)

RMR is a system of geo-mechanical classification developed by Z.T Bieniawski between 1972 and 1973. This method depends on six factors - JA1, JA2, JA3, JA4, JA5 & JB - used to evaluate RMR. These factors as obtained from field surveys. RMR is the summation of the six factors with a value ranging between 0 and 100 given by

$$\mathrm{RMR} = \mathrm{Ja1} + \mathrm{Ja2} + \mathrm{Ja3} + \mathrm{Ja4} + \mathrm{Ja5} + \mathrm{JB} \qquad \text{(Eq. 2.16)}$$

Several researchers have used RMR for calculating E_{rm}. The factors and empirical formulae are provided as follows.

Developed by Z.T Bieniawski

The modulus of elasticity E_m is given by

$$E_m = 2 \times \mathrm{RMR} - 100 \qquad \text{(Eq. 2.17)}$$

Developed by Serafin & Pereira

Serafin & Pereira (1983) provided an alternate way of evaluating E_{rm}

$$E_m(GPa) = 10^{(RMR-10)/40} \quad \text{(Eq. 2.18)}$$

Developed by Read et al (1999)

Read et al provided another method for evaluating E_{rm}

$$E_m(GPa) = 0.1(RMR/10)^3 \quad \text{(Eq. 2.19)}$$

Developed by Nicholson & Bieniawski (1990)

Nicholson & Bieniawski presented an empirical formula for calculating E_{rm}

$$E_m(GPa) = E_i/100(0.0028 + RMR^2 + 0.9\exp(RMR/22.82)) \quad \text{(Eq. 2.20)}$$

E_i = 50 GPa

Developed by Mitri et al (1994)

Mitri et al presented an empirical formula for calculating E_{rm}

$$E_m(GPa) = E_i(0.5(1 - \cos(\pi RMR/100))) \quad \text{(Eq. 2.21)}$$

E_i = 50 GPa

Developed by Hoek et al (1994)

Hoek et al presented an empirical formula for calculating E_{rm}

$$E_m(GPa) = (1 - D/2)\sqrt{\sigma_{ci}/100 \times 10^{((RMR-10)/40)}} \quad \text{(Eq. 2.22)}$$

where D = 0 and σ_{ci} = 100 MPa.

Method 5: Modulus of Elasticity of Sand Developed by Braja M. Das

Braja M. Das provided a simpler way to calculate modulus of elasticity using the standard penetration resistance value or N value obtained from field tests.

$$E\left(\frac{kN}{m^2}\right) = 766 \times N \qquad \text{(Eq. 2.23)}$$

where N is the standard penetration resistance value (SPT).

Literature has attempted to correlate unconfined compressive strength for rock with the Young's modulus (Chang et al. 2006), (Arslan et al. 2008). Strength and deformability characteristics of rocks are very consequential parameters for rock mass and material classification, as well as the design of the structure's foundations either upon or inside rocks, (Deere, Miller 1966) and (Bieniawski 1989).

	Equation	Coefficient of correlation (R)	Rock type
Wuerker (1959)	$E_t = 0.28\sigma_c + 5.83$	0.800	Sandstone Limestone
	$E_t = 0.57\sigma_c^{0.878}$	0.894	Shale Siltstone
Dhir and Sangha (1978)	$E_t = 0.19\sigma_c + 4.86$	0.936	Sandstone
	$E_t = 0.97\sigma_c^{0.69}$	0.875	Limestone
Lama and Vutukuri (1978)	$E_t = 0.15\sigma_c + 21.60$	0.448	Dolomite Sandstone Limestone
	$E_t = 1.93\sigma_c^{0.63}$	0.557	Shale Siltstone
Wilson (1980)	$E_t = 0.31\sigma_c$	–	Sandstone Siltstone Mudstone
	$E_t = 1.06\sigma_c^{0.729}$	0.863	Marble Silty Mudstone
Dennis et al. (1982)	$E_t = 0.13\sigma_c + 3.42$	0.715	Sandstone
	$E_t = 0.15\sigma_c^{0.76}$	0.788	Bituminous schist
Bell (1983)	$E_t = 0.285\sigma_c + 12.50$	0.350	Sandstone Limestone
	$E_t = 1.24\sigma_c^{0.783}$	0.902	Siltstone Shale
Sachpazis (1990)	$E_t = 0.257\sigma_c + 15.5$	0.856	Limestone
	$E_t = 0.50\sigma_c^{0.952}$	0.958	Dolomites
Rohde and Feng (1990)	$E_t = 0.057\sigma_c + 20.60$	0.293	Sandstone
	$E_t = 2.25\sigma_c^{0.523}$	0.503	
Arıkoğlu and Tokgöz (1992)	$E_t = 0.22\sigma_c + 7.30$	0.685	All above
	$E_t = 1.03\sigma_c^{0.730}$	0.812	Rocks
This study	$E_t = 0.27\sigma_c + 19.08$	0.810	Gypsum
	$E_t = 10.526\sigma_c^{0.2816}$	0.781	

Table 2.14 Young's Modulus for various rock types (Arslan et al. 2008)

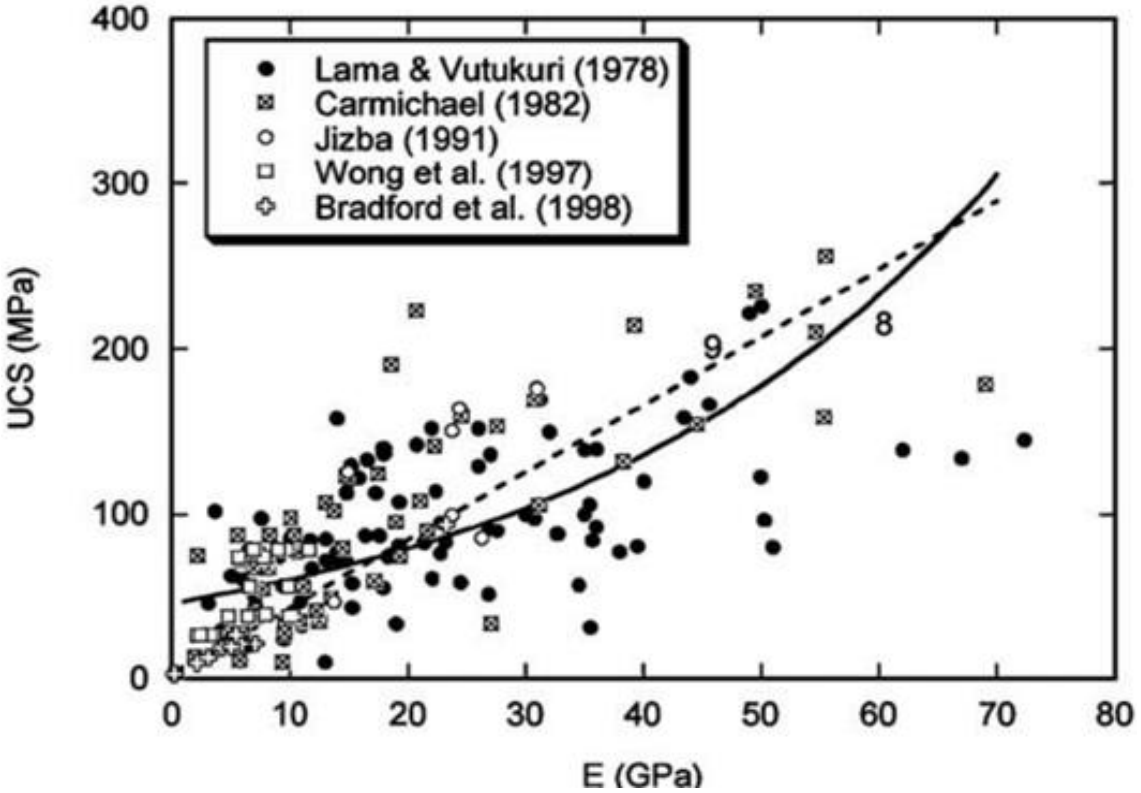

Fig. 2.5 UCS vs Modulus of elasticity (E) (Chang et al. 2006)

2.2.8 Poisson's Ratio

Poisson's ratio (n) can be defined as the ratio of lateral (radial) strain to vertical (axial) strain when subjected to uniaxial stress. The equation is expressed as follows:

$$\nu = \frac{-\varepsilon_r}{\varepsilon_a} \qquad \text{(Eq. 2.24)}$$

where

ν = Poisson’s ratio
ε_r = Radial strain
ε_a = Axial strain

When a sample of soil mass is subjected to compression or tension in the direction of the applied load, it will lead to contraction or extension of the soil mass in a direction perpendicular to the applied load. The ratio between these two quantities is exactly equal to Poisson’s ratio (Budhu 2010).

2.2.9 Over consolidation ratio

The ratio of the highest stress over the corresponding strain experienced for a soil mass is defined as the over consolidation ratio (OCR). The soil mass in its highest stress condition is said to be normally consolidated with an OCR value of 1.

2.2.10 Dilatancy

The exact description of volume changes due to imposed stress is fundamental to the modelling of the stress-strain behaviour of soils. The phenomenon of the coupling between volume and shape changes has been observed qualitatively and termed granular dilatancy by Osborne Reynolds (Reynolds, 1885) and, as a result, has influenced many concepts relating to in granular media and soil mechanics.

One of the earliest attempts to account for the increased shear strength due to dilatancy in dense sand was by D.W. Taylor (1948). Taylor used the term ‘interlocking’ to describe the effects of dilatancy. He calculated the power at peak strength for some direct shear-box data and found that the energy input is in part dissipated by a critical state friction component, and in part by the work needed to increase the volume, which is provided by the relationship.

$$\frac{\tau}{\sigma} = \mu + \frac{dy}{dx} \qquad \text{(Eq. 2.25)}$$

This shows that the peak strength of the dense granular material under normal stress is drawn from internal friction and interlocking (dilatancy). An increase in the effective stress reduces the interlocking, so that above a critical effective pressure there will not be an increase of volume but a reduction will occur instead.

2.3 Deep foundations

2.3.1 General

Deep foundations are structural components that, in comparison to shallow foundations, transfer load into deeper layers of earth materials. Deep foundations, generically referred to herein as piles, can be driven piles, drilled shafts, micro piles, and grouted-in-place piles. Vertical ground anchors (tie-downs) are also classified as deep foundations. Piles can be used in a group with a cap footing, or as a single pile/shaft supporting a column.

Piles foundations are long and slender structural elements in a foundation; the main aim of using piles being to transfer the load from the superstructure to the soil deep strata and from the top weak bearing capacity soil strata onto harder strata more compact or rock strata with high bearing capacity (Tomlinson and Boorman 2001). In addition to the aforementioned, piles are used in the cases of uplift or horizontal forces. These forces are due to permanent uplift form water pressure/high water table, wind load and seismic force acting on the structure.

2.3.2 Single pile foundation

The behaviour and analysis of a single pile has been studied extensively by several researchers. Total pile loads are transferred to the adjacent soil primarily by two mechanisms, first of all by the shaft resistance generated at the surface of the pile material with the adjoining soil and, secondly, by the load transferred to the base of the pile. The modulus of elasticity of the surrounding soil and the resulting settlement play an important role in ascertaining the pile capacity. Based on the type of pile material, the surrounding soil properties and the interface between the two results in a settlement of the pile which varies largely due to load transfer mechanism. A detailed explanation is made in the following section regarding the different types of piles.

2.3.3 Piled raft foundation and group piles

In recent years, combined Pile-Raft foundations have been studied extensively for the transfer of excessive loads from high-rise buildings, power plants, bridges, deep basements and special structures. The conventional foundation design using either only a raft foundation or Pile foundation is found to be conservative and technically insufficient to assess the accurate behaviour of the foundation system. Neglecting the stiffness of raft and using the pile stiffness alone yields uneconomical foundation design. Verification the combination of pile and raft foundation has been studied and developed by Clancy and Randolph (1993). Along with using accurate and realistic

values of soil properties, the use of Pile-Raft foundation system is likely to yield benefits in understanding the true behaviour of the soil- foundation-structure system and enable the transfer of higher loads to the soil. However, this study addresses the importance of verifying and utilizing realistic soil properties.

In literature, there are several bodies of research that focus on the parameters affecting the pile design, such as; the number of piles, length of piles, diameter of piles, pile spacing ratio, location of piles, stiffness of piles, distribution of load, level of load, raft thickness, raft dimensions and type of soil. Generally, group piles are used in groups to carry the large loads coming from the superstructure. The group may consist of three or more piles in general and, in some cases, two piles. The minimum spacing (centre to centre) of piles as suggested by some building codes are given (Bowles, 1996). The optimum spacing between piles that is generally recommended for use is 2.5 to 3.5 times the diameter of pile. For pile groups carrying lateral and/or dynamic loads, larger spacing is more efficient. Maximum spacing between piles is not specified in the building codes, however, spacing up to 8 D to 10 D can be used depending on the design.

The stresses and soil pressures developed from shaft friction or end bearing of a group of piles do overlap, and the soil may possibly fail in shear or settlement or can develop large settlement. In such cases, an increased pile spacing reduces the stresses; the resulting pile cap, however, would become large and expensive. The use of realistic soil parameters as studied in this research could resolve the technical deficiencies and provide an economical design.

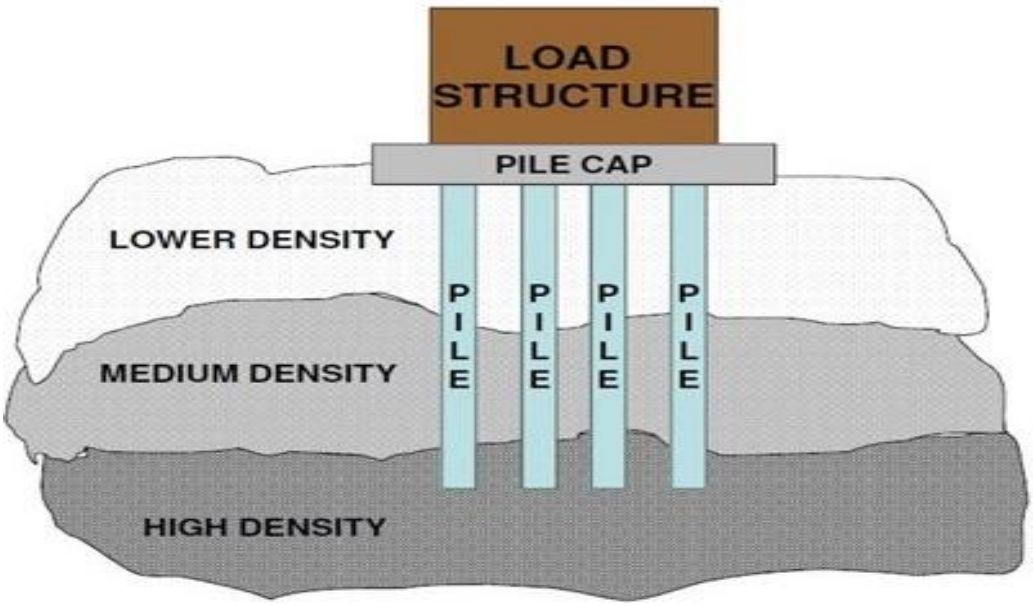

Fig. 2.6 Pile raft foundation

2.4 Classification of pile foundation

2.4.1 Based on type of pile material

Piles are primarily classified based on material composition and transfer mechanism of pile loads. It is common to use timber, steel and concrete piles based on specific requirements. This research is focused entirely on concrete piles.

Precast concrete:

Precast concrete piles, also known as 'prefabricated piles', are produced in a casting yard in a location away from the building site; in some cases, the casting yard may be situated close to the building site if sufficient space is available. According to Bowles (1996), the precast piles comprising of reinforcement are designed to withstand bending stresses during pick up and transport to the site, and bending moments from lateral loads, as well as to provide sufficient resistance to vertical loads and any tension forces developed during driving (Nawy 2008).

Pre-stressed piles:

In these piles, longitudinal reinforcement used in reinforced concrete piles are replaced by tensioned steel rods. This longitudinal reinforcement is designed to resist stresses in lifting and handling. Pre-stressed piles can be either pre-tensioned or post-tensioned (Jain 2005).

Cast-in-place piles:

Normally formed by drilling a hole in the ground and inserting an open-ended casing, the soil in the casing is removed and filled with concrete before the casing is removed. This usually consists of three specific types: cased, uncased and pedestal.

Composite piles:

Generally, the composite pile is composed of two or more materials: the upper part of the composite pile being made of cast in situ concrete and the lower part made of steel. However, due to the difficulty in connecting two different materials, they are rarely used in construction (Jain 2005).

Fig. 2.7 Types of concrete piles

2.4.2 Based on mechanism of load transfer

The pile load capacity depends upon the load transfer mechanism of the piles mechanism in to the soil. Piles can be classified based on the load transfer mechanism. These three categories as expanded upon below:

Friction piles:

The pile capacity of the friction pile is a result of soil adhesion and friction developed to the pile shaft due to soil-structure interaction, their load carrying capacity is from the skin friction and in this case the piles are called friction piles. The maximum pile load capacity of the pile depends on the pile length, which is the most important factor. There are many other affecting factors such as type of soil/rock and pile diameters (Shroff and Shah 2003).

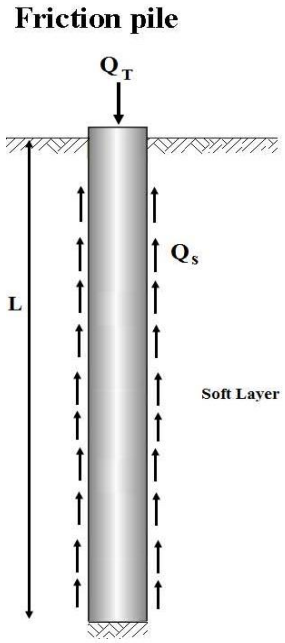

Fig. 2.8 Friction pile

End bearing piles:

Where the piles derive most of their load from end bearing - in other words, if the piles rest on rock or a hard soil stratum - then these piles are called end bearing piles. The pile load transfer mechanism occurs in the pile tip. The end bearing piles functions as a column to transfer the load through a weak soil stratum to the hard soil stratum such as rock layers. It is preferred to extend the piles into the rock if the bed rock is within a reasonable range. The ultimate/maximum pile load capacity depends on the load supported by the pile tip or end bearing. Thus, end bearing piles are also called point-bearing piles (Terzaghi et al. 1996).

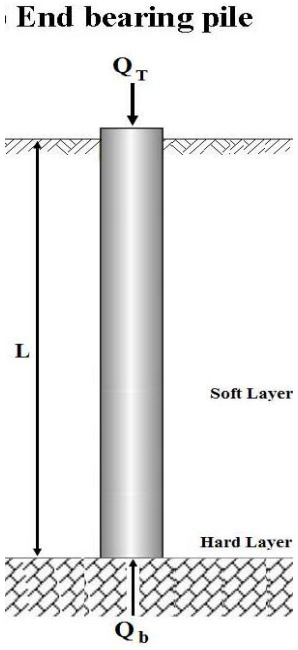

Fig. 2.9 End bearing pile

End bearing and friction piles:

Generally, the pile load capacity will be derived by two load transfer mechanisms, friction and end bearing. The ultimate pile load capacity is the total of the load carried by pile shaft friction and pile end bearing. To mobilise the shaft friction and base resistance, the pile should settle to gain the ultimate load capacity of the piles. The shaft resistance will be activated and, as the load gradually increases, the base resistance comes into action. The shaft resistance is fully developed when the pile settlement reaches 5-10 mm and the end bearing resistance is fully developed at a pile settlement of around 10 per cent of pile diameter (Prakash and Sharma 1990). Settlement should be less than 10 per cent to avoid pile failure for working piles test.

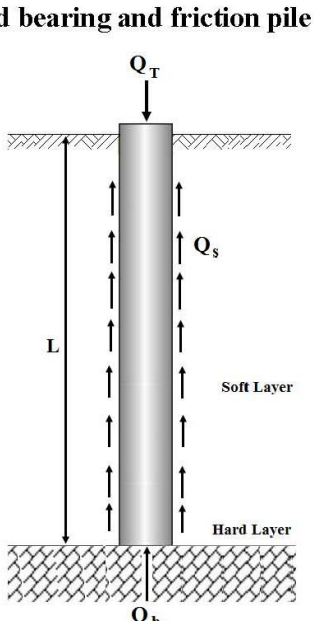

Fig. 2.10 End bearing and friction pile

2.4.3 Based on method of installation

Generally, there are two techniques for piles installation: driven piles and bored piles. Based on the installation methodology, the piles can be classified as per the following:

Bored or replacement piles:

Replacement piles cast in situ piles or bored piles are non-displacement reinforced concrete piles cast in situ to excavated holes. Initially, a borehole is constructed in the ground with the help of a drilling rig, then the pile is constructed by introducing a reinforcement cage into the borehole, followed by filling the hole with concrete. In case unstable soil is encountered in the site during the drilling of the hole, there are many techniques to stabilise the excavated soil, such as temporary casing or using support fluids including bentonite slurry or synthetic polymer fluids.

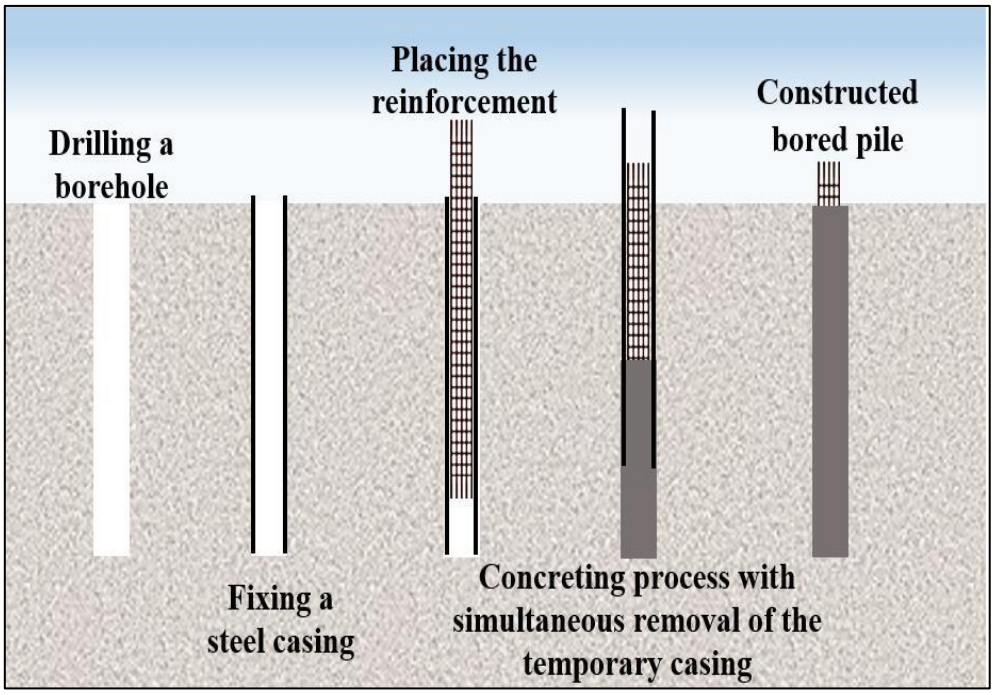

Fig. 2.11 Bored piles construction with temporary casing

For smaller piles diameter pile, the piles can be cast using short flight or continuous flight augers (CFA). The first step in drilling procedure auger to penetrate the soil up to the pile depth, then the auger is slowly removed while the concrete is gradually cast into the soil under controlled pressure using the tremie pipe. Once the concreting is completed, then the pile reinforcement cage is placed in the recently cast concrete (Azizi, 2000).

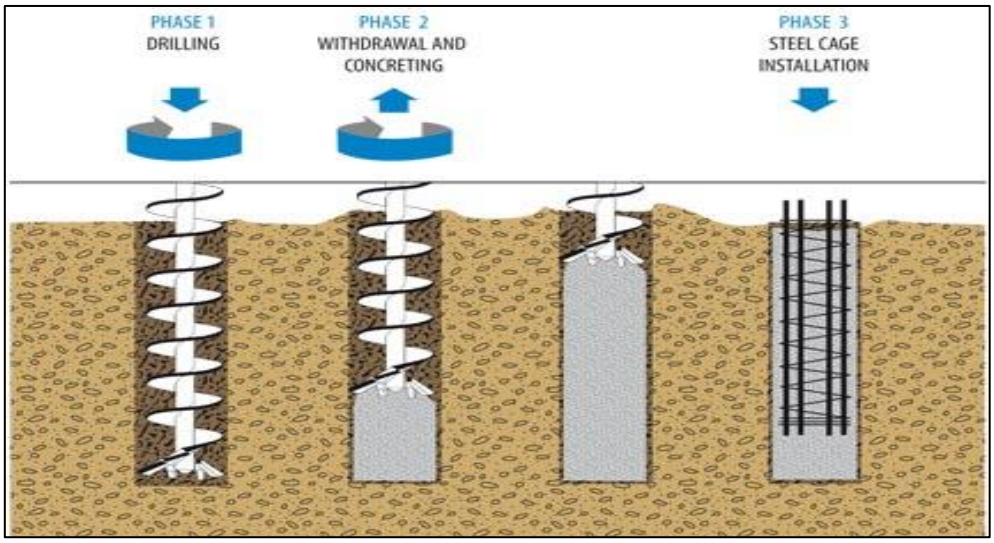

Fig. 2.12 CFA piles construction
(source http://www.alconstructionbelize.com/)

Driven or displacement piles:

Displacement piles or driven piles are usually made of steel, precast concrete or wood. They are defined as displacement piles, which are driven into the soil by hammering or vibrating. The driven mechanics causes displacement to the adjacent soil in the radial direction as the pile shaft penetrates the soil. Different piles cross sections can be used in construction and, as mentioned before, the driven piles are made of timber, steel tubes, steel boxes, precast or prestressed concrete and commonly driven into the soil by hammering, vibrating, screwing or jacking (Azizi, 2000).

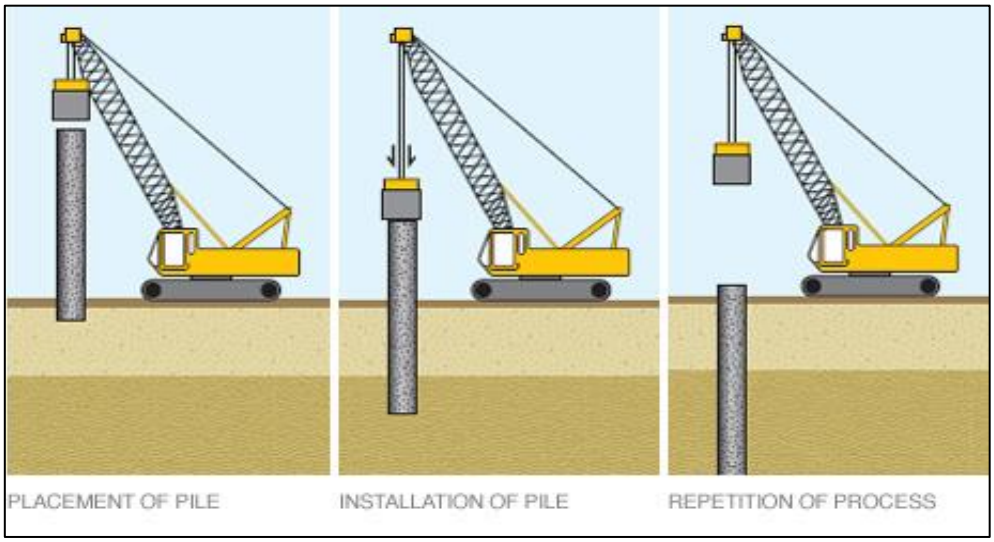

Fig. 2.13 Driven piles by hammering
(source: http://www.basiccivilengineering.com)

2.5 Methods of estimating pile load capacity

Generally, the methodology to estimate the pile capacity is to design the pile foundation, the failure criteria of pile foundation are shear failure and settlement. So, the pile foundation design must be safeguarded against the aforementioned failure criteria and should be within the allowable limits. The different methods used to determine the pile load capacity can be classified as follows:

- Static analysis based on convention approach
- Dynamic analysis
- Pile Load testing
- Correlation from field tests

In the following section, the above methods are explained in more detail.

2.5.1 Static analysis

Conventional approach or static analysis is used for the design of pile foundation depending on the geotechnical investigation. In this method, the soil-mechanics theory is applied for the computation of the pile load capacity based on geotechnical parameters from the soil investigation and ultimate load capacity (Q_u) calculated based on the following equation (Azizi, 2000).

$$Q_u = Q_s + Q_b - W \qquad \text{(Eq. 2.26)}$$

Q_u = Ultimate pile load capacity
Q_s = Ultimate skin friction
Q_b = Ultimate base resistance
W = Weight of pile

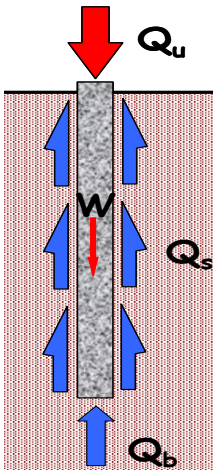

Fig. 2.14 Pile load capacity

2.5.2 Dynamic analysis

Usually, the use of driven piles for pile foundation is to optimise the design. The ultimate/maximum pile load capacity is obtained during the construction of piles as a function of resistance. The principle of re-calculating the pile capacity is the resistance during driving to penetrate the piles, which relies on the energy transferred during pile constriction by the impact hammer based on the ultimate load capacity equation. The equation assumes that the pile load capacity is equal to the dynamic resistance obtained during driving the pile (Council, 2007).

2.5.3 Pile load testing

Generally, pile load testing is conducted on all piling projects. The pile capacity is calculated based on the load tested and the pile settlement within the permissible limit. The pile load testing method is the most expensive method for determining the pile load capacity. On the other hand, it is the most reliable and accurate method to estimate the pile capacity because it tests all of the constructed piles (Smoltczyk, 2003).

2.5.4 Correlation with field tests

This method depends on the result of in situ soil tests to correlate and calculate the pile capacity. Field tests such as standard penetration test (SPT) and cone penetration test (CPT) are conducted to calculate the pile load capacity. The end bearing capacity is computed based on empirical equations where the shaft resistance is calculated based on SPT or CPT (Nejad, et al. 2009).

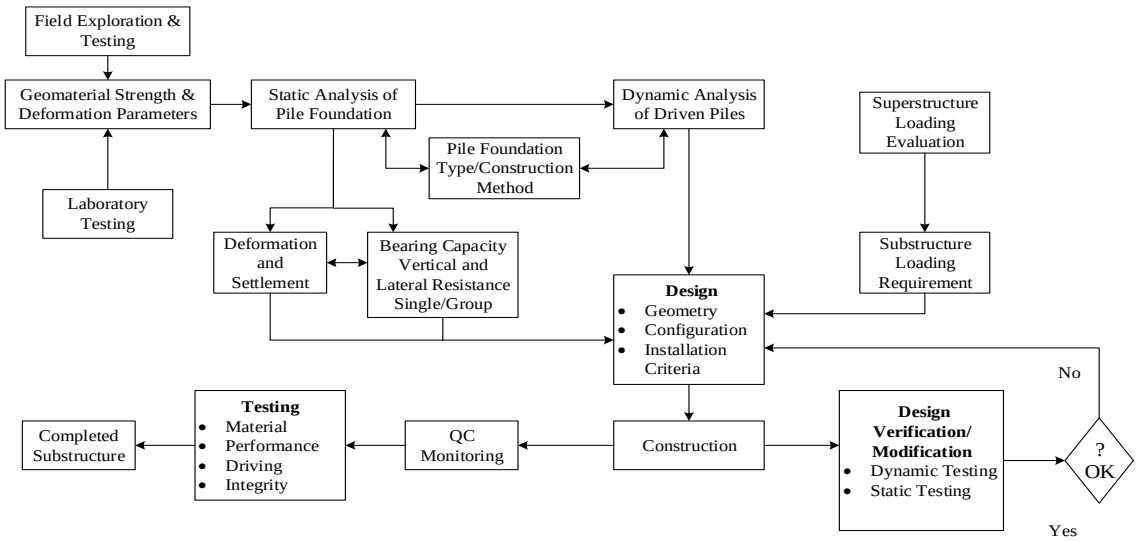

Fig. 2.15 Flow chart for pile design cycle

2.6 Load capacity of single pile in rock

2.6.1 Load transfer mechanism

The load transfer mechanism from a pile to the soil is complicated. Consider a length of pile L. The load on the pile is gradually increased from 0 to Q (z=0) at the ground surface. This load is resisted by the side skin friction developed along the pile shaft Q_1 and part by the soil below the tip of the pile Q_2. The total pile load transferred is the sum of Q_1 and Q_2 (Das 2015). In other words, part of the load will be carried by the skin

shaft friction (Q_1/Q_s) developed along the pile shaft and another part will be carried in base/tip resistance (Q_2/Q_b) developed at the pile base. Generally, the amount of the load is gradually increased, such as in the static load test, the relative settlement of the pile will also increase gradually. The maximum skin friction (Q_s) will develop at a pile settlement of 5 to 10 mm: however, the maximum/ultimate tip resistance (Q_b) will be developed when the base settlement about 10 - 25 percent of the pile diameter, at which point the lower limit applies to driven piles and the upper limit to bored piles (Das 2015). This shows the skin friction will develop a small pile settlement in comparison to tip resistance settlement.

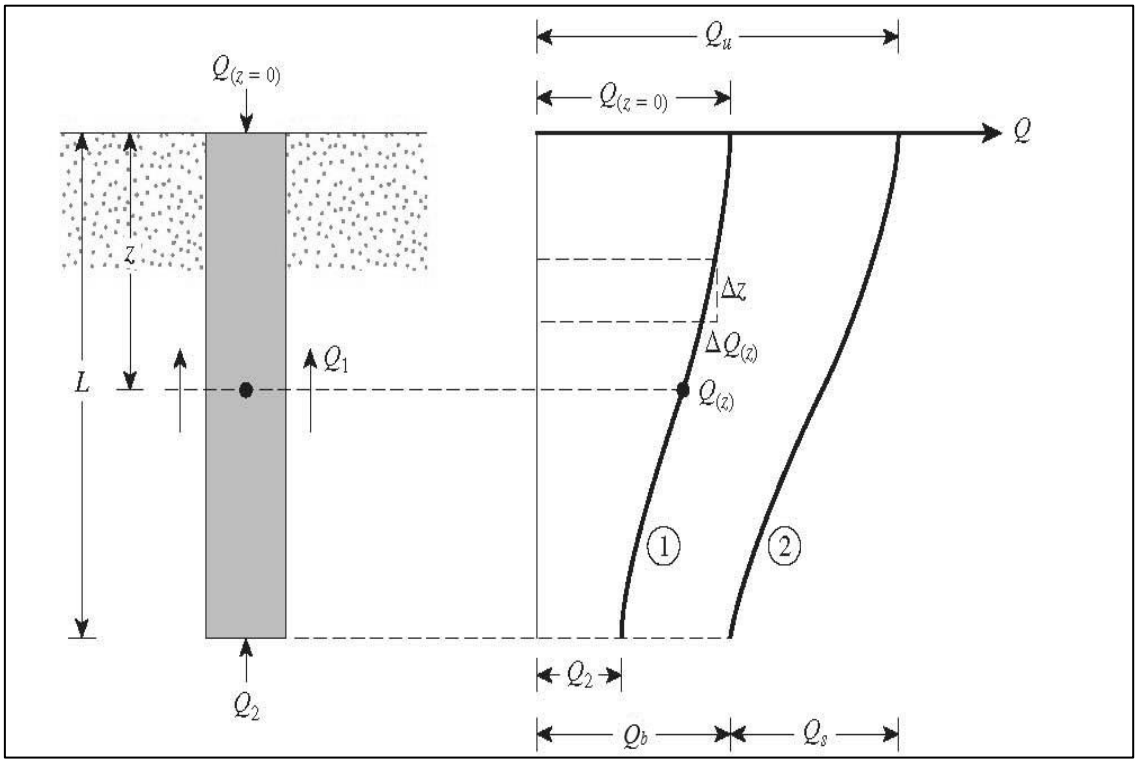

Fig. 2.16 Load transfer mechanism (DAS 7th edition)

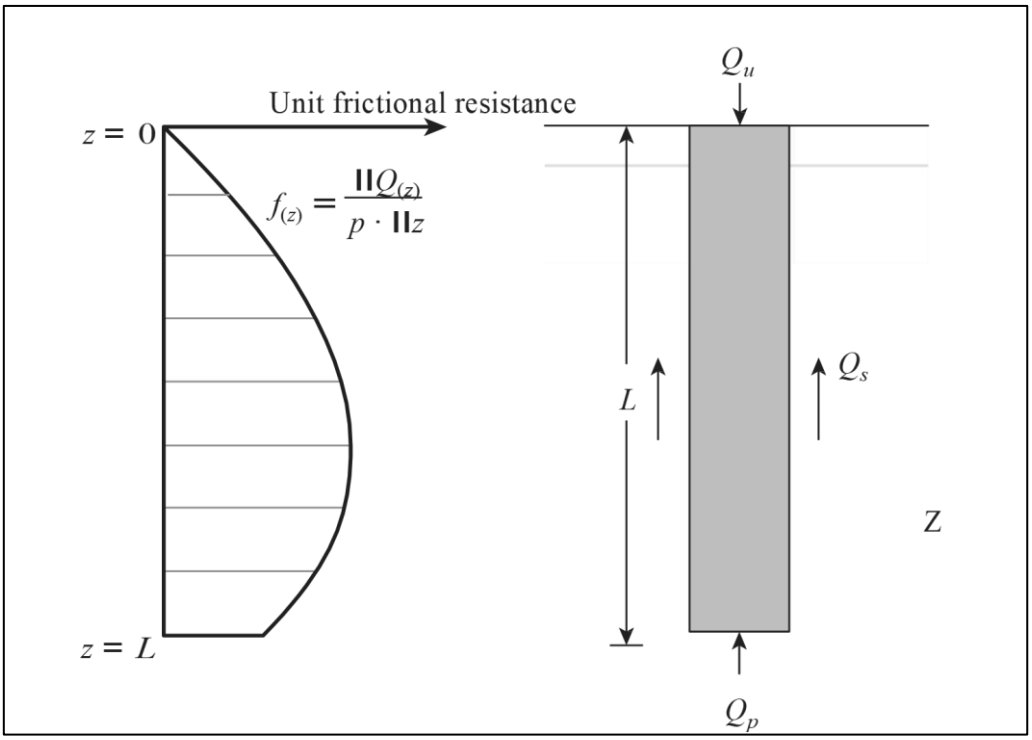

Fig. 2.17 Load transfer mechanism for pile tip (DAS 7th edition)

The failure mechanisms of single pile and shallow foundation are similar. The failure surface is developed at ultimate loading conditions. As shown in the figure below, the failure of the soil at the pile base/tip will be in punching mode. Zone I failure, known as 'triangular zone', is the failure develop at the pile tip at ultimate loading conditions; this zone is pushed downwards without creating any observable slip surface at the ground level. For piles in dense sand and stiff clay, a zone II failure will occur. This failure zone is known as the 'radial shear zone'.

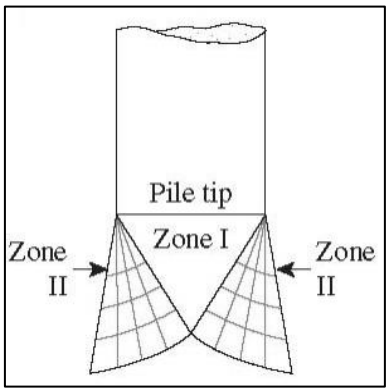

Fig. 2.18 Failure surface developed for single pile (DAS 7th edition)

2.6.2 Calculation of unit shaft resistance

The examination of skin friction formed along the pile shaft during the load transfer mechanism is a complex process, due to the dependency of pile-rock interaction on a number of variable factors, such as: rock material strength, rock socket roughness, normal stress formed, strength of concrete-rock bond, Poisson's ratio, Modulus ratio, extent of superficial deposition, polishing effect due to drilling process and length to diameter ratio of socket.

From the above factors, the length to diameter ratio of the socket is the most important factor in terms of determining the amount of skin friction developed. It will be not necessary to adopt a length greater than that of the required length to develop the available shaft resistance. The shaft resistance distribution corresponding to various length to diameter ratio of rock socket has been shown in the figure below:

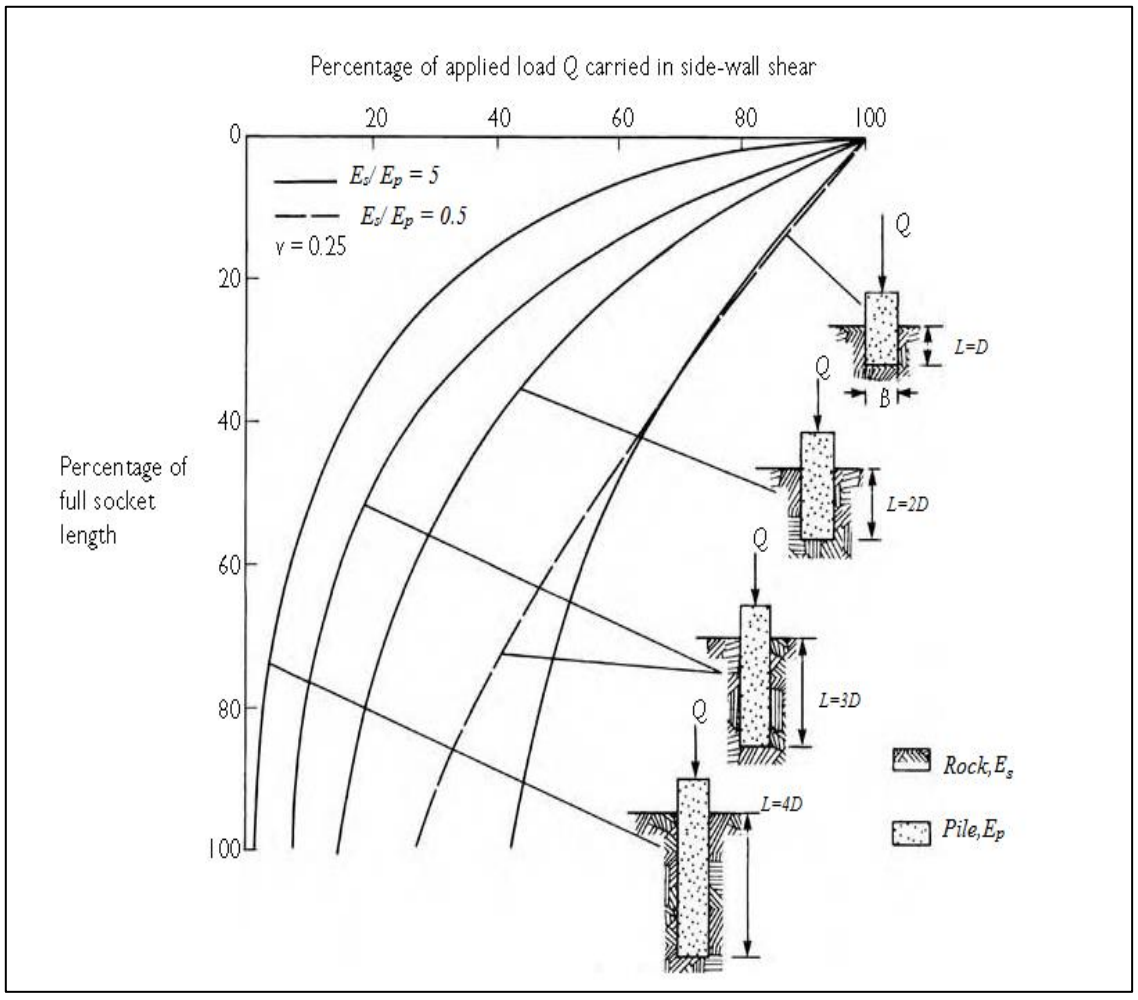

Fig. 2.19 Shaft resistance distribution based on L/D ratio (Tomlinson & Woodward 2007)

As seen in the above figure, if it is necessary to mobilise the base resistance in addition to shaft resistance, then the length of the rock socket should be maintained less than four times the diameter of pile (Tomlinson and Woodward 2007).

Various correlations have been developed between the skin friction developed in the rock socket and the unconfined compressive strength of the rock material. The most popular of these correlations are developed by Williams and Pells (1981), Horvarth (1978) and Rosenberg and Journeaux (1976). The unit skin frictional resistance (q_s) is related to the unconfined compressive strength (q_{uc}) by the following equation:

$$q_s = \alpha . \beta . q_{uc} \qquad \text{(Eq. 2.27)}$$

where

α = Reduction factor depending on q_{uc}
β = Correlation factor for rock mass discontinuity

The reduction factor depends on the adhesion developed at the pile-rock interface, which in turn depends on the rock socket roughness. As shown in the below figure, the reduction factor considers the effect developed due to the rock mass strength. It can also be seen that the value of the reduction factor, as proposed by William and Pells, is greater than the values proposed by Rosenberg and Journeaux, and that of Hovarth(Tomlinson and Woodward 2007). Some of the reasons for this variation are due to the effect of geological differences, variations in back analysis method and differences in the construction method adopted. A common practise is to consider an average of these correlations as a guideline for the initial design: additional information must be collected from the design reports of the past pile tests conducted in the area under consideration (Burland et al. 2012).

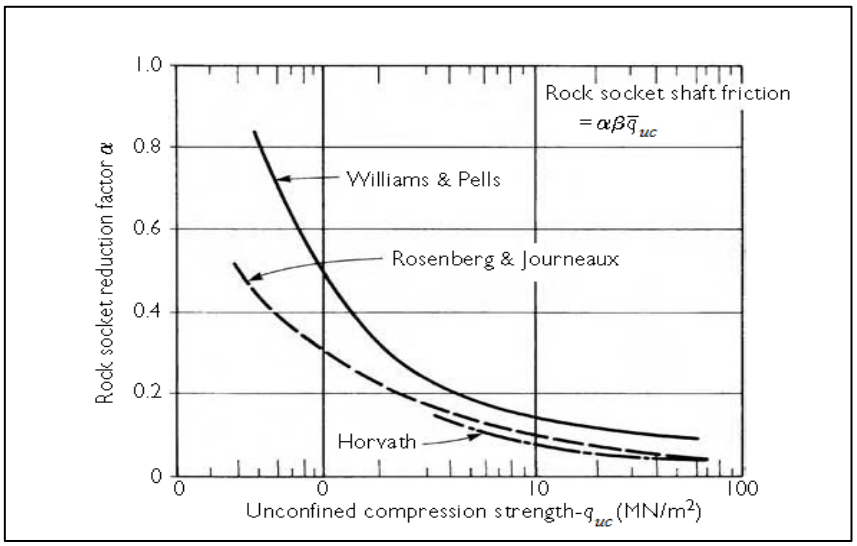

Fig. 2.20 Reduction Factor **α** (From Tomlinson & Woodward, 2007)

The correlation factor associated with the rock mass discontinuity is considered as unity in the methods proposed by Rosenberg and Journeaux, and by Hovarth. However, William and Pells considered the effect of rock mass discontinuity in determining the shaft resistance of the pile and related the value of the correlation factor to mass factor, j, as shown in the below figure. The mass factor can be defined as the ratio between the elastic modulus of the rock mass, E_m and the elastic modulus of intact rock substance, E_r. The rock mass property depends on the number of joints and the spacing between them. The most common methods used to determine of mass factor are seismic velocity measurement and load testing.

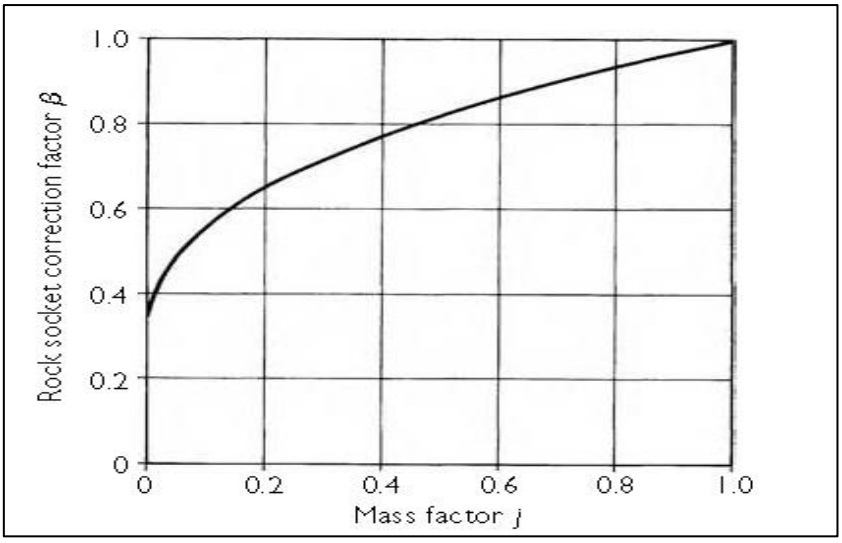

Fig. 2.21 Mass Factor (Tomlinson & Woodward, 2007)

When using the above correlations for the computation of unit shaft friction in mudstones, cautious consideration should be applied. In practise, the predicted values of mudstone rock strength are hardly achieved due to the high influence of rock polishing effect resulting from drilling operations (Burland et al. 2012).

Design method	**α**	**β**
Horvath and Kenney 1979	0.21	0.50
Carter and Kulhawy 1988	0.20	0.50
Williams et al. 1980	0.44	0.36
Rowe and Armitage 1984	0.40	0.57
Rosenberg and Journeaux 1976	0.34	0.51
Reynolds and Kaderbeck 1980	0.30	1.00
Gupton and Logan 1984	0.20	1.00
Reese and O'Neill 1988	0.15	1.00
Toh et al. 1989	0.25	1.00

Table 2.15 Values of α and β as proposed by several researchers (O'Neill et al 1995)

2.6.3 Calculation of unit base resistance

When soil parameters, such as angle of friction and cohesion, are available from the laboratory results, then the following equation can be used to calculate the unit base resistance developed beneath a pile base:

$$q_b = c.N_c + \gamma.L.N_q + \frac{\gamma.D.N_\gamma}{2} \qquad \text{(Eq. 2.28)}$$

where

N_c, N_q, N_γ = Bearing capacity factors
γ = Rock mass density
L = Length of the pile embedded in rock
D = Diameter of pile
L = Length of the pile embedded in rock
c = Cohesion

The first term of the above equation should be multiplied by 1.25 for square piles and 1.2 for circular piles. Also, the third term should be corrected by applying a correction factor of 0.8 for pile with square base and 0.7 for piles with circular base. However, the third term is usually neglected as the diameter/ width of pile foundation is relatively small compared to the length of the pile. So the above equation can be modified as follows for a circular pile (Tomlinson and Woodward 2007).

$$q_b = 1.2c.N_c + \gamma.L.N_q \qquad \text{(Eq. 2.29)}$$

A correlation has been established between the bearing capacity factors and angle of friction φ as shown in figure below.

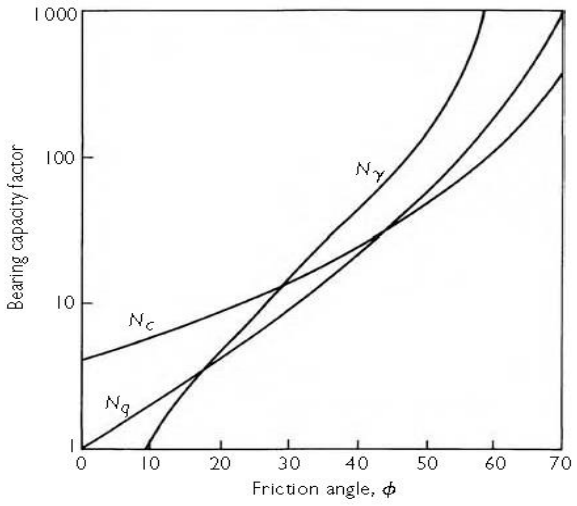

Fig. 2.22 Bearing Capacity Factor (Tomlinson & Woodward 2007)

2.7 Pile settlement calculation based on conventional methods

The single pile settlement subjected to axial load can be calculated using different methods. To calculate single pile settlement, generally there are three methodologies/approaches that can be used. The three design approaches are as per the following:

- Conventional methods: analysis based on empirical and analytical calculation.
- Experimental method: data based on the load-settlement test such as static load test.
- Numerical method: based on FEM analysis.

Pile foundation displacement depends on many variable factors. Usually it is hard to predict the pile settlement due to the many factors affecting the pile settlement, such as: the intensity of load applied; soil pile interaction; pile length and diameter; soil type; the nature of soil strata; soil stiffness; compressibility; bulk density; pile installation method in the state of soil stress; pile load distribution and the load end bearing tip.

The following section describes the estimation of total settlement for pile embedded in the soil using conventional methods. This is mainly composed of the following three mechanisms:

- Elastic shortening of pile
- Plie base settlement: displacement beneath the pile toe.
- Pile shaft displacement: settlement due to load transfer in soil along the pile shaft.

The following sub-sections of 2.7 explains the conventional design approach in detail (empirical and analytical methods) stated by different authors and discusses different methods of calculating settlement of piles. The following methods are widely used to calculate the pile settlement:

- Based on Wyllie approach
- Based on Bowles approach
- Based on Tomlinson approach
- Based on Das approach
- Based on Vesic approach

Many authors have developed empirical, analytical and semi-empirical. The present research discusses and focuses on the methods recommended by Bowles, Tomlinson, Das, Wyllie and Vesic.

2.7.1 Based on Wyllie approach

As per Wyllie (2003), calculating the settlement of a pile socketed into a rock based on the load mechanism and as per the following load procedure:

- Friction piles/shaft resistance only.
- End bearing piles/base resistance only.
- Shaft and end bearing piles/ combined base and shaft resistance.

The proposed computational method can accommodate the varying the modulus of elasticity of soil/rocks in the shaft and tip of the pile. The design method has been derived based on finite element analysis proposed by Pells and Turner (1979) and Rowe and Armitage (1987). The following three-stage-process shows the pile settlement due to axial loading, as per the below:

- The pile deformation starts with the elastic compression of the pile due to the growth of elastic shear strain at rock-structure interface, where it is not attached to the soil/rock.
- In the second stage, where the load is increasing, the load will be transferred to the pile tip due to initiation of slippage/movement at the rock-structure interface.
- In the last stage, the bond between the concrete and soil/rock is separated due to increasing settlement and due to the bond between the pile and the soil; the side shear resistance occurs at the pile sidewalls and the load will be transferred to the pile tip and generate base resistance. At this level, the shaft resistance shows plastic behaviour and slippage/movement occurs on the pile socket side walls.

Piles settlement calculation methods have been obtained for two type of settlement; elastic settlement and plastic settlement of the piles. To calculate the pile elastic settlement, it is assumed that pile comprise of an elastic enclosure bonded into the adjacent soil/rock and fully interfaced to soil/rock, which means that no slippage or movement happens at the rock-pile interface. In this case, the settlement due pile side friction is small and end bearing is not mobilised.

There are several pile socket conditions depending on methodology of construction and site soil characteristics. The pile load transfer mechanism is subject to pile socket conditions. To calculate the pile settlement and to accommodate the conditions, influence factor has been derived for the following conditions (Wyllie, 2003) as per the below:

- Shaft resistance (friction pile).
- Base resistance (end bearing pile).
- Friction and end bearing piles for a homogeneous rock socket.
- Friction and end bearing piles with different modulus of elasticity.

Settlement of friction piles:

The side wall resistance piles or friction piles to hold and to resist the working load in shaft resistance without any contribution from pile tip. The equation to calculate the pile settlement s_t has been proposed as follows:

$$s_t = \frac{Q_t . I_s}{D . E_s} \quad \text{(Eq. 2.30)}$$

where
Q_t = Total load applied
D = Diameter of pile
E_s = Modulus of deformation of rock forming the shaft
I_s = Elastic settlement influence factor shown in Fig. 2-23

The modulus of elasticity (E_s) value for the rock has been correlated with the soil/rock's unconfined compressive strength q_u values, taking into consideration safety factor of two. The following has been proposed by Rowe and Armitage (1987):

$$E_S = 110 . \sqrt{q_{uc}} \quad \text{(Eq. 2.31)}$$

where q_{uc} = Unconfined compressive strength of rock

There are many methods to estimate the modulus of elasticity (Es), as mentioned in section 2.2.7. The modulus of elasticity value depends on many factors such as rock degree of fracture or RQD. Hence, the relationship between rock quality characteristics and modulus of elasticity (E_s) should be considered and reduction should be applied to the modulus of elasticity (E_s) value in the above equation based on engineering sense for fractured rocks. The value of influence factor (I_s) has been correlated to the pile geometry and the modulus of elasticity of rock (E_s) and modulus of elasticity (E_p) for pile material. Based on the graph below, developed by Pells and Turner (1979), the value influence factor (I_s) depend on the modulus ratio R and L/D ratio. The values below have been obtained from Poisson's ratio of 0.25. However, a negligible effect on the influence factor has been proven for the value of Poisson's ration within a range of 0.15 - 0.3 for concrete material and 0.1 – 0.3 for rock material (Wyllie, 2003).

$$R = \frac{E_p}{E_s} \quad \text{(Eq. 2.32)}$$

where
L = Length of the piles
E_p = Modulus of elasticity of pile material

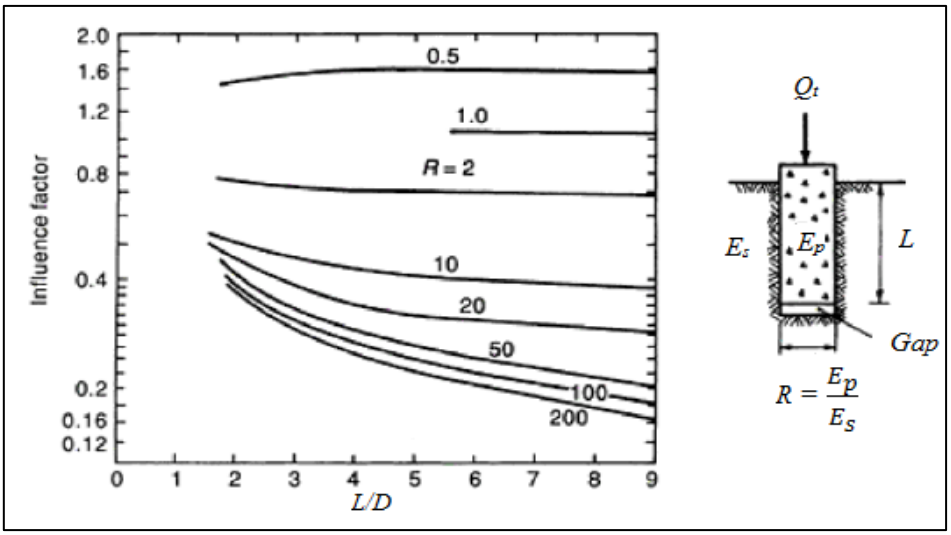

Fig. 2.23 Influence factor for side wall socketed piles (Pells & Turner, 1979)

The influence factor (I_s) values shown in the above figure assumes that the pile and soil/rock are the pile is fully bonded. However, reduction should be applied to the influence factor for piles recessed below the ground level. The pile recessed due to the pile socket passes through weak layers with low pile side friction or due to the using casing of upper portion; the pile settlement equation has been modified for recessed pile as per the below (Wyllie, 2003).

$$S_t = RF * \frac{Q_t . I_s}{D . E_s} \qquad \text{(Eq. 2.33)}$$

RF= Reduction Factor for recessed piles given in figure 2.24 below.

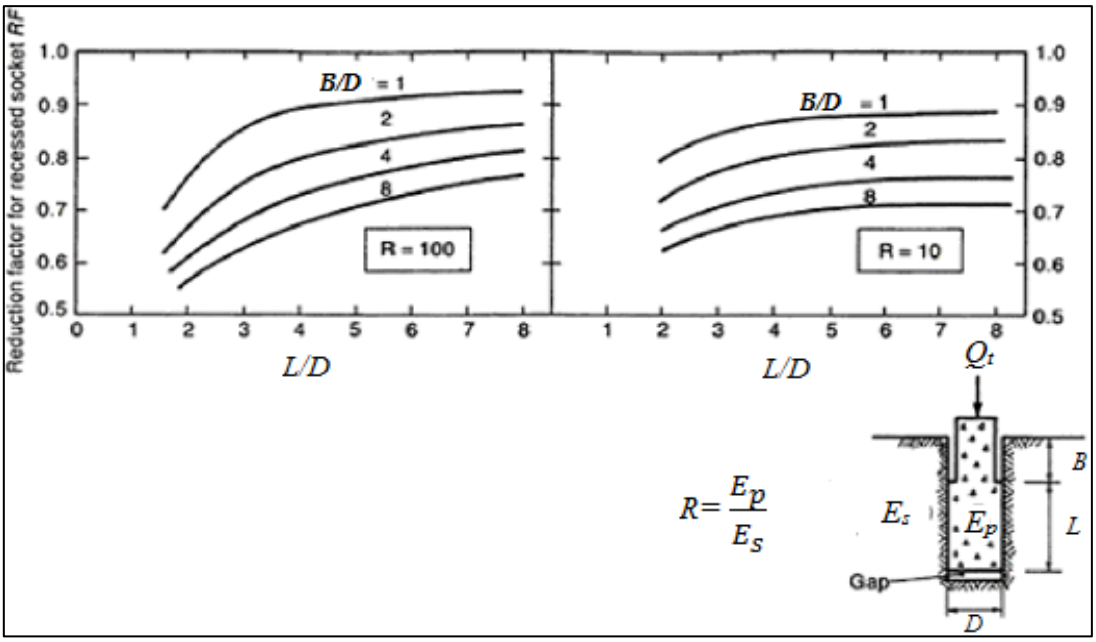

Fig. 2.24 Reduction factor for recessed piles (Pells & Turner, 1979)

Settlement of end bearing pile:

The calculation of settlement for end bearing piles will be related to a rigid footing resting on the surface. However, the pile displacement will be less than the rigid footing due to the area of pile tip, which is less when compared to the footing size and the rock mass area present in the pile base. To allow for this confinement in the settlement calculation, a reduction factor has been considered in the calculation. The reduction factor curve has been developed by Pells and Turner (1979) as shown below. Correlation between the ratio of pile length (L) to the pile diameter (D) and the ratio between modulus of pile material (E_p) to the modulus of rock at the pile base (E_b) as shown in the below figure. If the ratio of pile stiffness to rock stiffness under the pile tip (E_p/E_b) is greater than 50, then the pile is treated as a rigid footing and if this stiffness ratio is less than 50, then the pile is treated as a flexible footing (Wyllie, 2003).

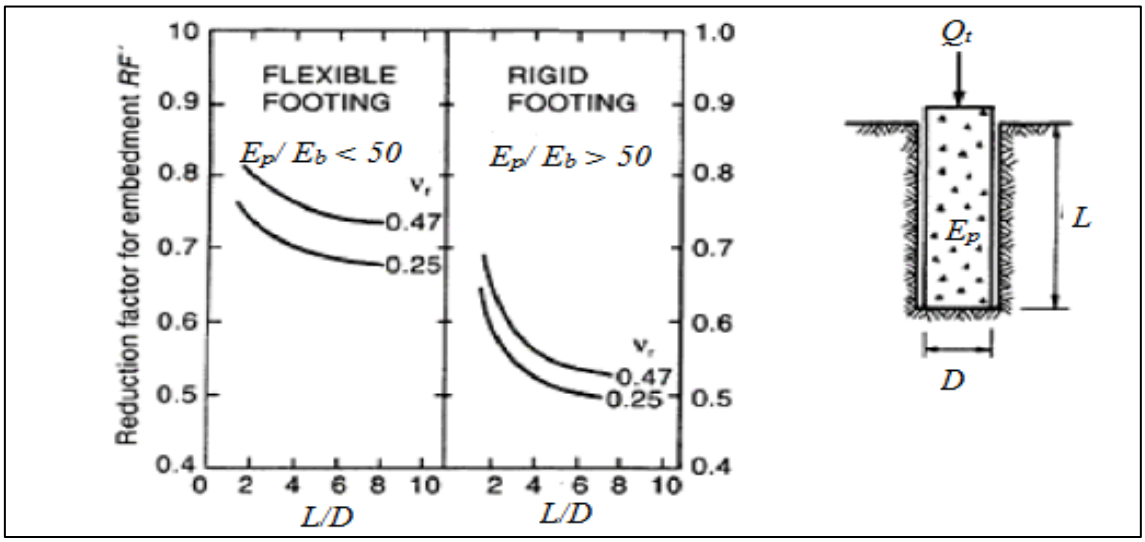

Fig. 2.25 Reduction factor for end bearing piles (From Pells & Turner, 1979)

So, considering the reduction factor, the settlement of an end bearing pile including for the elastic shortening of the pile shaft can be calculated as follows:

$$S_t = \frac{4Q_t}{\Pi D^2} * \left[\frac{L}{E_s} + \frac{RF'.C_d.D\,(1-\mu^2)}{E_b}\right] \qquad \text{(Eq. 2.34)}$$

RF'= Reduction factor for piles in end bearing
C_d = Shape and rigidity factor
= 0.85 for circular pile considered as flexible footing
= 0.79 for circular pile considered as rigid footing
μ = Poisson's ratio
E_b = Elastic modulus of the rock mass beneath the pile tip

Settlement of friction and end bearing piles:

The piles will resist the load in friction/shaft resistance and end bearing resistance. The pile settlement due to the load carried in pile shaft can be calculated with the equation shown below, by using the influence factor for an end bearing and socketed piles.

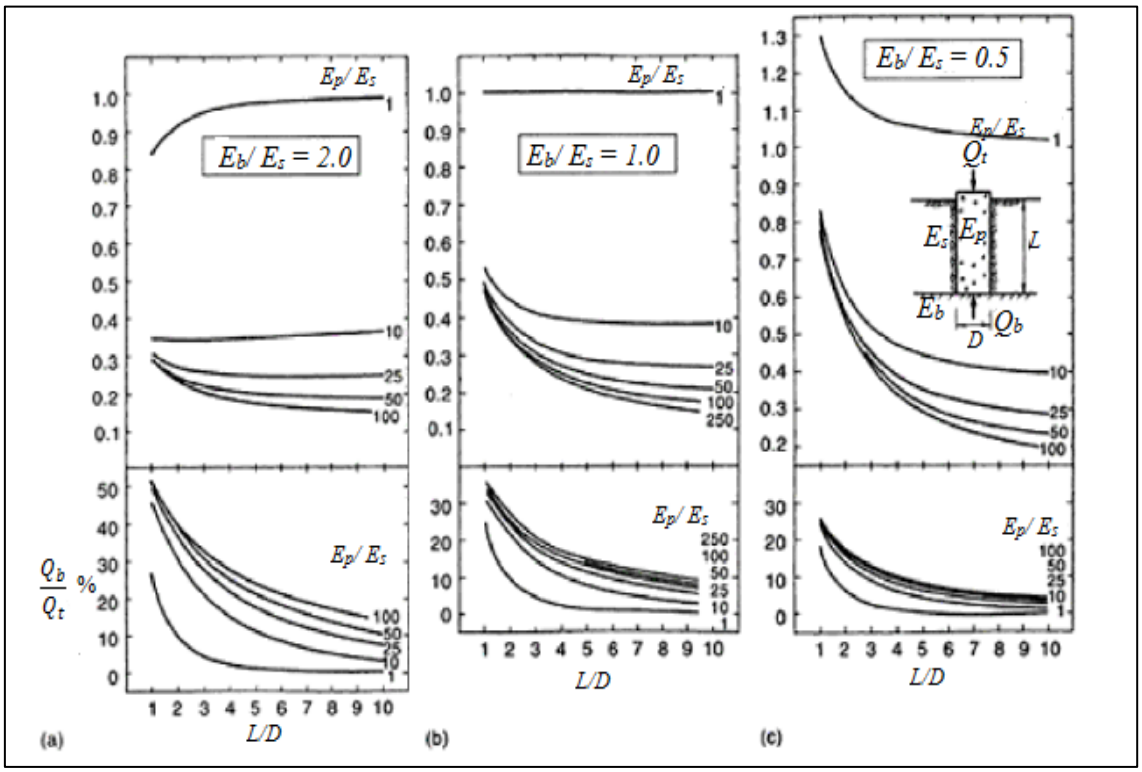

Fig. 2.26 Friction &end bearing piles Influence factor (Rowe & Armitage 1987)

Rowe and Armitage (1987) developed the above curve to be used to estimate the elastic behaviour of pile, considering full bonded between shaft of the pile and soil/rock. The curves show the difference in the influence factor with respect to modulus of elasticity of rock under the pile tip E_b and pile shaft E_s. The influence factor for end bearing with shaft resistance piles has a larger value than that for friction piles (Wyllie, 2003). By adding the settlement from previous equation (Eq. 2.33) the total settlement for shaft and end bearing pile can be expressed as below:

$$s_t = RF.\frac{Q_t.I_s}{D.E_s} + \frac{4Q_t}{\Pi D^2}.\left[\frac{L}{E_s} + \frac{RF'.C_d.D\,(1-\mu^2)}{E_b}\right] \qquad \text{(Eq. 2.35)}$$

For the load to be supported by the pile tip, it is important to check if the end bearing load will exceed the bearing capacity of soil/rock under the pile tip. The amount of the load carried in base resistance can be estimated by using the lower part of graph shown in the figure above.

2.7.2 Based on Joseph E. Bowles approach

As per Bowles (1997), the total pile total settlement (H_p) can be calculated as per the following equation:

$$H_p = \Delta H_a + \Delta H_{pt} \quad \text{(Eq. 2.36)}$$

where

ΔH_a = Elastic axial compression of pile.
ΔH_{pt}= Point pile settlement.

The elastic settlement of pile can be computed as the sum of settlements (ΔH_a) due to the average axial force acting on each pile segment of length (ΔL) with an average cross-sectional area, A_p, and modulus of elasticity, E_p. The first equation below calculates the pile elastic axial compression; the second term is for the elastic-plastic point settlement under the pile tip.

$$\Delta H_{s,s} = \frac{P.\Delta L}{A_p . E_p} \quad \text{(Eq. 2.37)}$$

$$\Delta H_a = \sum \frac{P.\Delta L}{A_p . E_p} \quad \text{(Eq. 2.38)}$$

The elastic plastic point settlement under the pile tip can be computed using the equation given below.

$$\Delta H_{pt} = \Delta q. D. \frac{1-\mu^2}{E_s} . m. I_s. I_F. F_I \quad \text{(Eq. 2.39)}$$

where

P = Total axial force acting on the pile
L = Length of the pile
A_p = Area of cross section of pile
E_p = Modulus of elasticity of pile
Δq = Bearing pressure at the pile tip
= Total axial load divided by the pile cross sectional area
$= Load/A_p$
D = Diameter of pile
μ = Poisson's ratio
E_s = Elastic modulus of soil beneath the pile tip
mI_s = Shape factor
= 1 for circular pile

based on the pile length (L) and pile diameter (D), the value of coefficient of embedment factor I_F can be as per the following values:

I_F = Embedment factor by Fox
= 0.55 if $L/D \leq 5$
= 0.50 if $L/D > 5$

The Reduction factor F_1 has the following cases:

F_1= Reduction factor = 0.25 for friction piles only, if the mobilised axial skin friction reduces the point load at the pile base, $P_p < 0$, thus the total load is mainly carried in skin friction.

F_1= Reduction factor = 0.75 for end bearing piles only, if the pile is end bearing. Also, could be consider minor skin friction for same case.

F_1= Reduction factor = 0.5 for friction & end piles, if the mobilised base resistance $P_b > 0$, and the total load is transmitted through bearing resistance and skin friction.

The tip zone movement due to the point load and the settlement of the pile due to the load transmitted along the pile shaft is accounted for by the factor F_1. In this technique, the total axial load and an estimated value of factor F_1 is used. The suggested value of F_1 must be modified to accommodate the various stratifications (Bowles 1997).

2.7.3 Based on M. J. Tomlinson approach

As per Tomlinson (2008), the load transfer mechanism between the soil and pile influences the axial elastic displacement of the pile. The settlement of a pile embedded in rock can be computed by the following equation (Tomlinson &Woodward 2007).

$$s_t = s_e + s_b + s_f \qquad \text{(Eq. 2.40)}$$

where

s_e= Axial compression of the material of the pile.
s_b = Deformation of the soil beneath the pile base due to the load acting at the pile tip
s_f = Settlement of the soil due to the load transfer along the pile shaft

The pile elastic shortening is calculated in accordance with Hooke's law. As per this law, the deformation of material is proportional to the applied stress within the elastic limit.

$$\text{i.e. } \varepsilon = \frac{\sigma}{E} \qquad \text{(Eq. 2.41)}$$

where

ε = Deformation
σ = Applied stress
E = Young's modules of material
linear deformation is the ratio of change in length to original length.

$$\varepsilon = \frac{\Delta L}{L} \qquad \text{(Eq. 2.42)}$$

where

ΔL = Change in length
L = Original length

By assembling the above equations for the value of deformation, the following fundamental formula is used to determine the variation in length of any material.

$$\Delta L = \frac{L \cdot \sigma}{E} \qquad \text{(Eq. 2.43)}$$

where

σ = Force acting per unit area = $\frac{F}{A}$
F = Applied force
A = Area of cross section

The above equation can be expressed as per the following:

$$\Delta L = \frac{L \,.\, F}{E \,.\, A} \qquad \text{(Eq. 2.44)}$$

The above equation cannot be applied for the computation of the elastic shortening of the pile material due to many reasons, such as the load transmitted to the soil by skin friction. The elastic shortening of pile relies on the mobilised side way resistance, which reduces the pile settlement. The above equation should be modified to accommodate the pile load transfer mechanism. The applied load is divided into skin friction load (Q_s) and end bearing load (Q_b) to calculate the elastic shortening of the pile. The following equation is modified to accommodate the effect of shaft resistance. The equation reduced by a factor (0.5) the elastic shortening as per the following.

$$s_e = \frac{(2Q_b + Q_s).L}{2E_p \,.\, A_p} \qquad \text{(Eq. 2.45)}$$

where

Q_b = Load carried by base resistance
Q_s = Load carried by skin resistance
L = Length of the pile
A_p = Area of cross section of pile
E_p = Modulus of elasticity of pile

Pile end bearing settlement, due to a point load acting at the pile tip, can be calculated by using the following equation

$$s_b = \frac{\pi}{4} \cdot \frac{Q_b}{A_b} \cdot \frac{D(1-\mu^2)}{E_b} . I_b \qquad \text{(Eq. 2.46)}$$

where

Q_b = Load acting at pile base per unit area = $\frac{Q_b}{A_p}$
D = Diameter of pile
A_b = Area of pile tip
μ = Poisson's ratio
E_b = Elastic modulus of soil beneath the pile tip
I_b = Influence factor (depends on L/D ratio)

When L/D ratio is greater than five, the influence factor (I_b) equal to 0.5 and the Poisson's ration is within the range of 0 to 0.25.

Pile friction settlement due to the load transferred along the pile shaft can be calculated using the following equation.

$$s_f = \frac{Q_s.I_s}{D.E_s} \qquad \text{(Eq. 2.47)}$$

where

E_s = Elastic modulus of soil surrounding the pile shaft
I_s = Influence factor

The soil-structure interaction during the load transfer mechanism is affected by pile length and diameter, pile concrete/material modulus of elasticity and the soil/rock modulus of elasticity. For the above factors, Pells and Turner have developed the diagram below, which was also initially proposed by Poulos and Mattes (1960) to find the influence factor (I_s) by correlating between the modulus ratio *R*, *L/D* ratio, as shown in the following figure.
where

$$R = \frac{E_p}{E_s} \qquad \text{(Eq. 2.48)}$$

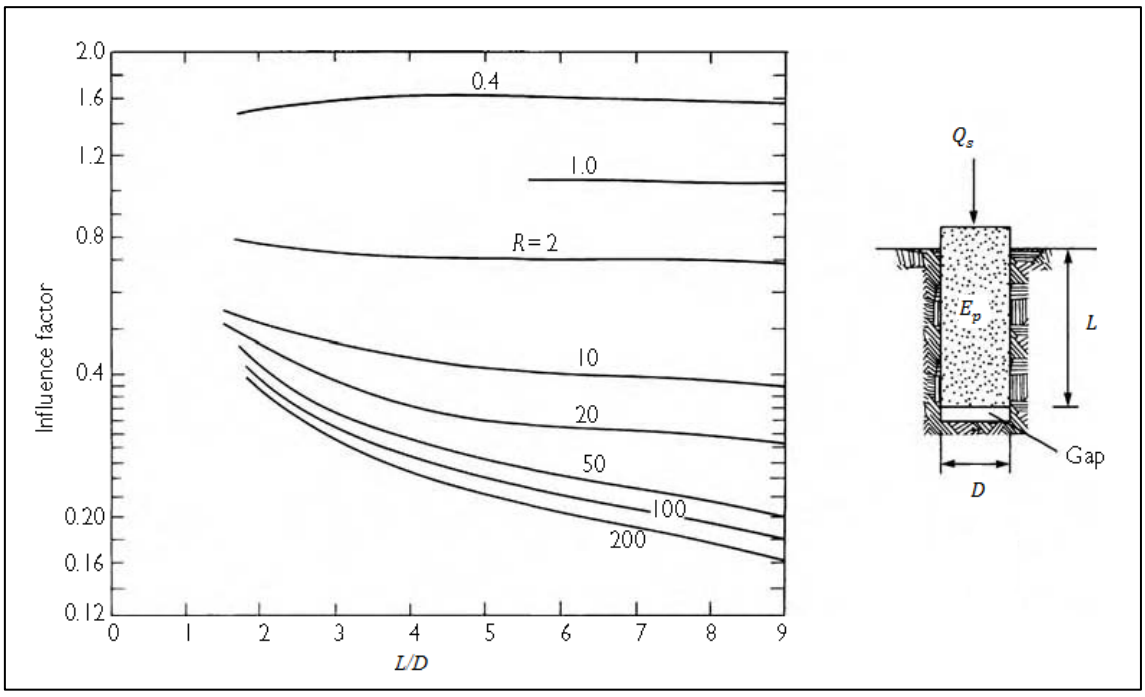

Fig. 2.27 Influence factor (Pells and Turner)

2.7.4 Based on Braja M. Das approach

In this method, the procedure of determining pile settlement is to separate the individual components based on the load transfer mechanism and the amount of settlement of pile. Pile settlement is the summation of the elastic compression of the pile shaft $s_{e(1)}$, elastic deformation of the soil beneath the pile base $s_{e(2)}$ and settlement of the soil due to the load carried by skin friction $s_{e(3)}$. This is given by using the following equation, as provided in Das (2011).

$$s_e = s_{e(1)} + s_{e(2)} + s_{e(3)} \quad \text{(Eq. 2.49)}$$

As per the elastic theory, first deformation component is derived by the below modified equation

$$s_{e(1)} = \frac{(Q_{wp} + \xi \cdot Q_{ws}) \cdot L}{E_p \cdot A_p} \quad \text{(Eq. 2.50)}$$

where

Q_{wp} = Load transferred to the pile base
Q_{ws} = Load transferred through skin friction
ξ = Reduction factor
L = Total pile length
E_p = Elasticity modulus of pile
A_p = Cross-sectional area of pile

As provided in the previous section, a reduction factor is applied to the frictional force to consider the settlement decreasing effect of skin friction. The magnitude of the reduction factor ξ is influenced by the frictional distribution along the pile shaft, and varies between 0.5 and 0.67 depending on the load transfer between the pile shaft and the soil surrounding the shaft, as given in the figure below. The hyperbolic function realistically reflects the behaviour of piles when loaded and accurately approximates load-settlement performance (Fleming 1992).

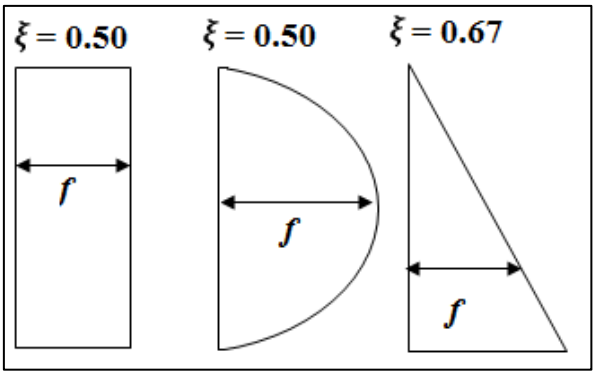

Fig. 2.28 Value of ξ for different distribution of skin friction

The difference in the frictional resistance of the shaft match with the curve, as shown in the figure below. The frictional force developed relating to the surface area of the shaft is defined as follows (Das 2011):

$$f_{(z)} = \frac{\Delta Q_{ws}}{p \cdot \Delta z} \qquad \text{(Eq. 2.51)}$$

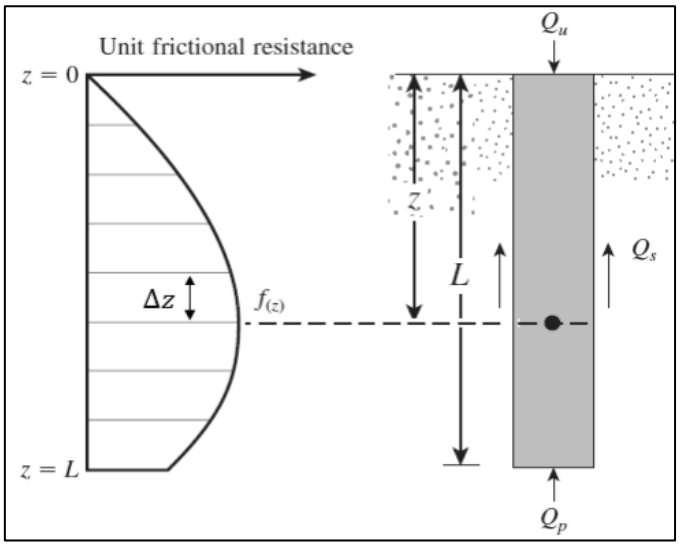

Fig. 2.29 Development of unit skin friction (modified from Das 2011)

The second deformation term in the equation evaluates the pile base settlement caused by the point load q_{wp}. The point load is defined as the ratio of the load transferred to the pile base to the cross-sectional area of the pile tip. For the influence factor I_{wp} (Das 2011) recommends a value of 0.85.

$$s_{e(2)} = \frac{q_{wp} \cdot B}{E_b}(1 - \nu^2) \cdot I_{wp} \qquad \text{(Eq. 2.52)}$$

The third component, the skin friction settlement is determined by the following equation.

$$s_{e(3)} = \left(\frac{Q_{ws}.B}{p.D}\right).\frac{B}{E_s}.(1-\nu^2).I_{ws} \qquad \text{(Eq. 2.53)}$$

where

p = Circumference of the pile
L = Total pile length
E_s= Elasticity modulus of soil surrounding the pile
I_{ws}= Influence factor

The expression inside the brackets $\left(\frac{Q_{ws}}{p \cdot D}\right)$ in the above equation is the average unit friction f distributed over the pile length. The influence factor I_{ws} defined by Vesic (1977) is calculated by the following empirical formula.

$$I_{ws} = 2 + 0.35\sqrt{\frac{D}{B}} \qquad \text{(Eq. 2.54)}$$

2.7.5 Based on Vesic approach

Vesic proposed two methods to calculate the pile settlement. An empirical approach was proposed in 1970, followed by a semi-empirical approach in 1977. Both methods will be explained as follows:

Empirical approach (1970)

The pile settlement s_t under working load conditions can be calculated using following equation:

$$S_t = \frac{D}{100} + \frac{Q_t\, L}{E_p.A_p} \qquad \text{(Eq. 2.55)}$$

where

s_t = Settlement of pile in inches
D = Diameter of pile in inches
L = Length of the pile in inches
Q_t = Total load acting on the pile in pounds (lbs)
E_p = Modulus of elasticity of pile in lbs/in.^{2}

Semi-empirical approach (1977)

As per Vesic (1977), the pile total settlement can be divided into three components as follows:

$$S_t = S_e + S_b + S_f \quad \text{(Eq. 2.56)}$$

where

s_e = elastic shortening settlement due to the elastic compression
s_b = pile base Settlement due to the load transmitted at the pile base.
s_f = Pile shaft settlement due to the load transmitted to the pile shaft.

Assuming the pile material to be elastic, the pile shaft total settlement s_e can be calculated as:

$$S_e = \frac{(Q_b + \xi . Q_s).L}{E_p . A_p} \quad \text{(Eq. 2.57)}$$

where

Q_b = Load carried by base resistance
Q_s = Load carried by skin resistance
L = Length of the pile
A_p = Area of cross section of pile
E_p = Modulus of elasticity of pile
ξ = factor depending on the distribution of skin friction along the pile shaft

The value of ξ depends on the load distribution. For example, for uniform or parabolic distribution of skin friction along the pile shaft $\xi = 0.5$. However, for the triangular distribution of shaft friction, a value of $\xi = 0.67$ is recommended (Vesic, 1977). Sharma and Joshi (1988) stated that the pile settlement based on the uniform or triangular distribution will not differ to a great degree depending on the ξ values. Hence, both the values of ξ (0.5/0.67) will give a logical pile settlement estimate (Prakash & Sharma, 1990).

Vesic developed a relationship based on the experimental studies conducted by testing piles of various types, embedded piles in soils with different diameters ranging from 5 to 46 cm, the relationship between different relative densities, the soil properties, ultimate point/end bearing resistance and settlement of pile. The following theoretical and empirical equation has been proposed to calculate the pile settlement due to end bearing load and pile friction load (Prakash & Sharma, 1990).

The pile base settlement (s_b) can be calculated as:

$$S_b = C_p . \frac{Q_b}{D . q_b} \quad \text{(Eq. 2.58)}$$

The pile shaft settlement (s_f) can be calculated as:

$$S_t = C_s . \frac{Q_s}{L . q_b} \quad \text{(Eq. 2.59)}$$

q_p= Load acting at pile base per unit area = $\frac{Q_b}{A_p}$

D = Diameter of pile

C_p= Empirical coefficient

C_s = 0.93+0.16 $\sqrt{\frac{L}{D.C_p}}$

As proposed by Vesic (1977), the typical values of coefficient C_p proposed are shown in the table below:

Soil Type	**Driven Piles**	**Bored Piles**
Sand (dense to loose)	0.02 – 0.04	0.09 – 0.18
Clay (stiff to soft)	0.02 – 0.03	0.03 – 0.06
Silt (dense to loose)	0.03 – 0.05	0.09 – 0.12

Table 2.16 C_p values for driven & bored piles (Prakash and Sharma, 1990)

2.8 Finite element method - numerical method

Numerical techniques are widely used to calculate the pile foundation settlement and obtain accurate pile settlement values. However, the level of calculation accuracy depends on the quality of soil parameters used in the analysis (Azizi, 2000).

There are many practical engineering problems for which we cannot obtain exact solutions. This inability to obtain an exact solution may be attributed to either the complex nature of governing differential equations or the difficulties that arise from dealing with the boundary and initial conditions. To deal with such problems, it is required to resort to numerical approximations. In contrast to analytical solutions which show the exact behaviour of a system at any point within the system, numerical solutions approximate exact solutions only at discrete points, called nodes. The first step of any numerical procedure is discretisation. This process divides the medium of interest into a number of small sub-regions and nodes. There are two common classes of continuum numerical methods:

- Finite difference methods
- Finite element methods

With finite difference methods, the differential equation is written for each node and the derivatives are replaced by difference equations. This approach results in a set of simultaneous linear equations. Although finite difference methods are easy to understand and employ in simple problems, they become difficult to apply to problems with complex geometries or boundary conditions. This situation is also true for problems with no isotropic material properties. In contrast, the finite element method uses integral formulations rather than difference equations to create a system of algebraic equations. Moreover, an approximate continuous function is assumed to represent the solution for each element. The complete solution is then generated by connecting or assembling the individual solutions, allowing for continuity at the inter-elemental boundaries. The basic steps involved in any finite element analysis consist of the following:

Pre-processing Phase

- Create and discretise the solution domain into finite elements; that is, subdivide the problem into nodes and elements.
- Assume a shape function to represent the physical behaviour of an element; that is, an approximate continuous function is assumed to represent the solution of an element.
- Develop equations for an element.
- Assemble the elements to present the entire problem. Construct the global stiffness matrix.
- Apply boundary conditions, initial conditions, and loading.

Solution Phase

- Solve a set of linear or nonlinear algebraic equations simultaneously to obtain nodal results, such as displacement values at different nodes or temperature values at different nodes in a heat transfer problem.
- Obtain other important information.

Post-processing Phase

At this point, you may be interested in values of principal stresses, heat fluxes, etc. In general, there are several approaches to formulating finite element problems:

- Direct Formulation
- The Minimum Total Potential Energy Formulation
- Weighted Residual Formulations

It is important to note that the basic steps involved in any finite element analysis - regardless of the way in which the finite element is modelled - will be same as per the above and will also be guided by the above.

The basic principle of FEA involves the following.

- Set geometry
- Discretise domain
- Set material parameters
- Set boundary conditions
- Apply loading
- Solve

2.9 Modelling in PLAXIS software

2.9.1 Introduction

PLAXIS is a company developing geotechnical software, using the finite element modelling approach. The software has the capability to simulate modelling in both two and three dimensions, with the soil properties and soil-structure interaction being modelled accurately. PLAXIS includes three main theories in its software for solving the FEM models, which are deformation, groundwater flow and consolidation. In this thesis, the version 'PLAXIS 2D Classic' is used and only static calculation is covered. The current research uses a static analytical approach. In this section PLAXIS 2D is presented for modelling. Subsequently, the material models available in PLAXIS are elaborated on. This section is based on the literature provided in PLAXIS manuals.

2.9.2 PLAXIS 2D

PLAXIS 2D enables the modelling of geotechnical problems either in a plane strain condition or as an axisymmetric model. In this dissertation, the problems are analysed using the axisymmetric approach. The general procedure while modelling in PLAXIS is to specify the model type. This is followed by defining the geometry with elements and corresponding materials, assigning loads and boundary conditions, creating a FEM-mesh, defining the initial condition, and performing the FEM-calculation. The procedure is detailed in this section on step-by step basis.

2.9.3 Principles of FEM analysis in PLAXIS

The efficient subsoil model derived is designed for the numerical solution of the soil-structure interaction to ascertain the accurate behaviour. The main purpose of the model is for the analysis of the distribution of forces and soil behaviour, including the influence of any subsoil or soil medium, without the need for expensive three-dimensional modelling. The relevant programs and their input data need not be too complicated as these demands do not match the physical complexity of the soil medium and, from the natural science point of view, can never be fulfilled in relation to the continuing rapid progress in the field of geo-mechanics. The prevalent gap in the current state of knowledge and practical design, using in many cases only the old "Winklerian" ideas, cannot be closed by further theoretical progress, even if it will prove useful in the future. It is necessary to include engineering ideas that are not just based on theoretical analysis but to interpret the behaviour and evaluate the accuracy subject to the model generated. The physical properties of the subsoil are expressed in a condensed form, despite their complex nature. The aim of this research is to develop a methodology

which may be used to consistently provide accurate soil properties in analysis and design and, ultimately, yield an economic design for the pile element.

The above is intended to address the problem orientation of the soil model represented and study soil behaviour from a geo-technical perspective. It is only a part of the whole model (structure + foundation + subsoil) which contains full information on this modelling, when the structure is composed of various two-dimensional elements. The present research deals only with constitutive soil model which satisfies the Mohr-Coulomb theory. Embedded Pile elements have been idealised in the two-dimensional models lying on subsoil. Pile loads have been applied as distributed loads at the top of the pile element. The soil layer has been discretised into element meshes to effect reasonable distribution of forces. The stiffening behaviour of the soil and the interface of the pile material at the surface with the soil are neglected in this research, as ensuring the same at site would not be possible with a reasonable degree of accuracy.

2.9.4 Material models

Soil is a non-linear, multi-phase, stress-dependent and time-dependent material. Hence, the material model, i.e. the constitutive relation between stress and strain, is complex. The constitutive relation can be modelled accurately. PLAXIS has implemented different material models as provided below, each of which may be suitable for different cases.

- Linear Elastic Model
- Mohr- Coulomb Model
- Hardening Soil Model
- Hardening Soil model with small-strain stiffness (HS small)
- Soft Soil Model (SS)
- Soft Soil Creep Model (SSC)
- Jointed Rock Model (JR)
- Modified Cam-Clay Model (MCC)
- NGI-ADP model (NGI-ADP)
- Sekiguchi-Ohta Model (Sekiguchi-Ohta)
- Hoek-Brown model (HB)

In this research, a linear Mohr- Coulomb soil model is considered. Hence the focus is on this type of constitutive soil.

Linear elastic model (Hooke's law)

Hooke's law is a linear elastic and isotropic relation between stress and strain. This constitutive relation is the simplest material model utilized in PLAXIS. It involves two input parameters; Young's module (E) and Poisson's ratio (v). This model is not suitable for the modelling of soil, due to soil exhibiting very complex behaviour. Hooke's law is, on the other hand, a good idealisation for material in structural elements, such as steel, which often behaves in a linear-elastic and isotropic way at lower stress states.

Mohr-Coulomb's model

The Mohr-Coulombs model (MC-model) is an elastic perfectly-plastic model. The general behaviour of an elastic perfectly plastic material is illustrated in Figure 5.3. The model requires five input parameters; E and v for the elasticity, M and c for plasticity and for the dilatancy. The model is isotropic and does not account for the stress-dependency of soil, i.e. in that soil has a tendency to stiffen with increased pressure. PLAXIS recommends using this material model in an initial simulation of soil because it is relatively fast and accurate.

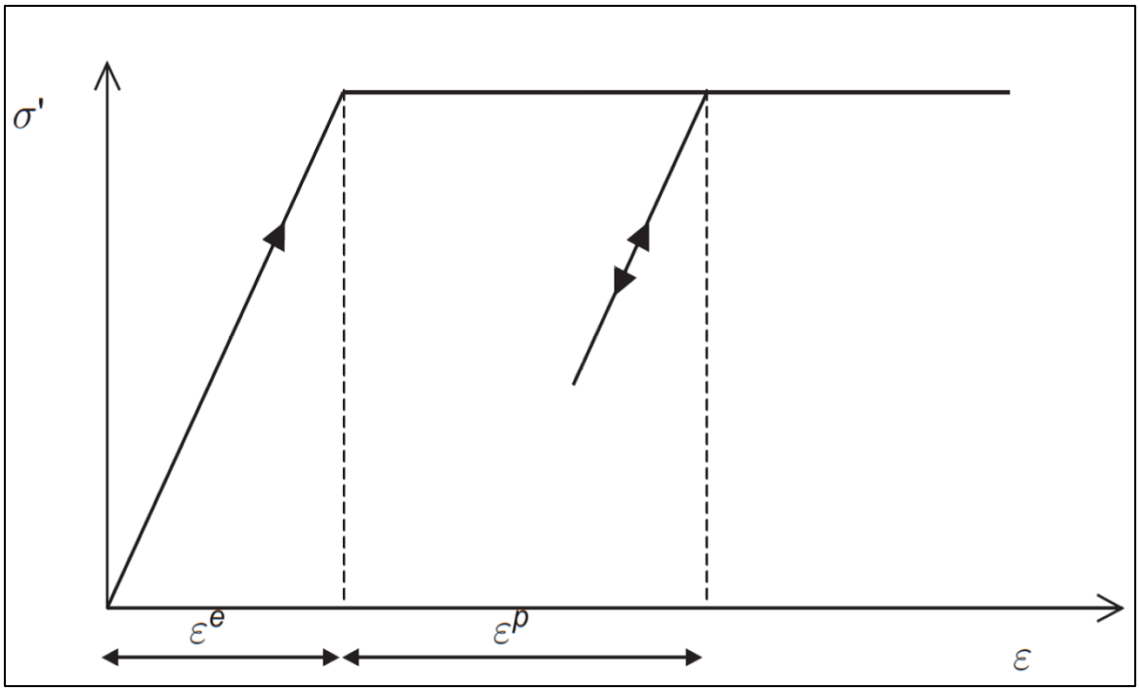

Fig. 2.30 Basic idea of an elastic perfectly plastic model

2.9.5 Plasticity and yield functions

When modelling plasticity, PLAXIS introduces functions called ‘yield functions’, which are equal to zero when the material behaves plastic. The Mohr-Coulomb yield condition consists of six yield functions, all expressed with principal stresses, the friction angle and the cohesion. The Mohr-Coulomb yield condition is an extension of the Coulomb friction law, and it obeys this law in any plane within the material. When the six functions are set to zero (i.e. acting plastic) they create a surface in the principal stress space called the ‘yield surface’, as illustrated in Fig. 2.31. When the material is exposed to stress states within this surface, it acts elastic and obeys Hooke’s law.

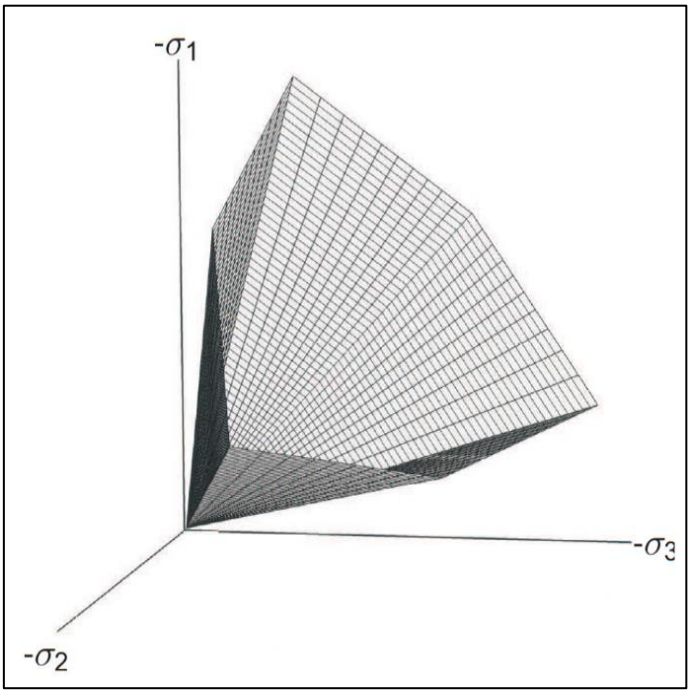

Fig. 2.31 Mohr-Coulombs yield surface in principal stress space

Perfectly plastic means that the constitutive relation is independent of the plastic strain and fully defined by the model’s input parameters. This leads to a fixed yield surface. In contrast, more advanced models that are plastic, not perfectly-plastic, have a yield surface that expands due to plastic strain.

2.9.6 Input parameters

When prescribing soil’s stiffness, PLAXIS recommends using E_{50} as stiffness when modelling initial loading and Eur when modelling unloading and reloading problems as excavations; where E50 is the Young’s modulus at 50 percent of the maximum stress-level occurred in a triaxle test and Eur is the Young’s module for soil when unloading and reloading. The latter is normally higher than for initial loading since the soil stiffens

due to increased stress-levels. When v is unknown, PLAXIS recommends using values in the range 0.3 to 0.4 and 0.15 to 0.25 for loading scenarios and reloading scenarios, respectively. When modelling sand without cohesive strength, PLAXIS will not perform well numerically. The cohesion should therefore be prescribed to a small value, in the order of magnitude $c \approx 0.2$ kPa. The computing time increases exponentially with increasing friction angle. Hence, one should avoid prescribing high values for the friction angle when doing rough time-limited calculations. According to the PLAXIS manual, the dilatancy angle for sand with a high friction angle is roughly $\psi = \varphi - 30°$. For sand with a friction angle less than 30°, and for clay, the dilatancy is close to zero.

2.9.7 Geometry and elements

When creating the profile of the geometry, it is essential to define points, geometry lines and clusters (areas). These are later assigned different properties. The clusters are given a soil element and a soil material, a geometry line is given either a structural element or a boundary condition. The different elemental models available in PLAXIS 2D are:

Soil element (volume element):

Basically, there are two different types of elements for soil modelling in PLAXIS 2D, either the six-noded or 15-noded triangular elements which have three or 12 stress points (i.e. Gaussian integration points) respectively. Fig 2.32 below explains the different elements.

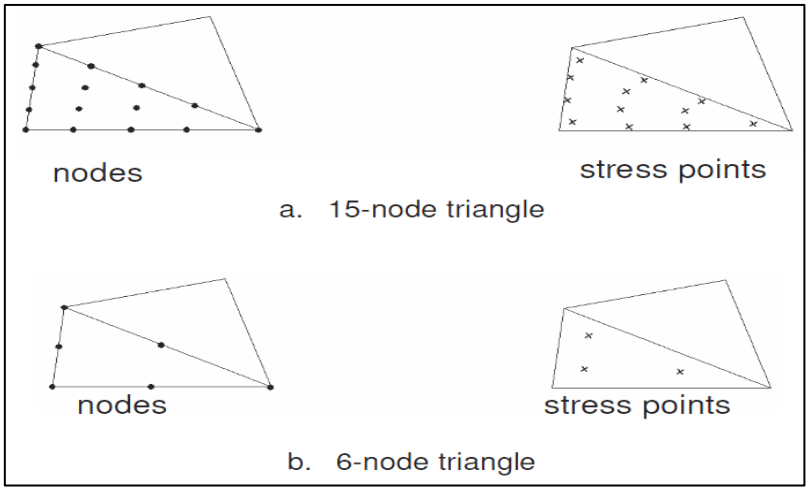

Fig. 2.32 Soil elements 15& 6 node tringle

The soil properties are assigned to a cluster by the choice of material model which is defined. The material model is important when modelling soil. The properties of soil required for different constitutive soil models are inputted in to PLAXIS.

Plate element:

The plate elements are composed of beam elements. Three degrees of freedom per node are present for beam element, with three respective five nodes when used with six nodes volume elements and 15 nodes volume elements respectively.

PLAXIS uses the Mindlin's beam theory, which governs both deflection due to shearing and bending; it also accounts for variations in change in length when exposed to axial force. The input parameters are; EA, axial stiffness, EI, bending stiffness, weight and v, Poisson's ration. FEM analysis can be carried out either by choosing elastic or elastoplastic behaviour. For including an elasto-plastic behaviour, limits of both the parameters are required to be set i.e. maximum bending moment and maximum axial force.

Geogrid element:

Geogrid is an element which only has tensile strength, i.e. no compressive strength or bending moment strength (as cables in structural mechanics). This is used for the modelling of soil reinforcement with geotextiles, which is often used in geotechnical structures to add tensile strength in soil. Geogrids may also be used with node-to-node anchor for modelling of tie backs, where the geogrid represents the grout and the node-to-node anchor represents the rod.

Interface element:

Interface elements are used for modelling the interaction between two materials. In FEM calculations, just one displacement is allowed in a specific node. Hence, in a node common for two elements with different material properties one (or same) displacement must be present. Where soil meets structural elements, this is unrealistic; one expects the soil to slip and gap relative to the structural element, e.g. a pile slipping relative the surrounding soil due to external loads. This is governed in PLAXIS by introducing the interface element, which has two nodes for every stress point. In the figure below two interface elements are illustrated, with corresponding volume element.

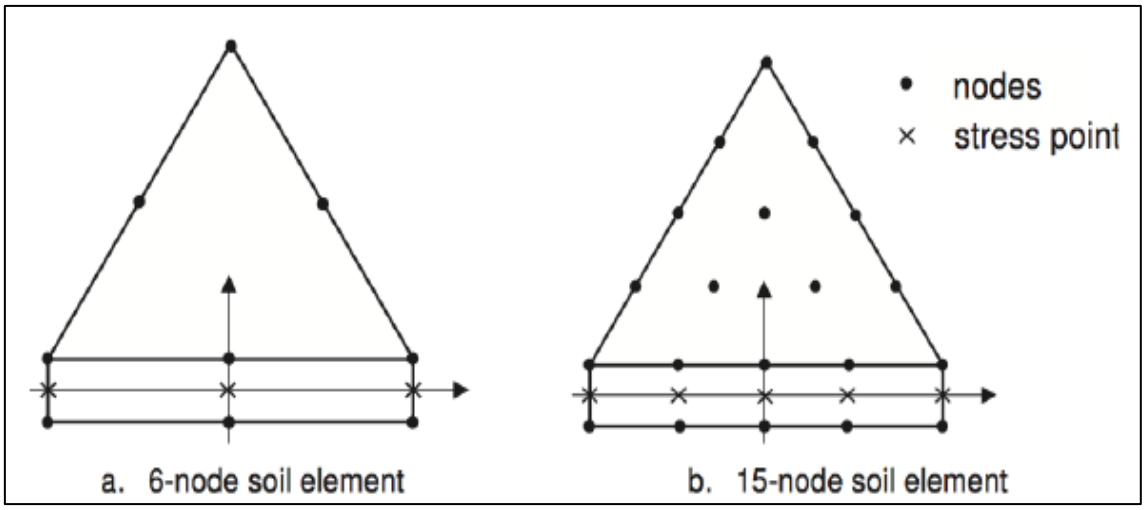

Fig. 2.33 Soil element coupled to an interface element (6 nodes & 15 nodes element)

The material of the interface element could also be defined by creating a new material, specific to the interface element. Another feature of the interface element is that it is impermeable. It could therefore be used in consolidation analysis and groundwater flow analysis to block groundwater flows. This feature is often used for preventing flow true plates, which are fully permeable in PLAXIS. The interface element could also be used to smooth the mesh around areas with high stress and strain gradient (e.g. sharp edges in stiff materials). Standard volume elements have difficulties to produce physical stress oscillation in such areas. Smoothening is created by applying interfaces around the area and activating them during mesh generation; during calculation, however, these should be deactivated.

Loads:

Two types of load could be applied in this version, i.e. distributed load and point load. These could be applied in x- and y-direction. Since the model is two dimensional, the point load is in fact a one-meter line load in the out-of-plane direction, i.e. N/m. Likewise, the distributed load has a thickness of one meter in the out-of-plane direction, i.e. N/m^2.

2.9.8 Mesh generating

PLAXIS has implemented an automatic mesh generator developed by Ingenieursbureau SEPRA. This generates an unstructured mesh with the chosen type of element, either six node or 15-node element. The program allows for five different coarseness levels of the global mesh, and it can also make the mesh finer in local parts of the model. The latter option is a convenient way to ensure having sufficient elements in parts exhibiting great stress and strain gradients, without creating a heavy (i.e. time consuming) mesh.

2.9.9 Initial condition

Prior to the main calculations in PLAXIS, the initial condition of the soil must be determined. This includes calculating both the initial effective stress-state and the initial water pressures in the soil.

Water pressures:

In PLAXIS, the initial water pressure could be generated in two ways, either directly from the phreatic level or by a steady state groundwater calculation. In both methods the user must define the phreatic levels, and, in the latter, it is possible to prescribe the groundwater head or discharge (it is only possible to set the discharge to zero). The groundwater calculation is based on the finite element method and uses the generated mesh, the permeability of the soil and the boundary conditions to calculate the water pressures.

Effective stress:

The initial stress state is in a two-dimensional analysis defined by the vertical stress together with the horizontal stress. As mentioned in Chapter 2, the vertical stress is caused either by external load or by the deadweight of the soil; the horizontal stress could further be calculated with knowledge of the coefficient K. PLAXIS calculates these two stresses in every stress point in the model for an initial condition. The initial condition implies no external loads and the vertical stresses are therefore calculated using the soils unit weight. The initial condition also implies the soil being at rest. The horizontal stresses are therefore calculated using the at-rest coefficient of lateral earth pressure, i.e. K_o.

2.9.10 Calculations

Once the geometry is set and the initial conditions are calculated, one can perform the main FEM calculation. There are three different types of calculations available for this stage, i.e. plastic calculation, consolidation calculation and safety calculation. Additionally, it is possible to account for large displacements in all types ('Updated mesh') and to perform dynamic calculations with an extension-program, neither of these features are taken in the account in this dissertation. The different calculation types are presented as follows:

Plastic calculation:

Plastic calculation is used for elastic-plastic deformation calculations, specifically when failure and stability of the object are analysed. Plastic calculation does not account for the time-dependent decay of excess pore pressure and is therefore not appropriate when analysing settlement in low permeable soil. On the other hand, this calculation type can be used when calculating settlement in high permeable soil or when the final settlement of a structure is calculated.

Consolidation analysis:

Water-saturated soil must drain water to develop settlement (due to water's incompressibility). In low permeable soil, such as clay, this is a time-consuming process and it is important to account for this process when analysing settlement. This is governed in the consolidation calculation. Hence, this calculation type is suitable for analysing time-dependent settlement for water-saturated and low permeable soil.

Safety analysis (PHI-C Reduction):

For safety analysis (i.e. calculating the safety factor), PLAXIS has implemented a calculation type called PHI-C Reduction. This is a plastic calculation where the strength parameters for soil and interfaces are reduced until failure. The safety factor for the object is then calculated as the available strength divided by the strength at failure. PLAXIS facilitates the use of arc length parameter, over-relaxation and extrapolation to improve the iteration process and capture the failure of the structure accurately. Design and safety factors are not in the scope of this work.

Staged construction:

A construction is, in practice, built in stages. To resemble and simulate this, the calculation process in PLAXIS is also divided into stages, called ‘calculation phases’. This is mainly to avoid failure during construction and to simulate excavation processes. The first calculation phase is always the earlier defined initial condition. One can then add an adequate number of phases where structural objects, loads and soil-clusters are activated or deactivated, successively, according to the planned construction process. It is also possible to change material data and the water condition and to pre-stress anchors.

2.9.11 Results

Once the calculations are completed, PLAXIS provides the user with different stress and deformation distribution. This is done using either the Output or Curves program, which are in-built. The Output program illustrates the stress and deformation distribution by use of arrows, contour lines or shading. The user is also provided with the final stresses and deformation for all nodes in tables. In the Curves program, the user is provided with curves and tables of the variation of displacement in specific points, as chosen by the user.

2.10 Evaluation of pile resistance by codes

2.10.1 Design of piles by Eurocode 7

Eurocode 7 introduces reliability into the design of piles. Partial factors for verification of Pile foundations are specified in Table 2.17 below.

Parameter	Model Factor	Resistance factors			
		R1	R2	R3	R4
Base Resistance	γb	-	1.1	1	-
Driven Pile		1	-	-	1.3
Bored Pile		1.25	-	-	1.6
CFA Pile		1.1	-	-	1.45
Shaft Resistance	γs	1	1.1	1	1.3
Total Resistance	γt	-	1.1	1	-
Driven Pile		1	-	-	1.3
Bored Pile		1.15	-	-	1.5
CFA Pile		1.1	-	-	1.4

Table 2.17 Eurocode 7 partial factors

Using the partial factors, the pile resistance is calculated by different approaches as follows.

- Design approach 1
- Design approach 2
- Design approach 3
- Design calculation
- Design by testing

The different approaches are outlined in the following sections.

Design Approach 1:

The philosophy of Design Approach 1 is to check reliability with two different combinations of partial factors. In combination 1 for pile foundations, partial factors are applied to actions and small factors to resistances, while ground strengths are left un-factored. This is achieved by employing factors from sets A1, M1 & R1. In combination 2 for pile foundations, partial factors are applied to resistances and variable actions, while permanent actions and ground strengths are left un-factored. This is achieved by employing factors from sets A2, M1 & R4. This is tabulated as follows:

Design Approach 1			**Combination 1**			**Combination 2**		
			A1	**M1**	**R1**	**A2**	**M1**	**R4**
Permanent Actions G	Unfavorable	γ_G	1.35	-	-	1	-	-
	Favorable	$\gamma_{G\,fav}$	1	-	-	1	-	-
Variable actions Q	Unfavorable	γ_Q	1.5	-	-	1.3	-	-
	Favorable	$\gamma_{Q\,fav}$	0	-	-	0	-	-
Material Properties X		γ_M	-	1	-	-	1	-
Base Resistance R_b	Driven Pile	γ_b	-	-	1	-	-	1.3
	Bored Pile		-	-	1.25	-	-	1.6
	CFA Pile		-	-	1.1	-	-	1.45
Shaft Resistance R_s		γ_s	-	-	1	-	-	1.3
Total Resistance R_c	Driven Pile	γ_t	-	-	1	-	-	1.3
	Bored Pile		-	-	1.15	-	-	1.5
	CFA Pile		-	-	1.1	-	-	1.4

Table 2.18 Eurocode 7, design approach 1

Design Approach 2:

This approach checks the reliability by applying partial factors to actions or actions effects and to resistance, while ground strengths are left un-factored. These factors are as per table 2.19 below:

Design Approach 2			Combination		
			A1	M1	R2
Permanent Actions G	Unfavorable Favorable	γ_G $\gamma_{G\,fav}$	1.35 1	- -	- -
Variable actions Q	Unfavorable Favorable	γ_Q $\gamma_{Q\,fav}$	1.5 0	- -	- -
Material Properties X		γ_M	-	1	-
Base Resistance Rb		γ_b	-	-	1.1
Shaft Resistance Rs		γ_s	-	-	-
Total Resistance Rc		γ_t	-	-	-

Table 2.19 Eurocode 7, design approach 2

Design Approach 3:

This approach checks the reliability by applying partial factors to actions and to material properties while resistances are left un-factored. The factors are tabulated as follows:

Design Approach 3			Combination			
			A1	A2	M2	R3
Permanent Actions G	Unfavorable Favorable	γ_G $\gamma_{G\,fav}$	1.35 1	1 1	- -	- -
Variable actions Q	Unfavorable Favorable	γ_Q $\gamma_{Q\,fav}$	1.5 0	1.3 0	- -	- -
Coefficient of Shearing Resistance (tan φ)		γ_φ	-	-	1.25	-
Effective Cohesion c'		$\gamma_{c'}$	-	-	1.25	-
Undrained Strength		γ_{cu}	-	-	1.4	-
Unconfined compressive strength		γ_{qu}	-	-	1.4	-
Weight Density		γ_s	-	-	1	-
Base Resistance Rb		γ_b	-	-	-	1
Shaft Resistance Rs		γ_s	-	-	-	-
Total Resistance Rc		γ_t	-	-	-	-

Table 2.20 Eurocode 7, design approach 3

Correlation Factors:

Correlation factors for calculating pile resistances form static load tests, ground tests and dynamic tests are tabulated as per below.

No of Tests	Static load tests		Ground Tests		No of tests	Dynamic Impact	
	ξ1	ξ2	ξ3	ξ4		ξ5	ξ6
1	1.4		1.4			1.6	1.5
2	1.3	1.2	1.35	1.27	2-4		
3	1.2	1.05	1.33	1.23			
4	1.1	1	1.31	1.2			
5	1	1	1.29	1.15	5-9	1.5	1.35
7	-	-	1.27	1.12			
10	-	-	1.25	1.08	10-14	1.45	1.3
					15-19	1.42	1.25
					≥20	1.4	1.25

Table 2.21 Eurocode 7, design by testing

Eurocode 7 allows for reduction in Correlation factors by 10 percent for static load tests when designing piles in groups. Correlation factors can be reduced by 15 percent for dynamic load tests if signal matching is used.

Evaluation of Characteristic Pile Resistance using Eurocode 7:

Eurocode 7 describes three procedures for obtaining the characteristic compressive resistance rock of pile:

- Directly from static pile load tests
- By calculation from profiles of ground test results
- By calculation from ground parameters

In the case of procedures a) and b), Eurocode 7 provides correlation factors to convert the measured pile resistances or pile resistances calculated from profiles of test results into characteristic resistances. In the case of procedure c), the characteristic pile resistance is calculated from ground parameter values.

The equilibrium equation to be satisfied in the ultimate limit state design of piles axially loaded in compression is:

$$F_{c;\,d} \leq R_{c;\,d}$$

$F_{c;\,d}$ is the design axial compression load and $R_{c;\,d}$ is the pile compressive design resistance.

2.10.2 Pile design as per IBC 2009

The pile design is dealt with in chapter 18; section 1807.2.8 of IBC 2009 deals with the allowable pier or pile loads. The determination of allowable loads on piles is calculated using the following:

- The allowable axial and lateral loads on piers or piles shall be determined by load test, static analysis or approved formulas.
- The factor of safety to be used for pier or pile design shall depend on the extent of field testing performed to verify capacity.
- If the ultimate capacity is assessed solely by static analysis, a minimum factor of safety of 3.0 shall be applied to the ultimate capacity to determine allowable load capacity.
- If only static analysis and dynamic field testing are performed, a minimum factor of safety of 2.5 shall be applied to the ultimate capacity to determine load capacity.
- If one or more static load tests are performed in addition to the analysis and tests mentioned above, a minimum factor of safety of 2.0 should be considered for determining the ultimate allowable capacity.
- A minimum factor of safety of 2.0 shall be used for occupiable structures provided that all of the conditions in pars. (a) to (e) are met. A minimum factor of safety of 1.5 may be used for non-occupiable structures, provided that the deep foundations are required only to control settlement, and it can be demonstrated that deep foundations are not required to prevent a bearing capacity failure.

Load tests on pile shall be conducted as per 1807.2.8.3 of IBC 2009:

Where greater compressive loads per pier or pile than permitted by section 1807.2.10 in IBC 2009 are desired, or where the design load for any pier or pile foundation is in doubt, control test piers or piles shall be tested in accordance with ASTM D 1143 or ASTM D 4945. At least one pier or pile shall be test loaded in each area of uniform subsoil conditions. Where required by the building official, additional piers or piles

shall be load tested where necessary to establish the safe design capacity. The resulting allowable loads shall not be more than one-half of that test load, which produces a permanent net settlement of not more than 0.01 inch per ton (0.0285 mm/kN) of test load, and not more than ¾ inch (19.1 mm). In subsequent driving of the balance of foundation piles, all piles shall be deemed to have a supporting capacity equal to the control pile where such piles are of the same type, size and relative length as the test pile, these are: installed using the same or comparable methods and equipment as the test pile; installed in similar subsoil conditions as the test pile and ;where the rate of penetration (e.g., net displacement per blow) of such piles is equal to or less than that of the test pile through a comparable driving distance.

Alternative determination of allowable load:

The ultimate capacity of the pile shall be defined as the load at which the average pile head deflection is defined as per the following equation. The calculation shall be predicated on an assumed end-bearing condition:

$$\delta = (\mathrm{PI}/\mathrm{AE}) + 0.15^2 + (\mathrm{B}/120) \qquad \text{(Eq. 2.60)}$$

where

δ = average pile head deflection, inches (mm)
P = applied load, pounds (N)
l = pile length, inches (mm)
A = transformed pile area of pile (to steel)
E = modulus of elasticity (of steel)
B = outside diameter (or width) of pile, inches (mm)

Allowable frictional resistance shall be evaluated as per clause 1807.2.8.4 of IBC 2009:

The assumed frictional resistance developed by any pier or uncased cast-in-place pile shall not exceed 1/6th of the bearing capacity of the soil at a minimum depth, as shown in Table 1804.2 in IBC 2009, up to a maximum of 500 pounds per square foot (24 kPa), unless a greater value is allowed by the building official after a soil investigation as specified in section 1802 in IBC 2009 is submitted. Frictional resistance and bearing resistance shall not be assumed to act simultaneously unless recommended by a soil investigation as specified in section 1802 in IBC 2009.

3 Subsoil condition in Business Bay and Downtown Dubai

3.1 Introduction

The United Arab Emirates (UAE) is located in the Middle East. Situated at the tip of the Arabian Peninsula between 22° 50 and 26° north latitudes and between 51° and 56° 25 east longitudes (23 49 N, 54 20 E), the UAE shares borders with the Kingdom of Saudi Arabia (KSA) and the Sultanate of Oman. It occupies a total of around 83,600 square kilometres and contains 200 islands. Dubai is one of the seven Emirates that form the UAE federation, located on the southern coast of the Persian Gulf along the Arabian Peninsula.

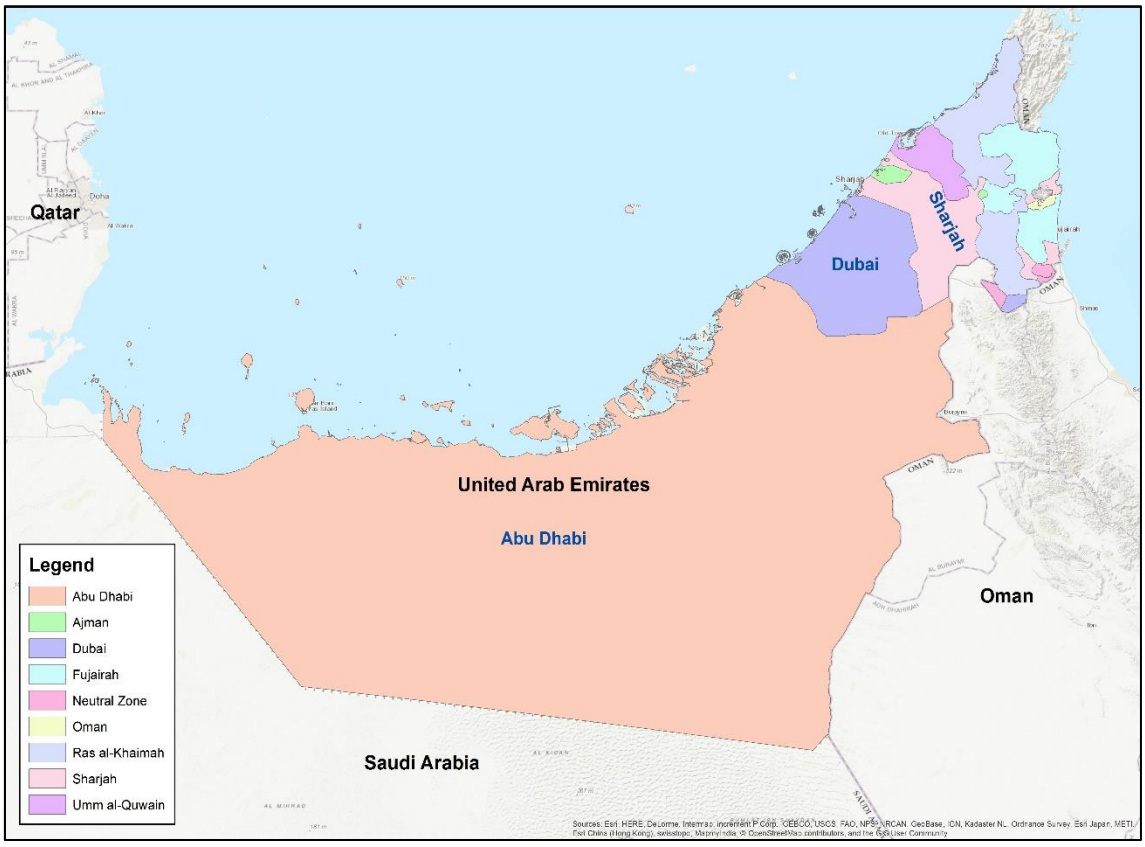

Fig. 3.1 Location of UAE & Dubai

The discussion presented in this chapter is limited to the geotechnical investigation of Business Bay and Downtown Dubai, a zone spanning 5,900,000 square metres and housing over 500 high-rise buildings. The geotechnical information that can be obtained from the investigation are endless; however, the main parameters that dictate the design consideration herein are based primarily on two parameters, those of: standard penetration value (SPT N-Value), and unconfined compressive strength (UCS). Unless otherwise specified, other geotechnical parameters presented are derived from or are co-related to the above two parameters.

Fig. 3.2 Schematic view of Business Bay and Downtown Dubai

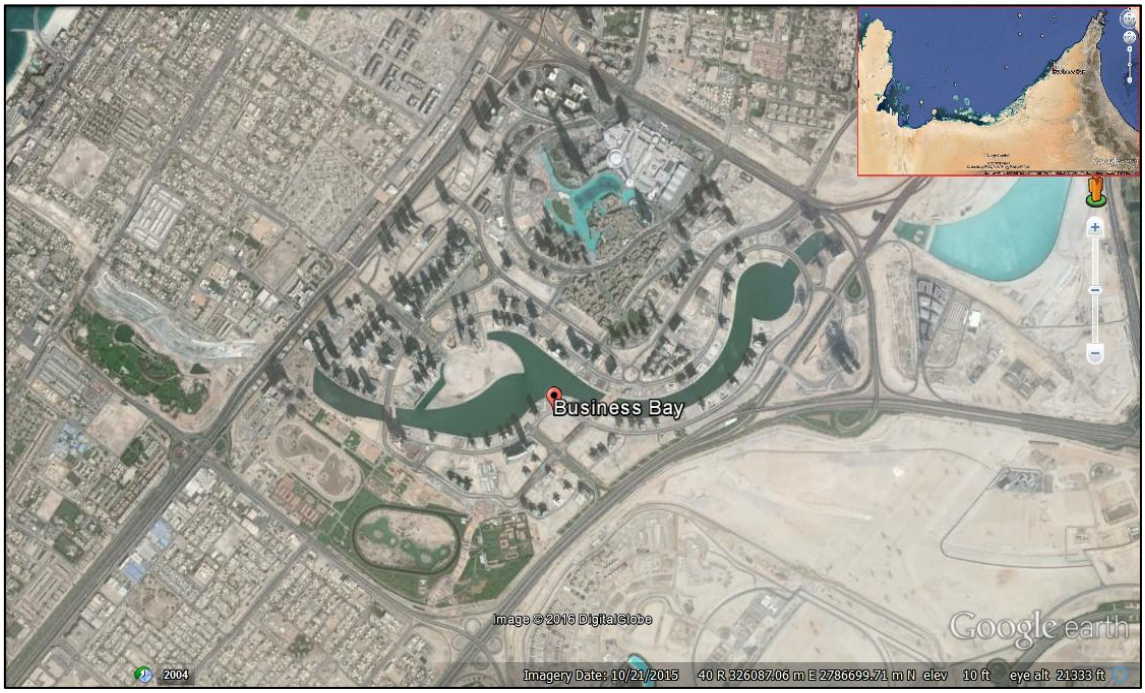

Fig. 3.3 Google Earth view of Business Bay and Downtown Dubai

3.2 Geology

3.2.1 Geology of the UAE

The general geology of the UAE has been substantially influenced by the deposition of marine deposits associated with the continuous sea level fluctuation during relatively recent geological times. Moreover, with the existing mountainous geology across the UAE, the country is considered to be a relatively low-lying area.

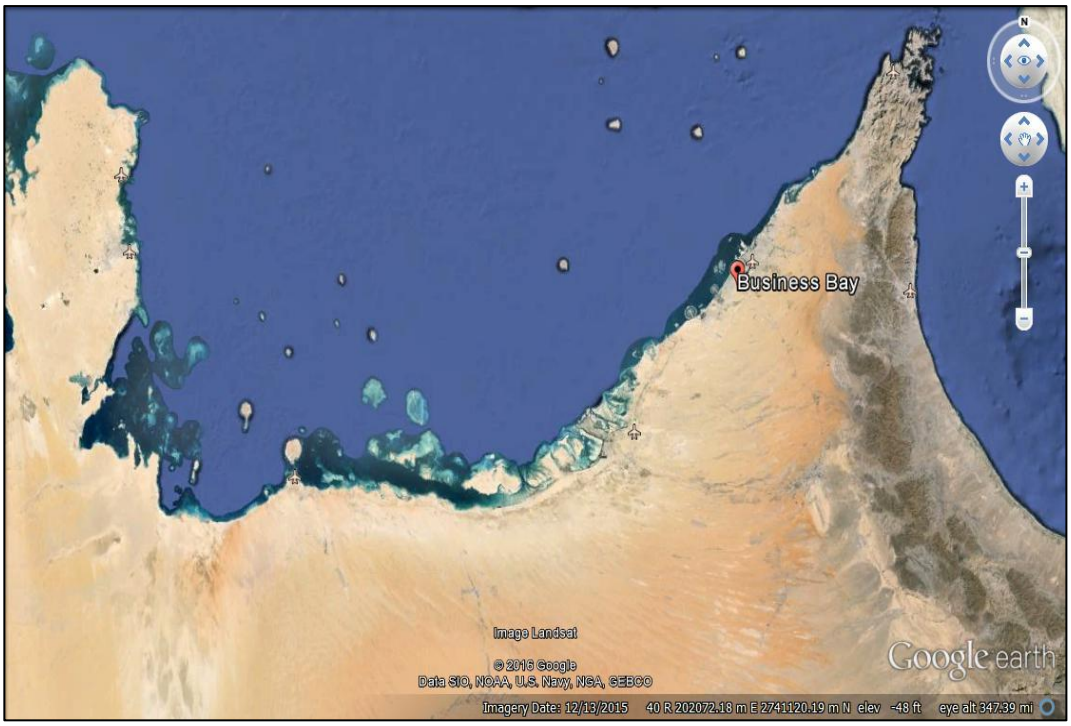

Fig. 3.4 General view of Dubai

3.2.2 Geology of Dubai

The emirate of Dubai covers an area of 3885 square kilometre and is characterised by a mainland consisting of desert and sand dunes along a coast line of over 50 km running along the Arabian Gulf. Occupying the northern part of UAE, the emirate of Dubai is bound by the emirates of Sharjah to the East, Abu Dhabi to West and South West, and the Arabian Gulf to the North and North West (Emad Y. Sharif, Mohd. J. Ahmed 2010).

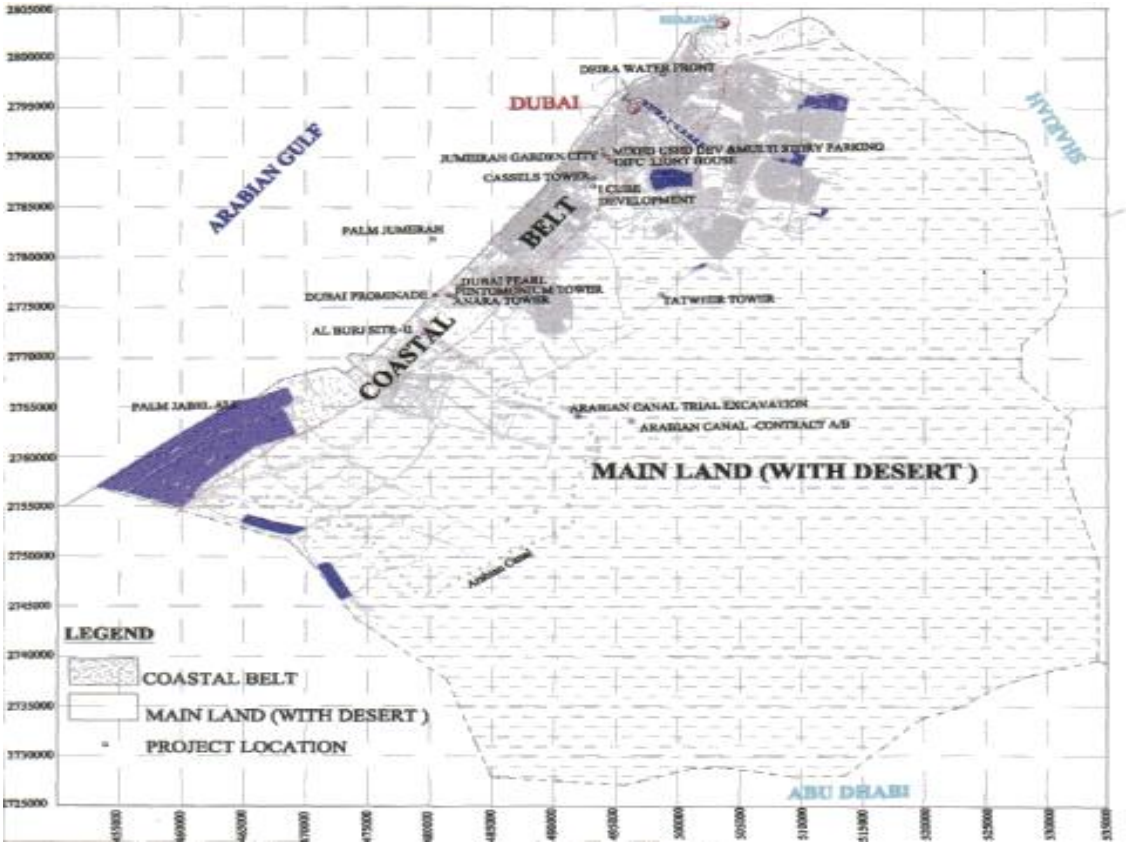

Fig. 3.5 Geology of Dubai

The interpreted soil and rock units revealed by sub-surface investigation in the Dubai area are an interlayered sequence of silty to fine sandy soils with shells, underlain by an inter-bedded sequence of sandstones (Arenaceous unit), siltstone/ claystone (Argillaceous unit), conglomerates (Rudaceous unit), and gypsum (sabkah) beds. The inter-bedding indicates facies variations due to fluctuating energy conditions in the depositional basin. The sabkah (evaporites) deposits with interbeds of siltstone/ claystone indicate a saline arid environment of depositions with restricted circulation. The rocks in general are sub-horizontally bedded with rolling dips of <10° and a regional dip towards north-northwest. The generalised stratigraphy of Dubai is presented in the table below:

Period	Lithologic Group	Thickness Approx. (m)	Elevation Approx. (m)	Description
Quaternaries	Over burden	<1 - 17	Varying	Includes all soils of following origins.
	Aeloian & Beach sands	1.0 – 3.5		**Aeolian:** Brownish, fine to very fine dune sand in the desert **Beach:** Light grey, medium to fine sand on the beach/coast.
Pleistocene	Recent Sediments	6-10	Varying	Loose to medium dense, brownish, silty fine sand with sea shells (deposited during the sea level fluctuations, due to eustatic changes).
	Recent Sabkah (Inland & Coastal)	0.5-2.5	<1 to +2.5	**Inland*:*** dark brownish coloured, poorly compacted, exposed in interdunal areas. **Coastal:** Light brownish coloured, friable/poorly compacted.
Early to Middle Tertiary	Rudite group of rocks	0.5-5.0	Varying	Inter-beds of reddish brown Polymictic conglomerates and calcirudite. Medium to fine gravels of basic/ igneous rock, sandstone, siltstone and cherts. Occur as interbeds only in arenites and argilities
	Arenite group of rocks (Sandstones)	5 - 35	+55 & -10	Grayish brown to light brown medium to fine grained sandstone with inter-beds of destructured (class 'D'; chemically weathered/ decomposed) sandstones. Pebbly/ gravelly calcareous sandstone/ calcarenites, conglomeratic calcareous sandstone. Gravels of gypsum also noticed locally.
	Argillite/ Lutite group of Rocks (Siltstone/ claystone)	+75	-35 to -200	Light grey to greenish grey calcareous siltstone with interbeds of conglomerate, gypsum and sandstone. conglomeratic siltstones with gravels of siltstone, sandstone, igneous/ ophiolite suit of rocks and crystalline gypsum. claystone/ siltstone with interlaminations and angular clasts of gypsum also noticed locally.
	Deep- seated / Paleo Sabkah deposits/ gypsum beds	+20	-95	Light grey to colourless/ transparent, crystalline gypsum/ anhydrite beds, hard and compact with inter laminations of siltstone (ME)/ clay (CE).

(Emad Y. Sharif, Mohd. J. Ahmed 2010)

Table 3.1 General stratigraphy of Dubai

Physiographic Unit	Soil & Rock Mass Category	Rock / Soil type	MASS PROPERTIES				MATERIAL PROPERTIES															
							Chemical			Strength								Physical				
			SPT 'N' Value	Permeability Cm/sec & LU)	Ed 2 (Mpa)	Shear wave velocity (Vs)	Cl %	So4 (g/l)	CaCo3 %	UCS (Mpa)	Point load (Is)	Modulus Es (Mpa)	Cohesion (Kpa) Peak	Angle of IF (φ°) Peak	Cohesion (Kpa) Residual	Angle of IF (φ°) Residual	particle density (Mg.m^3)	bulk density (Mg/m3	Moistur content (%)	Porosity (%)	Plasticity Index$_{I_p}$ (%)
MAIN LAND	U-I Overburden	Ia. Beach sand	X	X	X	X	0.01 to 1.90	0.1 to 2.2 (DS, 1&2)	52 to 76	NA	NA	X	7 to 33	31.6 to 42.6	<1 - 32.90	31.5 to 42.6	X	X	X	NA	NP
		Ia. Aeolian sand	2 to 10	2.7x10E-6 to 6.9x10E-5	X	X				NA	NA	X					2.55 - 2.77	X	6.6 - 28	NA	NP
		Ib.Recent marine sedimnt	2 to 38		X	X				NA	X	X					2.24 - 2.67	X	14 - 33	NA	32 - 35
		Ic. Recent Sabkah/ gypsum	X			X	0.05 - 1.35	1.4 - 1.6	X	0.08 - 1.12	X	X	X	X	X	X					
	RM III Rudaceous Group	Class 'D' conglomerate/ Calcirudites	>50	X	X	340 - 720	X	X	X	X							X	X	X	X	X
		Conglomerate/ Calcirudite (ClasA,B&C)	X	<1 - 100	8 to 57900	797-1194	0.0 to 4.7	0.1 to 2.8 (DS, 1 to 3)	<1 to 94.35	0.2 to 25	0.02 to 4		104to 542	26 to 69	38to 409	21 to 67		2.2 - 2.53	2 - 2.2	32 - 45	NP
	RM- II Arenaceous	Class 'D' sandstones	>50	X		370 - 700															
		Calcareous sandstone/ Calcarenite (ClasA,B&C)	X	<1 to 80		770-899				0.3 to 32	0.06 to 7.5	0.29 to 6.8	43 to 869 AV=	26 to 69 AV=	12 to 679 AV=	19 to 56 AV=	2.39 - 2.86	1.6 - 2.29	16 - 21	34 - 46	NP - 19
		Gravely calcareous sandstone (Clas A,B&C)	X			X															
	RM- I Argillaceous	Class 'D' siltstones	>50	X		330-580															
		Calcareous siltstone/ Calcisiltite (Clas A,B&C)	X	<1 to 100		770 - 928				0.3 to 44	0.01 to 6.7	1.86 to 2.20	35 to 849 AV=	21 to 74 AV=	9.6 to 724 AV=	18 to 72 AV=	2.5 - 2.68	1.23 - 2.08	2 to 18	38 - 46	24 - 77
		Gravely calcareous siltstone (Class A,B &C)	X			X												1.51 - 2.48			
		Stiff Clay/ highly plastic siltstone (Class A/B)	X	X	X	X	X	X	X	X	X	X	X	X	X	X	X	X	X	X	X
COASTAL BELT	U-I Overburden	Ia. Beach sand	2 to 20	X	X	X	0.01 to 4.63	0.1 to 2.8 (DS, 1 to 3)	62.12 to 97.7	NA			X	X	X	X					
		Ia.Aeolian sand	X	X	X	X							X	X	X	X			16 - 19		
		Ib.Recent marine sedimnt	8 to 40	X	X	X							7.7 - 10.4	32.7 - 34	7.1 - 10.2	32.1 - 33.3	2.65 to 2.80	2.02 - 2.28		X	NA
		Ic.Sabkah/ gypsum	X	X	X	X														NA	NA
	RM-III Rudaceous Group	Class 'D' conglomerate/ Calcirudites	>100	X	X	X	X	X	X	NA			X	X	X	X	X		20 -22	NA	NA
		Conglomerate/ Calcirudite (A/B/C)	X	X	7 to 11500	729 - 1000	0.01 to 2.9	0.1 to 2.2 (DS, 1 &2)	1.2 to 97.33	0.12 to 40.58	0.5	242 - 811	X	X	X	X		1.93	20 - 60	X	NA
	RM-II Arenaceous group	Class D sandstones	>50			520 - 612				NA			X	X	X	X				NA	NA
		Calcareous sandstone/ Calcarenite (clasA,B&C)	X	<1 to 103		615 -1125				0.0145 to 10.54	0.002 to 2.2	62 - 894	227	32.8	X	X		2.02 - 2.2	18 - 20	X	NA
		Gravely calcareous sandstone (ClasA,B &C)	X			X							X	X	X	X				X	NA
	RM- I Argillaceous group	Class 'D' siltstones	>50	X		X				NA			X	X	X	X				X	NA
		Calcareous siltstone/ Calcisiltite (Clas A,B&C)	X	<1 to 103		695 - 869				0.027 to 41.9	0.018 to 1.9	62 - 894	240 - 254	54.8	X	X		1.72 - 1.79	7 to 12		16.9 - 62.5
		Gravely calcareous siltstone (Class A,B &C)	X			729 - 1125							30.8	50.4	X	X					
		Deep seated Silt stone (Class A/B)	X	X	X	X	X	X	75 - 86	2.2 - 7.0	0.03 - 0.12	170 - 1624	252	31.8	X	X			27 - 48		32 - 113
	RM- IV	Deep seated Sabkah	X	X	X	X	1.6 - 1.7	1.35 - 1.5	X	1.9 - 16.3	0.94 -	377- 2304	X	X	X	X	X	X	X	X	X

NB: X- Data not available; 1- cm/sec for soils and LU for rock tests; 2- from pressure meter tests; NA- Not applicable,

Table 3.2 Generalised geotechnical parameters for Dubai

3.2.3 Geology of Business Bay

The Business Bay and Downtown Dubai areas are situated between the Coastal Belt and the Main Land terrains. The coastal belt zone is marked by raised beach deposits of calcareous Oolitic sand, locally forming fringing sandpits, shoals and small islands with coastal Sabkah evident along the coast and inland up to elevation of 2-4 m above sea level. The mainland zone is mostly occupied by the Aeolian desert sand dunes, with those dunes closer to the coastal belt being light coloured (light yellowish-brown) due to enrichment of carbonate source material from sea shells and rocks, whilst the inland dunes are of a darker colour (dark brown to brown) due to oxidation in an arid environment (Emad Y. Sharif & Mohd. J. Ahmed 2010).

The general stratigraphy in the Business Bay and Downtown Dubai areas can be broadly presented by the sub-surface characterisation presented in the table below:

Approximate Elevation DMD* (m)	Strata Description
5.00 to -3.00	SAND, locally interbedded by GRAVEL
-3.00 to -15.00	Very weak to weak CALCARENITE locally interbedded by SAND and GRAVEL
-15.00 to -23.00	Very weak to weak SANDSTONE, locally interbedded by SAND and CONGLOMERATE
-23.00 to -57.00	Alternating layers of weak to moderately weak, CALCISILTITE and CONGLOMERATE

*DMD – Dubai Municipality Datum

Table 3.3 General stratigraphy in Business Bay & Downtown Dubai

3.3 Geological and geotechnical structure mapping

3.3.1 gINT software

gINT software is a commercially available software. Its workflow is framed around a centralised data management system developed specifically for underground sub-surface management. gINT is built on a relationship structure between its various tables, as indicated below. These relationships form dependencies (Parent-Child) based on a rational structure.

gINT is an efficient tool for centralised data management of sub-surface information and is very powerful in handling multi-project reporting with built-in capabilities for producing boring and well log data management and reporting. It can be used as a reporting engine and manages data, and it is used as a standalone program for subsurface reporting. gINT can also be used as a subsurface data repository (geotechnical and geo environmental), and for creating contours, isopach and thematic maps (depths, soil classification). It enforces consistency across all data resources by using a centralised data storage, multi-project reporting and dramatically extended querying power via a MS SQL Server back-end.

The data obtained was from the 28 geotechnical investigation reports that were entered into gINT v8. Data entry was carried out in a user defined gINT template and gINT library compliant to AGS 3.1. The gINT database comprised of a total of 195 boreholes, specifically: 14 boreholes down to a depth of 25 meters, 44 boreholes down to a depth of between 25-40 meters, 100 boreholes down to a depth of between 40-60 meters, and 37 boreholes down to a depth of greater than 60 meters. To maximise efficiency, data entry was limited to the most essential field data that could be obtained from the available boreholes logs. In this way, consistency was achieved between the interpretations from the various geotechnical investigation reports, enabling a comprehensive and proper assessment of the prevailing sub-ground conditions. Refer to section 3.4.2 for more detailed information pertaining to boreholes, samples, testing regime and site conditions.

3.3.2 Geotechnical structure mapping

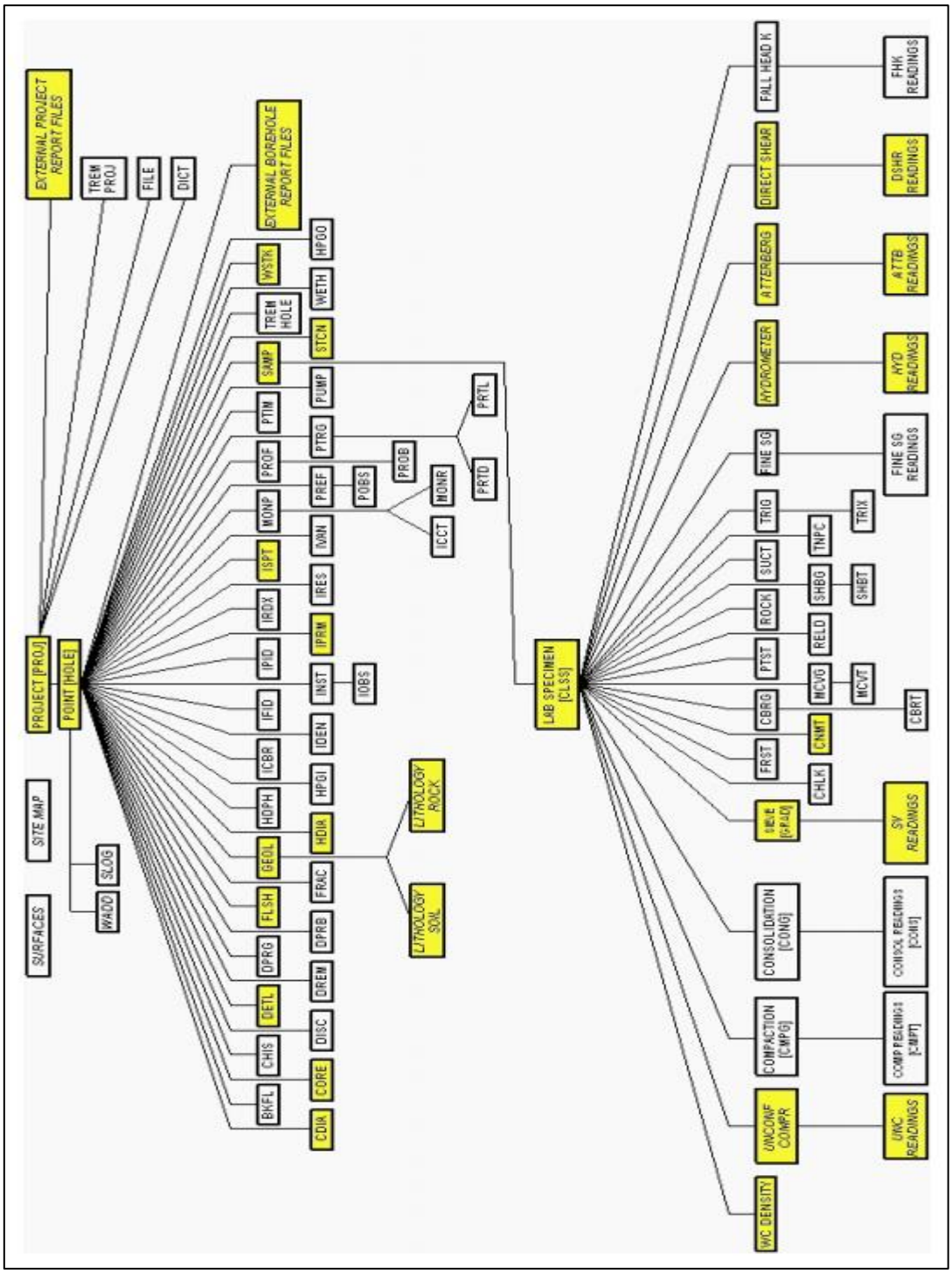

Fig. 3.6 gINT structural mapping

Parent Table	Direct Children	Description
PROJECT	PROJECTED, POINT	Defines the title and point ID (boreholes) related to the project
POINT	HOLE	Holds all the survey and general information related to the point. (eg. co-ordinates, elevation, drilling dates, operator and machinery)
POINT	CORE	Defines the information pertaining to the core runs carried out. (eg, TCR, SCR, RQD)
POINT	GEOL	Comprehensive description of the sub-surface
POINT	ISPT	Holds the information of the N values and their respective penetration.
POINT	SAMP	Holds the information for the various samples retrieved from the drilled point ID (borehole).
POINT	WSTK	Information regarding the water table encountered during drilling.
SAMP	CLSS	Samples chosen for testing.
CLSS	ROCK	Samples chosen for testing that were rock.
ROCK	UNCONF COMPR	Information of the unconfined compressive strength.

Table 3.4 Essential data structure map used

This data structure forms the basis of the data interpretation presented herein. The uniqueness of this structure lies in its compatibility with ASG 3.1; a standardised data transfer format published by the Association of Geotechnical and Geo-Environmental Specialists (AGS), commonly referred to as the 'AGS Format' (AGS, 1999). This data transfer format is now established as the UK industry standard for the electronic reporting of site investigation data. It has also been adopted as the national standard in other countries, notably Hong Kong, Singapore and Ireland. It is currently being implemented in governmental entities in the United Arab Emirates, such as ADM, DoT and RTA.

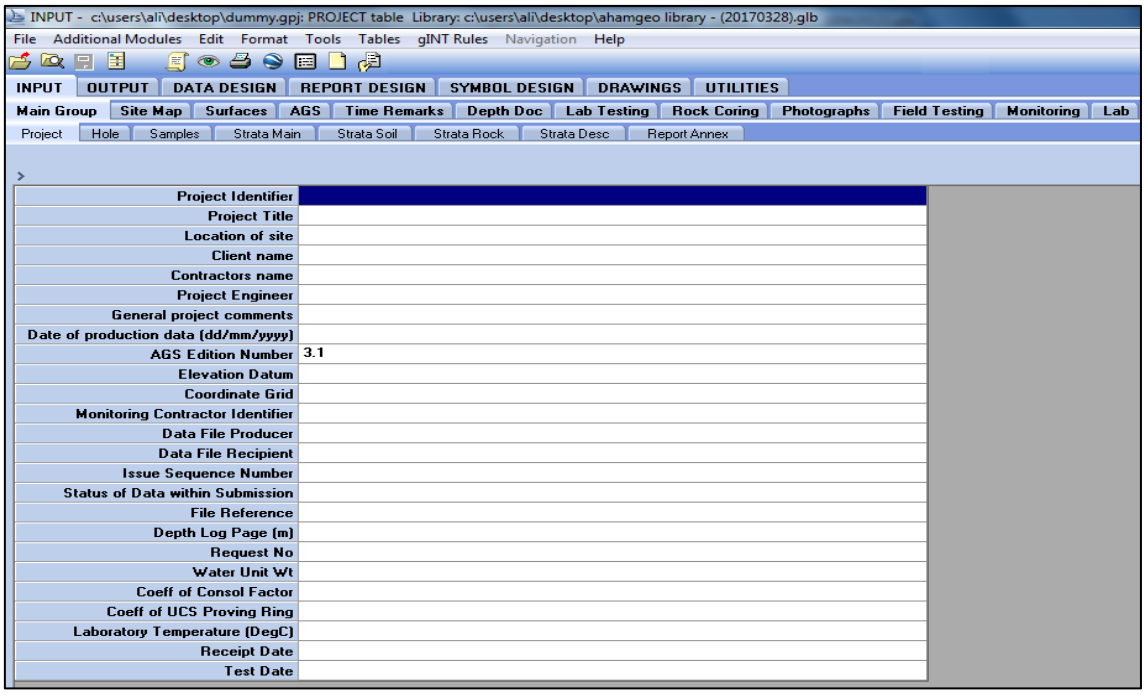

Fig. 3.7 Illustration of data entry (project table)

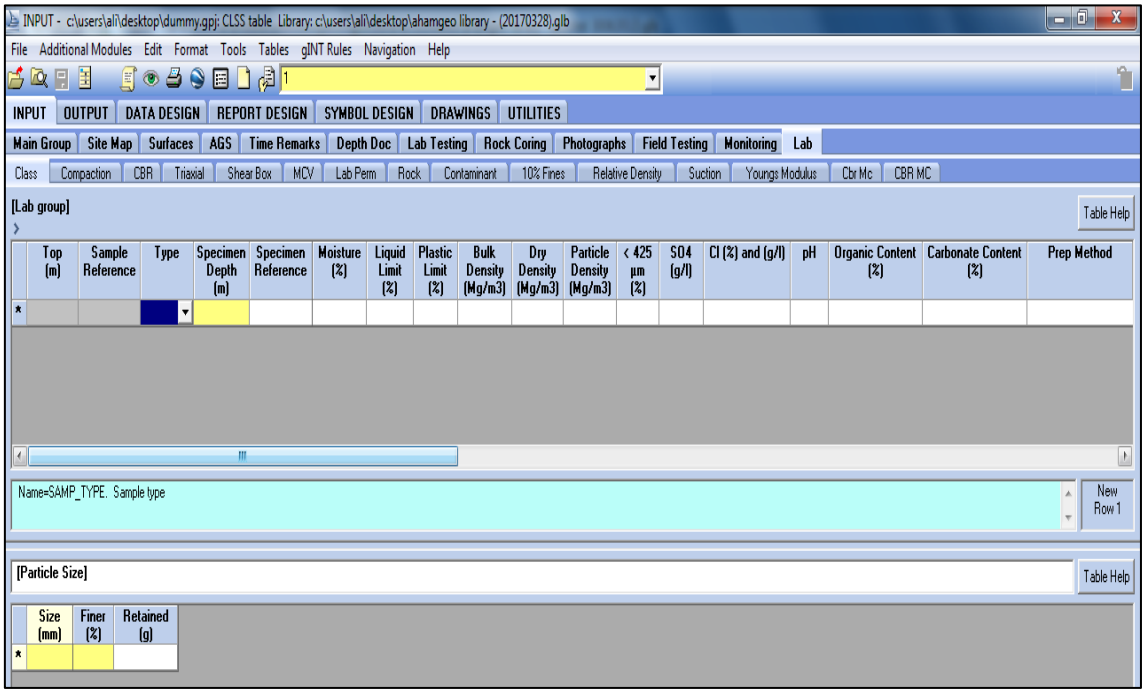

Fig. 3.8 Illustration of data entry in gINT (CLSS)

Boreholes location

The World Geodetic System -1984 (WGS84) is the base geographic Coordinate Reference System (CRS) for the emirate of Dubai. The details of this system are as follows:

WGS84 Bounds : 55.1000, 25.0000, 55.4000, 25.4000
Projected Bounds : 476444.9368, 2766055.8238, 506730.0070, 2810385.025

However, Dubai follows a unique transverse projection system, known as Dubai Local Transverse Mercator. The details of the system are as follows:

Grid system	:	DLTM (Dubai Local Transverse Mercator)
Latitude of origin	:	00-00-00.00N
Longitude of origin	:	55-20-00.00E
False Easting	:	500,000.00 metres
False Northing	:	0.00 meter
Scale Factor	:	1.000
Datum	:	WGS 84
Spheroid	:	WGS 84
Semi major axis	:	6378137.00
Flattening	:	1 / 298.257223563
Level Datum	:	DMD (Dubai Municipality Datum)

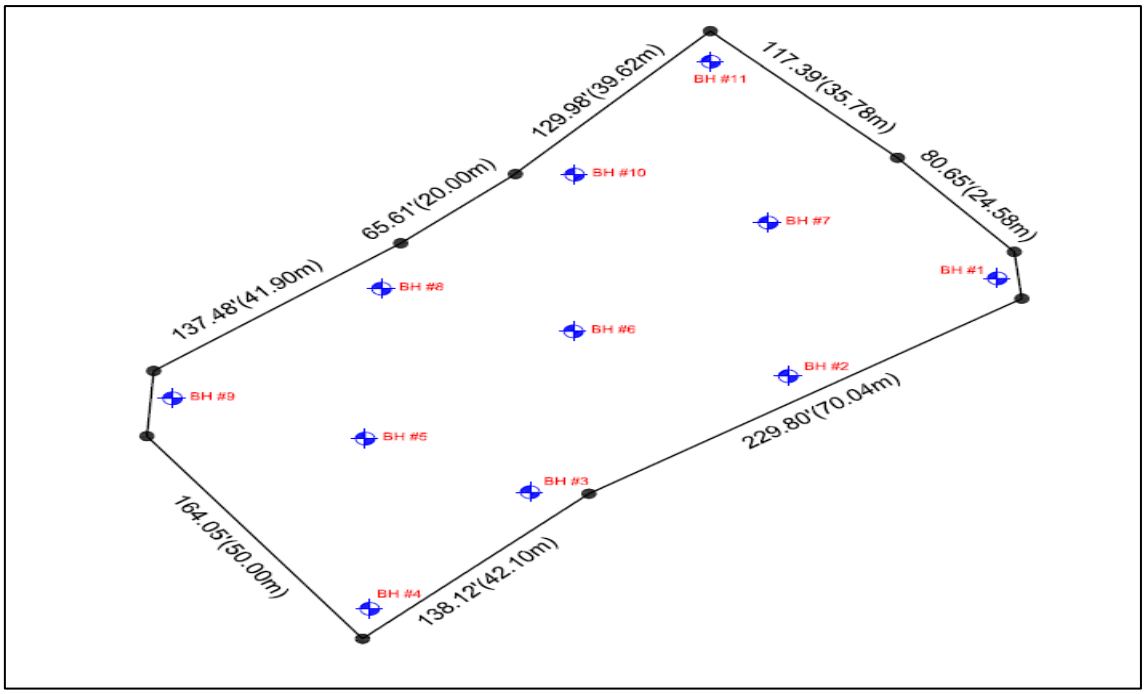

Fig. 3.9 Illustration of Boreholes locations

3.4 Ground investigation in Business Bay & Downtown Dubai

3.4.1 Introduction

Business Bay and Downtown Dubai are located in the heart of Dubai. Covering an area of around 5.9 square kilometres, these two locations will house more than 500 high rise towers, including the 'Burj Khalifa', currently the tallest building in the world. Over the past 15 years, there has been a dramatic increase in construction in the Gulf area, and particularly in Dubai. Business Bay and Downtown Dubai have experienced their share of this boom, with new construction sites being dug out more frequently than ever before. This advancement means that special attention should be paid to the geotechnical and foundation design; the parameters and properties of which are based entirely on geotechnical investigations. Realising its importance, the relevant Dubai authorities have set a mandate for geotechnical investigation to be undertaken prior to the design stage, ensuring that the works are carried out in accordance to a defined procedure.

3.4.2 Site Works

A total of 28 geotechnical reports, spanning between 2003 and 2013, were gathered to evaluate the sub-surface profile of the Business Bay area. The reports were reviewed and those presenting adequate data with proper topographic information were used. In total 28 reports were utilised, a summary of which are presented in Fig. 3.10 figure and Table 3.5 below.

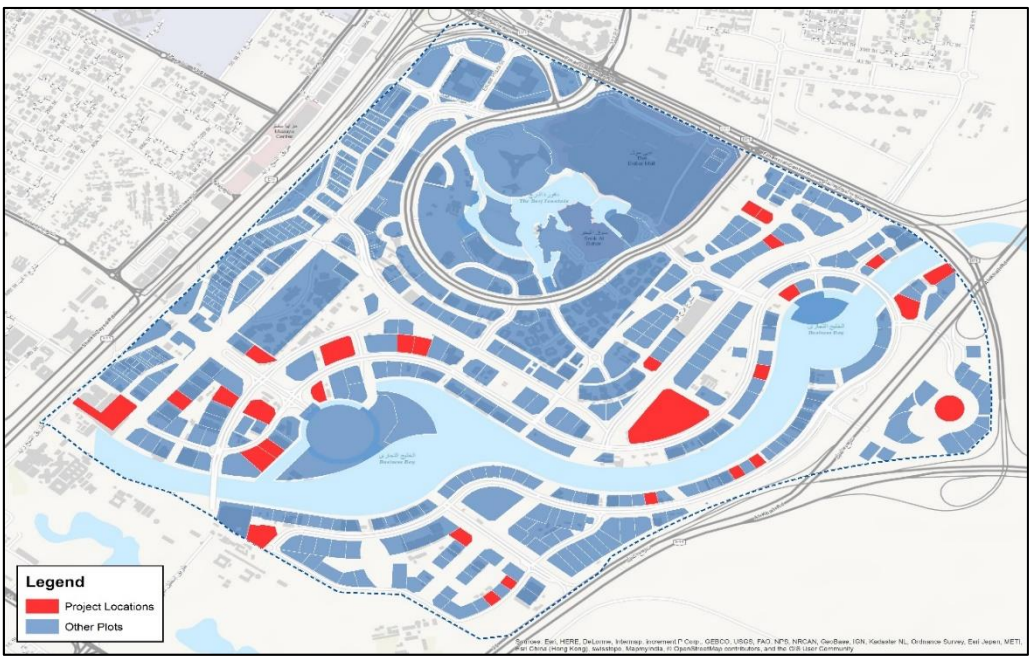

Fig. 3.10 Project locations

S. No.	Project No.
1	Project #1
2	Project #2
3	Project #3
4	Project #4
5	Project #5
6	Project #6
7	Project #7
8	Project #8
9	Project #9
10	Project #10
11	Project #11
12	Project #12
13	Project #13
14	Project #14
15	Project #15
16	Project #16
17	Project #17
18	Project #18
19	Project #19
20	Project #20
21	Project #21
22	Project #22
23	Project #23
24	Project #24
25	Project #25
26	Project #26
27	Project #27
28	Project #28

Table 3.5 Projects utilised in the study

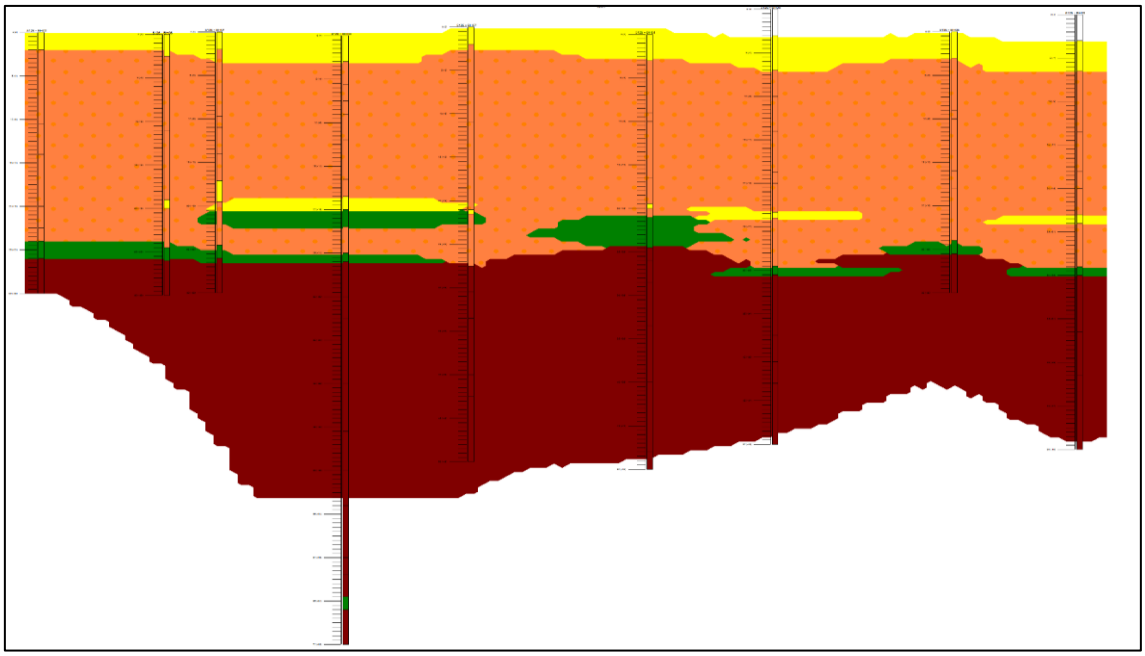

Fig. 3.11 Profile of the north-east side of Business Bay

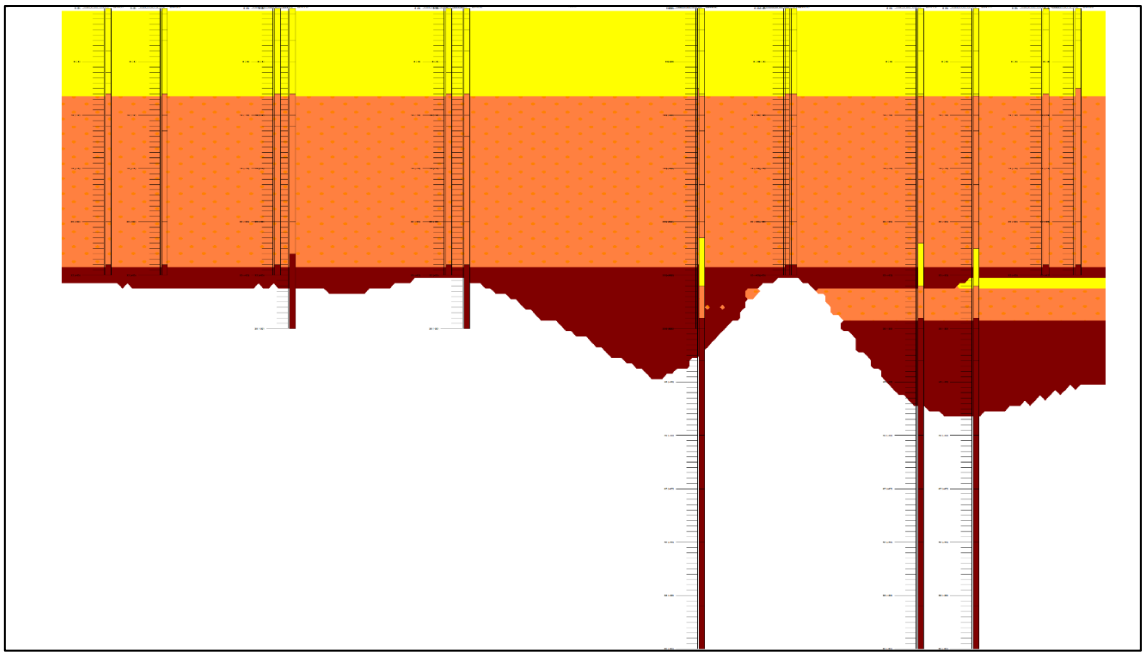

Fig. 3.12 Profile of the west side of Business Bay

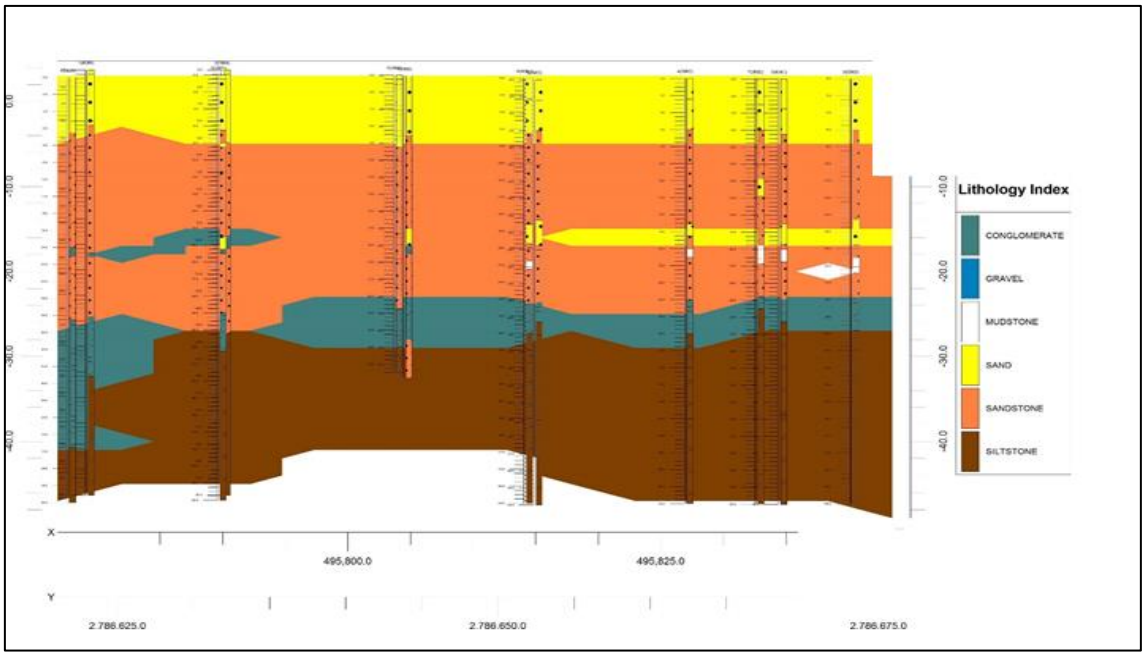

Fig. 3.13 Project profile in Business Bay

It is worth mentioning that the reports spanned over a large period of time, during which construction was taking place, for which several geotechnical contractors carried out the works. Hence, it was anticipated that variations in the underground would be encountered owing to the drilling techniques and competency of each of the drillers, as well as the uncertainty measurements of each of the contractors involved. In addition, construction could have affected the hydrology and ultimately the sub-surface. As indicated in Section 1 of this chapter, there are two main parameters that contribute to the findings of this report: unconfined compressive strength (UCS) and standard penetration test (SPT) N Value. The summary of these are presented in the table below and discussed in detail later.

Item	Unit	Total Number
Boreholes drilled	No.	195
Linear metres drilled	m	8766
SPT samples collected	No.	2234
Bulk samples collected	No.	151
Disturbed samples	No.	98
Rock core run retrieved	No.	4297

Table 3.6 Summary of geotechnical borings

The borehole depths ranged between 25m and 80m below the existing ground level. A summary of the boreholes depths are presented in the table below:

Borehole Depths below EGL (m)	Number of Boreholes
25	14
25 to 39	44
40 to 59	100
>= 60	37
Total	195

Table 3.7 Summary of borehole depths

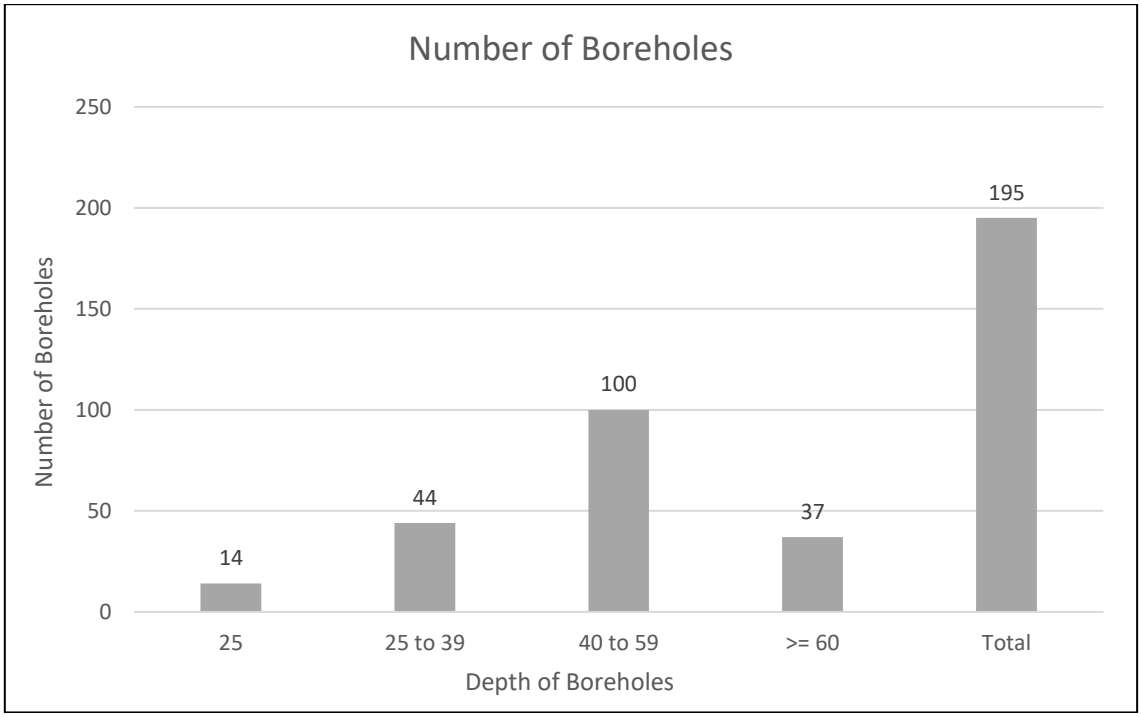

Fig. 3.14 Summary of borehole depths

The drilling procedures adopted during the investigation are as specified in the Code of Practice for site investigation BS 5930: 1999, which are in line with the common practice followed in Dubai and accredited by the local municipality. The generalised procedures used in-situ are:

- Standard Penetration Test (SPT) as per BS 1377: Part 9: 1990 - Test 3.3
- Cable Percussion boring as per BS 5930:1999, Sec 3, cl.20.5
- Rotary Drilling as per BS 5930:1999, Sec 3, cl.20.7

The commonly adopted issue of the standard was that released in 1999, to which all the field works were carried out. It should be noted that said release has been withdrawn and replaced with BS 5930:2015 and BS EN ISO 1997.

3.4.3 Laboratory Testing

The samples obtained from the drilled boreholes were subjected to classification, chemical and mechanical testing. These tests assist in providing geotechnical parameters that aid in the design.

Name	**Standard**
Classification test	
Sieve analysis	BS 1377: Part 2 1990 – AMD 9027 (96) Test 9.2
Hydrometer	BS 1377: Part 2 1990 – AMD 9027 (96) Test 9.5
Index Properties	
Atterberg limits	BS 1377: Part 2:1990 – AMD 9027 (96) 4.5/5.3/5.4
Specific gravity test	ASTM D 854:2002
Particle density and bulk density	BS 1377: 1990 Part 4
Moisture content of soil	BS 1377: 1990 Part 2
Chemical tests on soil and water	
Water soluble Sulphate content on soil	BS 1377: Part 3: 90 - Clause 5.3 & 5.4 - 9028 (96)
Water soluble Sulphate content on water	BS 1377: Part 3: 90 - Clause 5.3 & 5.4 - 9028 (96)
Water soluble Chloride content on soil	BS 1377: Part 3: 1990 - Clause 7.2 - AMD 9028 (96)
Water soluble Chloride content on water	BS 1377: Part 3: 1990 - Clause 7.2 - AMD 9028 (96)
pH on soil	BS 1377: Part 3: 1990 - Test 9 - AMD 9028 (96)*
pH on water	BS 1377: Part 3: 1990 - Test 9 - AMD 9028 (96)*
Carbonate content of soil	BS 1377: 1990 Part 3
Strength tests	
Shear strength determination by direct shear	BS 1377: 1990 Part 7
Tests on rock	
Unconfined compressive strength*	ASTM D 2938 (95); Preparation (ASTM D 4543)
Unconfined compressive strength with Stress-Strain measurements*	

*** Most samples do not comply with the preparation standard. However, the recent release of the ASTMD4543 -2008 allows for more flexibility in terms of sample tolerances.**

Table 3.8 Laboratory testing type

3.5 Soil properties for Business Bay and Downtown Dubai

3.5.1 Introduction

As will be apparent from the preceding discussions, the boreholes revealed that the sub-surface encountered is heterogeneous in terms of composition and compactness, making it an extremely laborious effort to try and identify the stratigraphy of the various sub-surface formations. As such, the aim of the following clauses is to attempt to demonstrate this fact, to provide comprehensive stratification data for Business Bay and Downtown Dubai.

3.5.2 Standard penetration test (SPT)

The standard penetration test (SPT) is probably the most essential in-situ test for soil and very weak rocks. In essence, this test is the resistance of the sub-surface to be penetrated by a split spoon sampler under an impact load of a donut hammer weighting 63.5 kg. This test is widely used and onto which many correlations have been built.

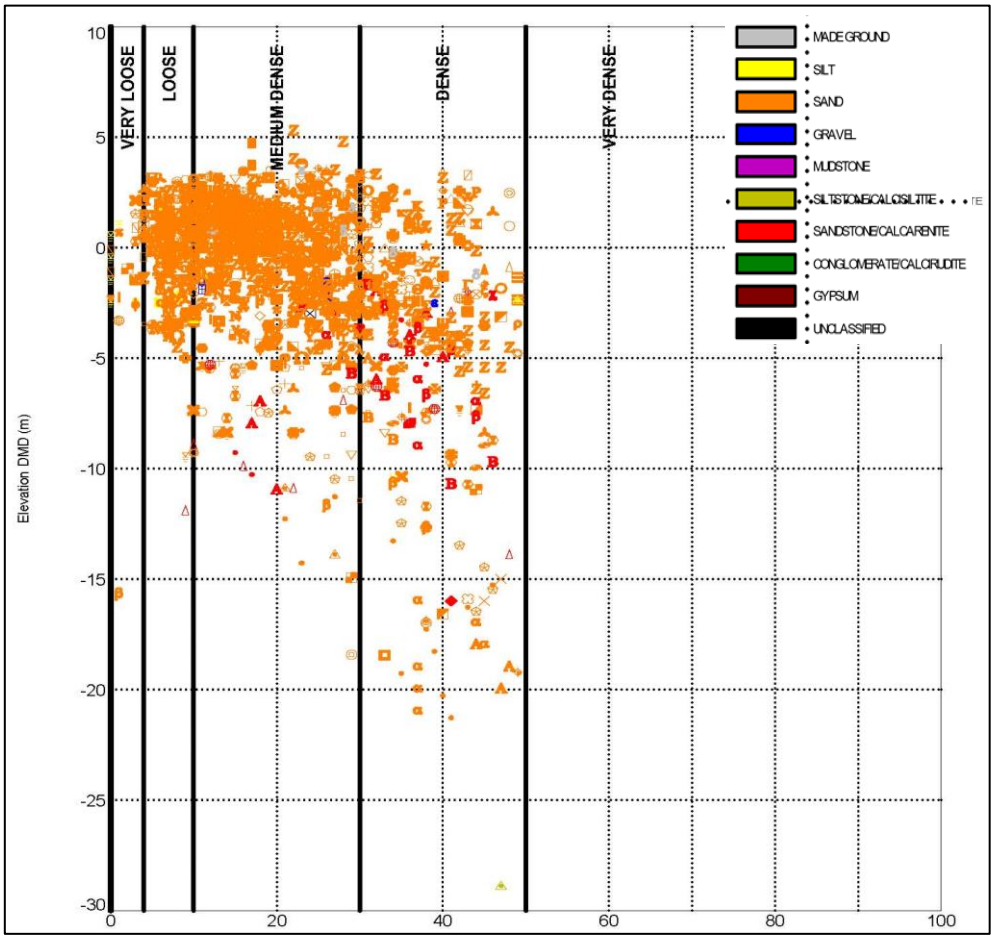

Fig. 3.15 Standard penetration test **(**SPT) vs elevation

In total, 1862 tests were carried out at various depths within the 195 drilled boreholes that form the structure of this chapter. Comprised mainly of sand, their compactness ranges from loose to dense at elevations between +5.0 to -3.0 m DMD. Most of the values indicate the presence of medium dense to dense sand. Although SPT values exist beyond the depth of -3.0 m DMD, they are of limited quantity and show the presence of sandstone and siltstone. Thus, it is safe to assume these as anomalies or non-intact rock core masses interbedded with layers of sand or gravel. Based on the outcome of these tests, it is reasonable to conclude that the top eight metres of soil in Business Bay and Downtown Dubai is mainly comprised of medium dense sand. Though this is a generalised assumption, it tends to match the average site conditions of the 28 geotechnical reports studied.

3.5.3 Unit Weight

The unit weight of the soil varies based on the size distribution and compactness of the encountered material. Even with such parameters being constant, the material composition of the soil will affect its unit weight. Referring to Chapter 2, for medium dense granular sand, the values range between 1.7 t/m^3 – 2.2 t/m^3, accordingly the value of 1.8 t/m^3 would seem adequate.

3.5.4 Angle of Internal friction

Soil strength parameters for both granular and cohesive soils may be related to SPT N-value. As discussed by McGregor and Duncan (1998), the existing correlations generally use the uncorrected SPT blow count, N. Generally, hammers delivering 60 per cent of the theoretical energy were used for SPT tests, and it seems likely that the data on which these correlations were based was obtained primarily from tests with such hammers (Aggour, 2002). However, this chapter ignores such correlations N60 and is based on the raw N value. Although these studies exhibit different results, the angle of internal friction varies by ±1. Hence, (Peck et al. 1974) has been adopted. The line in the figure below indicates the average SPT on site and its corresponding angle of internal friction.

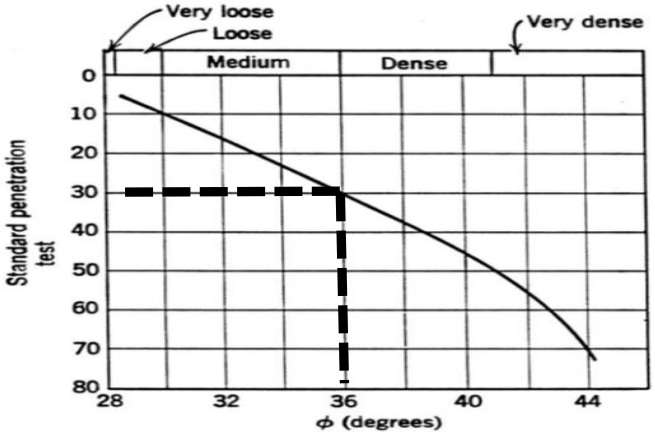

Fig. 3.16 Angle of internal friction (Peck et al. 1974)

3.5.5 Cohesion

Cohesion is the defined as the force that holds the molecules of the soil together. This type of force is more predominant in clay and silts, and is of low influence in granular soil with increasing influence proportional to the increase in silt/clay percentage. For soil layers, since the sub-surface conditions in the top eight meters comprises mainly of sand with varying silt/clay percentages, the cohesion value was determined to be of negligible value and 'zero' was adopted. For rock layers, the RMR procedure in Chapter 2 was followed and the resulting values presented in the findings of this clause.

3.5.6 Rock quality designation (RQD)

The data collected from the core drilling is highly scattered, providing no clear tendency and/or grouping scheme. It is also noted that there are a considerable amount of values that are 0 per cent, indicating red-flag zones (Deere 1988), which may be attributed to:

- Very weak sub-strata encountered
- Poor drilling techniques
- Feed pressure of the drilling machine
- Excess vibration of the rotary machine during drilling
- Rotation of the head of the drilling machine
- Type and size of core barrel used in the drilling
- Core breakage from handling
- Water pressure during the drilling
- Drilling polymer used
- Rock stress relief.

Fig. 3.17 Core box photograph

Fig. 3.18 Sample preparation

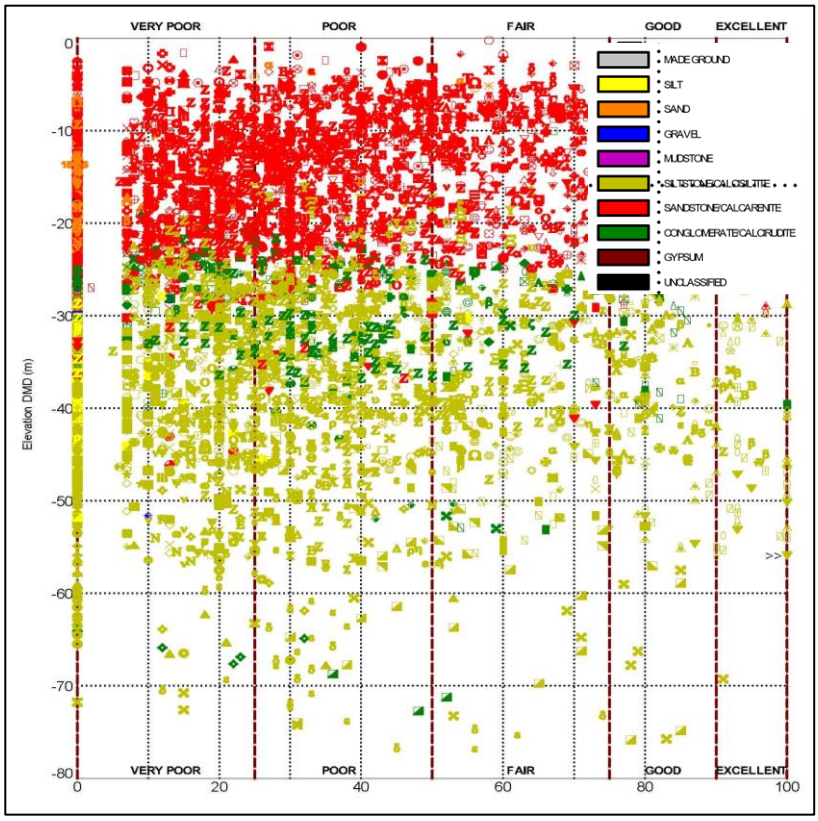

Fig. 3.19 Rock quality designation (RQD) vs elevation

3.5.7 Unconfined compressive strength (UCS)

The unconfined compressive strength (UCS) indicates the strength of the rock encountered.

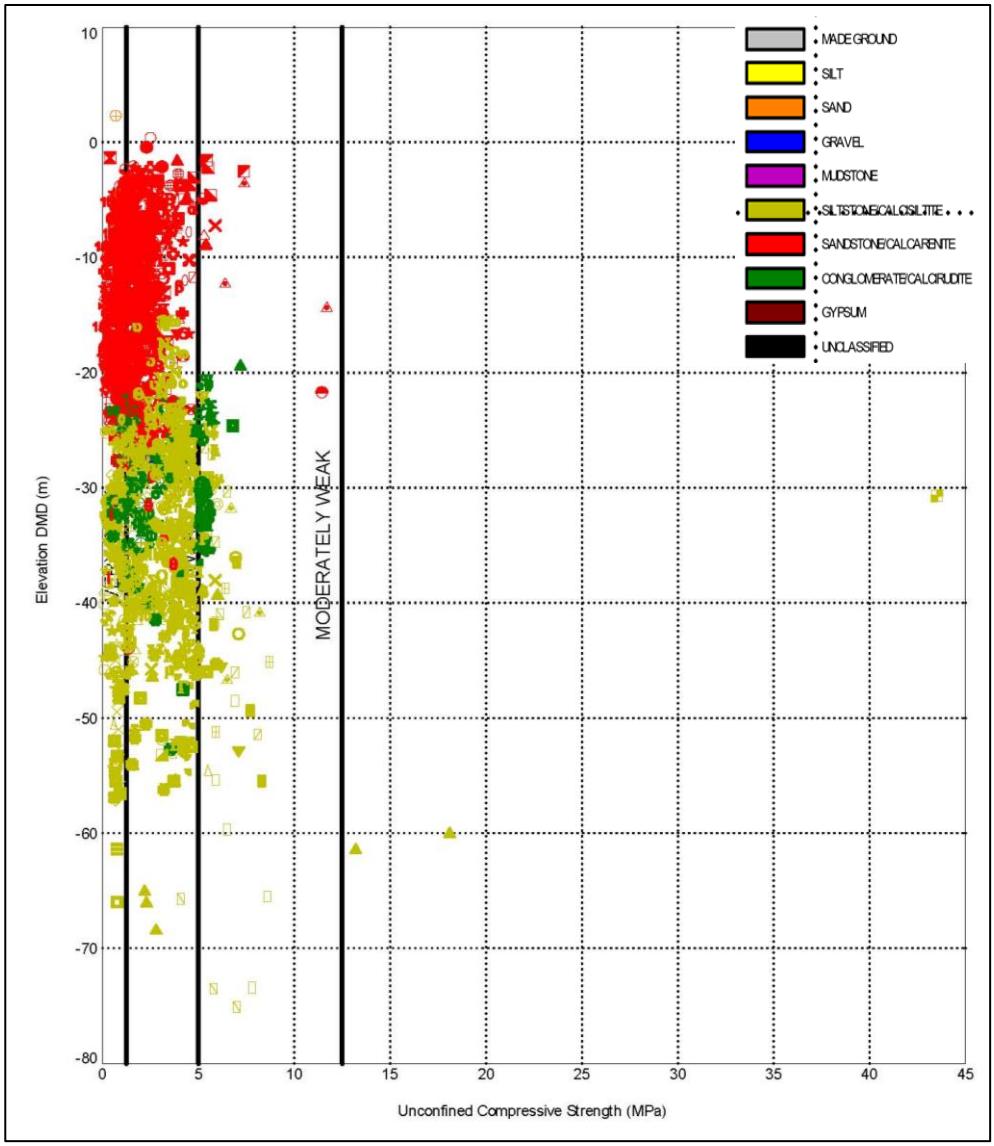

Fig. 3.20 Unconfined compressive strength (UCS) vs elevation

The results of the tests carried out on the samples retrieved from the drilled boreholes vary significantly. However, patterns can be visualised from the plot. The sandstone layer shows a decrease in strength as the depth increases, averaging weak strength closer to the very weak boundary. The conglomerate/siltstone layer shows a distinct weak strength that averages at the mid span of the weak strength range. As the depth increases below that layer, the siltstone layer shows the same features up to approximately -48.0 m DMD, beyond which it loses strength and falls into the very weak category.

3.5.8 Modulus of Elasticity (STRESS-STRAIN RELATIONSHIP)

The results below are based on the results of unconfined compressive strength test with Young's modulus measurements. The deformation of the sample is recorded by means of a dial gauge during the UCS test procedure, with the parameters being calculated as follows:

$$\text{Axial Strain (\%)} = \frac{\text{Change in Height of sample}}{\text{Original Height}} \; ; \; \varepsilon = \frac{\Delta}{\mathrm{L}}$$

$$\text{Axial Young's Modulus (MPa)} = \frac{\text{Compressive Stress}}{\text{Axial Strain}} \; ; E = \frac{\sigma}{\varepsilon}$$

There are three methods to calculate the Young's modulus for the resulting graph, these are:

- ASTM D7012-14 Clause 10.3.5.1 - Tangent Young's modulus at 50 per cent which is the stress divided by the strain when the sample has reached 50 per cent of the ultimate unconfined compressive strength (Refer figure 3a).
- ASTM D7012-14 Clause 10.3.5.2 - Average Young's modulus which is a best-fit line running through the straight-line portion of the stress-strain curve (Refer figure 3b).
- ASTM D7012-14 Clause 10.3.5.3 - Secant Young's modulus at break which is the maximum stress divided by the maximum strain at the peak point (Refer figure 3c).

The results presented in the graph below are the 'Secant Young Modulus':

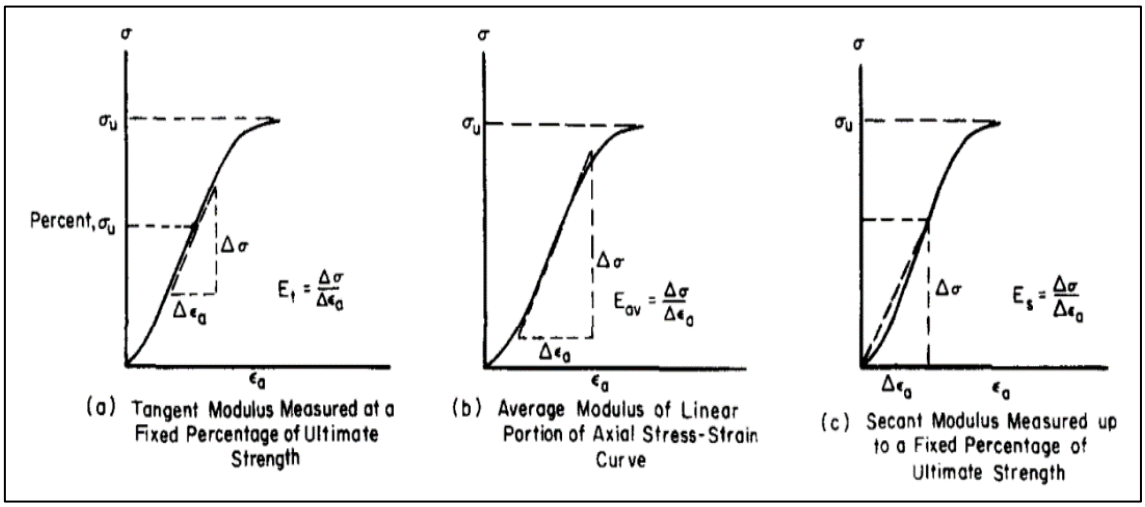

Fig. 3.21 Methods for calculating Young's modulus from axial stress-strain curve

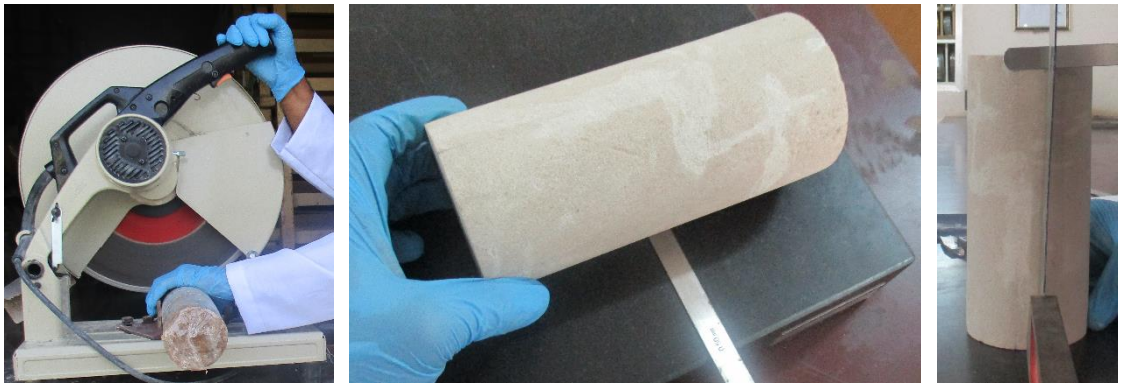

Fig. 3.22 Sample preparation: cutting (left), straightness (center), perpendicularity (right)

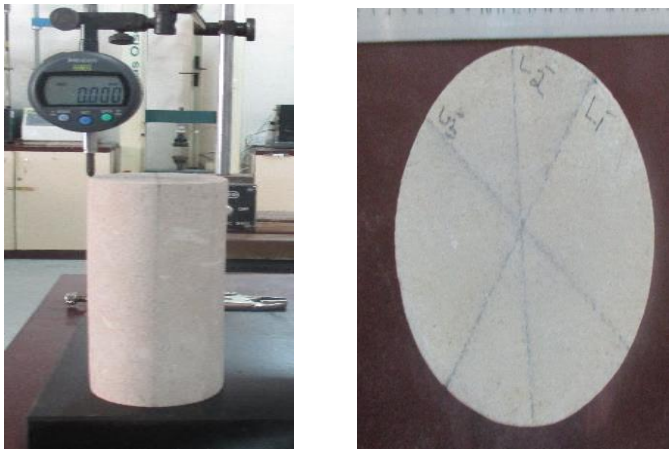

Fig. 3.23 Sample preparation: measure of surface flatness

Fig. 3.24 Sample testing and failure

3.5.9 Poisson's Ratio

In general, the Poisson's Ratio value for the weak/soft rock was assumed as 0.3.

3.5.10 Generalized sub-surface properties

Based on the outcome of the discussion presented in this chapter, the following table presents a rough and crude guide to the sub-surface conditions in Business Bay and Downtown Dubai.

Parameters	**Depth DMD (m)**				
	5.0 to -3.0	**-3.0 to -23.0**	**-23.0 to -32.0**	**-32.0 to -48.0**	**-48.0 to -75.0**
Description	Sand	Sandstone	Conglomerate/Siltstone	Siltstone	
Av. Bulk density: γ kN/m^3	18	20	20	20	20
Av. Angle of shearing resistance: Φ	30°	45°	45°	45°	45°
UCS MPa	-	1.3	3.0	3.0	1.5
Modulus of elasticity (E) MPa	-	5 - 50	30 – 100	30 – 100	90 – 150
Cohesion (c) kN/m^2	-	40-60	85-100	85-100	40-100

Table 3.9 Sub-surface conditions in Business Bay & Downtown Dubai

The bulk density of the sand was found to be 18 kN/m^3, increasing to 20 kN/m^3 for the subsequent rock layers. The same was the case for the angle of internal friction which was found to be 30° for the sand layer, increasing to 45° for the subsequent rock layers.

The rock layers extended down from an elevation beyond -3.0 metres DMD, down to -75.0 metres. The rock sub-surface comprised of 12 metres of very weak sandstone, followed by nine metres of weak conglomerate/siltstone, then 43 metres of weak through to very weak siltstone. The sandstone layer had an average unconfined compressive strength of 1.3 MPa, modulus of elasticity ranging between 5– 50 MPa and a cohesion value ranging between 40 – 60 kN/m^2. The following conglomerate/siltstone had an average unconfined compressive strength of 3.0 MPa, modulus of elasticity ranging between 30 – 100 MPa and a cohesion value ranging between 85 – 100 kN/m^2.

The underlying layer of siltstone was divided into two layers based on the strength properties of the revealed sub-surface. The top layer of siltstone had an unconfined compressive strength of 3.0 MPa, modulus of elasticity ranging between 30 – 100 MPa and a cohesion value ranging between 85 – 100 kN/m^2, while the lower layer had an unconfined compressive strength of 1.5 MPa, modulus of elasticity ranging between 90– 150 MPa and a cohesion value ranging between 40 – 100 kN/m^2.

4 Static load test field data

4.1 General

When it comes to the deep foundation, geotechnical field testing is required to determine the pile capacity. The piles design which is based on site investigation report and laboratory testing is verified by pile loading tests. Pile loading tests provide a relation between the displacement performance and the ultimate load of the tested pile. A significant distinction is made between the driven piles and the bored piles tested with the static load test. In Business Bay and Downtown Dubai, all the piles are bored piles; due to this, the following chapter focuses only on the bored pile. A review of different load tests will be given with the evaluation of the practiced field tests at project site.

4.2 Overview on Static Load Test

The Static Load Test can be performed for different configurations of load transfer:

- Compression
- Tension
- Lateral

This scientific work concentrates only on the compressive force applied to the piles as indicated in Fig. 4.1. The Standard Test Method for piles is called the 'Static Axial Compressive Load Test', which is described in ASTM D 1143. Furthermore, according to the method of pile loading, the compressive load test is divided into the maintained load test (ML) and constant rate of penetration (CRP) test as shown in Fig. 4.1. In the maintained load test procedure, the loading value for each step is kept constant for the planned time frame or until a definite displacement occurs. During the CRP test the measured rate for the settlement is constant, while the loading is adjusted in accordance with the pile movement.

This chapter will only refer to the maintained load test. During the implementation of the test the load transferred to the pile is continuously increased. The test pile is loaded until the maximum load equal to 1.5 times the expected working load is reached. Each loading step should be increased in increments of 25 per cent of the maximum load. The pile loading continues for two cycles, each cycle including the loading and unloading phases. During the first cycle, the pile is tested up to its working load, followed by load reduction until no force is applied. Again, the pile is reloaded in the second cycle to 150 per cent of the working load and finally unloaded.
The settlement of the pile that occurs after each step load is recorded when a defined period of time has elapsed. Table 4.1 indicates the difference in the types of loading

procedures based on loading test duration. As can be deduced from the table data, a common feature of all loading types is the reading interval in the first cycle, during which the maximum loading will reach 100 per cent. The holding period for the maximum load will be six hours and, after completing the first cycle, the unloading period should be undertaken for a minimum of one hour. In the second cycle, during which the maximum loading will reach 150 per cent, the holding period for the maximum load will be six hours for Type 1, 12 hours for Type 2 and 24 hours for Type 3 (as per Table 4.1). It should be noted that the minimum holding period mentioned in the table below is as per ASTM and Eurocode 7. Also, some pile tests were carried out in Business Bay and Downtown Dubai by using a smaller loading increments than mentioned in the tables below.

From this, the load-settlement curve is developed to evaluate the load bearing capacity of the pile. The failure criteria of the test appears as per the following:

- The maximum load of the pile is achieved once the pile moves downwards without increase in load.
- Total settlement of the pile exceeds 10 per cent of the pile diameter.

Preliminary Test Pile

The preliminary pile design (PTP) is carried out to evaluate the pile load capacity and displacement behaviour based on field investigation and desk study. The pile design is verified based on the pile test at site (PTP), with the outcome from the test used to finalise the pile design. Usually, the test load value for the (PTP) applied for load testing will be more or equal to two times of the working load or to be loaded until pile failure. The PTP pile will not be used as part of structure, also called ‘non–working piles’ (Murthy 2002).

Working Pile

Permanent piles or working piles are built to carry the working load of the structure. The working piles will be tested for static load up to 1.5 times the working load to confirm the pile design. Pile static load test will be conducted randomly for actual piles. As per the codes and local regulations, the percentage of tested piles should be not less than one per cent of the total number of the constructed piles.

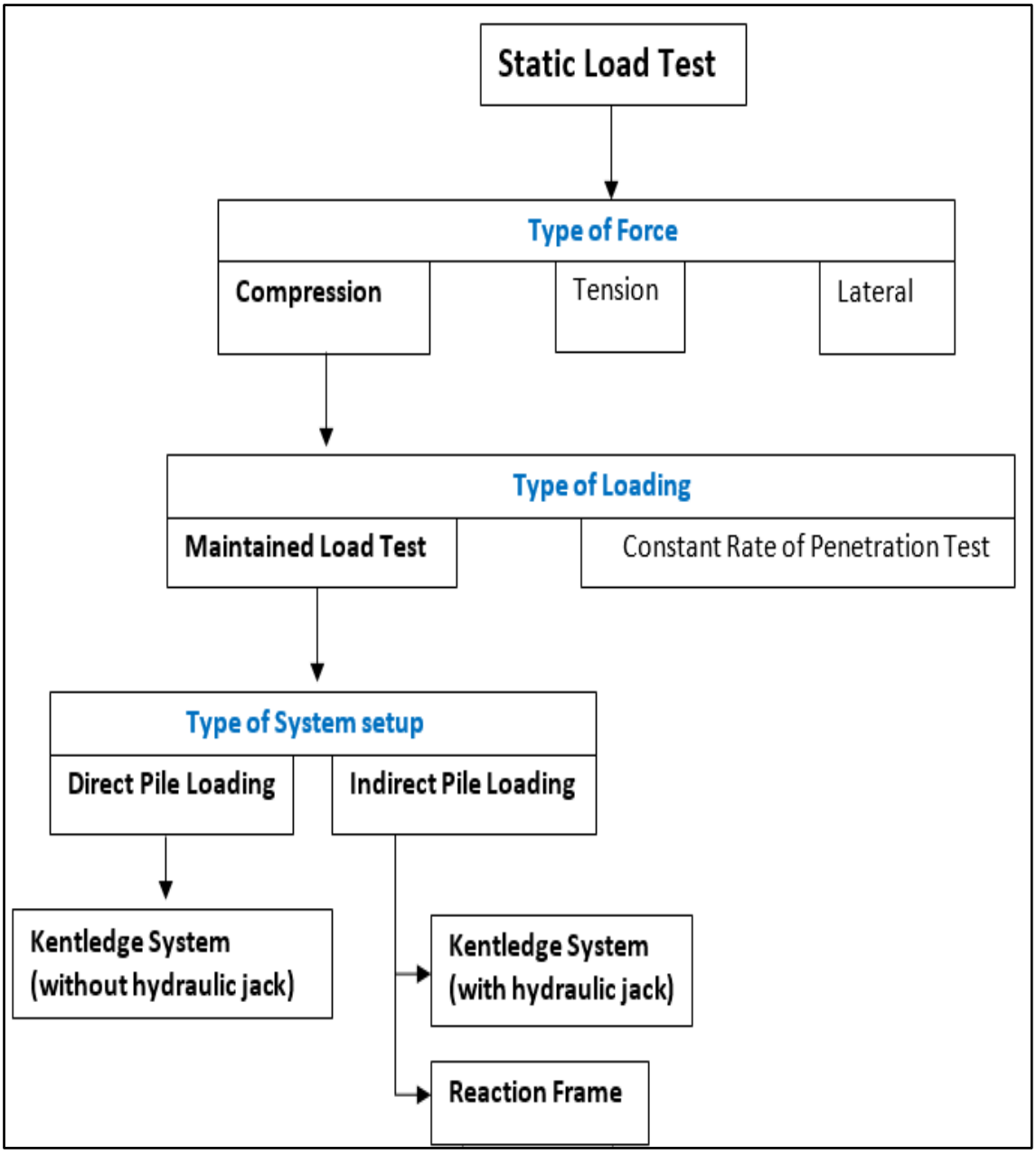

Fig. 4.1 Distinction between applicable types of Static Load Test

4.3 Mechanism of loading in Static Load Test

Based on the mechanism of loading, the pile load test can be mainly classified into the following two types:

4.3.1 Maintained load test

The pile is tested for a series of loading. In each stage, it is standard practice to increase the pile load in equal increments of 25 per cent, ensuring that sufficient time has elapsed between each load increments to allow only a small settlement to take place. The working pile is loaded to 1.5 times the working load capacity; however, the settlement should not exceed the permissible limit. This method is not used for the verification of ultimate load capacity of pile or to generate plunge as it is difficult to maintain the constant load for high settlement values (Burland, Chapman, & Engineers, 2012). The test is carried out in two cycles, with each cycle consisting of both the loading and unloading stages. During the first cycle, the pile is initially loaded in increments of 25 per cent until the working load capacity is reached, at which point the pile is unloaded in decrements of 25 per cent until zero. This loading and unloading phase completes the first cycle of the load test.

In the second cycle, the load test uses a similar procedure is used to that in first cycle, the only difference being that the pile will be loaded up to 1.5 times the working load. The time/settlement curve is recorded during each stage of the load increment after a specific time interval has elapsed (Tomlinson & Woodward, 2007). The minimum time for the holding of each load increment typically ranges from 30 to 60 mins in the loading phase and 10 mins in unloading phase.

Table 4.2 below illustrates the various types of loading procedure used during the maintained load test (ML test). As indicated in the table, the first loading cycle of all the three types follows the same loading procedure, with a holding time varying from five minutes to six hours during the loading phase and between five to 60 minutes in the unloading phase.

The difference between all three types of loading procedure is evident from the second cycle. During this cycle, the maximum holding time varies from six hours for Type-1, 12 hours for Type-2 and 24 hours for Type-3. The table represents the maximum holding time for specific load increments as recommended by ICE specification; however, the test can be conducted in lesser loading increments or with a shorter reading interval, as preferred by the investigator.

Finally, the load settlement relationship is established using the observed readings to verify the load bearing capacity of piles. The ultimate loading capacity of the pile is

evaluated at the failure criteria or when penetration exceeds 10 per cent of the pile diameter.

	Load %	Loading Interval		
		Type 1	**Type 2**	**Type 3**
1st Cycle	**0**	0	0	0
	25	0,5,15,30 min	0,5,15,30 min	0,5,15,30 min
	50			
	75			
	100	**0,5,15,30 min, 1 hr-6hrs**	**0,5,15,30 min, 1 hr-6hrs**	**0,5,15,30 min, 1 hr-6hrs**
	75	0,5,10 min	0,5,10 min	0,5,10 min
	50			
	25			
	0	0,5,15,30 min, 1 hr	0,5,15,30 min, 1 hr	0,5,15,30 min, 1 hr
2nd Cycle	**100**	0,5,15,30 min, 1 hr	0,5,15,30 min, 1 hr	0,5,15,30 min, 1 hr
	125			
	150	**0,5,15,30min, 1hr-6 hrs**	**0,5,15,30min, 1hr-12 hrs**	**0,5,15,30min, 1hr-24 hrs**
	125	0,5,10 min	0,5,10 min	0,5,10 min
	100			
	75			
	50			
	25			
	0	0,5,15,30 min, 1 hr	0,5,15,30 min, 1 hr	0,5,15,30 min, 1 hr

Table 4.1 Different loading procedures for ML test (ICE Specification, 1996)

Fig. 4.2 Static load test

4.3.2 Constant Rate of Penetration Test

This method was developed by Whitaker (1957) for the testing of the model pile. It was subsequently used for conducting full scale pile tests. In this method, the pile is loaded with a varying load to maintain a constant rate of penetration, with force applied at the top to maintain this constant penetration rate, which is continuously measured. The main objective of this test is to verify the ultimate pile load capacity. The data interpreted from the test is plotted as a graph of load versus penetration (Poulos & Davis, 1980).

Rate of penetration mm/s (mm/min)				
Major soil type	**SPERW 2007**	**BS8004**	**ASTM D1143-81**	**EN 1536 - 2000**
Fine-grained souls (e.g. clay)	0.01 (0.60)	0.0125 (0.75)	0.0042-0.021 (0.25-1.25)	0.01667 (1)
Course grained soils (e.g. sand or gravel)	0.02 (1.2)	0.025 (1.5)	0.0125-0.042 (0.75-2.5)	0.01667 (1)

Table 4.2 Examples of pile penetration rates (ICE Specifications)

The table above illustrates the typical penetration rates chosen for the CRP test as recommended by the ICE specifications, depending on the main type of soil encountered during pile installation. Due to these values of penetration rates, the test is comparatively quick to execute as there is no time-lapse for the consolidation or creep settlement of the soil. For example, a 750 mm diameter pile embedded in a clay soil can be tested for a penetration value of 10 per cent of the pile diameter (75 mm) in almost two hours (Burland et al., 2012). The CRP test is generally considered suitable for research purposes, but not for testing on site. Even though the test is comparatively faster, a greater capacity of loading and reaction system is needed to produce the required plunge (Burland et al., 2012).

4.3.3 Method of Equilibrium

This method was first developed by Mohan and Jain (1967) primarily to test the ultimate load capacity of piles and has been proven to provide reasonable settlement values. The main principle is to load the pile at stages of testing with a higher load value than required, then reduce the load to the required value. By using this process, the rate of settlement declines more quickly than it does in the ML test, and the equilibrium condition is able to be achieved in minutes rather than hours (Poulos & Davis, 1980).

As per the method suggested by Mohan and Jain, initially a load value of about one tenth of the estimated design load is applied over a time period of three to five minutes. The load is then maintained for approximately five minutes, before being allowed to decrease by itself through the downward movement of pile. In this way, the equilibrium conditions are attained in a few minutes. Then the next load increment is applied, and the process continues until the desired value of design load is reached. For higher load values, it is recommended to maintain the load initially for a time period of 10 to 15 minutes before being released. The total time required for the testing is approximately one third of the testing time required for the ML test (Poulos & Davis, 1980).

4.4 Types of Reaction System in Static Load Test

4.4.1 Direct Pile Loading

The loading of the pile can be conducted directly on the pile head or indirectly with the help of a loading jack (Fig. 4.1). The following section deals with different methods of applying load increments to the pile. Using this method, the load is transmitted into the pile directly by a platform built on cross beams (Fig. 4.2).

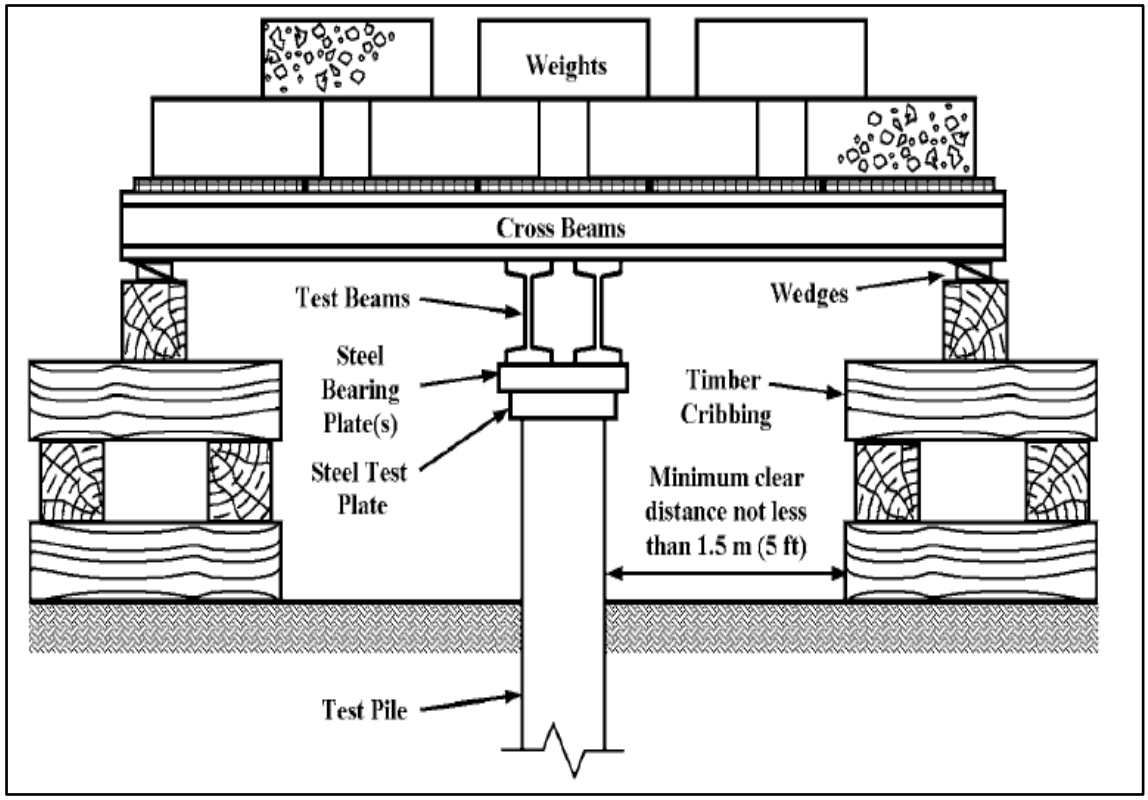

Fig. 4.3 Experimental setup for direct pile loading test

Usually, the ultimate load is identified by the indirect method of pile loading. This test consists of the installation time of a hydraulic jack between the test beams and test pile. Although the loading steps are similar, the system structure utilised to transfer the load to the pile differs. The indirect pile loading can be carried out by using either the reaction frame or the Kentledge system.

4.4.1 Indirect Pile Loading

Kentledge System:

The setup for the Kentledge Test is shown in (Fig. 4.4). In a symmetrical axis position the timber cribbing or concrete blocks are set on opposite sides of the test pile to support the cross beams. The load is applied on a platform above the cross beams until an increase of 10 percent greater than the design load is reached. The weight is transferred from the cross beams to the test beam centred on the test pile. While transferring the maximum load forces to the pile through the hydraulic jack, the lifting of dead load is not permitted. The load distribution to the cribbage and the test piles should be taken into consideration, with half of the total weight carried by each supporting pad (Chew 2009).

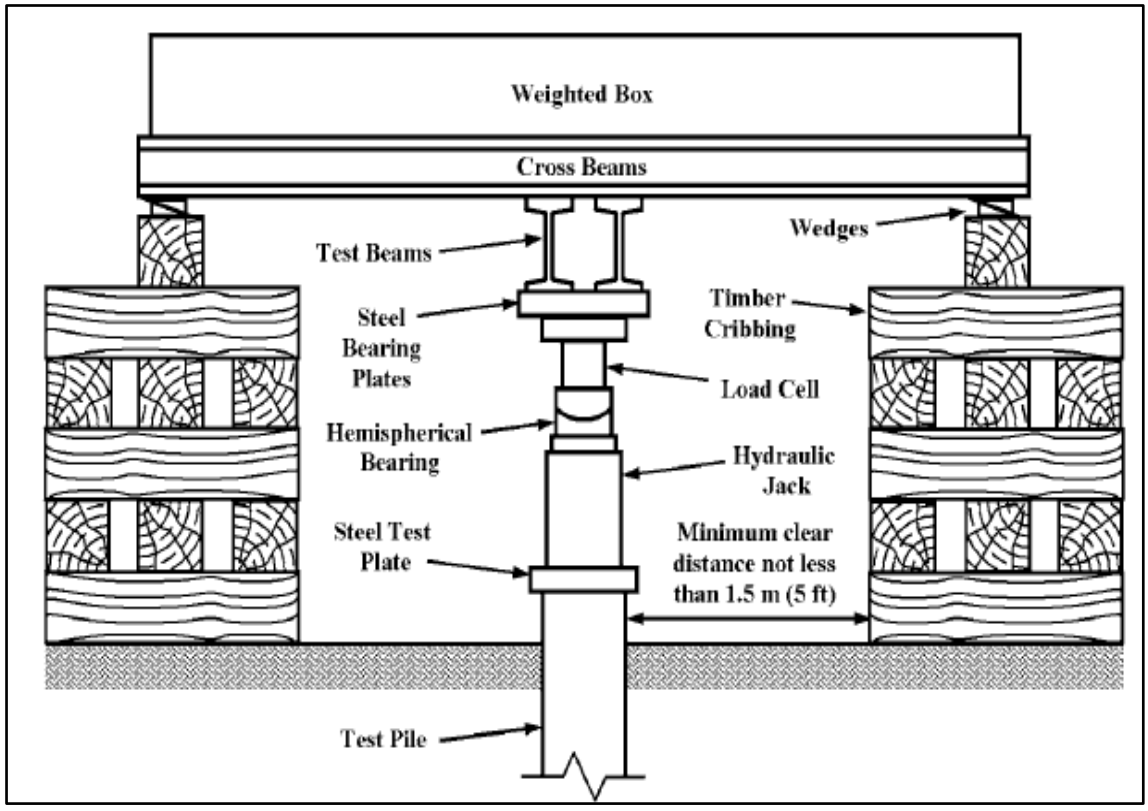

Fig. 4.4 Setup for Kentledge system

Reaction Frame:

A Reaction Frame is realised by building reaction piles on each side of the test pile, allowing a minimum clearance of 2.5 metres. The reaction piles either consist of tension piles or ground anchors, as illustrated in (Fig. 4.4). The hydraulic jack is then placed over the pile head once a steel plate has been installed between them. The loading of the pile is gauged by a load cell, fixed on a bearing block. The pressure in the test pile deriving from the hydraulic jack creating and ally pressure tension as the reaction force on the piles. These reaction piles are supposed to withstand the uplift force resulting from the beam whilst providing reaction force for the hydraulic jack to press the test pile into the ground (Poulos & Davis 1980).

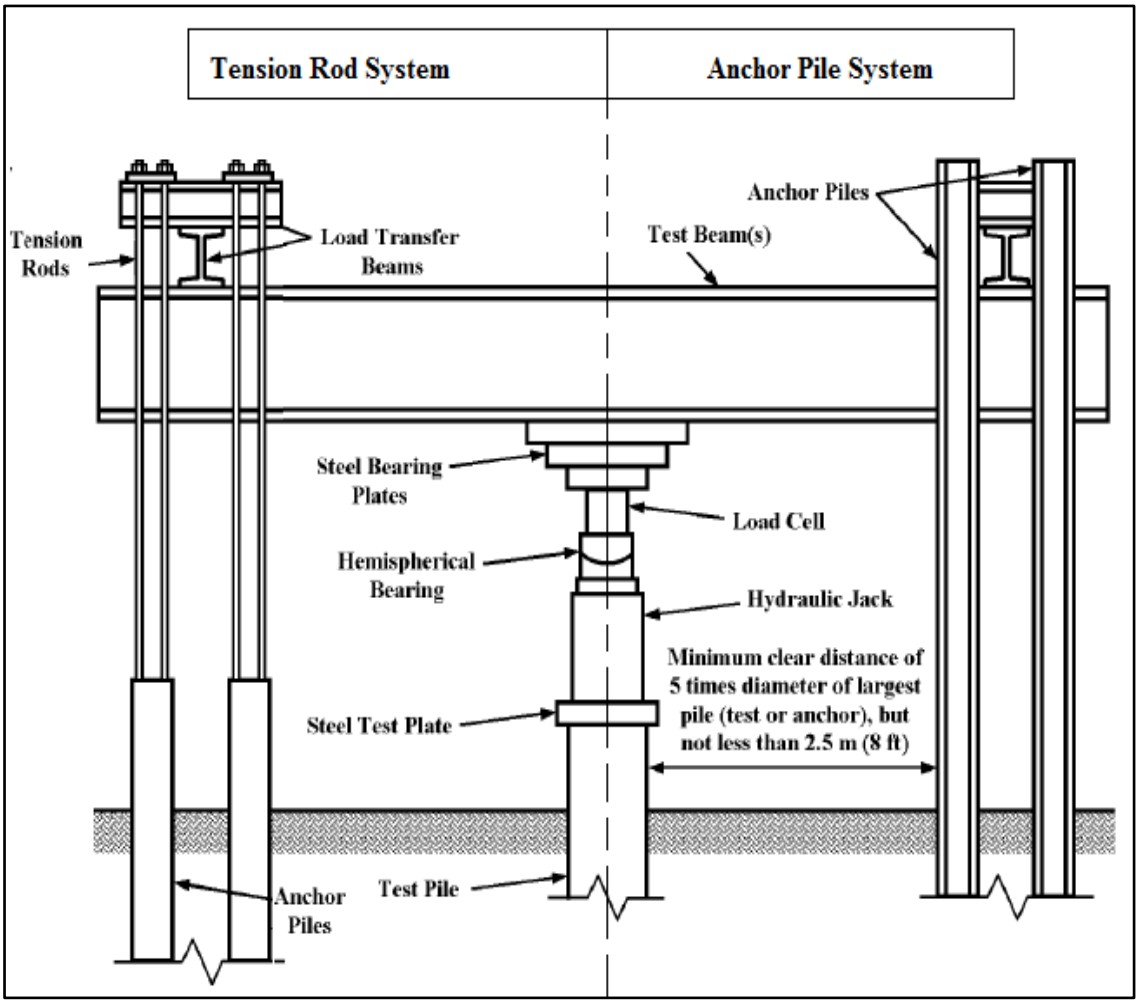

Fig. 4.5 Tension rods or anchor piles as a reaction system

Where cast in place piles are constructed and the installation of anchor piles is unfeasible, or the use of reaction frame is not possible due to insufficient capacity of the available soil, the Kentledge technique is preferred.

4.5 Overview on O-Cell Test

This method of pile testing is also called the ‘Bi-Directional Static Load Test’ based on measurement of two different pile resistance parameters. This type of test measures the compressive resistance at the bottom of the pile in addition to the skin friction. In comparison with the static load test, a main modification according to the setup in this test is the position of the jack, called the ‘Osterberg Cell’ or ‘O-Cell’, which is placed within the pile close to the bottom of the reinforced cage. First the pre-installation of the O-Cell inside the reinforcement is completed, then strain gages are placed in different pile levels and at the bottom of the pile. (Fig. 4.6)

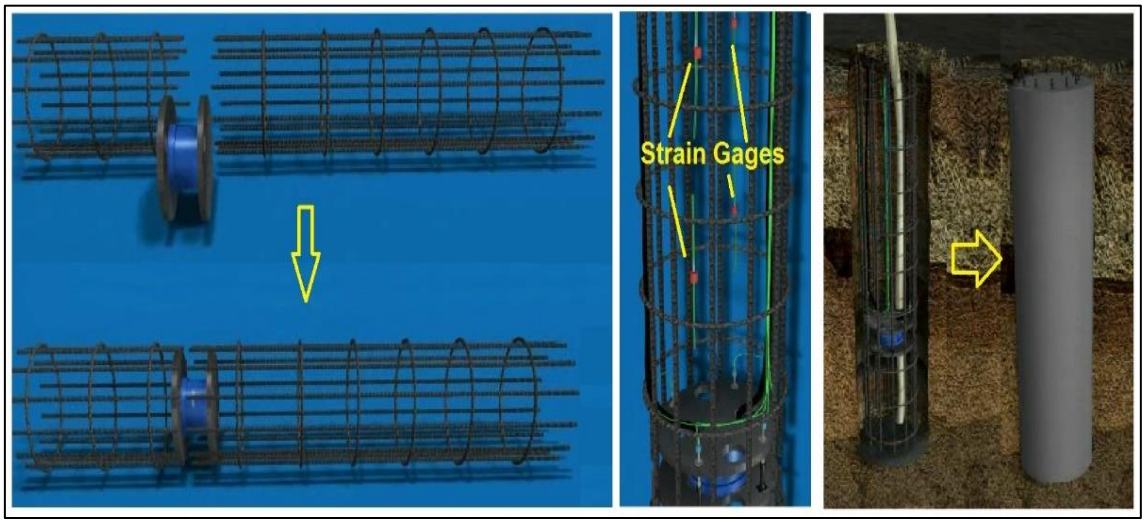

Fig. 4.6 Preparation of the test pile

Afterwards the pile is concreted; the O-Cell is hydraulically driven upwards as per (Fig. 4.7).

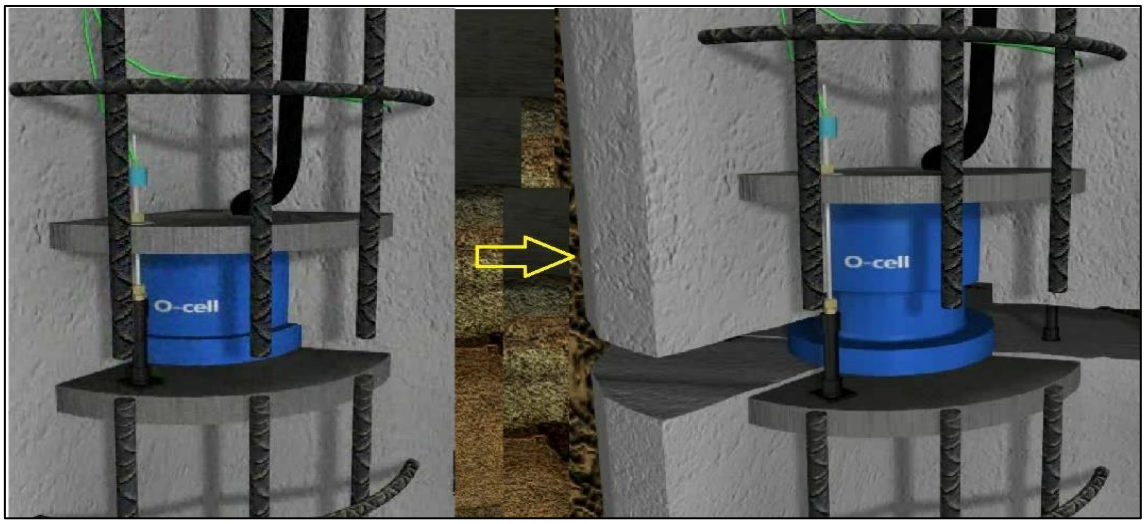

Fig. 4.7 Loading of the test pile by jack expansion

The equipment required for this test is illustrated in Fig. 4.7. During the loading process the extension of the O-Cell is recorded by movement transducers which are connected to a PC; this includes a data logger for recording the result data while applying the load on the pile with the help of a hydraulic control device. Moreover, the end bearing and pile friction is measured by the strain gages located along the pile and at the bottom of the pile (Chew 2009).

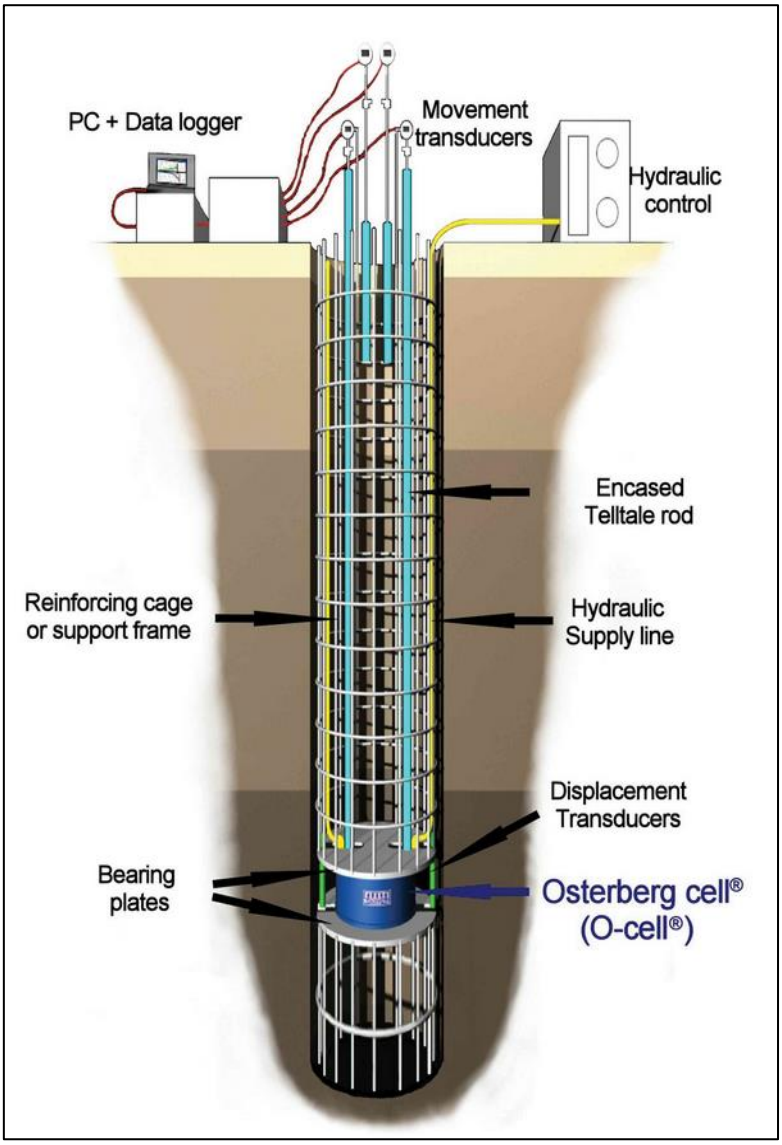

Fig. 4.8 Setup of O- Cell test

4.6 Evaluation of the field tests for Business Bay and Downtown project

The total numbers of the pile load tests in the Business Bay and Downtown Dubai areas are 116 piles. Among them were 113 piles tested with static load test and three piles tested with instrumented static load test. The description of each test will be defined in the following sections, with the exception of the end bearing test.

4.6.1 Static Load Test

The total numbers of the static load test in Business Bay are 113 piles; there are two different types of piles as per the following table

Type of Piles	Number of Piles	Percentage %
Working Piles	108	93.1%
Preliminary Piles	5	4.3%
Instrumented Piles	3	2.6%
Total	**116**	**100%**

Table 4.3 Type of piles tested at site

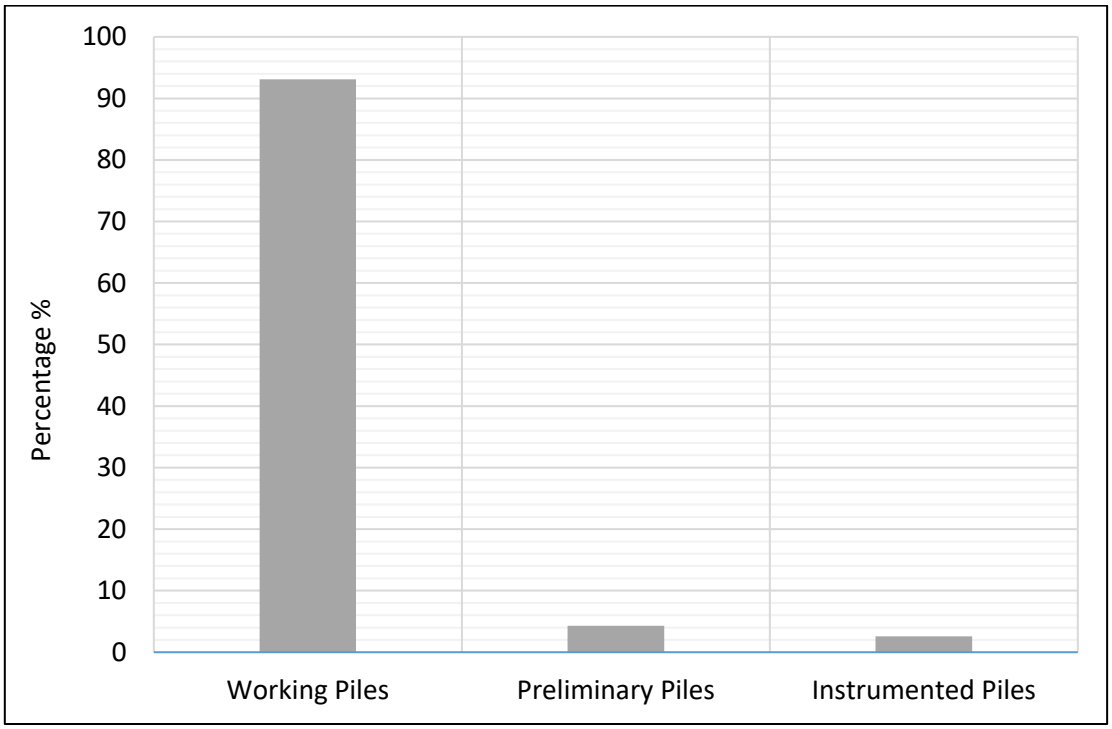

Fig. 4.9 Statistics for different types of piles

About 52 per cent of the total types of system setup for the static load test were carried out with reaction frame (Table 4.5). Most frequent types used at site were the anchor piles, as shown in (Fig. 4.10).

Fig. 4.10 Reaction frame including anchor piles at site

Type of system setup	Number of Piles	Percentage %
Kentledge System	61	54%
Reaction Frame	52	46%
Total	**113**	**100%**

Table 4.4 System setup applies at site

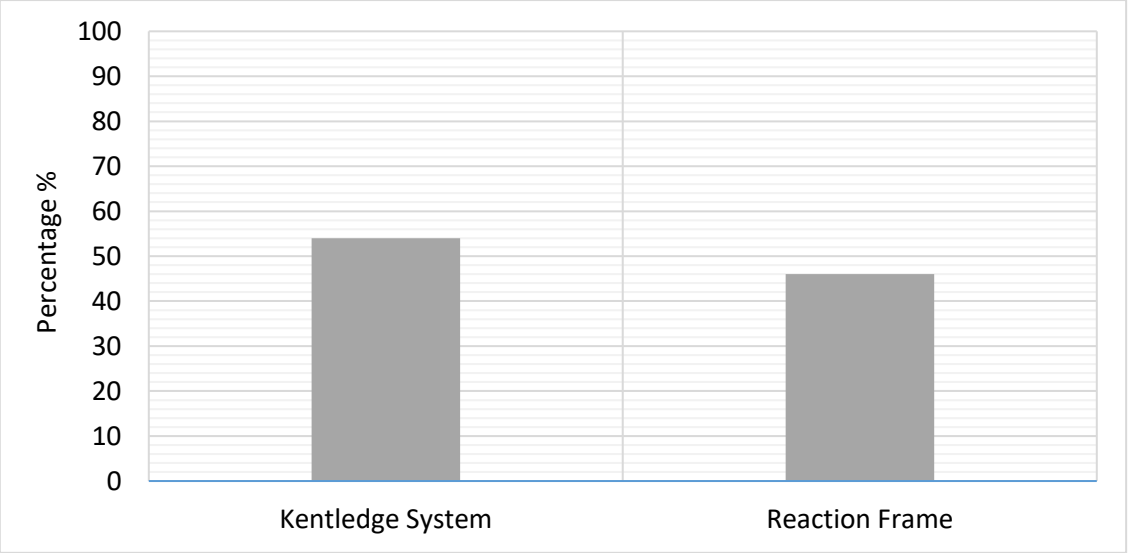

Fig. 4.11 Statistics for different types of system setup

Loading intervals	Number of Piles	Percentage %
Type 1	11	10 **%**
Type 2	50	44 **%**
Type 3	52	46 **%**
Total	**113**	**100 %**

Table 4. 1 Loading procedures carried out at site

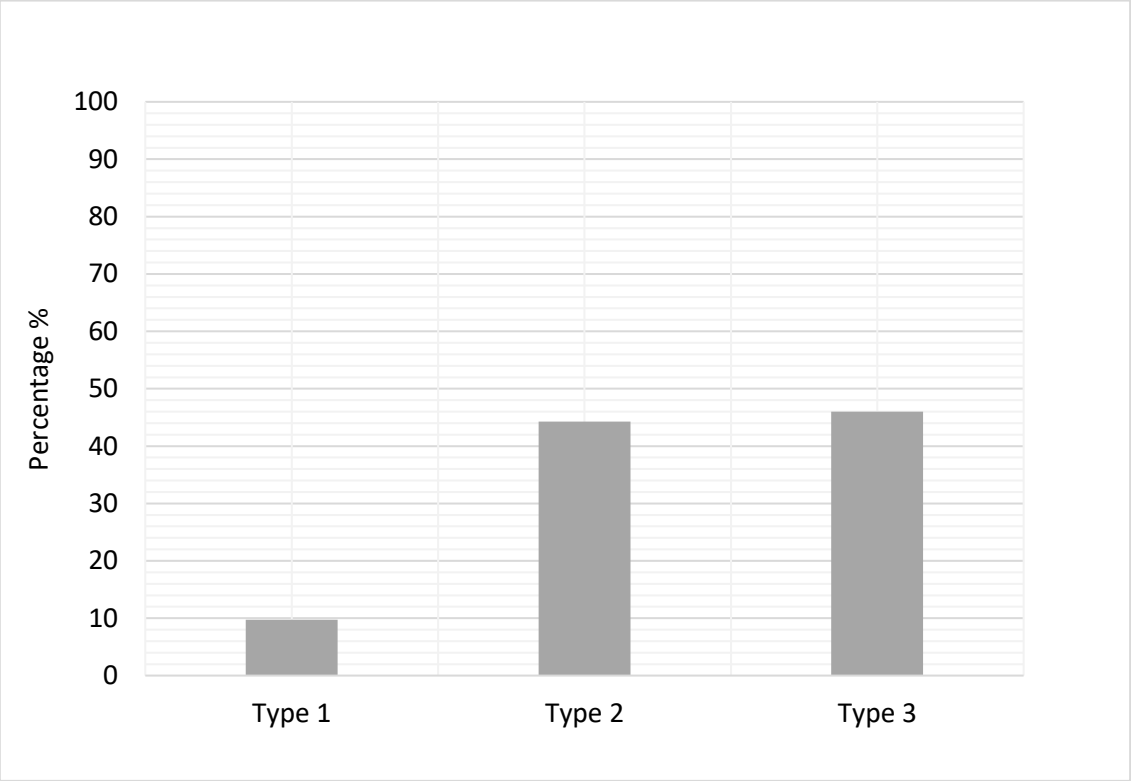

Fig. 4.12 Statistics for different types of loading procedures

4.6.2 Instrumented Static Load Test

The loading procedure and equipment for the instrumented static load test is similar to the standard static load test except for the strain gages, which are installed in different levels along the pile length. The strain gages are placed in opposite side to measure the settlement and friction of the outline pile surface. Moreover, the gages at the bottom of the pile provide an opportunity of measuring the end bearing capacity of the pile.

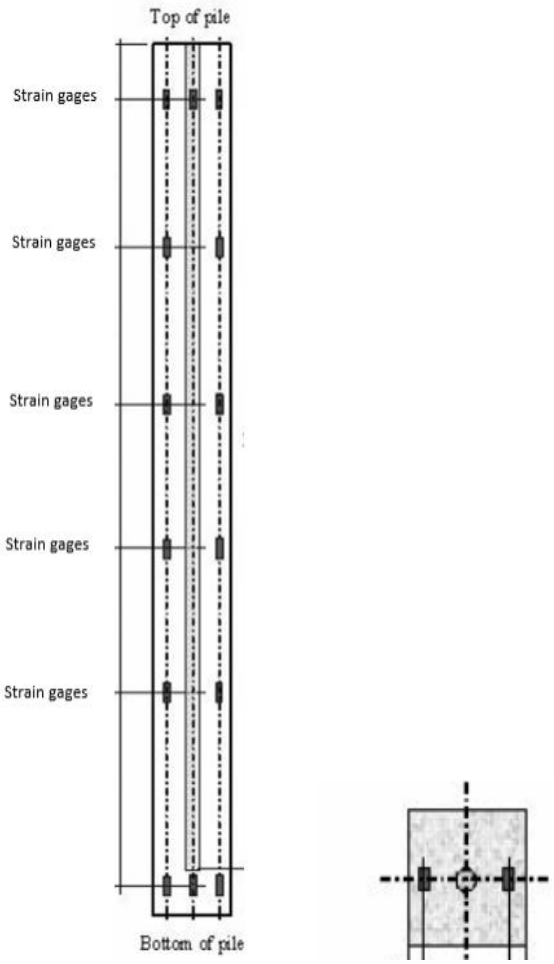

Fig. 4.13 Frontal view and cross section of the instrumented pile

When compared to the general static load test, the three instrumented piles were also loaded to 1.5 times the working load. Moreover, the loading and unloading stages are identical, which means an increment and decrement of 25 per cent working load in each loading step.

Before starting with the actual test, the test pile had to be prepared. A reinforcement cage is equipped with the mentioned strain gages at different heights as highlighted in (Fig. 4.14).

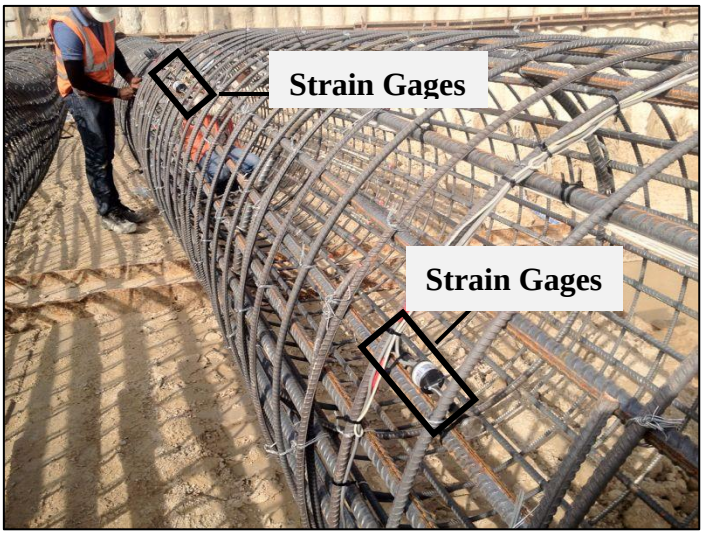

Fig. 4.14 Reinforcement cage with strain gages at site

After the strain gages have been fixed in the pile, the reinforcement cage is set up into the borehole and then the following concreting processes are performed (Fig. 4.15).

Fig. 4.15 Positioning of reinforced cage

Afterwards, the upper part of the test pile should be released from the surrounding soil, then the system setup described in section 4.2.2 is installed. After the completion of the arrangements, the static load test is conducted for three instrumented piles at site. The specifications of the piles equipped with gauges at different levels are given in Table 4.2

Pile	Pile Dia.	Pile Length	Working Load	Test Load	Cut off Level	Toe Level	Concrete Modulus of
	(mm)	(m)	(KN)	(KN)	(m)	(m)	(MN/ m^2)
P1	1300	44.0	23 393	32 089	-7.5	-51.5	30 000
P2	700	20.5	4 300	8 600	-11.7	-32.2	30 000
P3	1000	25.5	11 000	33 000	-7	-33	32 000

Table 4. 2 Instrumented piles load test details

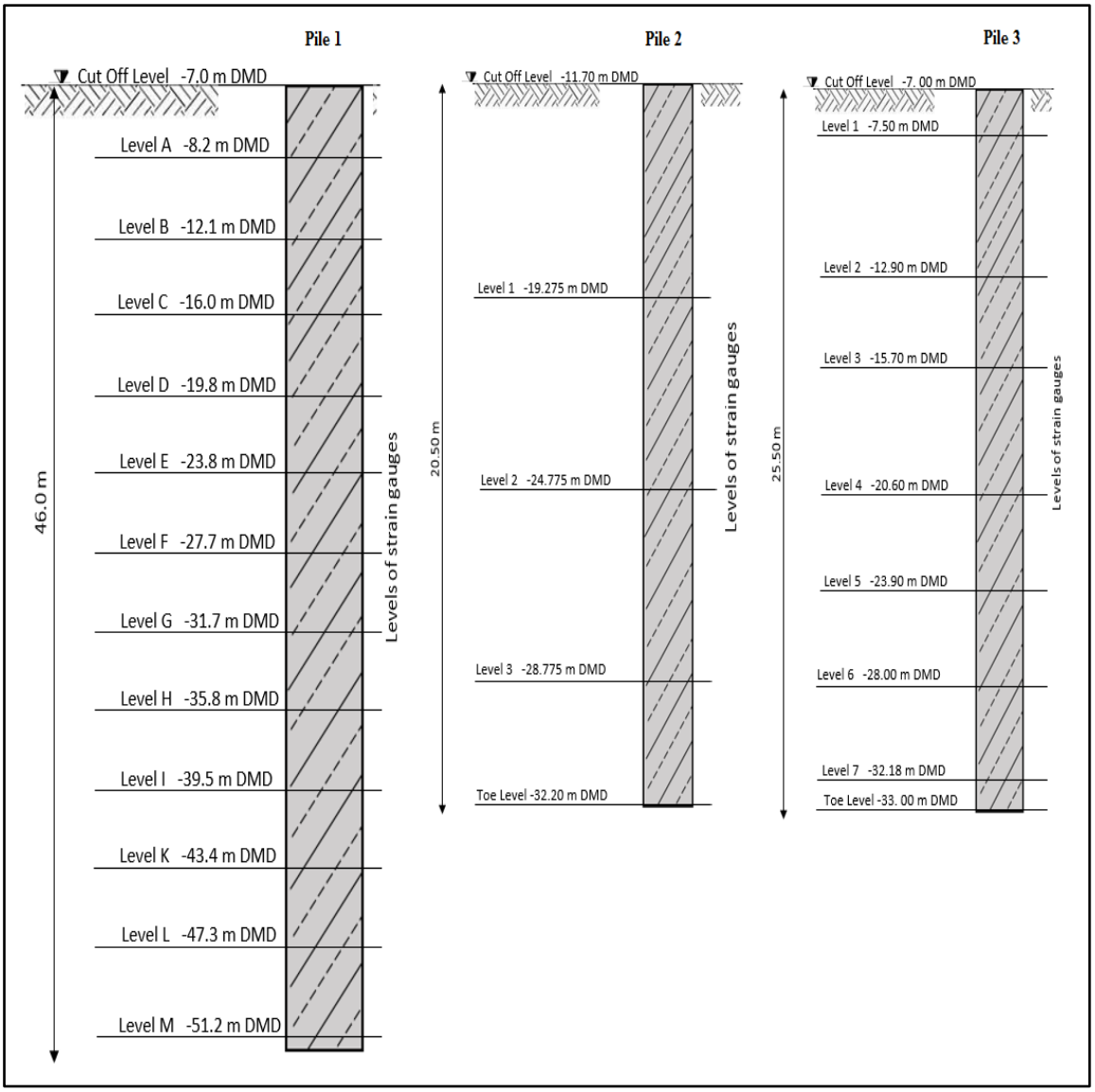

Fig. 4.16 Instrumental piles test

5 Analysis and FEM modelling of pile static load test

5.1 Introduction

5.1.1 Research methodology

In this research, a methodology is established to evaluate pile settlement by comparing the settlements' curve results obtained through conventional methods (empirical and analytical), numerical methods (finite element method, FEM models) and experimental methods (static load pile testing). The pile load settlement curves using different approaches is developed. A trial and error method is applied to evaluate more realistic values of soil modulus E_{mod} (modified modulus of elasticity) and back calculated from the FEM model. The revised or modified soil modulus E_{mod} is utilised in conventional method (analytical/empirical) and could be applied for piles and foundations design. Due to higher modulus of soil (E_{mod}) in the weak rock, the outcome of this approach indicates full utilisation of pile capacities leading to economical piles and foundation design.

Initially, in the conventional methods, the pile load settlement will be calculated using empirical and analytical methods. The approaches presented and explained by Braja Das, MJ Tomlinson & Bowles were used for the settlement calculation based on the soil parameters/properties from the soil laboratory testing. Generally, these outlined approaches can be referred to as approximate methods based on elastic theory. The modulus of elasticity (E_s) and the elastic shortening of pile concrete are the main parameters for the settlement analyses using these approaches. On the other hand, other methods stated by Wyllie and Vesic have been explained in the literature review but will not be used for the analysis in the study; this is due to the approach as mentioned by Das being established based on the semi empirical method recommended by Vesic in 1977. The approach mentioned by Tomlinson relies on the same principles adopted by Wyllie for the settlement analysis and, to avoid duplications of using similar approaches, for the analyses the pile load settlement. Thus, this research will use three conventional approaches as per Das, Tomlinson and Bowles.

Secondly, the pile load settlement will be calculated using numerical methods (finite element method, FEM models). A consistent and accurate analysis of the pile load settlement is conducted using the PLAIXS 2D based on the finite element method. In this method, the soil conditions and parameters obtained from the site investigation report in the first stage then, in the second stage, back calculation analysis for soil properties and specifically back calculation of Modulus of Elasticity (E_{mod}) to be obtained by the fitting the FEM settlement curve to pile settlement curve obtained from static load pile testing (experimental methods). By fitting the curve from actual test and FEM modelling an accurate value of modified Modulus of Elasticity (E_{mod}) can be reached.

Finally, for the experimental method, the pile load settlement curve is obtained from static load pile testing conducted at site for 116 piles. Type and procedures of tests was explained in detail in chapter 4. The test will be used in the back-calculation analysis of modified modulus of elasticity (E_{mod}) using FEM software (PLAXIS 2D) as explained previously.

In this research, a methodology is developed for recalculating the modified modulus of elasticity (E_{mod}) which will be used in piles and foundations design. As explained previously, this is done by using the pile static load test results to obtain E_{mod} through FEM model; as per Fig 5.1 showing the research methodology process flow.

5.1.2 Current practices

The current practice of calculating the piles settlements and capacities are based on standard methods using the procedures outlined in M J Tomlinson, Bowles & Braja Das. The pile static load tests are used more as a confirmation test to establish the pile load capacities considered in conventional methods (empirical and analytical). The use of factors of safety for shaft resistance and bearing resistance is a common feature in these methods and one generally followed in design offices. This approach to calculating the pile settlement and capacities relies on the soil properties obtained by laboratory testing of soil samples, as specified in the soil investigation reports. The numerous static load tests conducted and the settlement results observed clearly indicate that the piles have a larger load carrying capacity and low settlement. The drawback in the conventional methods (empirical and analytical) of using conservative modulus of elasticity (from soil investigation reports) and settlement values obtained thereof and use of factors of safety have resulted in decreasing the pile capacities. The Eurocode 7 provides guidelines for reducing the factors of safety if more preliminary static pile load tests (PTP) are conducted, as explained in chapter 2. However, this approach is still not popular in Dubai, UAE and it is required to carry out additional pile load tests as per Eurocode 7 for different pile diameters and lengths.

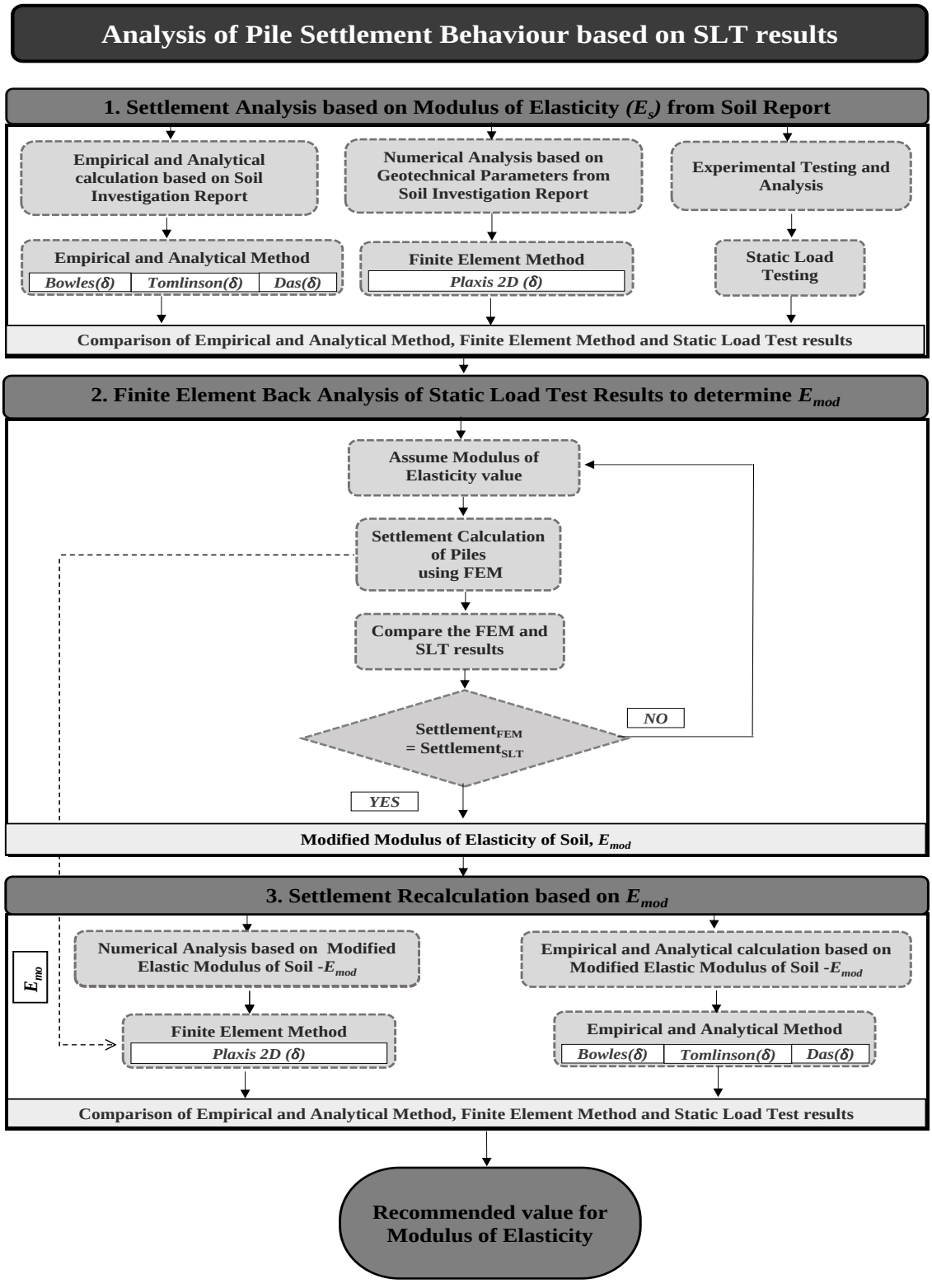

Note: Repeat the above analysis procedure for 116 piles

Fig. 5.1 Research methodology

5.2 Conventional methods settlement analysis using E_s from soil report

5.2.1 Introduction

In this section, the settlement behaviour of the piles P73 and P71 will be calculated based on the modulus of elasticity (E_s) values and other soil parameters from the soil report. Then the piles settlements results will be calculated using the conventional methods and finite elements methods (FEM) based on the soil report, prior to being compared with the static load test (SLT) in the following sections.

5.2.2 Soil and Pile Properties

The general soil profile for the project area has been divided into four layers. The design geotechnical parameters for this multi-layered soil system is provided in the soil investigation report (Table 5.1). However, those parameter values are used and required to calculate the pile settlement based on conventional methods (empirical and analytical equations) and numerical method (finite element method), the soil and geotechnical investigation report explained in detail for the entire Business Bay and Downtown project areas in Chapter 3, and for project 17 which include piles P71 and P73 (as per Chapter 6)**.**

Material Properties	**Unit**	**1st Layer**	**2nd Layer**	**3rd Layer**	**4th Layer**
	Level*	0 to -6 m	-6 to -29 m	-29 to -38 m	-38 to -60 m
Unit weight, γ	kN/m^3	18	20	20	20
Angle of friction, ϕ	(°)	33	45	45	45
Elastic Modulus, E	MN/m^2	15	50	100	60
Poisson's' ratio, μ	-	0.3	0.3	0.3	0.3
Cohesion, c	kN/m^2	-	46	100	62
Earth pressure at rest, K_o	(°)	0.46	0.29	0.29	0.29
Active earth pressure, K_a	(°)	0.29	0.17	0.17	0.17
Passive earth pressure, K_p	(°)	3.39	5.82	5.82	5.82

* Original ground level +3 to -1 DMD (Dubai Municipality Datum)

Table 5.1 Soil parameters provided in the soil investigation report

For empirical and analytical calculation, the soil profile is generalised as a single layer with weighted average of soil properties. The weighted average of soil parameters will be derived with respect to the thickness of each rock layer for the estimation of pile settlement. However, in order to avoid errors and interruptions during analysis, a slightly increased value was considered for Modulus of Elasticity of the weak rock (Es) as 70000 kN/m2 (70 Mpa). The top most layer of silty sand has not been considered in the pile design, due to the pile cut off level being at -7.00 DMD.

The analysis of pile settlement using the conventional methods (empirical and analytical equations) mentioned by all the three aforementioned authors and numerical methods (FEM, PLAXS 2D) requires information of certain soil materials parameters and pile materials properties. These geotechnical parameters/properties and the pile properties required for calculation are shown in Table 5.1 and Table 5.2 respectively.

Parameters	**Material Properties**	
Pile number	P 73	P 71
Cut off level (DMD)	-7	-7
Toe Level (DMD)	-47	-30
Working Load, WL (kN)	21393	7700
Test Load, TL (kN)	32089.5	11550
Length of Pile, L (m)	40	23
Concrete Grade, f_{cu} (N/mm^2)	70	70
Modulus of Elasticity of Pile, E_c (Mpa, Design)	31782	31782
Modulus of Elasticity of Pile, E_c (Mpa, Test)	33142.8	32316.2
Diameter of Pile, D (m)	1.3	0.8
Area of Pile, Ap (m^2) = π. D^2/4	1.328	0.503
Perimeter of Piles, p (m) = π. D	4.080	2.510
Poisson's Ratio ν	0.2	0.2

Table 5.2 Piles material properties

5.2.3 Calculation approaches of pile settlement using E_s from soil report

Approach 1: Calculation based on Das approach

As per the approach mentioned by Das, the total pile settlement caused due to a vertical axial load is divided in to three components; those components can be calculated as per the following equations, based on Das approach as explained in detail in Chapter 2:

(1) Elastic settlement of pile, $S_{e\,(1)}$

$$S_{e\,(1)} = \frac{(Q_{wb} + \xi . Q_{ws}).L}{A_p . E_p} \qquad \text{(Eq. 5.1)}$$

(2) Settlement caused by the load at the pile tip, Se (2)

$$S_{e\,(2)} = \frac{q_{wp} . D}{E_s} . (1 - v^2) . I_{wp} \qquad \text{(Eq. 5.2)}$$

(3) Settlement caused by the load transmitted along the pile shaft, $S_{e\,(3)}$

$$S_{e\,(3)} = \left(\frac{Q_{ws}}{p.L}\right) . \frac{D}{E_s} (1 - v^2) . I_{ws} \qquad \text{(Eq. 5.3)}$$

Total settlement = $s_e = s_{e(1)} + s_{e(2)} + s_{e(3)}$ (Eq. 5.4)

The calculation result for P73 using the soil report design parameters and the settlements results can be found below in Table 5.3 and Fig 5.2:

Load %	**Unit**	**0%**	**5%**	**10%**	**15%**	**20%**	**25%**	**50%**	**75%**	**100%**	**125%**	**150%**
Pile Load	kN	0	1069.65	2139.3	3208.95	4278.6	5348.25	10696.5	16044.75	21393	26741.25	32089.5
Shaft Load (Q_{ws})	kN	0	1069.65	2139.3	3208.95	4278.6	5348.25	10696.5	16044.75	21393	21393	21393
Tip Load (Q_{wb})	kN	0	0	0	0	0	0	0	0	0	5348.25	10696.5
$S_{e\,(1)}$	mm	0	0.51	1.01	1.521	2.03	2.54	5.07	7.61	10.14	15.21	20.29
$S_{e\,(2)}$	mm	0	0.00	0.00	0.00	0.00	0.00	0.00	0.00	0.00	57.88	115.76
$S_{e\,(3)}$	mm	0	0.44	0.87	1.31	1.75	2.18	4.36	6.55	8.73	8.73	8.73
S_e	mm	0	0.94	1.89	2.83	3.77	4.72	9.43	14.15	18.87	81.82	144.78

Table 5.3 Pile settlement calculation for P73 – Das

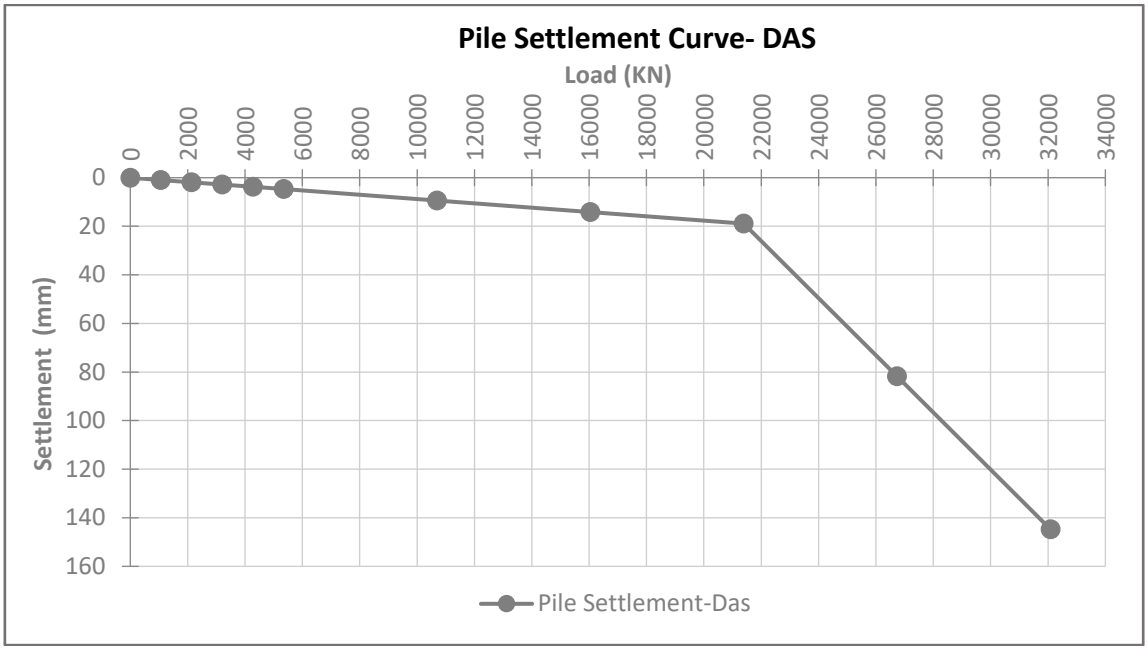

Fig. 5.2 Pile settlement curve P73 - Das approach

The same calculation for P71 is applied using the soil report design parameters the settlements results are as per Table 5.4 and Figure 5.3:

Load %	**Unit**	**0%**	**5%**	**10%**	**15%**	**20%**	**25%**	**50%**	**75%**	**100%**	**125%**	**150%**
Pile Load	kN	0	385	770	1155	1540	1925	3850	5775	7700	9625	11550
Shaft Load (Q_{ws})	kN	0	385	770	1155	1540	1925	3850	5775	7700	7700	7700
Tip Load (Qwb)	kN	0	0	0	0	0	0	0	0	0	1925	3850
$\mathbf{S_{e\,(1)}}$	mm	0	0.3	0.6	0.8	1.1	1.4	2.8	4.2	5.5	8.3	11.1
$\mathbf{S_{e\,(2)}}$	mm	0	0	0	0	0	0	0	0	0	33.9	67.7
$\mathbf{S_{e\,(3)}}$	mm	0	0.3	0.5	0.8	1.1	1.3	2.7	4.0	5.4	5.4	5.4
$\mathbf{S_e}$	mm	0	0.5	1.1	1.6	2.2	2.7	5.5	8.2	10.9	47.5	84.2

Table 5.4 Pile settlement calculation for P71 – Das

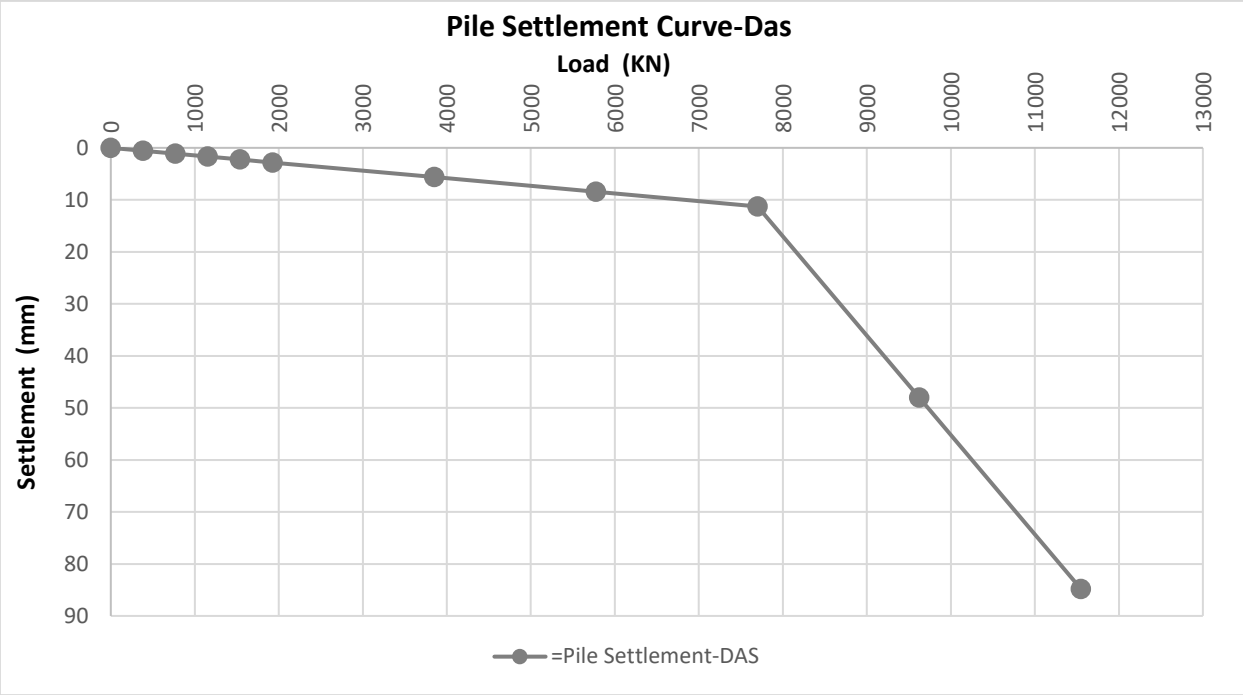

Fig. 5.3 Pile settlement curve P71- Das approach

Approach 2: Calculation based on Tomlinson approach

As per the method mentioned by Tomlinson (explained in detail in Chapter 2), the total settlement of the pile due to the elastic shortening of the pile material, and the soil displacements at the pile tip and the pile shaft due to the load transferred along the pile, can be calculated using the following equation:

$$s_t = s_e + s_b + s_f \qquad \text{(Eq. 5.5)}$$

where

s_e= Axial compression of the material of the pile.
s_b = Deformation of the soil beneath the pile base due to the load acting at the pile tip
s_f = Settlement of the soil due to the load transfer along the pile shaft

$$s_e = \frac{(2Q_b + Q_s).L}{2E_p.A_p} \qquad \text{(Eq. 5.6)}$$

$$s_b = \frac{\pi}{4}.\frac{Q_b}{A_b}.\frac{D(1-\mu^2)}{E_b}.I_b \qquad \text{(Eq. 5.7)}$$

$$s_f = \frac{Q_s.I_s}{D.E_s} \qquad \text{(Eq. 5.8)}$$

The calculation result for P73 using the soil report design parameters are as per Table 5.5 and Fig 5.4:

Load %	Unit	0%	5%	10%	15%	20%	25%	50%	75%	100%	125%	150%
Pile Load	kN	0	1070	2139	3209	4279	5348	10697	16045	21393	26741.3	32089.5
Shaft Load (Q_{ws})	kN	0	1070	2139	3209	4279	5348	10697	16045	21393	21393	21393
Tip Load (Q_{wb})	kN	0	0	0	0	0	0	0	0	0	5348.25	10696.5
S_e	mm	0	0.5	1.0	1.5	2.0	2.5	5.1	7.6	10.1	15.2	20.3
S_f	mm	0	1.4	2.8	4.2	5.6	7.1	14.1	21.2	28.2	28.2	28.2
S_b	mm	0	0	0	0	0	0	0	0	0	26.7	53.5
S_t	mm	0	1.9	3.8	5.8	7.7	9.6	19.2	28.8	38.4	70.2	102.0

Table 5.5 Pile settlement calculation for P73 – Tomlinson

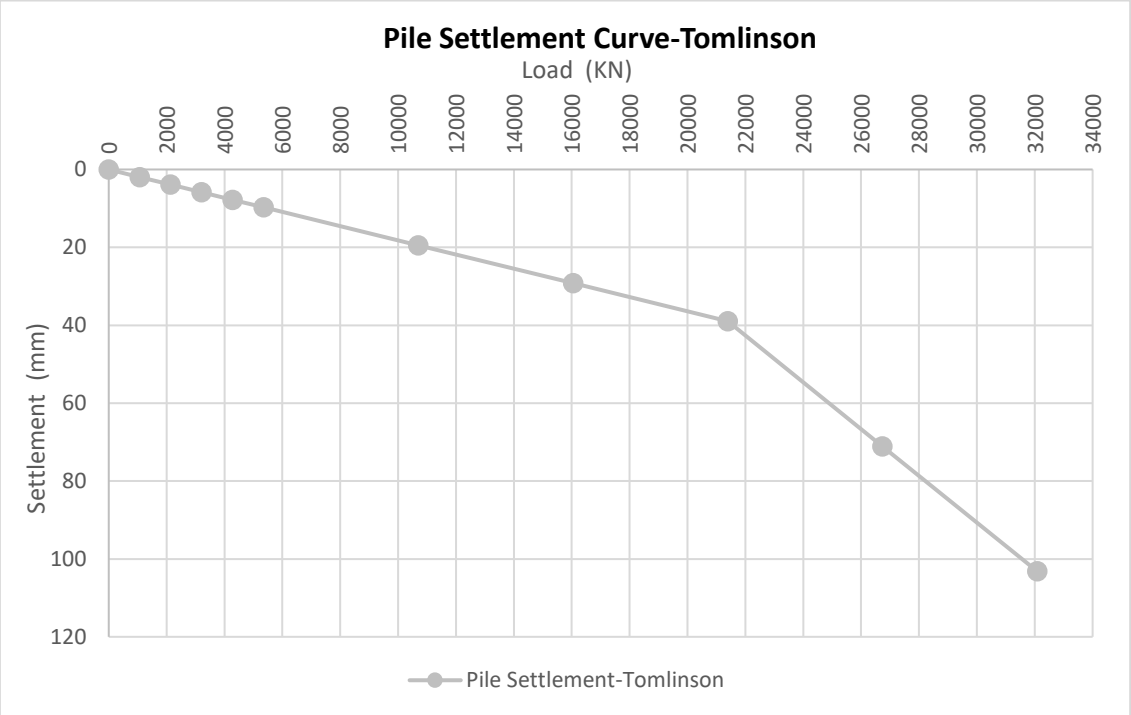

Fig. 5.4 Pile settlement curve P73- Tomlinson approach

The calculation result for P71 using the soil report design parameters for the settlements results are as per Table 5.6 and Fig 5.5:

Load %	Unit	0	5%	10%	15%	20%	25%	50%	75%	100%	125%	150%
Pile Load	kN	0	385	770	1155	1540	1925	3850	5775	7700	9625	11550
Shaft Load (Q_{ws})	kN	0	385	770	1155	1540	1925	3850	5775	7700	7700	7700
Tip Load (Q_{wb})	kN	0	0	0	0	0	0	0	0	0	1925	3850
S_e	mm	0	0.3	0.6	0.8	1.1	1.4	2.8	4.2	5.5	8.3	11.1
S_f	mm	0	0.8	1.7	2.5	3.3	4.1	8.3	12.4	16.5	16.5	16.5
S_b	mm	0	0	0	0	0	0	0	0	0	15.6	31.3
S_t	mm	0	1.1	2.2	3.3	4.4	5.5	11.0	16.5	22.0	40.5	58.9

Table 5.6 Pile settlement calculation for P71 – Tomlinson

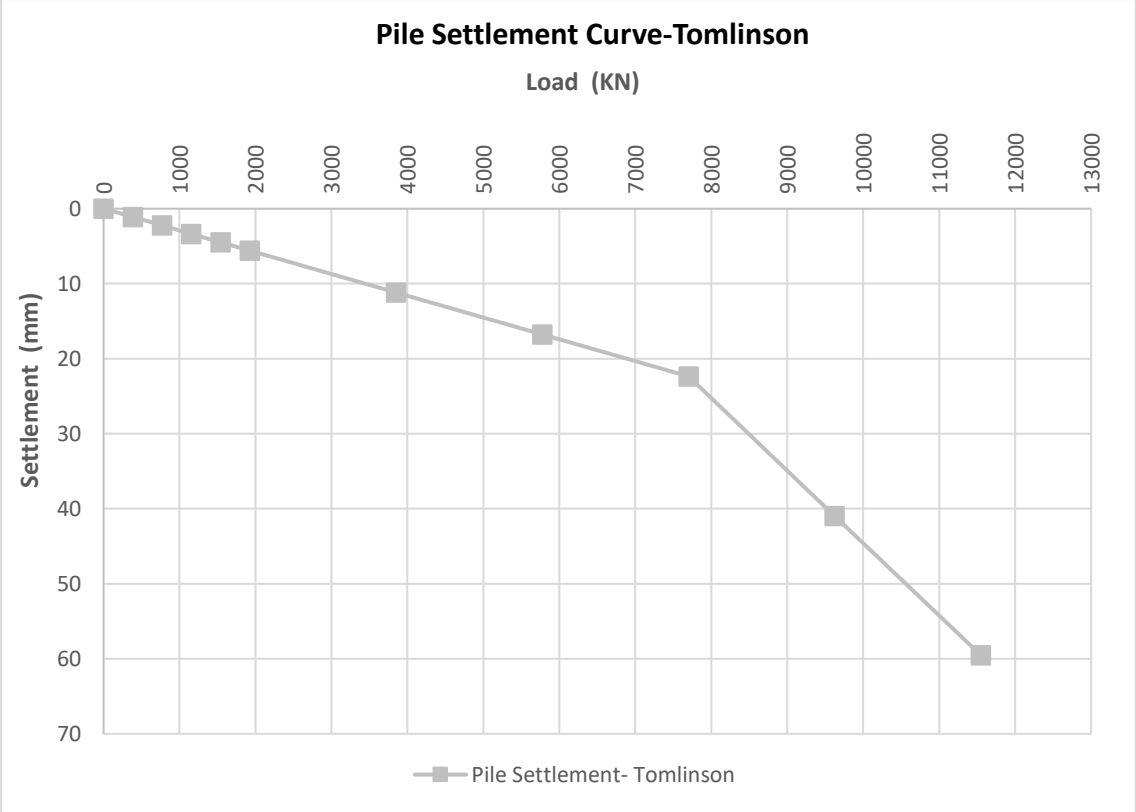

Fig. 5.5 Pile settlement curve P71- Tomlinson approach

Approach 3: Calculation Based on Bowles Approach

Based on the method mentioned by Bowles, the total pile settlement (H_p) can be calculated as per the following:

$$H_p = \Delta H_a + \Delta H_{pt} \quad \text{(Eq. 5.9)}$$

where

ΔH_a = Elastic axial compression of pile.
ΔH_{pt}= Point pile settlement.

The elastic settlement of pile can be computed as the sum of settlements (ΔH_a) due to the average axial force acting on each pile segment of length (ΔL) with an average cross-sectional area, A_p, and modulus of elasticity, E_p.

$$\Delta H_{s,s} = \frac{P.\Delta L}{A_p . E_p} \quad \text{(Eq. 5.10)}$$

$$\Delta H_a = \sum \frac{P.\Delta L}{A_p . E_p} \quad \text{(Eq. 5.11)}$$

The elastic plastic point settlement under the pile tip can be computed using the equation given below.

$$\Delta H_{pt} = \Delta q . D . \frac{1-\mu^2}{E_s} . m . I_s . I_F . F_I \quad \text{(Eq. 5.12)}$$

The values of reduction factor F1 depends on the load transfer mechanism of the pile. During the initial stages of pile loading, the load will be primarily carried in skin friction; hence factor F1 is considered as 0.25. However, with higher stages of loading, the base resistance will be developed and factor F1 will be taken as 0.5.

For P71 and P73, the piles are designed as friction piles for the working load conditions. Hence, the value of F_1 will be considered as 0.25 up to 100 per cent of working load; beyond this load limit, the base resistance is assumed to be mobilised and the factor F_1 will be taken as 0.5.

The calculation result for P73 using the soil report design parameters and the settlements results are as per Table 5.7 and Fig 5.6:

Load%	Unit	0%	5%	10%	15%	20%	25%
Pile Load	kN	0	1070	2139	3209	4279	5348
Shaft Load (Δq)	kN	0	806.3	1612.6	2418.8	3225.1	4031.4
ΔH_a	mm	0	1.0	2.0	3.0	4.1	5.1
ΔH_{pt}	mm	0	1.7	3.4	5.1	6.8	8.5
ΔH_p	mm	0	2.7	5.4	8.2	10.9	13.6

Load%	Unit	50%	75%	100%	125%	150%
Pile Load	kN	10697	16045	21393	26741.3	32089.5
Shaft Load (Δq)	kN	8062.8	12094.2	16125.6	20157.0	24188.4
ΔH_a	mm	10.1	15.2	20.3	25.4	30.4
ΔH_{pt}	mm	17.0	25.5	34.1	85.2	102.2
ΔH_p	mm	27.2	40.8	54.4	110.5	132.6

Table 5.7 Pile settlement calculation for P73 – Bowels

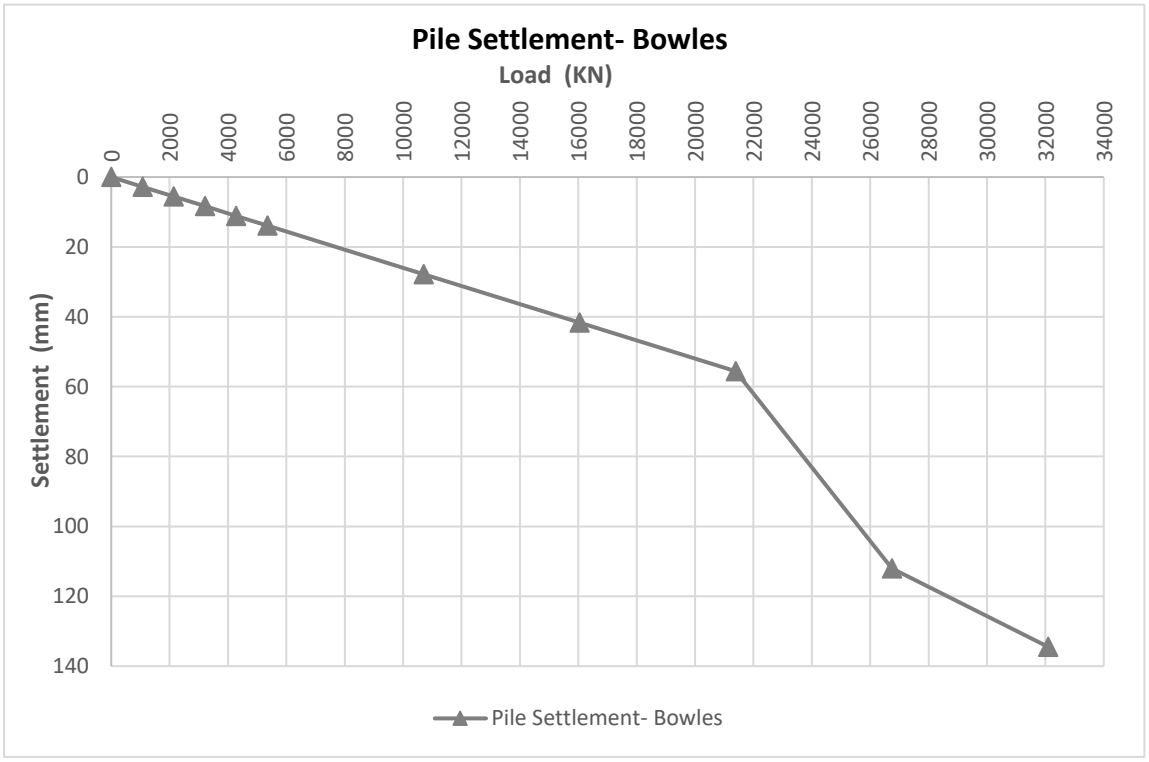

Fig. 5.6 Pile settlement curve P73- Bowles approach

The calculation result for P71 using the soil report design parameters and the settlements results are as per Table 5.8 and Fig 5.7:

Load %	Unit	0	5%	10%	15%	20%	25%	50%	75%	100%	125%	150%
Pile Load	kN	0	385	770	1155	1540	1925	3850	5775	7700	9625	11550
Shaft Load	kN	0	766.3	1532.6	2299.0	3065.3	3831.6	7663.2	11494.8	15326.4	19158.0	22989.6
ΔH_a	mm	0	0.6	1.1	1.7	2.2	2.8	5.5	8.3	11.1	13.9	16.6
ΔH_{pt}	mm	0	1.0	2.0	3.0	4.0	5.0	10.0	14.9	19.9	49.8	59.8
ΔH_p	mm	0	1.6	3.1	4.7	6.2	7.8	15.5	23.3	31.0	63.7	76.4

Table 5.8 Pile settlement calculation for P71 – Bowels

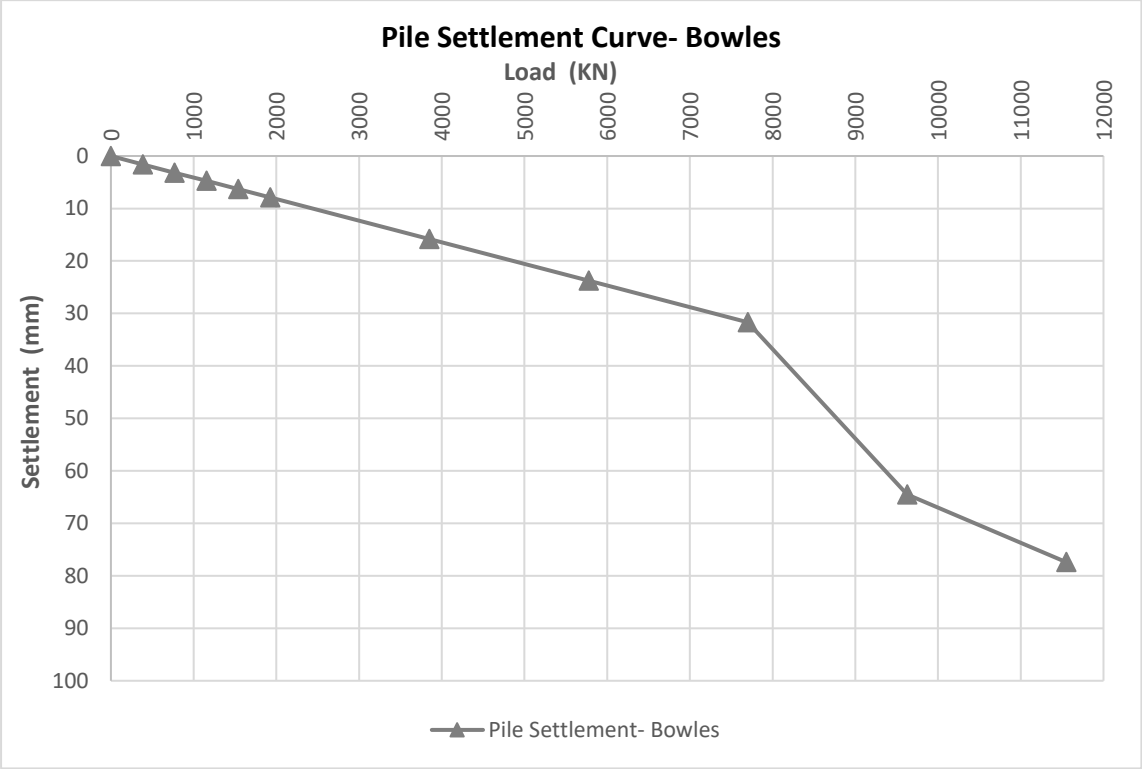

Fig. 5.7 Pile settlement curve P71- Bowles approach

5.2.4 Comparison between Conventional Methods using E_s from Soil Report

As described, all the piles were designed as friction piles and the end bearing was negligible. In our analysis, the end bearing base resistance was only assumed to be developed for loading conditions of more than 100 per cent of the working load values. In working load conditions of up to 100 per cent, only the shaft resistance and elastic shortening are developed. During this stage, the settlement of the pile is mainly due to the elastic shortening of pile material and the displacement of the soil around the pile shaft due to the load transferred through the shaft. However, after 100 per cent of the working load the settlement component due to the load transferred along the pile shaft remains constant and the mobilisation of base resistance will start. During this stage, even with minor load increases on loading values high settlement behaviour is shown by the piles (see Fig. 5.8 & Fig. 5.9). This further increases in the pile settlement after working loading (after 100 per cent) is caused due to the soil displacement at the pile base. This is due to the load being transferred along the pile tip and the elastic shortening component of the pile, which increased slightly. The settlement component due to the pile shaft remains constants during this stage, as explained previously.

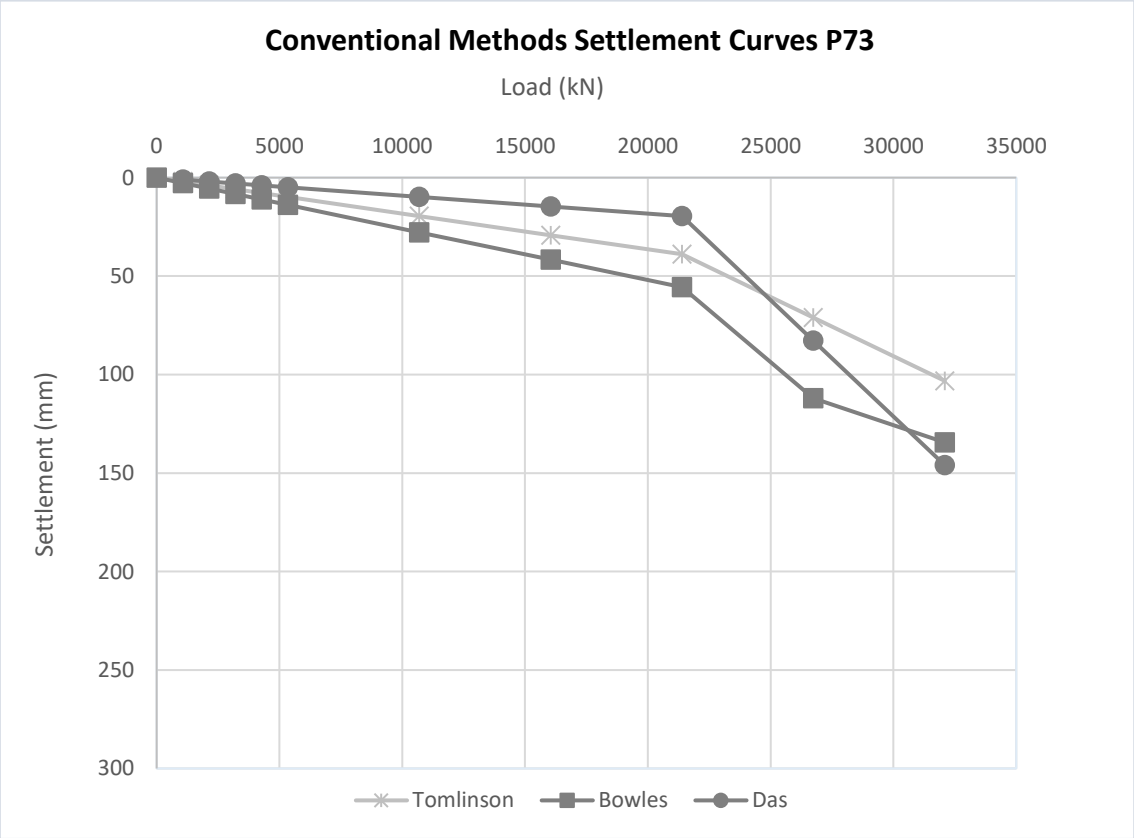

Fig. 5.8 Comparison between conventional methods settlements curves P73 based on E_s

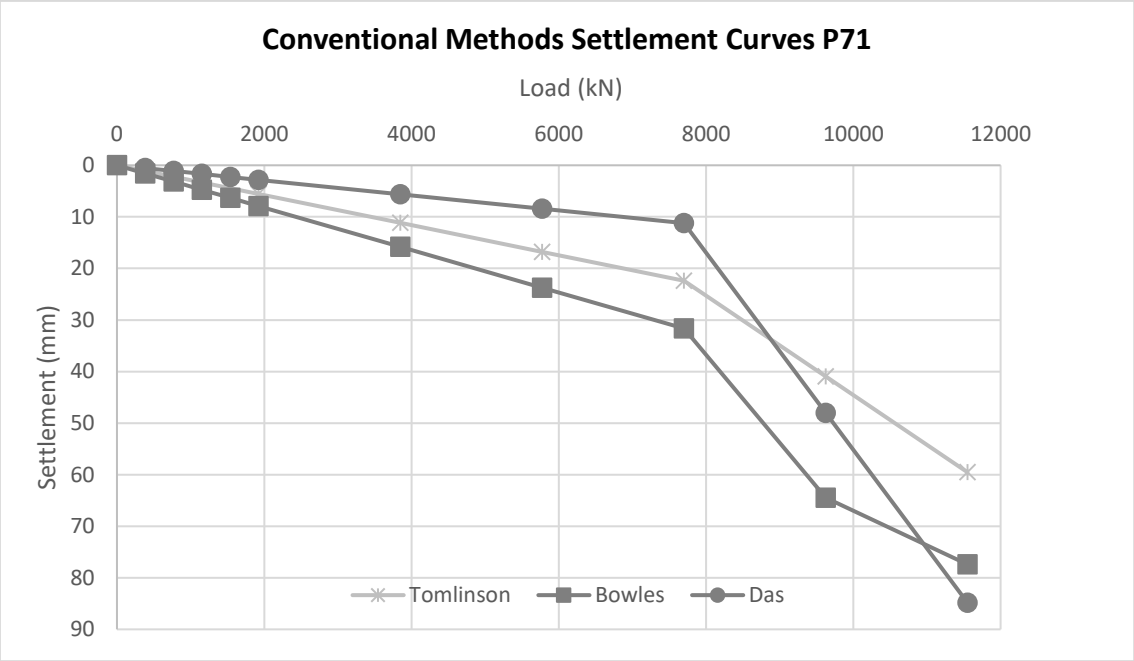

Fig. 5.9 Comparison between conventional methods settlements curves P71 based on E_s

The table below summarises the calculated settlement values of piles P 73 to P 71 for 100 per cent and 150 per cent of the working load conditions using the Bowles, Das and Tomlinson approaches. As seen in the above table, at 100 per cent of working load condition, the settlement values predicted by the Das approach is the lowest and the Bowles approach is the highest. On the other hand, at 150 per cent of working load when the base settlement take place, the settlement values predicted by Das method is the highest and the Tomlinson method is the lowest. Hence, it is evident that the base settlement component predicted by the Das method is the highest among all three of the applied methods.

Approach	**Load (%)**	**Settlement(mm)**	
		P73	**P71**
Bowles	100	55.4	31
Tomlinson		38.4	22
Das		**18.9**	**10.9**
Bowles	150	132.6	76.4
Tomlinson		**102**	**58.9**
Das		144.8	84.2

Table 5.9 Settlement values from empirical and analytical calculation based on E_s

5.3 FEM modelling of load test based on E_s from soil report Piles

5.3.1 Introduction to PLAXIS 2D

PLAXIS is a finite element package intended for the two-dimensional or three-dimensional analysis of deformation, stability and groundwater flow in geotechnical engineering. Geotechnical applications require advanced constitutive models for the simulation of the non-linear, time-dependent and anisotropic behaviour of soils and/or rock. In addition, since soil is a multi-phase material, special procedures are required to deal with hydrostatic and non-hydrostatic pore pressures in the soil. Although the modelling of the soil itself is an important issue, many geotechnical projects involve the modelling of structures and the interaction between the structures and the soil. PLAXIS is equipped with features to deal with various aspects of complex geotechnical structures.

In this research, PLAXIS 2D has been used for the modelling of static pile load tests. This modelling utilises the soil investigation report and in-situ pile load test results conducted. Conventional ways of pile analysis and design follows standard code procedures, which are followed universally. Several limitations in manual calculations that do not picture the behaviour of soil is accurately studied in the PLAXIS analysis. A detailed step-by-step modelling procedure is elaborated on in the following section, which outlines the soil profile and parameters considered along with the detailed analysis carried out to represent the actual site conditions.

5.3.2 Modelling procedure in PLAXIS 2D

PLAXIS 2D is used to carry out two-dimensional finite element analysis. The finite element model is defined by selecting the corresponding option in the Model drop specified in the software. Data input is entered relevant to the soil profile, soil properties, geometry of piles, discretisation of soil layers, pile loads and calculation methodology.

Step 1: Formation of soil and pile geometry using axisymmetric model

A plane strain model is utilised for geometries with uniform cross-section, corresponding stress state and loading scheme for a particular length perpendicular to the cross section (z-direction).
An axisymmetric model is used for circular structures with a (more or less) uniform radial cross section and loading scheme around the central axis, where the deformation and stress state are assumed to be identical in any radial direction. In this research, the axis-symmetric model is generated. A soil profile geometry of 55 m width x 54 m depth

is generated using rectangular coordinates. The soil stratigraphy is accurately assigned in the geometry as per the soil investigation report. The layers of the soil are assumed to be represented in horizontal layers that are uniform throughout the soil volume considered in the research. In a plane strain analysis, the displacements and strains in z-direction are assumed to be zero. However, normal stresses in z-direction are considered in the analysis.

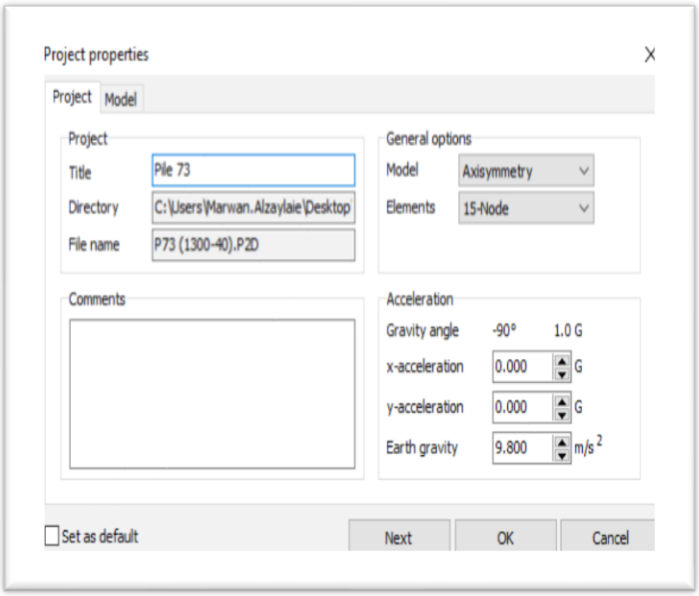

Fig. 5.10 Axisymmetric model 15 noded

A 15-node triangular element to model soil layers and other volume clusters are as shown in Figure 5.11 below.

nodes stress points a. 15-node triangle

Fig. 5.11 Position of nodes and stress points in soil elements

It provides a fourth order interpolation for displacements and the numerical integration involves twelve Gauss points (stress points). The type of element for structural elements and interfaces is automatically taken to be compatible with the soil element type selected. The 15-node triangle is a very accurate element that has produced high quality stress results for difficult problems, for example in collapse calculations for incompressible soils (Nagtegaal, Parks & Rice,1974, Sloan,1981 and Sloan & Randolph,1982). The 15-node triangle is particularly recommended for use in axis-symmetric analysis.

Step 2: Input and assign the soil layers' properties and constitutive soil model

Soil properties are input into PLAXIS using the soil mode view. The characteristics of the soil layers is entered in boreholes. Boreholes are locations in the draw area at which the information on the position of soil layers. Ground water table is input in the soil layers. The creation of material data sets and their assignment to soil layers are described in the following section.

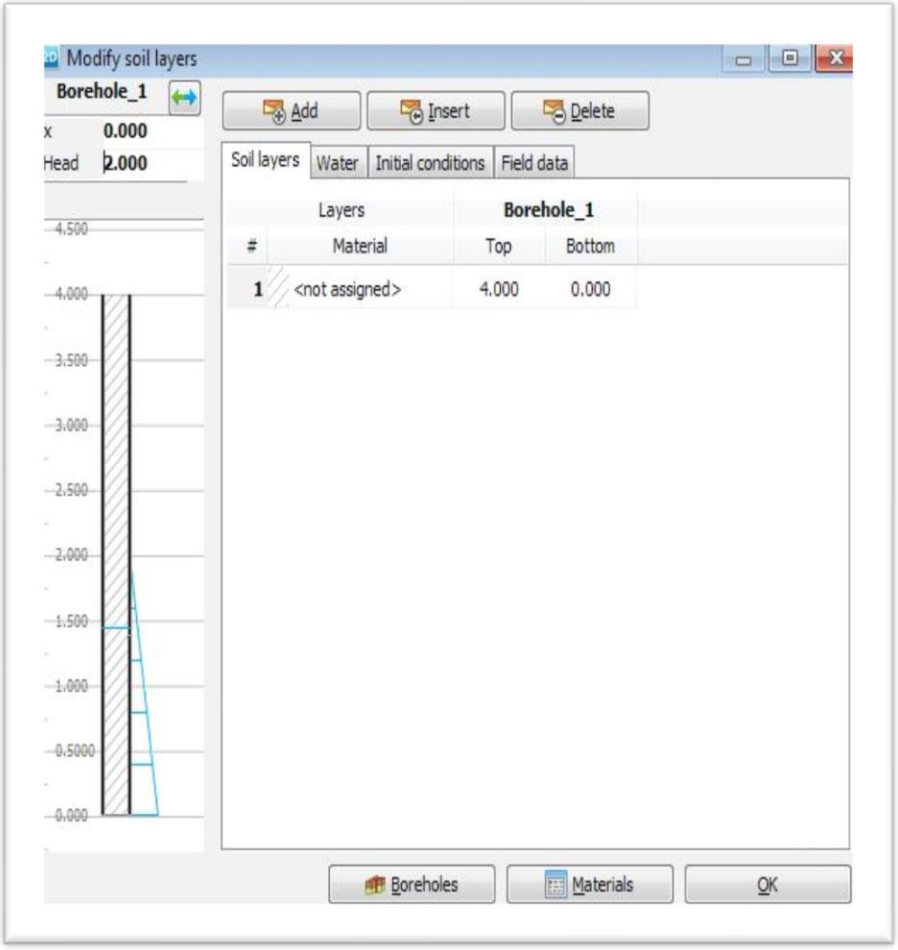

Fig. 5.12 Elevations of soil layers

In order to simulate the behaviour of the soil, a suitable soil model with appropriate material parameters are assigned to the geometry. In PLAXIS 2D, soil properties are collected in material data sets and the various data sets are stored in a material database. From the database, a data set is assigned to one or more soil layers. Different material data sets are inputted for different soil layers and assigned to soil profiles generated. PLAXIS 2D distinguishes between material data sets for soil and interfaces. In this research, for the study conducted a Mohr-Coulomb soil model is assumed. The layers of soil are considered to be fully drained as per the soil report. The material data is as shown in Fig 5.13 below. The proper values of soil are input in the general properties box according to the material properties listed in the Table below.

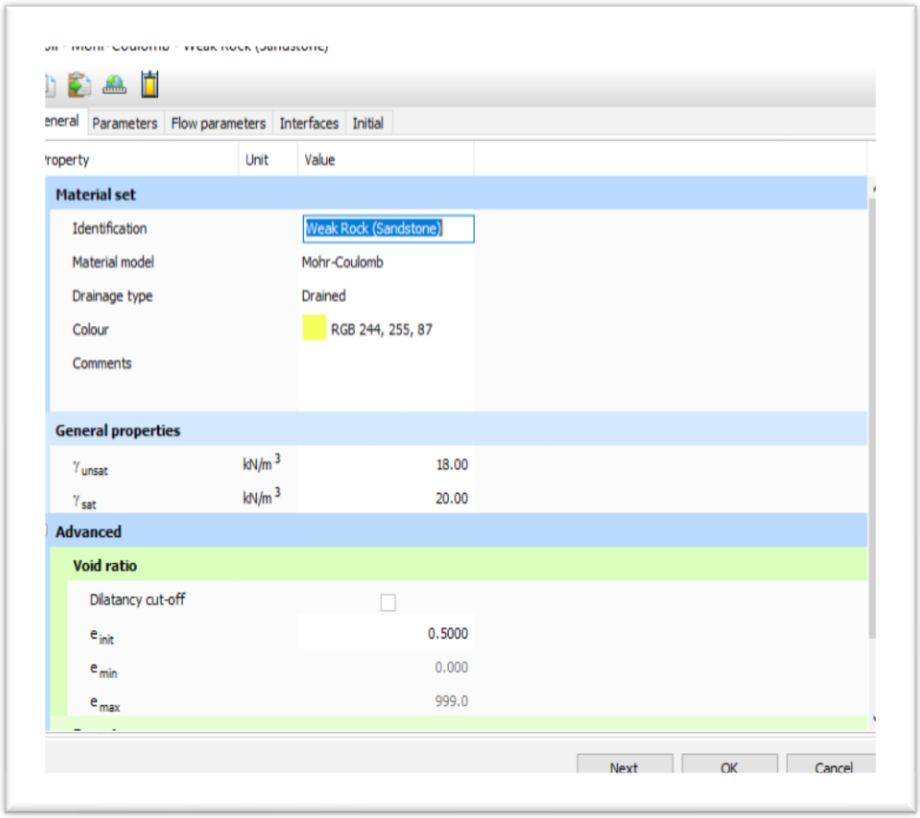

Fig. 5.13 Mohr-Coulomb soil model

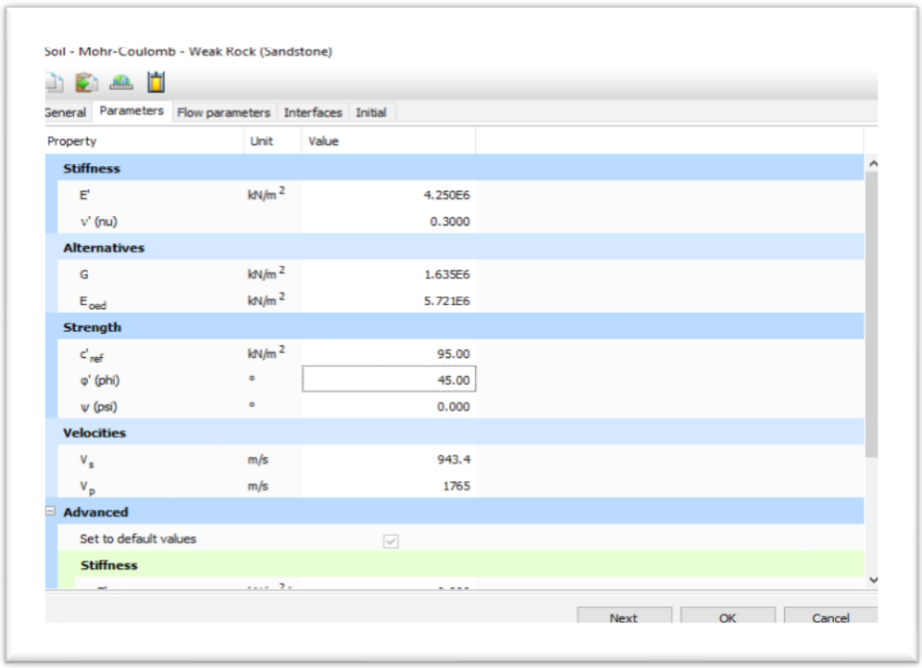

Fig. 5.14 Soil properties

A detailed description of each soil profile and their corresponding parameters are used to define the soil accurately. The table below shows the soil parameters used in this study. The created data set appears in the material sets, as follows:

Material Properties	Unit	Weak Rock Layer			Pile
		1st Layer	2nd Layer	3rd Layer	
		6 - 29 m	29 - 38 m	38-60 m	
Unit weight, γ	kN/m^3	20	20	20	25
Saturated Unit Weight γ_{sat}	kN/m^3	21	21	21	
Angle of Friction, ϕ	(^{o})	45	45	45	-
Elastic Modulus, E	MN/m^2	50	100	60	31781.9
Poisson's' ratio, μ	-	0.3	0.3	0.3	0.3
Cohesion, c	kN/m^2	46	100	62	-

Table 5.10 Material Properties

Step 3: Input and assign the pile element material properties

The structural elements are created in the 'structures mode' of the program where a uniform indentation will be created to model a very stiff structural element. In this research, the input for pile geometry is as carried out in PLAXIS modelling as follows.

The pile is defined as a column of half width of the pile diameter. Interface elements are placed along the pile to model the interaction between pile and the adjoining soil. Generally, PLAXIS recommends that the interface is extended about half a meter into the sandy layer. The interface is defined only on the side of the soil. This is necessary to include the proper damping effect of the soil.

The pile is made of concrete, hence modelling using a linear elastic model considering non-porous behaviour is selected in the structural elements tab in PLAXIS. The generated soil profile, pile element and the soil interface are shown in the figure below.

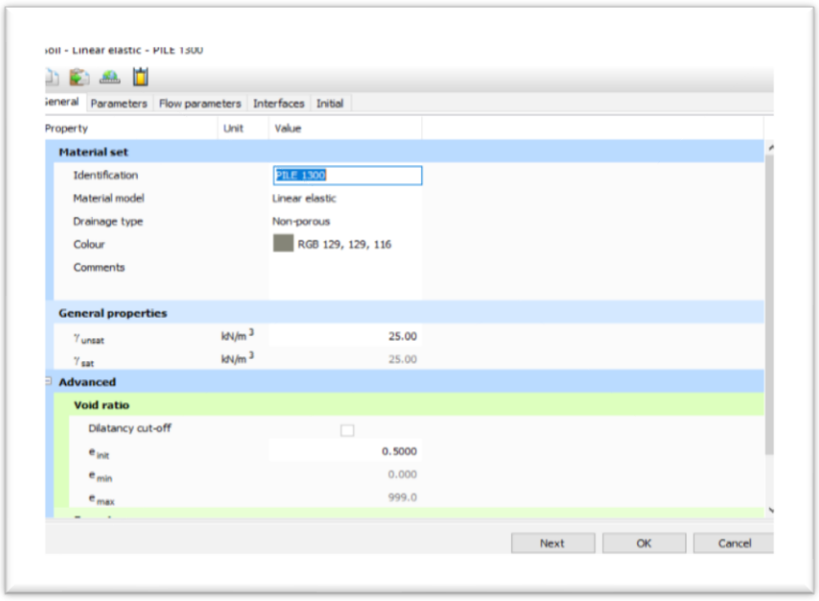

Fig. 5.15 Pile element material properties

Step 4: Assign soil-pile interface and boundary condition

Boundary conditions for the soil profile in an axisymmetric model are assigned using a standard fixity option. The boundary conditions of the soil profile at the edges are formed in such a way that only vertical displacements are permitted. The bottom of the soil profile is restrained from movement. The figure below shows the boundary condition which are assigned to the soil profile.

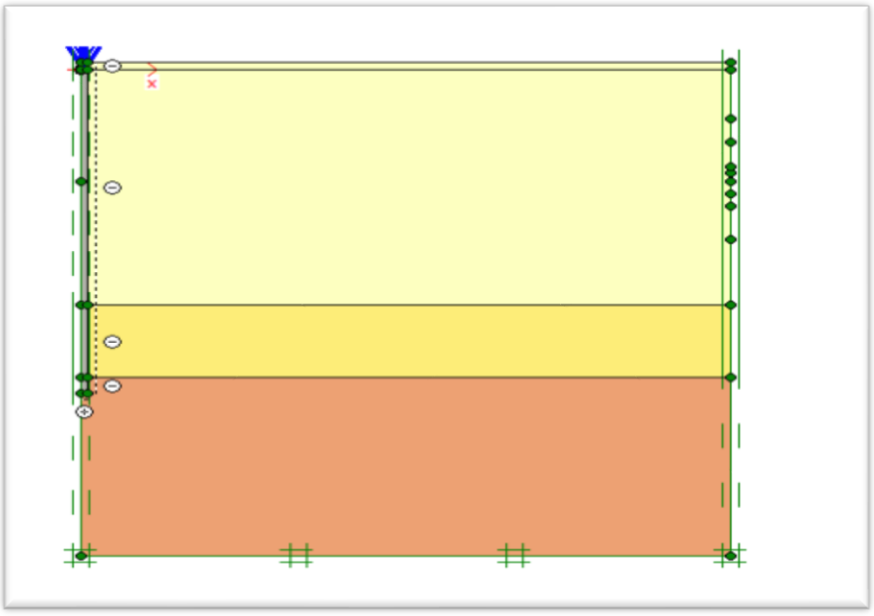

Fig. 5.16 Interface and boundary conditions

Step 5: Pile distributed load assignment

Loads can be assigned to existing geometric entities by right-clicking on the entity and selecting the corresponding option in the appearing menu. A geometric entity can be created and a load can be assigned to it simultaneously using the menu options. Although the input values of loads are specified in the structures mode, PLAXIS facilitates in the activation, deactivation or change of loads based on the staged construction.

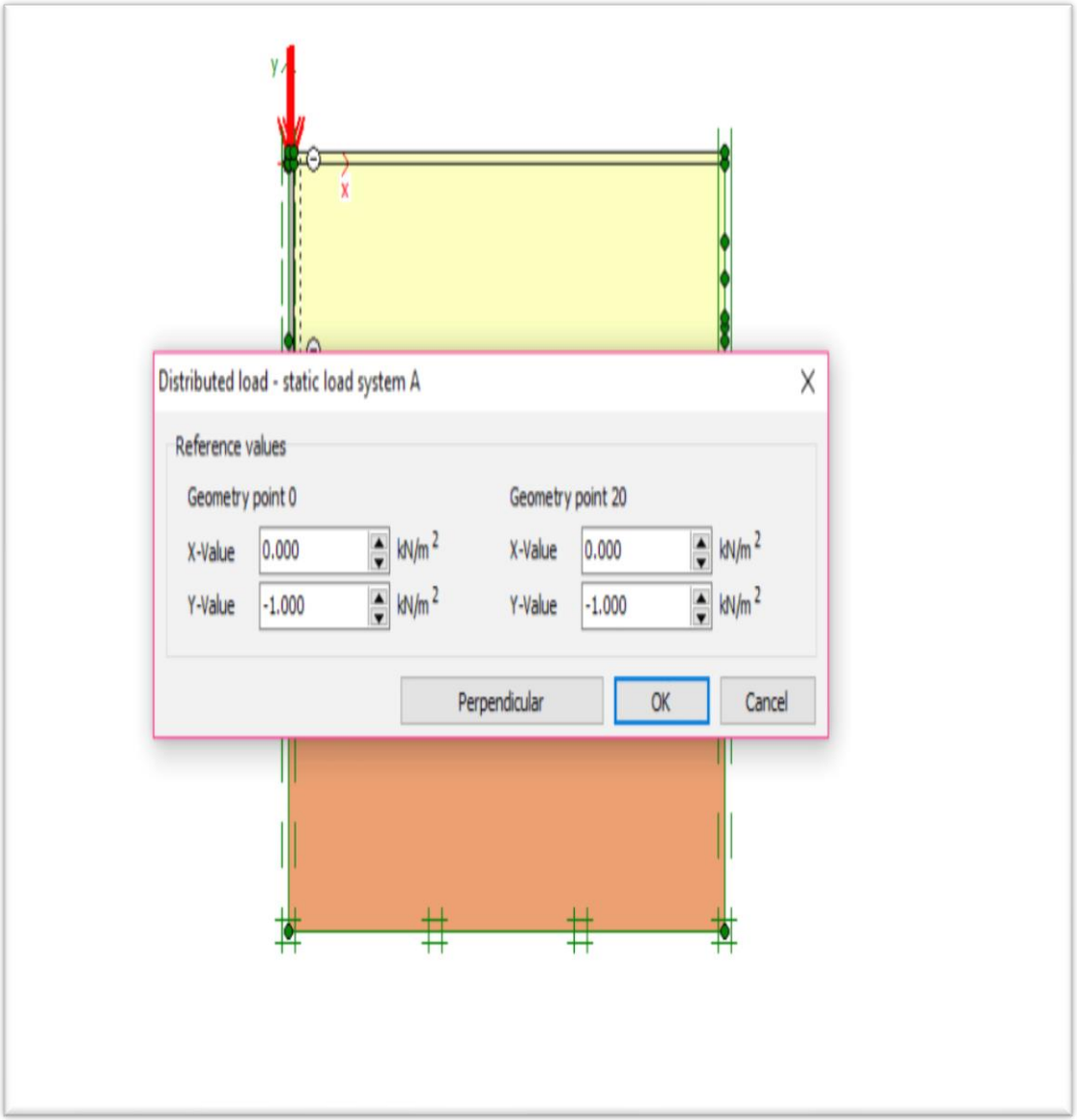

Fig. 5.17 Pile distributed load

Step 6: Mesh generation

When the geometry model is complete, the finite element mesh is generated. PLAXIS 2D allows for a fully automatic mesh generation in which the geometry is sub-divided into elements of the basic element type and compatible structural elements, as applicable. The mesh generation considers the position of points and lines in the model, so that the exact position of layers, loads and structures is accounted for in the finite element mesh. The generation process is based on a triangulation principle that searches for optimised triangles. In addition, to the mesh generation itself, a transformation of input data (properties, boundary conditions, material sets, etc.) from the geometry model (points, lines and clusters) to the finite element mesh (elements, nodes and stress points) is made. Mesh generation in PLAXIS can be selected in line with which suits the particular soil model and structural elements most efficiently. The elements in this research are meshed using the 'very fine' mesh option. The generated mesh appears in PLAXIS modelling as shown in the figure below.

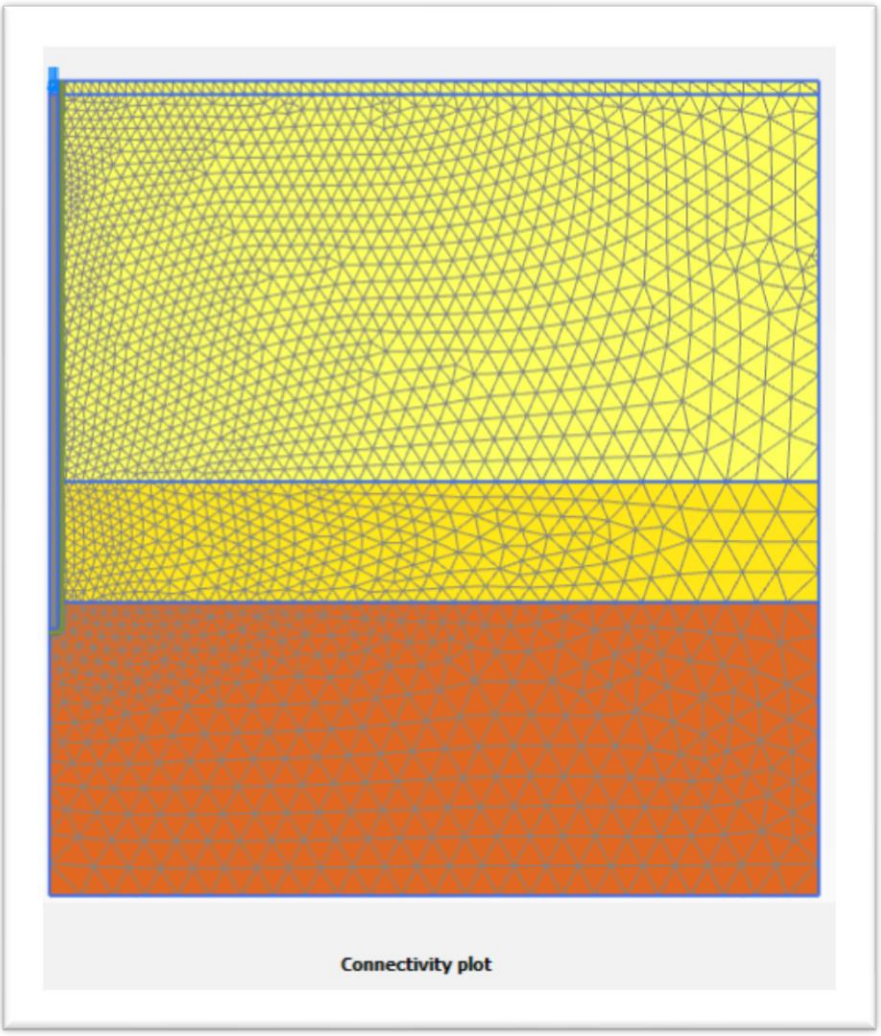

Fig. 5.18 Mesh generation

Step 7: Calculation type and analysis for construction phases

A plastic calculation is used to carry out an elastic-plastic deformation analysis, in which it is not necessary to take the change of pore pressure with time into account. Plastic calculation may be used for the limiting case of fully un-drained behaviour. In a plastic calculation, loading can be defined in the sense of changing the load and geometry configuration or pore pressure distribution by means of staged construction. The total level that is to be reached at the end of the calculation phase is defined by specifying a new geometry and load configuration and pore pressure distribution. Finite element calculations can be divided into sequential calculation phases. Each calculation phase corresponds to a particular loading or construction stage. The construction stages can be defined in the staged construction mode. The options available are Ko procedure and gravity loading for the initial phase to generate the initial stress state of soil. A 'groundwater flow only' option can be used only if groundwater flow analysis is to be performed. For deformation analysis options such as plastic, consolidation, safety, dynamic and fully occupied flow-deformation are available. In this research, a plastic calculation is selected for carrying out the analysis. The options for pore pressure calculation type for a plastic phase are:

- Phreatic
- Use pressures from previous phase
- Steady state groundwater flow

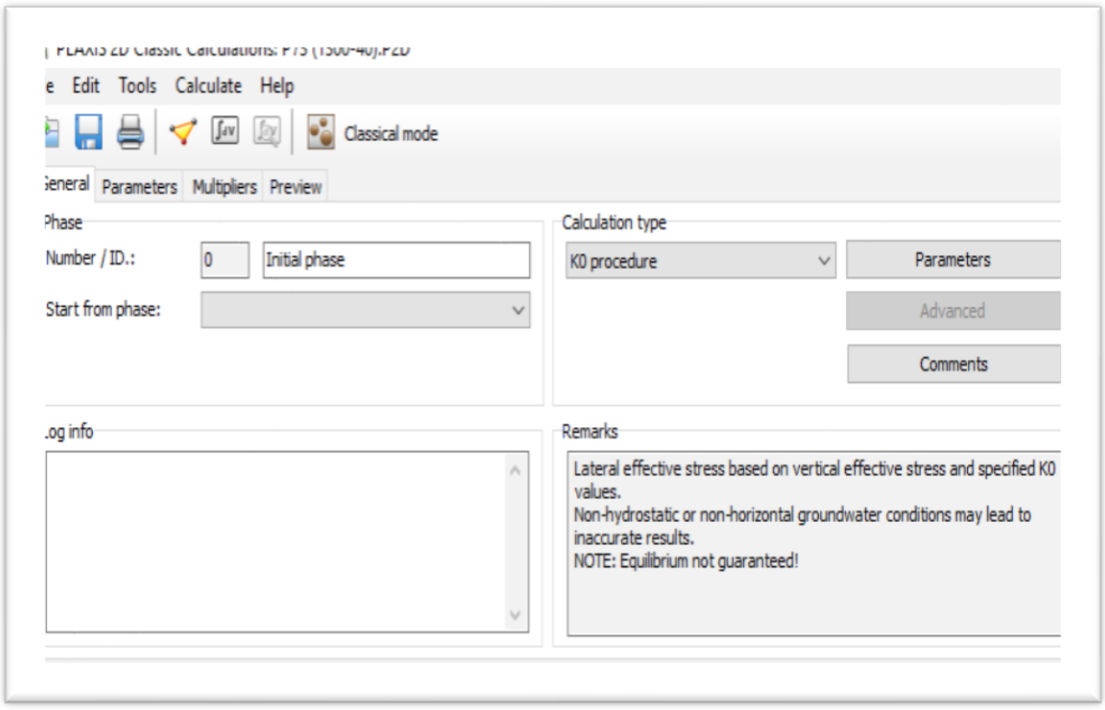

Fig. 5.19 Initial phase calculation type Ko procedure

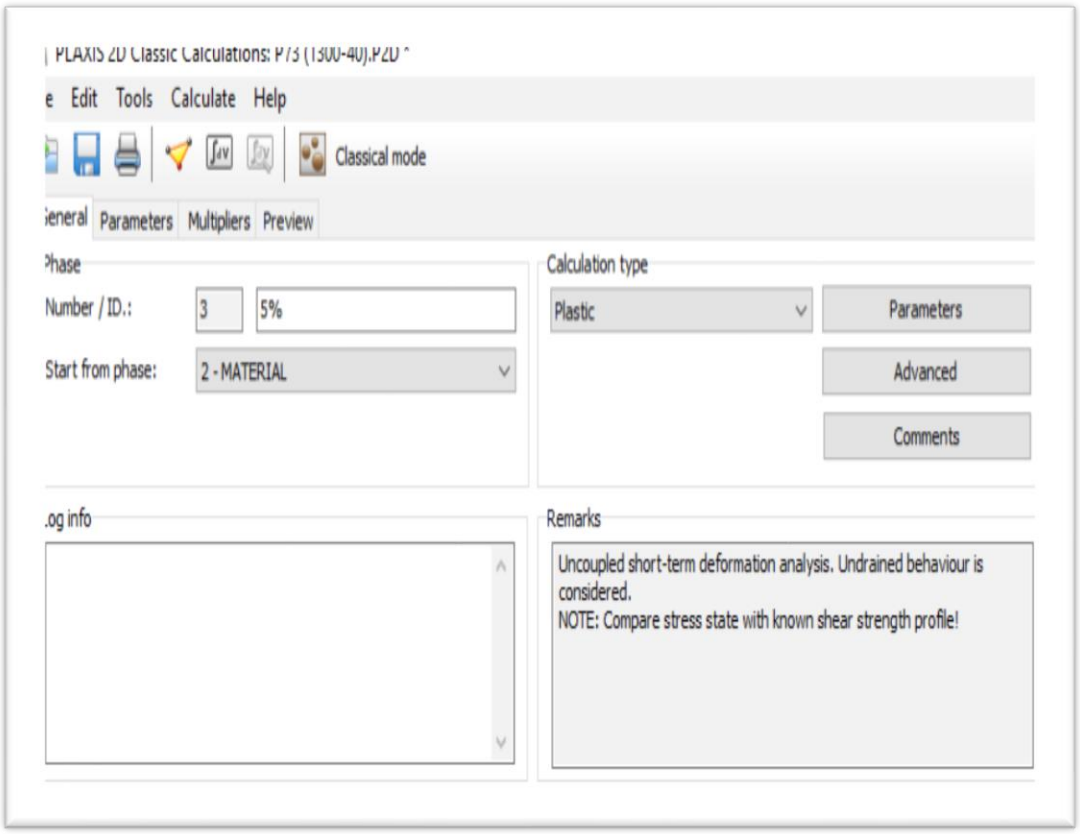

Fig. 5.20 Construction phases calculation type plastic

Step 8: Applying piles load incrementally for the loading phases

The distribution and the components of the static load are assigned in the first part of the load subtree. In the current study, pile loads are applied in different phases. The different phases of loading are consistent as per the static load tests carried out. Load increments are assigned for 5, 10, 15, 20, 25, 50, 75, 100, 125 and 150 per cent of the working capacity of loads. The loaded pile with the soil profile is as shown in the figure below.

PLAXIS allows for staged construction analysis. The pile static loads are applied in different stages. The soil in situ conditions and pile loading during the static load testing of the piles are simulated in the PLAXIS model.

During a calculation phase, soil and element objects in the geometry model are assigned as active and inactive elements. Initially, the soil profiles and pore pressures are activated in the initial stage to generate the stress conditions at rest. The first stage of analysis includes the pile element, along with the soil profile and water pressure, which are considered at one metre below the cut-off level of pile. The next subsequent stages of pile loading include the displacements of the soil and stresses developed in the first

stage. During these stages the rigid line interface elements are activated to stimulate frictional resistance and installation effects of pile.

The incremental increase in pile static loads to 150 per cent of the working capacity of piles and unloading of piles decremental is analysed in stages. The soil deformations and change in behaviour of soil profile, along with the pile element stresses and settlements, are observed in all the stages of construction. The figure below shows the construction stages considered in the staged construction analysis.

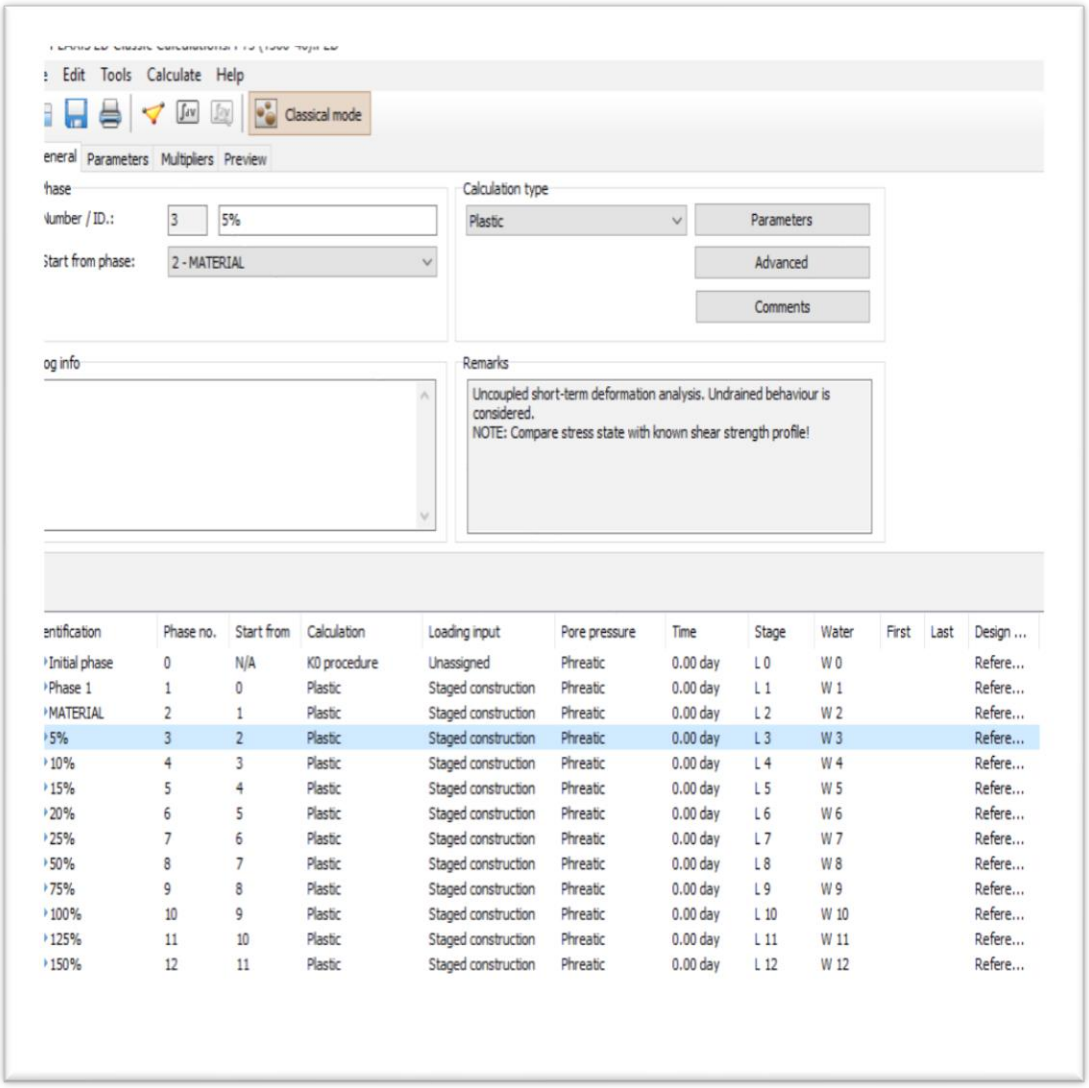

Fig. 5.21 Loading phases

Step 9: Run the model and draw load vs settlements curve

After the staged construction analysis, the analytical results are reviewed. Several points are selected along the length of pile to study the deformations and stresses. These points are selected prior to the calculation stage after the all the construction stages and pile loads are defined. The settlement values at the selected points for all stages of construction are identified. Pile settlement values obtained are as shown in the figures below.

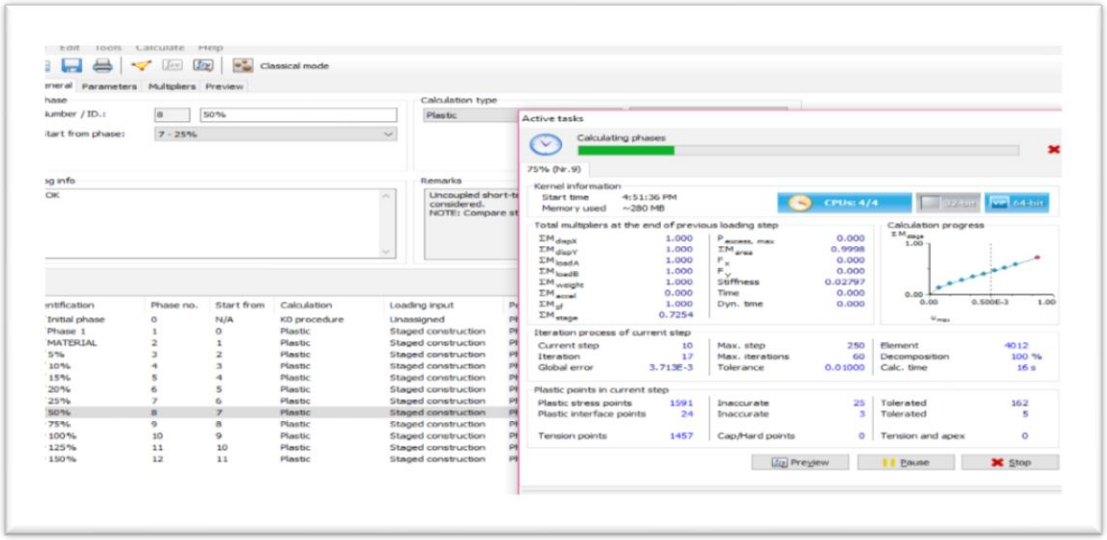

Fig. 5.22 Running the model

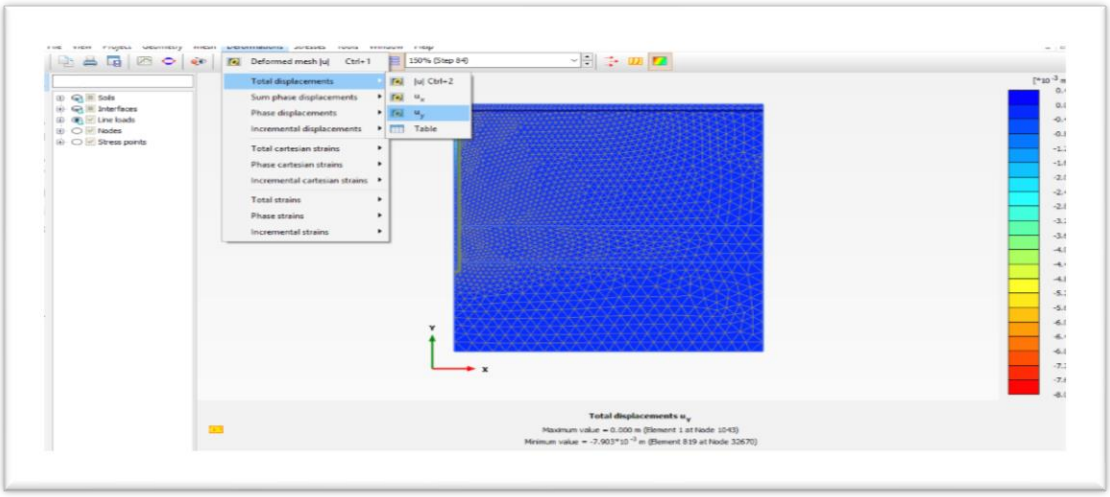

Fig. 5.23 Settlements result

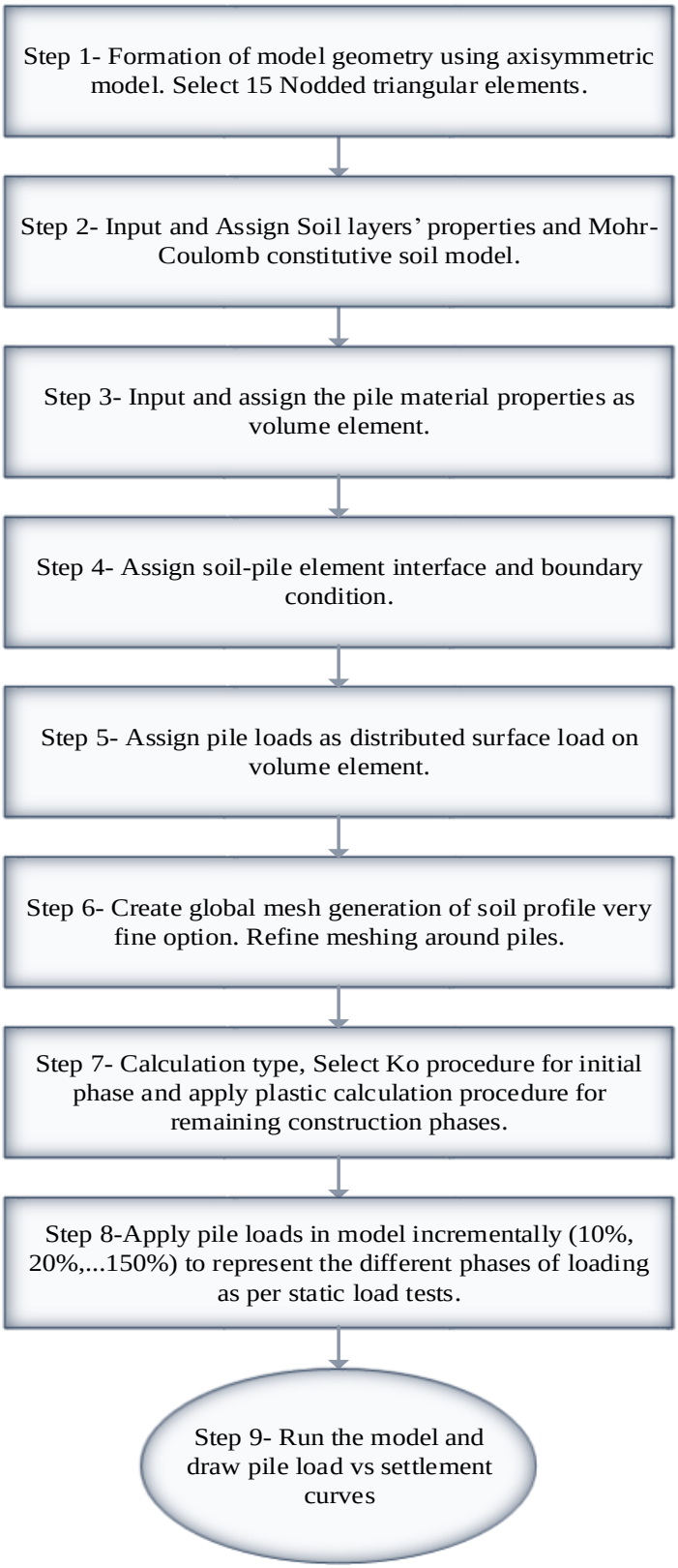

Fig. 5.24 Step by step procedure for PLAXIS 2D FEM analysis

5.3.3 FEM results for piles P73 and P71

Pile loads-settlement values and curves for P73 and P71, using FEM analysis based in geotechnical investigation report and modulus of elasticity from the investigation report, are shown in the tables and figures below:

Number	Load%	Load	Surface P	Settlement
0	0	0	0	0
1	5%	1069.65	806	0.97
2	10%	2139.3	1611	1.97
3	15%	3208.95	2417	2.97
4	20%	4278.6	3222	3.96
5	25%	5348.25	4028	4.96
6	50%	10696.5	8055	10.01
7	75%	16044.75	12083	15.25
8	100%	21393	16111	22.23
9	125%	26741.25	20139	44.85
10	150%	32089.5	24166	96.62

Table 5.11 Pile settlement calculation for P73 – PLAXIS 2D

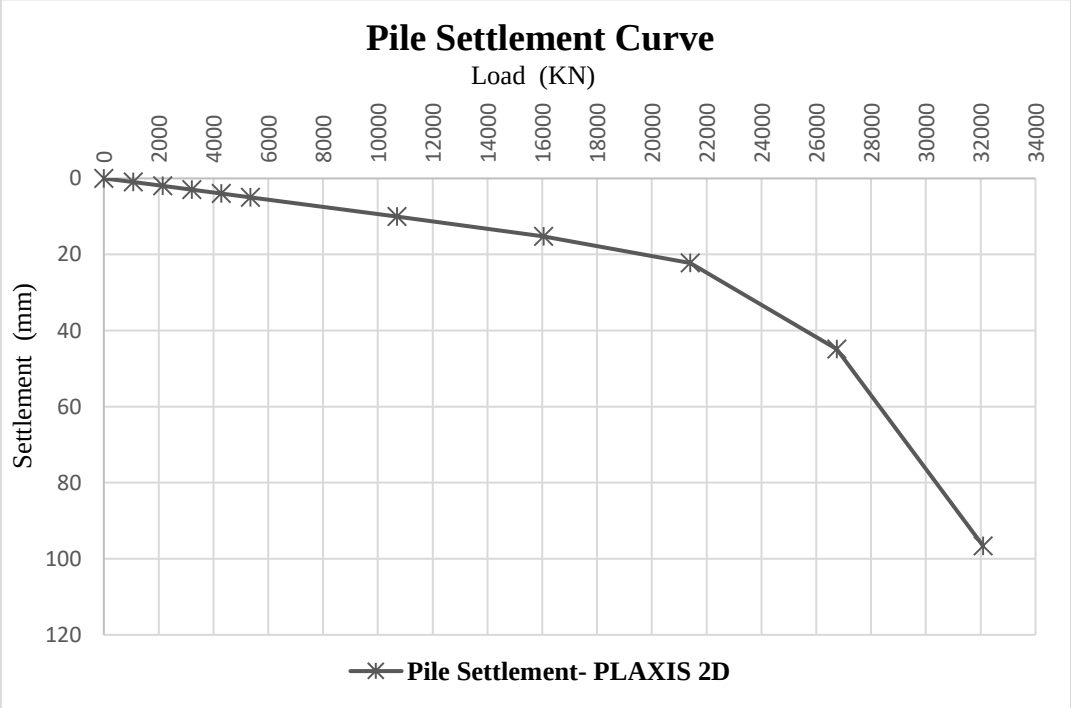

Fig. 5.25 Pile settlement curve P73- PLAXIS 2D

Number	Load%	Load	Surface P	Settlement
0	0	0	0	0
1	5%	385	766	0.67
2	10%	770	1531	1.35
3	15%	1155	2297	2.03
4	20%	1540	3063	2.7
5	25%	1925	3828	3.39
6	50%	3850	7656	6.83
7	75%	5775	11484	11.23
8	100%	7700	15313	29.83
9	125%	9625	19141	64.67
10	150%	11550	22969	102.2

Table 5.12 Pile settlement calculation for P71 – PLAXIS 2D

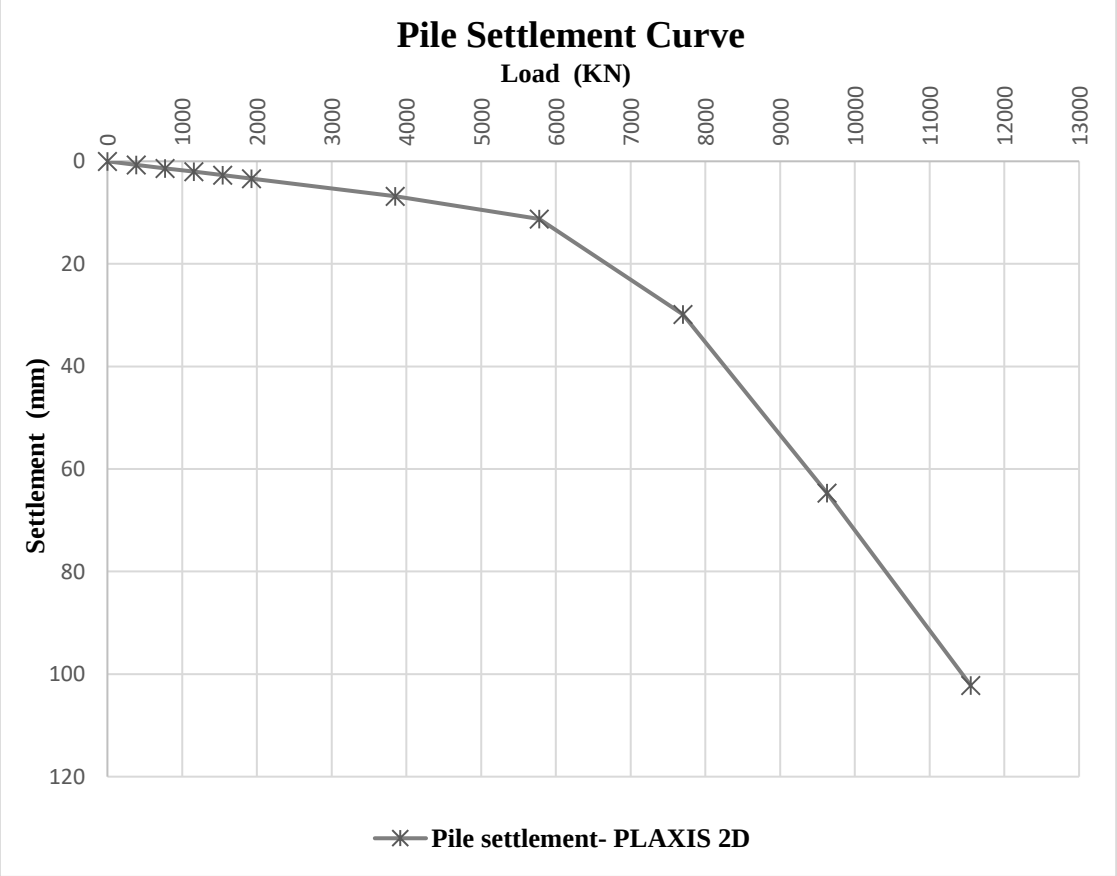

Fig. 5.26 Pile settlement curve P71- PLAXIS 2D

5.4 Static load tests result

5.4.1 Introduction

In this section, the static load test conducted for piles P76, P73 and P71 under consideration for the current study will be explained and, specifically, static load test results will be shown and explained. All test setup, instrumentation and test methods are explained in detail in Chapter 4. Three working piles out of 116 piles were chosen for this chapter and all static load test curves for 116 piles are available in Appendix 1 (Piles Summary Sheet). As explained previously, the piles generally tested for 1.5 times the design capacity/working load.

The cut of level for all piles is -7.5 DMD from the ground level; detailed information on working piles P76, P73 and P71 are given in the following table:

Pile Number & Type	Pile Diameter (mm)	Pile Length (m)	Working Load (kN)	Test Load (kN)	Toe Level (m)
P76 Instrumented	1.3	44	23190	32090	-51.5
P73	1.3	40	21393	32090	-47
P71	0.8	23	7700	11550	-30

Table 5.13 Working piles for static load test

5.4.2 Static load tests results for piles P73 & P71

% Load	Load (kN)	Settlement (mm)
0%	0	0.000
25%	5348.25	0.763
50%	10696.5	1.570
75%	16044.75	2.438
100%	21393	3.487
125%	26741.25	5.762
150%	32089.5	7.280

Table 5.14 Pile settlement results P73- static load test

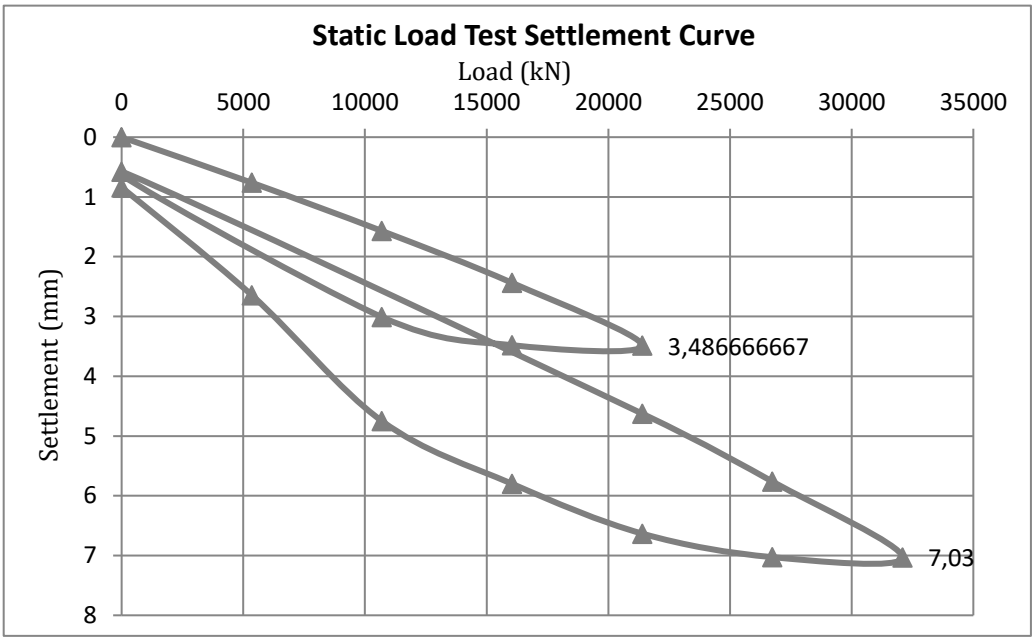

Fig. 5.27 Pile settlement curve P73-static load test

% Load	Load	Settlement
0%	0	0.000
10%	770	0.163
20%	1540	0.413
30%	2310	0.647
40%	3080	0.933
50%	3850	1.197
60%	4620	1.430
70%	5390	1.653
80%	6160	1.917
90%	6930	2.160
100%	7700	2.457
110%	8470	3.057
120%	9240	3.237
130%	10010	3.420
140%	10780	3.600
150%	11550	4.410

Table 5.15 Pile settlement results P71-static load test

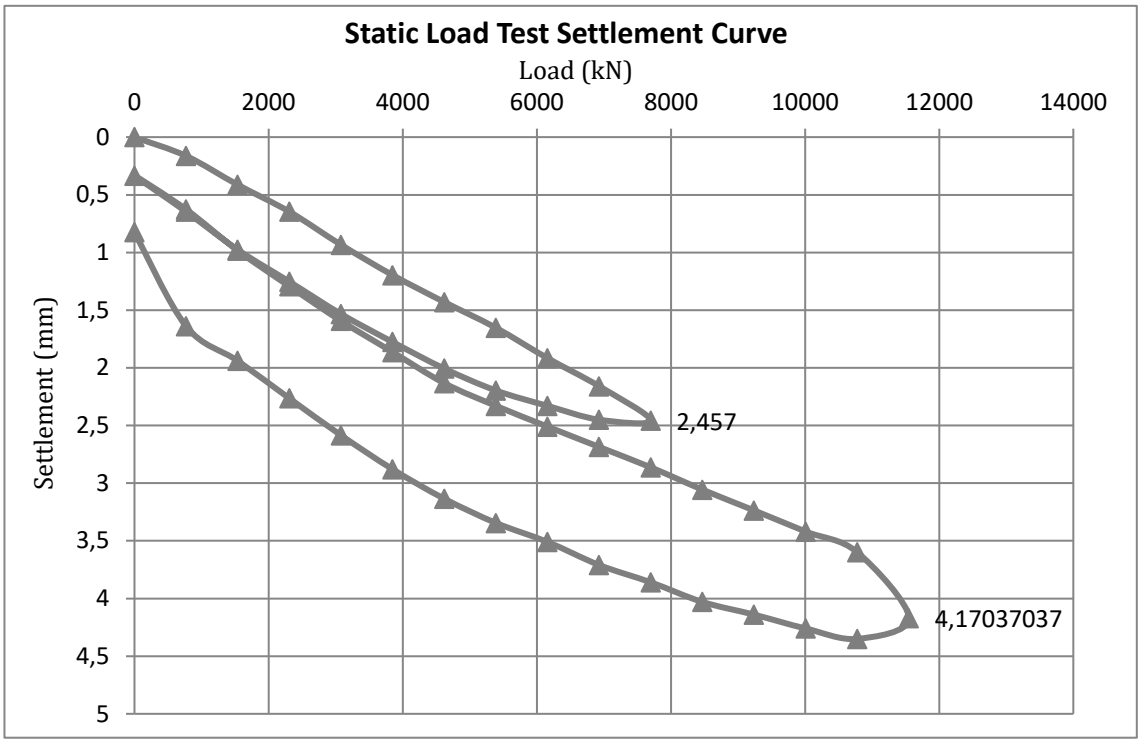

Fig. 5.28 Pile settlement curve P71- static load test

As per the project specification and design assumption, the acceptance criteria for the static load test was stated; the maximum settlement of the pile at working load should not exceed one per cent of the pile diameter.

As shown in above tables and figures, the maximum settlement values of all piles P73 and P71 are in compliance with the acceptance criteria, as mentioned in the project specifications and the design assumptions. Hence, the piles are capable for carrying the design loads in compression with small settlements, as shown above.

Furthermore, the above observations show that the maximum settlement from the static load is much less than the calculated settlement based on soil parameters from the soil investigation report, which also confirms the under-estimation of the soil parameters and over-design of the pile's lengths. This will be discussed in more detail in Sections 5.5 and 5.8.

5.4.3 Instrumented static load test results for pile P76

The objective of the instrumented static pile load test was to develop an understanding on the pile behaviour during the static load test and when the pile is exposed to various loading conditions. As per the pile design for P76, the maximum test load of 150 per cent working load for the pile was 34785 kN and the 100 per cent working load was 23190 kN. The table below details the loading stages:

% Load	Load	Settlement
0%	0.00	0.000
25%	5797.5	2.220
50%	11595	5.200
75%	17392.5	7.720
100%	23190	9.010
125%	28987.5	10.522
150%	34785	11.720

Table 5.16 Instrumented pile settlement results P76

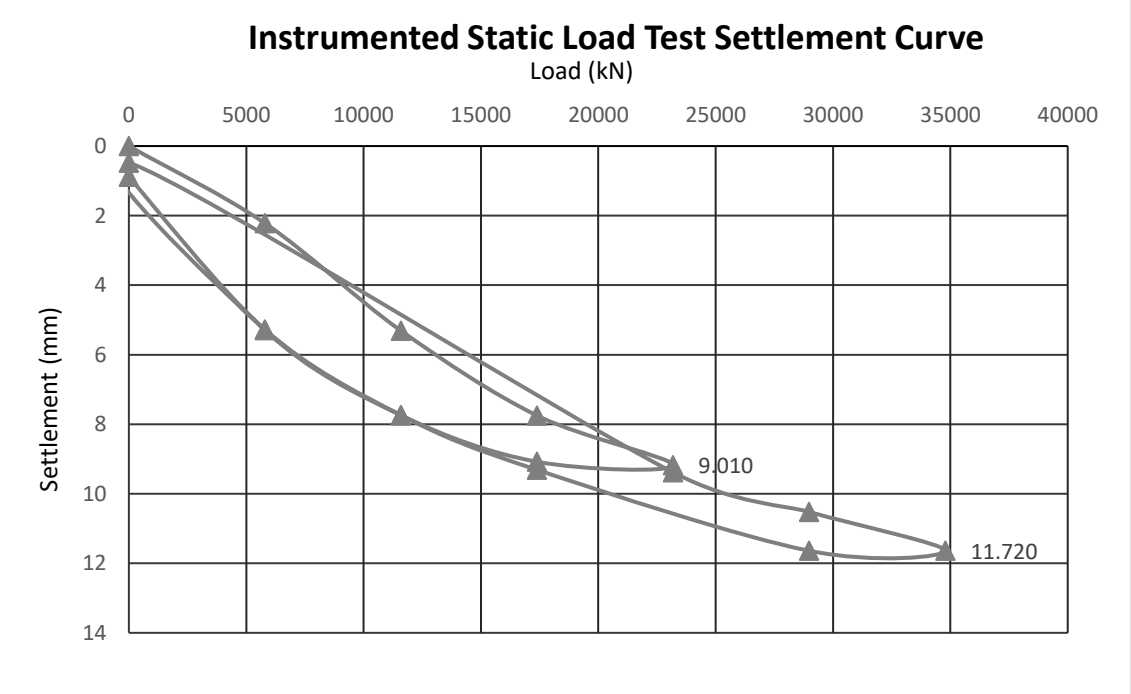

Fig. 5.29 Instrumented Pile settlement curve P76

As per the project specifications, the pile was equipped with a total of 48 Nos. vibrating wire strain gauges in sets of four, each installed at various levels, the details of which are as tabulated below:

Level	Installation Level DMD (m)	Quantity of Strain Gauge
A	-8.2	4 Nos
B	-12.1	4 Nos
C	-16.0	4 Nos
D	-19.8	4 Nos
E	-23.8	4 Nos
F	-27.7	4 Nos
G	-31.7	4 Nos
H	-35.8	4 Nos
I	-39.5	4 Nos
J	-43.4	4 Nos
K	-47.3	4 Nos
L	-51.2	4 Nos

Table 5.17 Instrumentation details & levels

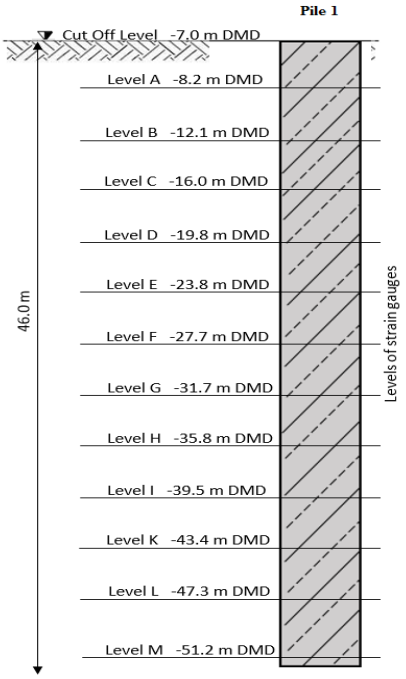

Fig. 5.30 Instrumentation details & levels

The following tables summarise the results and various obtained properties within the pile at the different levels during the various loading steps:

% of Load	Load (KN)	Elevation DMD (m)												Settlement (mm)
		-8.2	-12.1	-16	-19.8	-23.8	-27.7	-31.7	-35.8	-39.5	-43.4	-47.3	-51.2	
		Level A	Level B	Level C	Level D	Level E	Level F	Level G	Level H	Level J	Level K	Level L	Level M	
25%	**5798**	115	115	114	109	97	83	66	47	27	13	0	**0**	2.26
50%	**11595**	230	230	229	216	196	167	132	97	58	30	4	**0**	5.31
75%	**17393**	345	345	343	330	296	254	200	150	97	52	13	**0**	7.78
100%	**23190**	460	460	460	443	395	342	270	200	132	67	30	**0**	9.29
125%	**28988**	579	578	575	557	494	428	339	255	176	99	45	**0**	10.55
150%	**34785**	691	690	690	677	595	521	414	308	215	132	63	**0**	11.72

Table 5.18 Micro strain readings (ms)

% of Load	Load (KN)	Elevation DMD (m)												Settlement (mm)
		-8.2	-12.1	-16	-19.8	-23.8	-27.7	-31.7	-35.8	-39.5	-43.4	-47.3	-51.2	
		Level A	Level B	Level C	Level D	Level E	Level F	Level G	Level H	Level J	Level K	Level L	Level M	
25%	**5798**	5777	5777	5726	5475	4872	4169	3315	2361	1356	653	0	**0**	2.26
50%	**11595**	11553	11553	11503	10850	9845	8389	6630	4872	2913	1507	201	**0**	5.31
75%	**17393**	17330	17330	17229	16576	14868	12759	10046	7535	4872	2612	653	**0**	7.78
100%	**23190**	23106	23106	23106	22252	19841	17179	13562	10046	6630	3365	1507	**0**	9.29
125%	**28988**	29084	29033	28883	27979	24814	21499	17028	12809	8841	4973	2260	**0**	10.55
150%	**34785**	34710	34659	34659	34006	29887	26170	20796	15471	10800	6630	3165	**0**	11.72

Table 5.19 Load transfer between levels (kN)

% of Load	Load (KN)	Elevation DMD (m)										
		-8.2	-12.1	-16	-19.8	-23.8	-27.7	-31.7	-35.8	-39.5	-43.4	-51.2
		Level A to B	Level B to C	Level C to D	Level D to E	Level E to F	Level F to G	Level G to H	Level H to I	Level I to J	Level J to K	Level K to M
25%	**5798**	8	11	24	46	52	62	68	71	52	49	8
50%	**11595**	8	11	49	71	100	119	119	131	96	90	21
75%	**17393**	8	14	49	115	141	179	166	175	150	131	49
100%	**23190**	8	8	62	160	175	235	229	223	213	125	103
125%	**28988**	11	18	65	207	216	289	273	257	251	179	150
150%	**34785**	11	8	49	267	242	346	343	302	270	226	207

Table 5.20 Calculated unit skin friction (kN/m^2)

% of Load	Load (KN)	Elevation DMD (m)											Settlement (mm)
		-8.2	-12.1	-16	-19.8	-23.8	-27.7	-31.7	-35.8	-39.5	-43.4	-47.3	-51.2	
		Level A	Level B	Level C	Level D	Level E	Level F	Level G	Level H	Level J	Level K	Level L	Level M	
25%	**5798**	100	100	99	94	84	72	57	41	23	11	0	**0**	2.26
50%	**11595**	100	100	99	94	85	73	57	42	25	13	2	**0**	5.31
75%	**17393**	100	100	99	95	85	74	58	43	28	15	4	**0**	7.78
100%	**23190**	100	100	100	96	86	74	58	43	29	15	6	**0**	9.29
125%	**28988**	100	100	100	97	86	74	59	44	30	17	8	**0**	10.55
150%	**34785**	100	100	100	98	86	75	60	44	31	19	9	**0**	11.72

Table 5.21 Percentage load transfer between levels (%)

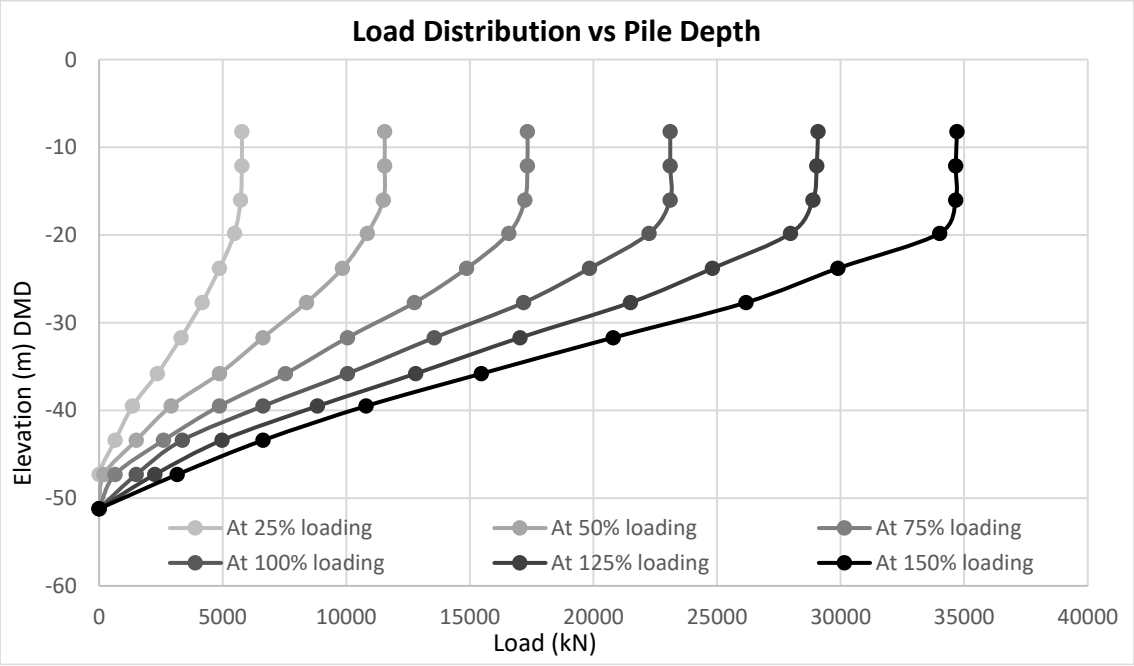

Fig. 5.31 Load distribution vs depth

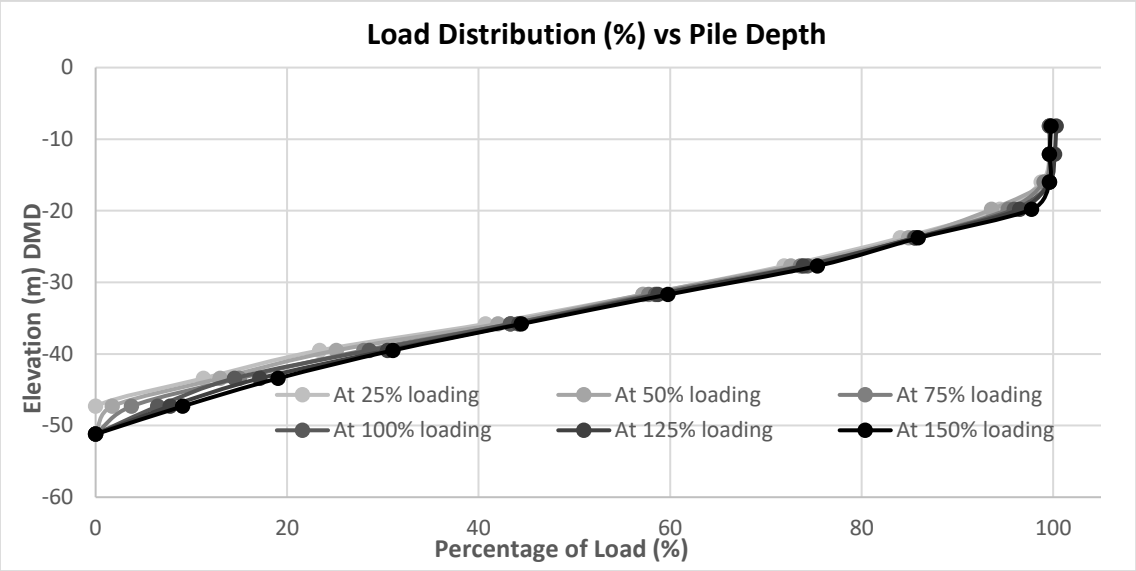

Fig. 5.32 Load distribution percentage vs depth

Based on the load transferred to the pile at each level along the pile depth, as shown in the above figures and tables, it was found that the loads were taken mainly by friction and there is no load transfer to the pile tip even with 150 per cent of working load, which also proves that the length of the pile is overestimated. Further discussion on this topic can be found in Sections 5.5 and 5.8.

5.5 Conventional methods, FEM and SLT settlement curves using E_s-soil report

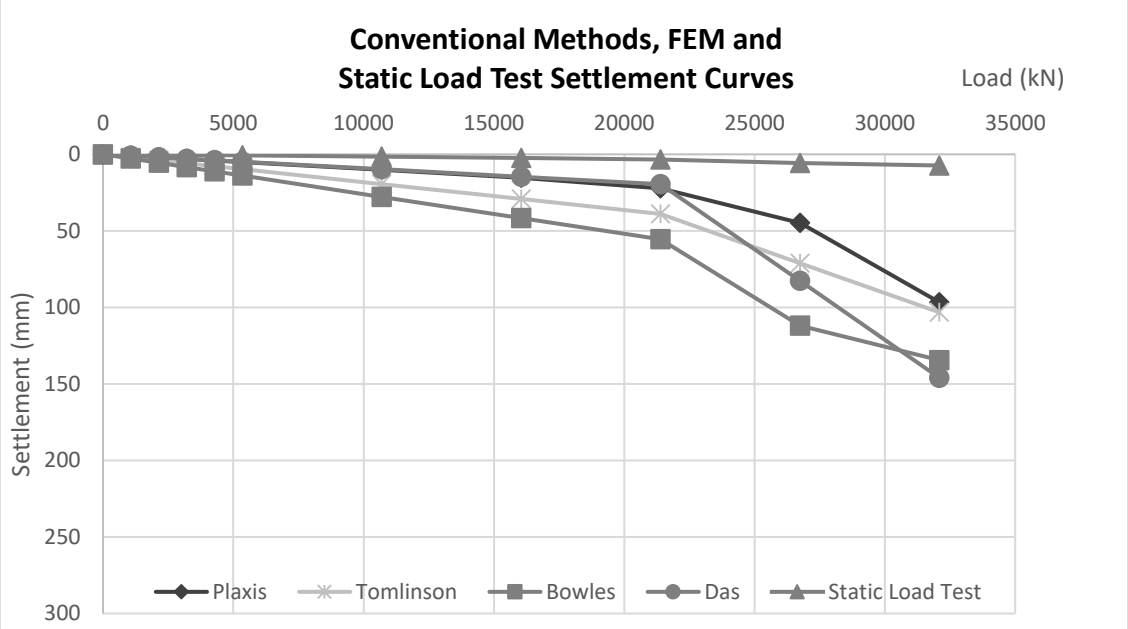

Fig. 5.33 Comparison curves for P73 using E_s soil report for different methodologies

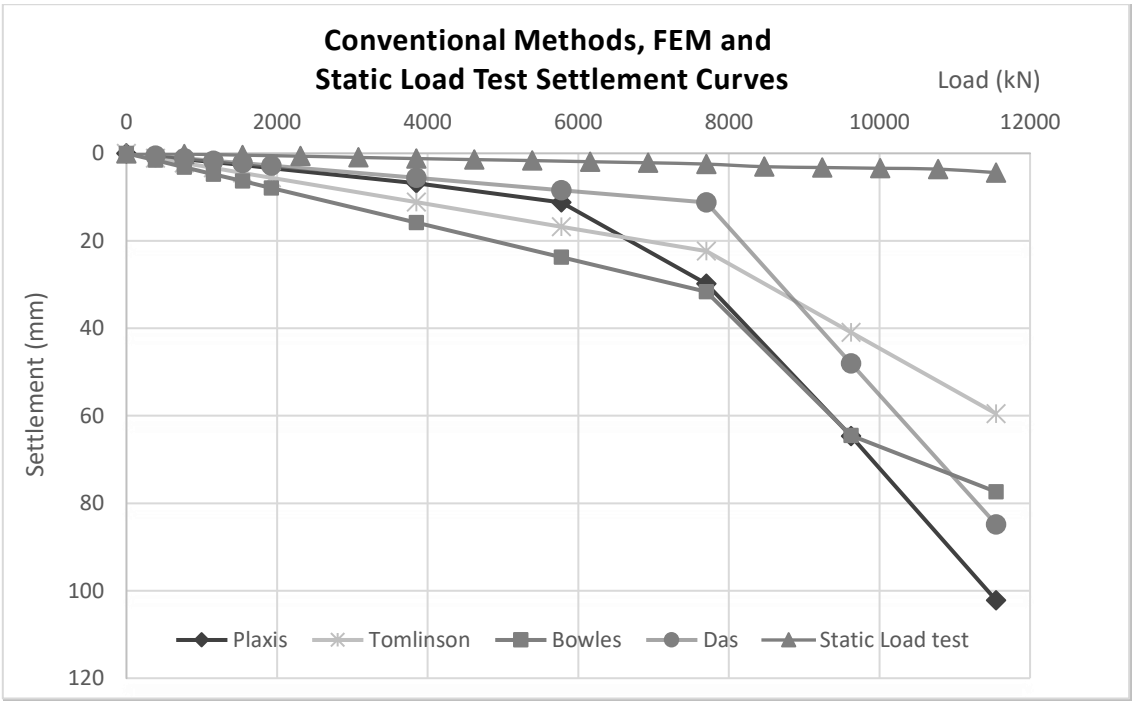

Fig. 5.34 Comparison curves for P71 using E_s soil report for different methodologies

As described in the research methodology in Section 5.1.1, the load settlement behaviour of the piles was determined using conventional methods (empirical and analytical calculations) and the finite element analysis based on the geotechnical

parameters obtained from the geotechnical soil investigation report. The settlement values calculated for the piles P73 and P71 corresponding to 100 per cent and 150 per cent of loading conditions, as shown below:

Approach		Load (%)	Settlement(mm)	
			P73	P71
Static Load Test		100 %	3.48	2.55
Conventional Method	Bowles		54.4	31
	Tomlinson		38.4	22
	Das		18.9	10.9
FE Analysis			22.2	29.8
Static Load Test		150 %	7.03	4.18
Conventional Method	Bowles		132.6	76.4
	Tomlinson		102	58.9
	Das		144.8	84.2
FE Analysis			96.62	102.2

Table 5.22 Settlement values obtained for different methodologies using E_s soil report

As seen in Table 5.15, the settlement values obtained by the Das method and the finite element method are less in comparison with others at 100 per cent of the working load condition; the settlement values obtained by Bowles and Tomlinson method differ greatly from the settlement values obtained by the finite element method. Amongst all the empirical methods, the settlement values calculated by the Bowles method significantly vary from the finite element analysis results. Therefore, it should be considered that this method only provides a rough approximation of the settlement prediction.

However, the settlement values significantly increased in the case of empirical and analytical methods when the applied loading condition exceeded 100 per cent of the working load values and the variation also increased with finite element results. The main reason for this is the theoretical assumption used for the conventional methods (empirical and analytical calculation), where the piles are designed as friction pile for 100 per cent of the working load and any further increases in the loads being carried in base resistance, causing further settlements.

For increased clarity relating to the comparisons, the load settlement behaviour obtained using the different computational methodologies, along with the static load test results can, be plotted as shown in Fig 5.33 and 5.34.

As detailed in these graphs, all piles possess a similar load settlement behaviour when subjected to compressive axial loading. The nearly linear relationship exhibited in the initial portions of load settlement graph indicates that the axial load is carried in skin friction/shaft resistance in that region. Comparing the load settlement behaviour exhibited between the conventional calculations and finite element analysis of piles in terms of load transfer mechanism, it can be interpreted that in up to 100 per cent of loading conditions, the load is carried in shaft resistance; the change in slope of the graph beyond this point depicts the development of base resistance in piles. However, in comparison with the static load test results, the FEM analysis and conventional methods show a huge variation in the load settlement behaviour.

Based on the comparative study, the predicted settlement values were much higher than the settlement values obtained by static load testing. As previously explained in the literature review, the predicted settlement values are highly dependent on the modulus of elasticity of the soil. In fact, the empirical and analytical methods used for the settlement analysis are collectively known as approximation methods based on the theory of elasticity. Also, as explained in the Section 5.2.3, the material models used for soil is the Mohr-Coulomb model, for which the modulus of elasticity is an important input parameter. Thus, the predicted settlement values are highly affected by the accuracy of elastic modulus of soil, which is obtained by the empirical correlation of UCS values determined in the laboratory testing as shown in Section 2.2.3. Hence, it can be concluded that the laboratory tests only provide a fair estimate of the elastic modulus of soil; the main reasons for this underestimation being the inefficiencies and errors in sampling undisturbed soil samples for laboratory tests. In addition, the laboratory tests do not consider the pile installation effect on the surrounding soil, which has a significant impact on the stiffness of the near soil zones, which is remoulded and densified during the process of pile installation.

Additionally, the modulus of elasticity is computed based on the empirical relationship with the soil parameters; this empirical correlation is based on site specific data, local conditions and the assumption that the future models the past. Thus, the results determined by empirical correlation can differ highly from the real in-situ soil stiffness conditions.

5.6 Determination of modified modulus of elasticity E_{mod} using FEM back-analysis

5.6.1 Introduction

Based on the previous comparative study, the value of settlement calculated using the Soil parameters from the geotechnical investigation report varied highly from the static load test settlement results. As explained before, the load settlement behaviour of the pile is dependent on the weak rock modulus of elasticity. The discrepancy between the calculated settlement based on (Es) and the settlement from static load test values were mainly due to the under estimation of the modulus of elasticity (Es) of the soft rock. Therefore, in this section the modified value of elastic modulus of the soil (E_{mod}) will be determined using the back analysis of static load results using the finite element method (FEM).

5.6.2 Back-analysis procedure for determining modified modulus of elasticity

In this section, the FEM back analysis of the soil parameters, specifically the modulus of elasticity (E_{mod}), will be back calculated based on the static load test results. The settlement curve obtained during the static load test will be used as the reference value for the FEM back analyses of soil parameters in the PLAXIS 2D program. The FEM back analysis is a complex trial and error procedure where the computed data is compared with the deformation / settlement values obtained from each loading stages of the static load test (5,10, 15.....150 per cent). The modulus of elasticity values is continuously adjusted in the FEM model and the entire process repeated until the values of settlement from the FEM model coincides with the static load test to obtain the modulus of elasticity (E_{mod}). The load settlement curve will be plotted for each pile (116 Piles) by using FEM back analysis and the modulus of elasticity value. Corresponding to which, the settlement curve obtained through the finite element analysis resembles the load settlement behaviour of pile; during static load testing is chosen as modified modulus of elasticity (E_{mod}).

FEM modelling and analysis using PLAXIS 2D will be conducted as per the procedure explained in Section 5.3.2. As previously clarified, the pile extends through three different weak layers of rock. The material characteristics provided for the pile and weak rock layer in Table 5.1 and 5.2 will be used as the initial input data for the FEM back analysis. All the parametric values in the table, except for modulus of elasticity, will remain unchanged during the back analysis of static load test (SLT). However, during some simulations, it will be required to increase the cohesion values to fulfil the Mohr Coulomb's failure criteria used in the material modelling of rock. Also based on the availability cubes test results, the actual modulus of elasticity of concrete will be used.

5.6.3 Results analysis and interpretation

Due to the back analysis conducted on piles P73 and P71 for the static load test result, the load settlement graphs obtained are shown in Figures 5.35 and 5.36. Detailed results of back analysis for incremental loading stages 5, 10, 15 per cent up to a total loading condition of 150 per cent (1.5 times) as shown in Table 5.23 and 5.24.

Number	Load%	Load	Surface P	Settlement
0	0	0	0	0
1	5%	1069.65	806	0.054
2	10%	2139.3	1611	0.11
3	15%	3208.95	2417	0.16
4	20%	4278.6	3222	0.23
5	25%	5348.25	4028	0.3
6	50%	10696.5	8055	0.83
7	75%	16044.75	12083	1.6
8	100%	21393	16111	2.55
9	125%	26741.25	20139	3.64
10	150%	32089.5	24166	4.62

Table 5.23 Pile settlement calculation for P73 – PLAXIS 2D

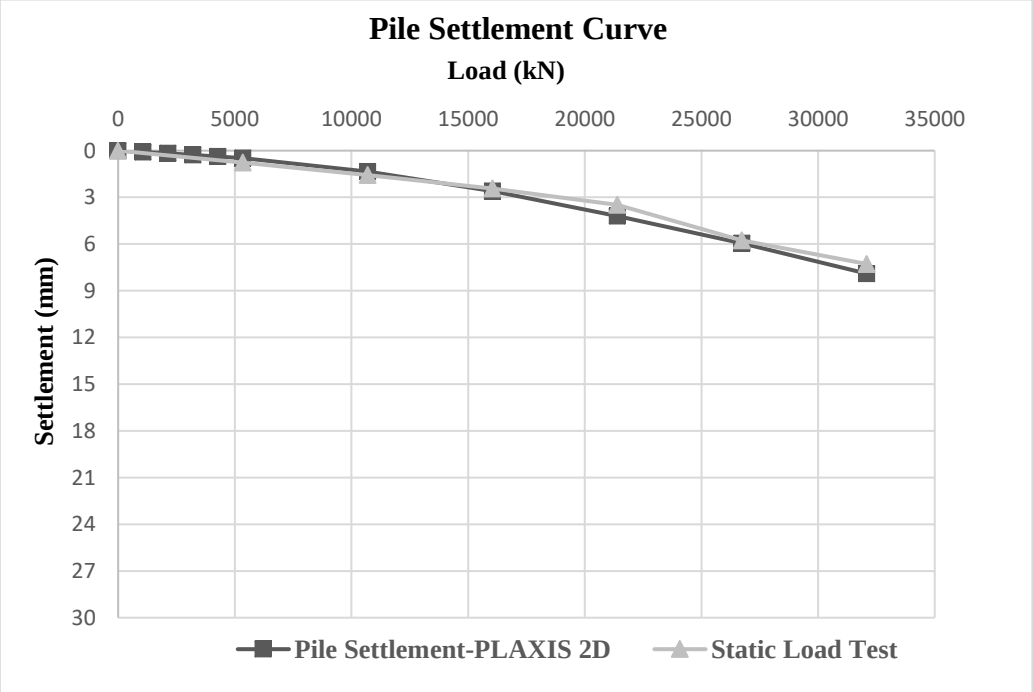

Fig. 5.35 Pile settlement curve P73- PLAXIS 2D

Number	Load%	Load	Surface P	Settlement
0	0	0	0	0
1	5%	385	766	0.054
2	10%	770	1531	0.11
3	15%	1155	2297	0.16
4	20%	1540	3063	0.23
5	25%	1925	3828	0.3
6	50%	3850	7656	0.83
7	75%	5775	11484	1.6
8	100%	7700	15313	2.55
9	125%	9625	19141	3.64
10	150%	11550	22969	4.62

Table 5.24 Pile settlement calculation for P71 – PLAXIS 2D

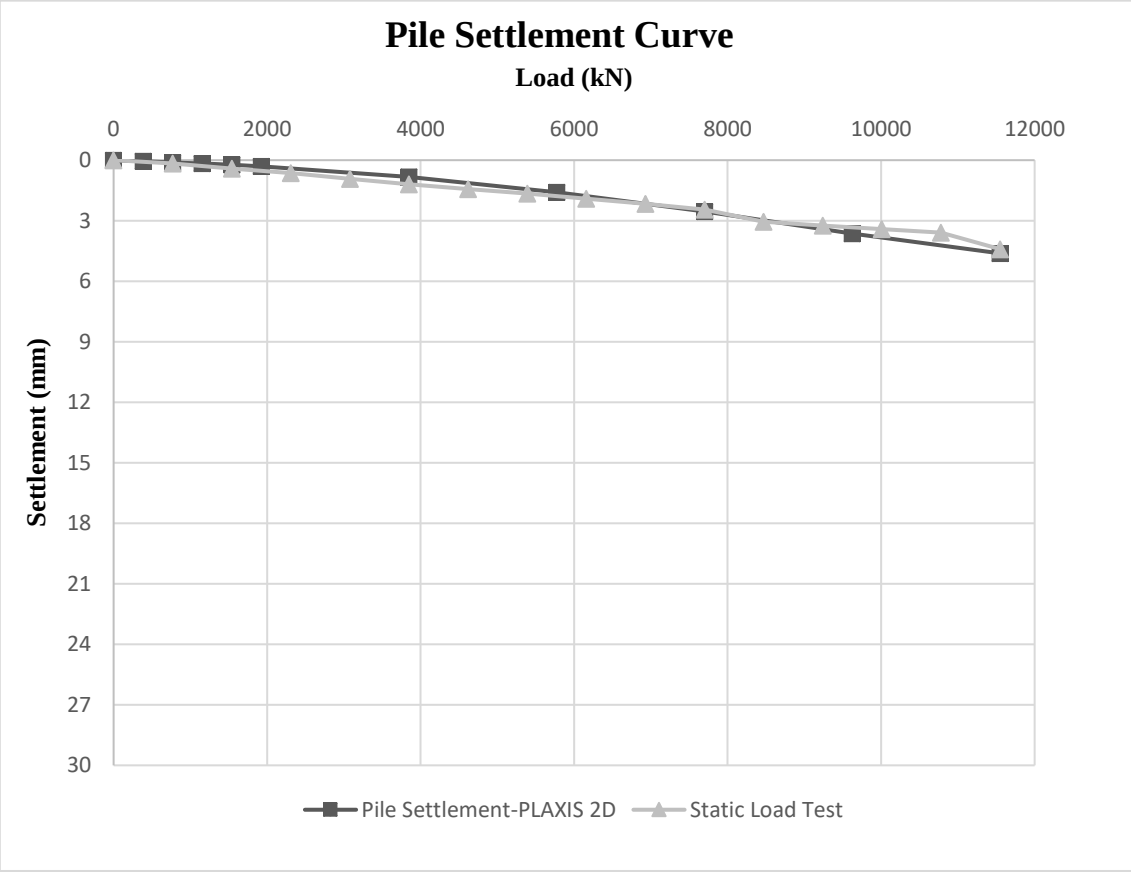

Fig. 5.36 Pile settlement curve P71- PLAXIS 2D

The modulus of elasticity values of each soft/weak rock layers are increased till the desired settlement (actual settlement from SLT) values are obtained from the finite FEM. As represented by Figure 5.36, the depth of the domain to be investigated is limited at 54 m depth, corresponding to the thickness of the three weak layers of rock. However, as the length of the pile P73 is 40 m and pile P71 is 23 m, thus in the case of pile P71 with 23 m lengths, the influence zone of pile will not extend through the three layers of rock. Hence, the settlement of pile P71 will not be sensitive to the modulus of elasticity of the bottom layers of rock. Therefore, for pile P71 the modulus of elasticity for the bottom layers are assigned in a similar manner to the modulus of elasticity of rock in the influence zone of pile during back analysis. The results of the back analysis were obtained after an average of 10 to 15 iterations with different values of modulus of elasticity by fitting the numerically computed curves using PLAXIS 2D with the static load test results (SLT). As shown in Figure 5.35 and 5.36, the load settlement curve obtained using the soil parameters from the soil report in the initial FEM analysis has now been adjusted to approximately match with the static load test results (SLT). However, there were minor differences between the back-analysis settlement results and SLT settlement results which are acceptable. This difference is on the conservative side for calculating the modified module of elasticity (E_{mod}). The table below summarises the settlement values obtained from FEM and the settlement from static load test (SLT) for P73 and P71 corresponding to 100 and 150 per cent of loading conditions, which is very similar.

Approach	**Load (%)**	**Settlement(mm)**	
		P73	**P71**
Static Load Test (SLT)	100%	3.48	2.55
FEM Back-Analysis		**4.2**	**2.55**
Static Load Test (SLT)	150%	7.03	4.18
FEM Back-Analysis		**7.9**	**4.62**

Table 5.25 Pile settlement values obtained for FE back analysis and static load test

The matching modified modulus of elasticity (E_{mod}) values back calculated from FEM to obtain the above settlements behaviour as static load test (SLT) results for P73 and P71 as per the table below:

Rock Layer		Modulus of Elasticity (MPa)			
		P73 (-7 to -40 DMD)		P71 (-7 to -30 DMD)	
		E [MN/m²]	**c** [kN/m²]	**E** [MN/m²]	**c** [kN/m²]
Soil Report	Layer-1 (-6 to-29 DMD)	**65**	50	**65**	50
	Layer-2 (-29 to -38 DMD)	**100**	100	**100**	100
	Layer-3 (-38 to -60 DMD)	**60**	62	**60**	62
Back-Analysis	Layer-1 (-6 to-29 DMD)	**4250**	95	**5000**	75
	Layer-2 (-29 to -38 DMD)	**5000**	100	**5000**	100
	Layer-3 (-38 to -60 DMD)	**5000**	95	**5000**	62

Table 5.26 Modulus of elasticity E_{mod} values from back analysis

As shown in the above table, the modulus of elasticity E_{mod} values obtained from the FEM back-analysis of static load test significantly change from the values from the soil investigation report. However, for comparison purposes, the increment in modulus of elasticity values and the corresponding increasing were determined for P73 and P71 factors, as shown in the table below:

Pile #	Length [m]	Dia. [m]	Working Load [kN]	Test Load[kN]	E Soil Report (E_s) [MN/m²]	E Back Calculated (E_{mod}) [MN/m²]	Increment in E
P73	40	1.3	21393	32089.5	65	4250	70.8 times
					100	5000	50.0 times
					60	5000	80.6 times
P71	23	0.8	7700	11550	65	5000	83.3 times
					100	5000	50.0 times
					60	5000	80.6 times

Table 5.27 Increment in modulus of elasticity

The modified modulus of elasticity (E_{mod}) value has increased by a factor of 50 to 80 times of the values obtained from the soil investigation report, the reasons for this primarily being the underestimation of weak rock properties, the human effect in laboratory testing, the methods of calculation of modulus of elasticity being conservative and ignoring the effect of confinement of the rock at site.

5.7 Settlement analysis using E_{mod} from back-analysis

5.7.1 Introduction

In this section, the settlement behaviour of the P73 and P71 will be recalculated based on the modulus of elasticity (E_{mod}) values, back calculated using FEM from the static load test results. This recalculation of the piles settlements using the conventional methods benefit in determining the effect of the modulus of elasticity (E_{mod}) values in piles settlement values and comparing this with the FEM and the static load test (SLT)

5.7.2 Modified soil properties

Comparable to conventional methods calculations performed in section 5.2.2 using weighted average of modulus of elasticity (Es) from the soil investigation report, similarly in this section the weighted average of the modulus of elasticity (E_{mod}) values will be used for the settlement calculation using the conventional methods. The modulus of elasticity (E_{mod}) values obtained for each layer are used to calculate the weighted average of the modulus of elasticity with respect to the thickness of each layer, as well as the effect of layers in the pile based on the pile length.

Pile	Rock layer	Layer Thickness	E_{mod}	Weighted Average E_{mod}
#	#	(m)	MPa	MPa
P73	Layer 1	23	**4250**	**4600**
	Layer 2	9	**5000**	
	Layer 3	22	**5000**	
P71	Layer 1	23	**5000**	**5000**
	Layer 2	9	**5000**	
	Layer 3	22	**5000**	

Table 5.28 Weighted average of E_{mod} values for piles P73 &P71

The geotechnical parameters and pile properties required for the settlement are calculated using the conventional method calculation (empirical and analytical), as shown in table below. Other influence factors and parameters required for the settlement calculation using conventional methods (Das, Bowles & Tomlinson approaches) were considered as per the previous calculations performed in Section 5.2.2.

Parameters	**Pile Number**	
	P73	**P71**
Load (kN)	21393	7700
Length of Pile, L (m)	40	23
Modulus of Elasticity of Pile (Test), E_p (MPa)	33142.8	33142.8
Diameter of Pile, D (m)	1.3	0.8
Area of Pile, A_p (m^2)	1.330	0.500
Perimeter of Piles	4.080	2.510
Poisson's Ratio	0.3	0.3
Modulus of Elasticity, E_{mod} (MPa)	**4600**	**5000**

Table 5.29 Soil & pile properties used in conventional method calculations

5.7.3 Conventional method calculation of pile settlement based on E_{mod}

The settlement behaviour showed by P73 and P71 during the calculations using conventional methods (empirical and analytical calculations) based on the modified elastic modulus (E_{mod}) values - using the three different approaches as per Das, Bowles and Tomlinson - are shown in the figures below. The increase in modulus of elasticity values (E_{mod}) brought significant changes in the calculated load settlement behaviours and the settlement curve of P73 and P71 particularly when compared to the previous settlement values and the load settlement graph carried out based on Es from the soil investigation report (section 5.2.2)

The settlement curves obtained by the Das and Tomlinson approaches using modified modulus of elasticity (E_{mod}) values are as shown in the figures below. However, for settlement curves obtained by the Bowles approach, this varies from the other two computational methods. The improvement on the settlement curves calculated based on this latter approach is less and more linear in comparison to the previous analysis behaviour obtained by using the (E_{mod}) value.

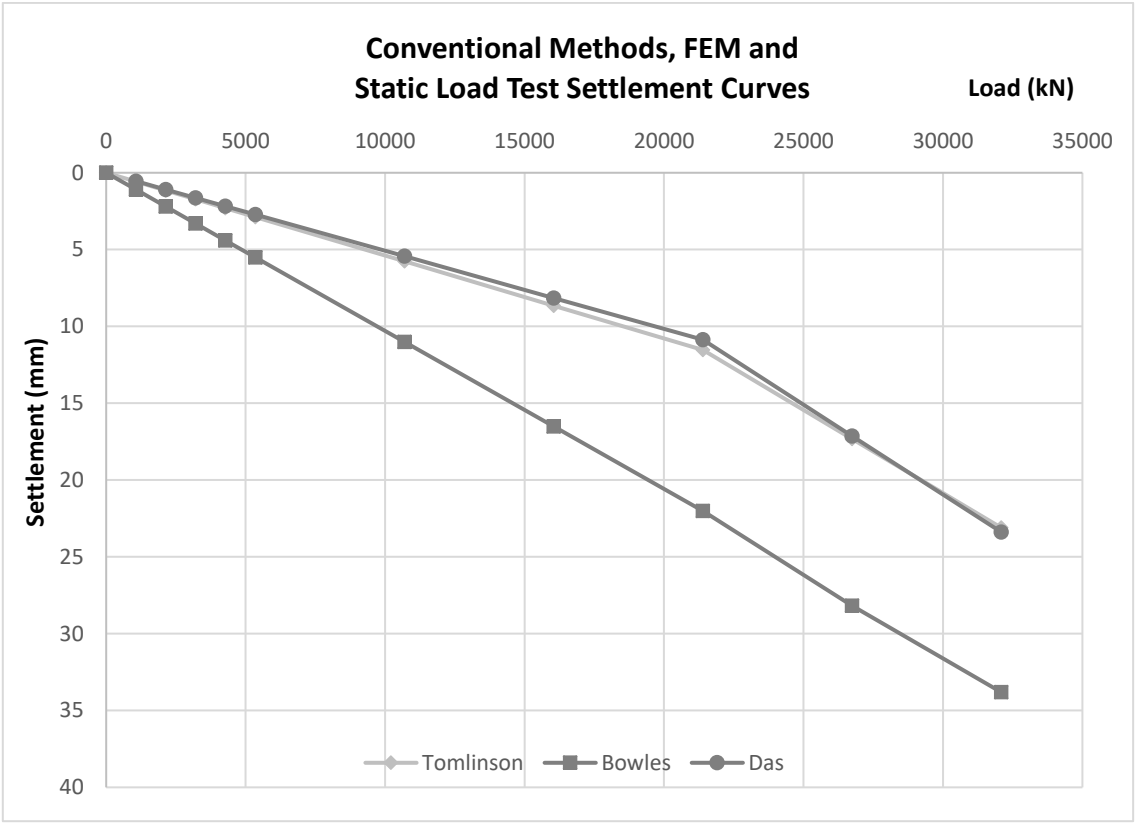

Fig. 5.37 Conventional methods settlements curves P73 using E_{mod} back-calculated

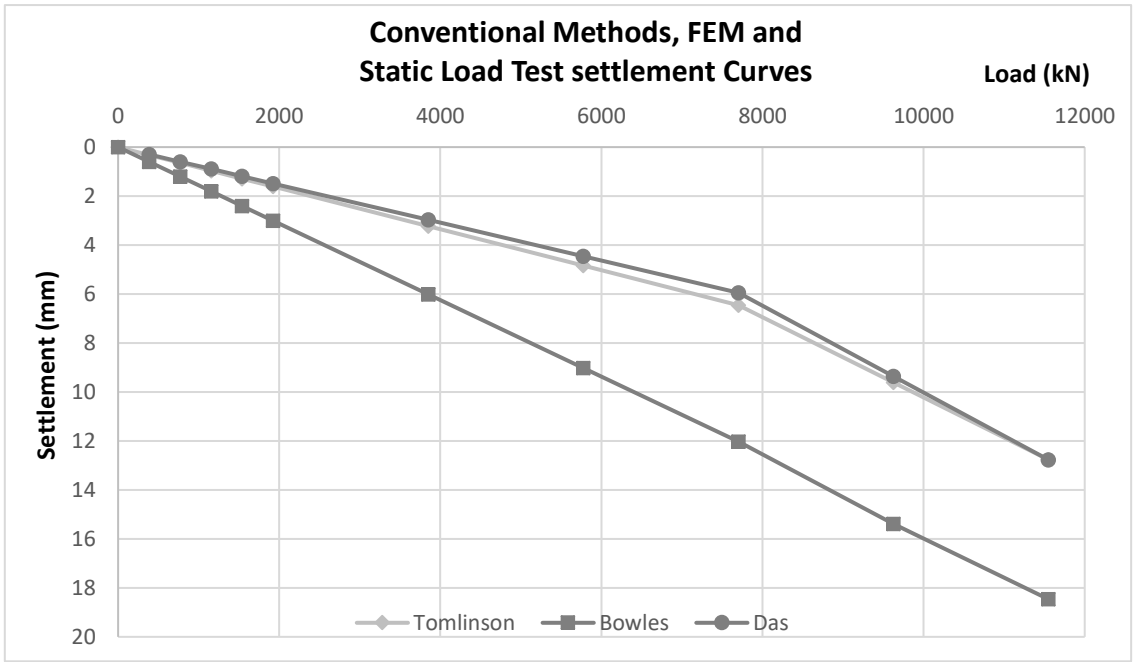

Fig. 5.38 Conventional methods settlements curves P73 using E_{mod} back-calculated

The table below summarises the settlement values of P73 and P71 based on modified modulus of elasticity (E_{mod}) values for 100 and 150 per cent of the working load using the conventional methods of the Bowles, Das and Tomlinson approaches.

Approach	Load (%)	Settlement(mm)		Reduction in settlement (%)	
		P73	P71	P73	P71
Bowles	100%	20	11.2	60%	62%
Tomlinson		10.9	6.1	70%	71%
Das		9.9	5.5	41%	47%
Bowles	150%	30.7	16.8	75 %	76 %
Tomlinson		21.9	12.1	77%	79%
Das		21.3	11.9	84%	86%

Table 5.30 Settlement values for P73 and P71 from conventional methods calculation based on E_{mod}.

As clarified earlier, the piles are designed as friction piles, so the working load will be carried by ultimate shaft resistance up 100 per cent of the working load, and any further load beyond 100 per cent will be carried in base resistance. This stands even though the settlement will be mainly caused by the elastic shortening of the pile and displacement due to the load transferred through the shaft, with the base resistance being less in comparison to the elastic shortening of piles.

As shown in the above table and figures, and as discussed previously, the settlement values obtained by the Das and Tomlinson approaches are less than the values obtained using the Bowles method. In 100 per cent of working load, almost twice the values obtained by Das and Tomlinson approach and in 150 per cent of working load, and 1.5 times of the settlement values. As explained in the previous paragraph, the settlement is mainly due to elastic shortening; if the settlement from elastic shortening excluded all approaches it will give similar values.

Combined, the aforementioned factor leads to the conclusion that the lengths of the piles are over-estimated and the working load is not reaching the pile tip, in addition to the fact that most of the piles (116 piles) are over-designed. Additionally, when comparing the settlement values given in the table with the previous values calculated using the modulus of elasticity (Es) from the soil investigation report, the above table shows the reduction in percentage obtained in the settlement values corresponding to 100 and 150 per cent of the working load conditions for the various conventional methods. At 100 per cent of loading conditions, the percentage reduction in the settlement is maximised when using the Tomlinson approach and minimised when using the Das approach. On the other hand, at 150 per cent of working load conditions, the percentage reduction is maximised when using the Das approach and minimised when using the Bowles approach.

5.8 Comparison between conventional methods, FEM and SLT

This section displays the comparison between all methods FEM, conventional methods and the static load test. The load settlement behaviour of P73 and P71 has been determined based on the back calculated modified modulus (E_{mod}) values. The settlement values obtained for piles P73 and P71 using different approaches, FEM and static load test result has been tabulated in the table below.

Approach		Load (%)	Settlement(mm)	
			P73	P71
Static Load Test		100%	3.49	2.5
Conventional Methods	Bowles		20	11.2
	Tomlinson		10.9	6.1
	Das		9.9	5.5
FE Analysis			4.2	2.55
Static Load Test		150%	7.28	4.41
Conventional Methods	Bowles		30.7	16.8
	Tomlinson		21.9	12.1
	Das		21.3	11.9
FE Analysis			7.9	4.62

Table 5.31 Pile settlement values obtained for different analysis procedures using E_{mod}.

To obtain clarity for the comparison between all the methods based on (E_{mod}), the settlement curves behaviour obtained using the different computational procedures along with the static load test results have been plotted, as shown in the figures below:

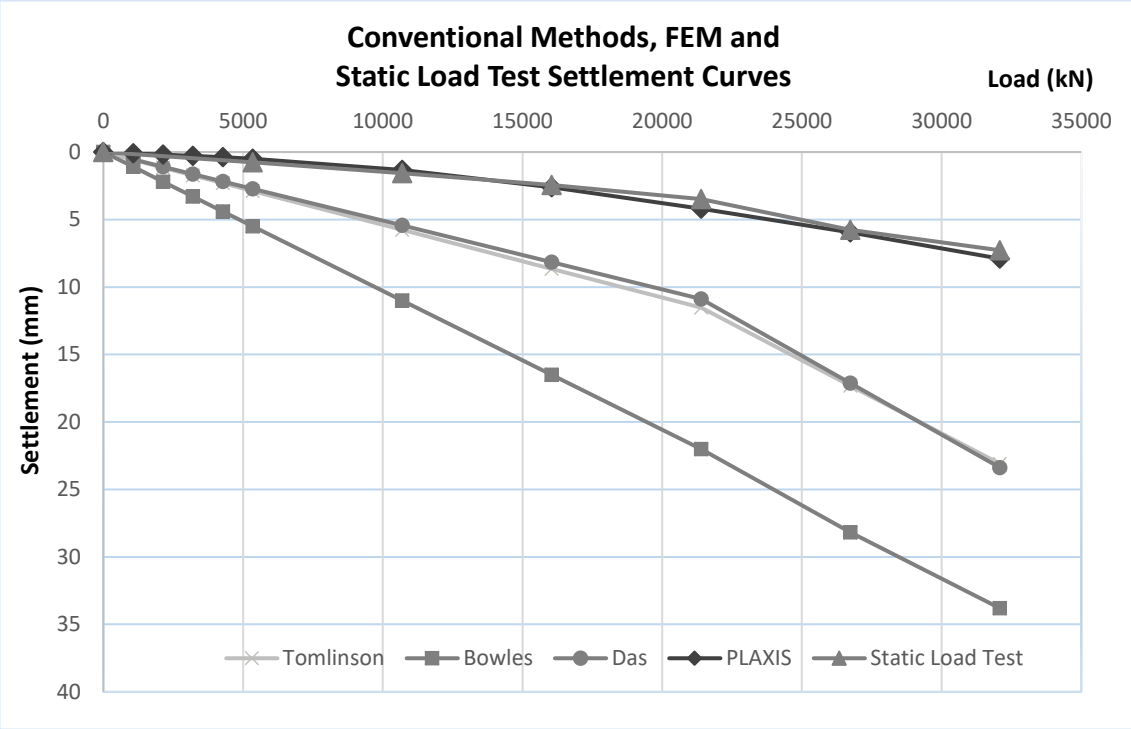

Fig. 5.39 Settlement curves for all methodologies for P73 using E_{mod} back-calculated

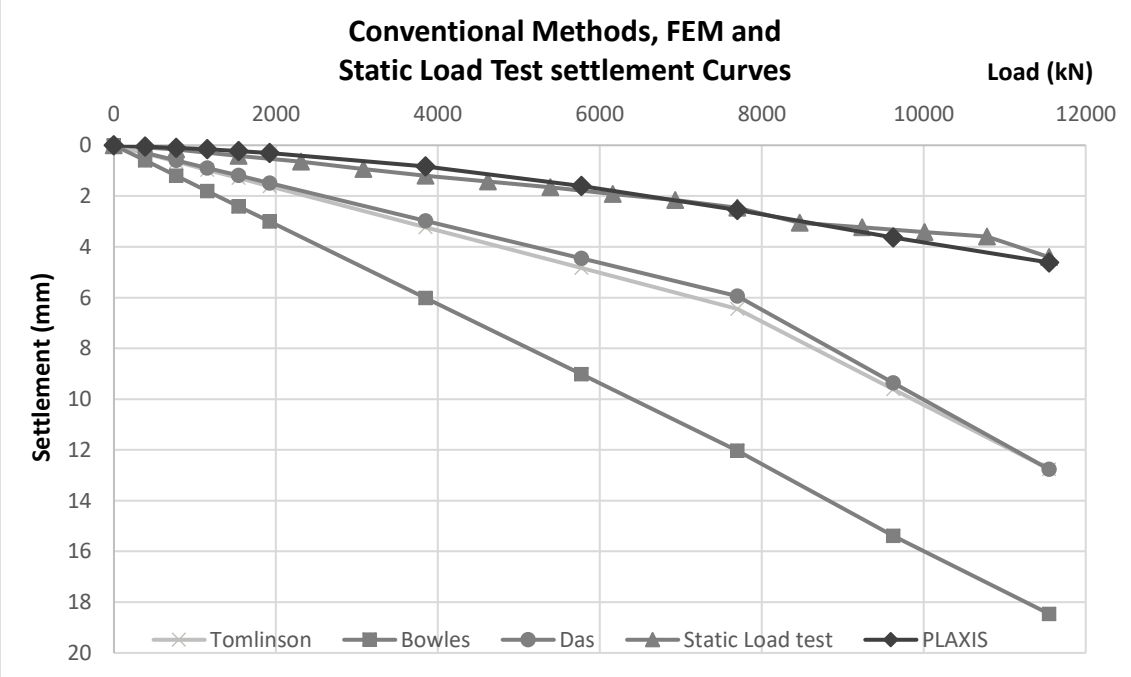

Fig. 5.40 Settlement curves for all methodologies for P71 using E_{mod} back-calculated

As per the preceding graphs, the load settlement behaviour curve evaluated using the different procedures follow a similar shape for P73 and P71. The nearly linear relationship exhibited in the initial portions of the load settlement graph indicates that

the axial load is carried in the shaft resistance. Comparing the load settlement performance exhibited by the conventional methods, the finite element analysis (FEM) and static load test (SLT) results of piles in terms of load transfer mechanism, it can be understood that for up to 100 per cent of the working load, the load is carried in shaft resistance for conventional methods. In the case of finite element analysis (FEM) and static load test results, however, the applied axial load is mainly carried in shaft resistance up to the maximum applied load of 150 per cent, which also can be proven by the FEM result - as shown in the figures below - and by the instrumented static load test which shows no load transfer to the pile tip (Section 5.4.3). This difference in the load transfer mechanism is the reason for high settlement values obtained by the conventional methods (empirical and analytical methods) when the applied loading condition exceeds 100 per cent of the working load conditions, even though (as previously mentioned) the effect of the settlement due base/tip resistance loading is less when compared to elastic shortening due to the high value of modified modulus of elasticity (E_{mod}).

The elastic shortening settlement component of P73 and P71 has been computed using the total length L of the pile in all three empirical and analytical approaches. However, at actual loading conditions, the overall length of the pile will not be contributing to the shaft resistance or frictional capacity of the pile. The length of pile which contributes to the shaft resistance is known as 'effective length' ($L_{effective}$). Mostly, the effective length will be shorter than the total length of the pile; this is confirmed from the instrument static load test (Section 5.4.3) and FEM model by PLAXIS, both of which are shown in the figures below.

For the pile design, mainly based on the modulus of elasticity of rock and rock quality designation (RQD) for pile settlement calculation, and for pile capacity calculation based on unconfined compressive strength (UCS) and RQD, the mentioned parameters and other parameters used in pile design are from the soil report. This generally underestimated the parameters due to a number of factors, such as the human impact on laboratory testing. This will lead to overestimating the pile length, hence the applied load will not have an influence on the last part of the piles. Therefore, in using the conventional methods settlement calculations to consider the total length of the pile (L) which is greater than the pile length effect by load, the effective length ($L_{effective}$). Using the full length of pile in settlement calculation will result in extensive settlement in comparison to FEM calculation and static load test (SLT). Otherwise, using the $L_{effective}$ in conventional method settlement calculation will give an adjacent result for FEM and the static load test (SLT). On the other hand, the conventional methods equation could be used to estimate and calculate the exact pile length required for design or, in other words, measurement of the effective length ($L_{effective}$) should be used for design purposes.

The load settlement curve obtained from FEM analysis matches that of the static load test results, with very negligible deviations in the settlement curve. The main reasons for this negligible deviation is the pile installation effect not being fully considered in the FEM modelling. In the FEM analysis, the pile is completely cylindrical with a uniform diameter throughout the full pile length. However, during the process of drilling, there may be a number of undulations created along the pile sides and the pile out of vertically accepted tolerance. That will lead to create a minor non-uniformity along the shaft surface which effects the SLT curve. Moreover, the loading time of static load test has also not been considered in the FEM analysis.

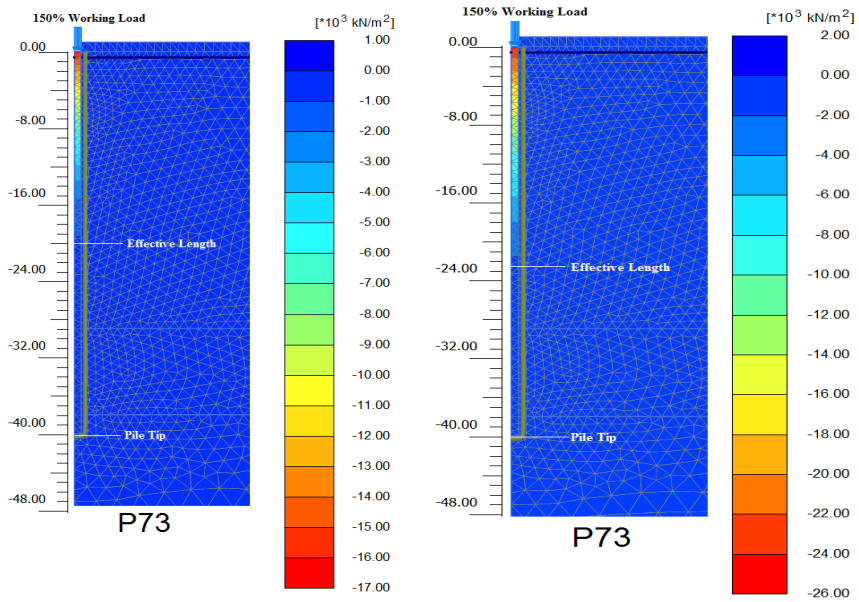

Fig. 5.41 Stress on pile P73 showing no stress on the lower part

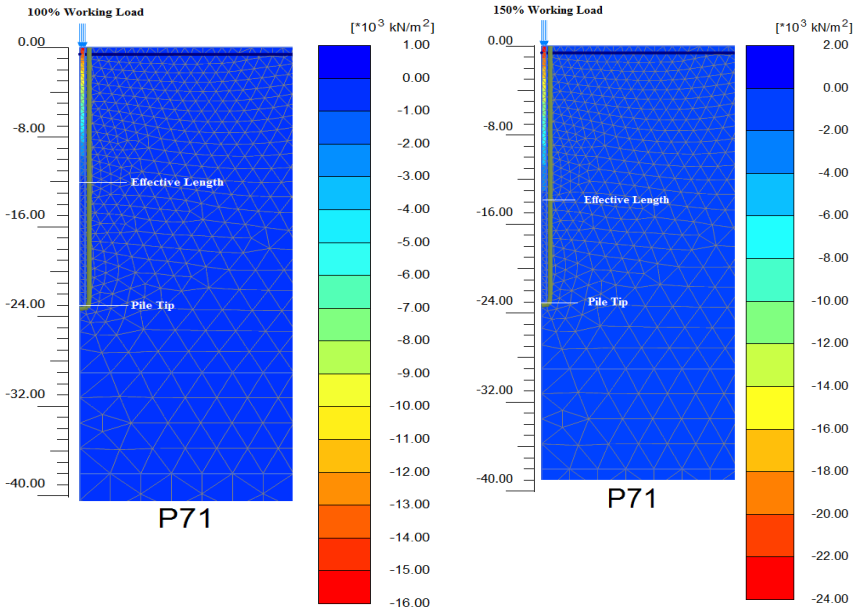

Fig. 5.42 Stress on pile P71 showing no stress on the lower part

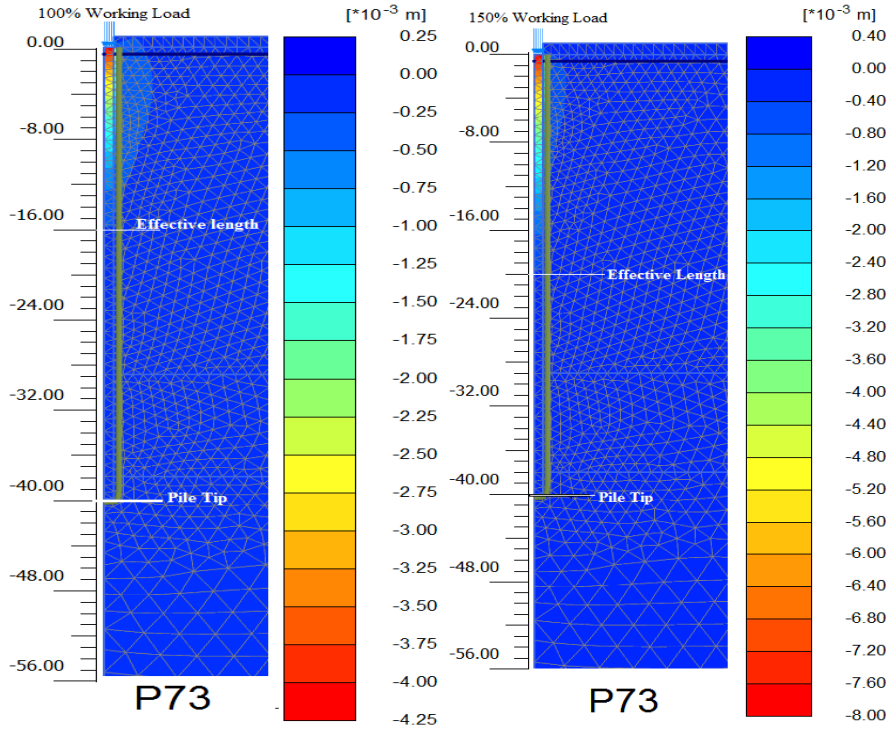

Fig. 5.43 Displacement influence on pile P73 showing no displacement on the lower part

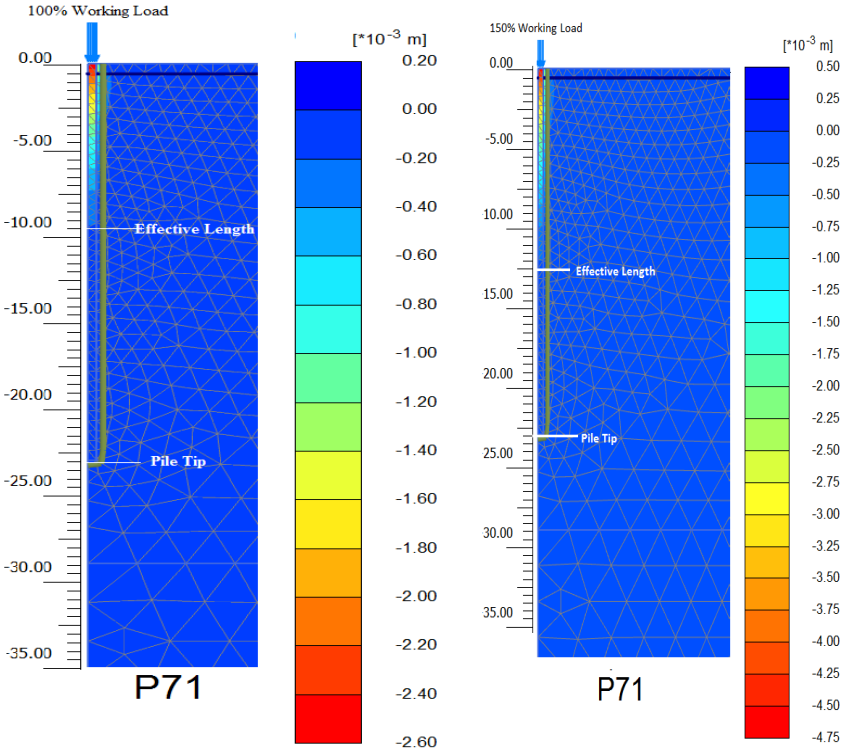

Fig. 5.44 Displacement influence on pile P71 showing no displacement on the lower part

5.9 Verification using MIDAS GTS 2D for piles P71 & P73

5.9.1 Introduction to MIDAS

MIDAS is 2D and 3D finite eliminate software which provides a numerical model for the project design. The FEM models are created using the accurate software and the analysis performed by MIDAS obtains relatively safe results. In this section, the analysis using MIDAS GTS software is used to compare and verify the results from PLAXIS 2D for pile P73 and pile P71. The objective of the research is to simulate the pile static load test conducted at site using MIDAS GTS NX, then comparing it with PLAXIS 2D. The analysis functions available within the software includes: static analysis, dynamic analysis, flow-stress coupling analysis, seepage analysis, construction stage analysis and consolidation analysis (Cai 2011). In this research, the axisymmetric model is created to simulate the static load tests for P73 and P71. The following section explains the step-by-step modelling procedure for MIDAS GTS.

5.9.2 Modelling procedure in MIDAS GTS

This section will explain the step-by-step modelling procedure for the static load test. The modelling procedure will be as per the following steps:

- Soil pile geometry
- Material modelling
- Defining properties
- Mesh generation and interface elements
- Boundary conditions
- Assigning loads
- Construction staging and analysis

As an outcome from the software, the pile load settlement behaviour will be obtained from the FEM model. More detail explanations for each stage of the FEM modelling simulation are as follows:

Step 1: Formation of soil pile geometry

An axisymmetric model has been created using MIDAS to simulate static load test and to analyse the load settlement behaviour of a single pile. The model geometry is a rectangle of 55 m width and 54 metre depth, as shown in the below figure. The model size has been determined in such a way as to to avoid the disturbances from the boundary condition and created by the reaction of the surrounding rock against the pile load into the simulation process (MIDAS GTS NX).

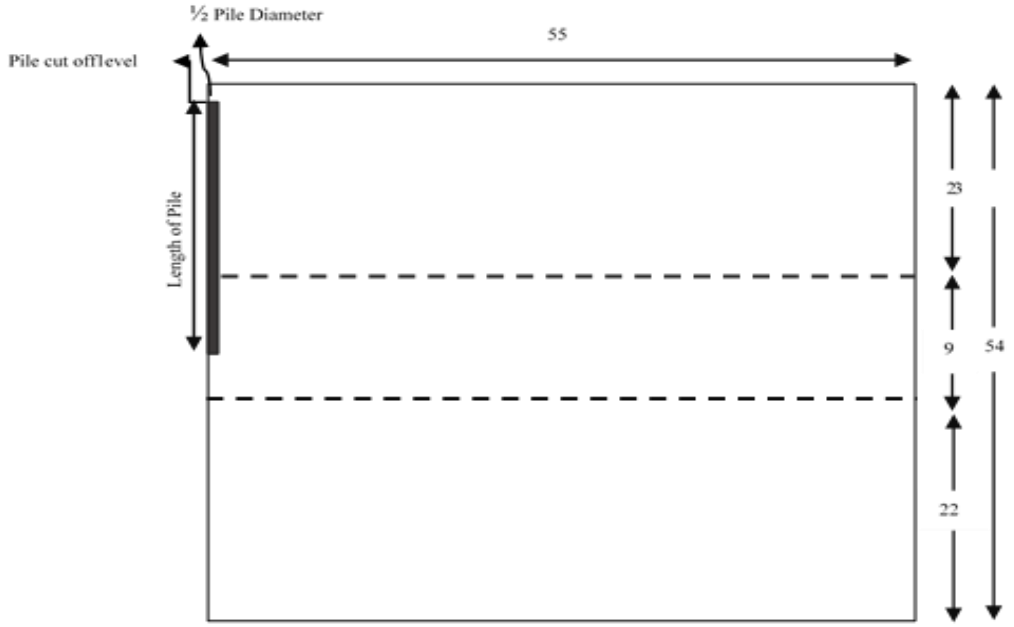

Fig. 5.45 Soil pile model Geometry

Step 2: Material modelling and constitutive law selection

The material model for the concrete pile and weak rock should be inputted. The data should be identical to PLAXIS data, using the same material model. The pile was modelled as an isotropic elastic material and the required input data for the pile model are concrete Young's modulus E, Poisson's ratio μ and unit weight γ. For the rock, the Mohr Coulomb model was used as the basic material for representing the elasto-plastic behaviour of the surrounding rock. This model requires six input parameters, which are: rock model of elasticity, Poisson's ratio μ, angle of friction ϕ, cohesion c, unit weight γ, angle of dilatancy ψ. permeability properties and drained/undrained. The soil and pile material characteristics used as input data are shown in the table below:

Material Properties	**Unit**	**Weak Rock Layer**			**Pile**
		1st Layer	**2nd Layer**	**3rd Layer**	
		6 - 29 m	**29 - 38 m**	**38-60 m**	
Unit weight, γ	kN/m^3	20	20	20	25
Saturated Unit Weight γ_{sat}	kN/m^3	21	21	21	
Angle of Friction, ϕ	(°)	45	45	45	-
Elastic Modulus, E	kN/m^2	50000	100000	60000	33142.8
Poisson's' ratio, μ	-	0.3	0.3	0.3	0.2
Cohesion, C	kN/m^2	46	100	62	-
Earth pressure at rest, K_o	(°)	0.29	0.29	0.29	-

Table 5.32 Soil and pile material characteristics for FEM analysis

Step 3: Defining properties to the soil-pile model

Once the material modelling and all material properties have been inputted in the software, it is then required to define the pile and rock properties. The schematic figure representation rock and pile properties are shown below.

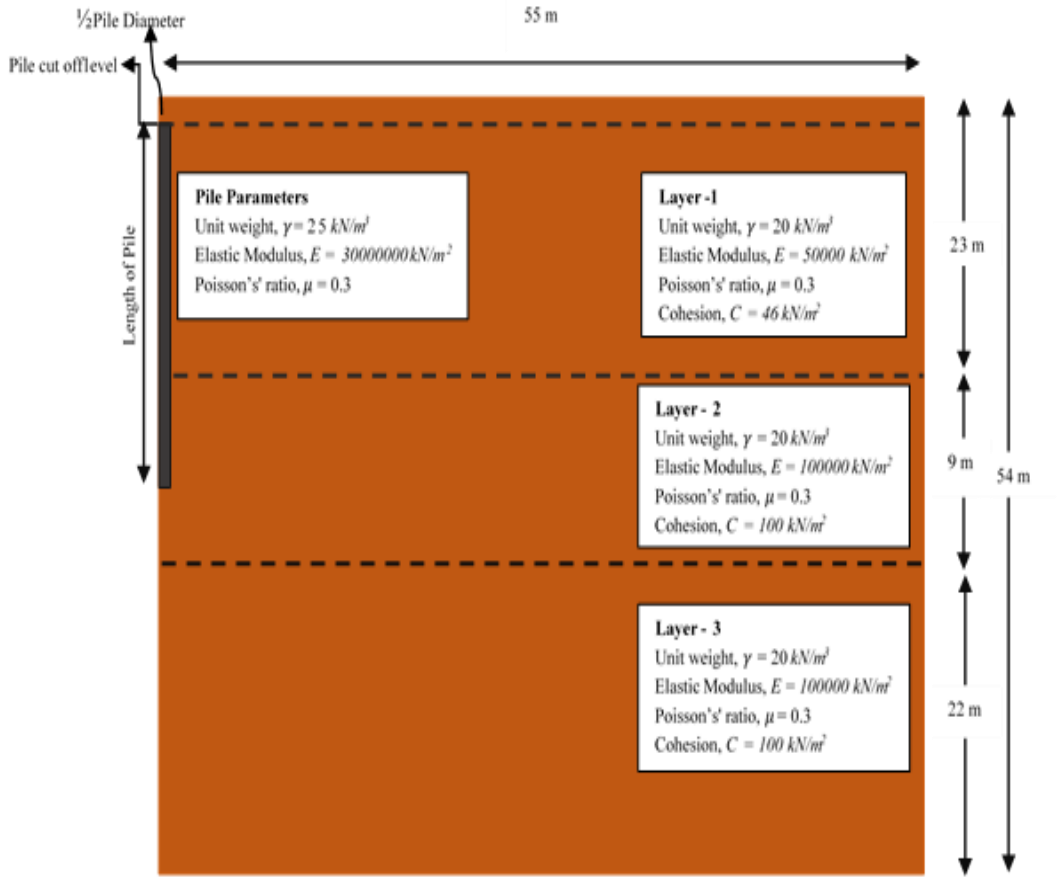

Fig. 5.46 Properties assigned to the pile and rock

Step 4: Mesh generation and interface elements

In the software, there is possibility to choose from quadrilateral, triangular and tri-quad 2D plane elements for mesh generation. In this model, the soil and pile models were divided into finer elements using a triangular element of size 0.2 mm and 2 mm respectively. The mesh generated for the three-layered soil system and pile model in the FEM program and the system generated adjacent to the rock pile interface is refined by creating finer mesh elements to achieve better results with a sufficient degree of accuracy. Also, the rock pile interface is simulated by creating interface elements with a reduction factor of 1.0, as shown in the figure below.

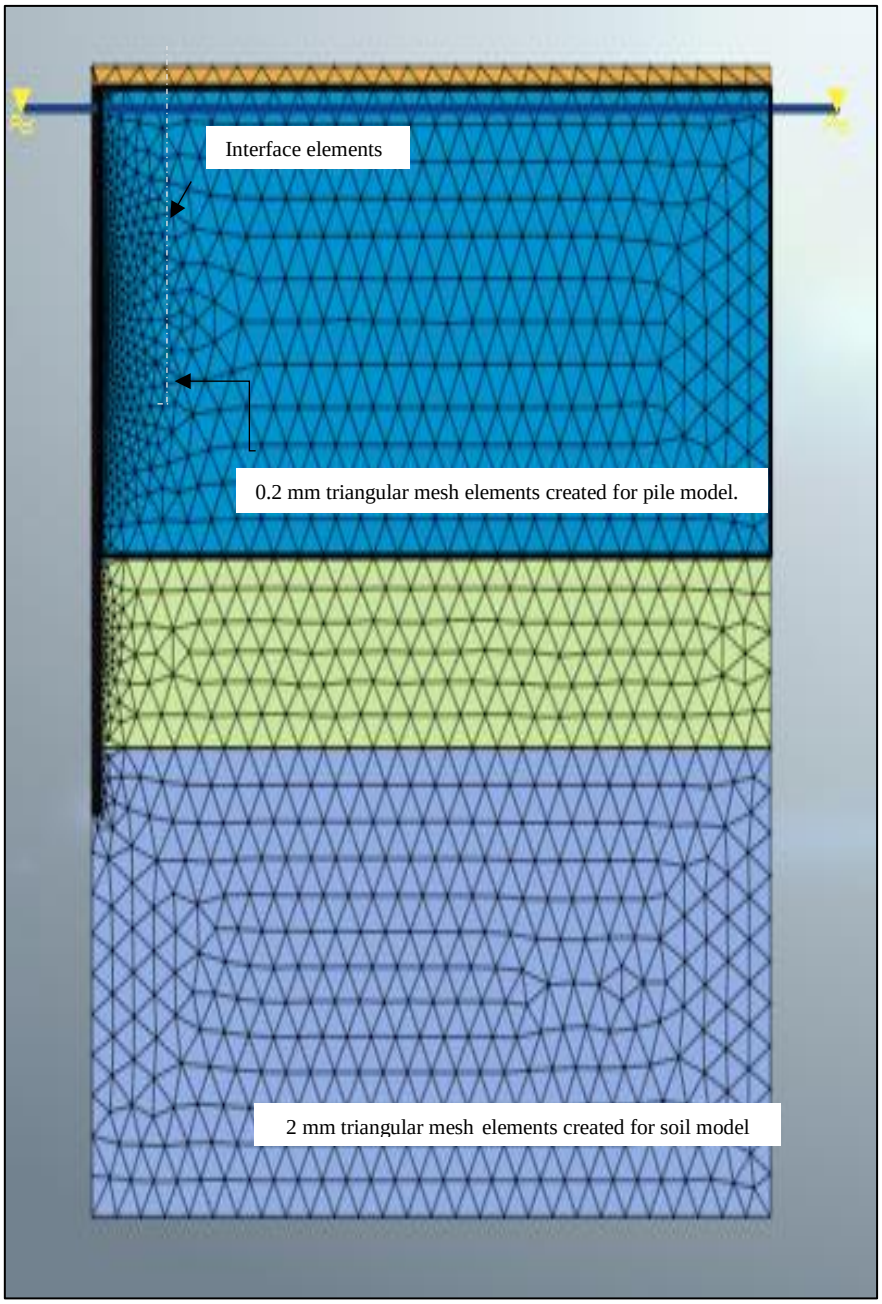

Fig. 5.47 Model meshed system

Step 5: Applying Boundary Conditions

After mesh generation, the boundary conditions are presented in the model. The boundary conditions were formed at the mesh edges in such a way that only vertical movements (i.e. u = 0) while confining any movements (i.e. u = v = 0) at the bottom horizontal boundary. The figure below shows the model boundary conditions.

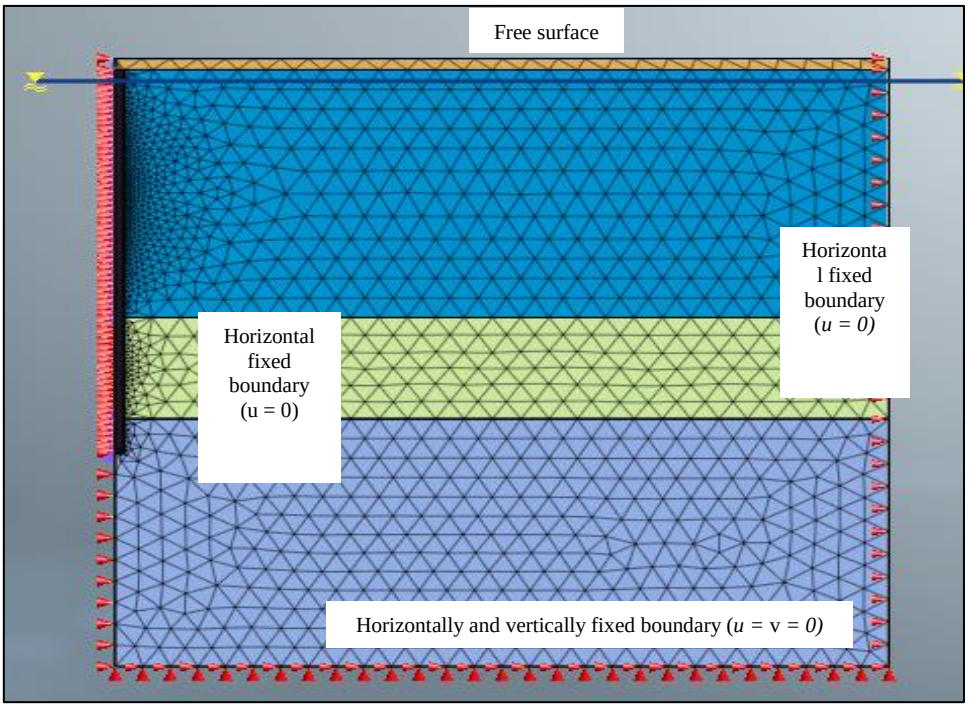

Fig. 5.48 Boundary conditions applied for soil pile model

Step 6: Assigning static loads to the pile

Firstly, the self-weight of the model is activated for the all mesh sets of the model. Then the test load conditions are applied on the pile elements in stages, similar to the loading mechanism in the static load testing. The total test load was applied as uniform pressure load acting on the top edge of the pile element. The maximum pressure loads applied, corresponding to the test load conditions of the pile, are tabulated as per the table below.

Number	Load%	Load	Surface P
0	0	0	0
1	0.05	385	766
2	0.1	770	1531
3	0.15	1155	2297
4	0.2	1540	3063
5	0.25	1925	3828
6	0.5	3850	7656
7	0.75	5775	11484
8	1.0	7700	15313
9	1.25	9625	19141
10	1.50	11550	22969

Table 5.33 Imposed load/pressure on pile P71

Number	Load%	Load	Surface P
0	0	0	0
1	0.05	1069.65	806
2	0.1	2139.3	1611
3	0.15	3208.95	2417
4	0.2	4278.6	3222
5	0.25	5348.25	4028
6	0.5	10696.5	8055
7	0.75	16044.75	12083
8	1.0	21393	16111
9	1.25	26741.25	20139
10	1.50	32089.5	24166

Table 5.34 Imposed load/pressure on pile P73

The pressure loads were imposed on the pile in increments of 10, 20, 30,40,50 ……, 140, 150 per cent, simulating the pile static loading conditions of the pile. The schematic representation of the pressure load acting on the pile top is shown in the figure below.

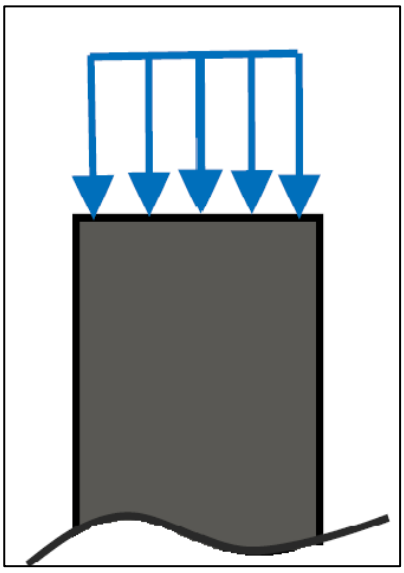

Fig. 5.49 Pressure load acting on top of pile element

Step 7: Construction Staging and Analysis

To define the construction stage, the mesh sets and loading conditions are activated and deactivated the mesh sets and loading conditions by sequence, which is applied to simulate the installation effect of pile in the soil strata. The material properties for pile, rock and

water level can also be justified for each step. The following stages show how the piles were simulated in the model:

- Stage 1: Rock and pile materials were activated along with a rigid interface and the water level defined at one metre below ground level/pile cut off level to simulate the dewatering conditions at site.
- Step 2: The rigid interface elements were deactivated and the line interface elements activated to stimulate the pile installation effect and the frictional resistance mobilised at the soil pile interface. The top one metre layer of rock above the pile was deactivated to avoid any heaving. During the construction stages, the settlement has been reset to zero to neglect the settlement caused by the activation of the existing rock and pile construction effect.
- Step 3: The loading phase has been performed by activating the uniform distributed load at the pile top in incremental stages of 10, 20, 30 …..through to 150 per cent.

The analysis was then performed: the result of pile vertical settlement of the pile is shown in the figure below:

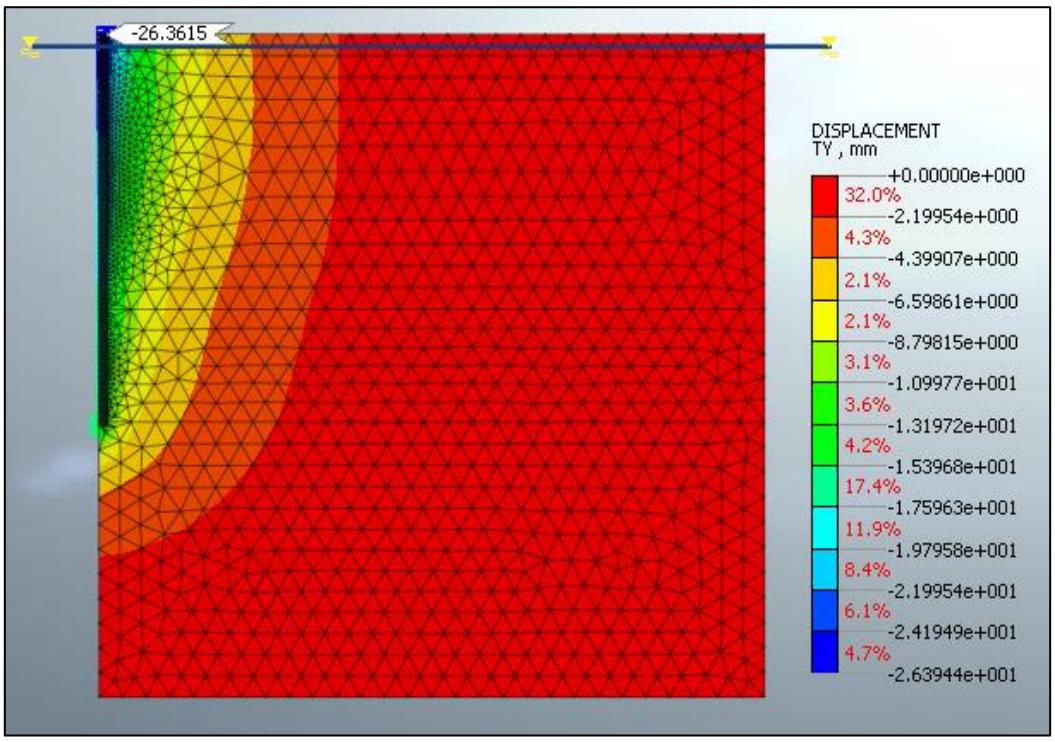

Fig. 5.50 Pile vertical settlement

5.9.3 Compression between PLAXIS 2D and MIDAS GTS 2D

In this section, the settlement from PLAXIS and MIDAS GTS is compared by using the same soil parameters used in back calculation for Piles P71 and P73. The table below shows the soil and pile design parameters for P71 used in the software.

Pile Information P71	Cut off Level	-7	m
	Toe Level	-30	m
	Pile length	23	m
	Pile Diameter	0.8	kN
	Working Load	7700	m
	Area of Pile	0.5029	kN
	Test Load	11550	m^2
	Concrete Modulus (E_c)	33142.8	MN/m^2
Soil Properties			
Layer 1 (6-29)	Poisson ratio, m	0.3	
	Young's Modulus of soil (E_s)	5000	MN/m^2
	Cohesion	75	kN/m^2
	Angle of friction	45°	
Layer 2 (29-38)	Poisson ratio, m	0.3	
	Young's Modulus of soil (E_s)	5000000	MN/m^2
	Cohesion	100	kN/m^2
	Angle of friction	45°	
Layer 3 (38-60)	Poisson ratio, m	0.3	
	Young's Modulus of soil (E_s)	5000000	MN/m^2
	Cohesion	62	kN/m^2
	Angle of friction	45°	

Table 5.35 Input data and materials properties for P71

The settlement results for P71 is summarised in the table and figure below:

#	%	Load [kN]	Surface P [kN/m^2]	Settlement (PLAXIS) [mm]	Settlement (MIDAS) [mm]
0	0	0	0	0.00	0.00
1	0.05	385	766	0.05	0.04
2	0.1	770	1531	0.11	0.07
3	0.15	1155	2297	0.16	0.11
4	0.2	1540	3063	0.23	0.15
5	0.25	1925	3828	0.30	0.19
6	0.5	3850	7656	0.83	0.57
7	0.75	5775	11484	1.60	1.18
8	1.0	7700	15313	2.55	2.05
9	1.25	9625	19141	3.64	3.21
10	1.50	11550	22969	4.62	4.66

Table 5.36 Settlement results from PLAXIS 2D and MIDAS GTS P71

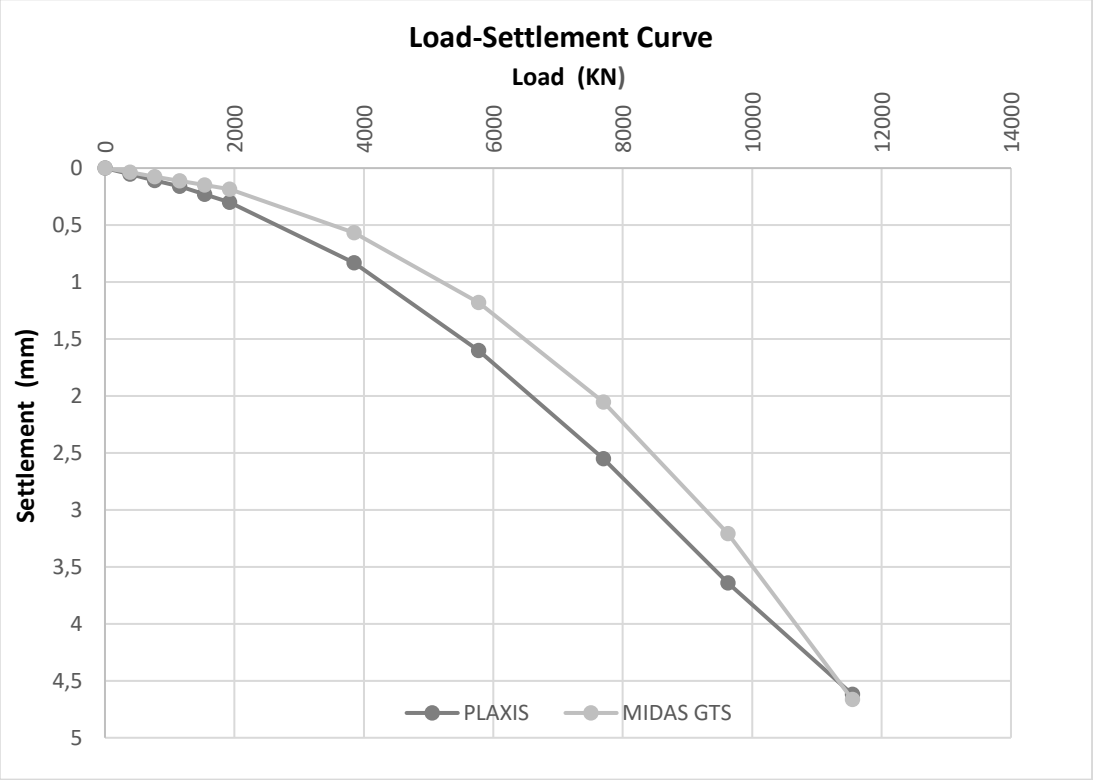

Fig. 5.51 Load vs settlement curve PLAXIS- MIDAS GTS P71

The table below shows the soil and pile design parameters for P73 used in the software.

Pile Information P73	Cut off Level	-7	m
	Toe Level	-47	m
	Pile length	40	m
	Pile Diameter	1.3	m
	Working Load	21393	kN
	Area of Pile	1.3279	m^2
	Test Load	32089.5	kN
	Concrete Modulus (Ec)	33142.8	MN/m^2
Soil Properties			
Layer 1 (6-29)	Poisson ratio, m	0.3	
	Young's Modulus of soil (Es)	4250	MN/m^2
	Cohesion	95	kN/m^2
	Angle of friction	45°	
Layer 2 (29-38)	Poisson ratio, m	0.3	
	Young's Modulus of soil (Es)	5000	MN/m2
	Cohesion	100	kN/m2
	Angle of friction	45°	
Layer 3 (38-60)	Poisson ratio, m	0.3	
	Young's Modulus of soil (Es)	5000	MN/m^2
	Cohesion	95	kN/m^2
	Angle of friction	45°	

Table 5.37 Input data and materials properties for P73

The settlement results for P73 is summarised in the table and figure below.

#	%	Load	Surface P	Settlement (PLAXIS)	Settlement (MIDAS)
0	0	0	0	0	0.00
1	0.05	1069.65	806	0.089	0.08
2	0.1	2139.3	1611	0.18	0.16
3	0.15	3208.95	2417	0.28	0.23
4	0.2	4278.6	3222	0.38	0.31
5	0.25	5348.25	4028	0.49	0.39
6	0.5	10696.5	8055	1.34	1.20
7	0.75	16044.75	12083	2.6	2.49
8	1.0	21393	16111	**4.2**	**4.31**
9	1.25	26741.25	20139	5.96	6.67
10	1.50	32089.5	24166	**7.9**	**9.63**

Table 5.38 Settlement results from PLAXIS 2D and MIDAS GTS P73

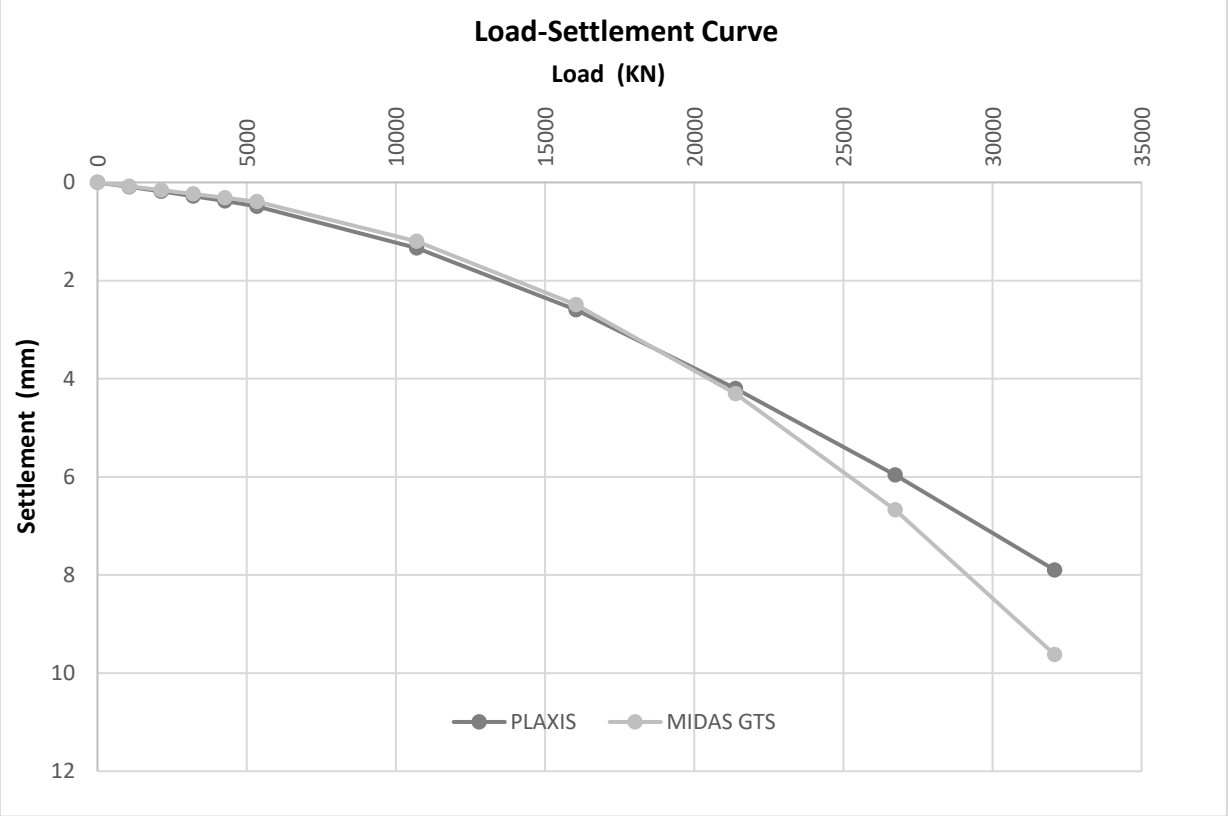

Fig. 5.52 Load vs settlement curve PLAXIS- MIDAS GTS P73

As shown above in P71, the difference between PLAXIS 2D and MIDAS GTS was + 0.04 mm; which is much less and almost similar. In P73 the difference was 1.73 mm, which is acceptable due to the length of pile (44 m). On the other hand, for P73, the value E_{mod} back-calculated using MIDAS GTS is higher than when PLAXIS is used.
For pile 73, the values of (E_{mod}) back-calculated using MIDAS GTS in comparison to PLAXIS is shown in the table below.

Soil Layers	**Back-calculated (E_{mod})**	**PLAXIS**	**MIDAS GTS**	
Layer 1 (6-29)	Young's Modulus of soil (E_{mod})	**4250**	**5500**	MN/m^2
Layer 2 (29-38)	Young's Modulus of soil (E_{mod})	**5000**	**5500**	MN/m^2
Layer 3 (38-60)	Young's Modulus of soil (E_{mod})	**5000**	**5500**	MN/m^2

Table 5.39 Values of (E_{mod}) using MIDAS GTS & PLAXIS

The back-calculated values are obtained from the curve below.

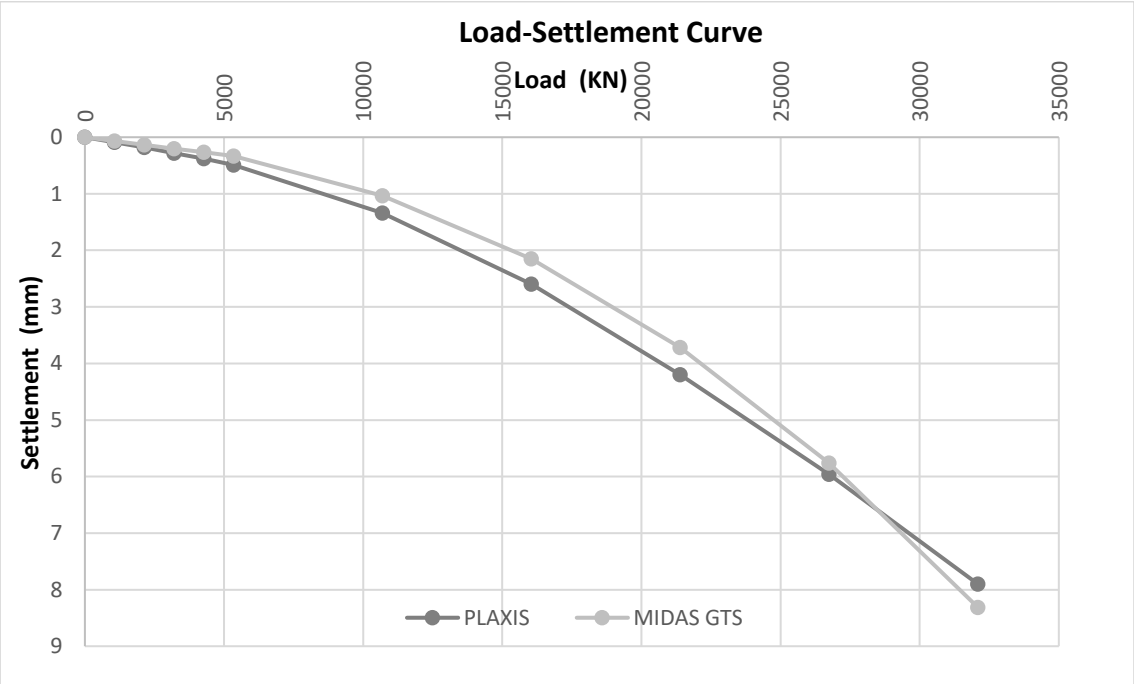

Fig. 5.53 MIDAS GTS Load-settlement curve using new back-calculated E_{mod} for P73

5.10 Modified modulus of elasticity E_{mod} for 116 piles back-calculated from SLT

5.10.1 Introduction

In this section, a similar study to the previous analysis for piles P73 and P71 is conducted for 116 piles, representing 28 projects and including approximately 45 towers. As explained previously, the load settlement behaviour of the pile is highly dependent on the weak rock modulus of elasticity and the discrepancy between the calculated settlement based on (Es); the settlement from static load test values were mainly due to the under-estimation of the modulus of elasticity (Es) of the weak rock. Therefore, in this section the modified value of elastic modulus of the soil (E_{mod}) will be determined using the back analysis of static load results via the finite element method (FEM) for the 116 Piles. The pile summary sheet for all 116 piles can be referred to in Appendix A.

5.10.2 Summary of Result of E_{mod} for 116 piles

Pile #	Length [m]	Diameter [m]	Working Load [kN]	Test Load [kN]	$E_{Soil\ Report}$ (Es) [MN/m²]	$E_{Back\ Calculated}$ (Emod) [MN/m²]	Increment in E
P1	21	1.2	15000	22500	120	8000	67 times

Table 5.40 $E_{Soil\ Report}$ (E_s) and $E_{Back\ Calculated}$ from load test (E_{mod}), Project 1

Pile #	Length [m]	Diameter [m]	Working Load [kN]	Test Load [kN]	$E_{Soil\ Report}$ (Es) [MN/m²]	$E_{Back\ Calculated}$ (Emod) [MN/m²]	Increment in E
P2	18.5	0.6	2880	4320	90	2350	26 times
P3	19.5	0.75	3961	5941.5	90	4000	44 times
P4	27	1.2	9425	14137.5	90	2000	22 times
P5	20	1.2	7728	11592	90	1000	11 times

Table 5.41 $E_{Soil\ Report}$ (E_s) & $E_{Back\ Calculated}$ from load test (E_{mod}), Project 2.

Pile #	Length [m]	Diameter [m]	Working Load [kN]	Test Load [kN]	$E_{Soil\ Report}$ (Es) [MN/m²]	$E_{Back\ Calculated}$ (Emod) [MN/m²]	Increment in E
P6	18.2	0.9	8400	12600	90	2000	22 times
P7	22.2	1.2	15000	22500	90	2000	22 times
P8	22.2	1.2	17000	25500	90	2500	28 times
P9	22.2	1.2	15000	22500	90	2000	22 times
P10	18.2	0.9	8400	12600	90	1800	20 times
P11	18.2	0.9	8400	12600	90	2000	22 times

Table 5.42 $E_{Soil\ Report}$ (E_s) and $E_{Back\ Calculated}$ from load test (E_{mod}), Project 3

Pile #	Length [m]	Diameter [m]	Working Load [kN]	Test Load [kN]	$E_{Soil\ Report}$ (Es) [MN/m²]	$E_{Back\ Calculated}$ (Emod) [MN/m²]	Increment in E
P12	14.4	0.6	2540	3810	78	2200	28.2 times
					90	2200	24.4 times
					216	2200	10.2 times
					192	2200	11.5 times
P13	23.1	0.8	6447	9670.5	78	2500	32.1 times
					90	2500	27.8 times
					216	2500	11.6 times
					192	2500	13.0 times
P14	23	1	8400	12600	78	2500	32.1 times
					90	2500	27.8 times
					216	2500	11.6 times
					192	2500	13.0 times
P15	23.3	1.2	12700	19050	78	2500	32.1 times
					90	2500	27.8 times
					216	2500	11.6 times
					192	2500	13.0 times

Table 5.43 $E_{Soil\ Report}$ (Es) and $E_{Back\ Calculated}$ from load test (Emod), Project 4

Pile #	Length [m]	Diameter [m]	Working Load [kN]	Test Load [kN]	$E_{Soil\ Report}$ (Es) [MN/m²]	$E_{Back\ Calculated}$ (Emod) [MN/m²]	Increment in E
P16	19	0.8	6029	9043.5	85	3000	35.3 times
P17	17.4	0.7	5050	7575	85	2000	23.5 times
P18	17.4	0.7	5050	7575	85	1500	17.6 times
P19	17.4	0.7	5050	7575	85	3000	35.3 times
P20	19	0.8	6029	9043.5	85	1300	15.3 times

Table 5.44 $E_{Soil\ Report}$ (Es) and $E_{Back\ Calculated}$ from load test (Emod), Project 5

Pile #	Length [m]	Diameter [m]	Working Load [kN]	Test Load [kN]	$E_{Soil\ Report}$ (Es) [MN/m²]	$E_{Back\ Calculated}$ (Emod) [MN/m²]	Increment in E
P21	22.5	0.8	6000	9000	109	1500	13.8 times
					180	1500	8.3 times
P22	25.5	1	11000	16500	109	2000	18.3 times
					180	2000	11.5 times
P23	25	1	10000	15000	109	2000	18.3 times
					180	2000	11.1 times

Table 5.45 $E_{Soil\ Report}$ (Es) and $E_{Back\ Calculated}$ from load test (Emod), Project 6

Pile #	Length [m]	Diameter [m]	Working Load [kN]	Test Load [kN]	$E_{Soil\ Report}$ (Es) [MN/m²]	$E_{Back\ Calculated}$ (Emod) [MN/m²]	Increment in E
P24	18	1	6850	10275	84	3000	35.7 times
					180	3000	16.7 times
P25	17	0.8	5000	7500	84	3000	35.7 times
					180	3000	16.7 times

Table 5.46 $E_{Soil\ Report}$ (E_s) and $E_{Back\ Calculated}$ from load test (E_{mod}), Project 7

Pile #	Length [m]	Diameter [m]	Working Load [kN]	Test Load [kN]	$E_{Soil\ Report}$ (Es) [MN/m²]	$E_{Back\ Calculated}$ (Emod) [MN/m²]	Increment in E
P26	23.5	1	7300	10950	78	4000	51.3 times
					120	4000	33.3 times

Table 5.47 $E_{Soil\ Report}$ (E_s) and $E_{Back\ Calculated}$ from load test (E_{mod}), Project 8

Pile #	Length [m]	Diameter [m]	Working Load [kN]	Test Load [kN]	$E_{Soil\ Report}$ (Es) [MN/m²]	$E_{Back\ Calculated}$ (Emod) [MN/m²]	Increment in E
P27	14	1	6873	10309.5	84	1000	11.9 times
P28	14	1	7382	11073	84	2500	29.8 times
P29	23	1	10551	15826.5	84	4500	53.6 times
P30	8.5	0.7	3509	5236.5	84	2000	23.8 times
P31	15	0.7	4467	6700.5	84	2000	23.8 times
P32	13	0.8	4903	7354.5	84	1000	11.9 times
P33	18.5	0.8	6333	9499.5	84	3500	41.7 times

Table 5.48 $E_{Soil\ Report}$ (E_s) and $E_{Back\ Calculated}$ from load test (E_{mod}), Project 9

Pile #	Length [m]	Diameter [m]	Working Load [kN]	Test Load [kN]	$E_{Soil\ Report}$ (Es) [MN/m²]	$E_{Back\ Calculated}$ (Emod) [MN/m²]	Increment in E
P34	25.5	0.9	6000	9000	60	5000	83.3 times
P35	23	1.2	10500	15750	60	6000	100 times
P36	23	1.2	8000	12000	60	3000	50.0 times
P37	24	0.9	5000	7500	60	2750	45.8 times
P38	27	0.9	6000	12000	60	4000	66.7 times
P39	30	1.2	10000	20000	60	3500	58.3 times

Table 5.49 $E_{Soil\ Report}$ (E_s) and $E_{Back\ Calculated}$ from load test (E_{mod}), Project 10

Pile #	Length [m]	Diameter [m]	Working Load [kN]	Test Load [kN]	$E_{Soil\ Report}$ (Es) [MN/m²]	$E_{Back\ Calculated}$ (Emod) [MN/m²]	Increment in E
P40	20	0.75	5950	8925	60	6000	100 times
P41	23.5	0.75	6250	9375	60	6000	100 times
P42	21	0.75	6250	9375	60	8750	145.8 times
P43	21	0.75	6250	9375	60	5600	93.3 times
P44	17	0.75	5300	7950	60	4500	75.0 times
P45	23.5	0.75	6250	9375	60	6000	100 times
P46	20	0.75	5950	8925	60	4500	75.0 times
P47	20	0.75	5950	8925	60	6500	108.3 times
P48	17	0.75	5300	7950	60	6000	100 times
P49	19	0.75	5600	8400	60	6000	100 times

Table 5.50 $E_{Soil\ Report}$ (E_s) and $E_{Back\ Calculated}$ from load test (E_{mod}), Project 11

Pile #	Length [m]	Diameter [m]	Working Load [kN]	Test Load [kN]	$E_{Soil\ Report}$ (Es) [MN/m²]	$E_{Back\ Calculated}$ (Emod) [MN/m²]	Increment in E
P50	27	1.2	11000	16500	72	6000	83.3 times
P51	22.25	1	5900	8850	72	1500	20.8 times

Table 5.51 $E_{Soil\ Report}$ (E_s) and $E_{Back\ Calculated}$ from load test (E_{mod}), Project 12

Pile #	Length [m]	Diameter [m]	Working Load [kN]	Test Load [kN]	$E_{Soil\ Report}$ (Es) [MN/m²]	$E_{Back\ Calculated}$ (Emod) [MN/m²]	Increment in E
P52	20	0.8	11708.3	17562.45	100	2500	25 times

Table 5.52 $E_{Soil\ Report}$ (E_s) and $E_{Back\ Calculated}$ from load test (E_{mod}), Project 13

Pile #	Length [m]	Diameter [m]	Working Load [kN]	Test Load [kN]	$E_{Soil\ Report}$ (Es) [MN/m²]	$E_{Back\ Calculated}$ (Emod) [MN/m²]	Increment in E
P53	24	1.2	7830.4	15660.80	90	20000	25 times
P54	27	1.2	8886.7	17773.40	90	20000	222.2 times
P55	14.5	0.75	2270	3405	90	11000	122.2 times
P56	13	0.75	2250	3375	90	6000	66.7 times
P57	21	1.2	6480	9720	90	12000	133.3 times
P58	24	0.75	4420	8840	90	12000	133.3 times
P59	25	1.2	6960	10440	90	20000	222.2 times

Table 5.53 $E_{Soil\ Report}$ (E_s) and $E_{Back\ Calculated}$ from load test (E_{mod}), Project 14

Pile #	Length [m]	Diameter [m]	Working Load [kN]	Test Load [kN]	$E_{Soil\ Report}$ (Es) [MN/m²]	$E_{Back\ Calculated}$ (Emod) [MN/m²]	Increment in E
P60	21	0.75	5564	8346	90	2000	22.2 times
P61	20	0.75	5000	7500	90	3500	38.9 times
P62	21	0.75	5664	8496	90	3500	38.9 times
P63	24.5	1	9714	14571	90	3500	38.9 times
P64	24.5	1	9714	14571	90	3500	38.9 times
P65	20.5	0.75	5000	7500	90	2000	22.2 times
P66	19.5	1	7400	11100	90	2000	22.2 times

Table 5.54 $E_{Soil\ Report}$ (Es) and $E_{Back\ Calculated}$ from load test (Emod), Project 15

Pile #	Length [m]	Diameter [m]	Working Load [kN]	Test Load [kN]	$E_{Soil\ Report}$ (Es) [MN/m²]	$E_{Back\ Calculated}$ (Emod) [MN/m²]	Increment in E
P67	36.5	1.2	16900	25350	72	1500	20.8 times
P68	36.5	1.2	16900	25350	72	2500	34.7 times
P69	30.1	0.9	9000	13500	72	3500	48.6 times
P70	23	0.75	4000	6000	72	7000	97.2 times

Table 5.55 $E_{Soil\ Report}$ (Es) and $E_{Back\ Calculated}$ from load test (Emod), Project 16

Pile #	Length [m]	Diameter [m]	Working Load [kN]	Test Load [kN]	$E_{Soil\ Report}$ (Es) [MN/m²]	$E_{Back\ Calculated}$ (Emod) [MN/m²]	Increment in E
P71	23	0.8	7700	11550	60	5000	83.3 times
					100	5000	50.0 times
					62	5000	80.6 times
P72	22	0.8	7500	11250	60	3000	50.0 times
					100	3000	30.0 times
					62	3000	48.4 times
P73	40	1.3	21393	32089.5	60	4250	70.8 times
					100	5000	50.0 times
					62	5000	80.6 times
P74	34	1.3	18000	27000	60	2700	45.0 times
					100	2700	27.0 times
					62	2700	43.5 times
P75	31.30	1.3	16400	24600	60	1450	24.1 times
					100	1450	14.5 times
					62	1450	23.4 times
P76	46	1.3	21393	32089.5	60	2000	33.3 times
					100	2100	20.0 times
					62	2200	33.9 times

Table 5.56 $E_{Soil\ Report}$ (Es) and $E_{Back\ Calculated}$ from load test (Emod), Project 17

Pile #	Length [m]	Diameter [m]	Working Load [kN]	Test Load [kN]	$E_{Soil\ Report}$ (Es) [MN/m²]	$E_{Back\ Calculated}$ (Emod) [MN/m²]	Increment in E
P77	31	1	11367	17050.5	60	4000	66.6 times
P78	27.5	1.2	13865	20797,5	60	3500	58.3 times
P79	15	0.75	3910	5865	60	900	15.0 times

Table 5.57 $E_{Soil\ Report}$ (E_s) and $E_{Back\ Calculated}$ from load test (E_{mod}), Project 18

Pile #	Length [m]	Diameter [m]	Working Load [kN]	Test Load [kN]	$E_{Soil\ Report}$ (Es) [MN/m²]	$E_{Back\ Calculated}$ (Emod) [MN/m²]	Increment in E
P80	17.4	0.6	4010	6015	90	1250	13.9 times

Table 5.58 $E_{Soil\ Report}$ (E_s) and $E_{back\text{-}Calculated}$ from load test (E_{mod}), Project 19

Pile #	Length [m]	Diameter [m]	Working Load [kN]	Test Load [kN]	$E_{Soil\ Report}$ (Es) [MN/m²]	$E_{Back\ Calculated}$ (Emod) [MN/m²]	Increment in E
P81	38	1.2	18000	27000	60	6500	108.3 times
P82	38	1.2	18000	27000	60	3500	58.3 times
P83	38	1.2	18250	27375	60	5000	83.3 times
P84	13	0.8	3800	5700	60	2500	41.7 times
P85	13	0.8	3800	5700	60	2500	41.7 times

Table 5.59 $E_{Soil\ Report}$ (E_s) and $E_{back\text{-}Calculated}$ from load test (E_{mod}), Project 20

Pile #	Length [m]	Diameter [m]	Working Load [kN]	Test Load [kN]	$E_{Soil\ Report}$ (Es) [MN/m²]	$E_{Back\ Calculated}$ (Emod) [MN/m²]	Increment in E
P86	20	0.8	7000	10500	85	3600	42.4 times
P87	20	0.8	7000	10500	85	3600	42.4 times
P88	24	1.2	12700	19050	85	4200	49.4 times
P89	22	1.2	12700	19050	85	1600	18.8 times

Table 5.60 $E_{Soil\ Report}$ (E_s) and $E_{back\text{-}Calculated}$ from load test (E_{mod}), Project 21

Pile #	Length [m]	Diameter [m]	Working Load [kN]	Test Load [kN]	$E_{Soil\ Report}$ (Es) [MN/m²]	$E_{Back\ Calculated}$ (Emod) [MN/m²]	Increment in E
P90	32	1.2	10500	15750	55	4500	81.8 times
P91	32	1.2	11100	16650	55	4000	72.7 times
P92	45	1.2	16660	24990	55	4000	72.7 times
P93	32	1.2	9050	13575	55	1500	27.3 times
P94	25	1.2	8400	12600	55	1150	20.9 times
P95	25	1.2	8400	12600	55	4000	72.7 times

Table 5.61 $E_{Soil\ Report}$ (E_s) and $E_{back\text{-}Calculated}$ from load test (E_{mod}), Project 22

Pile #	Length [m]	Diameter [m]	Working Load [kN]	Test Load [kN]	$E_{Soil\ Report}$ (Es) [MN/m²]	$E_{Back\ Calculated}$ (Emod) [MN/m²]	Increment in E
P96	20	0.9	3000	4500	75	3000	40 times
P97	30	1.2	8600	12900	75	3000	40 times
P98	20	0.6	1900	2850	75	3000	40 times
P99	39	1.2	17300	25950	75	15000	200 times

Table 5.62 $E_{Soil\ Report}$ (Es) and $E_{back\text{-}Calculated}$ from load test (Emod), Project 23

Pile #	Length [m]	Diameter [m]	Working Load [kN]	Test Load [kN]	$E_{Soil\ Report}$ (Es) [MN/m²]	$E_{Back\ Calculated}$ (Emod) [MN/m²]	Increment in E
P100	18	0.75	2289	3433.5	42	2000	47.6 times
P101	22.50	0.9	3612	5418	42	1500	35.7 times
P102	23	1	4420	6630	42	4500	107 times

Table 5.63 $E_{Soil\ Report}$ (Es) and $E_{back\text{-}Calculated}$ from load test (Emod), Project 24

Pile #	Length [m]	Diameter [m]	Working Load [kN]	Test Load [kN]	$E_{Soil\ Report}$ (Es) [MN/m²]	$E_{Back\ Calculated}$ (Emod) [MN/m²]	Increment in E
P103	15	0.75	3000	4500	24	1400	58.3 times
					60	2000	33.3 times
P104	18	1	5480	8220	24	6000	250 times
					60	10000	167 times

Table 5.64 $E_{Soil\ Report}$ (Es) and $E_{back\text{-}Calculated}$ from load test (Emod), Project 25

Pile #	Length [m]	Diameter [m]	Working Load [kN]	Test Load [kN]	$E_{Soil\ Report}$ (Es) [MN/m²]	$E_{Back\ Calculated}$ (Emod) [MN/m²]	Increment in E
P105	19.5	0.75	4770	7155	75	1700	22.7 times
P106	24	1	9100	13650	75	2000	26.7 times
P107	24	1.2	12570	18855	75	4500	60.0 times
P108	33	1.2	15500	23250	75	4500	60.0 times

Table 5.65 $E_{Soil\ Report}$ (Es) and $E_{back\text{-}Calculated}$ from load test (Emod), Project 26

Pile #	Length [m]	Diameter [m]	Working Load [kN]	Test Load [kN]	$E_{Soil\ Report}$ (Es) [MN/m²]	$E_{Back\ Calculated}$ (Emod) [MN/m²]	Increment in E
P109	23	0.7	3430	5145	60	4000	66.7 times
P110	23	1	5500	8250	60	1050	17.5 times
P111	25	1.2	7070	10605	60	1000	16.7 times
P112	22	0.8	4080	6120	60	1350	22.5 times
P113	23	1.5	9740	14610	60	1400	23.3 times

Table 5.66 $E_{Soil\ Report}$ (Es) and $E_{back\text{-}Calculated}$ from load test (Emod), Project 27

Pile #	Length [m]	Diameter [m]	Working Load [kN]	Test Load [kN]	E $_{Soil\ Report}$ (Es) [MN/m²]	E $_{Back\ Calculated}$ (Emod) [MN/m²]	Increment in E
P114	25	1	8258	12387	60*	5000	83.3 times
					60*	8000	133.3 times
P115	32	1.2	13652	20478	60*	4000	66.7 times
					60*	9500	158.3 times
P116	19	0.75	4142	6213	60*	1500	25.0 times
					60*	2500	41.7 times

*Different cohesion value for layer 1 & 2

Table 5.67 $E_{Soil\ Report}$ (E_s) and $E_{back\text{-}Calculated}$ from load test (E_{mod}), Project 28

5.10.3 Results Analysis and Interpretation

From the tables in the section above, the modulus of elasticity values obtained for several piles (116 piles) and different projects /plots are significantly diverse - from 900 Mpa to 15000 Mpa - and the increment in modulus of elasticity (E_{mod}) varied from 11 times to 200 times. As explained previously, this variation is totally acceptable as the UCS values obtained by the laboratory testing of rock samples also had a high variation range. This difference exhibited in the UCS values of various rock samples collected from different boreholes at the site shows the huge area and different projects. The deference between modulus of elasticity, (E_{mod}) values will reduce as per the plot/project.

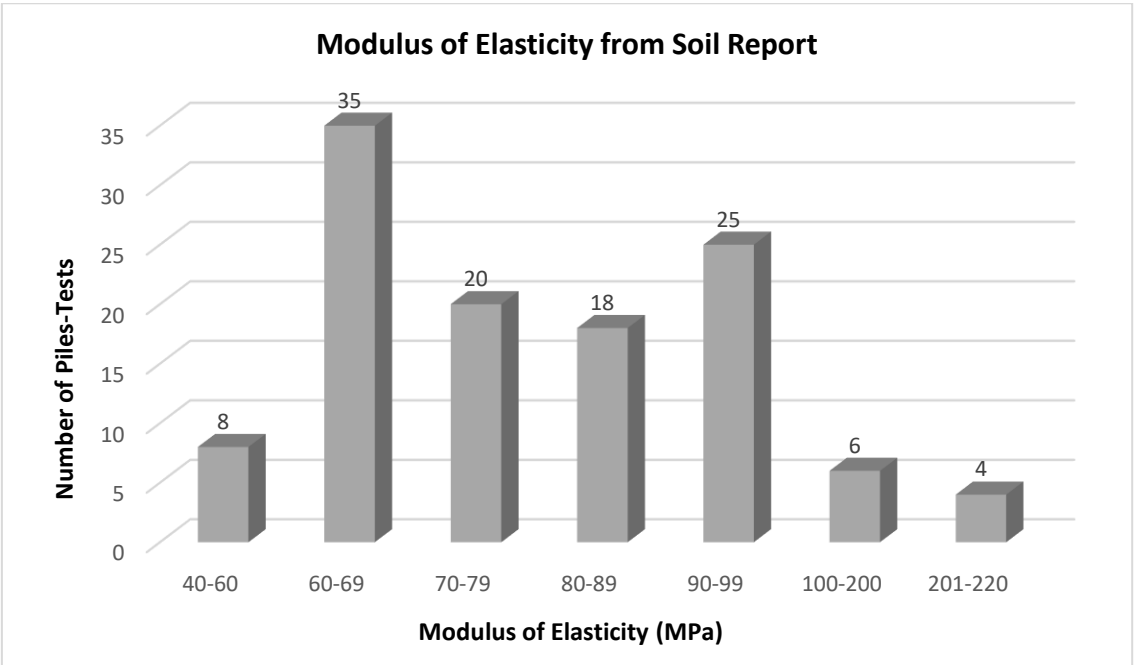

Fig. 5.54 Modulus of elasticity from soil report E_s vs number of piles-tests

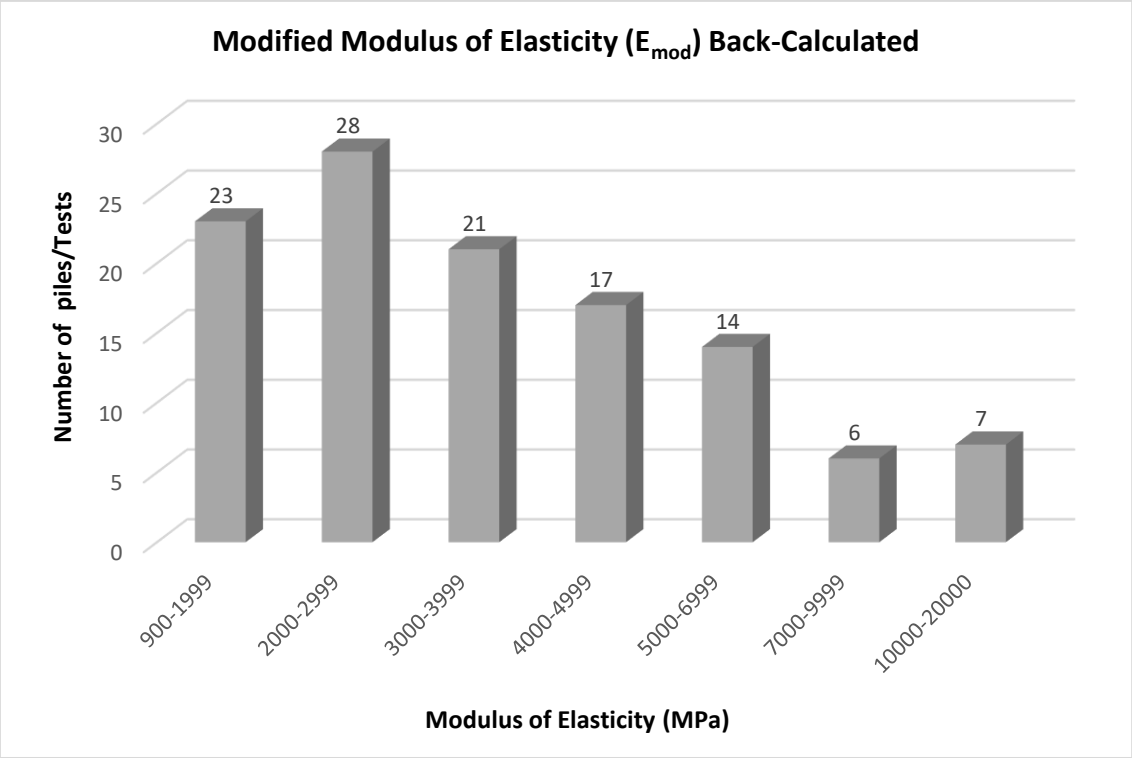

Fig. 5.55 Modulus of elasticity back-calculated E_{mod} vs number of piles-tests

6 Paramount Towers: A Case Study Project

6.1 Introduction

This case study deals with one of the high-rise buildings under construction in the Business Bay area. Project 17, called ‘Paramount Towers’, covers an area of 2922 m^2 and is bordered from the west by an existing car park with undeveloped roads and plots on the other sides. This multi-storey structure is comprised of four towers, is over 270 meters in height and will have a total of 64 floors when completed. Three of the towers will be used as service apartment buildings, whereas the fourth will accommodate hotel/service apartments.

The substructure of the towers is designed to be on pile foundations to transfer the load from the raft to the piles, without considering the weak rock under the raft. The foundation system of the four buildings has more than 600 piles under the raft. The static load test conducted on six of the working piles of the foundation system will be analysed in the case study.

Fig. 6.1 Project site location in Business Bay

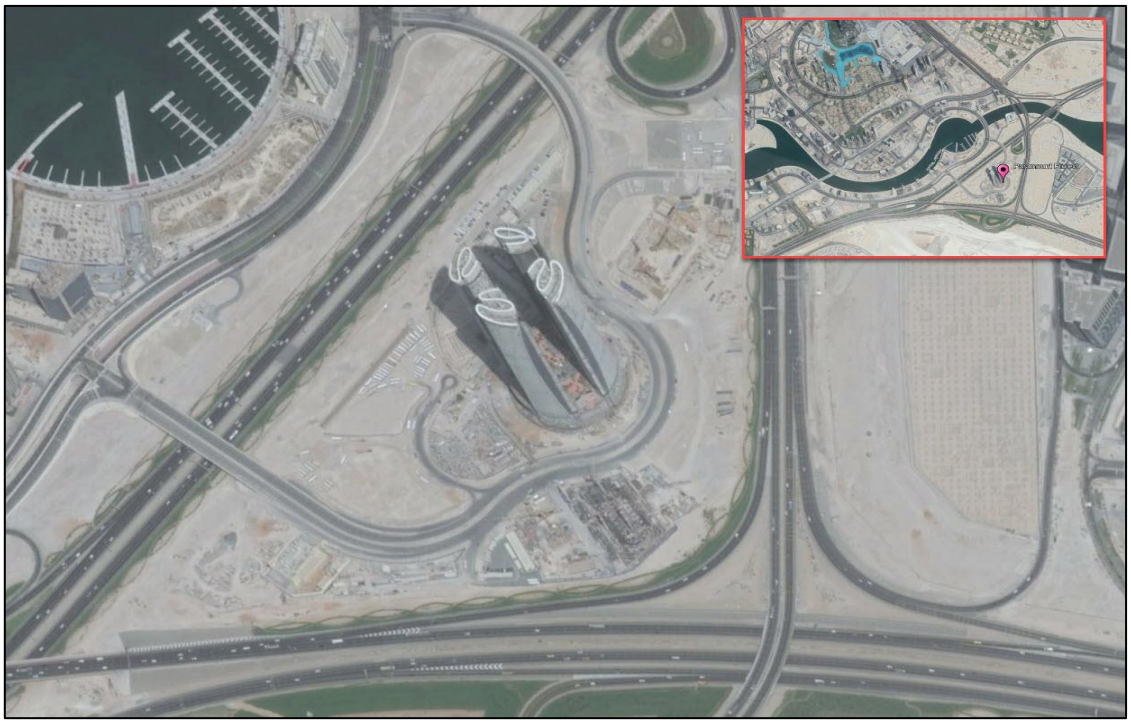

Fig. 6.2 A closer view of Paramount Towers

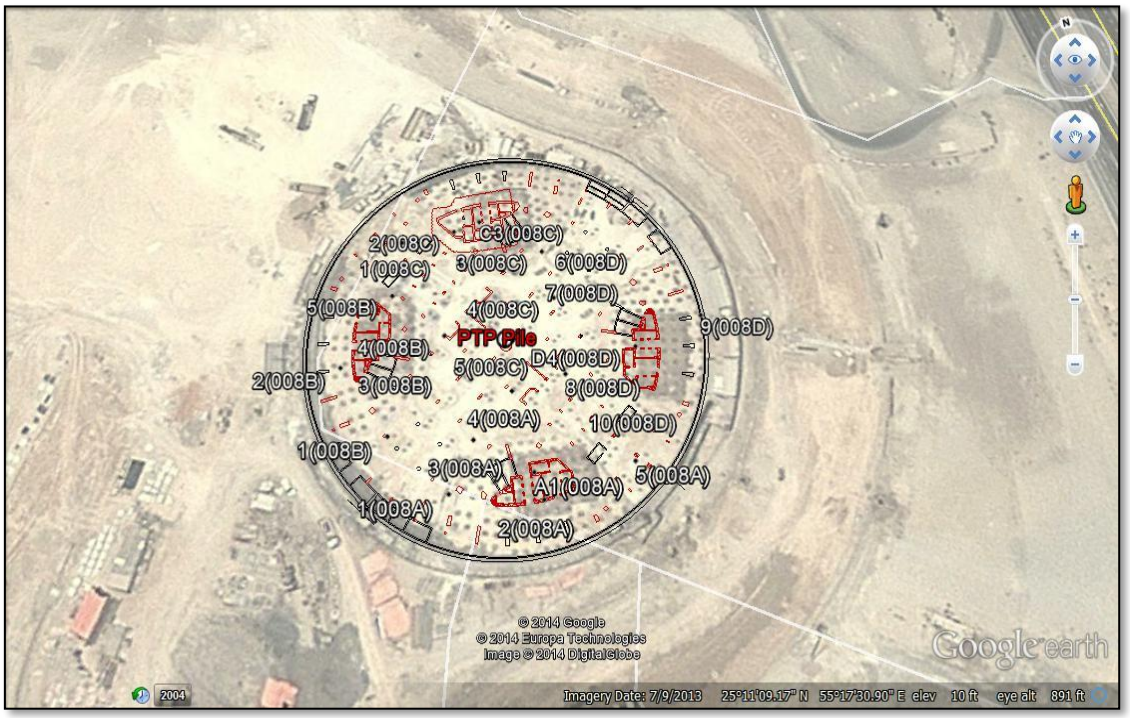

Fig. 6.3 Boreholes and PTPs locations

The geotechnical investigation report includes the drilling of a total of 14 boreholes, two cable percussive boreholes down to 35.5 meters each and 12 cable percussive boreholes. This is followed by rotary drilling, of which two boreholes were down to 35 meters each, six boreholes were down to 50 meters each and four boreholes were down

to 60 meters each. This is comprised of drilling 10 cable percussive boreholes, followed on by rotary drilling down to 50 meters each.

6.2 Site works

The site works for the proposed by the consultant for the towers can be summarised as follows:

Type	No.	Location	Elevation DMD (m)	Total Depth (m)	Remarks
Cable Percussive followed by Rotary drilling	A1	008 A	-1	60	Confirmation boreholes in 2013
	B2	008 B	-1	60	
	C3	008 C	-1	60	
	D4	008 D	-1	60	
	1	008 A	2.8	50	Phase 1 Initial boreholes in 2010
	1	008 B	3.7	50	
	2	008 A	2.4	50	
	2	008 B	3.15	50	
	3	008 A	3.7	50	
	3	008 B	3.1	50	
	4	008 A	3.1	35	
	5	008 A	1.9	35	
Cable Percussive	4	008 B	3	35.5	
	5	008 B	3	35.5	
Cable Percussive followed by Rotary drilling	1	008C	3.1	50	Phase 2 in 2012
	2	008C	3	50	
	3	008C	2.61	50	
	4	008C	2.69	50	
	5	008C	2.54	50	
	6	008D	2.65	50	
	7	008D	2.62	50	
	8	008D	2.74	50	
	9	008D	2.5	50	
	10	008D	2.6	50	

Table 6.1 Exploratory borehole location

Laboratory testing was carried out on the samples retrieved from within the drilled boreholes, with special emphasis placed on the unconfined compressive strength of the rock core samples.

6.3 Site geology and soil profile

Based on the findings of the soil investigation report, the following table presents a general subsurface lithology for Phases I and II.

EGL (m)	Elevation DMD (m)	Strata Description
0.0 to -0.5	3.0 to 2.5	Brown SAND with few shell fragments.
0.5 to -6.0	2.5 to -3.0	Light yellowish brown to light grey SAND with few cemented bands.
6.0 to -7.0	-3.0 to -4.0	Brown SAND with many sandstone bands and little gypsum.
7.0 to -36.0	-4.0 to -33.0	Brown to reddish brown, gypsiferous SANDSTONE embedded with shell fragments & brown mottled grey and white CONGLOMERATE embedded with gypsum.
36.0 to -60.0	-33.0 to -57.0	Off-white mottled grey gypsiferous SILTSTONE locally interbedded with gravel locally interbedded with sandstone bands.

Table 6.2 Site geology phase 1 (A&B)

EGL (m)	Elevation DMD (m)	Strata Description
0.0 to -6.0	2.7 to -3.5	Medium dense to dense SAND with rare shell fragments
6.0 to -21.0	-3.5 to -18.5	Very weak to weak brown SANDSTONE interbedded with cemented sand bands
21.0 to -22.0	-18.5 to -19.5	Very weak to weak MUDSTONE
22.0 to -26.0	-19.5 to -23.5	Very weak to weak reddish brown gypsiferous SANDSTONE with cemented bands
26.0 to -29.0	-23.5 to -26.5	Moderately weak to moderately strong CONGLOMERATE
29.0 to -35.5	-26.5 to -32.0	Moderately weak CALCISILTITE
35.5 to -51.2	-32.0 to -47.5	Very weak to weak gravelly SILTSTONE

Table 6.3 Site geology phase 2 (C&D)

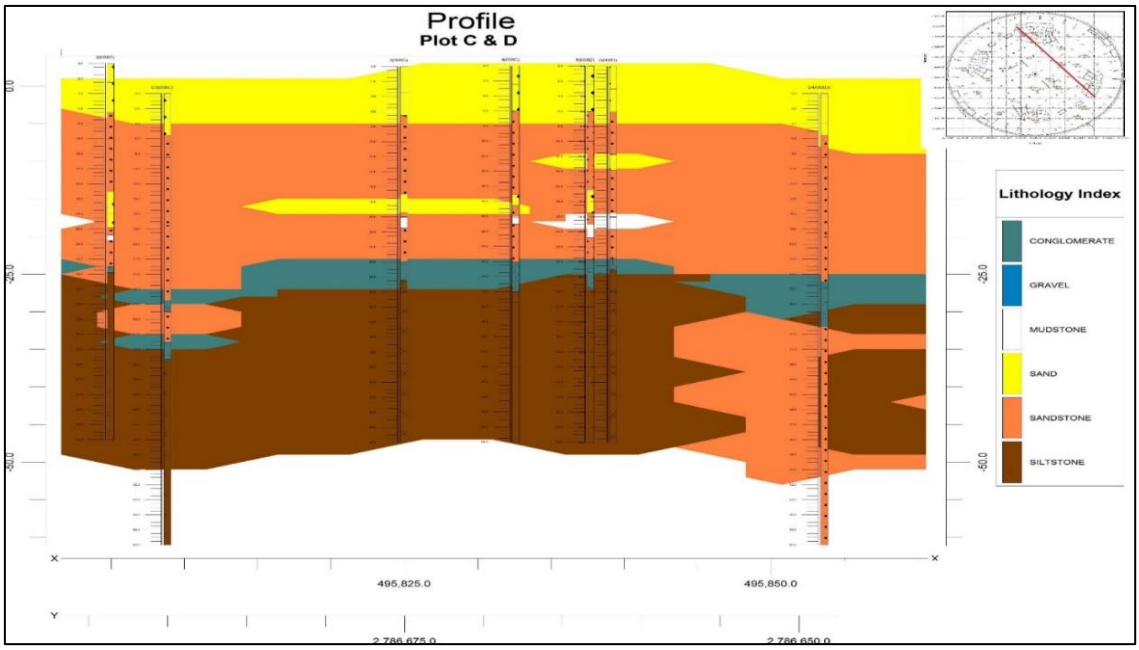

Fig. 6.4 Soil profile for phase 2 (C&D)

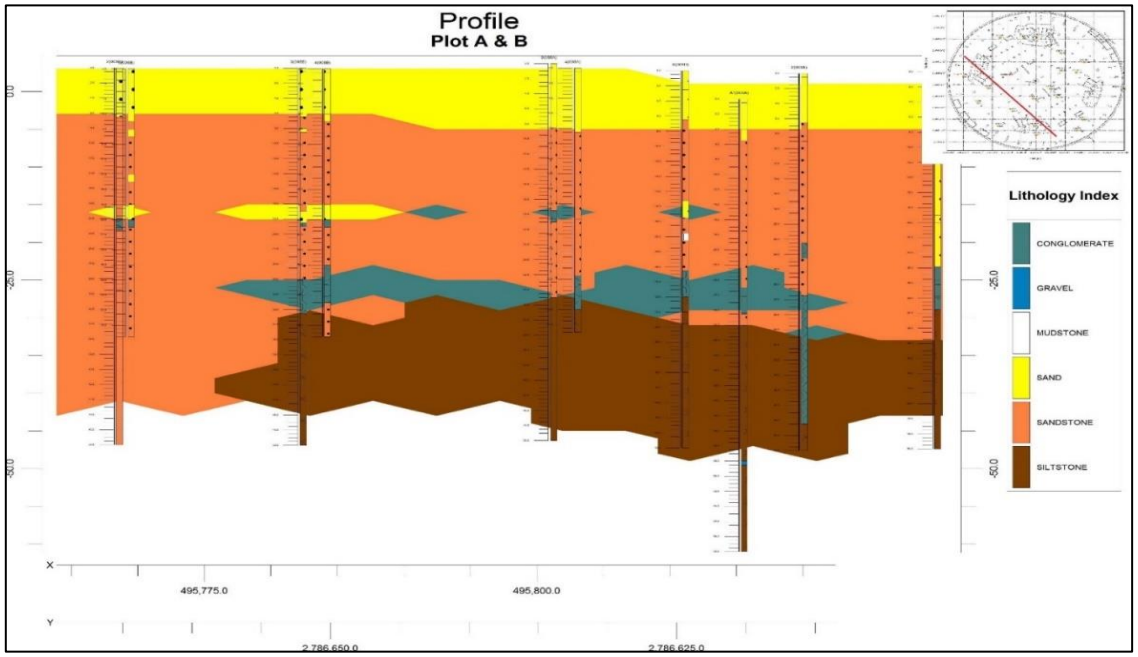

Fig. 6.5 Soil profile for phase 1 (A&B)

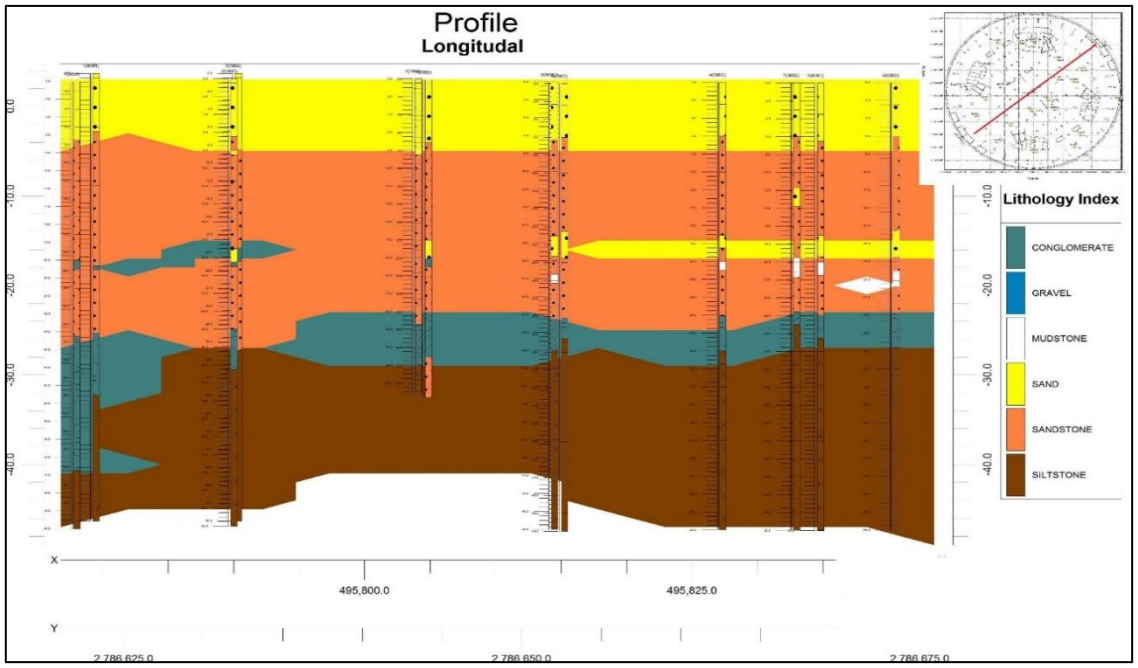

Fig. 6.6 General longitudinal soil profile for the site

6.4 Soil investigation and properties

The following table summarises the results of the laboratory testing carried out from samples retrieved from within the drilled boreholes.

Elevation DMD (m)	Unconfined Compressive Strength (MPa)			
	Initial Boreholes		Phase II	
	Average	Std. Deviation	Average	Std. Deviation
-4.00	0.69	*	1.16	0.43
-5.00	0.77	0.11	0.63	0.33
-6.00	0.75	0.10	0.48	*
-7.00	0.94	*	1.09	1.03
-8.00	0.73	0.31	2.32	1.41
-9.00	0.99	0.16	2.08	0.28
-10.00	0.94	*	0.83	0.44
-11.00	1.02	0.33	0.53	*
-12.00	1.27	0.56	1.41	*
-13.00	1.02	0.13	1.57	1.20
-14.00	0.82	0.48	3.77	0.21
-15.00	1.07	0.49	-	-
-16.00	-	-	-	-
-17.00	1.09	0.13	6.23	*
-18.00	1.08	0.38	1.55	0.64
-19.00	-	-	1.17	*

Elevation DMD (m)	Unconfined Compressive Strength (MPa)			
	Initial Boreholes		Phase II	
	Average	Std. Deviation	Average	Std. Deviation
-20.00	1.10	0.23	1.34	1.08
-21.00	0.23	*	0.73	*
-22.00	1.06	0.45	0.27	*
-23.00	0.84	0.25	0.61	0.42
-24.00	0.61	*	21.07	16.37
-25.00	1.43	0.55	7.32	8.42
-26.00	2.35	1.31	20.36	*
-27.00	2.04	*		
-28.00	2.04	*	3.58	3.78
-29.00	3.94	0.21	6.76	4.99
-30.00	1.32	0.79	7.68	2.22
-31.00	0.96	0.68	5.59	*
-32.00	1.94	1.33	4.57	3.82
-33.00	0.90	*	-	-
-34.00	0.49	*	2.18	2.67
-35.00	0.81	0.14	1.27	*
-36.00	0.82	0.18	2.58	*
-37.00	0.74	0.07		
-38.00	2.36	*	1.12	*
-39.00	1.03	*		
-40.00	1.15	0.34		
-41.00	1.14	*		
-42.00				
-43.00	1.06	0.46		
-44.00	2.71	2.19		
-45.00				
-46.00			5.94	3.82
-47.00				
-48.00	0.68	*		
-49.00	0.64	*		
-50.00				
-51.00	1.07	*		
-52.00	0.84	0.03		
-53.00	0.76	*		
-54.00	0.83	*		
-55.00				
-56.00	0.75	0.15		
-57.00	0.66	0.12		

Elevation DMD (m)	Unconfined Compressive Strength (MPa)			
	Initial Boreholes		Phase II	
	Average	Std. Deviation	Average	Std. Deviation
-58.00	0.66	*		
-59.00	0.80	0.15		
-60.00	0.74	0.16		

* Insufficient data to produce standard deviation

Table 6.4 Summary of unconfined compressive strength (UCS)

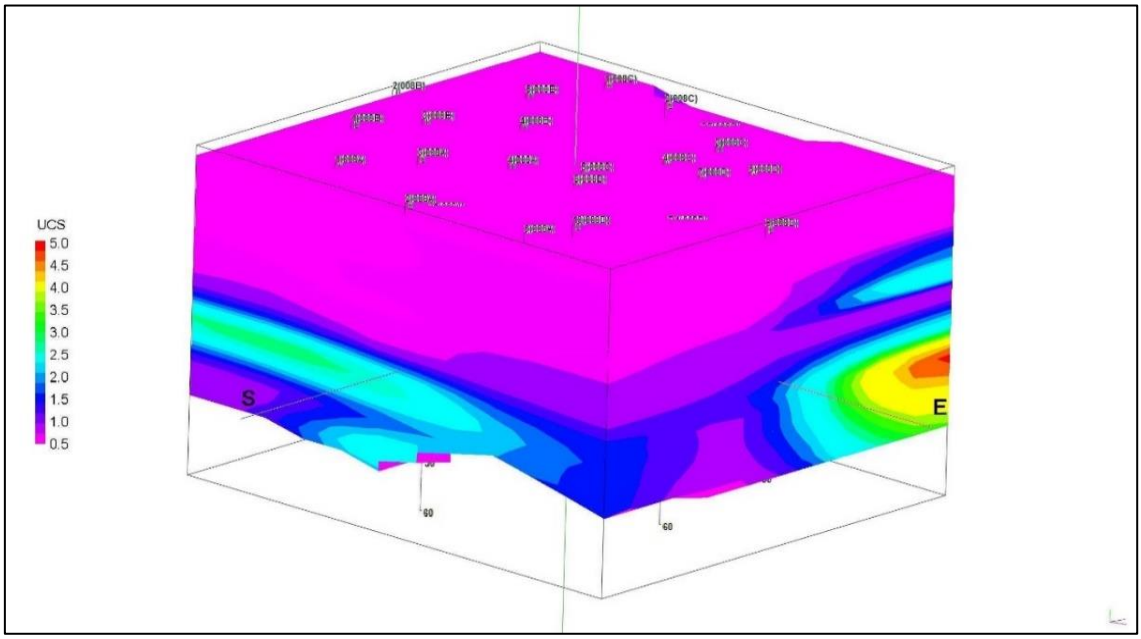

Fig. 6.7 Unconfined compressive strength (UCS) values 3D view

The data obtained from the initial report in Phase 1 shows a lower unconfined compressive strength when compared to the findings of Phase 2. Furthermore, the values obtained from Phase II seem relatively high in comparison to the general stratigraphy of the Business Bay area.

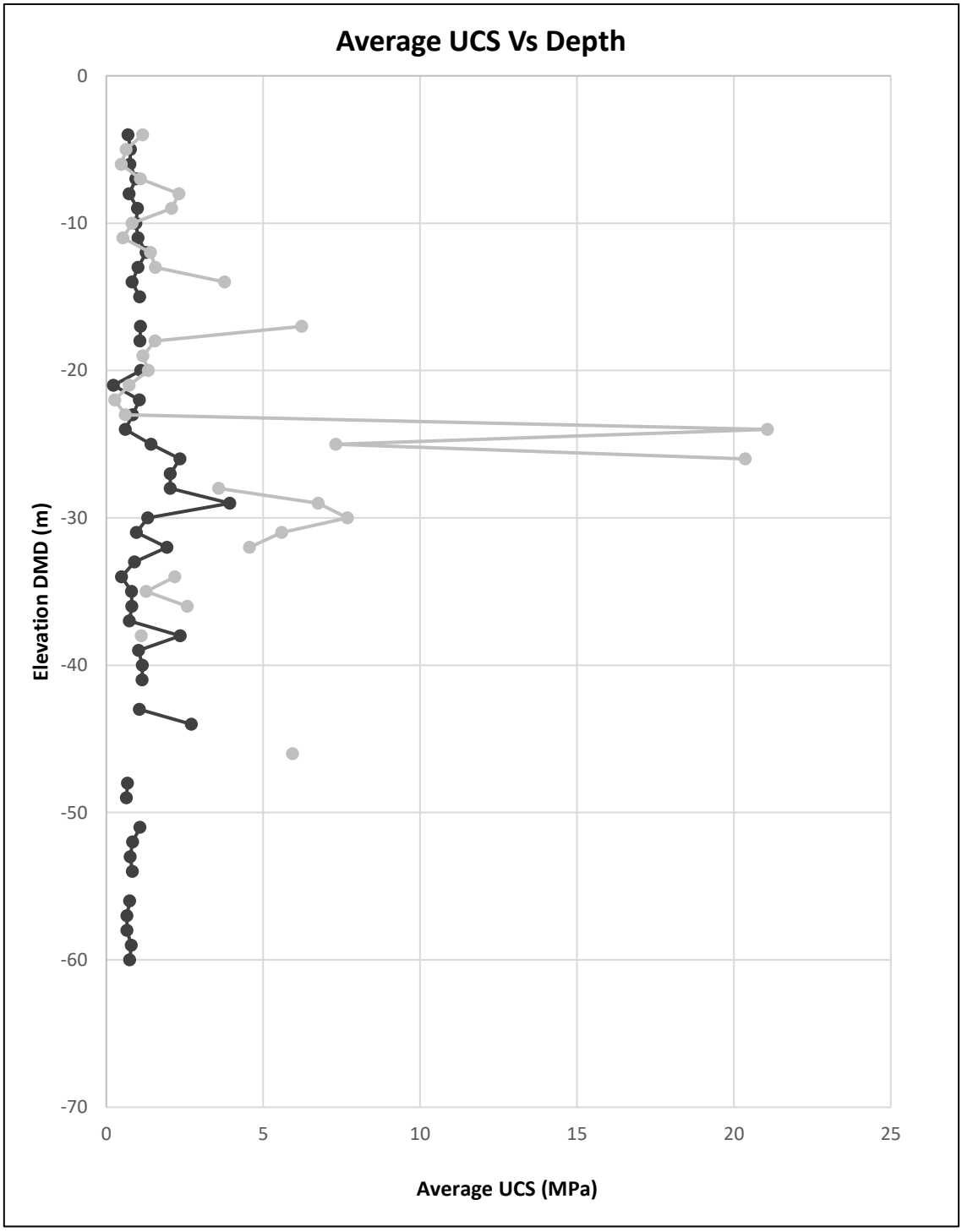

Fig. 6.8 Average unconfined compressive strength (UCS) values vs depth (Phase 1&2)

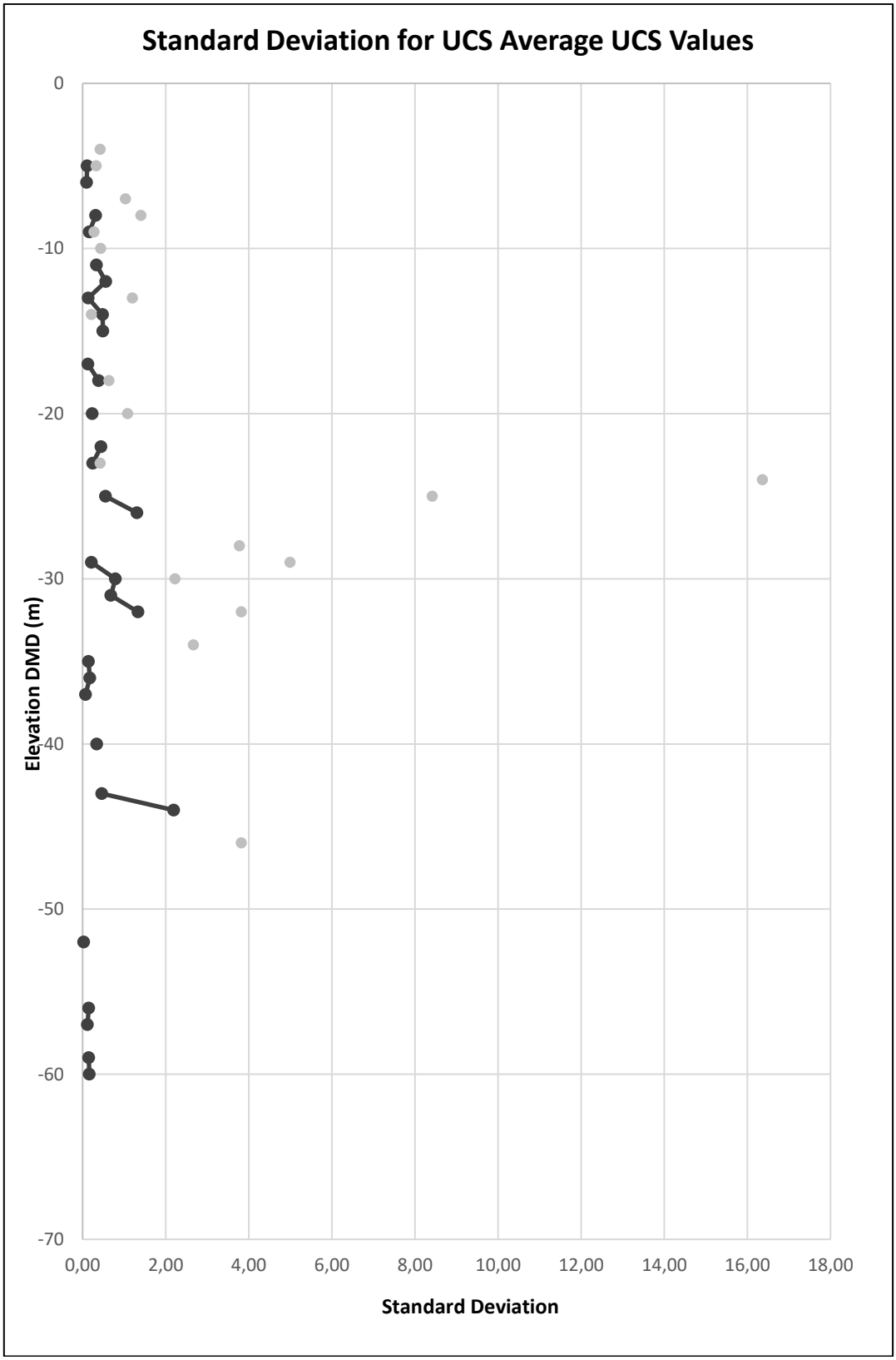

Fig. 6.9 Standard deviation for average UCS values (Phase 1&2)

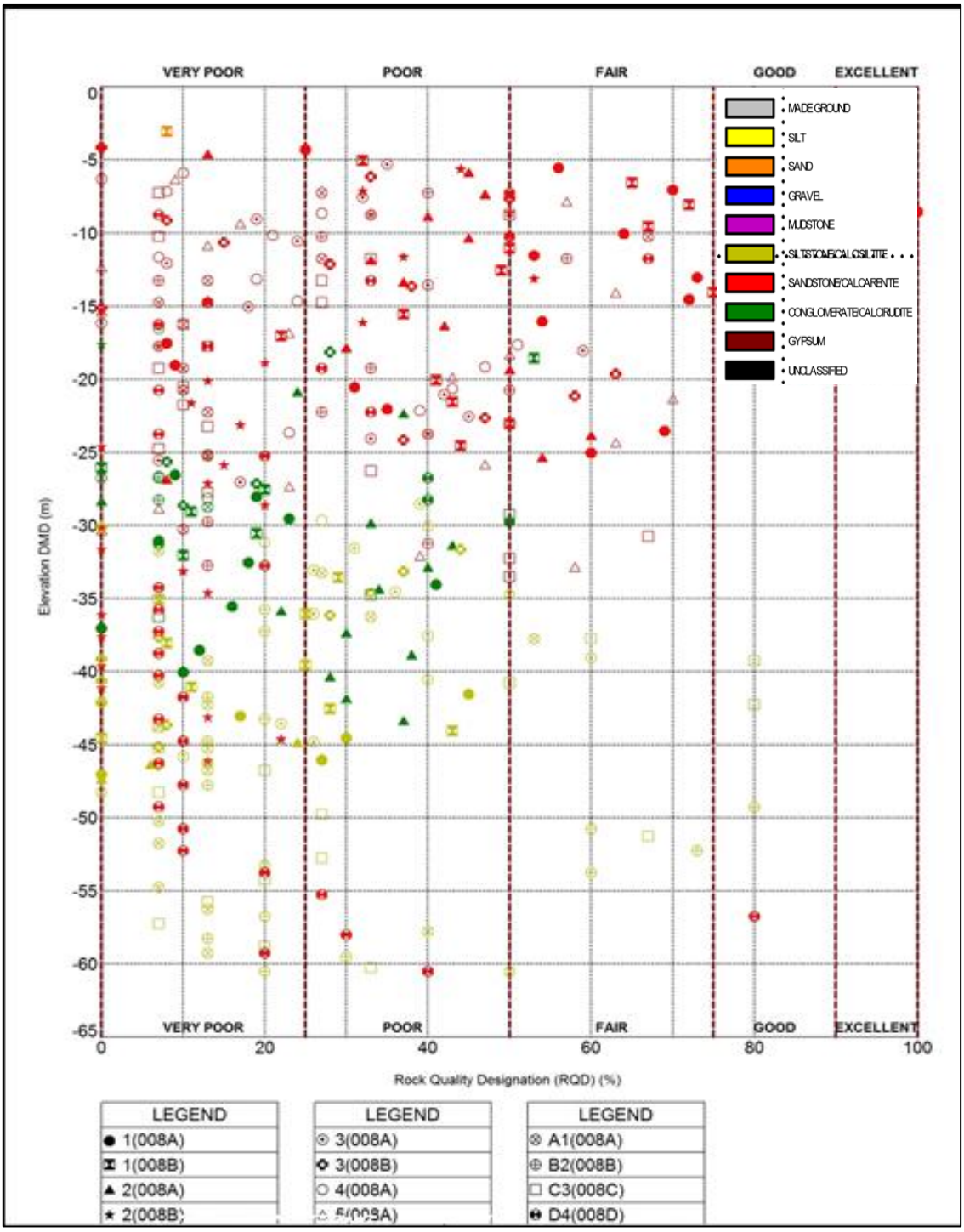

Fig. 6.10 Range of RQD for recovered cores from Phase I (A&B)

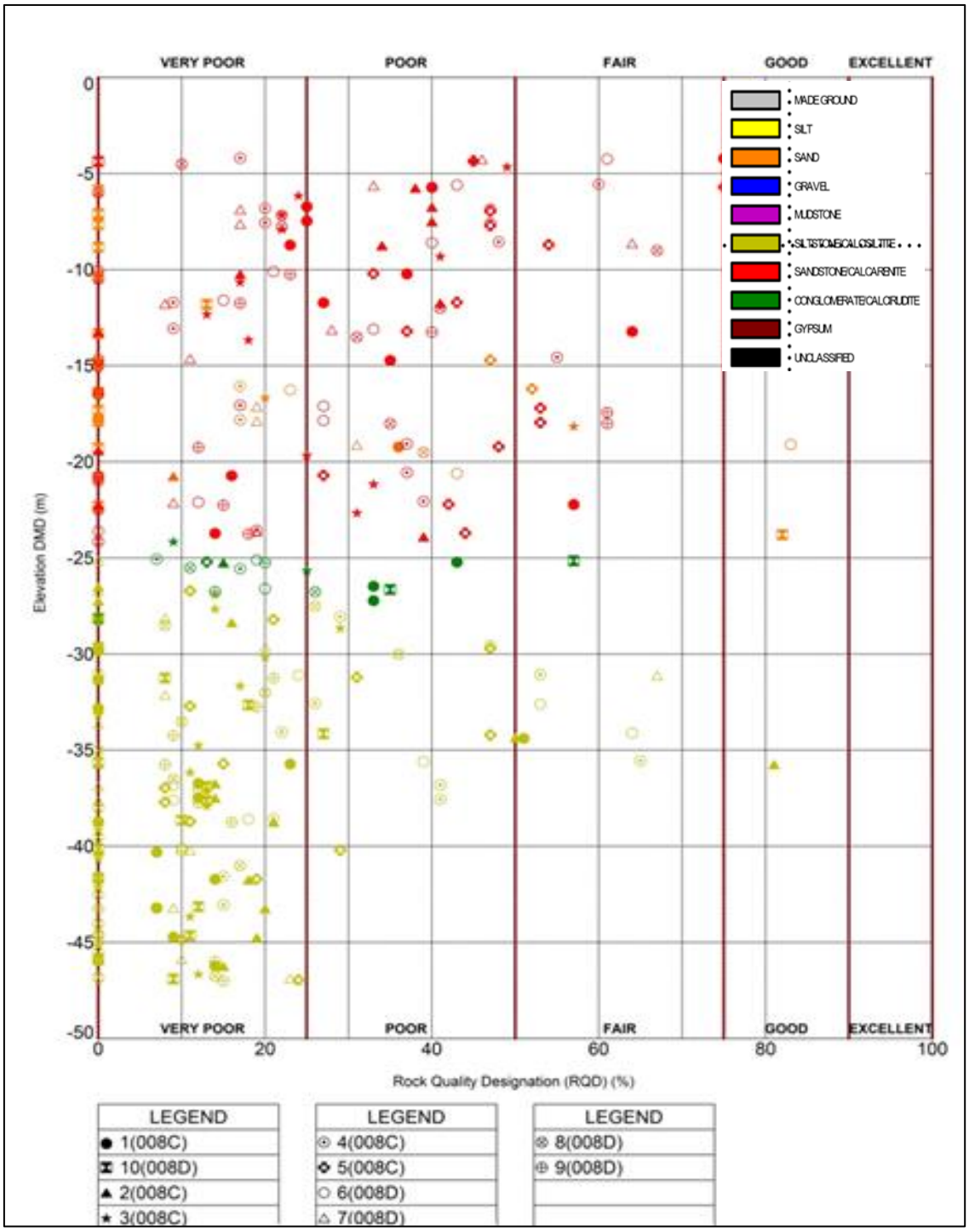

Fig. 6.11 Range of RQD for recovered cores from phase II (C&D)

It is apparent from the above comparison that the strength of the layers varies significantly between the findings of the two reports. In addition, the standard deviation showed a wide range for samples tested at the same depths. Upon taking a further detailed review of the drilled boreholes log sheets, it was noticed that the cores recovered showed a very poor Rock Quality Designation (RQD), with most runs showing an RQD of 0%; this may be due to various factors, including but not limited to:

- Very weak sub-strata encountered
- Feed pressure of the drilling machine
- Excess vibration of the rotary machine during drilling
- Rotation of the head of the drilling machine
- Type and Size of core barrel used in the drilling
- Water pressure during the drilling
- Drilling polymer used

Points two to seven are major factors that affect the core recovery, since these can be controlled in such a manner to obtain a better core recovery in the weakest of the soil-stratas. In addition, the extracted core samples may have been subjected to excess vibration and developed minor cracks within the core itself during handling and transportation, hence leading to initial deformation during the unconfined compressive strength and so resulting in lower rock strength. The summary of the soil properties is presented in the table below.

Soil Parameters	**Depth below the average ground level (m)**			
	+3.0 to -6.0 DMD	**-6.0 to -29.0 DMD**	**-29.0 to -38.0 DMD**	**-38.0 to -60.0 DMD**
Average Bulk Density: γ kN/m^3	18	20	20	20
Av. Angle of Shearing Resistance: Φ	33	45	45	45
Av. Coefficient of Rest Pressure: K_o	0.46	0.29	0.29	0.29
Av. Coefficient of Active Pressure: K_a	0.29	0.17	0.17	0.17
Av. Coefficient of Passive Pressure: K_p	3.39	5.82	5.82	5.82
Module of Elasticity: E_s, MPa	15	50	100	60
Cohesion: c, kN/m^2	-	46	100	62

Table 6.5 Summary of the soil parameters for entire site

6.5 Determination of modified modulus of elasticity back-calculated from SLT

In this section the same procedure will be followed and implemented in Project 28 (see Chapter 5). The modified value of elastic modulus of the soil (E_{mod}) will be determined using the back analysis of static load results (SLT) using the finite element method PLAXIS 2D for six piles, specifically: P76, P75, P74, P73, P72 and P71. The soil parameters are mentioned in the previous section. The following table summarises the material properties for all the aforementioned piles.

Parameters	**Pile Number**					
	P76	**P75**	**P74**	**P73**	**P72**	**P71**
Working Load (kN)	23190	16400	18000	21393	7500	7700
Test Load (kN)	34785	24600	27000	32090	11250	11550
Cut off Level (DMD)	-7.0	-7.0	-7.0	-7.0	-7.0	-7.0
Toe Level (DMD)	51.0	38.3	-41.0	-47.0	-29.0	-30.0
Length of Pile (m)	44	31.3	34	40	22	23
f_{cu}, Compressive Strength (Design, N/mm^2)	70	70	70	70	70	70
Modulus of Elasticity of Pile, E_p (Design, MPa)	31782	31782	31782	31782	31782	31782
f_{cu}, Compressive Strength (Test, N/mm^2)	80.5	76	72	80.5	78	74
Modulus of Elasticity of Pile, Ep (Test, MPa)	33142.8	32640	32051.6	33142.8	32830.6	32316.2
Diameter of Pile (m)	1.3	1.3	1.3	1.3	0.8	0.8

Table 6.6 Piles material properties

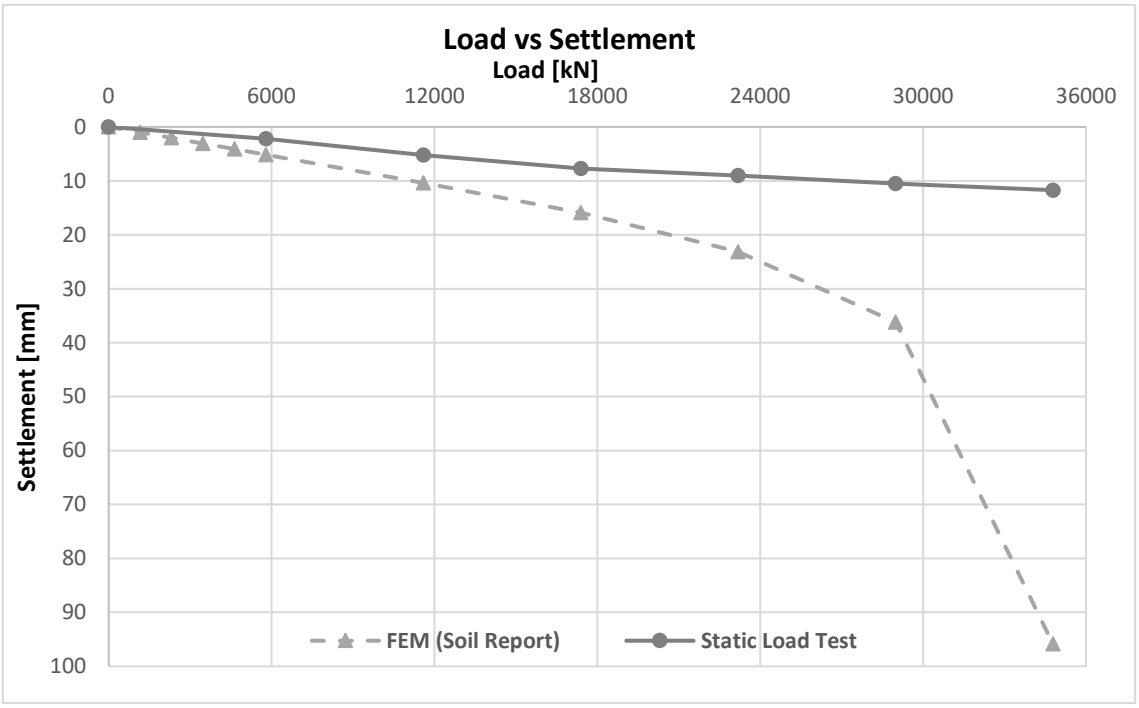

Fig. 6.12 Modelling by using modulus of elasticity Es from soil report P76

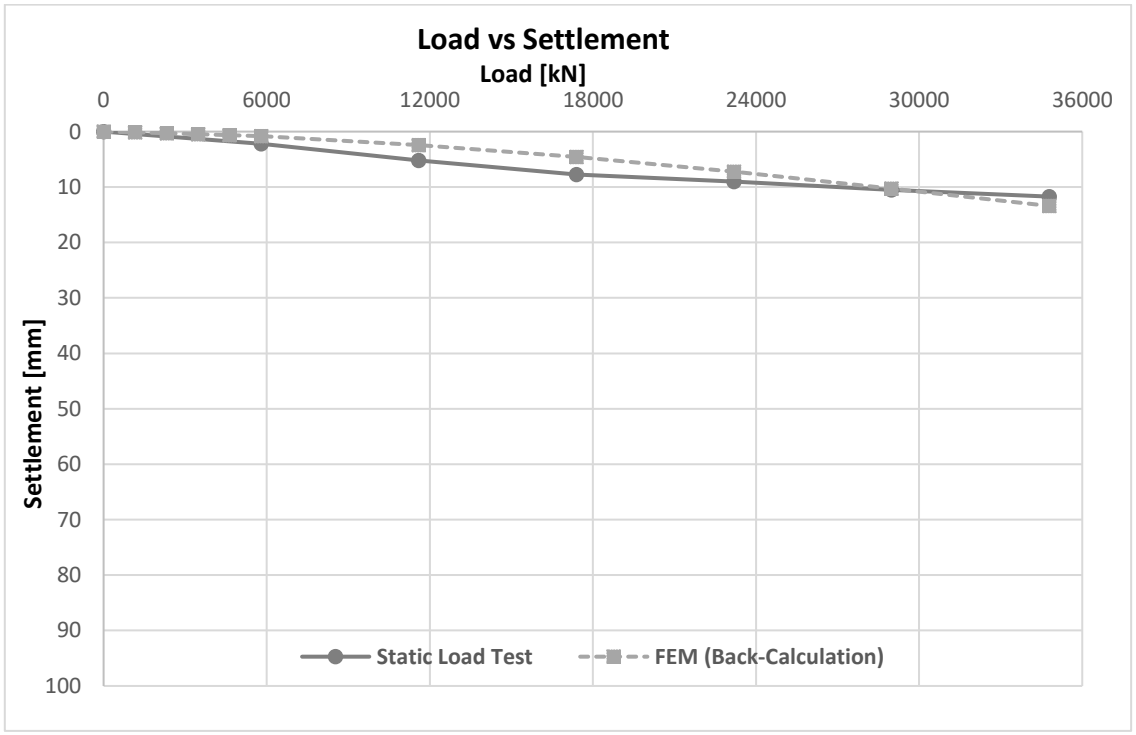

Fig. 6.13 Back-analysis of modulus of elasticity E_{mod} from SLT P76

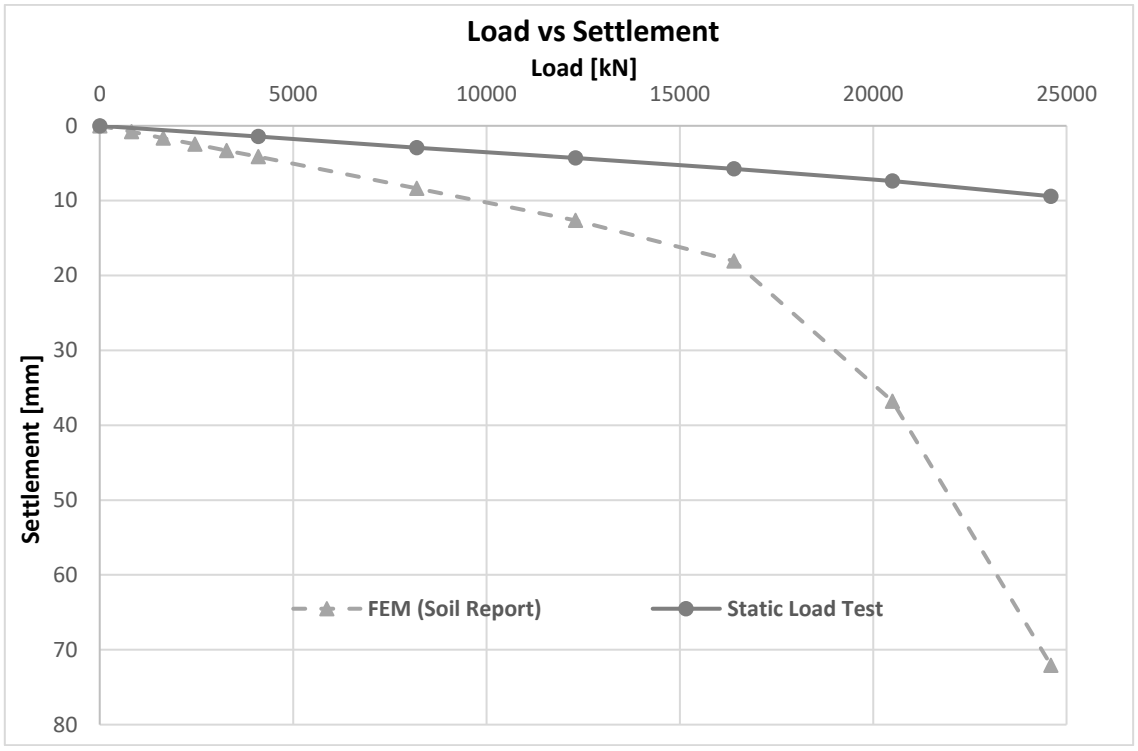

Fig. 6.14 Modelling by using modulus of elasticity Es from soil report P75

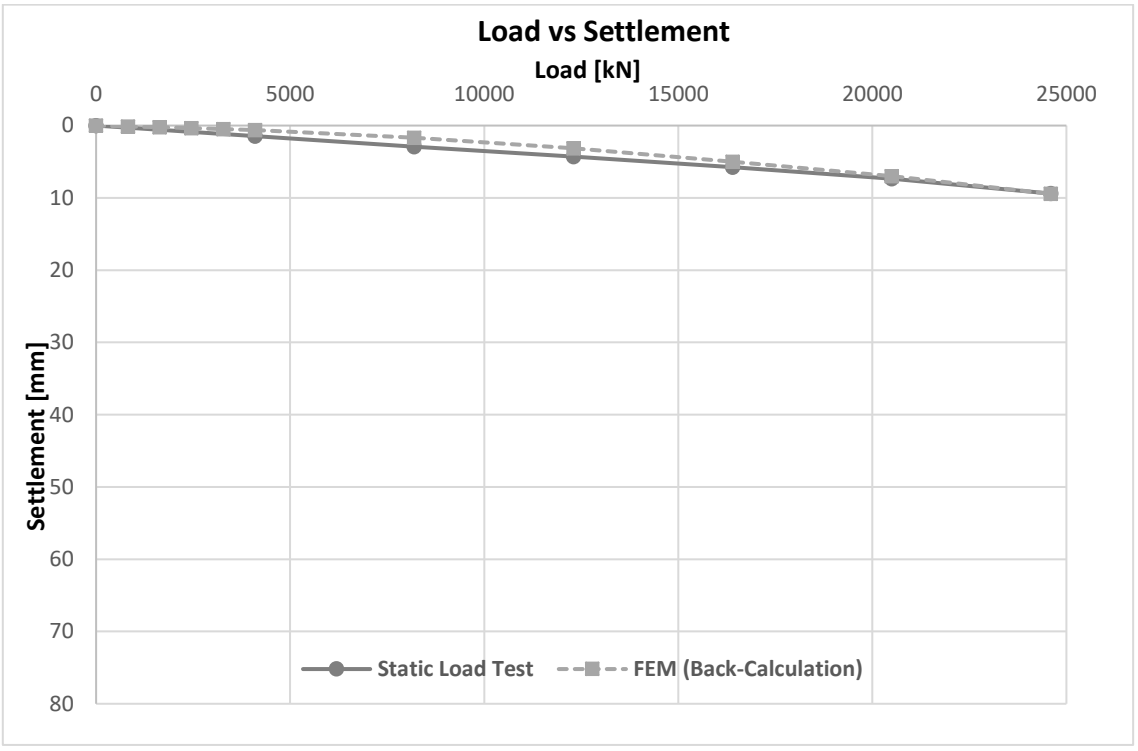

Fig. 6.15 Back-analysis of modulus of elasticity E_{mod} from SLT P75

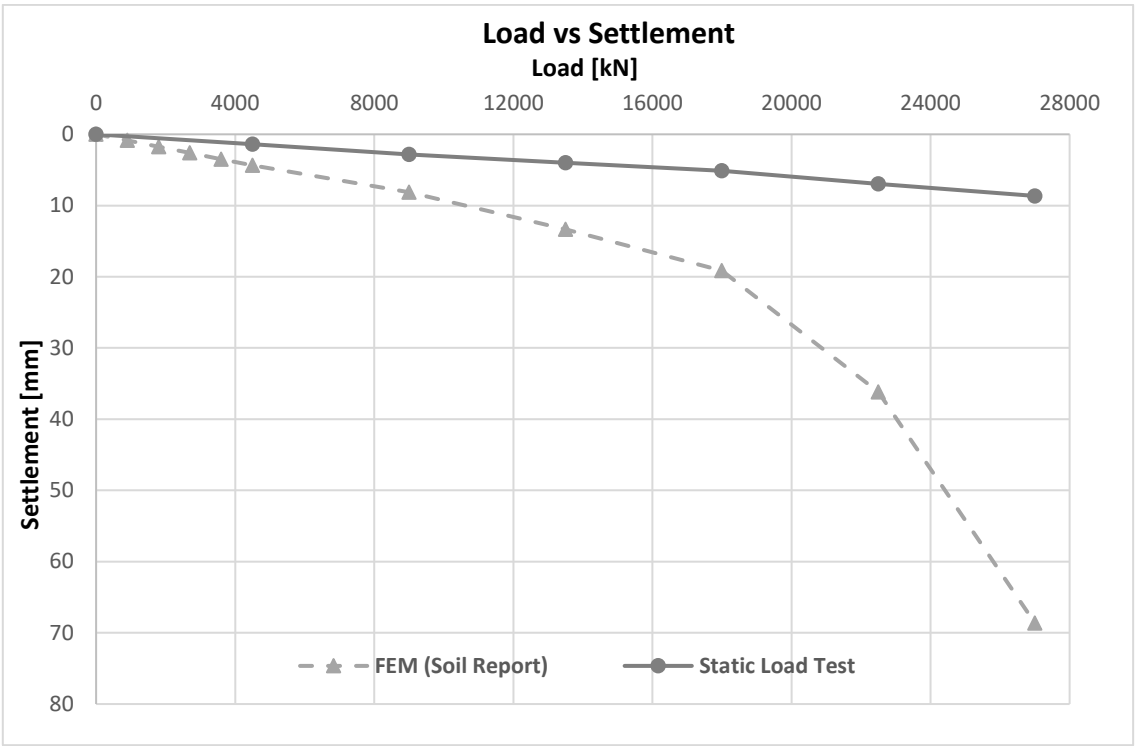

Fig. 6.16 Modelling by using modulus of elasticity Es from soil report P74

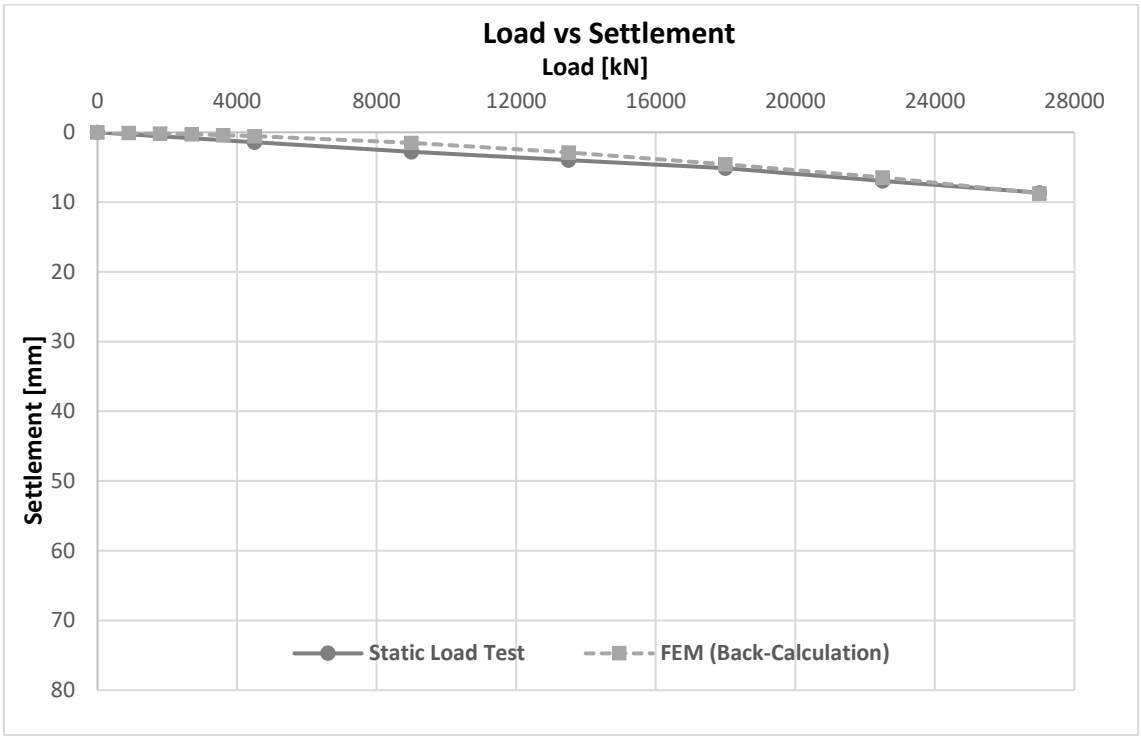

Fig. 6.17 Back-analysis of modulus of elasticity E_{mod} from SLT P74

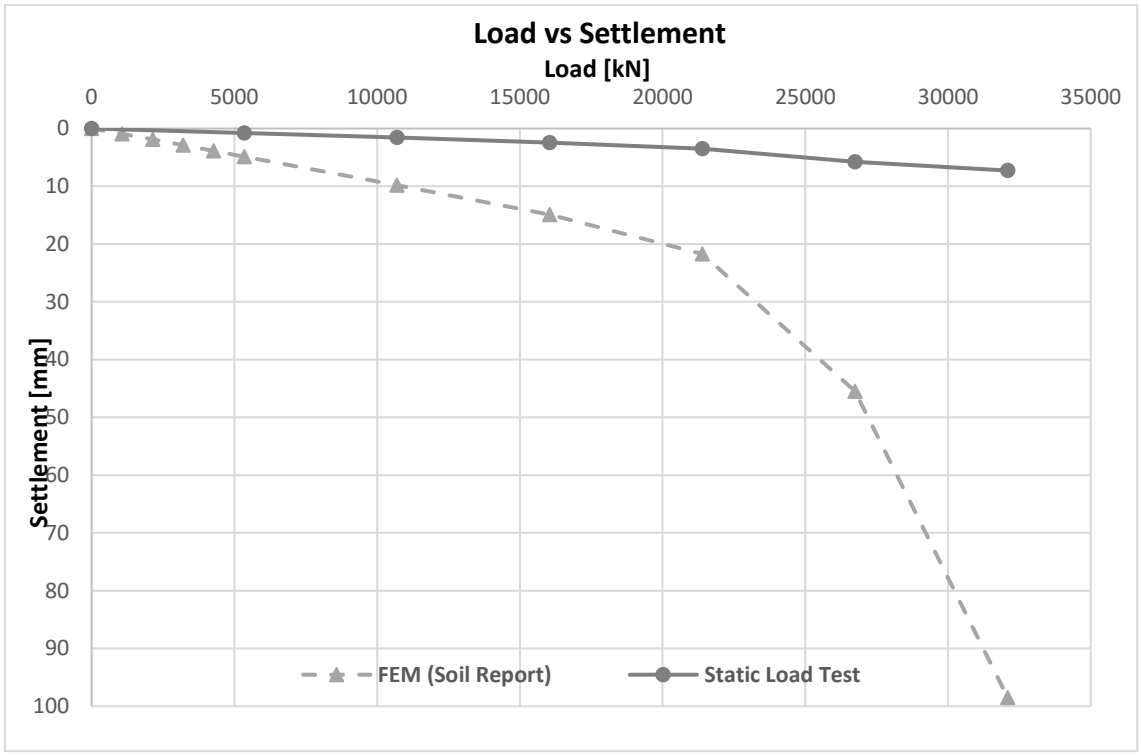

Fig. 6.18 Modelling by using modulus of elasticity Es from soil report P73

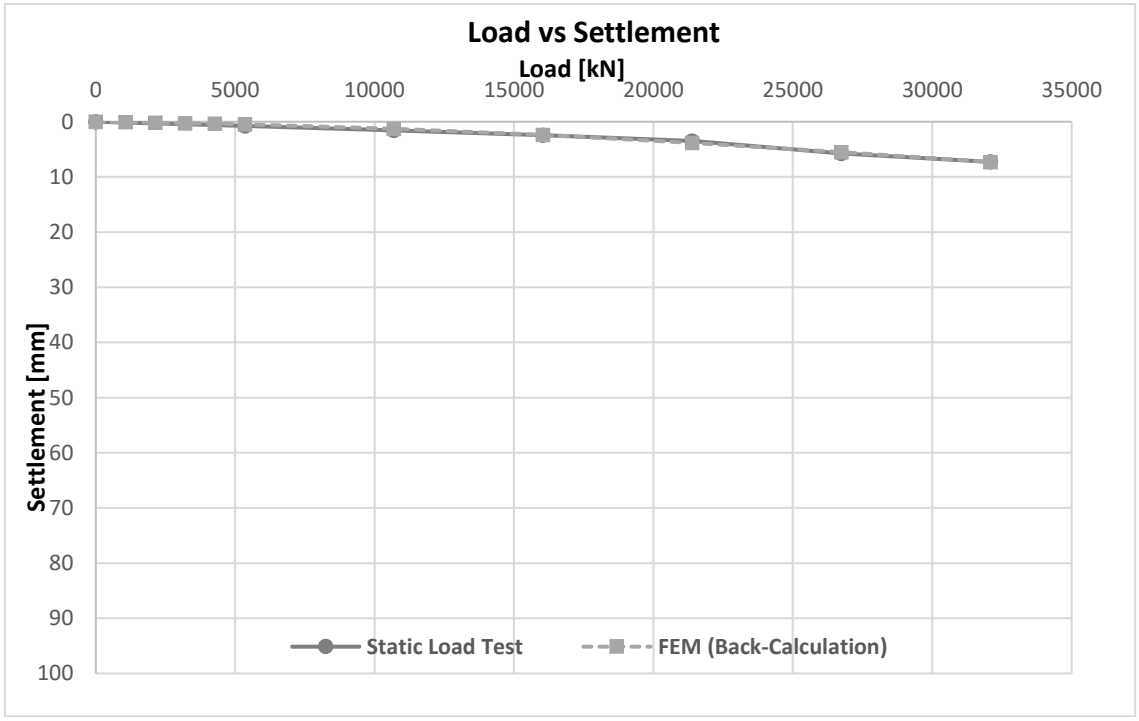

Fig. 6.19 Back-analysis of modulus of elasticity E_{mod} from SLT P73

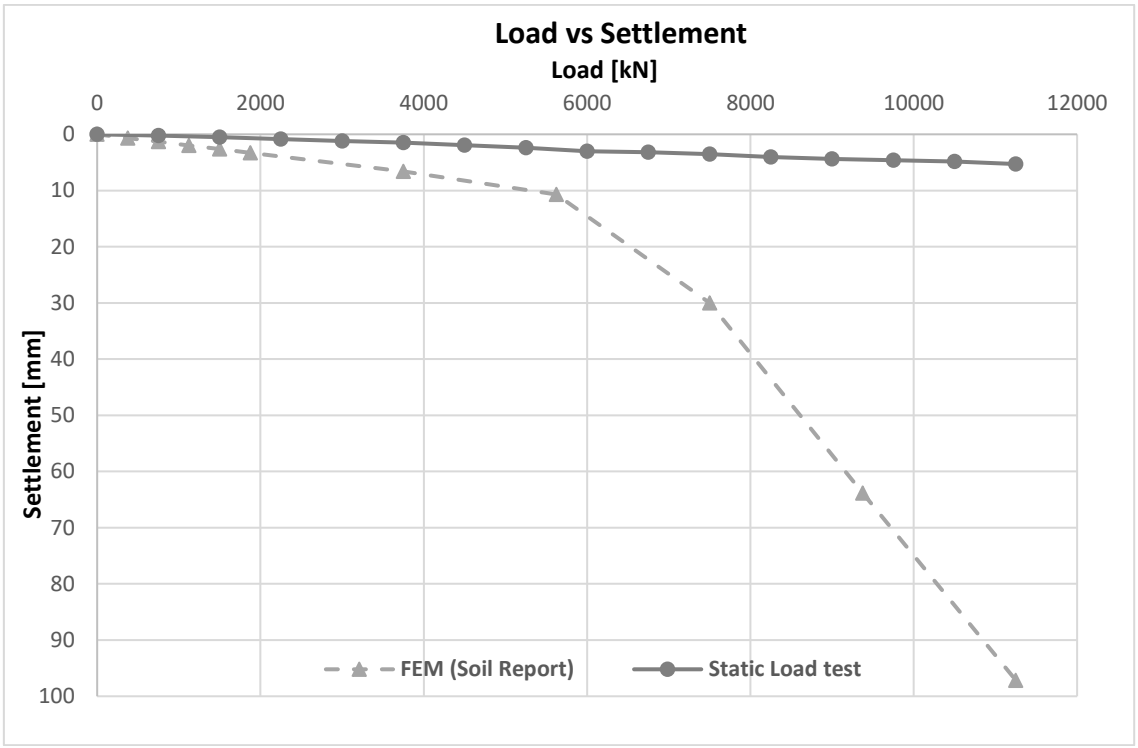

Fig. 6.20 Modelling by using modulus of elasticity Es from soil report P72

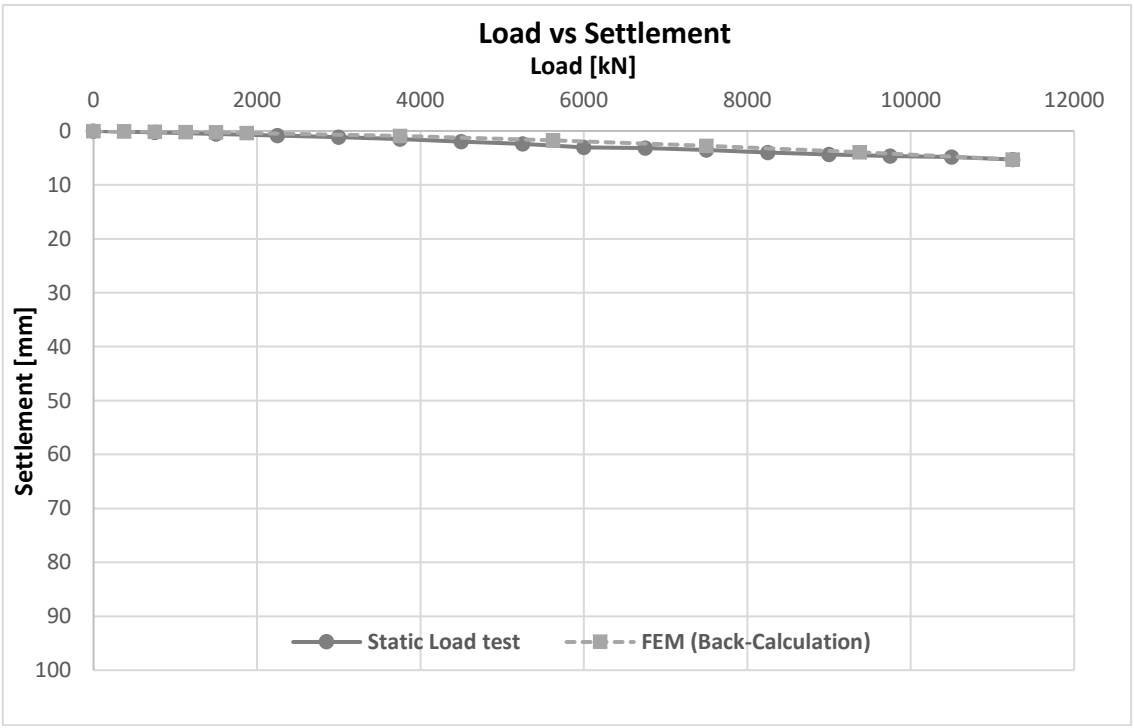

Fig. 6.21 Back-analysis of modulus of elasticity E_{mod} from SLT P72

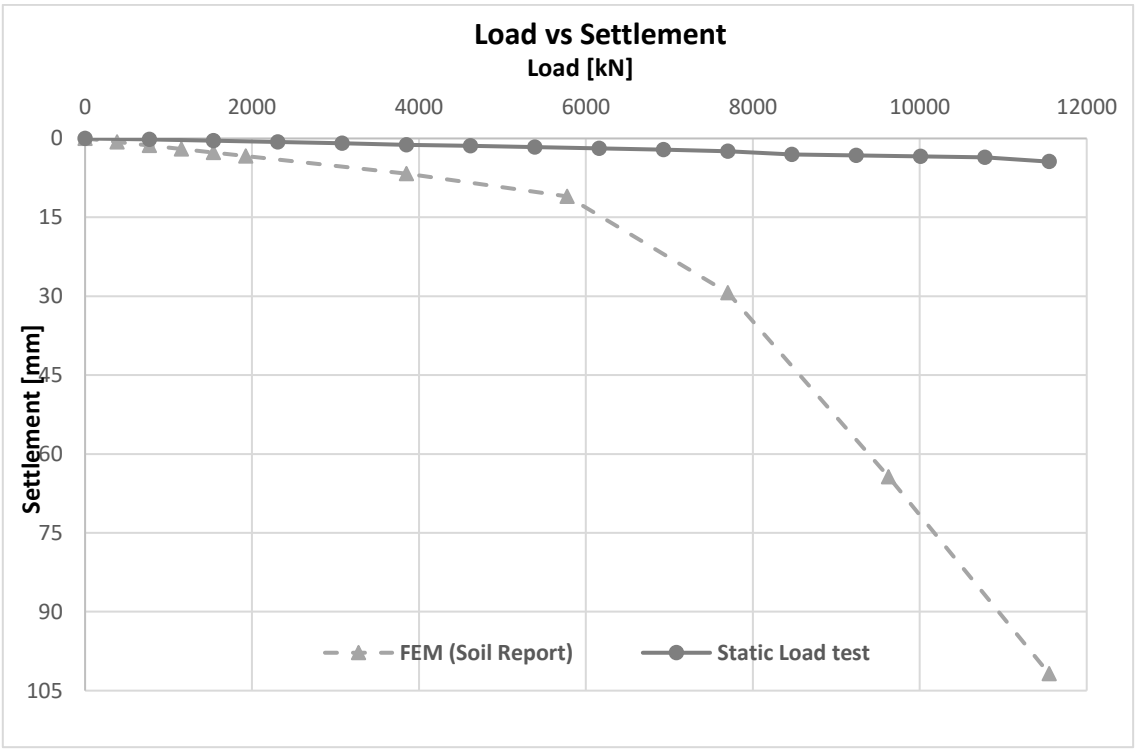

Fig. 6.22 Modelling by using modulus of elasticity Es from soil report P71

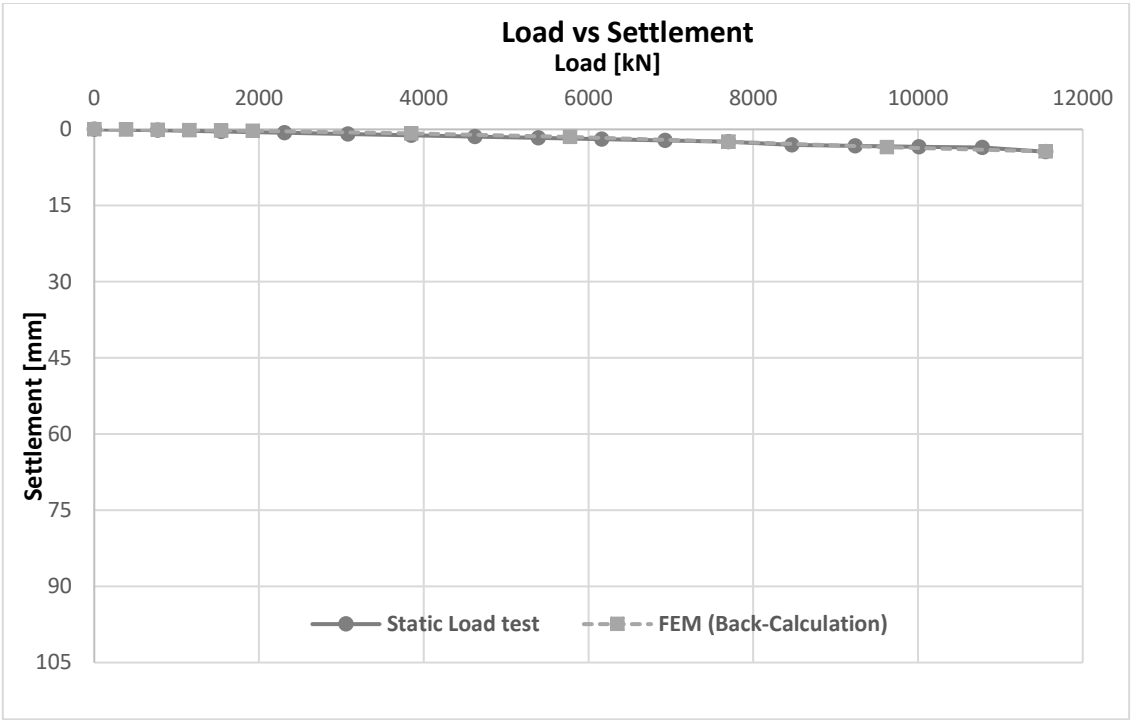

Fig. 6.23 Back-analysis of modulus of elasticity E_{mod} from SLT P71

Pile #	Length [m]	Diameter [m]	Working Load [kN]	Test Load [kN]	$E_{Soil\ Report}$ (Es) [MN/m²]	$E_{Back\ Calculated}$ (Emod) [MN/m²]	Increment in E
P71	23	0.8	7700	11550	60	5000	83.3 times
					100	5000	50.0 times
					62	5000	80.6 times
P72	22	0.8	7500	11250	60	3000	50.0 times
					100	3000	30.0 times
					62	3000	48.4 times
P73	40	1.3	21393	32089.5	60	4250	70.8 times
					100	5000	50.0 times
					62	5000	80.6 times
P74	34	1.3	18000	27000	60	2700	45.0 times
					100	2700	27.0 times
					62	2700	43.5 times
P75	31.30	1.3	16400	24600	60	1450	24.1 times
					100	1450	14.5 times
					62	1450	23.4 times
P76	46	1.3	21393	32089.5	60	2000	33.3 times
					100	2000	20.0 times
					62	2100	33.9 times

Fig. 6.24 Summary for back-calculated modulus of elasticity

6.6 Modulus of elasticity (E_{mod}) recommended value for case study project 17

Based on the back analysis conducted on the static load test results for P76, P75, P74, P73, P72 and P71, the following table details the values of E_{mod} for each pile:

Rock Layer (DMD)	Modulus of Elasticity, E_{mod} (MPa)					
	P76	**P75**	**P74**	**P73**	**P72**	**P71**
Layer 1 (-6 to -29)	2000	1450	2700	4250	3000	5000
Layer 2 (-29 to -38)	2000	1450	2700	5000	3000	5000
Layer 3 (-38 to -60)	2100	1450	2700	5000	3000	5000

Table 6.7 Modulus of Elasticity E_{mod} values for each layer

From the above table, the modulus of elasticity E_{mod} values achieved from all piles ranged from 1450 to 5000 MPa. The range of modulus of elasticity values obtained for each layer of soil has been schematically represented, as shown in the figure below.

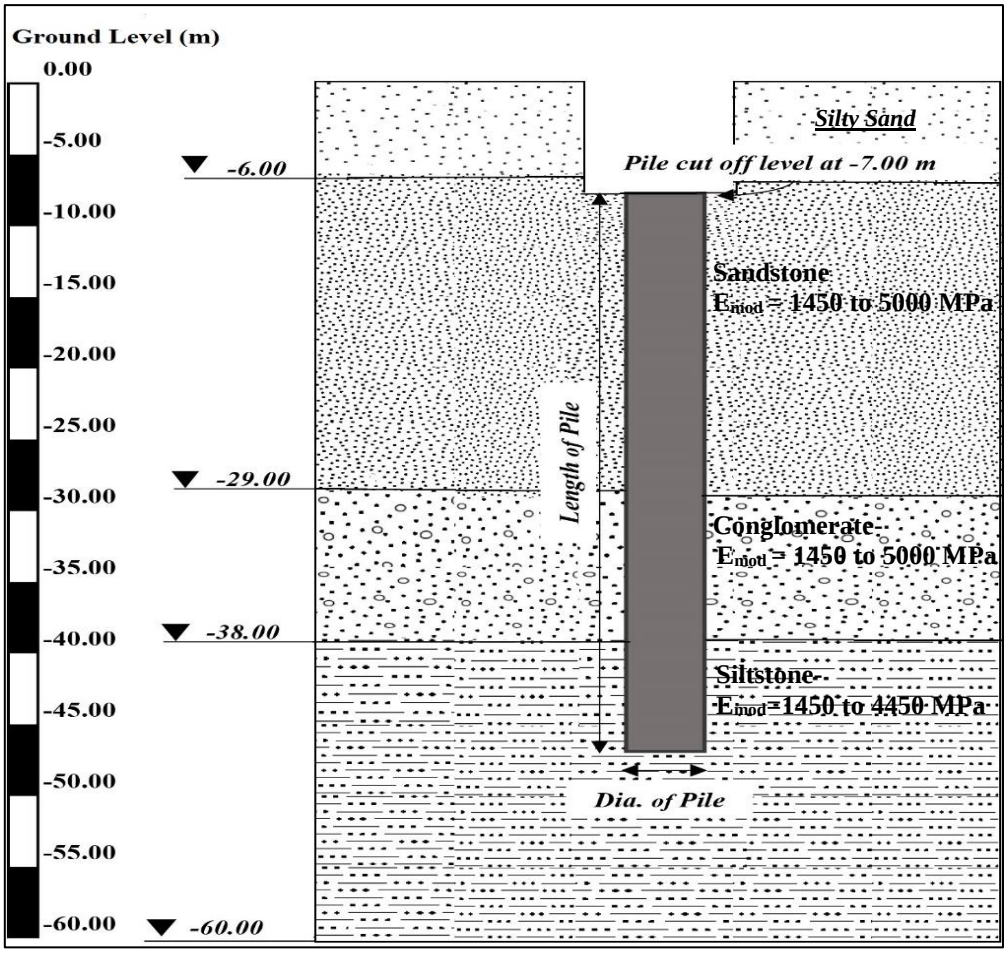

Fig. 6.25 Range of E_{mod} values over soil depth

Referring to the figure above, the modulus of elastic value of upper layer of silty sand has not been considered in FEM analysis because the foundation and pile cut off level is at -7.00 DMD (Dubai Municipality Datum). Therefore, this layer will be excavated and removed from the site.

The modulus of elasticity values shown corresponds to the stiffness conditions of the weak rock at different locations in the Project 17 site. However, a representative value of modulus of elasticity E_{mod} should be determined for the entire project site for the purpose of the design. There are many ways and approaches by which to determine this, such as selecting the best fit values by observing the trend of the plot as the representative values of modulus of elasticity; the same method has been used to determine the representative UCS and RQD values. However, where RQD and UCS are concerned, many locations were available to determine the general trend of the plot across the project site, with comparison being made with the static load test. Therefore, due to the high values of E_{mod}, to ensuring a safe design, the minimum modulus of elasticity founded during the FEM modelling should be recommended for the design. Representative values for the modules of elasticity for the entire site shown in the table below.

Rock Layer	Recommended value of E_{mod} (MPa)
Layer-1	1450
Layer-2	1450
Layer-3	1450

Fig. 6.26 Recommended value of modulus of elasticity E_{mod} for Project 17

6.7 Foundation settlement during construction

In this section, the observation of the foundation of the project for the four towers has been monitored by the surveying equipment and the monitoring started after casting the foundation until the concrete structure (without finishing). The table below summarises the foundation settlement in the core area during construction.

Readings	Date	Construction Stages	Level/height	Settlement
1st reading	16th April 2015	20th floor	106.1 m	5 mm
2nd reading	1st July 2015	30th floor	140.2 m	6 mm
3rd reading	5th October 2015	40th floor	176.8 m	6 mm
4th reading	28th December 2015	50th floor	209.8 m	14 mm
5th reading	4th April 2016	60th floor	242.8 m	14 mm
6th reading	19th August 2016	60th floor	242.8 m	15 mm

Table 6.8 Summary of building settlement during construction

Based on the above results, the foundation is not moving and the settlement recorded is small in comparison to the building load. In this case the weight of the structural skeleton of the building caused only 15 mm settlement. The figure below shows the settlement during construction.

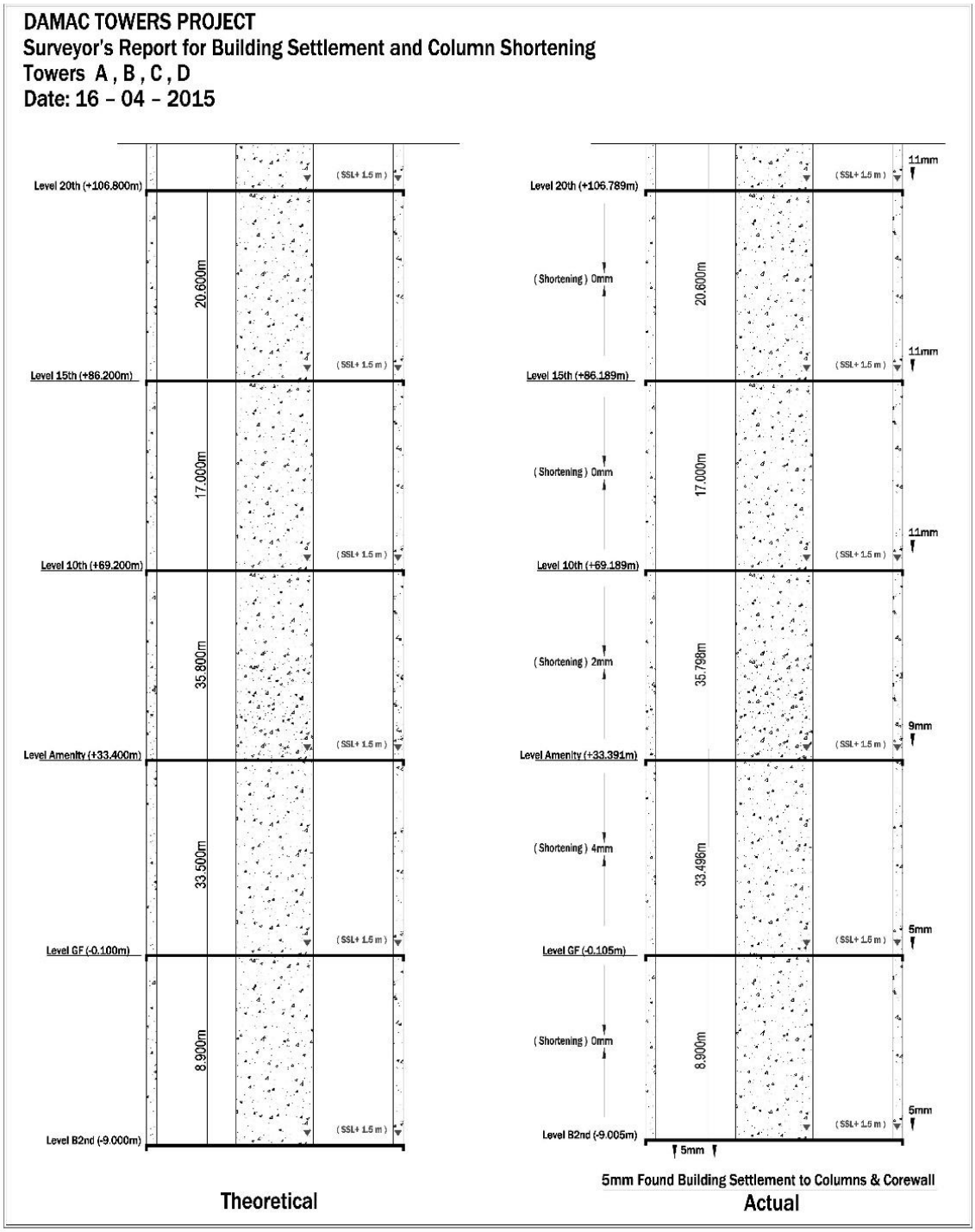

Fig. 6.27 Building settlement for 20 floors

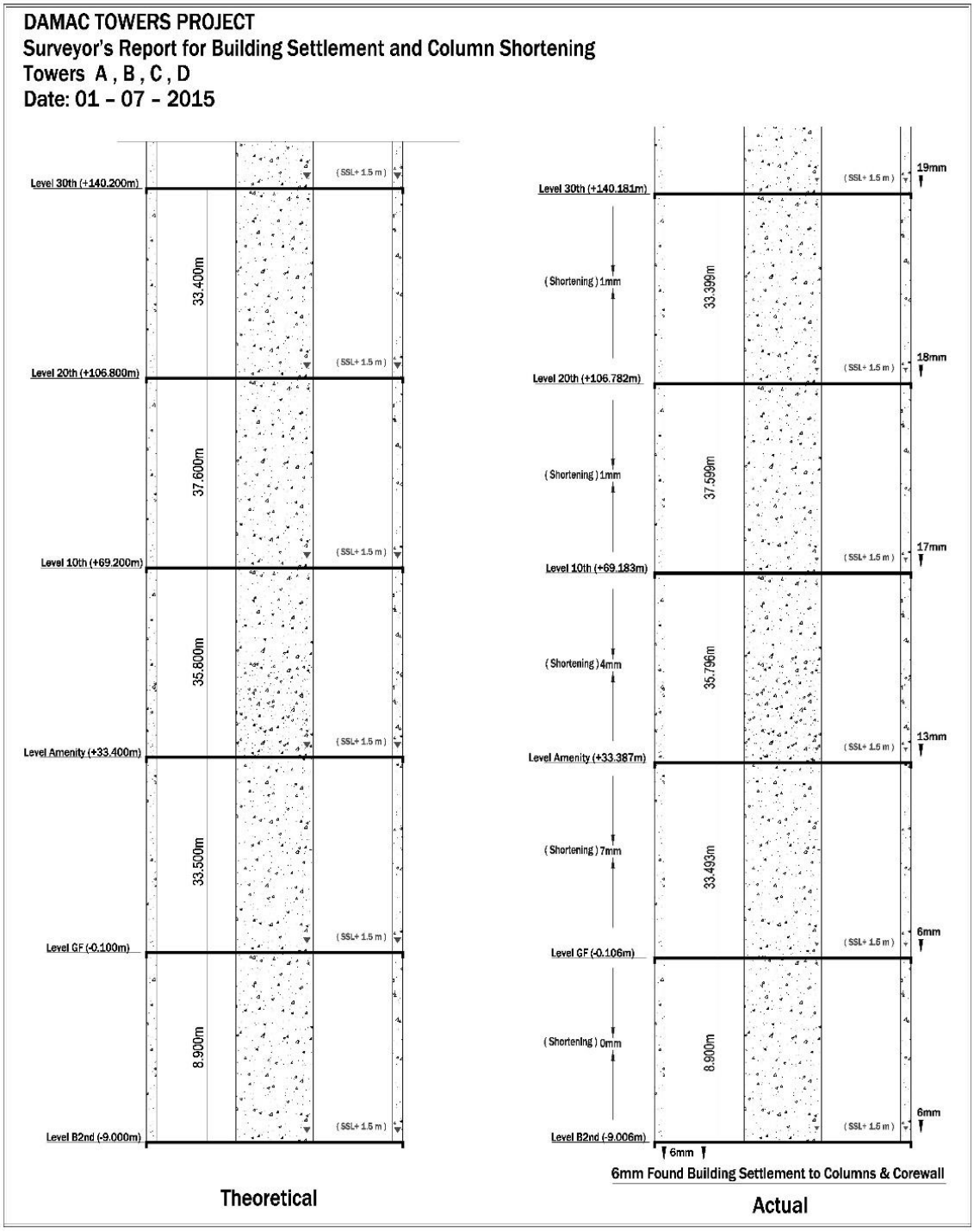

Fig. 6.28 Building settlement for 30 floors

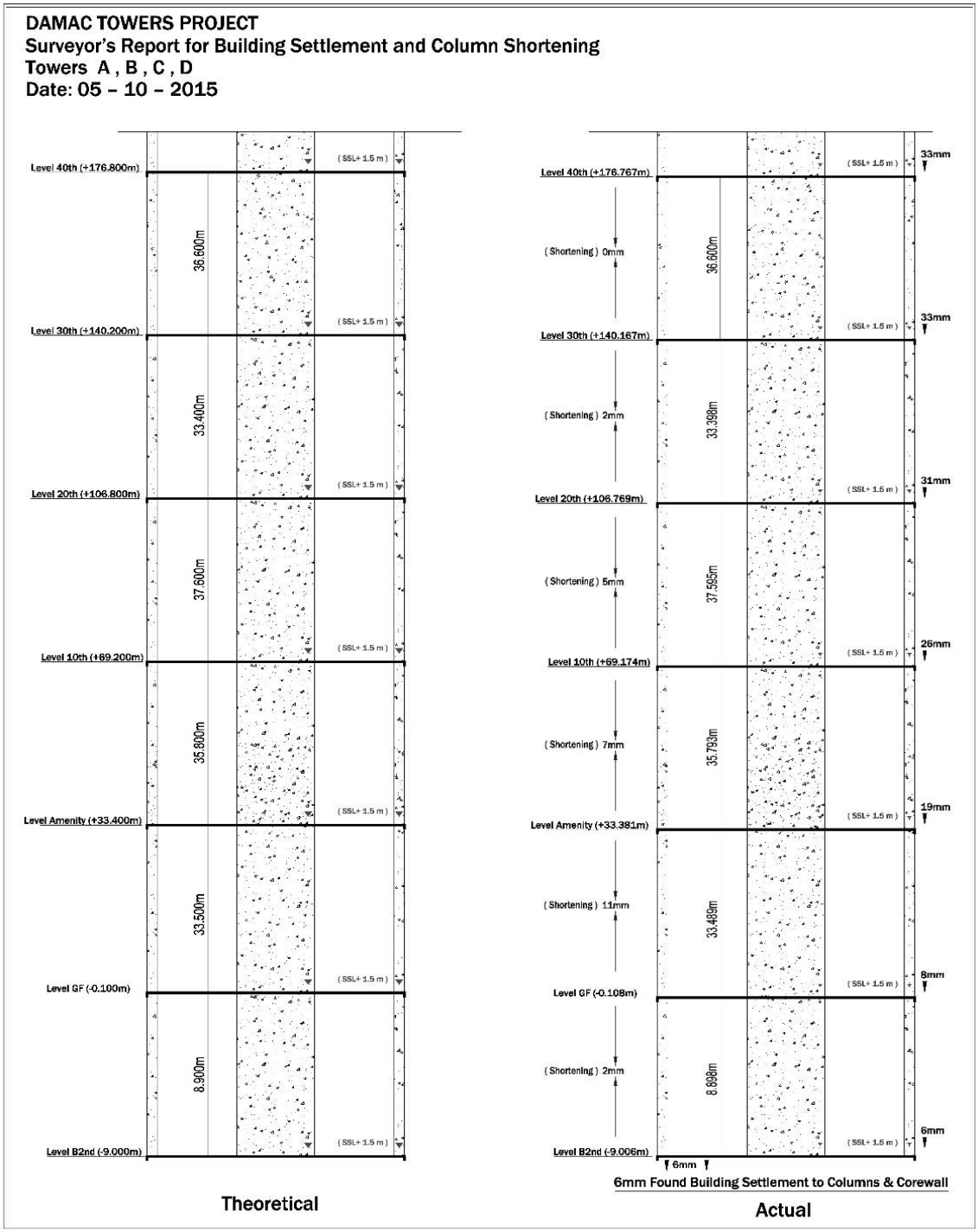

Fig. 6.29 Building settlement for 40 floors

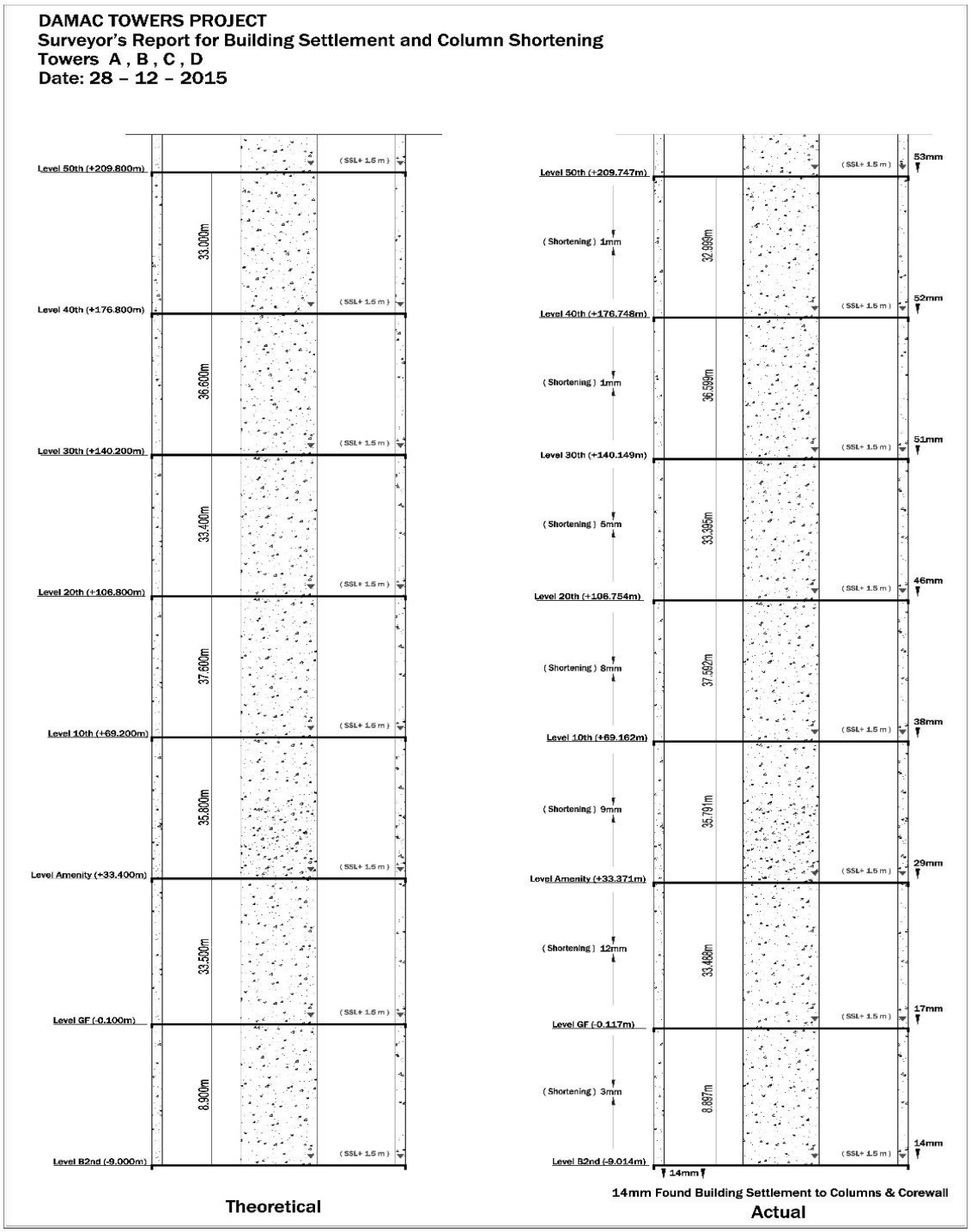

Fig. 6.30 Building settlement for 50 floors

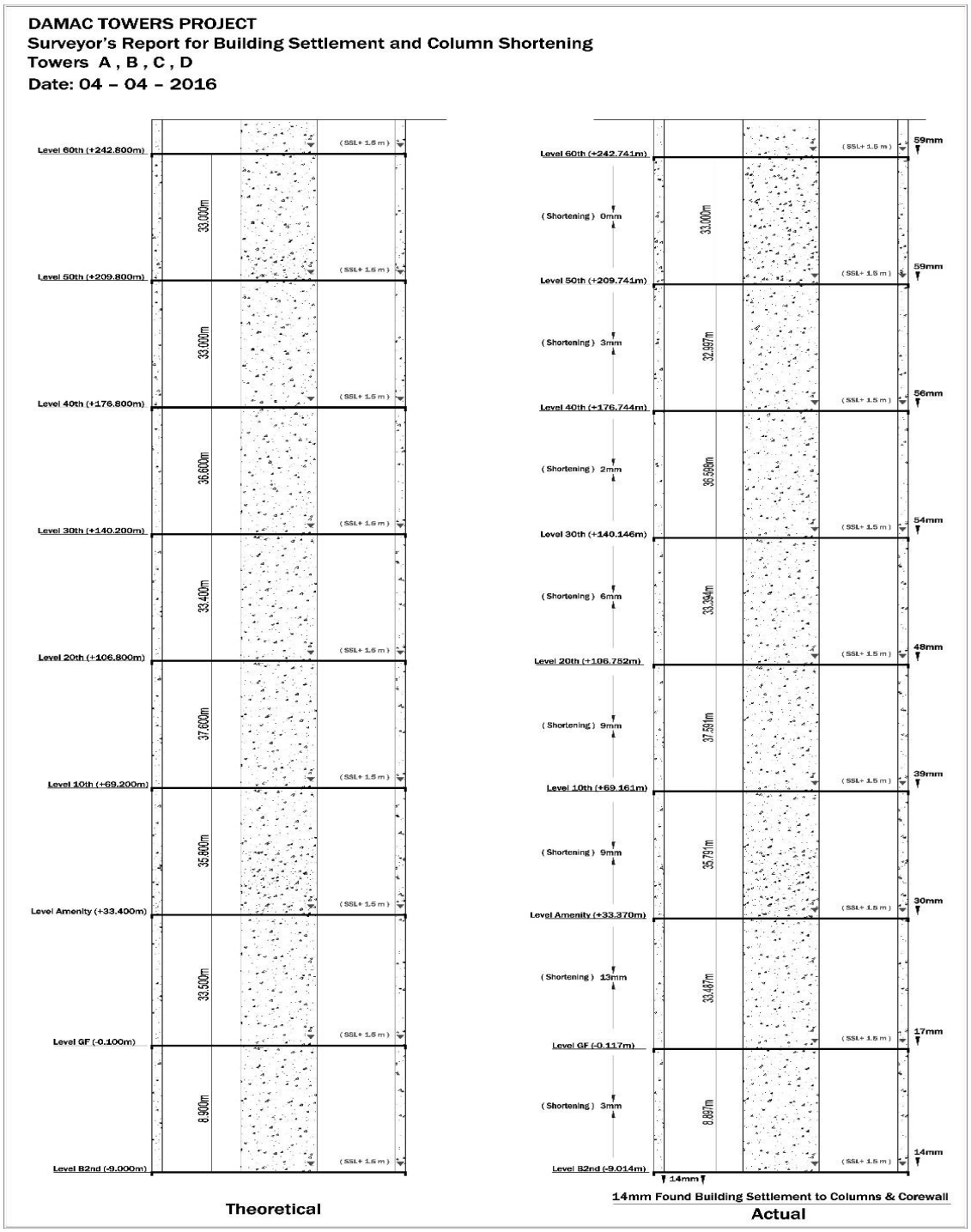

Fig. 6.31 Building settlement for 60 floors

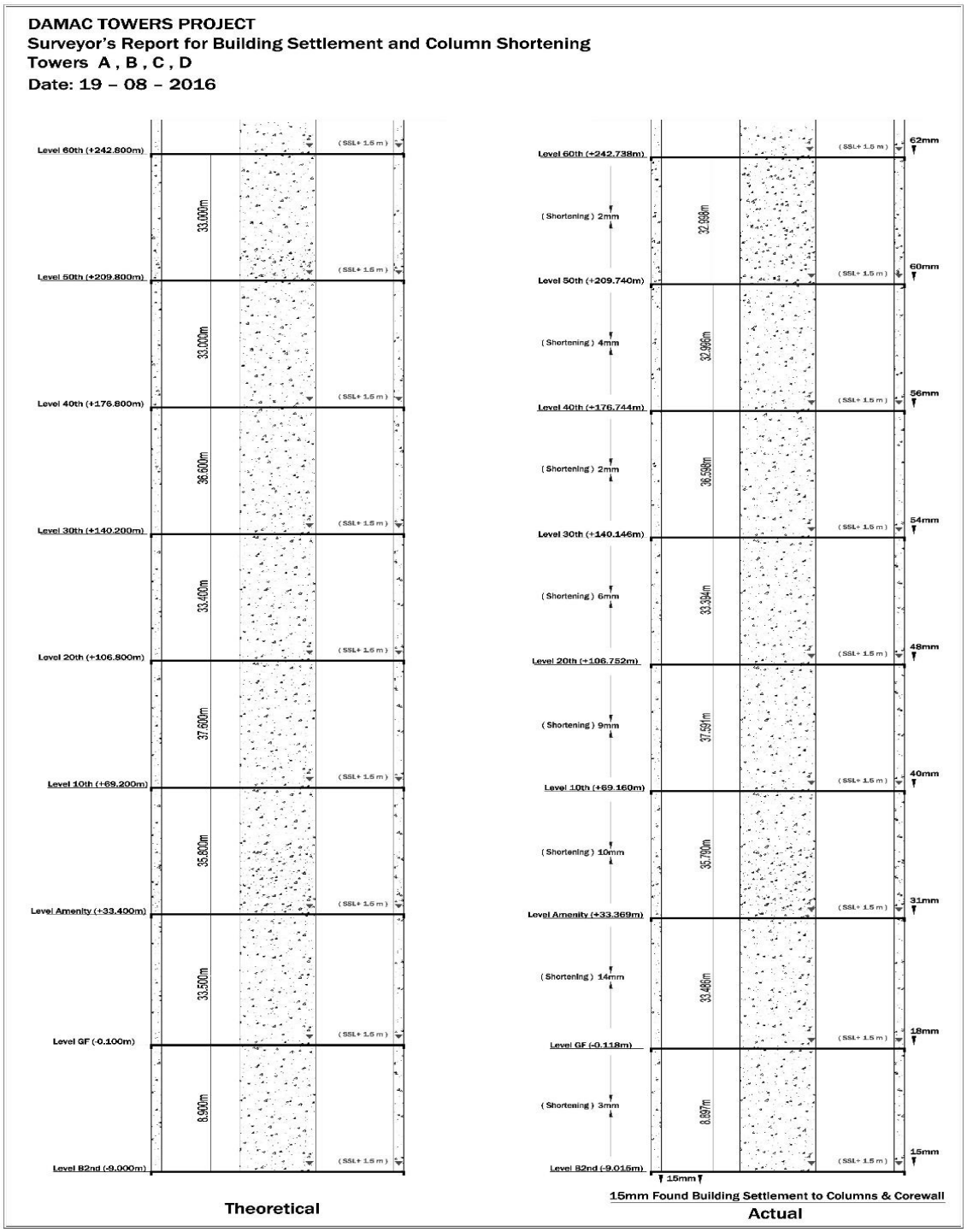

Fig. 6.32 Building settlement for 60 floors

7 Conclusions

A comprehensive study has been conducted to identify the influence of soil parameters, back calculating the elastic modulus of weak rock on the predicted load settlement behaviour of pile by stimulating the static load test using finite element analysis. The results of 116 static load tests conducted on the pile relating to high-rise buildings in the Business Bay and Downtown Dubai areas has been considered for the analysis. The results obtained through conventional methods (empirical and analytical equations), numerical method (finite element method, FEM models) and experimental methods (static load pile testing) has primarily been adopted for the analysis.

Initially, the modulus of elasticity values recommended within the soil investigation reports were used for the load settlement analysis. The comparative study of the conventional and finite element analysis results, along with the static load test results, showed significant variations. The predicted settlement values were highly over-estimated when compared to the static load test results. The variations obtained in the settlement values of conventional and static load test results were beyond the comparable and agreeable limits. The finite element method was initially assumed to be able to deliver better results as the in-situ soil conditions were perfectly simulated using the geotechnical parameters from the soil investigation report during the analysis; however, the finite element results still showed variance, as per the static load test results. The overall trend for the load settlement graphs for both the conventional and finite element results show more similarities in terms of load settlement values.

As explained previously, the load settlement computational methods are highly dependent on the modulus of elasticity of the soil. The conventional equations of settlement are based on the theory of elasticity. Moreover, in the finite element analysis, the material models used for pile and soil are elastic, as is the case for the Mohr-Coulomb model, for which the modulus of elasticity is an important input parameter. Thus, it can be interpreted that the high variation levels seen in the predicted settlement values is mainly due to the dependency on the underestimated values of modulus of elasticity, E_s.

More reliable and accurate values of elastic modulus of weak rocks E_{mod} were back calculated by the stimulation of static load test results using the finite element analysis. Based on this modified modulus of elasticity E_{mod}, the load settlement behaviour of the piles was re-analysed using the conventional methods for determining the influence of the E_{mod} values in the accuracy and reliability of the predicted settlement values by the three empirical and analytical approaches. Compared to the initial analysis results using E_s from the soil report, the use of modified values of E_{mod} in the conventional analysis has bought significant reductions in the predicted settlement values, bringing them into to a comparable range to that of the static load results. However, the elastic shortening settlement component of the piles computed using conventional methods were using the

total length of the pile, whereas the effective length contributing to the skin friction will be less than this total embedded length; the trend of over-designing the pile dimensions is a contributing factor towards the decrease in effective length. Thus, the variations observed between the conventional and the static load test results are as can be expected.

The modulus of elasticity values calculated during the finite element back analysis of static load test significantly differed from the values obtained from the soil investigation report. The back-calculated values of modulus of elasticity E_{mod} have increased by a factor of 11 to 200 times the values obtained from the soil investigation report. This modified elastic modulus values represents the actual stiffness condition at various location in Business Bay and Downtown Dubai. Thus, in order to ensure a safe design, the lowest value of modified elastic modulus was recommended as per the case study conducted in Chapter 6.

Based the above findings, it can be interpreted that the design of pile foundation based on the modulus of elasticity from the soil investigation report will lead to uneconomical over-design of the pile foundation. It is evident that the 116 static load test results used for the analysis were preliminarily designed based on the geotechnical parameters from the soil report, which leads to additional over-design of the pile dimensions than as per the required standards, resulting in additional material and labour having to be used, and increased costs for equipment.
In summary, the key findings that can be interpreted from the present study are as follows:

- The modulus of elasticity (Es) values determined from empirical correlation of the laboratory test results underestimates the actual soil parameters at site; the settlement analysis based on modulus of elasticity (Es) values proves to be highly over-estimated in relation to the load settlement behaviour of the pile in comparison to those of the static load test results.

- The FEM back analysis of the static load test results shows it to be an effective method for accurate estimation of the modified modulus of elasticity $E_{mod,}$ which represents the actual rock stiffness conditions at site. The back-calculated values of the modulus of elasticity E_{mod} increased by a factor of 11 to 200 times the values obtained from the soil investigation report.

- The concrete modulus of elasticity tested at site should be used in the back-analysis process to avoid the limited influence on the modified modulus of elasticity.

- The conventional (empirical and analytical) methods settlement calculations based on the modified modulus of elasticity E_{mod} values and using the effective length of the pile affected by load appear to be a reasonable method to obtain accurate settlement values in line with expectation.

- The numerical analysis technique based on finite element method provides an accurate estimate of the expected settlement values under static loading conditions.

- The geotechnical design for pile foundation based on the soil parameters and modulus of elasticity from the soil investigation report will lead to uneconomical over-design.

- The pile static load test results can be used in combination with the FEM back analysis method to determine the modified elastic modulus E_{mod} of rock. Using E_{mod} will have a huge impact on the design optimization; in addition cost efficiencies related to the design of pile foundations can be achieved.

- The instrumented static load test demonstrated there is no load transfer to the last part and tip of the pile, even with 150% of working load.

- For the case studies, the minimum modulus of elasticity (1450 MPa) found during the FEM modelling from all static piles tests conducted at site should be recommended for the design and as representative values for the modules of elasticity for the site.

- The foundation settlement recorded only 15 mm after completing the structural skeleton; the settlement recorded is much less when compared to the building load, which shows that the rock below the foundation has been underestimated or not taken into account during the design stage.

- Optimization of the deep foundation design by using the modified modulus of elasticity (E_{mod}) will lead to economical building foundations and green construction

- Based on the research results a major saving of surrounding resources such as concrete, steel, energy consumption, cost, time & manpower is possible.

References

Arslan, A. T.; Koca, M. Y.; Aydogmus, T.; Klapperich, H.; Yılmaz, H. R. (2008)
Correlation of Unconfined Compressive Strength with Young's Modulus and Poisson's Ratio in Gypsum from Sivas (Turkey). In Rock Mech Rock Eng 41 (6), 941–950. DOI: 10.1007/s00603-007-0145-8.

Akgüner, C., & Kirkit, M. (2012).
Axial bearing capacity of socketed single cast-in-place piles. Soils and Foundations, 52(1), 59-68.

Azizi, F. (2000)
Applied analyses in geotechnics. London; New York: E & FN Spon.

Bell, F. G. (2004)
Engineering Geology and Construction, Taylor & Francis.

Bieniawski, Z. T. (1989)
Engineering rock mass classifications. A complete manual for engineers and geologists in mining, civil, and petroleum engineering. New York: Wiley.

Bond, A., & Harris, A. (2008).
Decoding eurocode 7. CRC Press.

Bowles, J. E. (1997)
Foundation Analysis and Design, McGraw-Hill.

Bowles, Joseph E. (1996)
Foundation analysis and design. 5th ed. New York: McGraw-Hill; [Online:] Knovel.

Budhu, M. (2010)
Soil Mechanics and Foundations, 3rd Edition, John Wiley & Sons, Incorporated.

Burland, J. B., Chapman, T. and Engineers, I. o. C. (2012)
ICE Manual of Geotechnical Engineering: Geotechnical engineering principles, problematic soils and site investigation, ICE.

Chang, Chandong; Zoback, Mark D.; Khaksar, Abbas (2006)
Empirical relations between rock strength and physical properties in sedimentary rocks. In Journal of Petroleum Science and Engineering Vol. 51 (3-4), 223–237. DOI: 10.1016/j.petrol.2006.01.003.

Clayton, Christopher R. I.; Simons, Noel Edward; Matthews, Marcus C. (1982)
Site investigation.

Council, N. R. (2007)
Load and resistance factor design (LRFD) for deep foundations: TRB.

Craig, R. F. (2004).
Craig's soil mechanics. CRC Press.

Das, B. M. (2007)
Advanced Soil Mechanics, Taylor & Francis.

Das, B. M. (2015)
Principles of Foundation Engineering, Cengage Learning.

Das, B. M. and Sobhan, K. (2013)
Principles of Geotechnical Engineering, SI Edition, Cengage Learning.

Deere, D. (1988)
The Rock Quality Designation (RQD) Index in Practice: ASTM International.

Deere, Don Uel; Miller, R. P. (01-Jan-66)
Engineering classification and index properties for intact rock. DTIC Document.

Emad Y. Sharif, Mohd. J. Ahmed (2010)
Engineering Geology of Dubai. First Edition. United Arab Emirates: ACES (1).

Fang, Hsai-yang (1991)
Foundation engineering handbook. 2. ed. New York, NY: VanNostrand Reinhold.

Fleming, W. G. K. (1992).
A new method for single pile settlement prediction and
analysis. Geotechnique, 42(3), 411-425.

Ghamgosar, M., Fahimifar, A., & Rasouli, V. (2010).
Estimation of rock mass deformation modulus from laboratory experiments in Karun Dam. In ISRM International Symposium-EUROCK 2010. International Society for Rock Mechanics.

Jain, B. C. P. A. K. J. A. K. (2005)
Building Construction, Laxmi Publications.

Jalali, M. M., Golmaei, S. H., Jalali, M. R., Borthwick, A., Ahmadi, M. K. Z., & Moradi, R. (2012)
Using Finite Element method for Pile-Soil Interface (through PLAXIS and ANSYS). Journal of Civil Engineering and Construction Technology, Vol. 3(10), 256-272.

Kwong, A. K. L., Lau, C. K., Lee, C. F., Ng, C. W. W., Pang, P. L. R., Yin, J. H., & Yue, Z. Q. (2001)
Soft Soil Engineering: Taylor & Francis.

Lakusic Stjepan, Bashar Tarawneh, Mounir Matraji (2014)
Ground improvement using rapid impact compaction: case study in Dubai. In JCE 66. DOI: 10.14256/JCE.1083.2014.

Lee, I. K., White, W., & Ingles, O. G. (1983).
Geotechnical Engineering. Pitmans Books Limited.

Lindeburg, Michael R. (2001)
Civil engineering reference manual for the PE exam. 8th ed. Belmont, CA: Professional Publications.

Naveen, B. P., Sitharam, T. G., & Vishruth, S. (2011).
Numerical simulation of vertically loaded piles. Young, 21(22.00), 25-00.

Aggour, M. Sherif (2002)
UPDATING BEARING CAPACITY – SPT GRAPHS. Maryland State Highway Administration Office of Policy and Research.

Marsland, A. (1986)
The Choice of Test Methods in Site Investigations. In Geological Society, London, Engineering Geology Special Publications Vol. 2 (1), 289–297.

Meyerhof, G. G. (1976)
Bearing capacity and settlement of pile foundations. In Journal of the Geotechnical Engineering Division, ASCE Vol. 102 (1), 195–228.

Naval Facilities Engineering Command (1986a)
FOUNDATIONS ANTD EARTH STRUCTURES. DESIGN MANUAL 7.02.

Naval Facilities Engineering Command (1986b)
Soil Mechanics. DESIGN MANUAL 7.01.

Nawy, E. G. (2008)
Concrete construction engineering handbook, 2nd ed., Boca Raton: CRC Press.

Nazir, R., Moayedi, H., Mosallanezhad, M., & Tourtiz, A. (2015).
Appraisal of reliable skin friction variation in a bored pile. Proceedings of the Institution of Civil Engineers-Geotechnical Engineering, 168(1), 75-86.

Nejad, F. P., Jaksa, M. B., Kakhi, M., & McCabe, B. A. (2009)
Prediction of pile settlement using artificial neural networks based on standard penetration test data. Computers and Geotechnics, Vol. 36(7), 1125-1133.

Omer, J. R., Delpak, R., & Robinson, R. B. (2010).
An empirical method for analysis of load transfer and settlement of single piles. Geotechnical and Geological Engineering, 28(4), 483-501.

Peck, Ralph B.; Hanson, Walter Edmund; Thornburn, Thomas Hampton (1974)
Foundation engineering. [By] Ralph B. Peck, Walter E. Hanson, Thomas H. Thornburn. 2nd ed. New York, etc.: Wiley.

Plaxis, B. V. (2010).
PLAXIS 2D Reference Manual. PO Box, 572, 2600.

Poulos, H. G., & Davis, E. H. (1980)
Pile foundation analysis and design. New York; Chichester: Wiley.

Prakash, S. and Sharma, H. D. (1990)
Pile foundations in engineering practice, New York; Chichester: Wiley.

Prakash, S., & Sharma, H. D. (1990). Pile Foundations in Engineering Practice: Wiley.
Punmia, B. C. and Jain, A. K. (2005) Soil Mechanics and Foundations, Laxmi Publications Pvt Limited.

Reddy, J. R. (1999) Civil Engineering (O.T.), Laxmi Publications Pvt Limited.
Rosenberg, P. and Journeaux, N.L. (1976) Friction and end bearing tests on bedrock for high capacity socket design. Canadian Geotechnical Journal, Vol. 13(3), 324-333.

Rowe, R.K. and Armitage, H.H., (1987)
A design method for drilled piers in soft rock. Canadian Geotechnical Journal, Vol. 24(1), 126-142.

Rowe, R.K. and Armitage, H.H., (1987)
Theoretical solutions for axial deformation of drilled shafts in rock. Canadian Geotechnical Journal, Vol. 24(1), 114-125.

Schuppener, B. (2007).
Eurocode 7: Geotechnical Design-Part 1: General rules-its implementation in the European Member states. In Proc. 14th European Conference on Soil Mechanics and Geotechnical Engineering, Madrid.

Sew, I. D. G. S., Chin, I. T. Y., & Shong, I. L. S. (2003).
A brief guide to design of bored piles under axial compression–a Malaysian approach. In Seminar and Exhibition on Bridge Engineering, Kulala Lumpur, Malaysia pp. 8-22.

Shroff, A. V. and Shah, D. L. (2003)
Soil mechanics and geotechnical engineering, Rotterdam: Balkema.

Smoltczyk, U. (2003)
Geotechnical Engineering Handbook, Procedures (Vol. 2): John Wiley & Sons.

Standard, British: 5930 (1981)
Code of Practice for Site Investigations. In British Standards Institution, London, p. 147.

Terzaghi, K., Peck, R. B. and Mesri, G. (1996)
Soil Mechanics in Engineering Practice, Wiley.

Tomlinson, M. and Woodward, J. (2007)
Pile Design and Construction Practice, Fifth Edition, CRC Press.

Tomlinson, M. J. and Boorman, R. (2001)
Foundation design and construction, 7th ed. ed., Harlow: Prentice Hall.

Tomlinson, M., & Woodward, J. (2007)
Pile Design and Construction Practice, Fifth Edition: CRC Press.

Vesic, A. S. (1977)
'Design of pile foundations', NCHRP synthesis of highway practice, (42).

Waltham, T. (2009).
Foundations of engineering geology. CRC Press.

Wehnert, M., & Vermeer, P. A. (2004).
Numerical analyses of load tests on bored piles. Numerical methods in geomechanics–NUMOG IX, 505-511.

Wyllie, D. C. (2003)
Foundations on Rock: Engineering Practice, Second Edition, Taylor & Francis.

List of figures

List of tables

Mitteilungen des Institutes und der Versuchsanstalt für Geotechnik der Technischen Universität Darmstadt

---

Mitteilungen der Versuchsanstalt für Bodenmechanik und Grundbau der TH Darmstadt
Hrsg.: o. Prof. Dr.-Ing. Herbert Breth

Nr. 1 Beitrag zur Berechnung von Gründungsbalken und einseitig ausgesteiften Gründungsplatten unter Einbeziehung der Steifigkeit von rahmenartigen Hochbauten.
Dr.-Ing. Heinrich Sommer, Februar 1965

Nr. 2 Aktuelle Probleme im Staudammbau.
Veröffentlichungen in den Jahren 1966 und 1967

Nr. 3 Über den Einfluß eines dünnwandigen, im Boden verlegten Rohres auf das Tragverhalten des Bodens.
Dr.-Ing. Karl-Heinz Schwinn, Januar 1968

Nr. 4 Das Tragverhalten des Frankfurter Tons bei im Tiefbau auftretenden Beanspruchungen.
Prof. Dr.-Ing. Herbert. Breth, Dipl.-Ing. Ekkehart Schultz, Dipl.-Ing. Dieter Stroh, April 1970

Nr. 5 Zur Frage der Erosionssicherheit unterströmter Erdstaudämme.
Dr.-Ing. Klaus Günther, Juni 1970

Nr. 6 Ermittlung der rheologischen Zustandsgleichung eines Lehmes mit Hilfe einer neuentwickelten Versuchsapparatur.
Dr.-Ing. Dietrich Fedder, Dezember 1970

Nr. 7 Beiträge in den Jahren 1968 bis 1970.

Nr. 8 Der Einfluß der Steifigkeit von Stahlbetonskelettbauten auf die Verformung und die Beanspruchung von Gründungsplatten auf Ton.
Dr.-Ing. Heinz Heil, Juni 1971

Nr. 9 Der Einfluß von Fundamentlasten auf die Größe und Verteilung des Erddrucks auf biegsame, abgesteifte Baugrubenwände.
Dr.-Ing. Robert Wanoschek, März 1972

Nr. 10 Das Verformungsverhalten des Frankfurter Tons beim Tunnelvortrieb.
Dipl.-Ing. Gerd Chambosse, Februar 1972

Nr. 11 Beiträge in den Jahren 1972 und 1973.

Nr. 12 Messungen an einer verankerten Baugrubenwand.
Dipl.-Ing. Wolfhard Romberg, Dezember 1973

Nr. 13 Berechnung verankerter Baugruben nach der Finite Element Methode.
Dr.-Ing. Dieter Stroh, Juni 1974

Nr. 14 Ein Beitrag zur Klärung des Tragverhaltens einfach verankerter Baugrubenwände.
Dr.-Ing. Gert-Peter Schmitt, Juli 1974

Nr. 15 Verformungsverhalten des Baugrundes beim Baugrubenaushub und anschließendem Hochhausbau am Beispiel des Frankfurter Tons.
Dr.-Ing. Peter Amann, Prof. Dr.-Ing. Herbert Breth, Dr.-Ing. Dieter Stroh, Juni 1975

Nr. 16 Ermittlung des Tragverhaltens einer mehrfach verankerten Baugrubenwand durch Modellversuche.
Dr.-Ing. Reinhard Wolff, Juni 1975

Nr. 17 Die instationäre Brunnenströmung im anisotropen Grundwasserleiter mit freier Oberfläche.
Dr.-Ing. Thomas Klüber, November 1975

Nr. 18 Spannungen und Verformungen in hohen Dämmen im Bauzustand.
Dr.-Ing. Gunter Hardt, Januar 1976

Nr. 19 Beiträge in den Jahren 1974 bis 1977

Sonderheft:
Beiträge zu Staudammbau und Bodenmechanik.
Festschrift zum 65. Geburtstag von o. Prof. Dr.-Ing. H. Breth, Darmstadt, 1978

Nr. 20 Spannungen und Verformungen in hohen Steinschüttdämmen im Bauzustand unter besonderer Berücksichtigung von Talform und Hangrauhigkeit.
Dr.-Ing. Heinz Czapla, März 1979

Nr. 21 Beitrag zur Berechnung von Gründungsplatten - Eine vergleichende Studie.
Dr.-Ing. Horst Rückel, August 1979

Nr. 23 Beitrag zum Spannungs- Verformungsverhalten der Böden.
Dr.-Ing. M. Ulvi Arslan, Dr.-Ing. Rainer Wanninger, August 1980

Nr. 24 Entwicklungstendenzen beim Bau und der Berechnung oberflächennaher Tunnel in bebautem Stadtgebiet.
Dr.-Ing. Rolf Katzenbach, November 1981

Mitteilungen des Institutes für Grundbau, Boden- und Felsmechanik der TH Darmstadt
Hrsg.: Prof. Dr.-Ing. Eberhard Franke

Sonderheft:
Beiträge zu Staudammbau und Bodenmechanik.
Festschrift zum 70. Geburtstag von o. Prof. em. Dr.-Ing. H. Breth
Darmstadt, 1983

Nr. 25 Großversuche zur Ermittlung des Tragverhaltens von Pfahlreihen unter horizontaler Belastung.
Dr.-Ing. Hans-Gottfried Schmidt, Januar 1986

Sonderheft:
Beiträge zum Symposium Pfahlgründungen, 12./13.3.1986 in Darmstadt.
Darmstadt, 1986

Nr. 26 Pfahlgruppen in geschichtetem Boden unter horizontaler dynamischer Belastung.
Dr.-Ing. Hans Georg Hartmann, April 1986

Nr. 27 Zur Frage der Standsicherheit verankerter Stützwände auf der tiefen Gleitfuge.
Dr.-Ing. Michael H. Heibaum, April 1987

Nr. 28 Tragverhalten von Pfahlgruppen unter Horizontalbelastung.
Dr.-Ing. Eberhard Klüber, März 1988

Nr. 29 Untersuchungen über den Primärspannungszustand in bindigen überkonsolidierten Böden am Beispiel des Frankfurter Untergrundes.
Dr.-Ing. Hermann Mader, Februar 1988

Nr. 30 Coulombsches Extremalprinzip und Schranken des Erddrucks.
Prof. Dr.-Ing. Thomas Dietrich und Dr.-Ing. Ulvi Arslan, Juni 1989

Nr. 31 Beitrag zur Beschreibung des Materialverhaltens bindiger Böden unter allgemeiner nichtmonotoner Belastung.
Dr.-Ing. Gerhard Muth, Juli 1989

Mitteilungen des Institutes und der Versuchsanstalt für Geotechnik der TU Darmstadt
Hrsg.: Prof. Dr.-Ing. Rolf Katzenbach

Nr. 32 Festvorträge zum Festkolloquium am 1. Oktober 1993 anläßlich des 80. Geburtstages von em. Prof. Dr.-Ing. Herbert Breth.
Darmstadt, November 1994

Nr. 33 Vorträge des 1. Darmstädter Geotechnik-Kolloquiums am 14.7.1994.
Darmstadt, Dezember 1994

Nr. 34 Vorträge zum 2. Darmstädter Geotechnik-Kolloquium am 30.3.1995.
Darmstadt, Dezember 1995

Nr. 35 Vorträge zum 3. Darmstädter Geotechnik-Kolloquium am 21.3.1996.
Darmstadt, März 1996

Nr. 36 Ein Berechnungsmodell zum Tragverhalten der Kombinierten Pfahl-Plattengründung.
Dr.-Ing. Yasser El-Mossallamy, Dezember 1996

Nr. 37 Vorträge zum 4. Darmstädter Geotechnik-Kolloquium am 13.3.1997.
Darmstadt, März 1997

Nr. 38 Vorträge zum Workshop Baugrund-Tragwerk-Interaktion am 21.November 1997.
Darmstadt, November 1997

Nr. 39 Vorträge zum 5. Darmstädter Geotechnik-Kolloquium am 19.3.1998.
Darmstadt, März 1998

Nr. 40 Beitrag zum Grenzverformungsverhalten und zur Gebrauchstauglichkeit horizontaler mineralischer Deponiebarrieren.
Dr.-Ing. Lorenz Edelmann, August 1998

Nr. 41 Flachglas-Elemente als dauerhafte Schadstoffsperre in Deponiebasisabdichtungen - Integrierte-Glas-Sandwich-Dichtung (IGSD) -.
Dr.-Ing. Heinrich Weiler, November 1998

Nr. 42 Experimentelle und numerische Untersuchungen zum Tragverhalten von Pfahlgründungen im Fels.
Dr.-Ing. Jörg Holzhäuser, November 1998

Nr. 43 Vorträge zum 1. Darmstädter Baurechts-Kolloquium am 14. Januar 1999 an der TU Darmstadt.
Darmstadt, Januar 1999

Nr. 44 Vorträge zum 6. Darmstädter Geotechnik-Kolloquium am 11. März 1999.
Darmstadt, März 1999

Nr. 45 Einfluß der Kapillarität auf die Mehrphasenströmung bei der Sanierung von Mineralölschadensfällen im Boden.
Dr.-Ing. Matthias Vogler, März 1999

Nr. 46 Vorträge zum 2. Berlin-Darmstädter Baurechts-Kolloquium am 15. Oktober 1999 in Berlin.
Darmstadt, Oktober 1999

Nr. 47 Vorträge zum Darmstädter Fortbildungsseminar Kombinierte Pfahl-Plattengründung (KPP).
Darmstadt, Dezember 1999

Nr. 48 Untersuchungen zur Viskoplastizität und Festigkeit von Steinsalz.
Dr.-Ing. Conrad Boley, Dezember 1999

Nr. 49 Experimentelle und theoretische Untersuchung der Stabilisierungsmöglichkeiten und des Verhaltens von tropischen Lateritböden.
Dr.-Ing. Girma Boled-Mekasha, Dezember 1999

Nr. 50 Vorträge zum 2. Workshop Baugrund-Tragwerk-Interaktion am 17.März 2000.
Darmstadt, März 2000

Nr. 51 Vorträge zum 7. Darmstädter Geotechnik-Kolloquium am 23. März 2000.
Darmstadt, März 2000

Nr. 52 Beiträge anlässlich des 50. Geburtstages von Herrn Professor Dr.-Ing. Rolf Katzenbach.
Darmstadt, Mai 2000

Nr. 53 In-situ-Messungen und numerische Studien zum Tragverhalten der Kombinierten Pfahl-Plattengründung.
Dr.-Ing. Oliver Reul, Juli 2000

Nr. 54 Vorträge zum 3. Darmstadt-Berliner Baurechts-Kolloquium am 20. Oktober 2000 an der TU Darmstadt.
Darmstadt, Oktober 2000

Nr. 55 Vorträge zum 8. Darmstädter Geotechnik-Kolloquium am 15. März 2001.
Darmstadt, März 2001

Nr. 56 Vorträge zum 4. Berlin-Darmstädter Baurechts-Kolloquium am 28. September 2001 in Berlin.
Darmstadt, September 2001

Nr. 57 Experimentelle und numerische Untersuchungen zur Gleislagestabilität.
Dr.-Ing. Stefan A. Heineke, Dezember 2001

Nr. 58 Vorträge zum 9. Darmstädter Geotechnik-Kolloquium am 14. März 2002.
Darmstadt, März 2002

Nr. 59 Trag- und Verformungsverhalten tiefer Baugruben in bindigen Böden unter besonderer Berücksichtigung der Baugrund-Tragwerk- und der Baugrund-Grundwasser-Interaktion.
Dr.-Ing. Christian Moormann, Juli 2002

Nr. 60 Energiepfahlanlagen mit Saisonalem Thermospeicher.
Dr.-Ing. Annette Ennigkeit, September 2002

Nr. 61 Vorträge zum 5. Darmstadt-Berliner Baurechts-Kolloquium am 18. Oktober 2002 an der TU Darmstadt.
Darmstadt, Oktober 2002

Nr. 62 Vorträge zum 3. Workshop Baugrund-Tragwerk-Interaktion am 30. Oktober 2002.
Darmstadt, Oktober 2002

Nr. 63 Beitrag zur Modellierung des Tragverhaltens Kombinierter Pfahl-Plattengründungen (KPP) unter Verwendung geotechnischer Messungen.
Dr.-Ing. Bernd Lutz, Dezember 2002

Nr. 64 Vorträge zum 10. Darmstädter Geotechnik-Kolloquium am 13. März 2003.
Jubiläumskolloquium, Darmstadt, März 2003

Nr. 65 Festschrift zum 90. Geburtstag von em. Prof. Dr.-Ing. Herbert Breth am 29. Juni 2003.
Darmstadt, Juni 2003

Nr. 66 Experimentelle und numerische Untersuchungen zum Verhalten von granularen Materialien unter zyklischer Beanspruchung.
Dr.-Ing. Gerd Festag, September 2003

Nr. 67 Vorträge zum 6. Berlin-Darmstädter Baurechts-Kolloquium am 30. Oktober 2003 in Berlin.
Darmstadt, Oktober 2003

Nr. 68 Vorträge zum 11. Darmstädter Geotechnik-Kolloquium am 18. März 2004.
Darmstadt, März 2004

Nr. 69 Vorträge zum 7. Darmstadt-Berliner Baurechts-Kolloquium am 28. Oktober 2004 an der TU Darmstadt.
Darmstadt, Oktober 2004

Nr. 70 Experimentelle und numerische Untersuchungen zum Tragverhalten von Ortbetonpfählen mit variabler Bodenverdrängung.
Dr.-Ing. Alexander Schmitt, Dezember 2004

Nr. 71 Vorträge zum 12. Darmstädter Geotechnik-Kolloquium am 17. März 2005.
Darmstadt, März 2005

Nr. 72 Beitrag zur Klärung des Trag- und Verformungsverhaltens horizontal belasteter Kombinierter Pfahl-Plattengründungen.
Dr.-Ing. Jens Turek, März 2006

Nr. 73 Vorträge zum 13. Darmstädter Geotechnik-Kolloquium am 16. März 2006.
Darmstadt, März 2006

Nr. 74 Vorträge zum 8. Berlin-Darmstädter Baurechts-Kolloquium am 6. Oktober 2006 in Berlin.
Darmstadt, Oktober 2006

Nr. 75 Experimentelle und numerische Untersuchungen zur Baugrund-Fahrweg-Interaktion von Bahnstrecken auf gering tragfähigem Baugrund.
Dr.-Ing. Marc Ittershagen, März 2006

Nr. 76 Vorträge zum 14. Darmstädter Geotechnik-Kolloquium am 15. März 2007.
Darmstadt, März 2007

Nr. 77 Nonlinear response of laterally loaded piles in soft Bangkok clay.
Dr.-Ing. Sathaporn Pokpong, August 2007

Nr. 78 Erdwiderstand in homogenem und geschichtetem Baugrund – Experimente und Numerik.
Dr.-Ing. Christian Gutberlet, Februar 2008

Nr. 79 Vorträge zum 15. Darmstädter Geotechnik-Kolloquium am 13. März 2008.
Darmstadt, März 2008

Nr. 80 Prozessorientierte Kooperation in der geotechnischen Bauplanung.
Dr.-Ing. Johannes Giere, März 2009

Nr. 81 Vorträge zum 16. Darmstädter Geotechnik-Kolloquium am 19. März 2009.
Darmstadt, März 2009

Nr. 82 Dreidimensionale, zeitvariante stoffliche Modellierung von granularem Steinsalz.
Dr.-Ing. Stefan Wachter, Mai 2009

Nr. 83 Möglichkeiten und Grenzen experimenteller und numerischer Modellbildungen zur Optimierung geotechnischer Verbundkonstruktionen.
Dr.-Ing. habil. Christian Moormann, Mai 2009

Nr. 84 Entwicklung von Grund- und Böschungsbruch – Experimente und Numerik.
Dr.-Ing. Gregor Bachmann, August 2009

Nr. 85 Effects of seismic soil-structure interaction on the bearing capacity factors for shallow strip footings.
Dr.-Ing. Alexis Nzahabwanimana, September 2009

Nr. 86 Vorträge zum 17. Darmstädter Geotechnik-Kolloquium am 18. März 2010.
Darmstadt, März 2010

Nr. 87 Vorträge zum Festkolloquium “50 Jahre Geotechnik an der TU Darmstadt” am 25. Juni 2010. Darmstadt, Juni 2010

Nr. 88 Vorträge zum 18. Darmstädter Geotechnik-Kolloquium am 17. März 2011.
Darmstadt, März 2011

Nr. 89 Vorträge zum 9. Berlin-Darmstädter Baurechts-Kolloquium am 07. April 2011 in Berlin.
Darmstadt, April 2011 (in Vorbereitung)

Nr. 90 Optimized Use of Combined Pile-Raft Foundation Design for High-Rise Buildings on Semi-Soft Soils.
Dr.-Ing. Henok Fikre, Dezember 2011

Nr. 91 Vorträge zum 19. Darmstädter Geotechnik-Kolloquium am 15. März 2012.
Darmstadt, März 2012

Nr. 92 Vorträge zum 20. Darmstädter Geotechnik-Kolloquium am 21. März 2013.
Jubiläumskolloquium, Darmstadt, März 2013

Nr. 93 Vorträge zum 21. Darmstädter Geotechnik-Kolloquium am 20. März 2014.
Darmstadt, März 2014

Nr. 94 Vorträge zum 22. Darmstädter Geotechnik-Kolloquium am 12. März 2015.
Darmstadt, März 2015

Nr. 95 Simulation des mechanischen Verhaltens einer Deponie unter Berücksichtigung der spezifischen Stoffeigenschaften und zeitvarianten Randbedingungen.
Dr.-Ing. Jörg Gutwald, September 2015

Nr. 96 Serviceability and safety in the design of rigid inclusions and combined pile-raft foundations.
Dr.-Ing. Cécilia Bohn, September 2015

Nr. 97 Vorträge zum 23. Darmstädter Geotechnik-Kolloquium am 10. März 2016.
Darmstadt, März 2016

Nr. 98 Handbuch zur Wiedernutzung von Bestandsgründungen, Dezember 2016

Nr. 99 Oberflächennahe Geothermiesondenanlagen – von der Praxisstudie zur modellbasierten Analyse ihrer Temperaturfahnenausbreitung.
Dr.-Ing. Isabel Wagner, Dezember 2016

Nr. 100 Einsatz effizienzoptimierter geothermischer Systeme zur Schnee- und Eisfreihaltung von Verkehrsflächen.
Dr.-Ing. Thomas Waberseck, März 2017

Nr. 101 Vorträge zum 24. Darmstädter Geotechnik-Kolloquium am 16. März 2017.
Darmstadt, März 2017

Nr. 102 Stiffness and strength of Dubai sedimentary rock.
Dr.-Ing. Marwan Alzaylaie, Dezember 2017

Darmstadt Geotechnics
Ed.: Prof. Dr.-Ing. Rolf Katzenbach

No. 1 3rd Darmstadt-Geotechnical Conference. 21 March 1996, Darmstadt
No. 2 4th Darmstadt-Geotechnical Conference. 13 March 1997, Darmstadt
No. 3 5th Darmstadt-Geotechnical Conference. 19 March 1998, Darmstadt
No. 4 International Conference on Soil-Structure Interaction in Urban Civil Engineering. Volume I + II, 8/9 October 1998, Darmstadt
No. 5 6th Darmstadt Geotechnical Conference. 11 March 1999, Darmstadt
No. 6 2nd Workshop Soil-Structure Interaction. 17 March 2000, Darmstadt
No. 7 7th Darmstadt Geotechnical Conference. 23 March 2000, Darmstadt
No. 8 8th Darmstadt Geotechnical Conference. 15 March 2001, Darmstadt
No. 9 9th Darmstadt Geotechnical Conference. 14 March 2002, Darmstadt
No. 10 3rd Workshop Soil-Structure Interaction. 30 October 2002, Darmstadt
No. 11 10th Darmstadt Geotechnical Conference. 13 March 2003, Darmstadt
No. 12 11th Darmstadt Geotechnical Conference. 18 March 2004, Darmstadt
No. 13 12th Darmstadt Geotechnical Conference. 17 March 2005, Darmstadt
No. 14 13th Darmstadt Geotechnical Conference. 16 March 2006, Darmstadt
No. 15 14th Darmstadt Geotechnical Conference. 15 March 2007, Darmstadt
No. 16 15th Darmstadt Geotechnical Conference. 13 March 2008, Darmstadt
No. 17 16th Darmstadt Geotechnical Conference. 19 March 2009, Darmstadt
No. 18 International Conference on Deep Foundations – CPRF and Energy Piles. 15 May 2009, Frankfurt am Main
No. 19 17th Darmstadt Geotechnical Conference. 18 March 2010, Darmstadt
No. 20 18th Darmstadt Geotechnical Conference. 17 March 2011, Darmstadt
No. 21 Particle Image Velocemitry Measuring Methods for Soil Movements in Geotechnics, December 2011, Darmstadt
No. 22 19th Darmstadt Geotechnical Conference, 15 March 2012, Darmstadt
No. 23 20th Darmstadt Geotechnical Conference, 21 March 2013, Darmstadt
No. 24 21th Darmstadt Geotechnical Conference, 20 March 2014, Darmstadt

Appendix 1 Tiles Summary Results

Pile Summary Sheet
P1

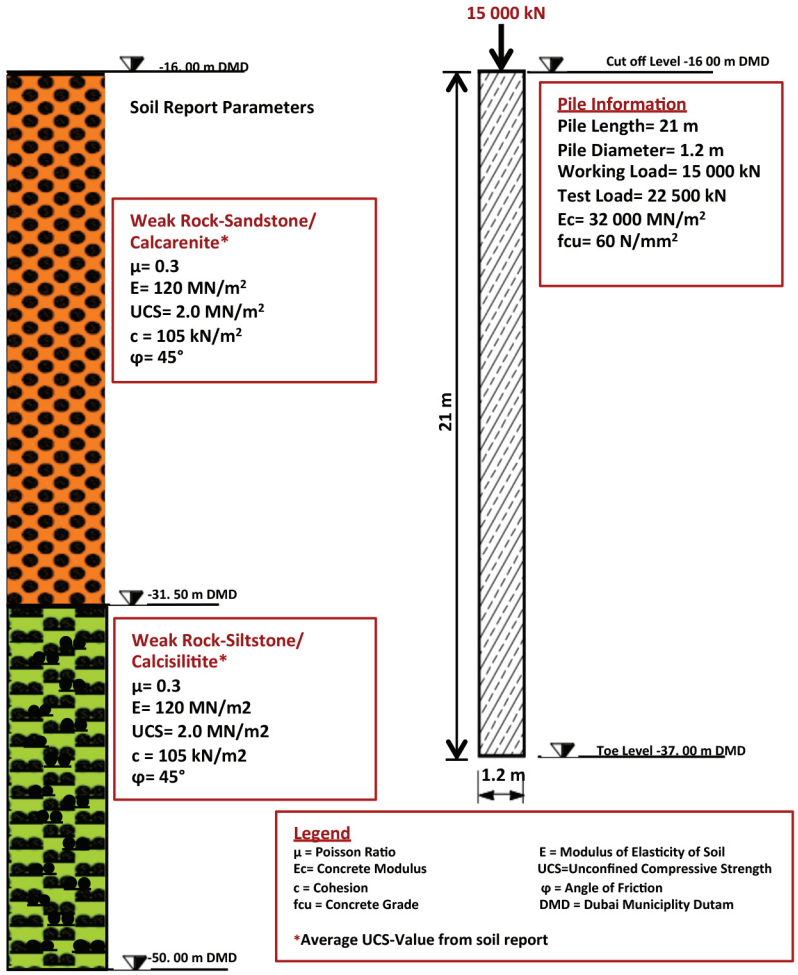

Pile Information
Pile Length= 21 m
Pile Diameter= 1.2 m
Working Load= 15 000 kN
Test Load= 22 500 kN
Ec= 32 000 MN/m²
fcu= 60 N/mm²

Legend

μ = Poisson Ratio
Ec= Concrete Modulus
c = Cohesion
fcu = Concrete Grade
E = Modulus of Elasticity of Soil
UCS=Unconfined Compressive Strength
φ = Angle of Friction
DMD = Dubai Municiplity Dutam

*Average UCS-Value from soil report

Modelling by using Soil Report Parameters

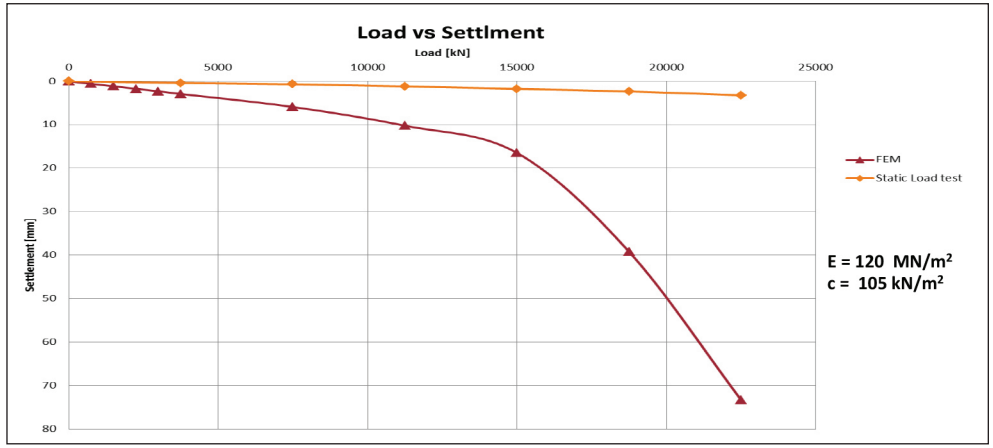

E = 120 MN/m²
c = 105 kN/m²

Back-Analysis of Soil Properties from Load Test

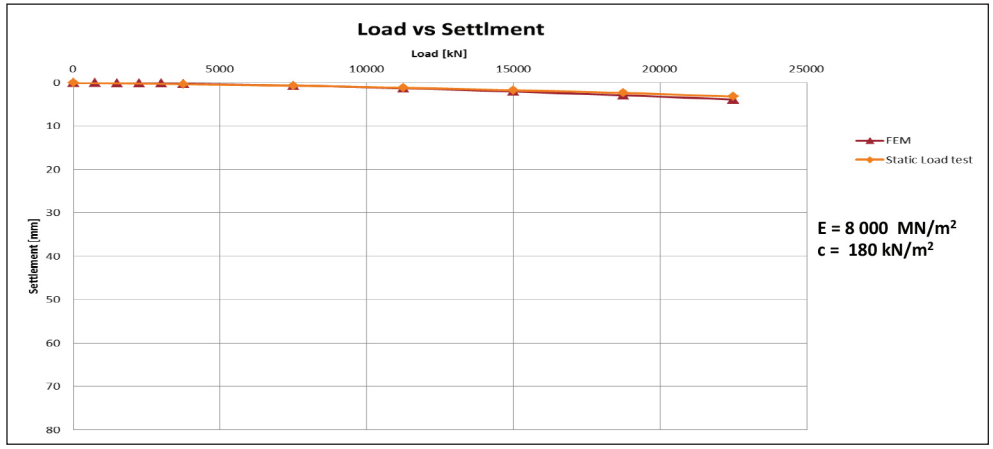

E = 8 000 MN/m²
c = 180 kN/m²

Pile Summary Sheet
P2

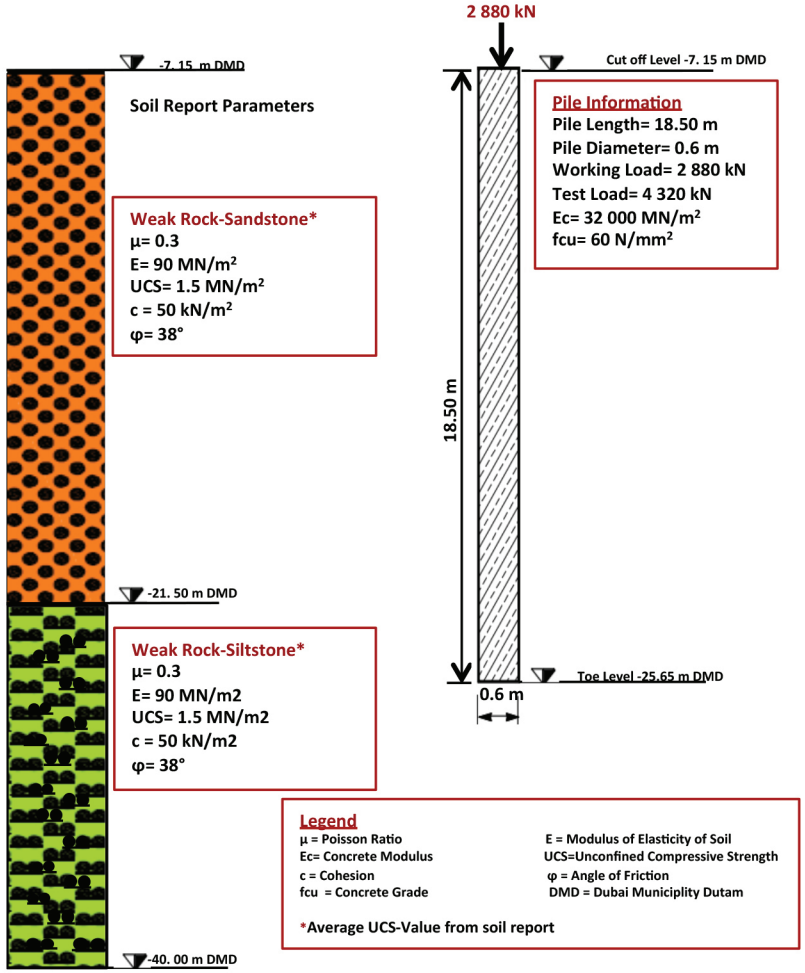

Modelling by using Soil Report Parameters

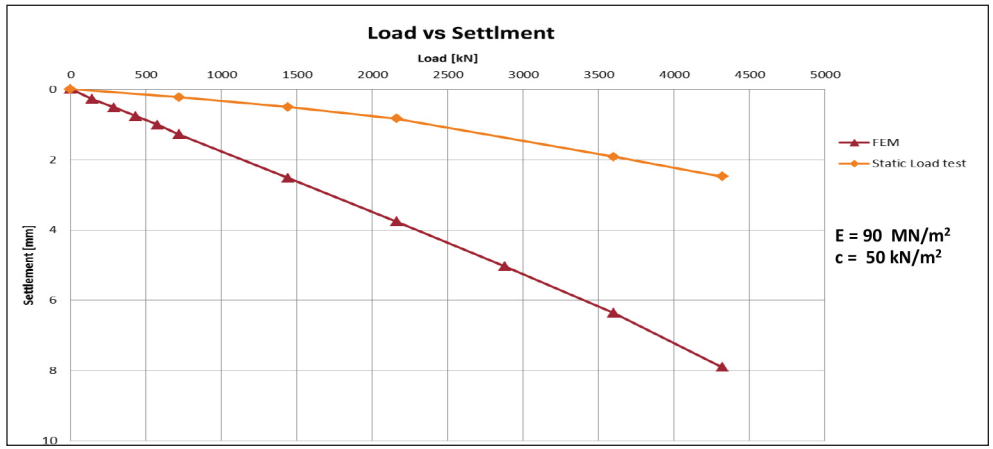

Back-Analysis of Soil Properties from Load Test

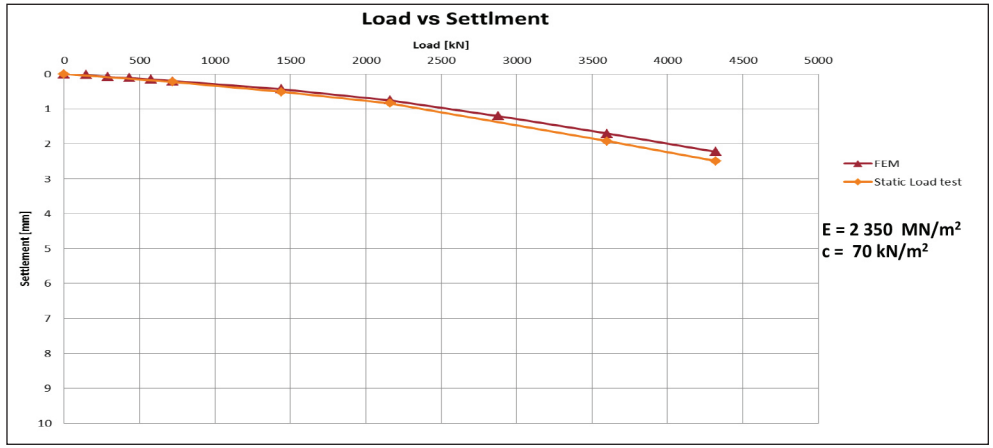

Pile Summary Sheet
P3

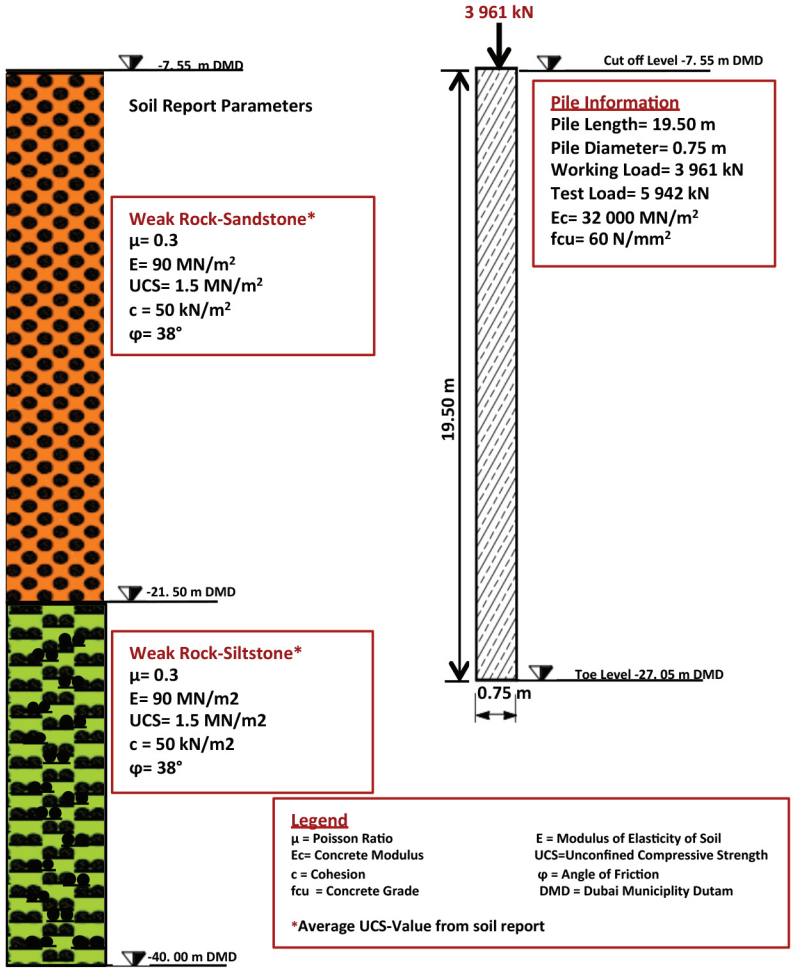

Modelling by using Soil Report Parameters

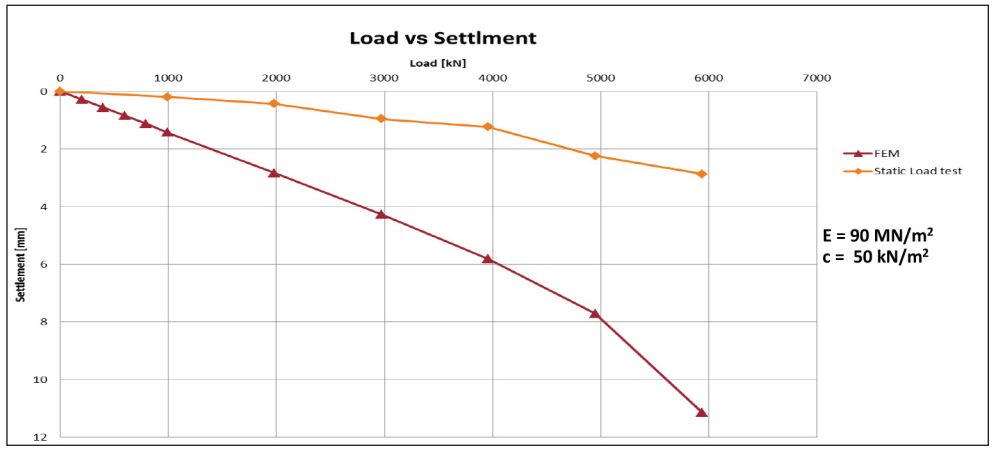

Back-Analysis of Soil Properties from Load Test

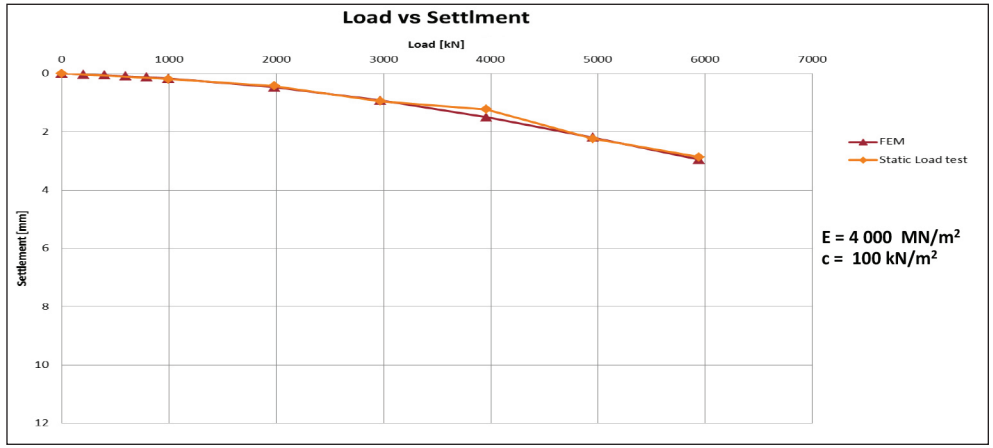

Pile Summary Sheet
P4

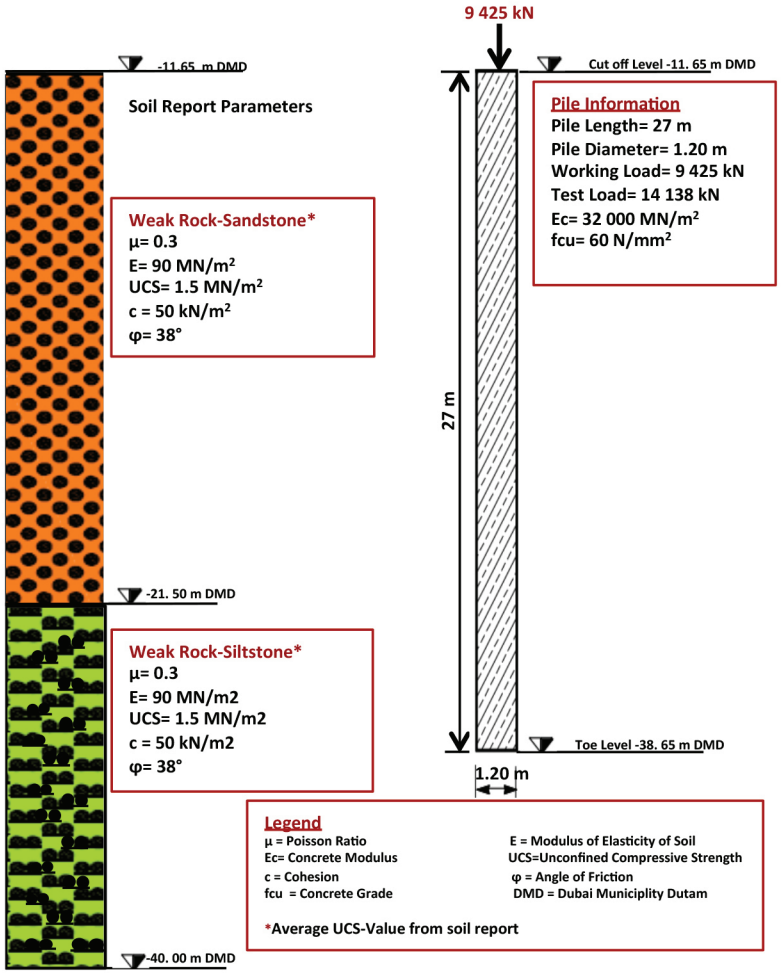

Modelling by using Soil Report Parameters

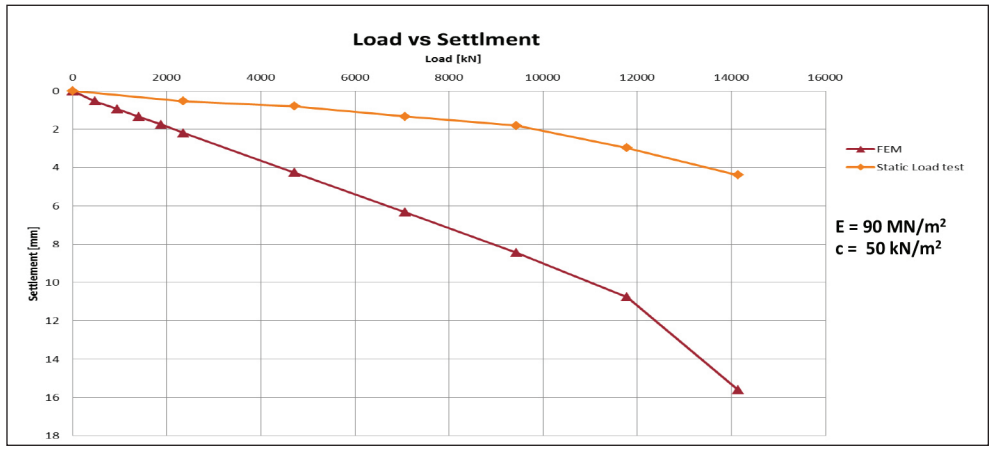

Back-Analysis of Soil Properties from Load Test

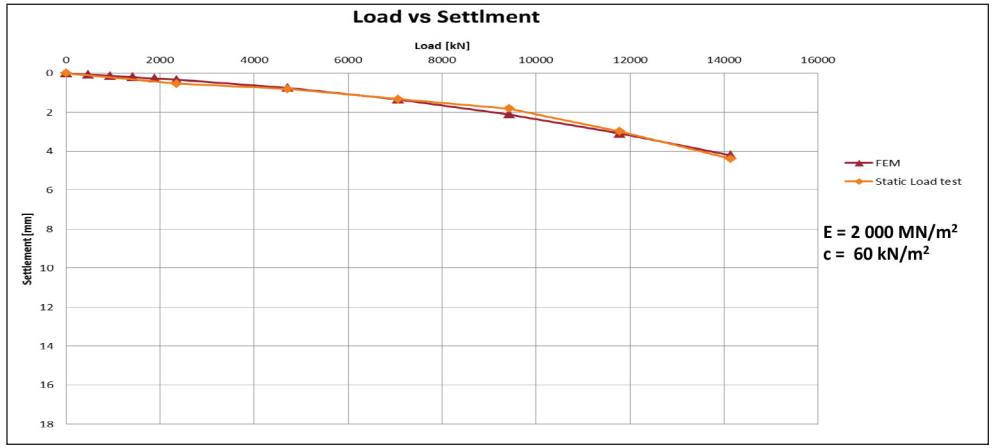

Pile Summary Sheet
P5

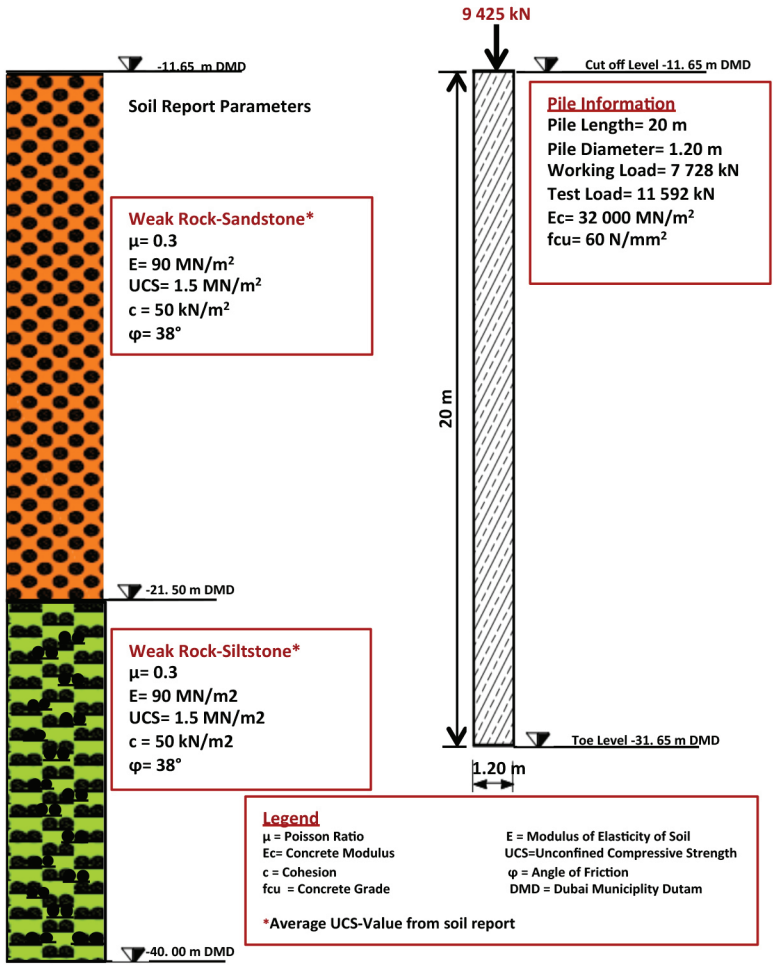

Modelling by using Soil Report Parameters

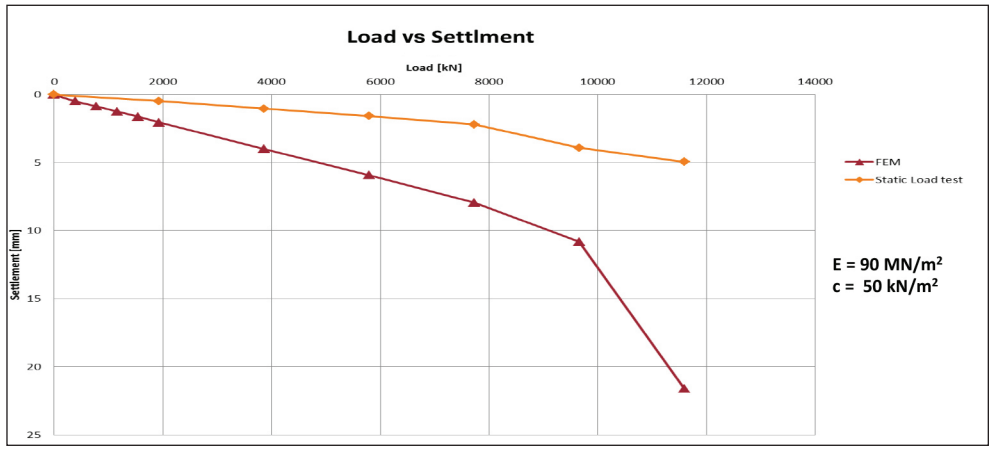

Back-Analysis of Soil Properties from Load Test

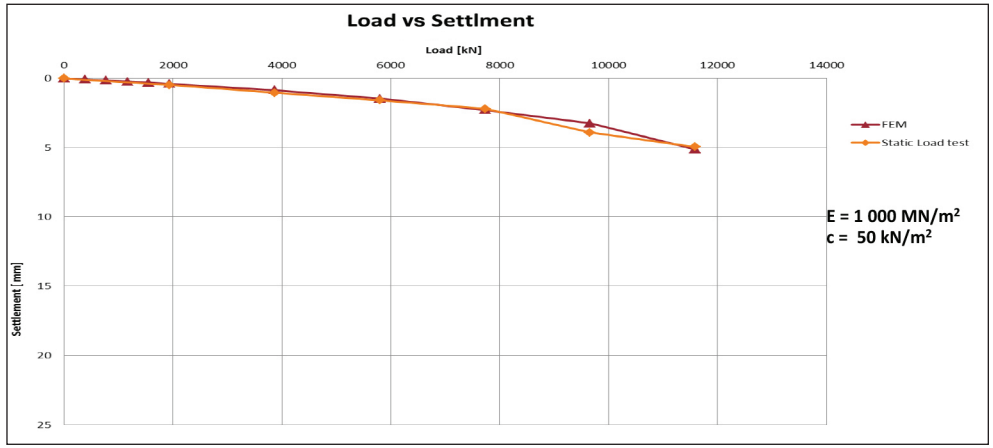

Pile Summary Sheet
P6

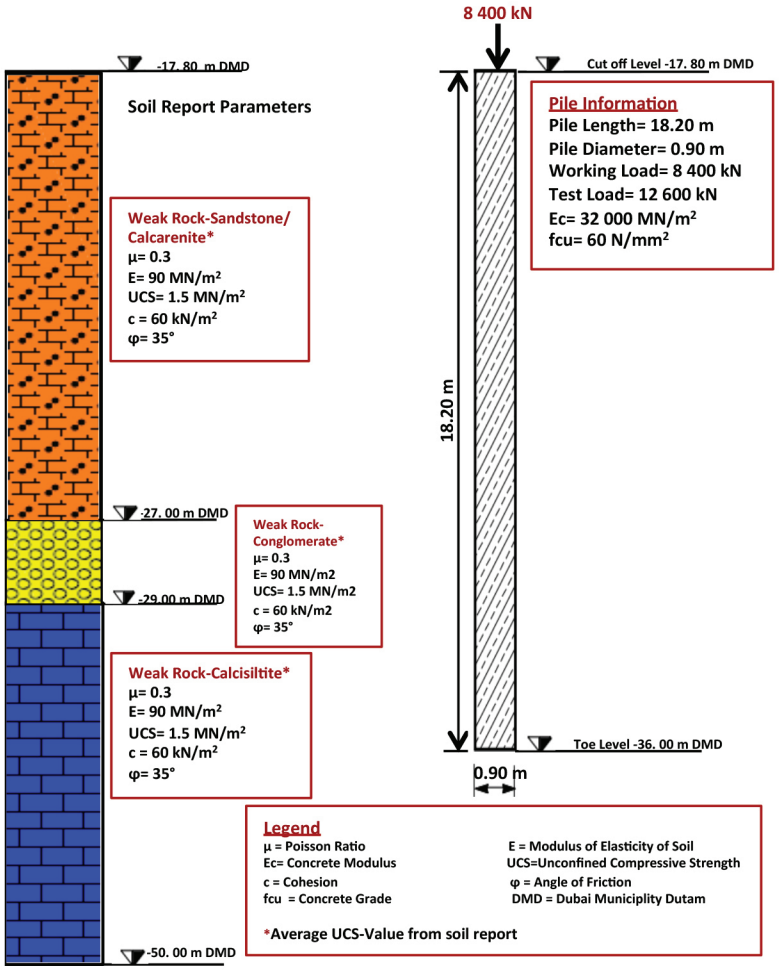

Pile Information
Pile Length= 18.20 m
Pile Diameter= 0.90 m
Working Load= 8 400 kN
Test Load= 12 600 kN
Ec= 32 000 MN/m²
fcu= 60 N/mm²

Legend
μ = Poisson Ratio
Ec= Concrete Modulus
c = Cohesion
fcu = Concrete Grade
E = Modulus of Elasticity of Soil
UCS=Unconfined Compressive Strength
φ = Angle of Friction
DMD = Dubai Municiplity Dutam

*Average UCS-Value from soil report

Modelling by using Soil Report Parameters

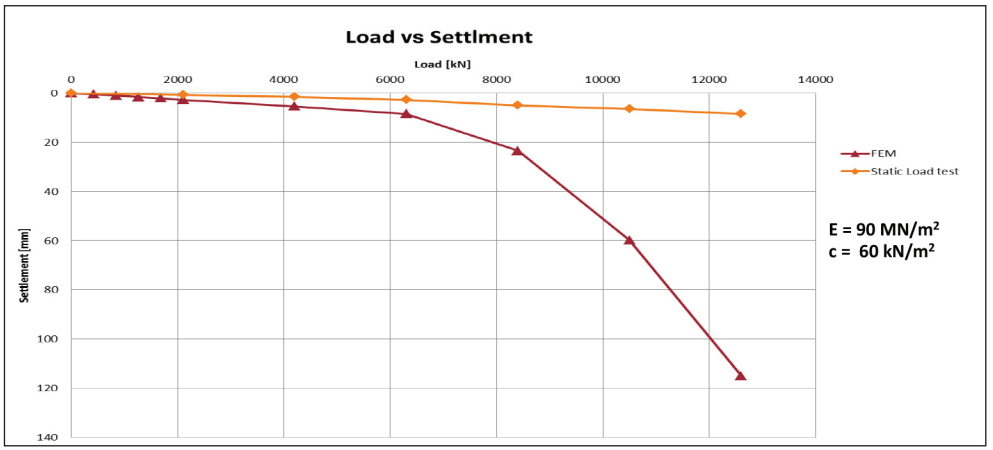

Back-Analysis of Soil Properties from Load Test

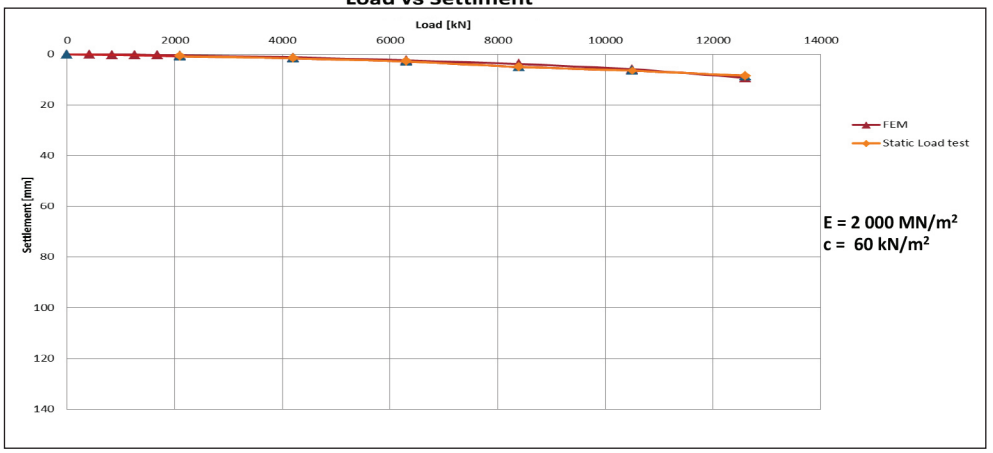

Pile Summary Sheet
P7

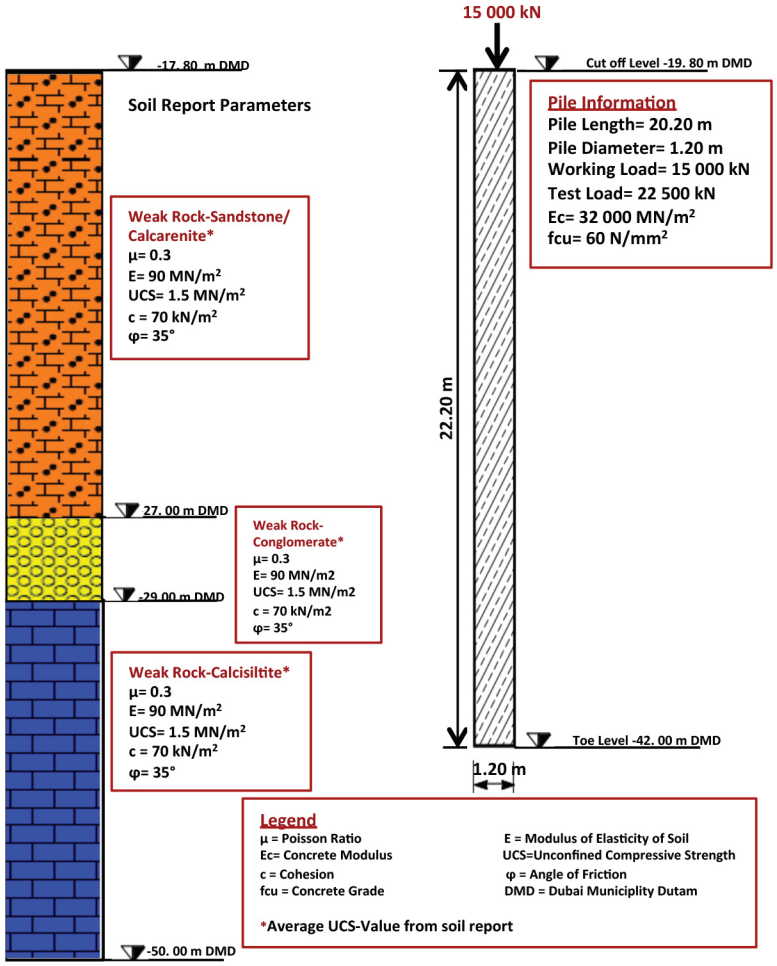

Modelling by using Soil Report Parameters

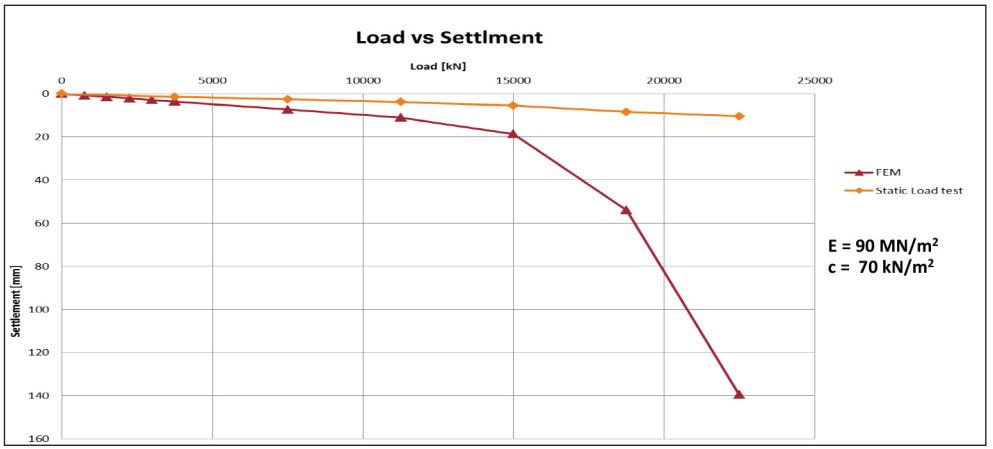

Back-Analysis of Soil Properties from Load Test

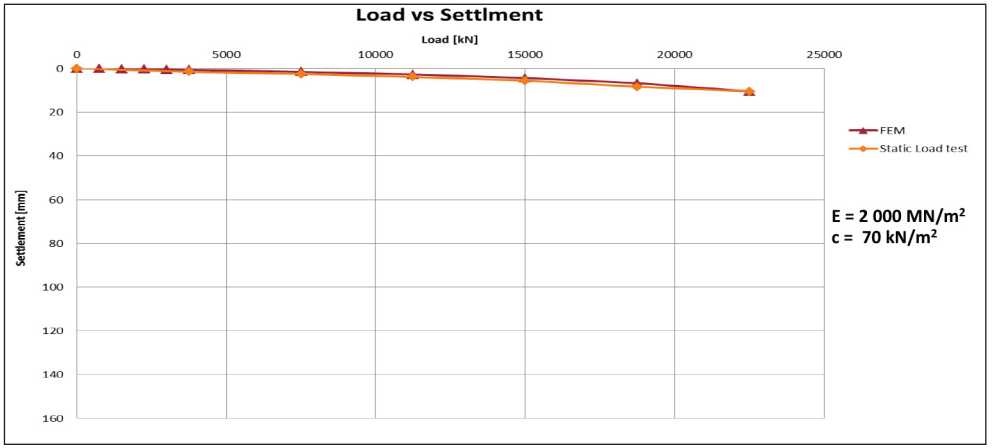

Pile Summary Sheet
P8

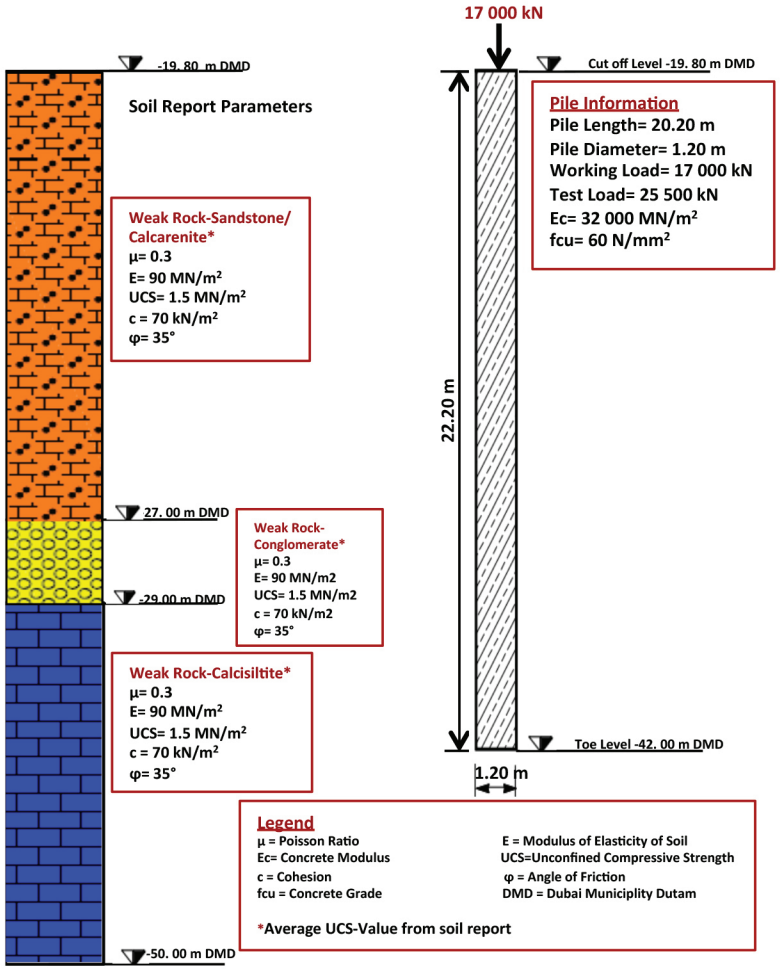

Pile Information
Pile Length= 20.20 m
Pile Diameter= 1.20 m
Working Load= 17 000 kN
Test Load= 25 500 kN
Ec= 32 000 MN/m²
fcu= 60 N/mm²

Modelling by using Soil Report Parameters

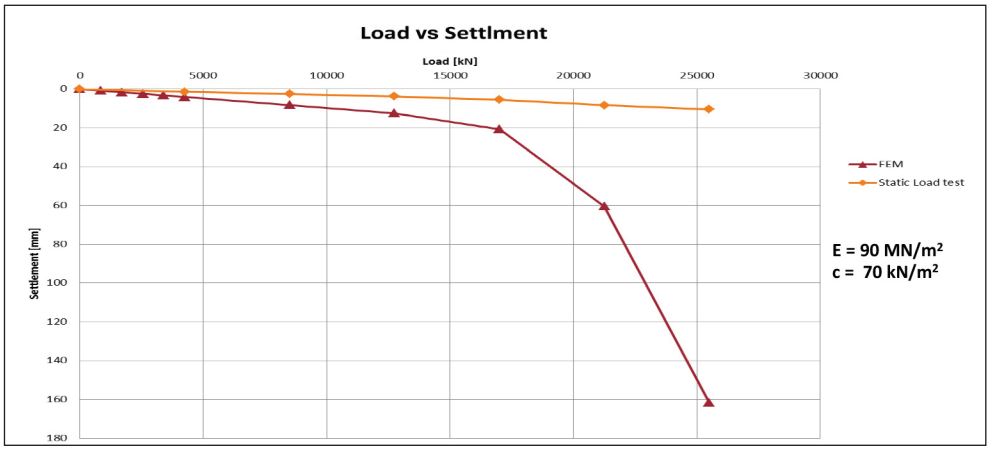

Back-Analysis of Soil Properties from Load Test

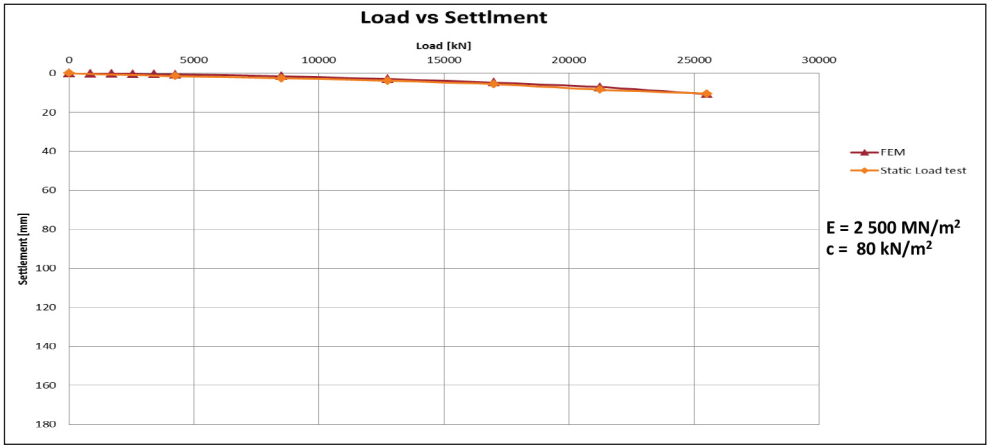

Pile Summary Sheet
P9

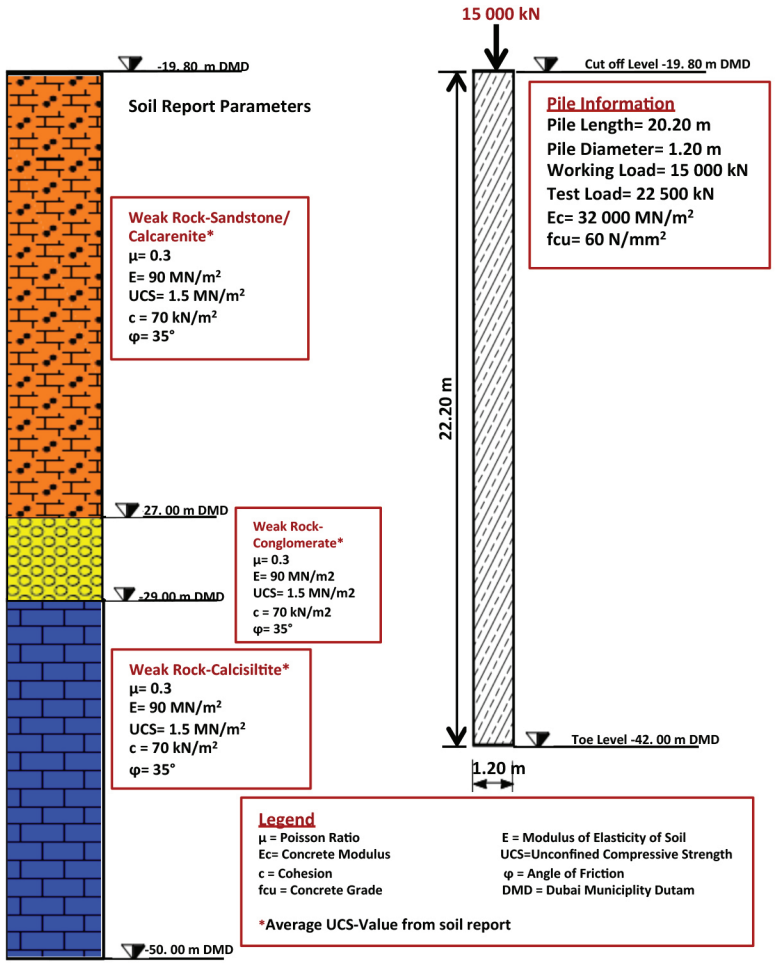

Pile Information
Pile Length= 20.20 m
Pile Diameter= 1.20 m
Working Load= 15 000 kN
Test Load= 22 500 kN
Ec= 32 000 MN/m²
fcu= 60 N/mm²

Legend

μ = Poisson Ratio	E = Modulus of Elasticity of Soil
Ec= Concrete Modulus	UCS=Unconfined Compressive Strength
c = Cohesion	φ = Angle of Friction
fcu = Concrete Grade	DMD = Dubai Municiplity Dutam

*Average UCS-Value from soil report

Modelling by using Soil Report Parameters

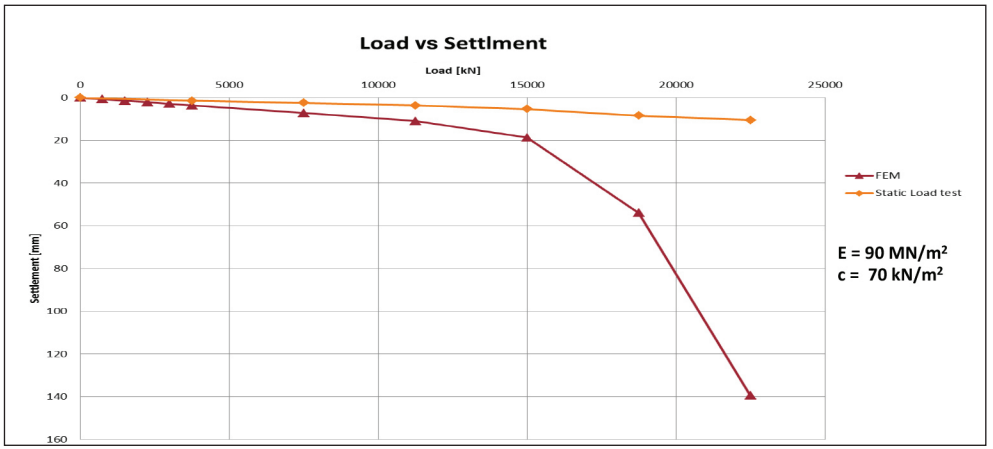

Back-Analysis of Soil Properties from Load Test

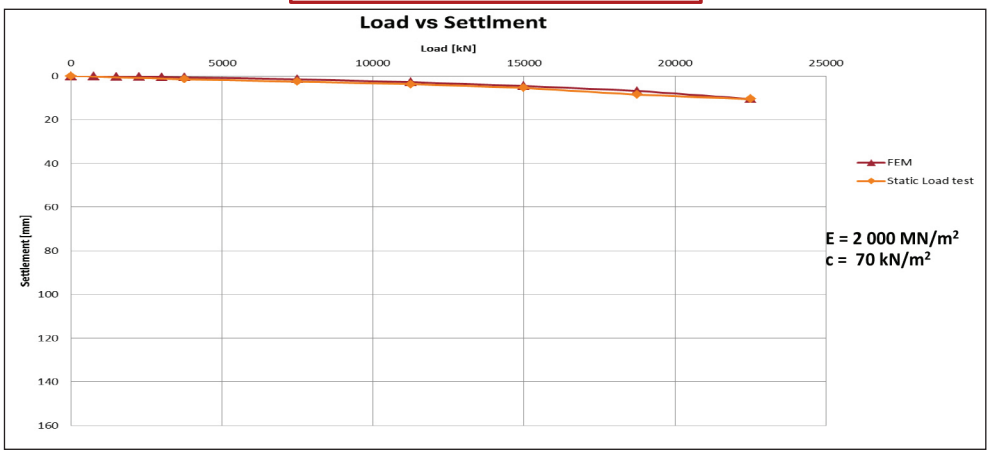

Pile Summary Sheet
P10

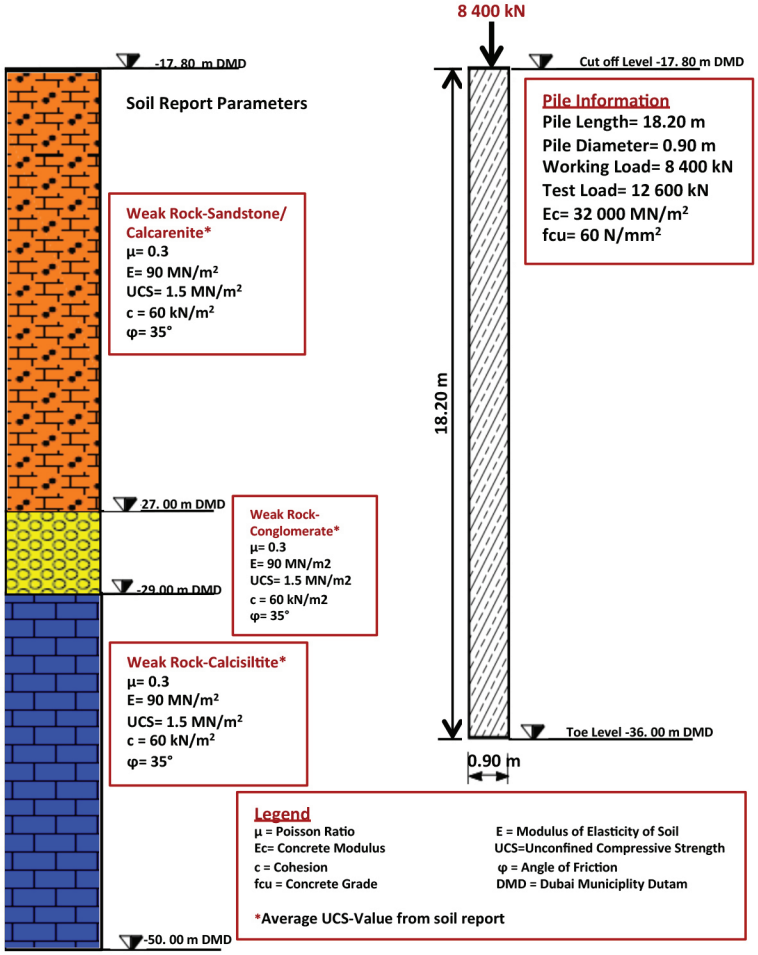

Modelling by using Soil Report Parameters

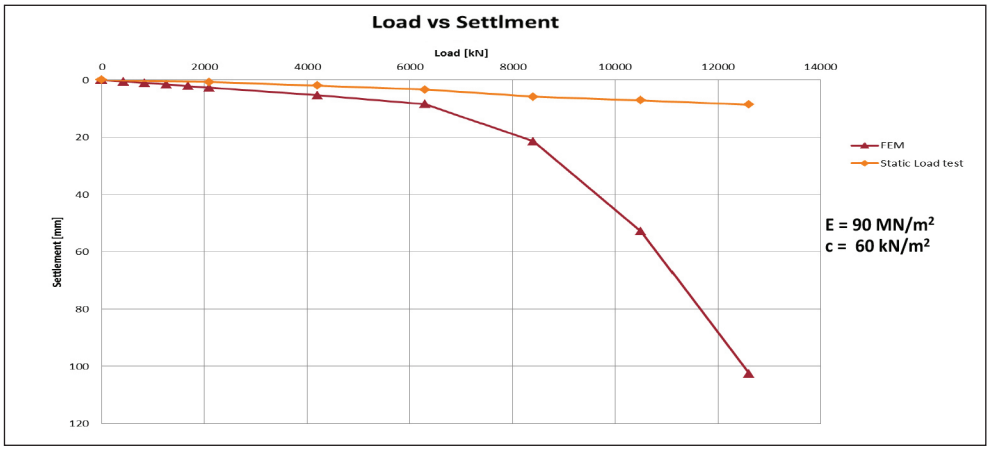

Back-Analysis of Soil Properties from Load Test

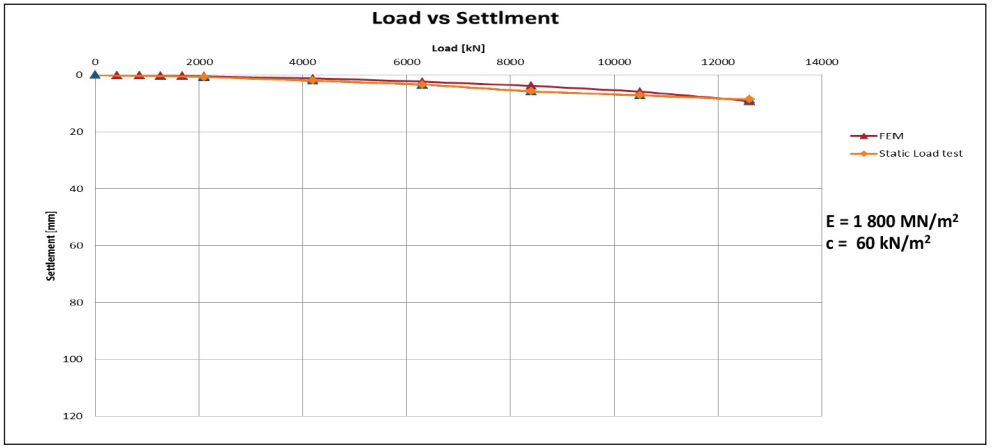

Pile Summary Sheet
P11

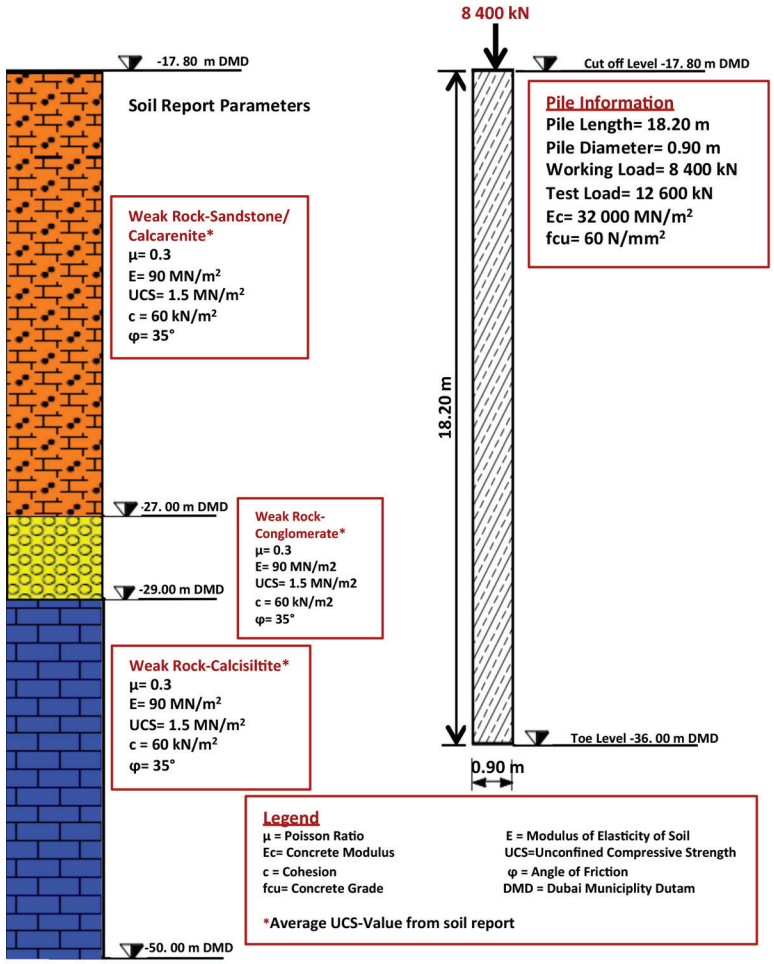

Modelling by using Soil Report Parameters

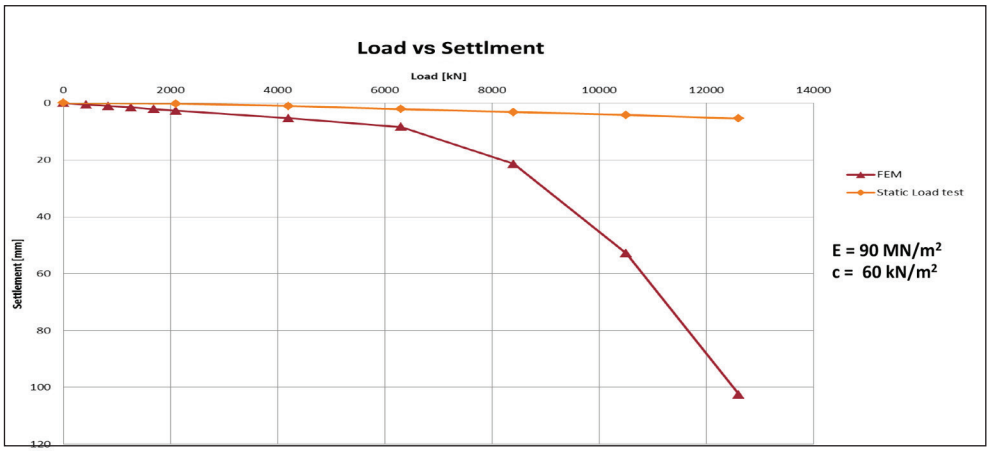

Back-Analysis of Soil Properties from Load Test

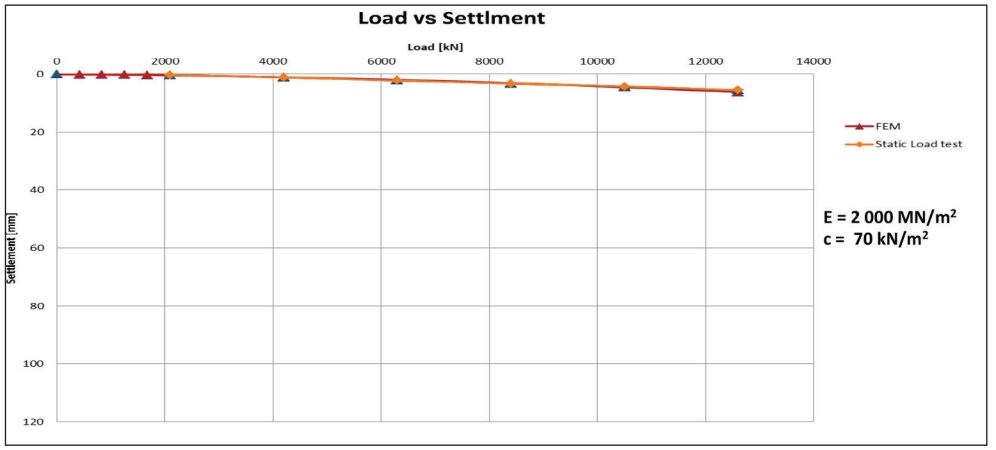

Pile Summary Sheet
P12

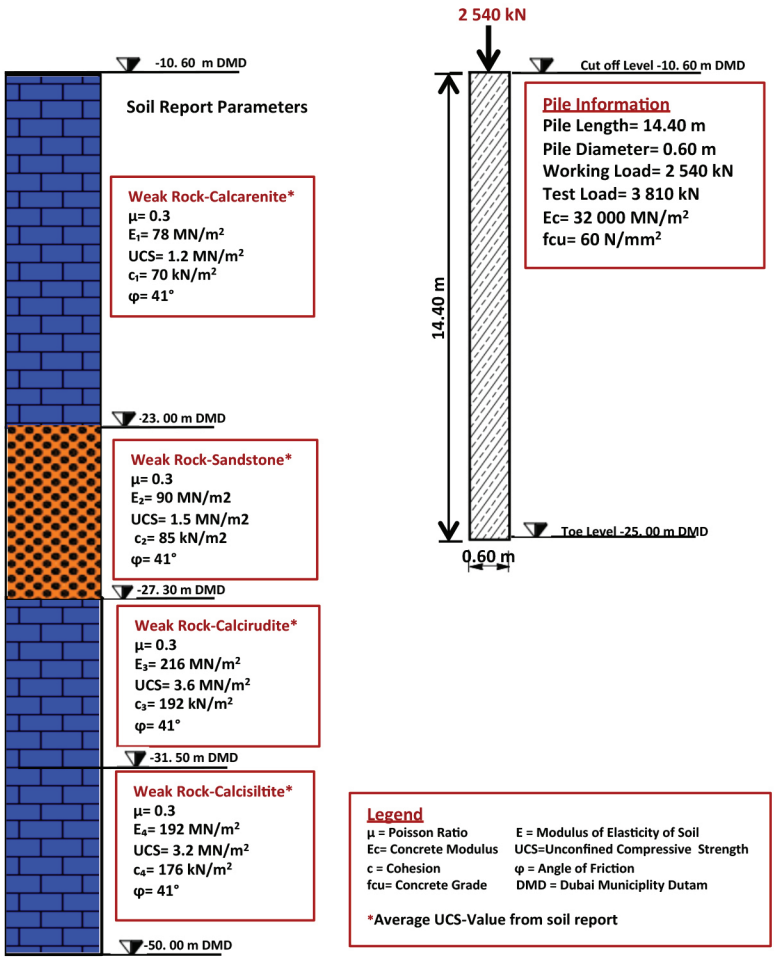

Pile Information
Pile Length= 14.40 m
Pile Diameter= 0.60 m
Working Load= 2 540 kN
Test Load= 3 810 kN
Ec= 32 000 MN/m²
fcu= 60 N/mm²

Legend

μ = Poisson Ratio	E = Modulus of Elasticity of Soil
Ec= Concrete Modulus	UCS=Unconfined Compressive Strength
c = Cohesion	φ = Angle of Friction
fcu= Concrete Grade	DMD = Dubai Municiplity Dutam

*Average UCS-Value from soil report

Modelling by using Soil Report Parameters

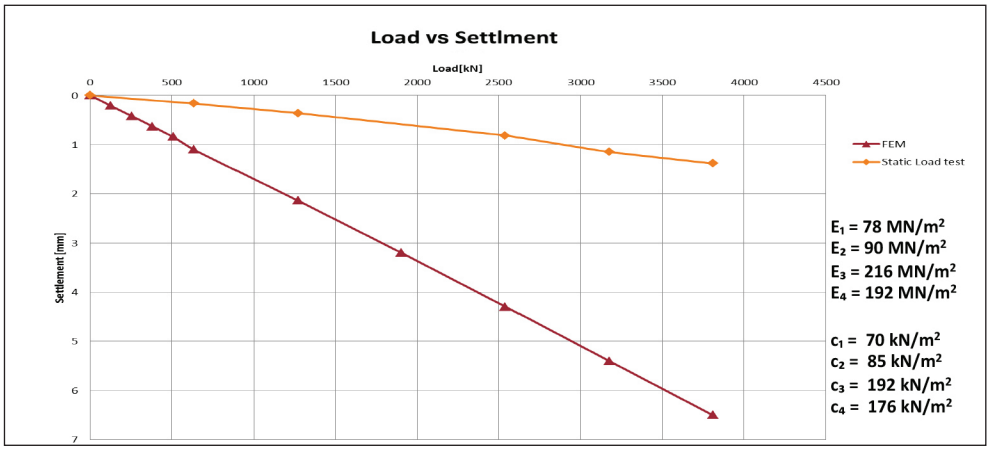

Back-Analysis of Soil Properties from Load Test

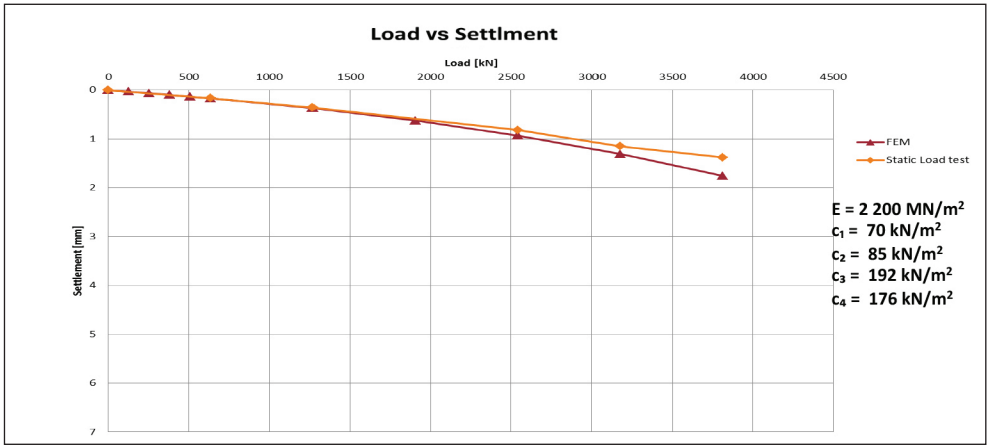

Pile Summary Sheet
P13

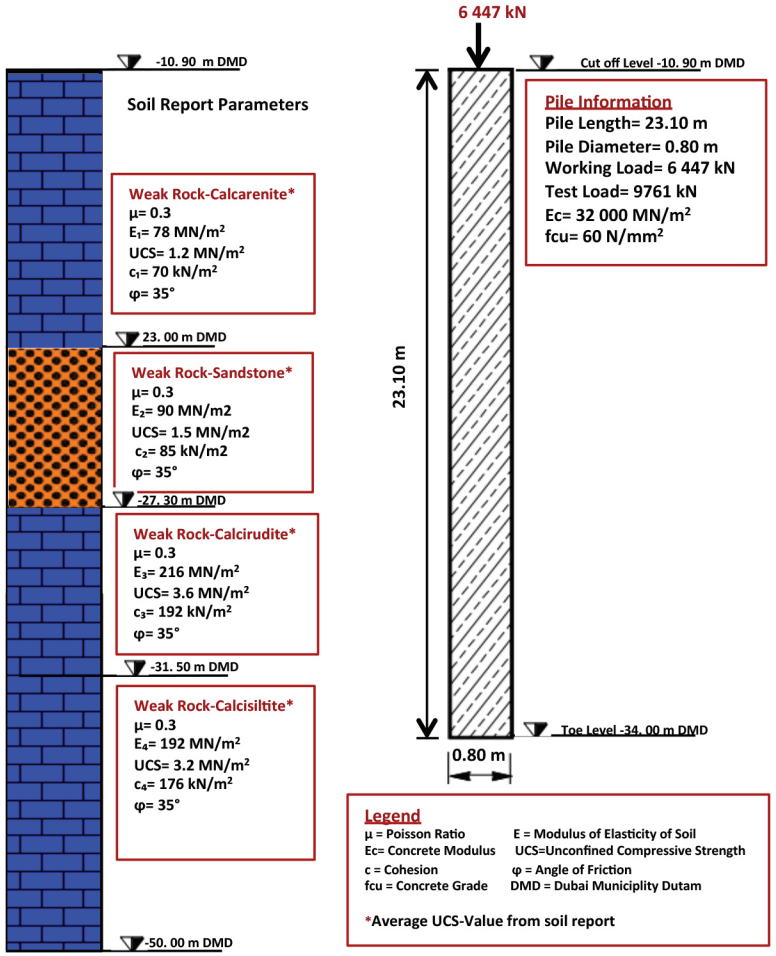

Pile Information
Pile Length= 23.10 m
Pile Diameter= 0.80 m
Working Load= 6 447 kN
Test Load= 9761 kN
Ec= 32 000 MN/m²
fcu= 60 N/mm²

Legend
μ = Poisson Ratio
E = Modulus of Elasticity of Soil
Ec= Concrete Modulus
UCS=Unconfined Compressive Strength
c = Cohesion
φ = Angle of Friction
fcu = Concrete Grade
DMD = Dubai Municiplity Datam

*Average UCS-Value from soil report

Modelling by using Soil Report Parameters

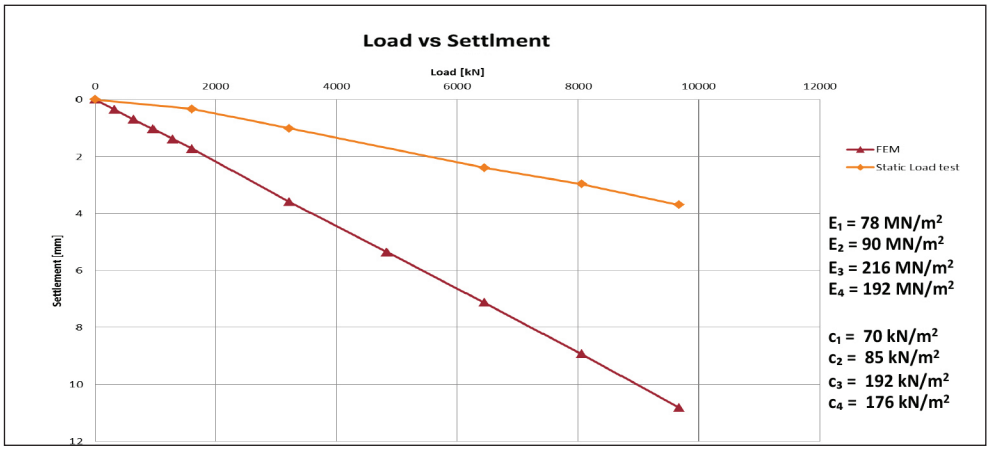

E_1 = 78 MN/m²
E_2 = 90 MN/m²
E_3 = 216 MN/m²
E_4 = 192 MN/m²

c_1 = 70 kN/m²
c_2 = 85 kN/m²
c_3 = 192 kN/m²
c_4 = 176 kN/m²

Back-Analysis of Soil Properties from Load Test

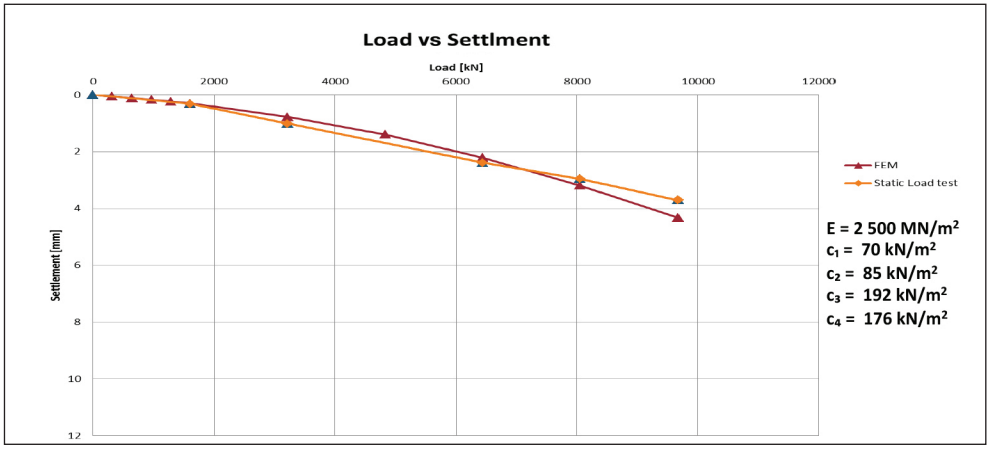

E = 2 500 MN/m²
c_1 = 70 kN/m²
c_2 = 85 kN/m²
c_3 = 192 kN/m²
c_4 = 176 kN/m²

Pile Summary Sheet
P14

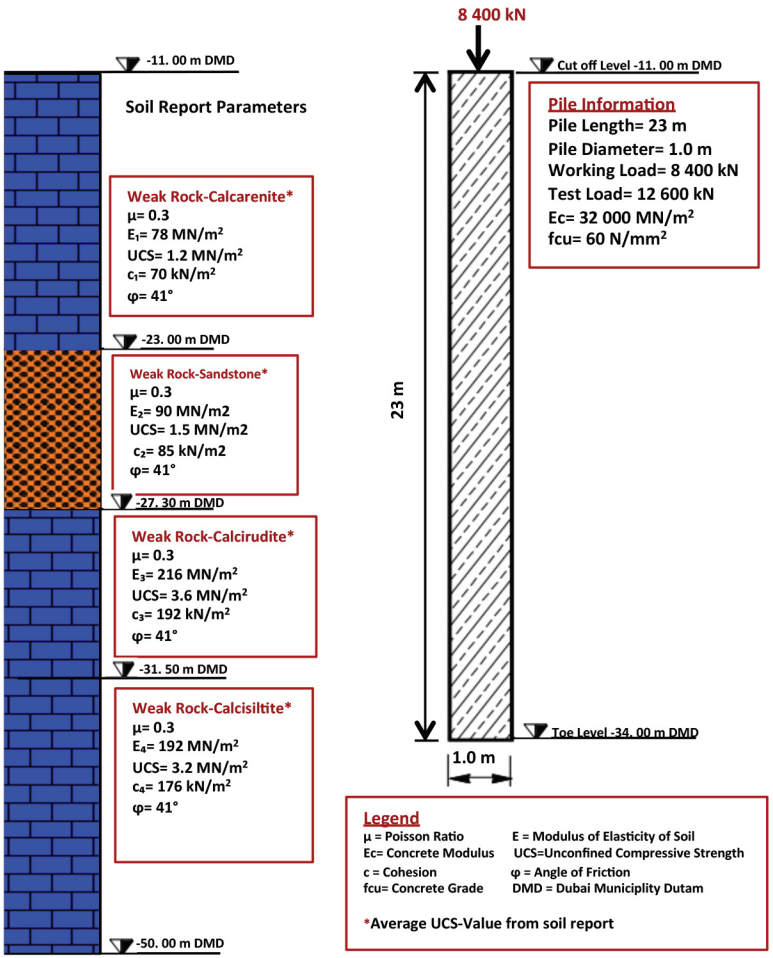

Pile Information
Pile Length= 23 m
Pile Diameter= 1.0 m
Working Load= 8 400 kN
Test Load= 12 600 kN
Ec= 32 000 MN/m²
fcu= 60 N/mm²

Legend
μ = Poisson Ratio
E = Modulus of Elasticity of Soil
Ec= Concrete Modulus
UCS=Unconfined Compressive Strength
c = Cohesion
φ = Angle of Friction
fcu= Concrete Grade
DMD = Dubai Municiplity Dutam

*Average UCS-Value from soil report

Modelling by using Soil Report Parameters

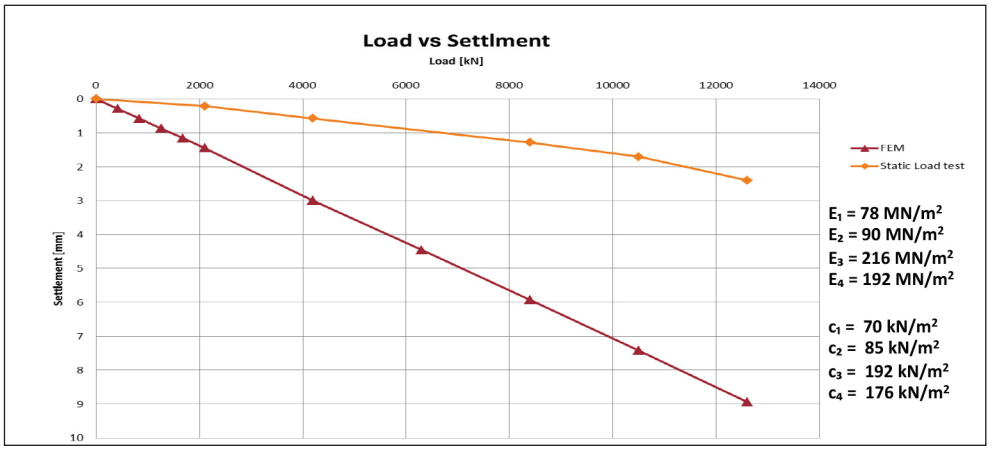

Back-Analysis of Soil Properties from Load Test

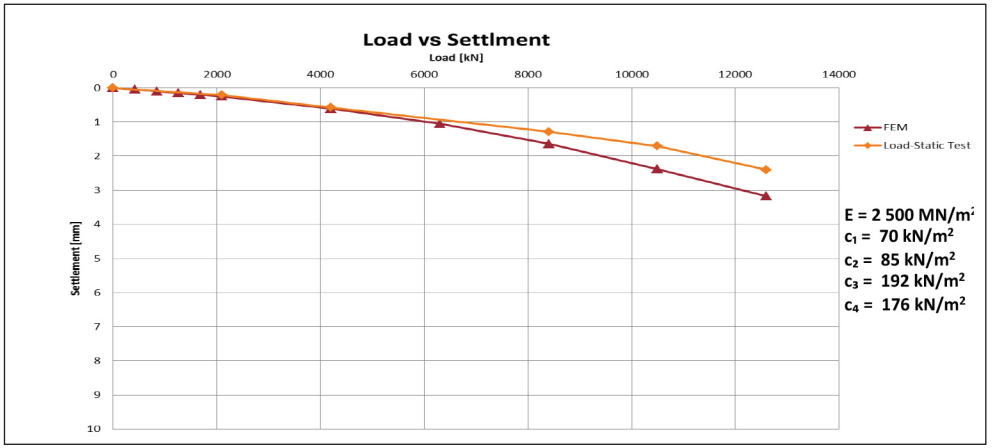

Pile Summary Sheet
P15

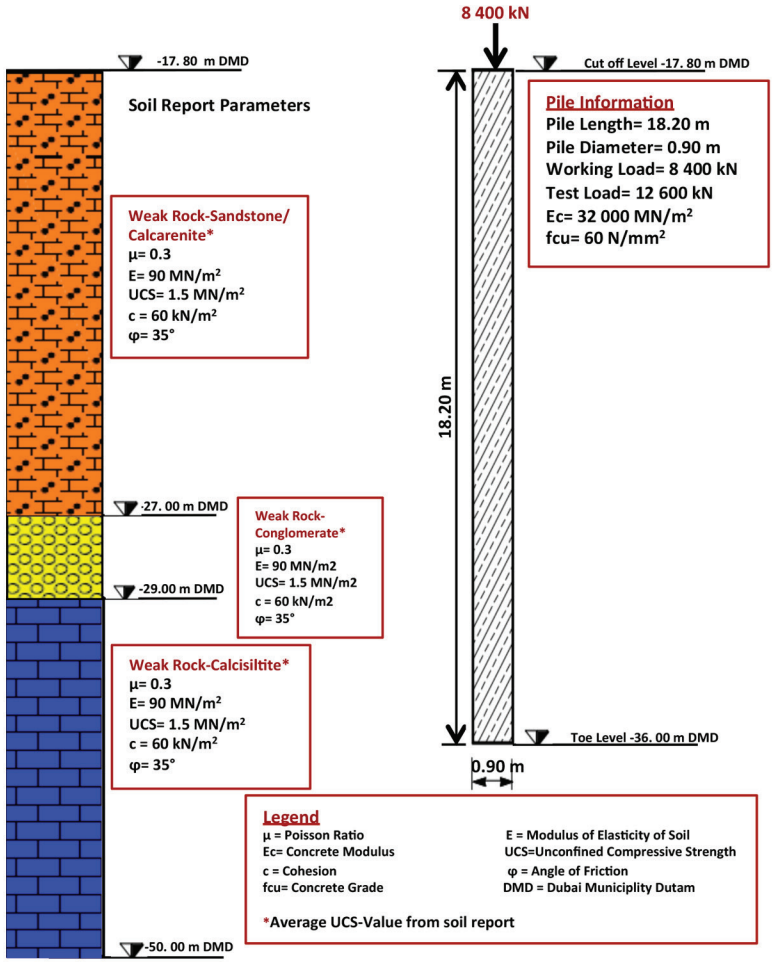

Modelling by using Soil Report Parameters

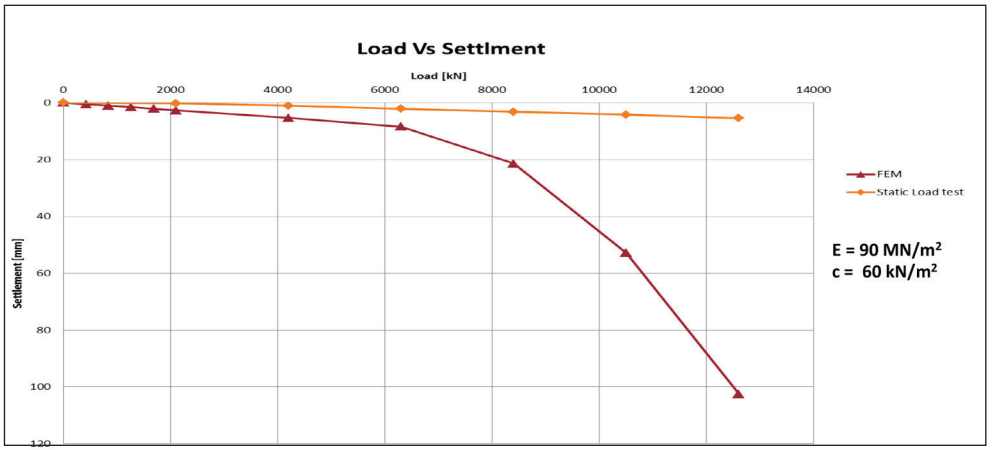

Back-Analysis of Soil Properties from Load Test

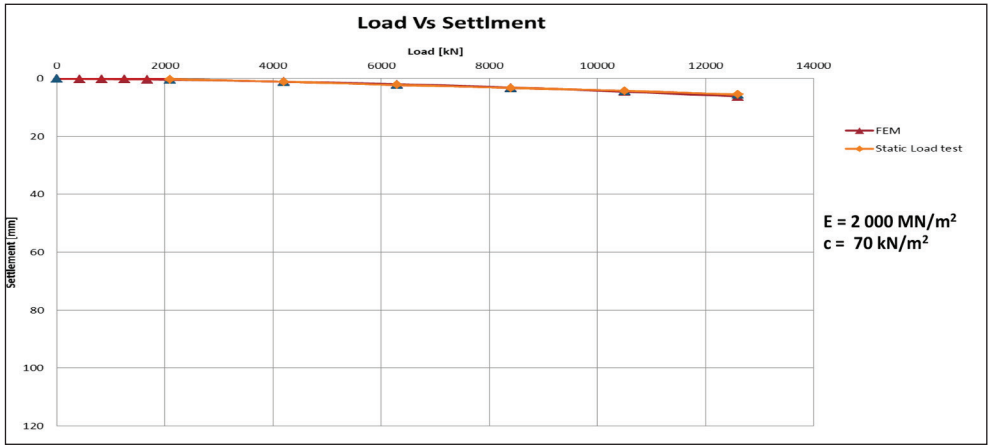

Pile Summary Sheet
P16

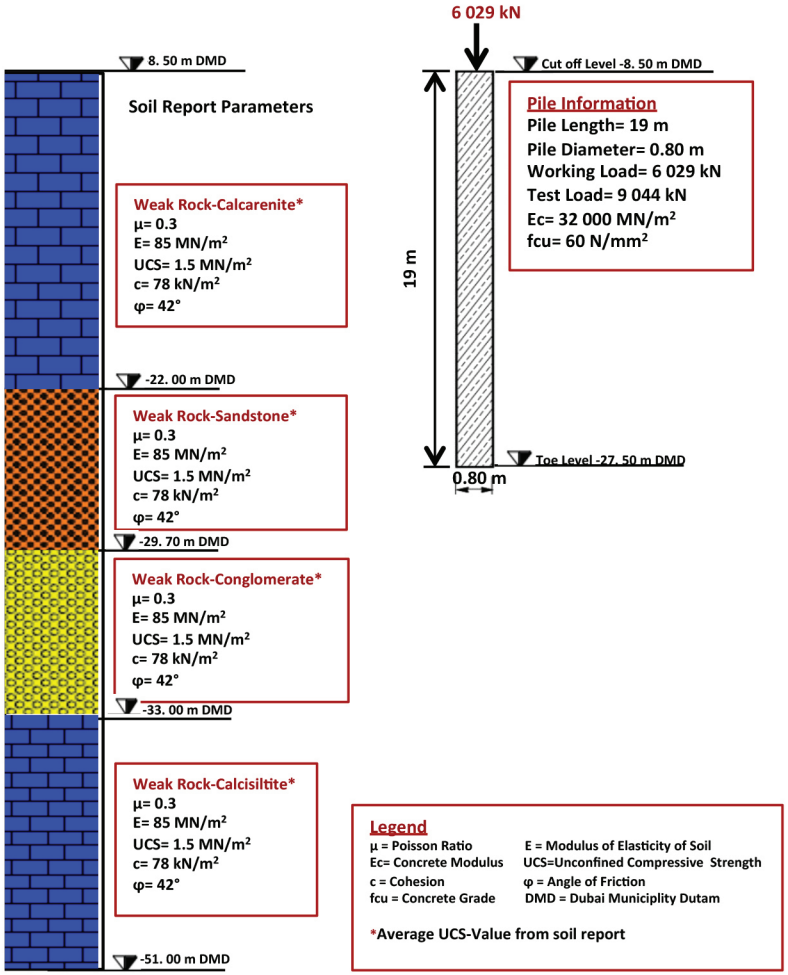

Pile Information
Pile Length= 19 m
Pile Diameter= 0.80 m
Working Load= 6 029 kN
Test Load= 9 044 kN
Ec= 32 000 MN/m²
fcu= 60 N/mm²

Legend
μ = Poisson Ratio
E = Modulus of Elasticity of Soil
Ec= Concrete Modulus
UCS=Unconfined Compressive Strength
c = Cohesion
φ = Angle of Friction
fcu = Concrete Grade
DMD = Dubai Municiplity Dutam

*Average UCS-Value from soil report

Modelling by using Soil Report Parameters

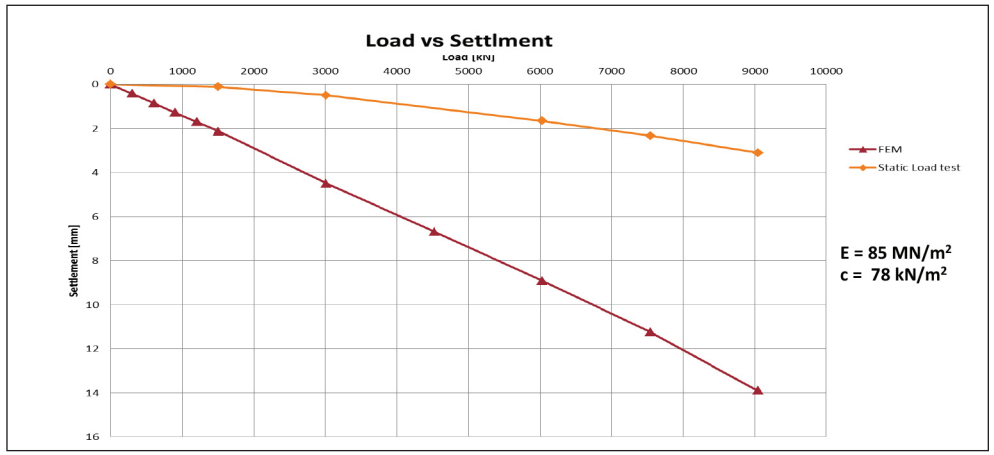

Back-Analysis of Soil Properties from Load Test

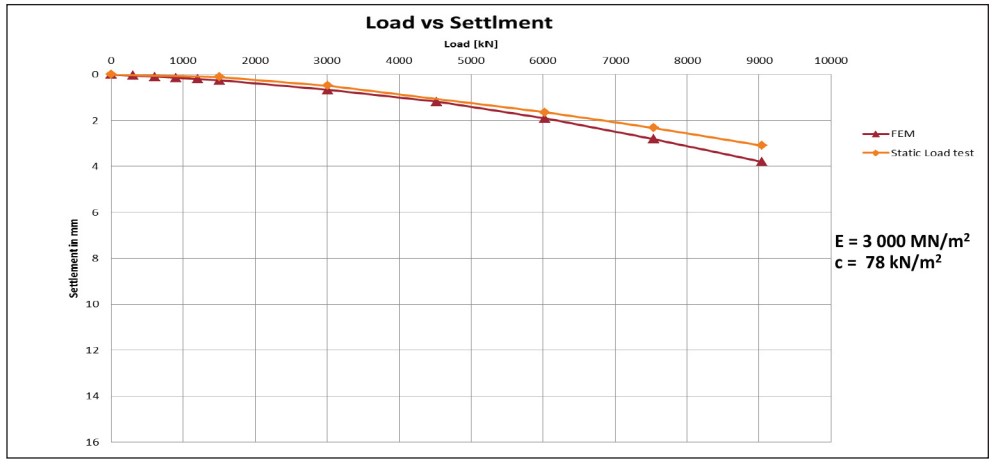

Pile Summary Sheet
P17

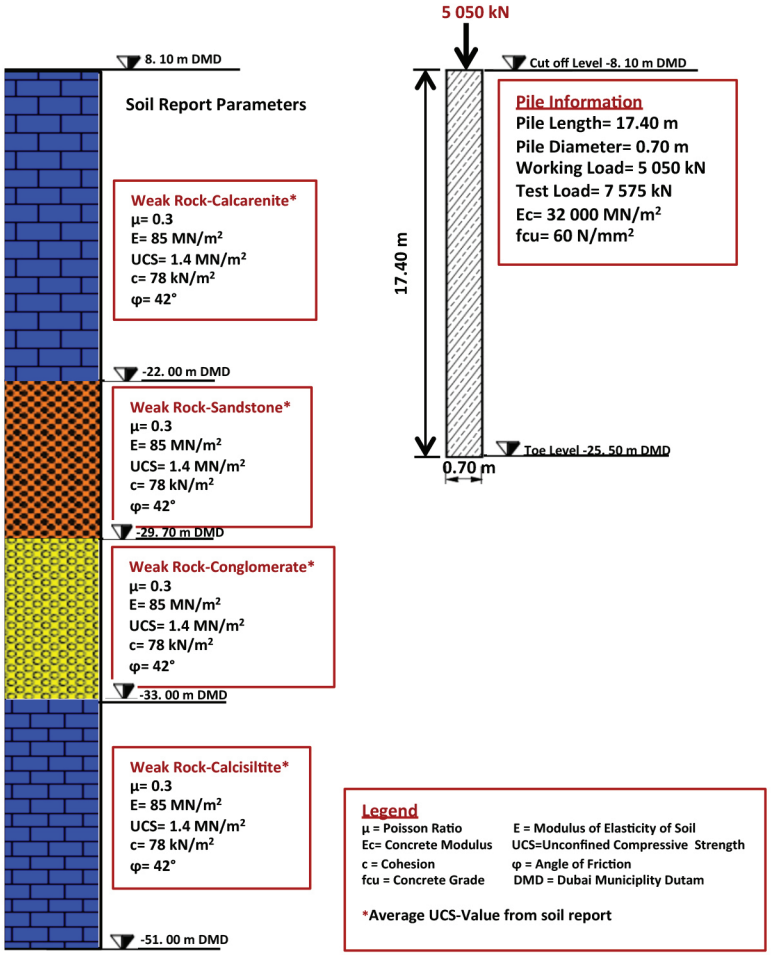

Pile Information
Pile Length= 17.40 m
Pile Diameter= 0.70 m
Working Load= 5 050 kN
Test Load= 7 575 kN
Ec= 32 000 MN/m²
fcu= 60 N/mm²

Legend

μ = Poisson Ratio	E = Modulus of Elasticity of Soil
Ec= Concrete Modulus	UCS=Unconfined Compressive Strength
c = Cohesion	φ = Angle of Friction
fcu = Concrete Grade	DMD = Dubai Municiplity Dutam

*Average UCS-Value from soil report

Modelling by using Soil Report Parameters

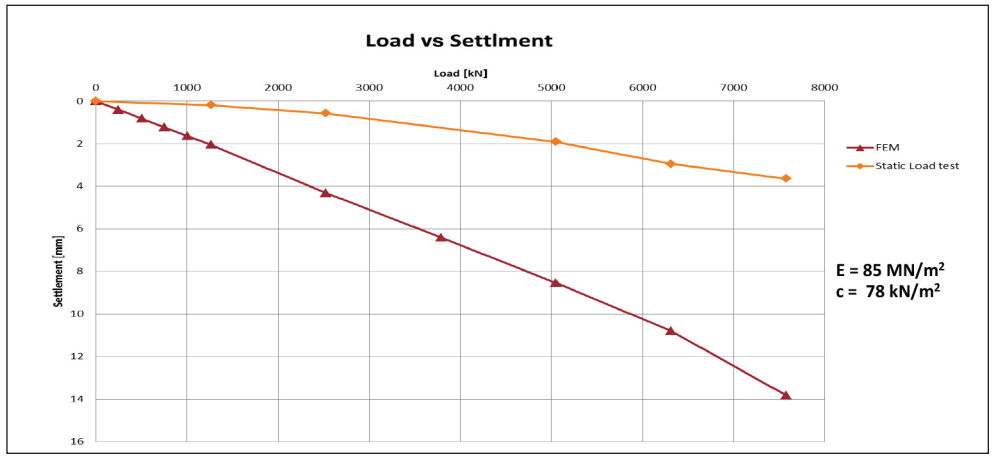

Back-Analysis of Soil Properties from Load Test

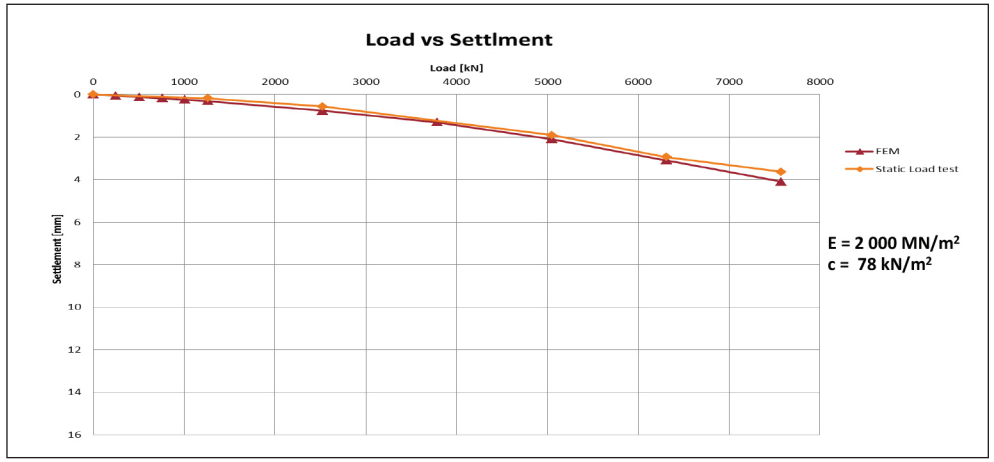

Pile Summary Sheet
P18

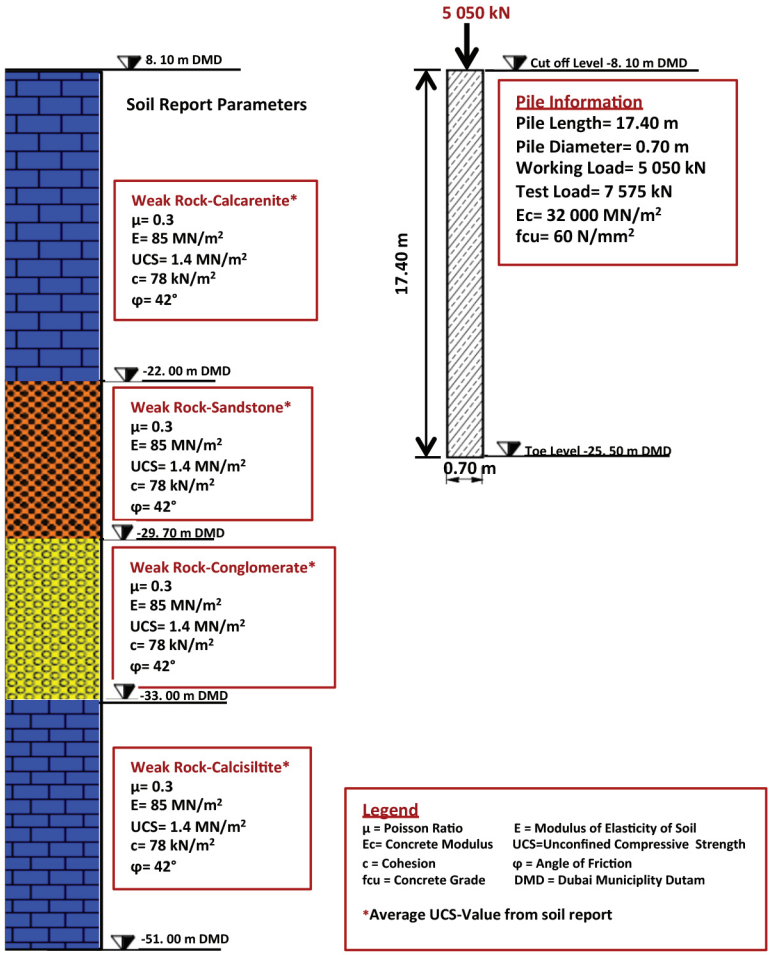

Pile Information
Pile Length= 17.40 m
Pile Diameter= 0.70 m
Working Load= 5 050 kN
Test Load= 7 575 kN
Ec= 32 000 MN/m²
fcu= 60 N/mm²

Legend

μ = Poisson Ratio	E = Modulus of Elasticity of Soil
Ec= Concrete Modulus	UCS=Unconfined Compressive Strength
c = Cohesion	φ = Angle of Friction
fcu = Concrete Grade	DMD = Dubai Municiplity Dutam

*Average UCS-Value from soil report

Modelling by using Soil Report Parameters

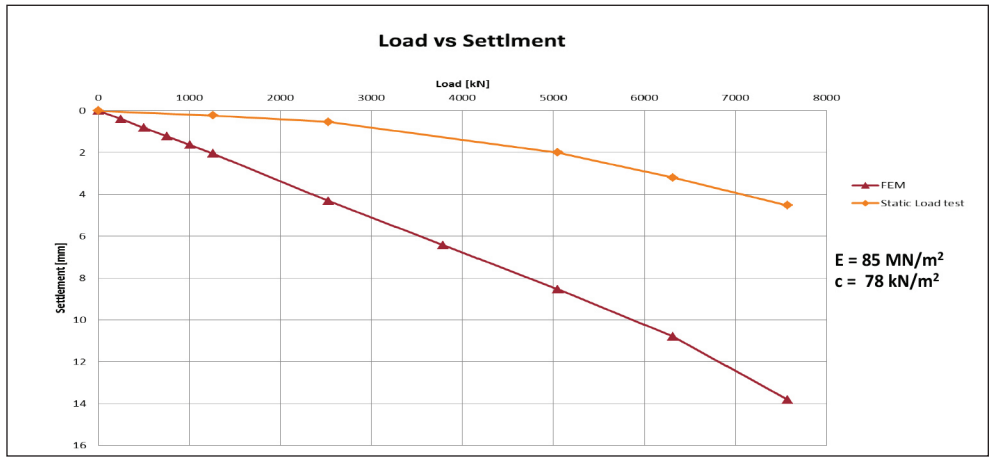

Back-Analysis of Soil Properties from Load Test

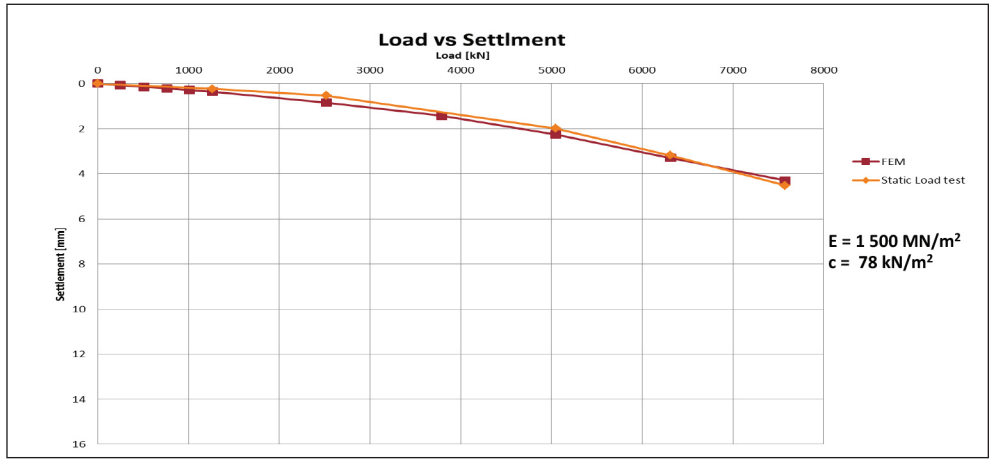

Pile Summary Sheet
P19

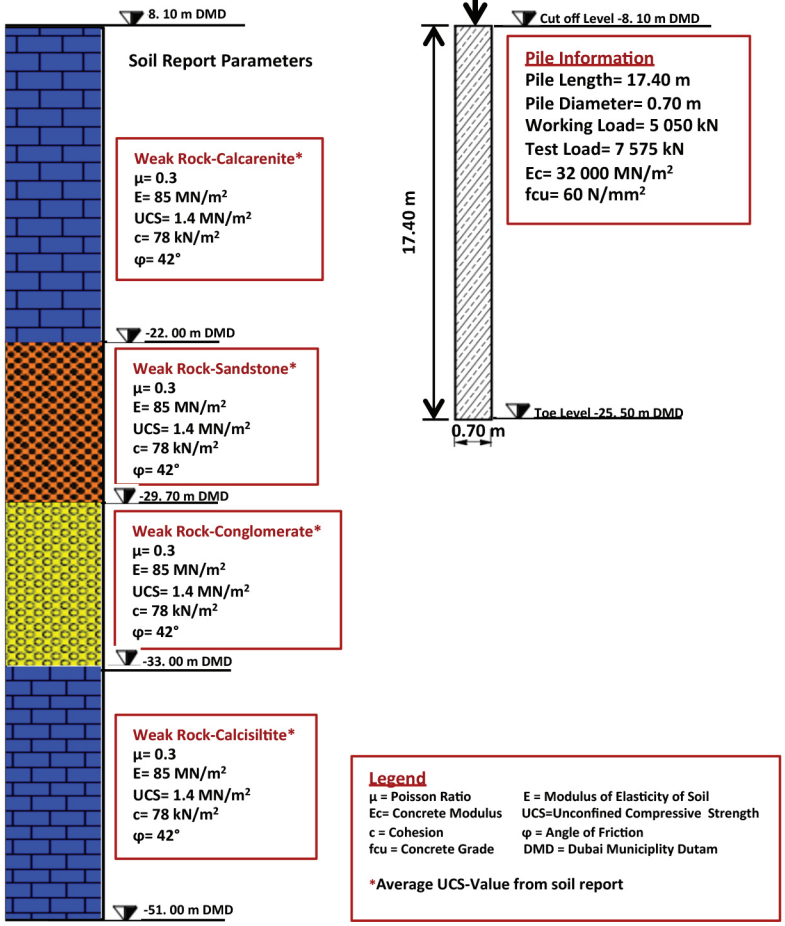

Pile Information
Pile Length= 17.40 m
Pile Diameter= 0.70 m
Working Load= 5 050 kN
Test Load= 7 575 kN
Ec= 32 000 MN/m²
fcu= 60 N/mm²

Legend

μ = Poisson Ratio	E = Modulus of Elasticity of Soil
Ec= Concrete Modulus	UCS=Unconfined Compressive Strength
c = Cohesion	φ = Angle of Friction
fcu = Concrete Grade	DMD = Dubai Municiplity Dutam

*Average UCS-Value from soil report

Modelling by using Soil Report Parameters

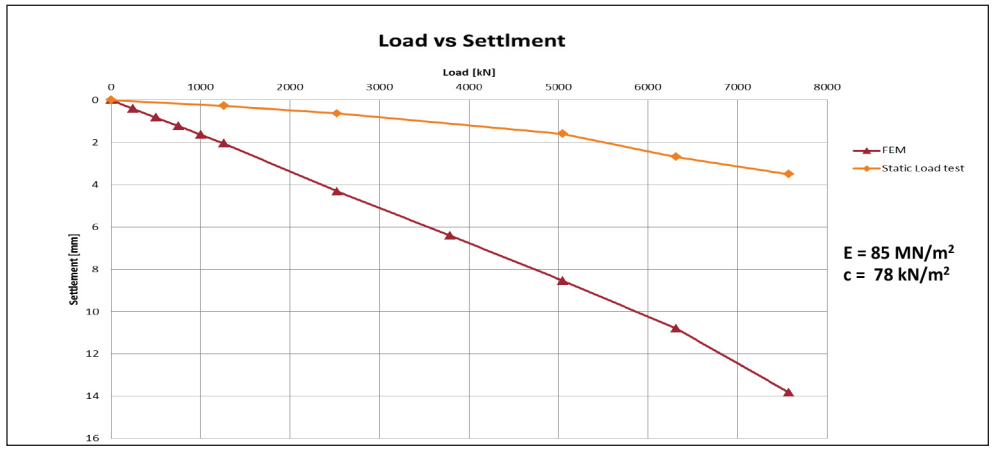

Back-Analysis of Soil Properties from Load Test

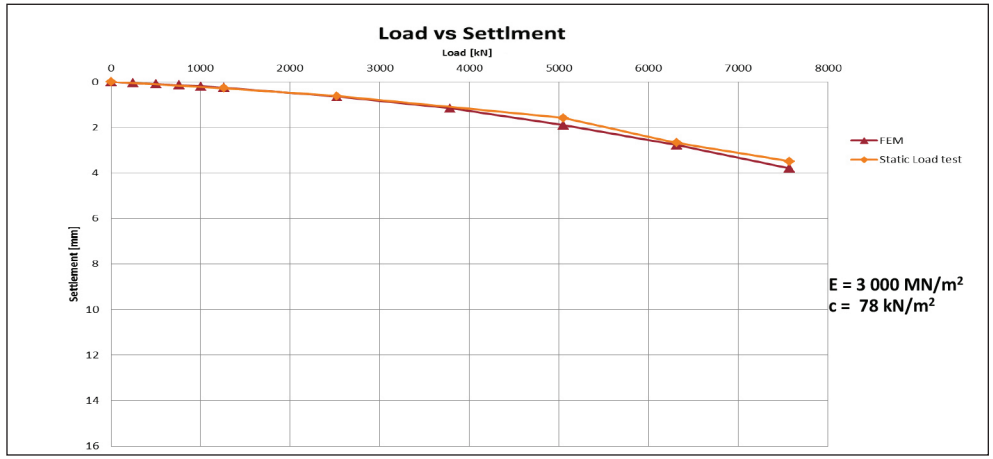

Pile Summary Sheet
P20

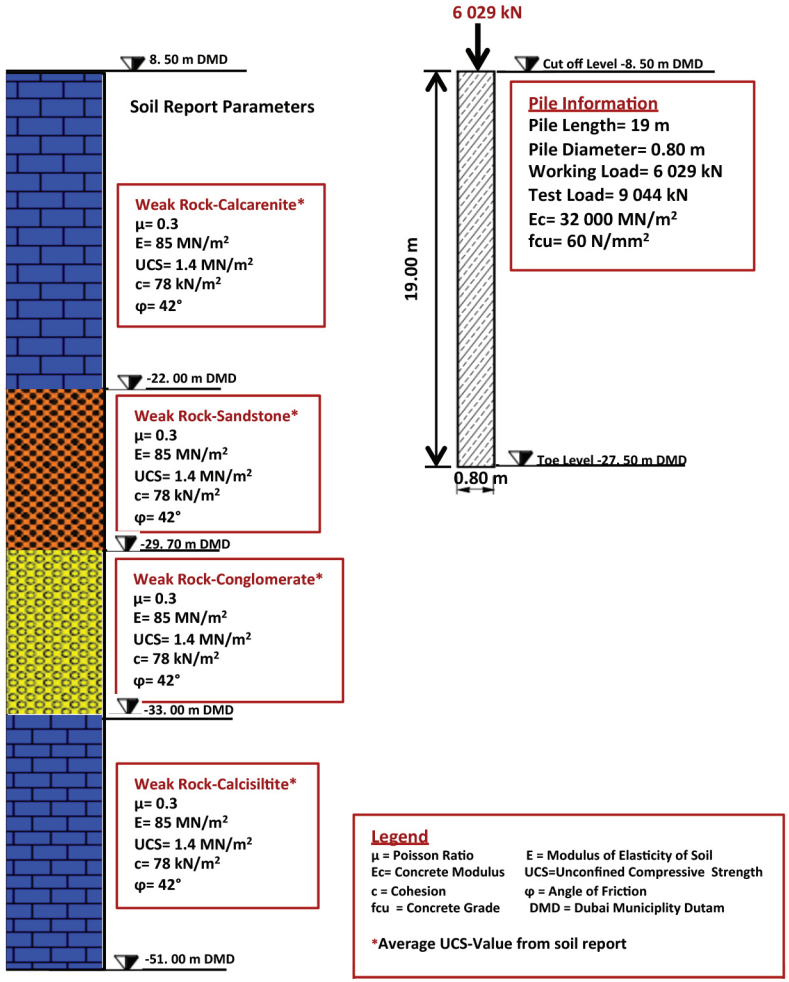

Pile Information
Pile Length= 19 m
Pile Diameter= 0.80 m
Working Load= 6 029 kN
Test Load= 9 044 kN
Ec= 32 000 MN/m²
fcu= 60 N/mm²

Legend

μ = Poisson Ratio	E = Modulus of Elasticity of Soil
Ec= Concrete Modulus	UCS=Unconfined Compressive Strength
c = Cohesion	φ = Angle of Friction
fcu = Concrete Grade	DMD = Dubai Municiplity Dutam

*Average UCS-Value from soil report

Modelling by using Soil Report Parameters

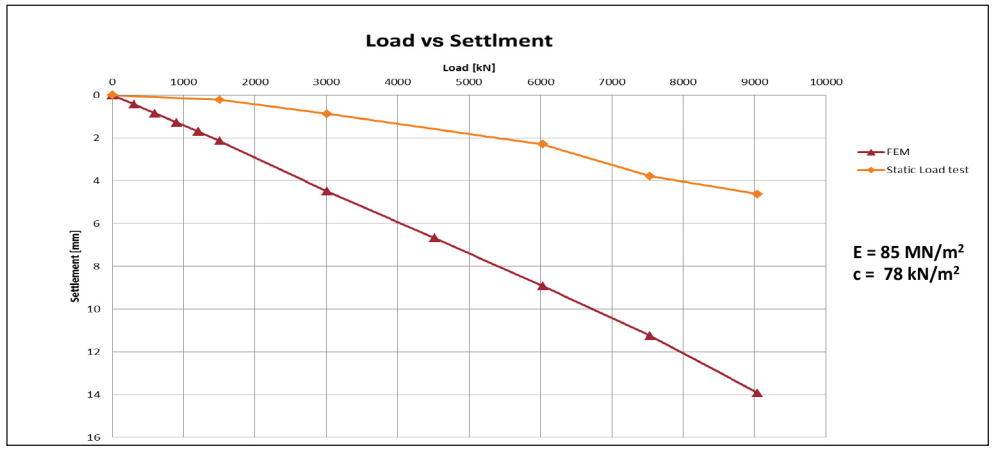

Back-Analysis of Soil Properties from Load Test

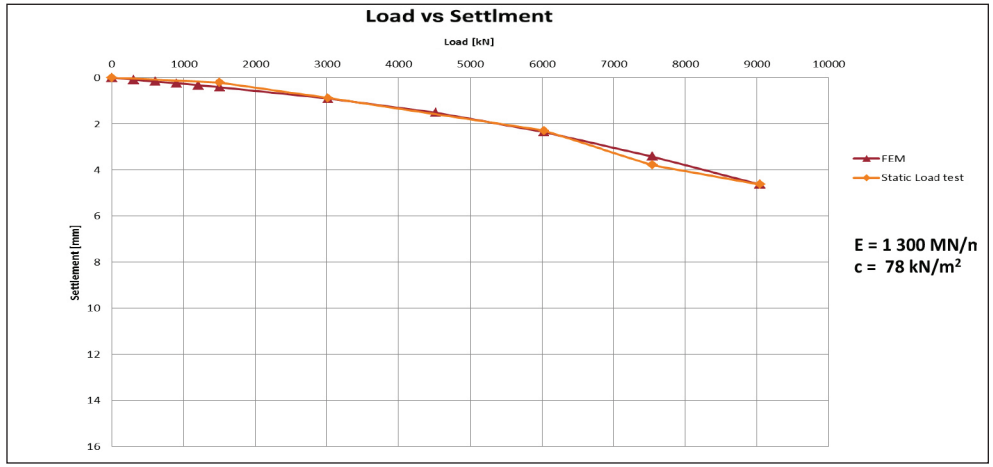

Pile Summary Sheet
P21

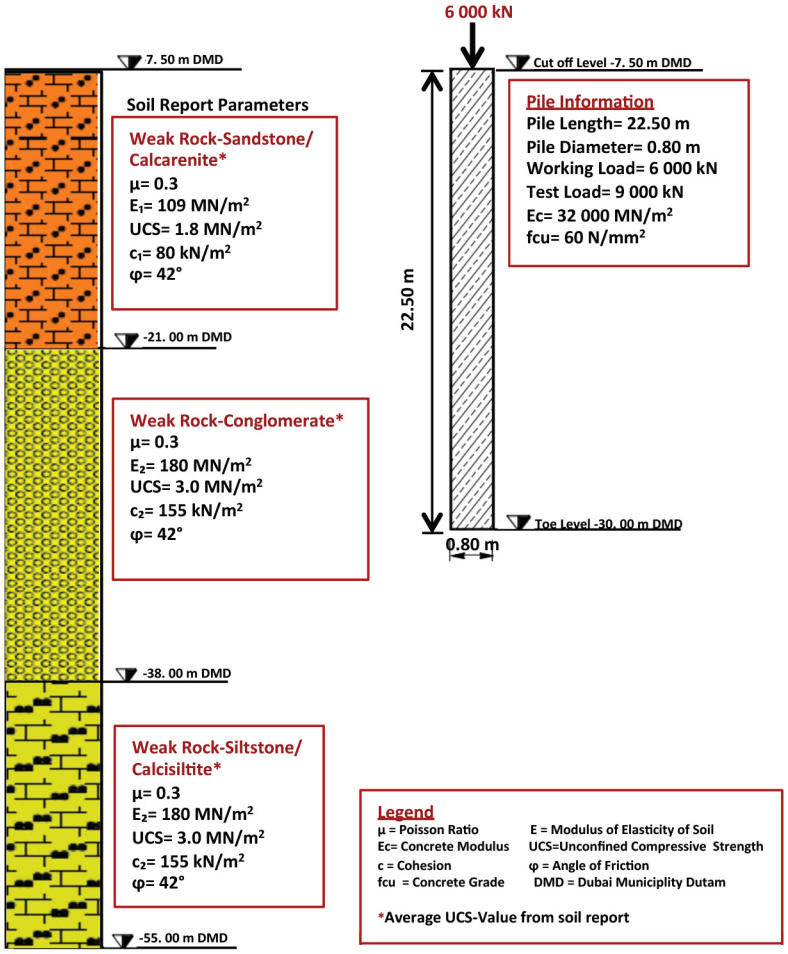

Legend

μ = Poisson Ratio — E = Modulus of Elasticity of Soil
Ec= Concrete Modulus — UCS=Unconfined Compressive Strength
c = Cohesion — φ = Angle of Friction
fcu = Concrete Grade — DMD = Dubai Municiplity Dutam

*Average UCS-Value from soil report

Modelling by using Soil Report Parameters

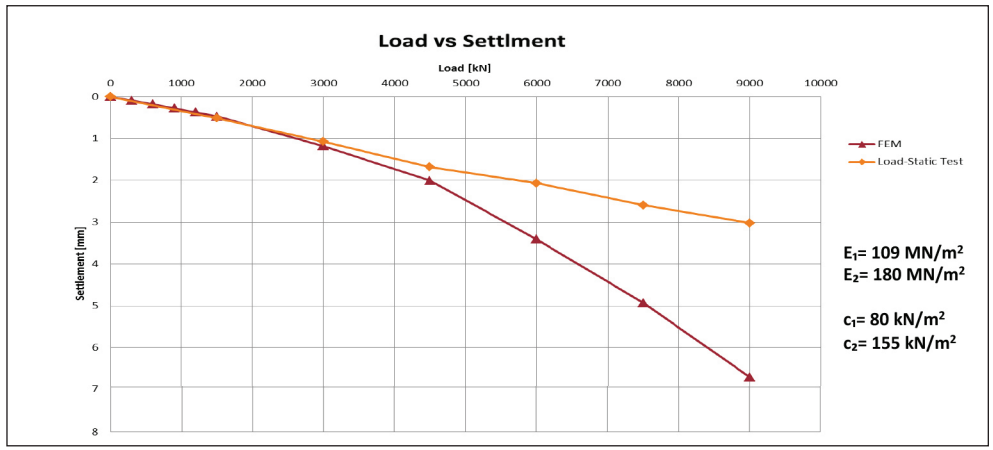

Back-Analysis of Soil Properties from Load Test

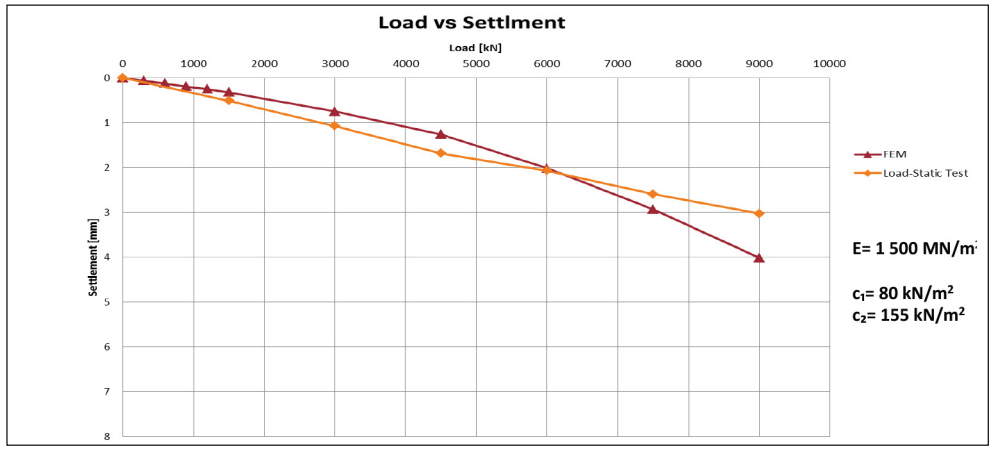

Pile Summary Sheet
P22

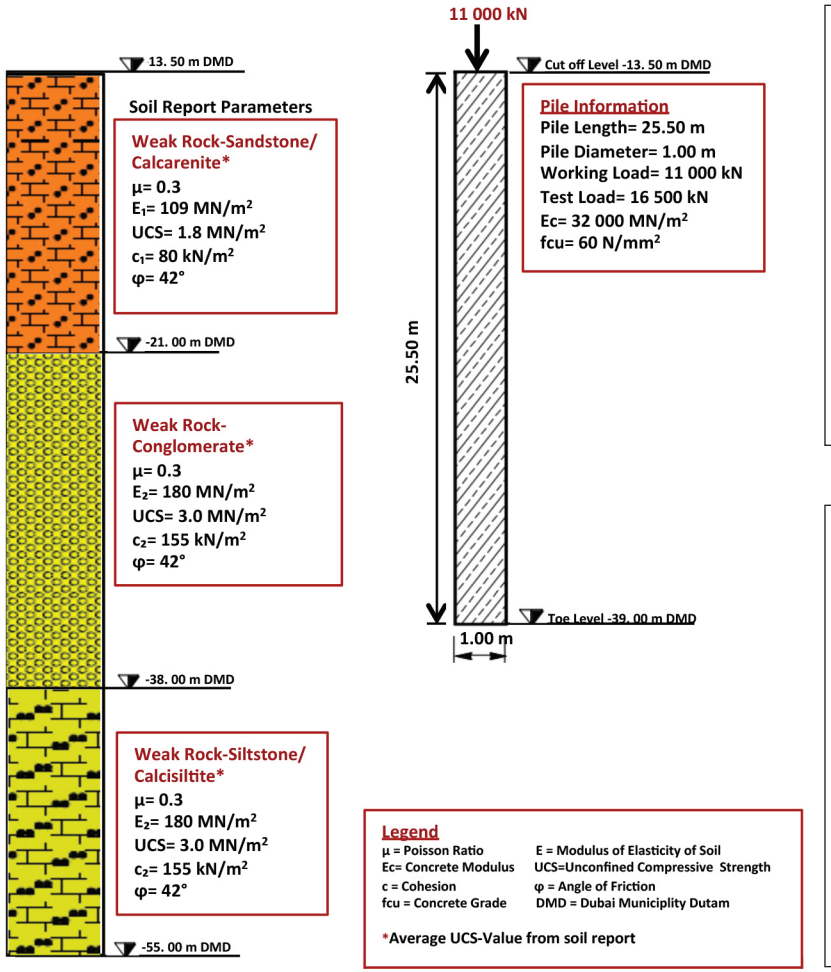

Legend

μ = Poisson Ratio	E = Modulus of Elasticity of Soil
Ec= Concrete Modulus	UCS=Unconfined Compressive Strength
c = Cohesion	φ = Angle of Friction
fcu = Concrete Grade	DMD = Dubai Municiplity Datum

*Average UCS-Value from soil report

Modelling by using Soil Report Parameters

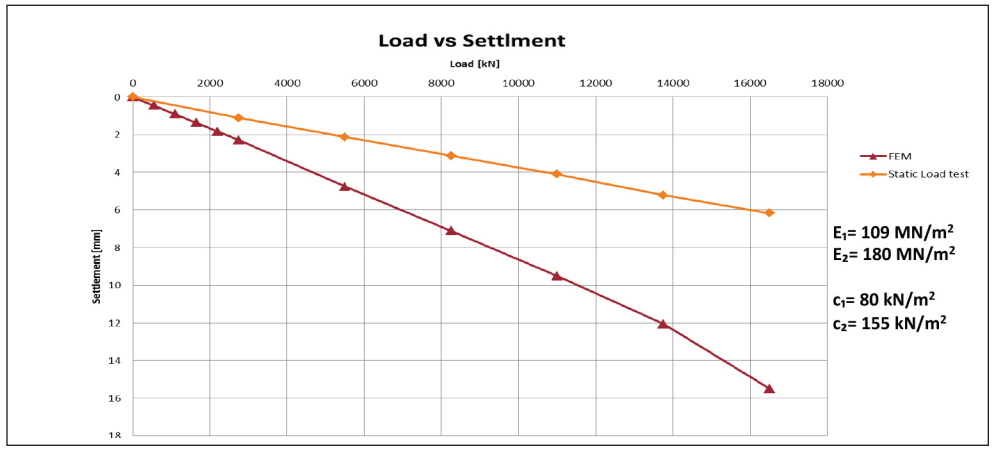

Back-Analysis of Soil Properties from Load Test

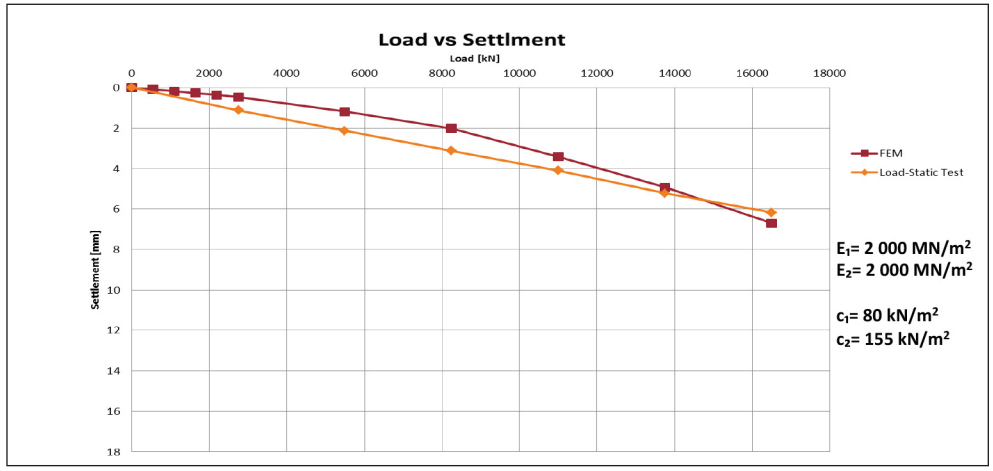

Pile Summary Sheet
P23

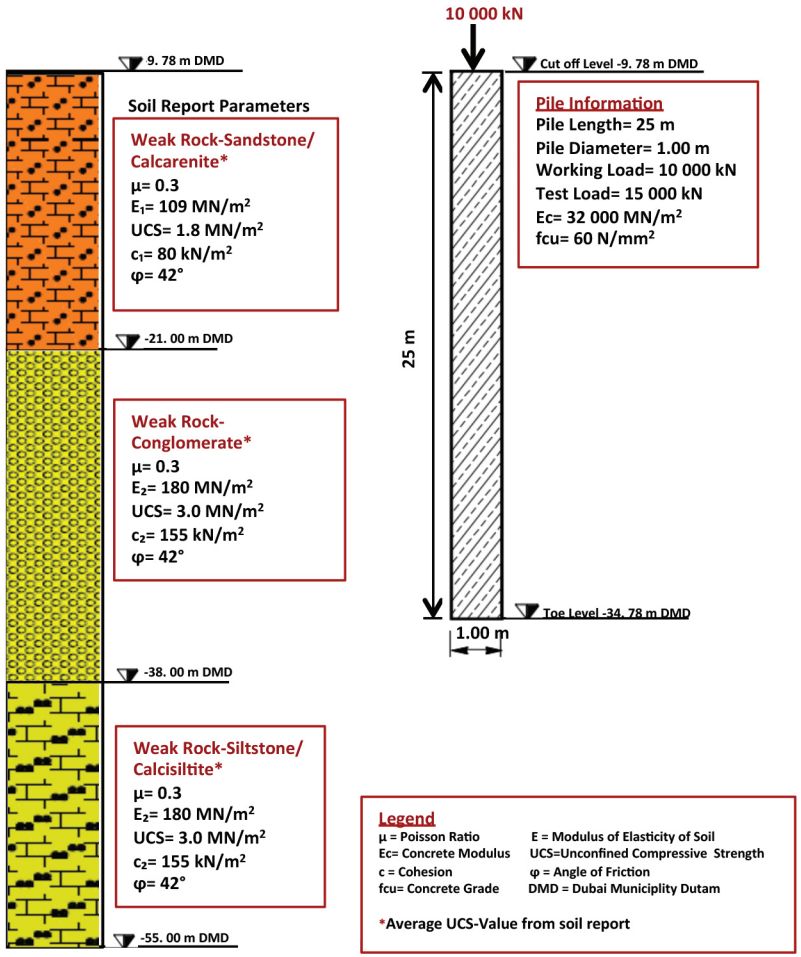

Pile Information
Pile Length= 25 m
Pile Diameter= 1.00 m
Working Load= 10 000 kN
Test Load= 15 000 kN
Ec= 32 000 MN/m²
fcu= 60 N/mm²

Legend

μ = Poisson Ratio	E = Modulus of Elasticity of Soil
Ec= Concrete Modulus	UCS=Unconfined Compressive Strength
c = Cohesion	φ = Angle of Friction
fcu= Concrete Grade	DMD = Dubai Municiplity Dutam

*Average UCS-Value from soil report

Modelling by using Soil Report Parameters

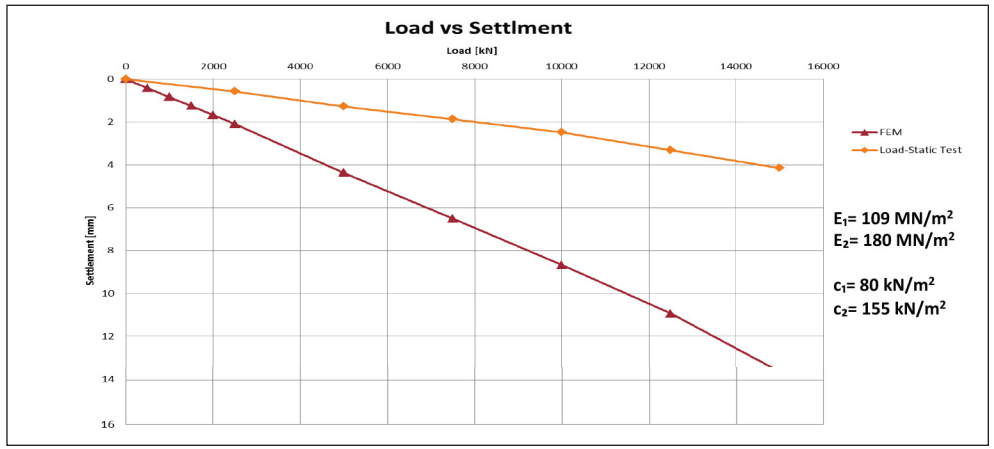

Back-Analysis of Soil Properties from Load Test

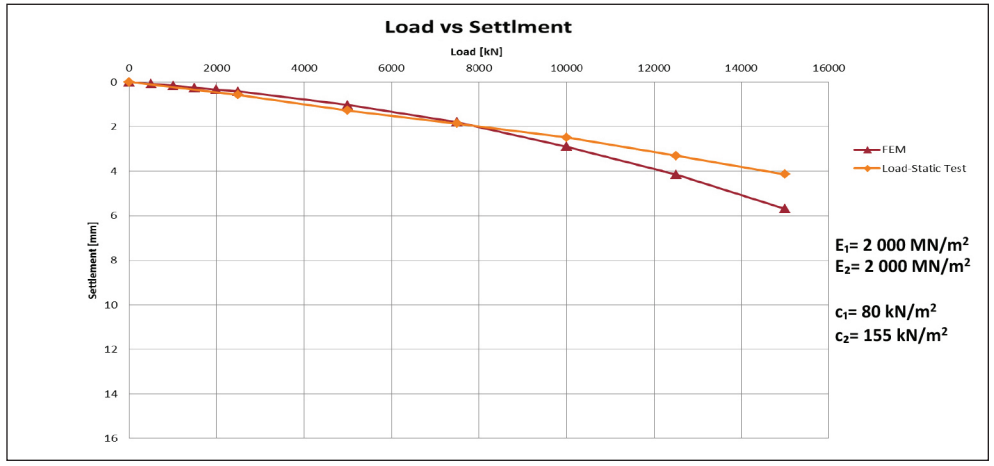

Pile Summary Sheet
P24

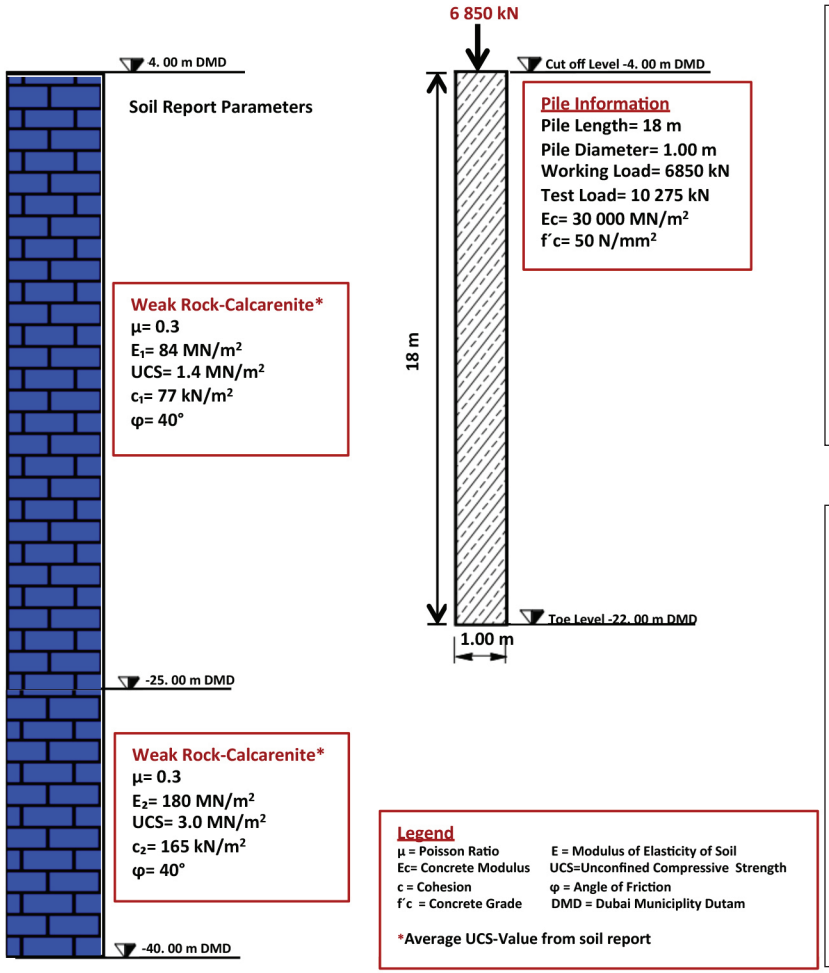

Weak Rock-Calcarenite*
μ= 0.3
E_1= 84 MN/m²
UCS= 1.4 MN/m²
c_1= 77 kN/m²
φ= 40°

Pile Information
Pile Length= 18 m
Pile Diameter= 1.00 m
Working Load= 6850 kN
Test Load= 10 275 kN
Ec= 30 000 MN/m²
f´c= 50 N/mm²

Weak Rock-Calcarenite*
μ= 0.3
E_2= 180 MN/m²
UCS= 3.0 MN/m²
c_2= 165 kN/m²
φ= 40°

Legend

μ = Poisson Ratio	E = Modulus of Elasticity of Soil
Ec= Concrete Modulus	UCS=Unconfined Compressive Strength
c = Cohesion	φ = Angle of Friction
f´c = Concrete Grade	DMD = Dubai Municiplity Dutam

*Average UCS-Value from soil report

Modelling by using Soil Report Parameters

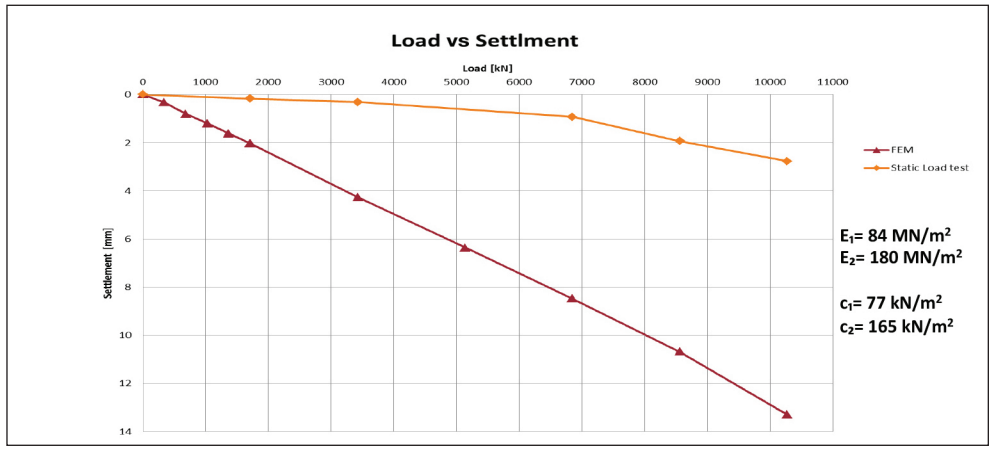

E_1= 84 MN/m²
E_2= 180 MN/m²
c_1= 77 kN/m²
c_2= 165 kN/m²

Back-Analysis of Soil Properties from Load Test

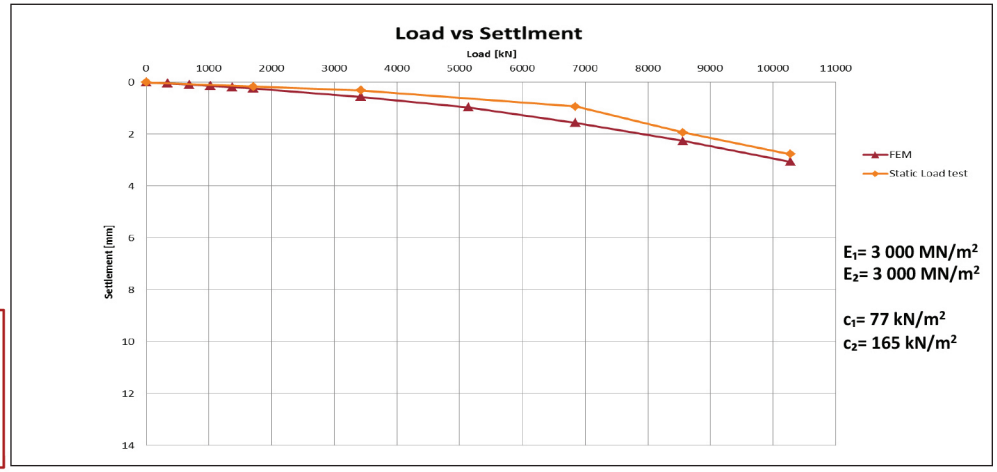

E_1= 3 000 MN/m²
E_2= 3 000 MN/m²
c_1= 77 kN/m²
c_2= 165 kN/m²

Pile Summary Sheet
P25

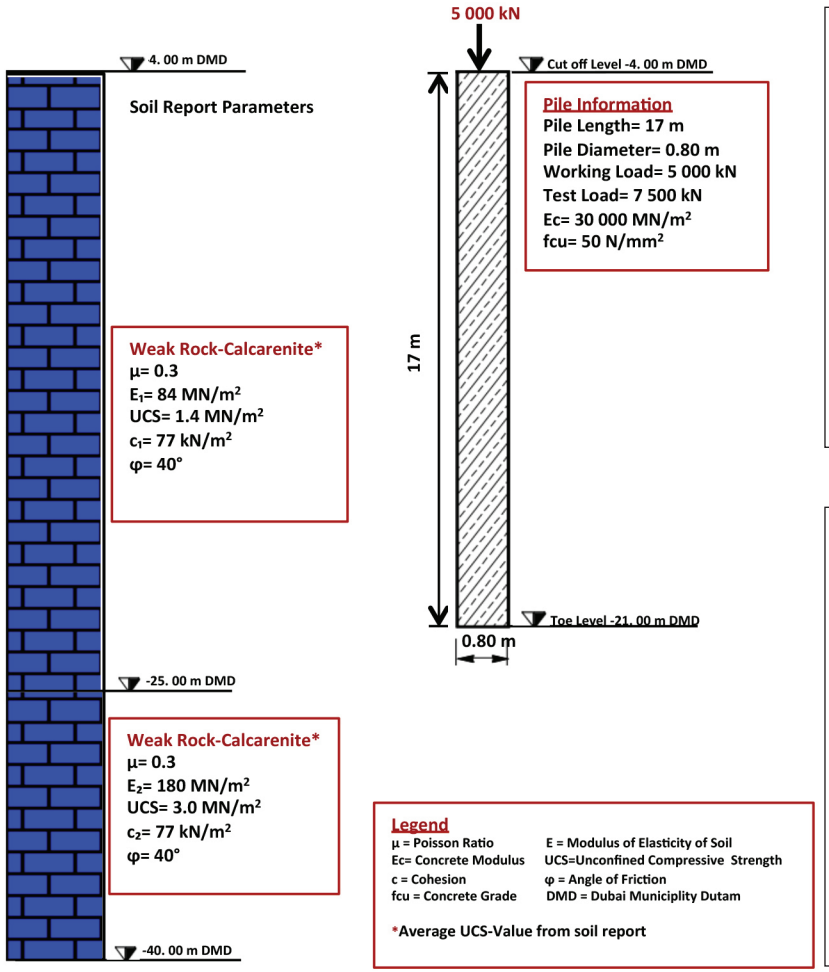

Pile Information
Pile Length= 17 m
Pile Diameter= 0.80 m
Working Load= 5 000 kN
Test Load= 7 500 kN
Ec= 30 000 MN/m²
fcu= 50 N/mm²

Legend

μ = Poisson Ratio	E = Modulus of Elasticity of Soil
Ec= Concrete Modulus	UCS=Unconfined Compressive Strength
c = Cohesion	φ = Angle of Friction
fcu = Concrete Grade	DMD = Dubai Municiplity Dutam

*Average UCS-Value from soil report

Modelling by using Soil Report Parameters

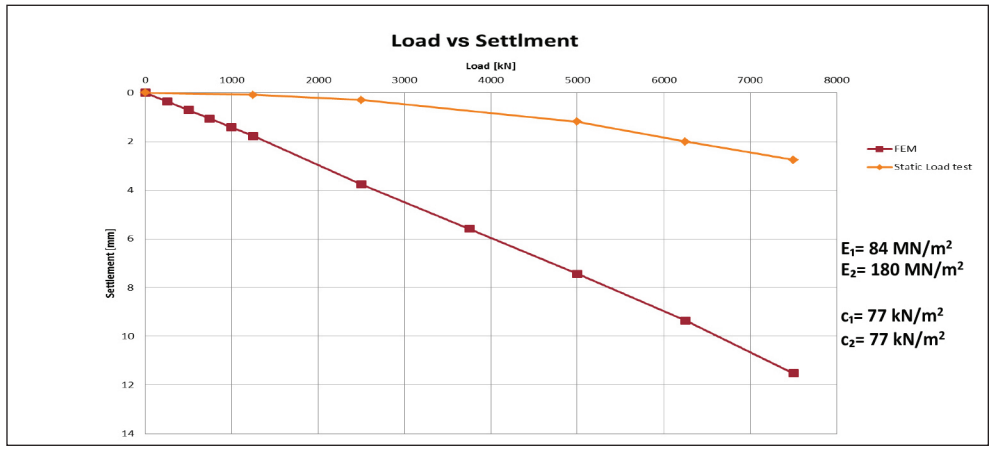

Back-Analysis of Soil Properties from Load Test

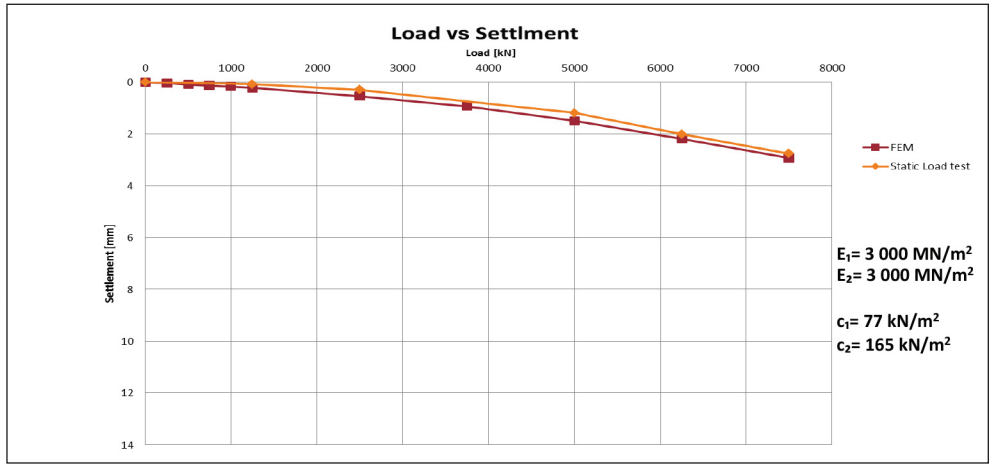

Pile Summary Sheet
P26

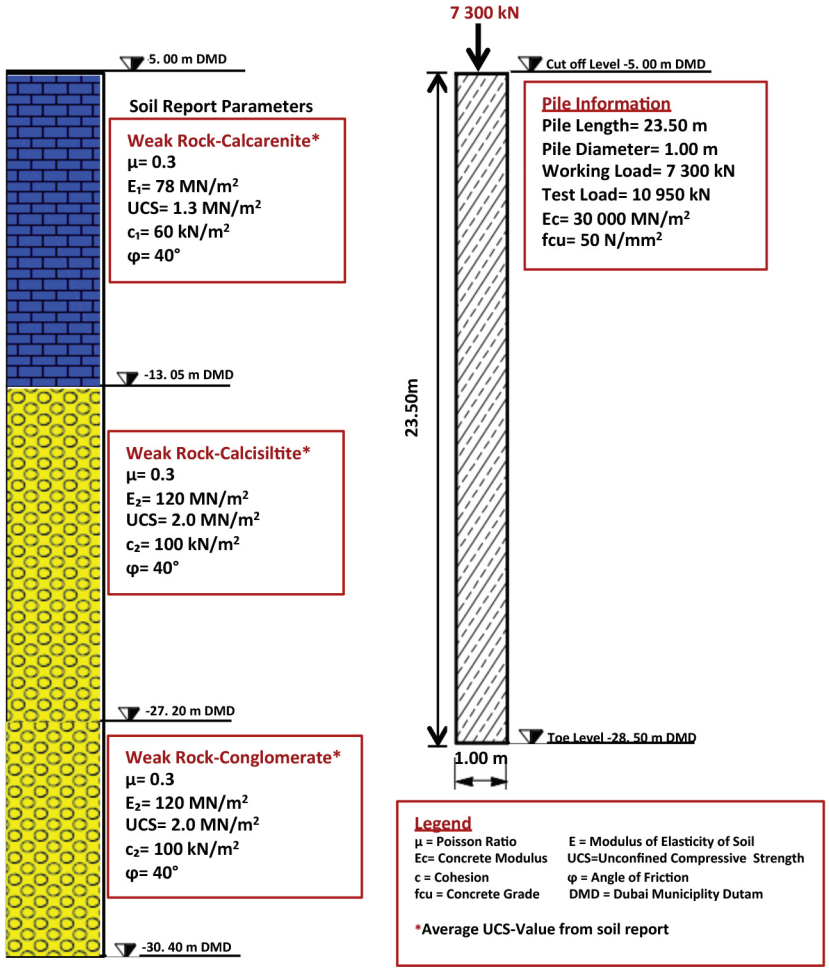

Pile Information
Pile Length= 23.50 m
Pile Diameter= 1.00 m
Working Load= 7 300 kN
Test Load= 10 950 kN
Ec= 30 000 MN/m²
fcu= 50 N/mm²

Legend

μ = Poisson Ratio — E = Modulus of Elasticity of Soil
Ec= Concrete Modulus — UCS=Unconfined Compressive Strength
c = Cohesion — φ = Angle of Friction
fcu = Concrete Grade — DMD = Dubai Municiplity Dutam

*Average UCS-Value from soil report

Modelling by using Soil Report Parameters

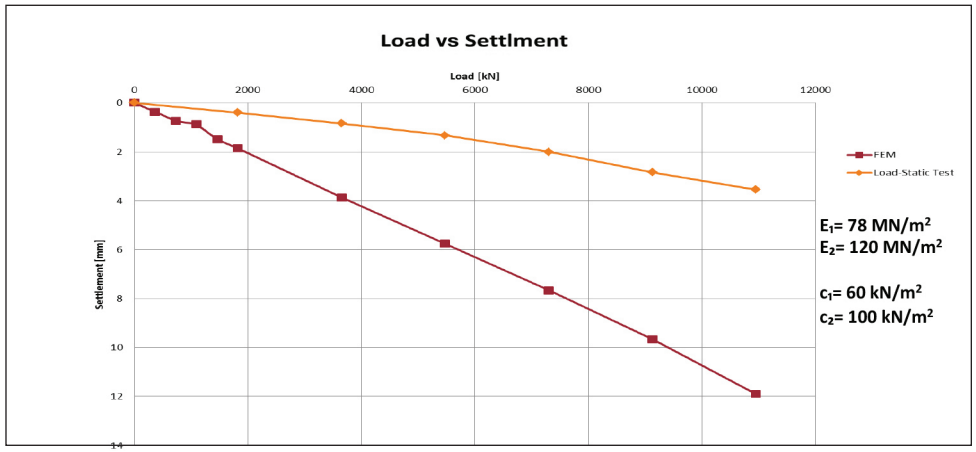

Back-Analysis of Soil Properties from Load Test

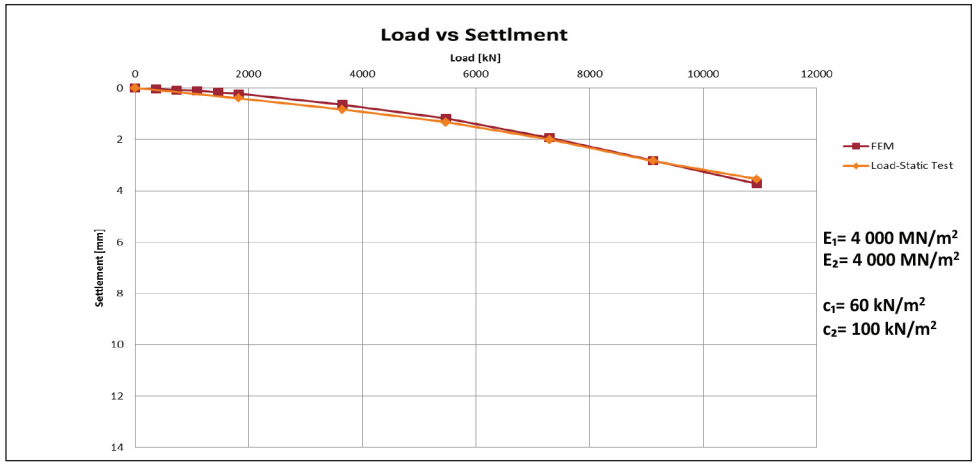

Pile Summary Sheet
P27

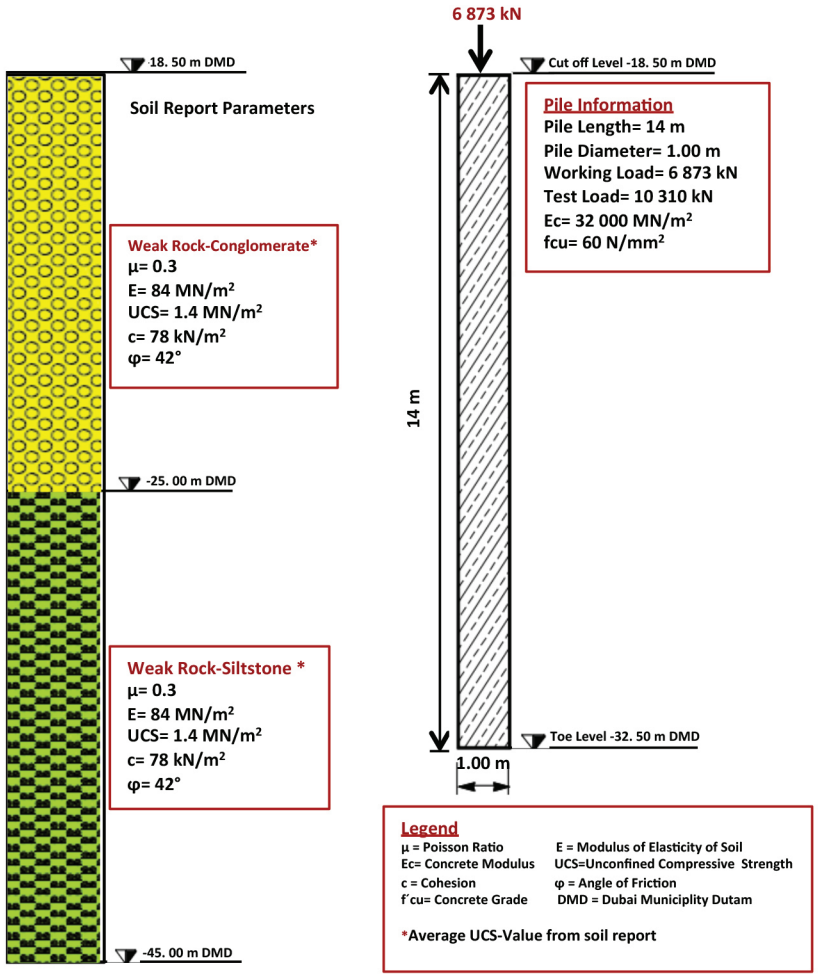

Pile Information
Pile Length= 14 m
Pile Diameter= 1.00 m
Working Load= 6 873 kN
Test Load= 10 310 kN
Ec= 32 000 MN/m²
fcu= 60 N/mm²

Legend

μ = Poisson Ratio	E = Modulus of Elasticity of Soil
Ec= Concrete Modulus	UCS=Unconfined Compressive Strength
c = Cohesion	φ = Angle of Friction
f´cu= Concrete Grade	DMD = Dubai Municiplity Dutam

*Average UCS-Value from soil report

Modelling by using Soil Report Parameters

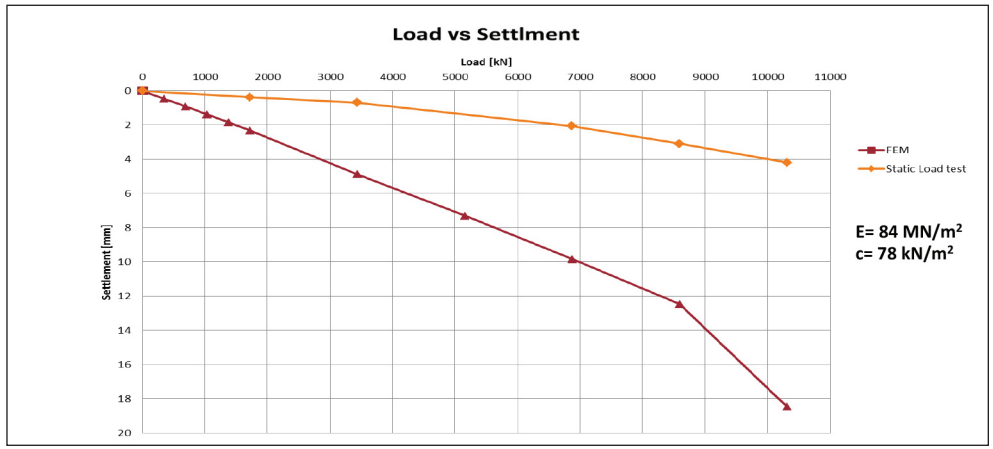

E= 84 MN/m²
c= 78 kN/m²

Back-Analysis of Soil Properties from Load Test

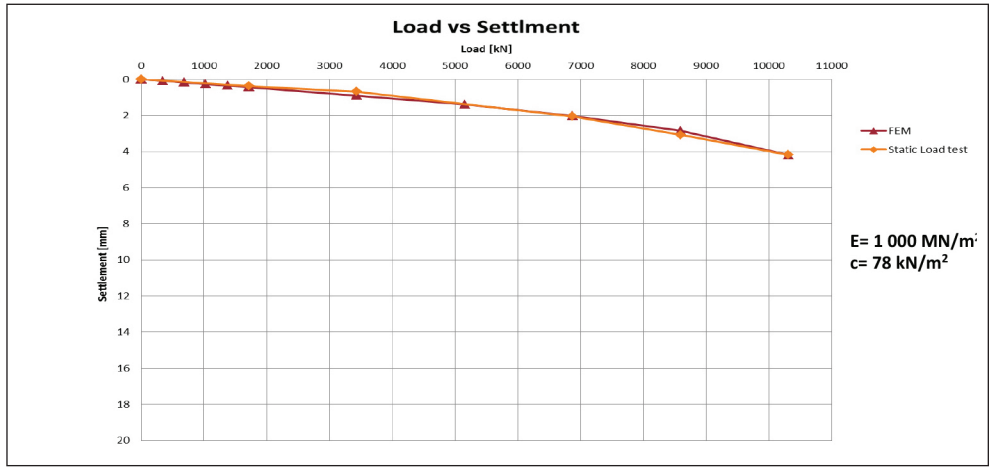

E= 1 000 MN/m²
c= 78 kN/m²

Pile Summary Sheet
P28

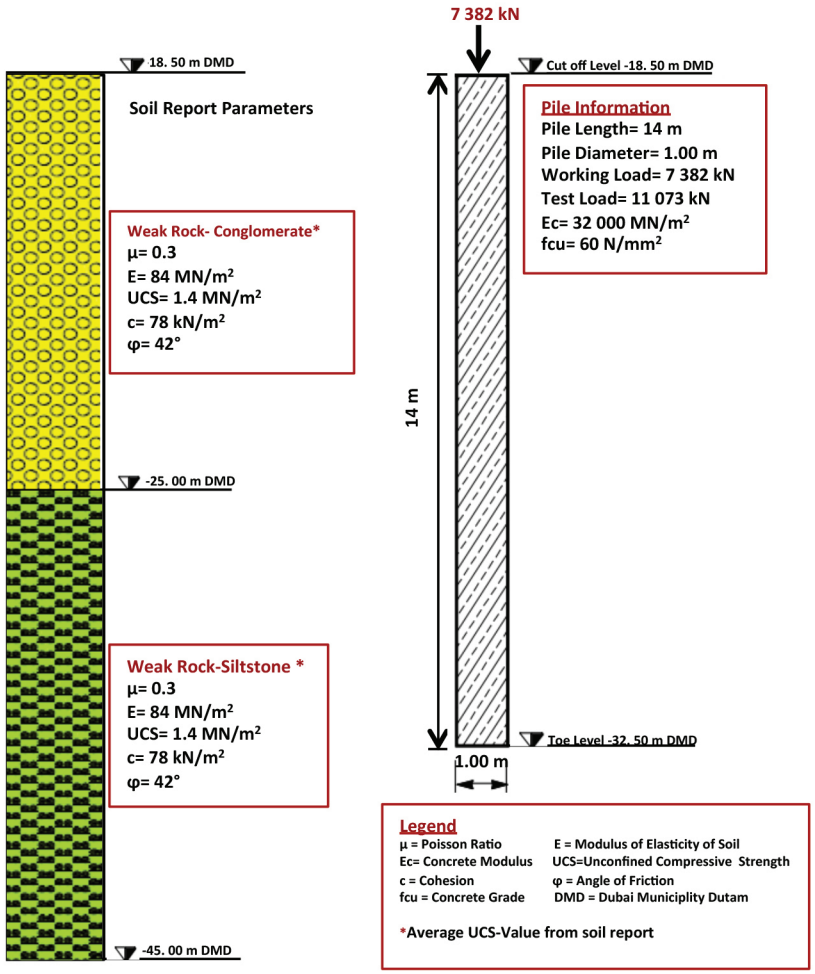

Pile Information
Pile Length= 14 m
Pile Diameter= 1.00 m
Working Load= 7 382 kN
Test Load= 11 073 kN
Ec= 32 000 MN/m²
fcu= 60 N/mm²

Legend

μ = Poisson Ratio	E = Modulus of Elasticity of Soil
Ec= Concrete Modulus	UCS=Unconfined Compressive Strength
c = Cohesion	φ = Angle of Friction
fcu = Concrete Grade	DMD = Dubai Municiplity Dutam

*Average UCS-Value from soil report

Modelling by using Soil Report Parameters

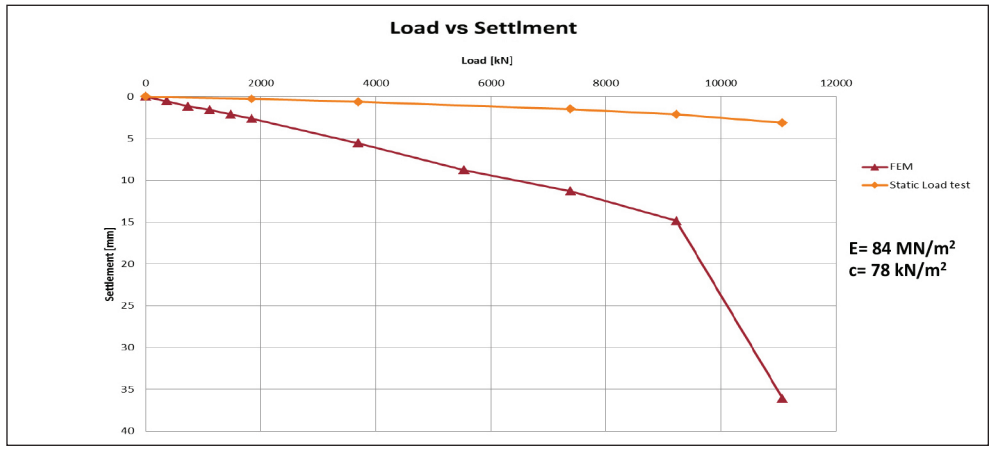

Back-Analysis of Soil Properties from Load Test

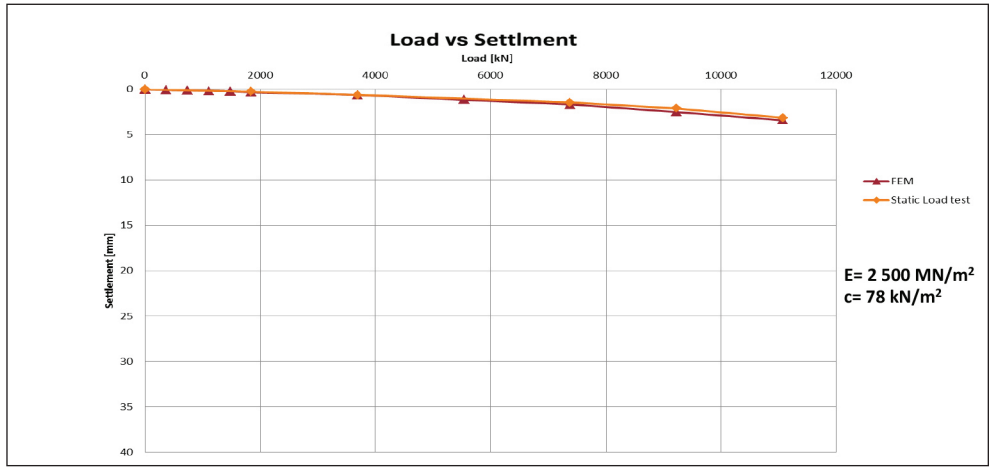

Pile Summary Sheet
P29

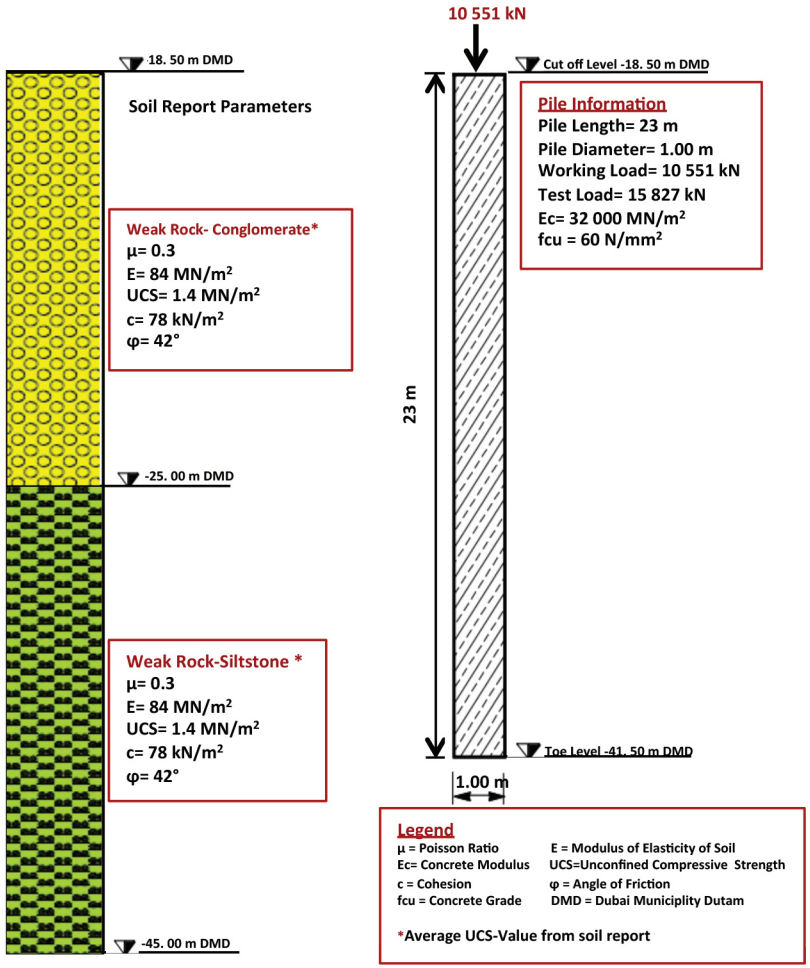

Modelling by using Soil Report Parameters

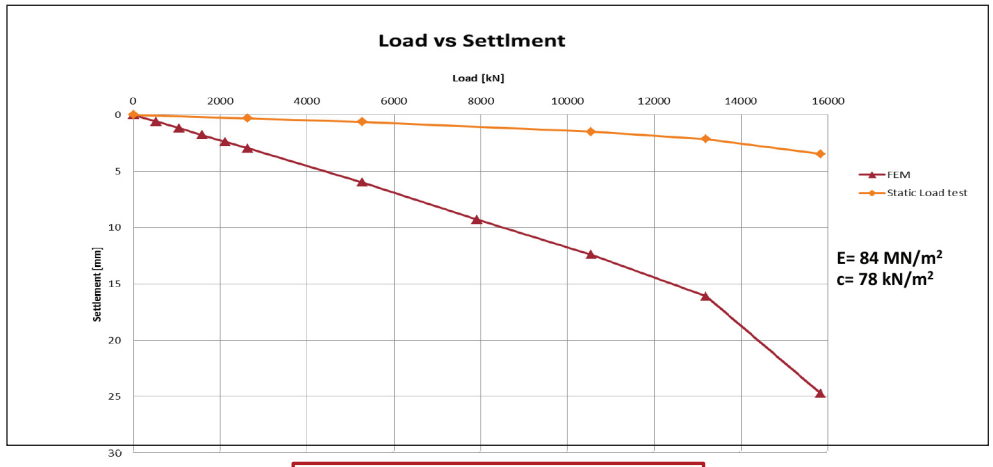

Back-Analysis of Soil Properties from Load Test

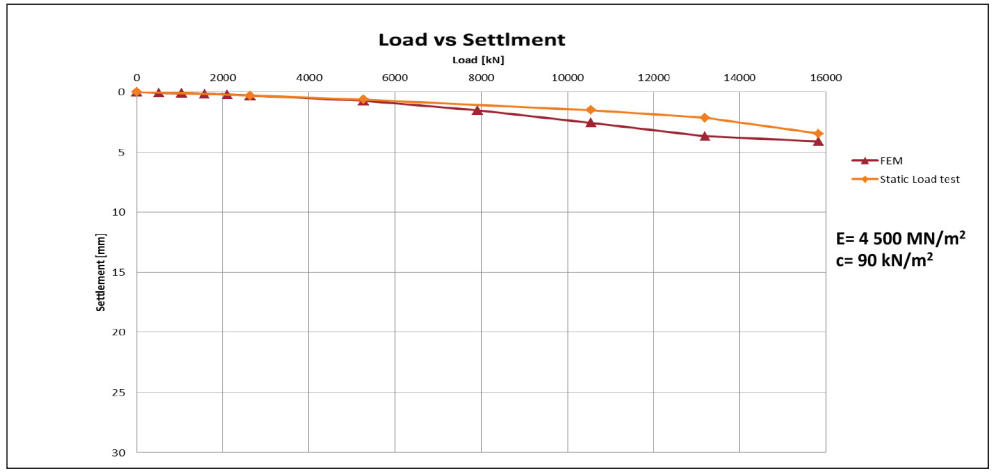

Pile Summary Sheet
P30

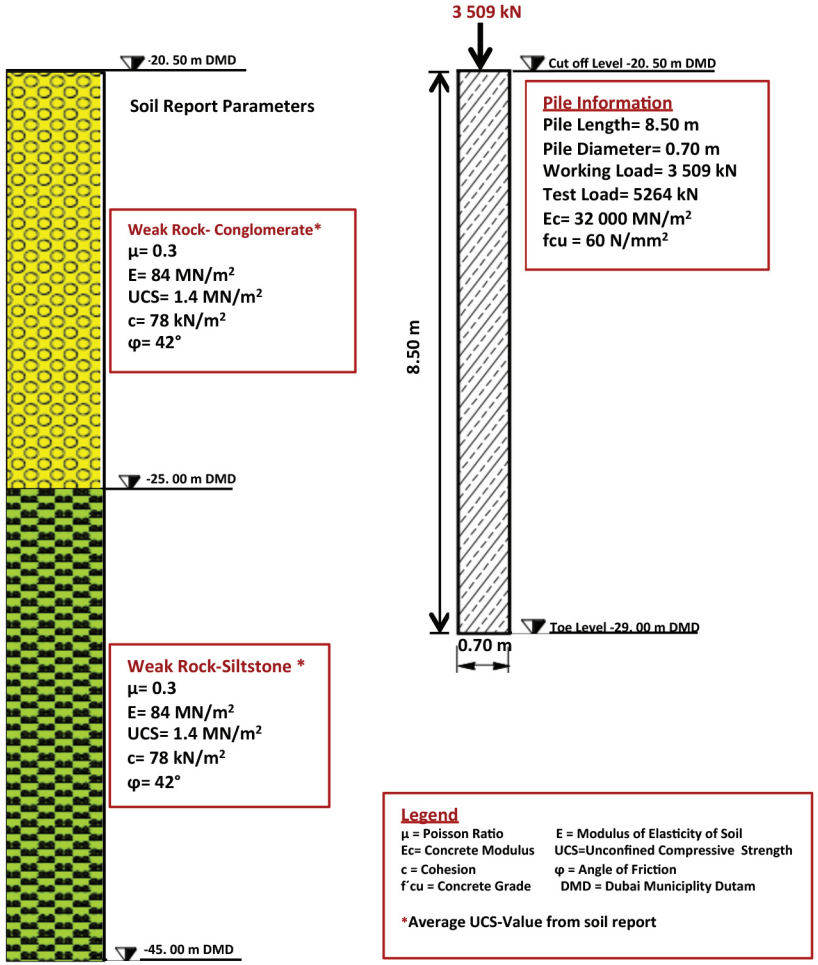

Legend

μ = Poisson Ratio — E = Modulus of Elasticity of Soil
Ec= Concrete Modulus — UCS=Unconfined Compressive Strength
c = Cohesion — φ = Angle of Friction
f´cu = Concrete Grade — DMD = Dubai Municiplity Dutam

*Average UCS-Value from soil report

Modelling by using Soil Report Parameters

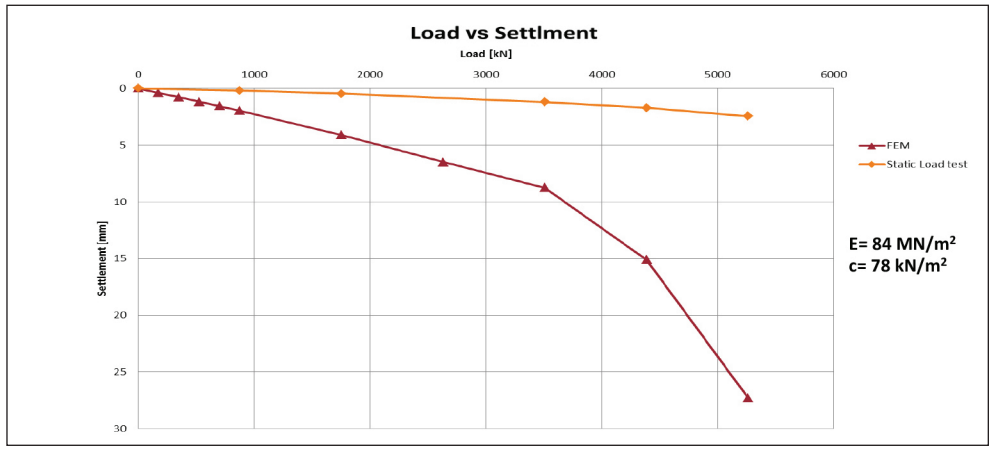

Back-Analysis of Soil Properties from Load Test

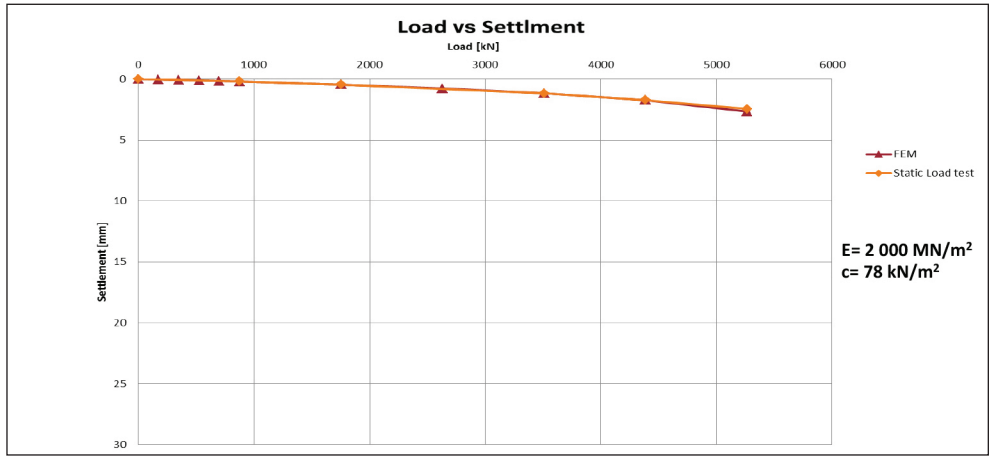

Pile Summary Sheet
P31

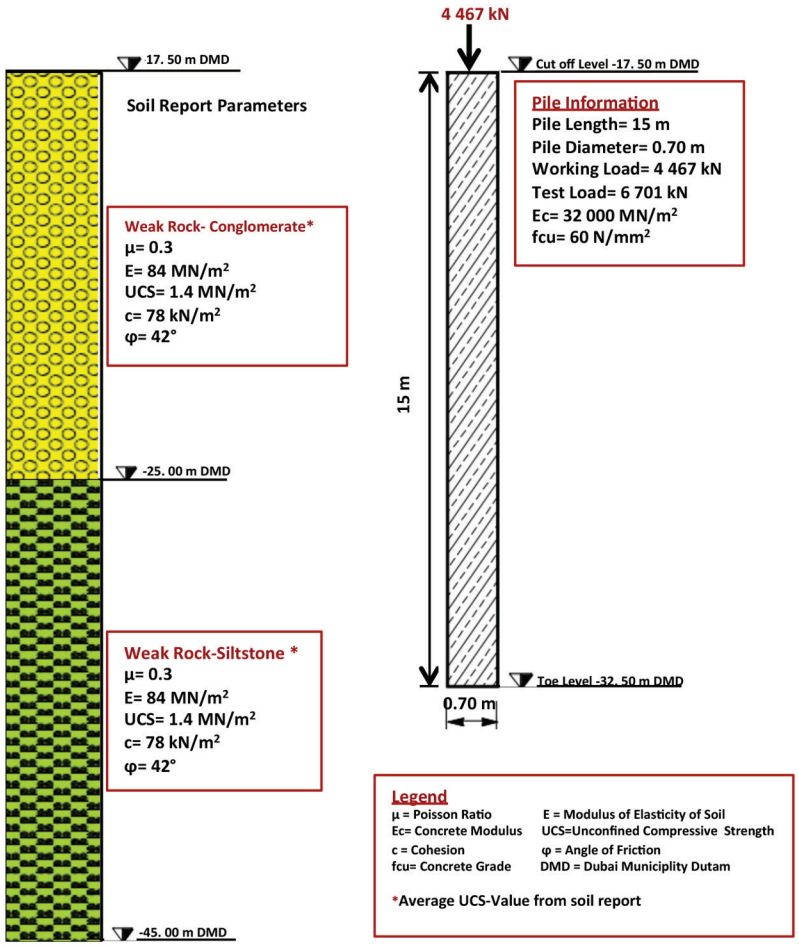

Pile Information
Pile Length= 15 m
Pile Diameter= 0.70 m
Working Load= 4 467 kN
Test Load= 6 701 kN
Ec= 32 000 MN/m²
fcu= 60 N/mm²

Legend

μ = Poisson Ratio	E = Modulus of Elasticity of Soil
Ec= Concrete Modulus	UCS=Unconfined Compressive Strength
c = Cohesion	φ = Angle of Friction
fcu= Concrete Grade	DMD = Dubai Municiplity Dutam

*Average UCS-Value from soil report

Modelling by using Soil Report Parameters

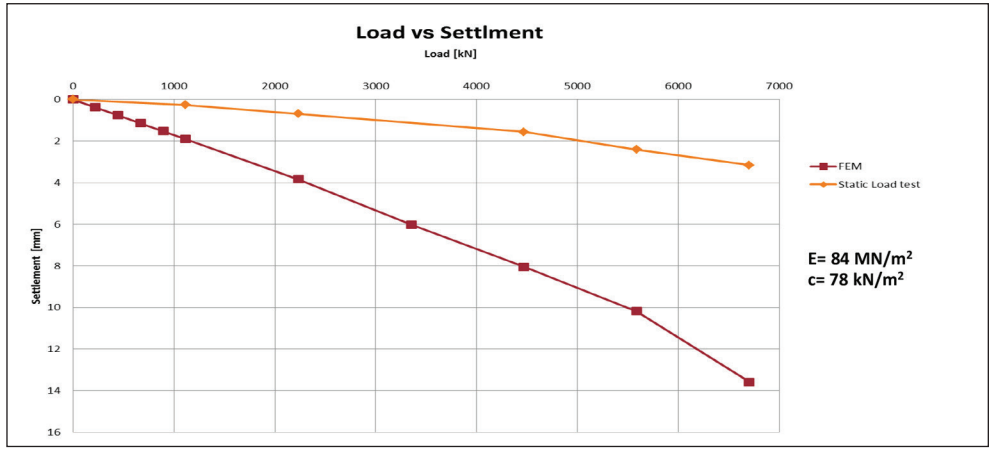

Back-Analysis of Soil Properties from Load Test

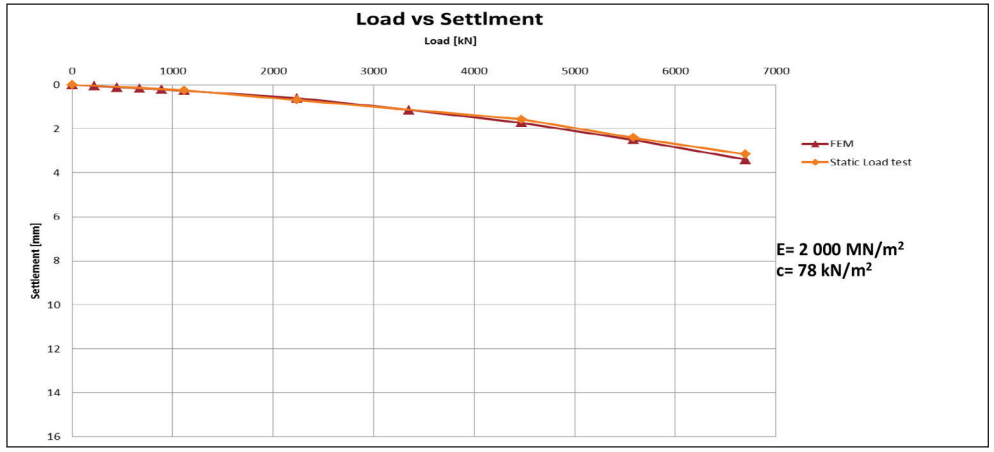

Pile Summary Sheet
P32

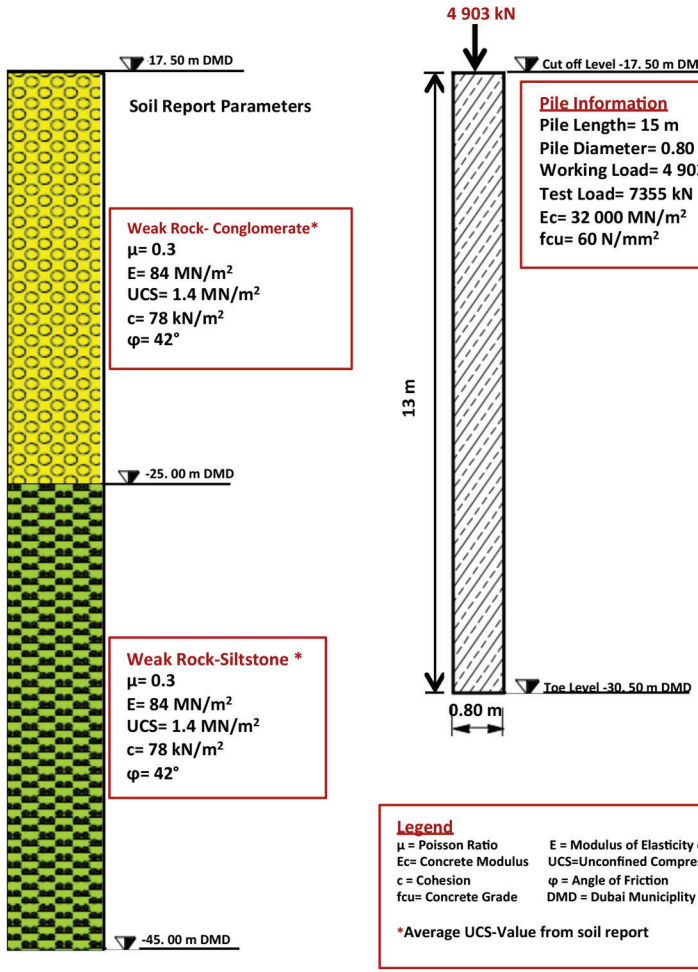

Pile Information
Pile Length= 15 m
Pile Diameter= 0.80 m
Working Load= 4 903 kN
Test Load= 7355 kN
Ec= 32 000 MN/m²
fcu= 60 N/mm²

Legend

μ = Poisson Ratio	E = Modulus of Elasticity of Soil
Ec= Concrete Modulus	UCS=Unconfined Compressive Strength
c = Cohesion	φ = Angle of Friction
fcu= Concrete Grade	DMD = Dubai Municiplity Dutam

*Average UCS-Value from soil report

Modelling by using Soil Report Parameters

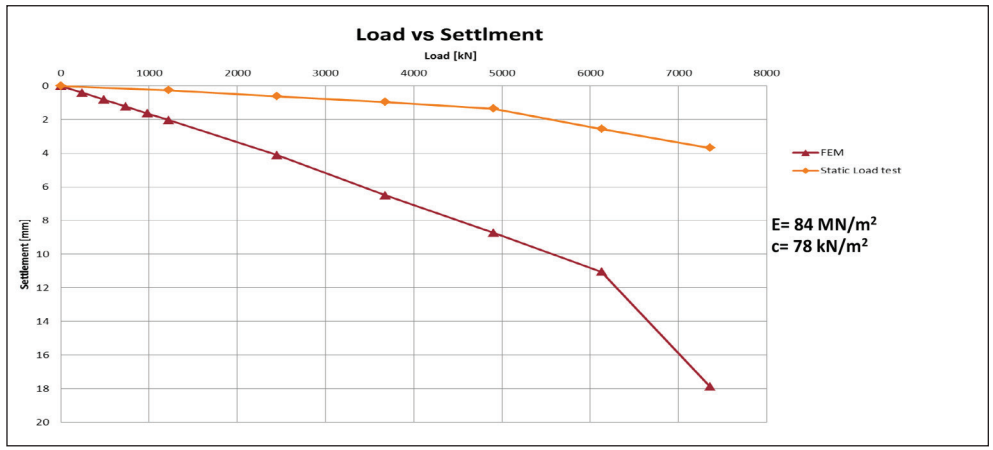

Back-Analysis of Soil Properties from Load Test

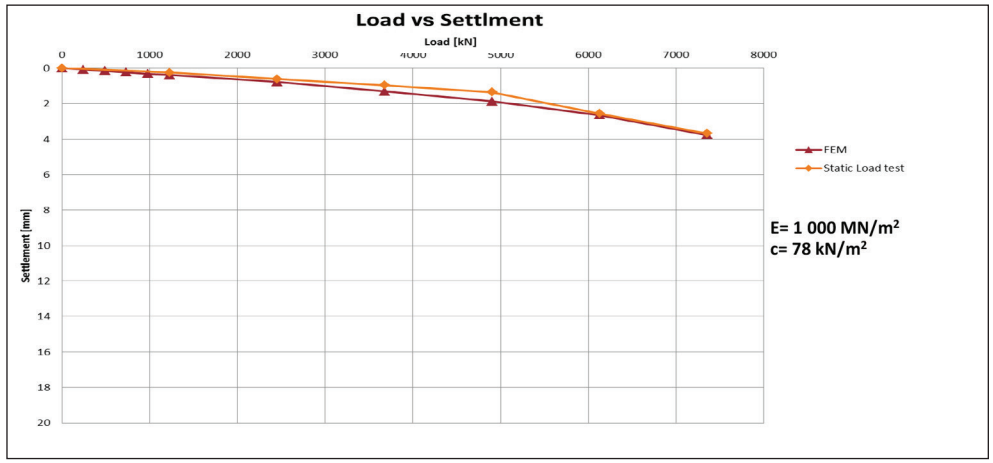

Pile Summary Sheet
P33

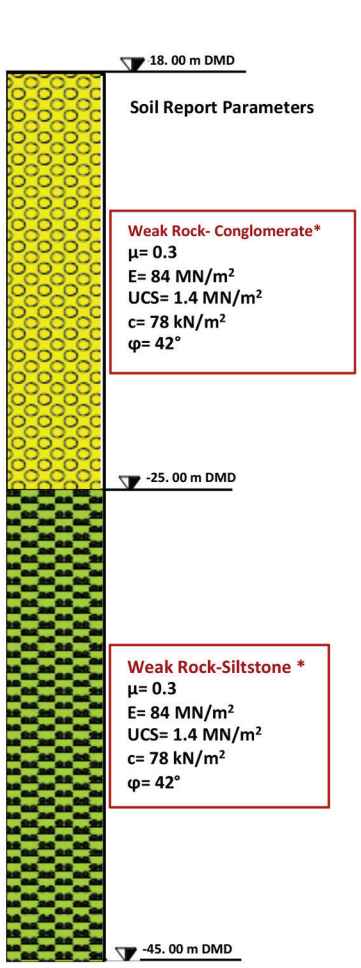

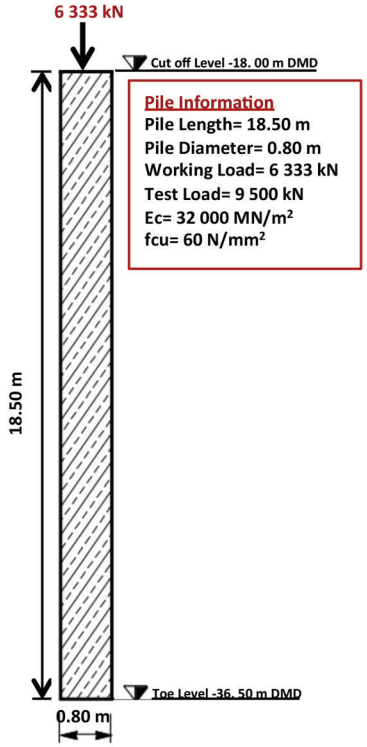

Pile Information
Pile Length= 18.50 m
Pile Diameter= 0.80 m
Working Load= 6 333 kN
Test Load= 9 500 kN
Ec= 32 000 MN/m²
fcu= 60 N/mm²

Legend

μ = Poisson Ratio	E = Modulus of Elasticity of Soil
Ec= Concrete Modulus	UCS=Unconfined Compressive Strength
c = Cohesion	φ = Angle of Friction
fcu= Concrete Grade	DMD = Dubai Municiplity Dutam

*Average UCS-Value from soil report

Modelling by using Soil Report Parameters

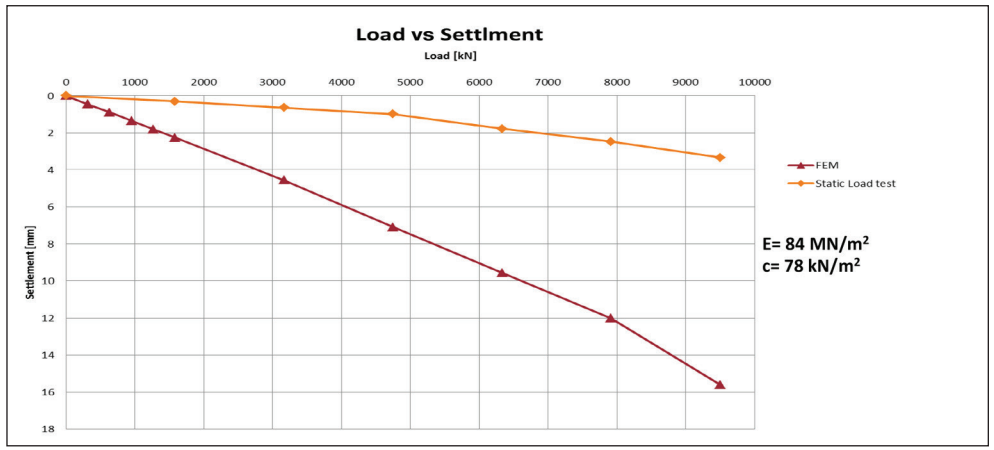

Back-Analysis of Soil Properties from Load Test

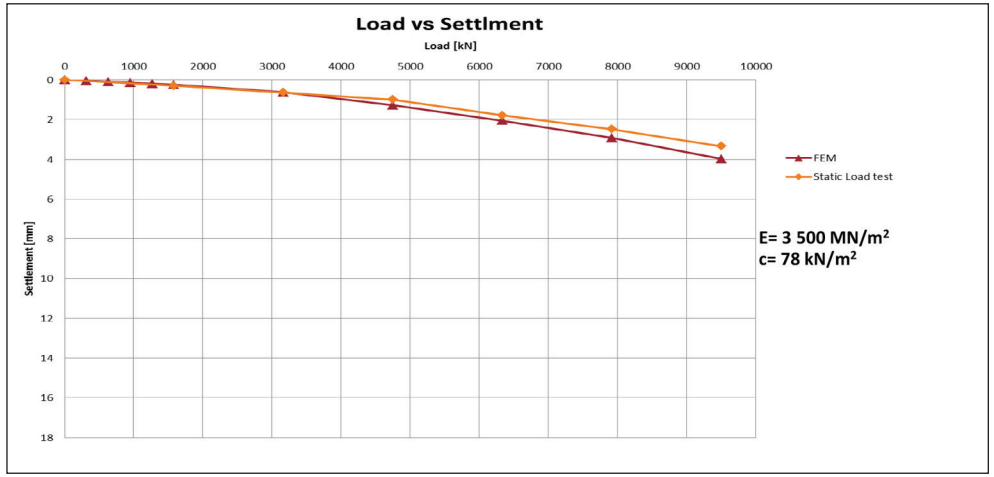

Pile Summary Sheet
P34

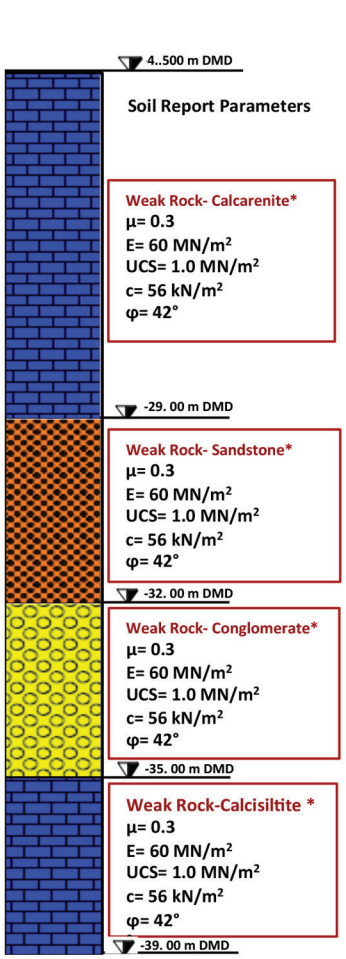

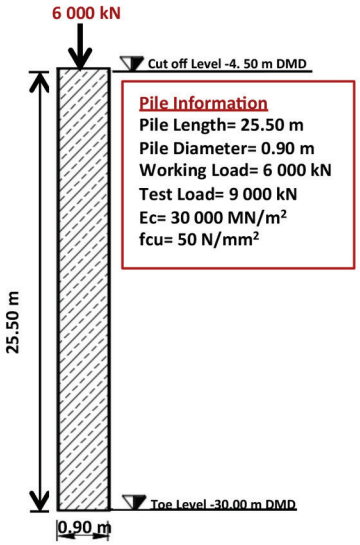

Pile Information
Pile Length= 25.50 m
Pile Diameter= 0.90 m
Working Load= 6 000 kN
Test Load= 9 000 kN
Ec= 30 000 MN/m²
fcu= 50 N/mm²

Legend

μ = Poisson Ratio	E = Modulus of Elasticity of Soil
Ec= Concrete Modulus	UCS=Unconfined Compressive Strength
c = Cohesion	φ = Angle of Friction
fcu= Concrete Grade	DMD = Dubai Municiplity Dutam

*Average UCS-Value from soil report

Modelling by using Soil Report Parameters

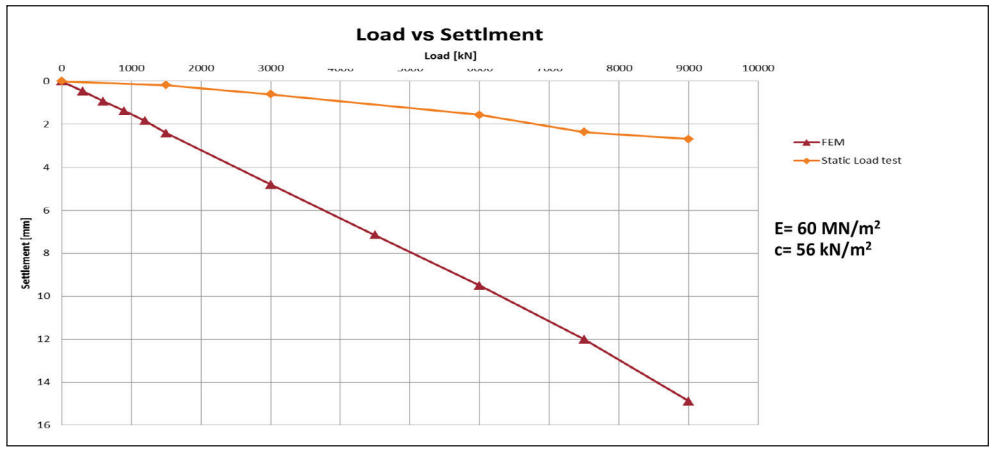

Back-Analysis of Soil Properties from Load Test

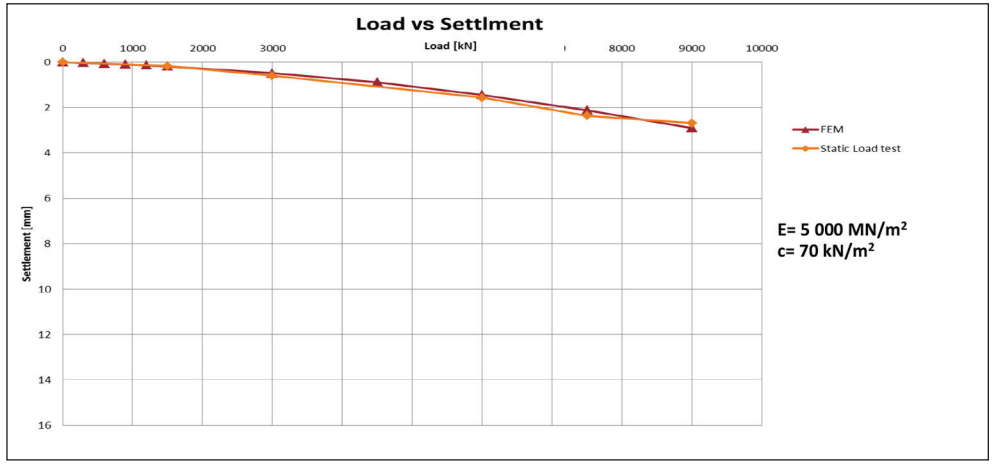

Pile Summary Sheet
P35

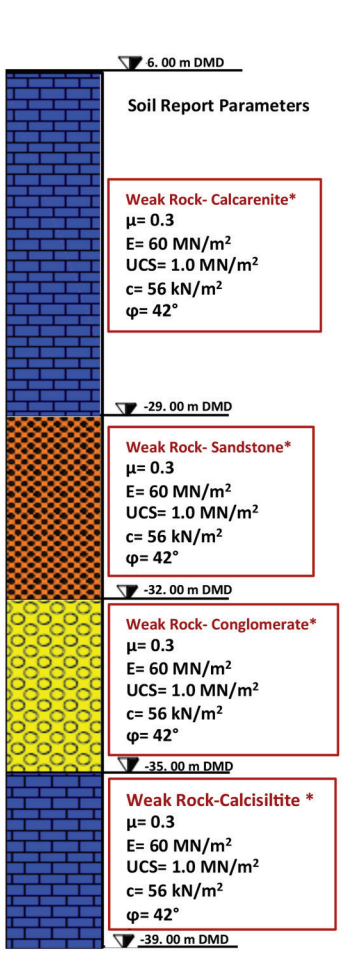

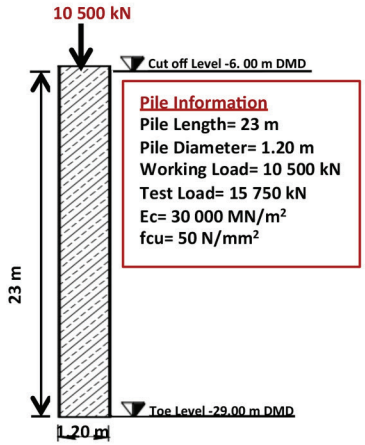

Pile Information
Pile Length= 23 m
Pile Diameter= 1.20 m
Working Load= 10 500 kN
Test Load= 15 750 kN
Ec= 30 000 MN/m²
fcu= 50 N/mm²

Legend

μ = Poisson Ratio	E = Modulus of Elasticity of Soil
Ec= Concrete Modulus	UCS=Unconfined Compressive Strength
c = Cohesion	φ = Angle of Friction
fcu = Concrete Grade	DMD = Dubai Municiplity Dutam

*Average UCS-Value from soil report

Modelling by using Soil Report Parameters

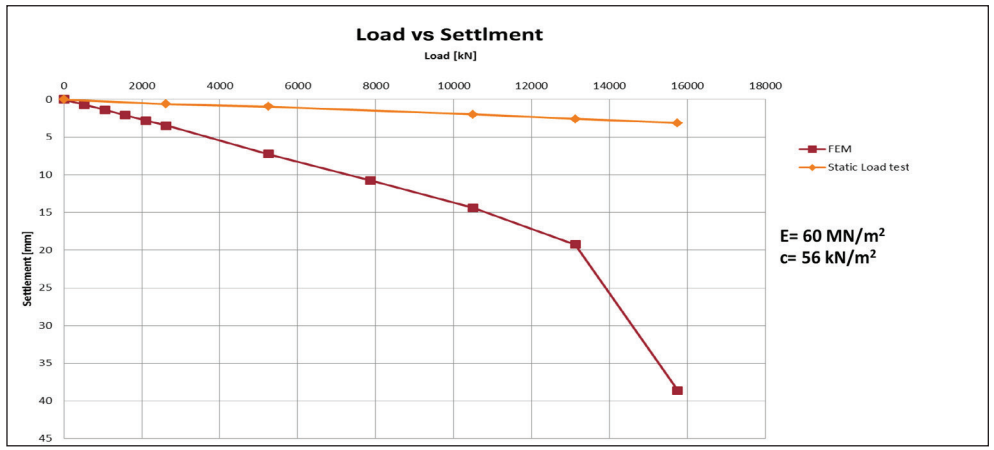

Back-Analysis of Soil Properties from Load Test

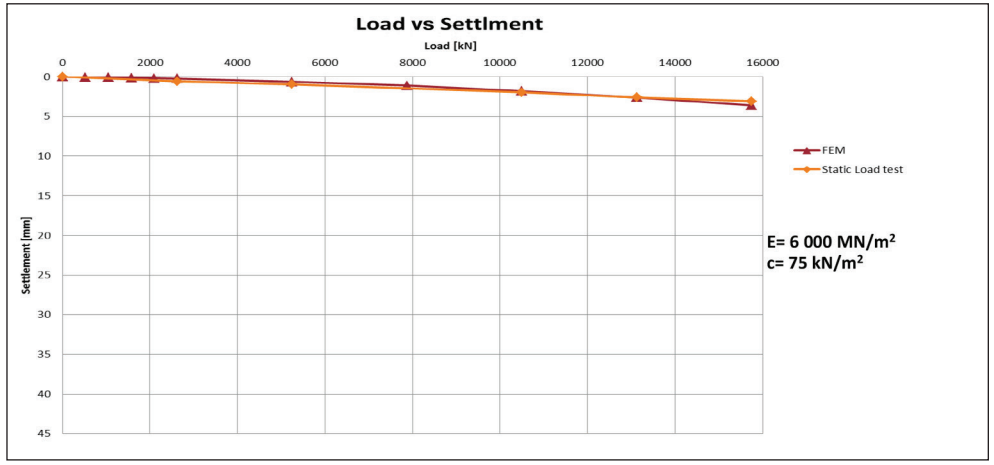

Pile Summary Sheet
P36

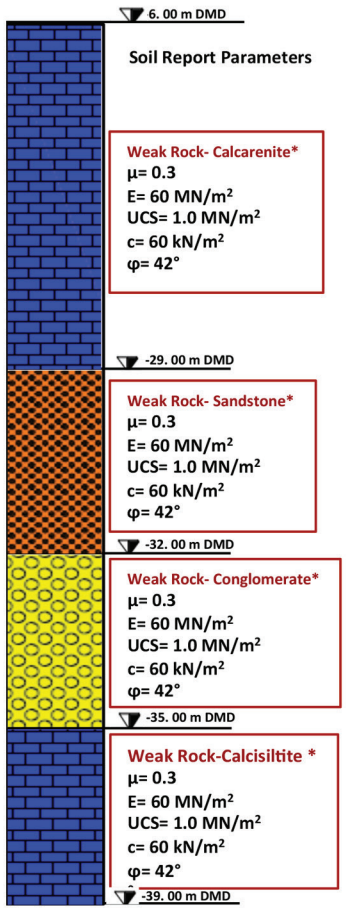

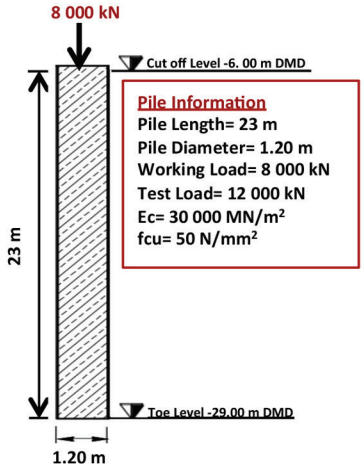

Pile Information
Pile Length= 23 m
Pile Diameter= 1.20 m
Working Load= 8 000 kN
Test Load= 12 000 kN
Ec= 30 000 MN/m²
fcu= 50 N/mm²

Legend

μ = Poisson Ratio	E = Modulus of Elasticity of Soil
Ec= Concrete Modulus	UCS=Unconfined Compressive Strength
c = Cohesion	φ = Angle of Friction
fcu = Concrete Grade	DMD = Dubai Municiplity Dutam

*Average UCS-Value from soil report

Modelling by using Soil Report Parameters

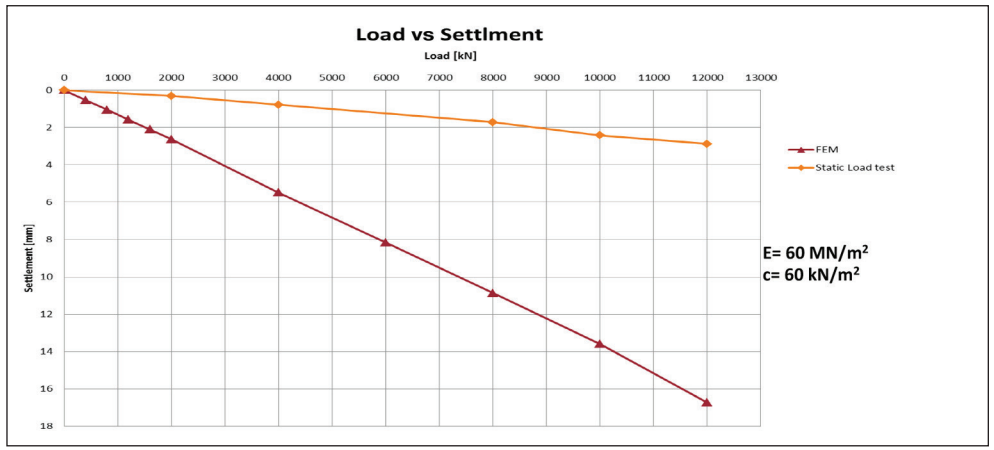

Back-Analysis of Soil Properties from Load Test

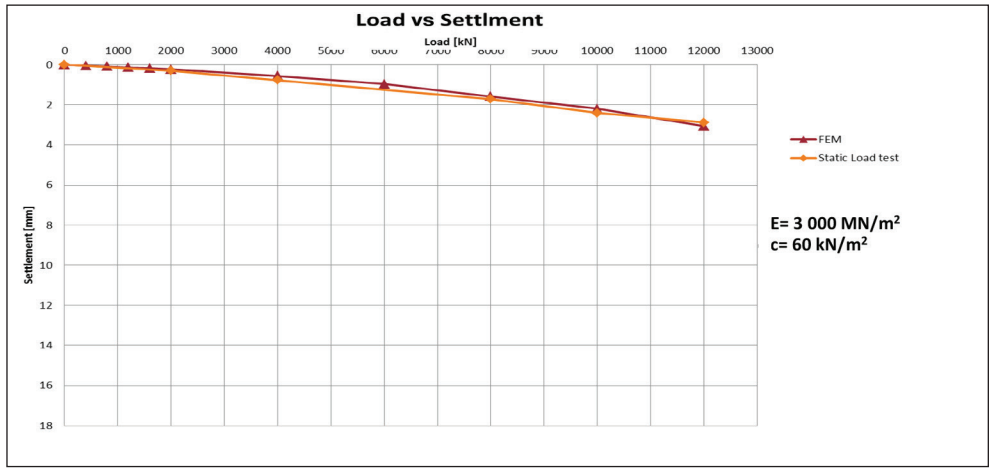

Pile Summary Sheet
P37

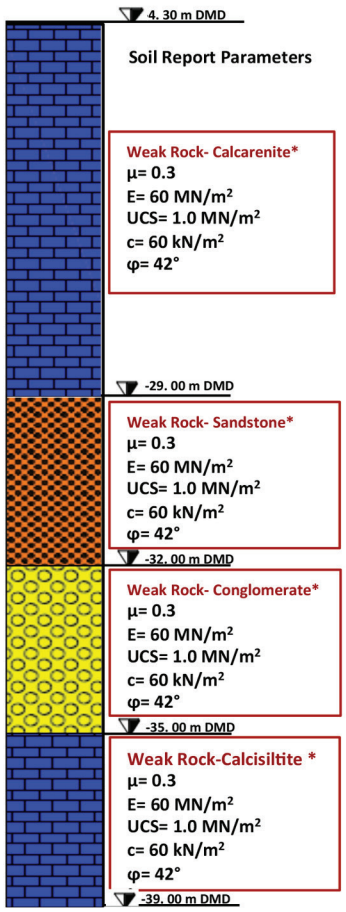

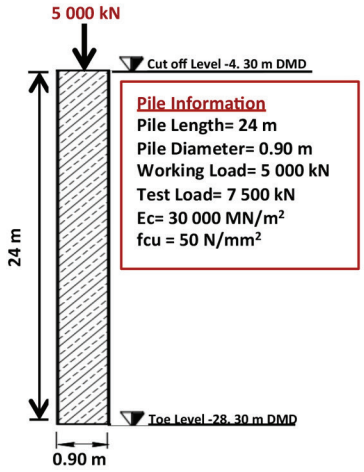

Pile Information
Pile Length= 24 m
Pile Diameter= 0.90 m
Working Load= 5 000 kN
Test Load= 7 500 kN
Ec= 30 000 MN/m²
fcu = 50 N/mm²

Legend

μ = Poisson Ratio	E = Modulus of Elasticity of Soil
Ec= Concrete Modulus	UCS=Unconfined Compressive Strength
c = Cohesion	φ = Angle of Friction
fcu = Concrete Grade	DMD = Dubai Municiplity Dutam

*Average UCS-Value from soil report

Modelling by using Soil Report Parameters

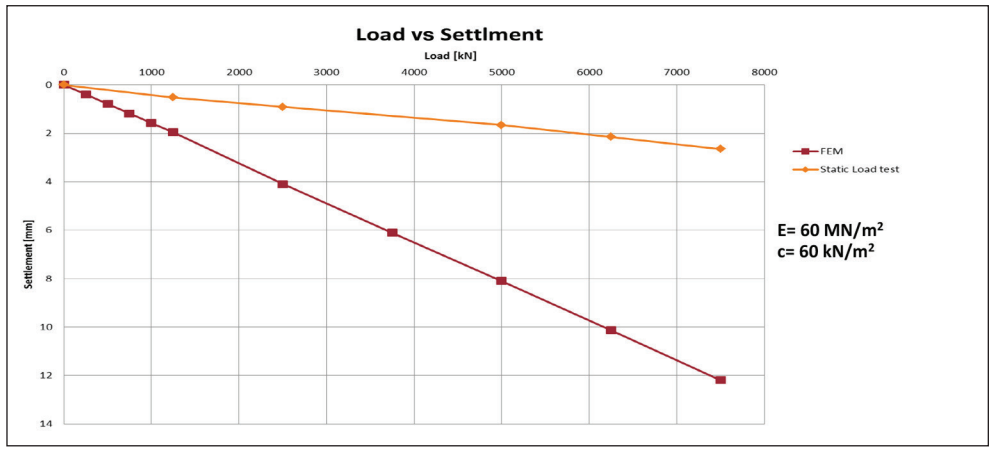

Back-Analysis of Soil Properties from Load Test

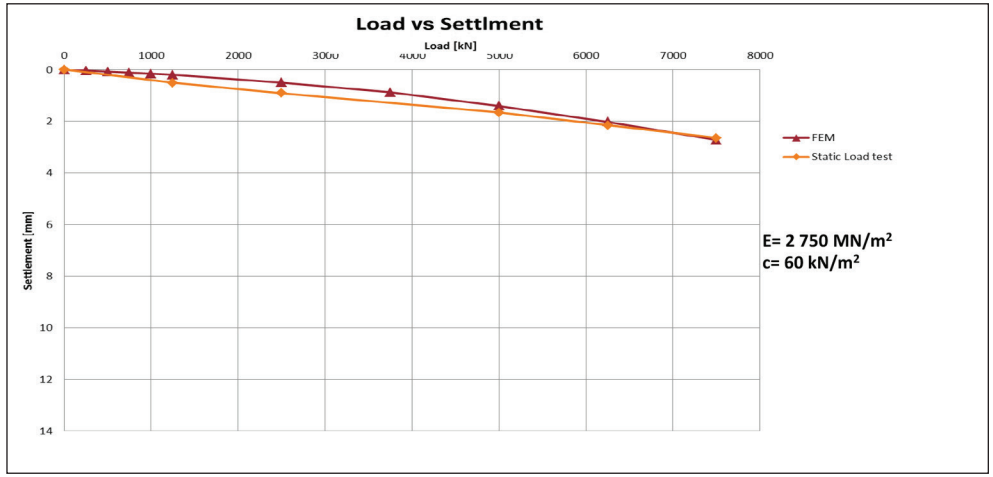

Pile Summary Sheet
P38

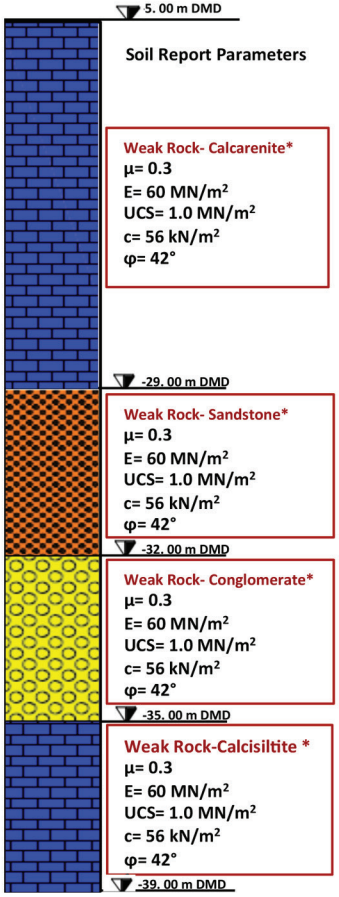

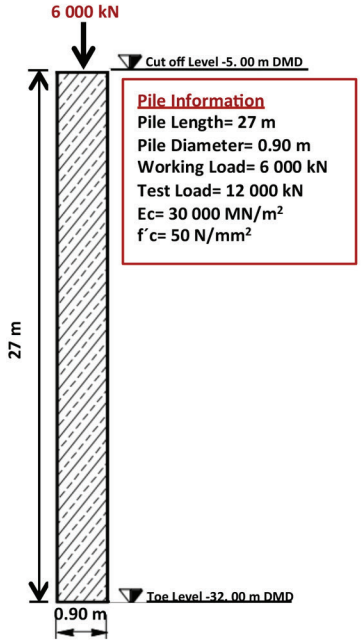

Pile Information
Pile Length= 27 m
Pile Diameter= 0.90 m
Working Load= 6 000 kN
Test Load= 12 000 kN
Ec= 30 000 MN/m²
f´c= 50 N/mm²

Legend

μ = Poisson Ratio	E = Modulus of Elasticity of Soil
Ec= Concrete Modulus	UCS=Unconfined Compressive Strength
c = Cohesion	φ = Angle of Friction
f´c = Concrete Grade	DMD = Dubai Municiplity Dutam

*Average UCS-Value from soil report

Modelling by using Soil Report Parameters

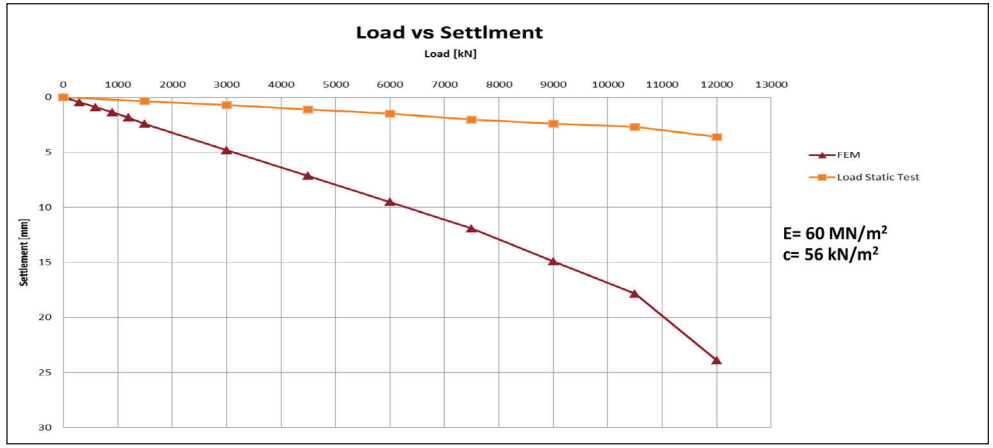

Back-Analysis of Soil Properties from Load Test

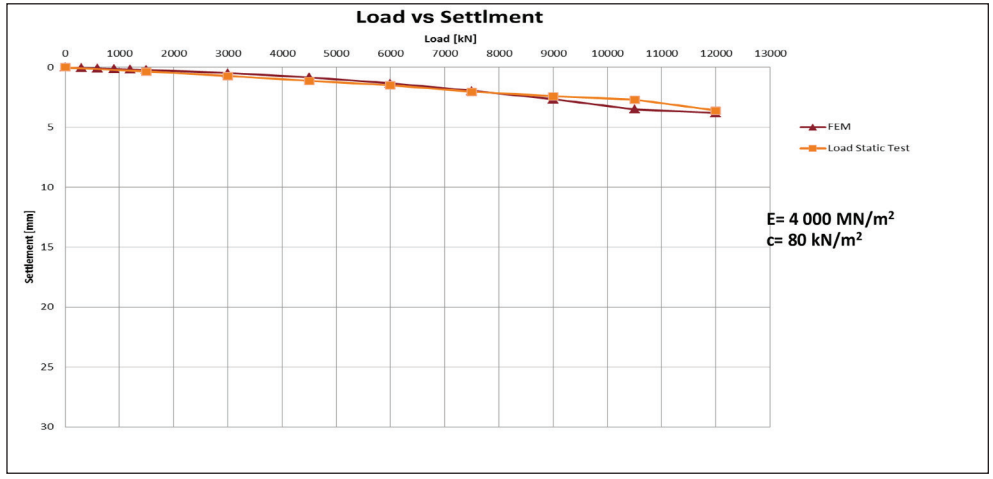

Pile Summary Sheet
P39

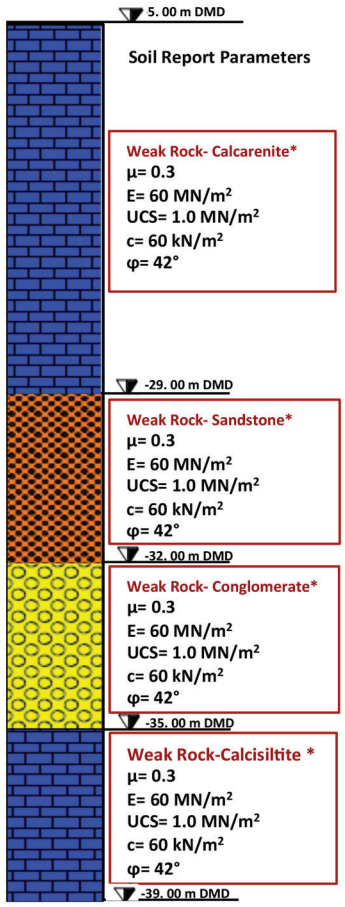

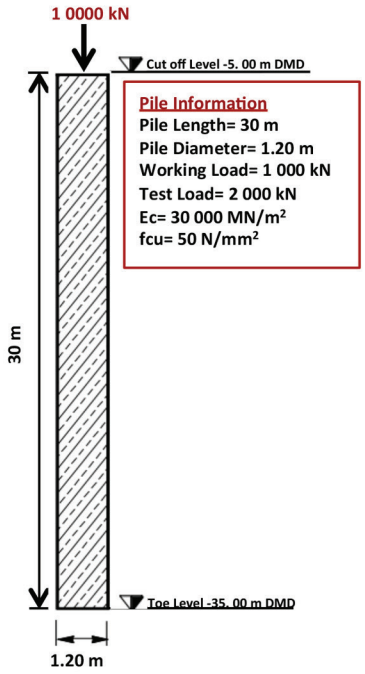

Pile Information
Pile Length= 30 m
Pile Diameter= 1.20 m
Working Load= 1 000 kN
Test Load= 2 000 kN
Ec= 30 000 MN/m²
fcu= 50 N/mm²

Legend

μ = Poisson Ratio	E = Modulus of Elasticity of Soil
Ec= Concrete Modulus	UCS=Unconfined Compressive Strength
c = Cohesion	φ = Angle of Friction
fcu = Concrete Grade	DMD = Dubai Municiplity Dutam

*Average UCS-Value from soil report

Modelling by using Soil Report Parameters

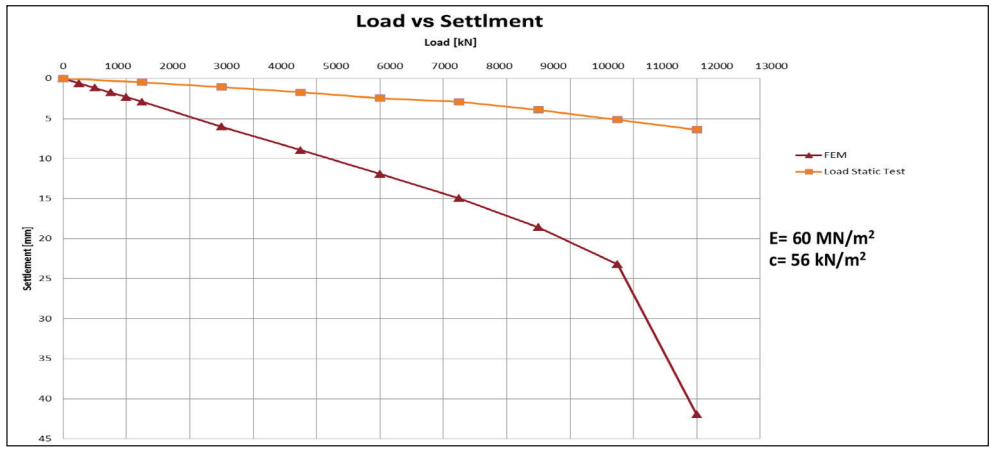

Back-Analysis of Soil Properties from Load Test

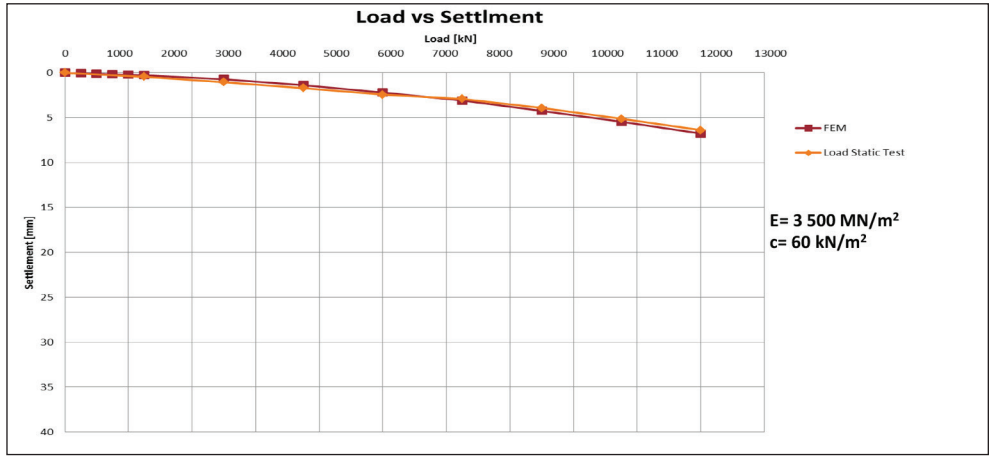

Pile Summary Sheet
P40

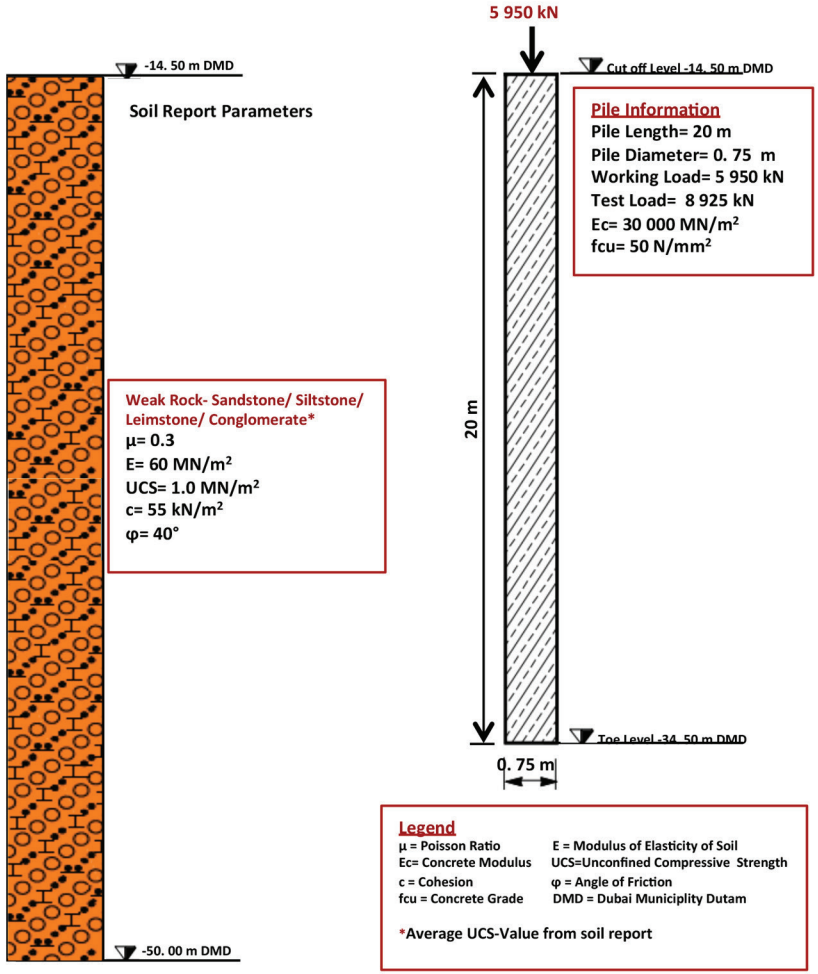

Pile Information
Pile Length= 20 m
Pile Diameter= 0. 75 m
Working Load= 5 950 kN
Test Load= 8 925 kN
Ec= 30 000 MN/m²
fcu= 50 N/mm²

Legend

μ = Poisson Ratio	E = Modulus of Elasticity of Soil
Ec= Concrete Modulus	UCS=Unconfined Compressive Strength
c = Cohesion	φ = Angle of Friction
fcu = Concrete Grade	DMD = Dubai Municiplity Dutam

*Average UCS-Value from soil report

Modelling by using Soil Report Parameters

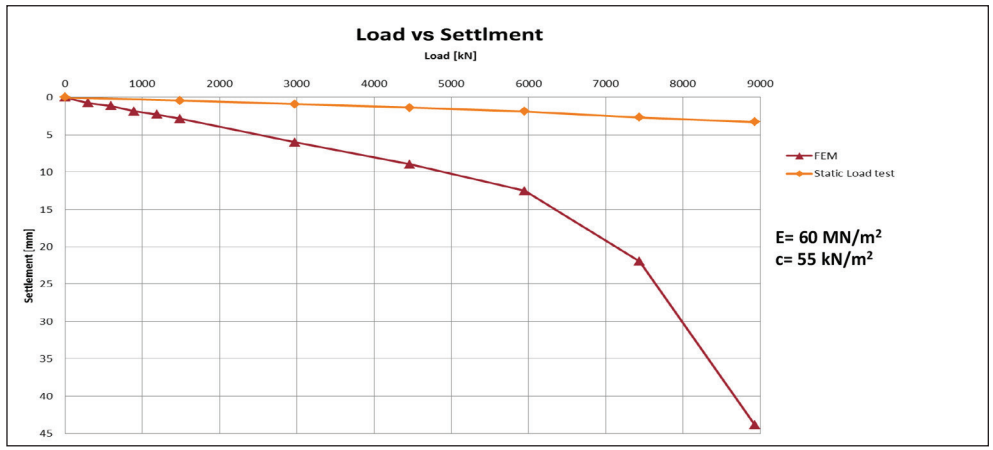

Back-Analysis of Soil Properties from Load Test

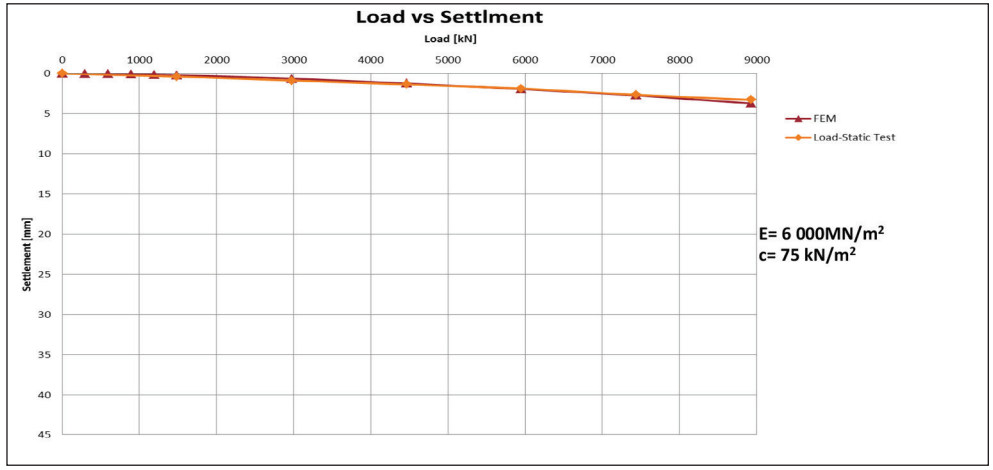

Pile Summary Sheet
P41

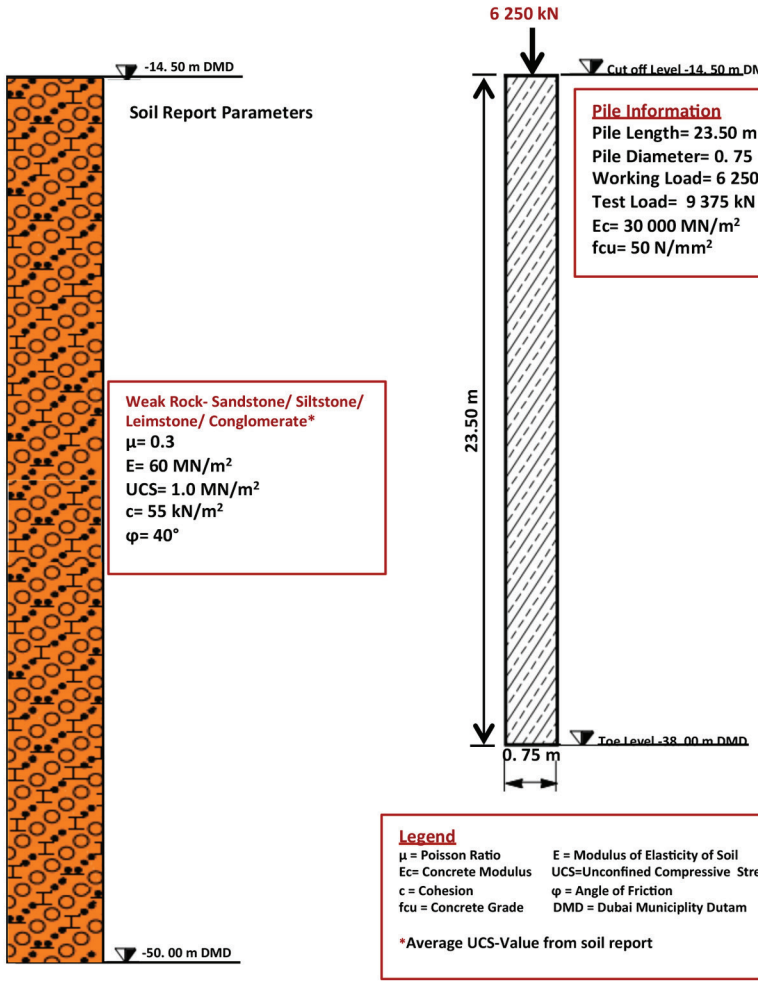

Pile Information
Pile Length= 23.50 m
Pile Diameter= 0. 75 m
Working Load= 6 250 kN
Test Load= 9 375 kN
Ec= 30 000 MN/m²
fcu= 50 N/mm²

Legend

μ = Poisson Ratio	E = Modulus of Elasticity of Soil
Ec= Concrete Modulus	UCS=Unconfined Compressive Strength
c = Cohesion	φ = Angle of Friction
fcu = Concrete Grade	DMD = Dubai Municiplity Dutam

*Average UCS-Value from soil report

Modelling by using Soil Report Parameters

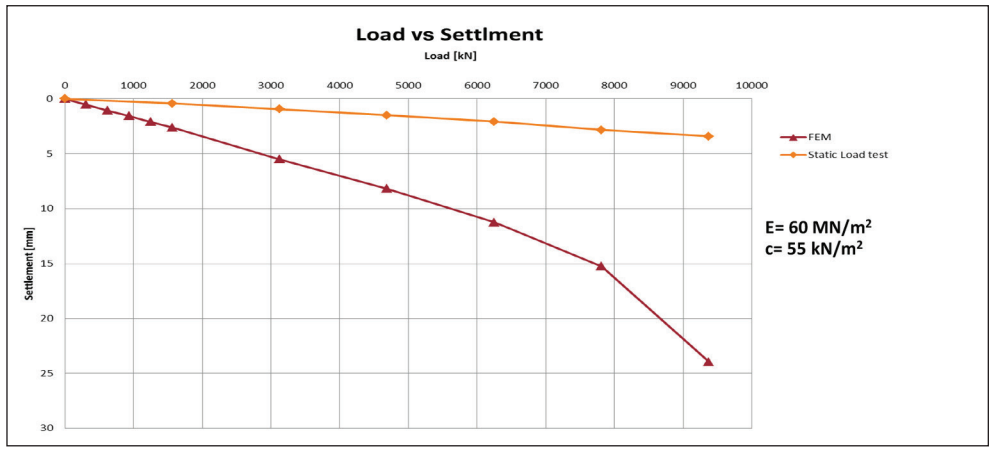

Back-Analysis of Soil Properties from Load Test

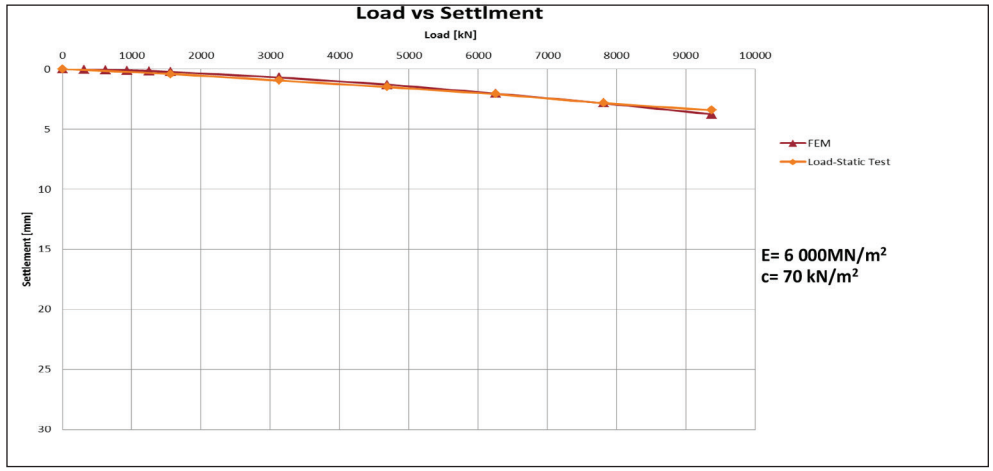

Pile Summary Sheet
P42

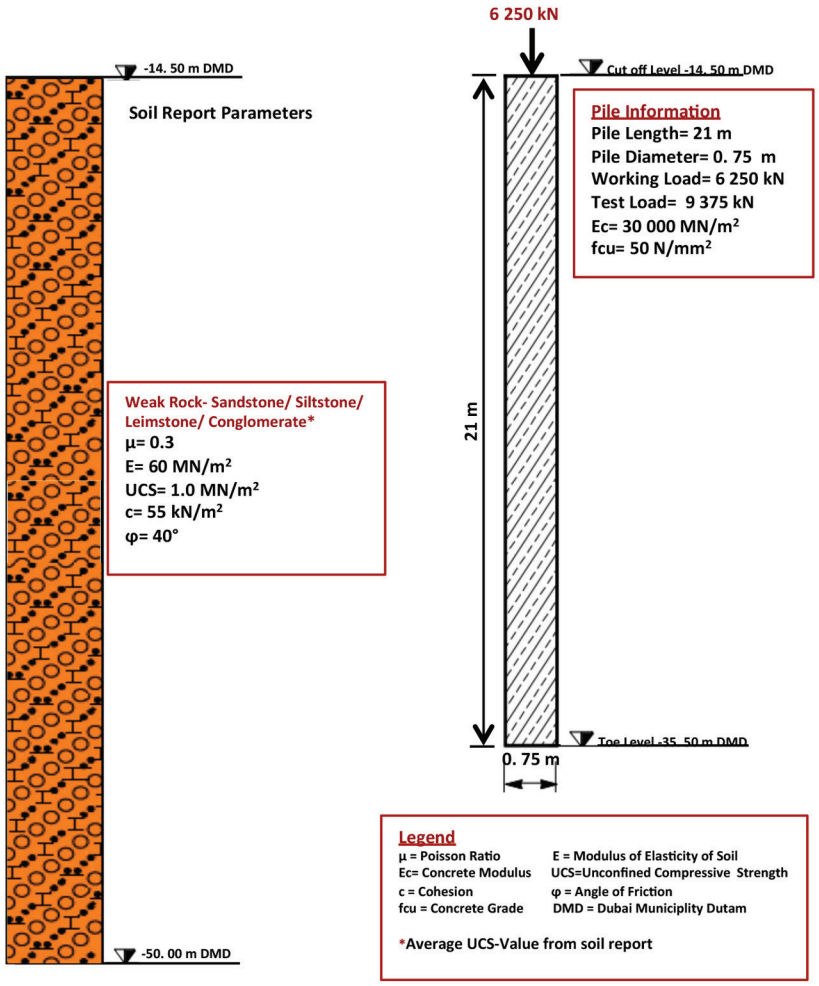

Pile Information
Pile Length= 21 m
Pile Diameter= 0. 75 m
Working Load= 6 250 kN
Test Load= 9 375 kN
Ec= 30 000 MN/m²
fcu= 50 N/mm²

Legend

μ = Poisson Ratio	E = Modulus of Elasticity of Soil
Ec= Concrete Modulus	UCS=Unconfined Compressive Strength
c = Cohesion	φ = Angle of Friction
fcu = Concrete Grade	DMD = Dubai Municiplity Dutam

*Average UCS-Value from soil report

Modelling by using Soil Report Parameters

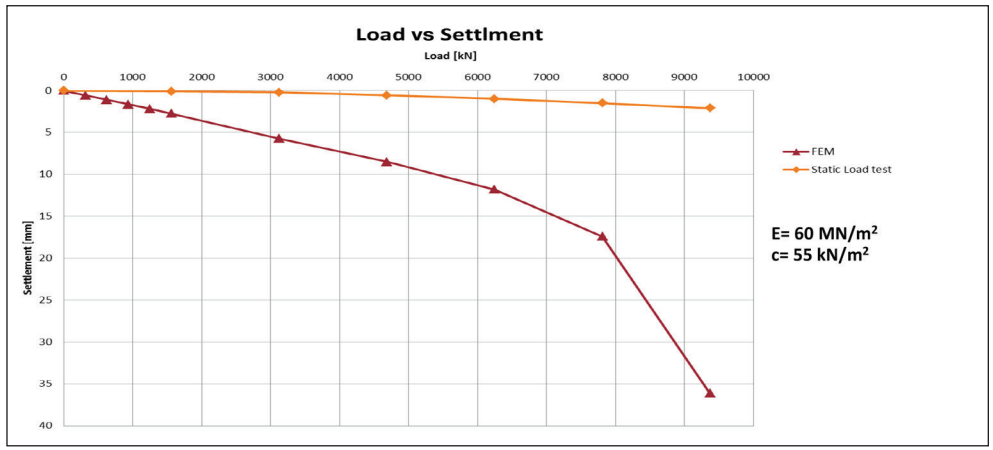

Back-Analysis of Soil Properties from Load Test

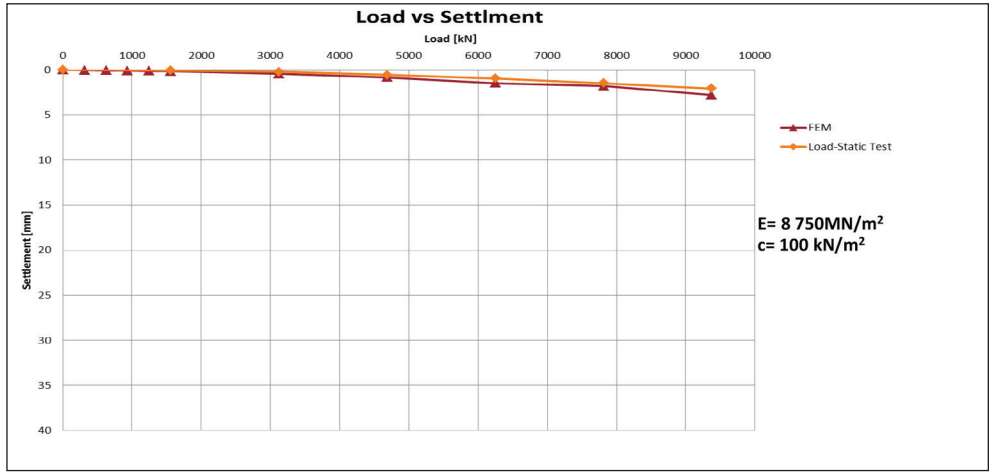

Pile Summary Sheet
P43

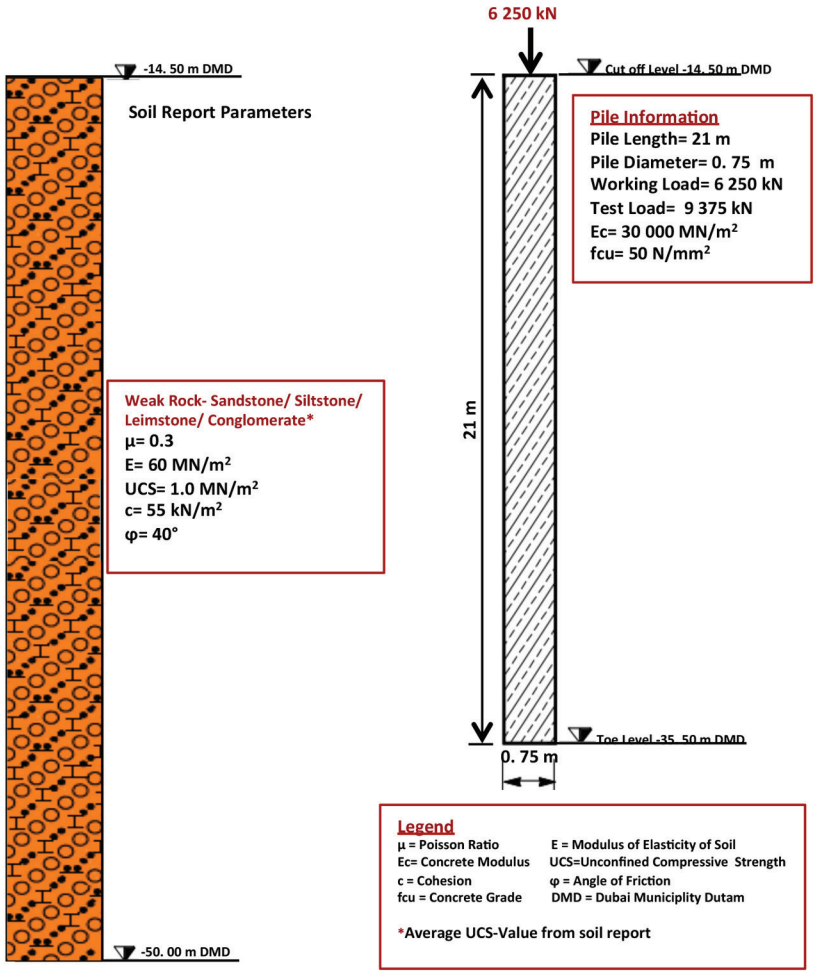

Pile Information
Pile Length= 21 m
Pile Diameter= 0. 75 m
Working Load= 6 250 kN
Test Load= 9 375 kN
Ec= 30 000 MN/m²
fcu= 50 N/mm²

Legend

μ = Poisson Ratio	E = Modulus of Elasticity of Soil
Ec= Concrete Modulus	UCS=Unconfined Compressive Strength
c = Cohesion	φ = Angle of Friction
fcu = Concrete Grade	DMD = Dubai Municiplity Dutam

*Average UCS-Value from soil report

Modelling by using Soil Report Parameters

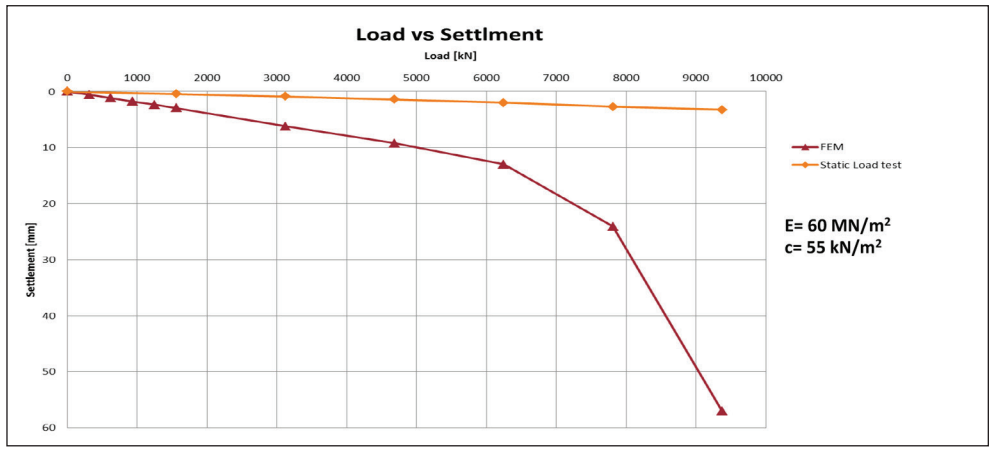

Back-Analysis of Soil Properties from Load Test

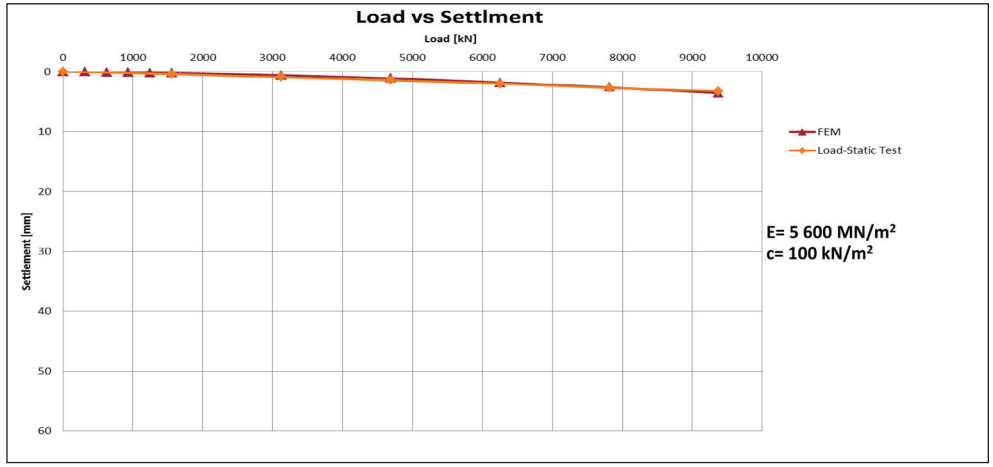

Pile Summary Sheet
P44

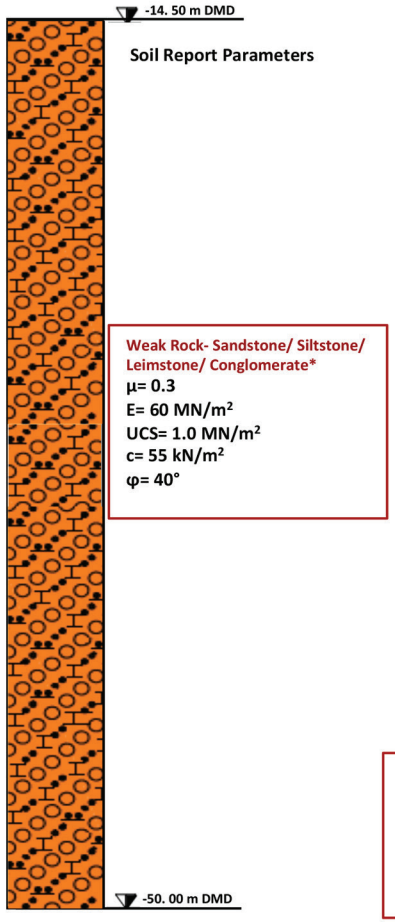

Weak Rock- Sandstone/ Siltstone/ Leimstone/ Conglomerate*
μ= 0.3
E= 60 MN/m²
UCS= 1.0 MN/m²
c= 55 kN/m²
φ= 40°

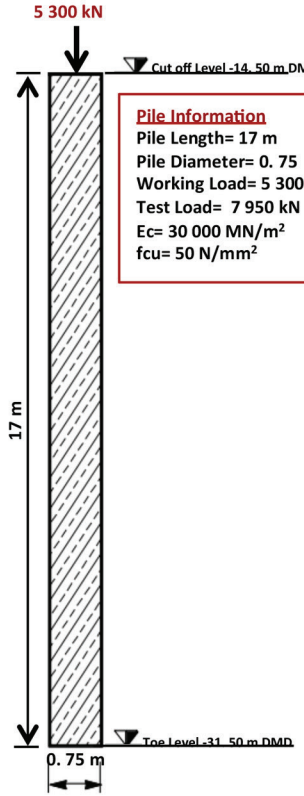

Pile Information
Pile Length= 17 m
Pile Diameter= 0. 75 m
Working Load= 5 300 kN
Test Load= 7 950 kN
Ec= 30 000 MN/m²
fcu= 50 N/mm²

Legend

μ = Poisson Ratio	E = Modulus of Elasticity of Soil
Ec= Concrete Modulus	UCS=Unconfined Compressive Strength
c = Cohesion	φ = Angle of Friction
fcu = Concrete Grade	DMD = Dubai Municiplity Dutam

*Average UCS-Value from soil report

Modelling by using Soil Report Parameters

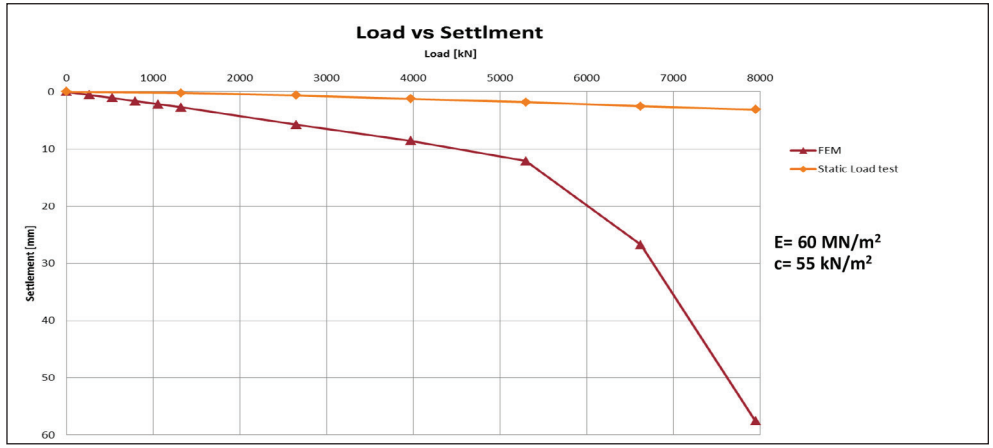

Back-Analysis of Soil Properties from Load Test

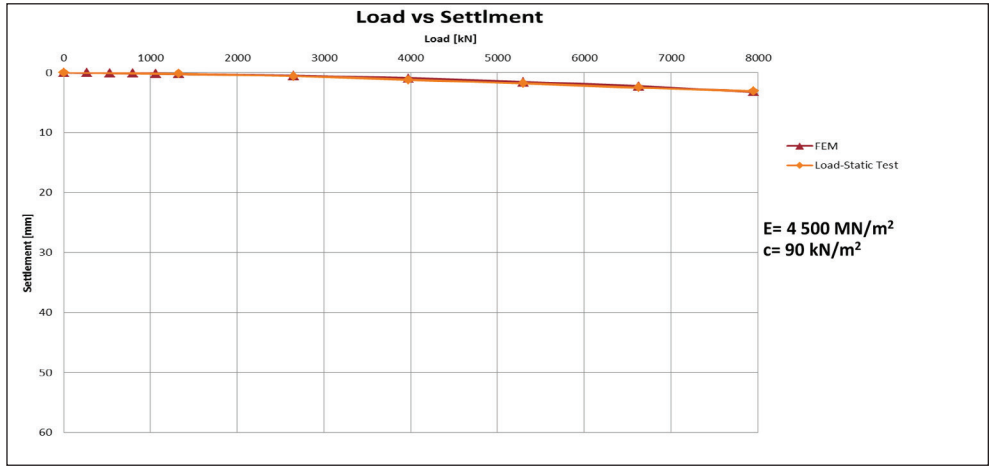

Pile Summary Sheet
P45

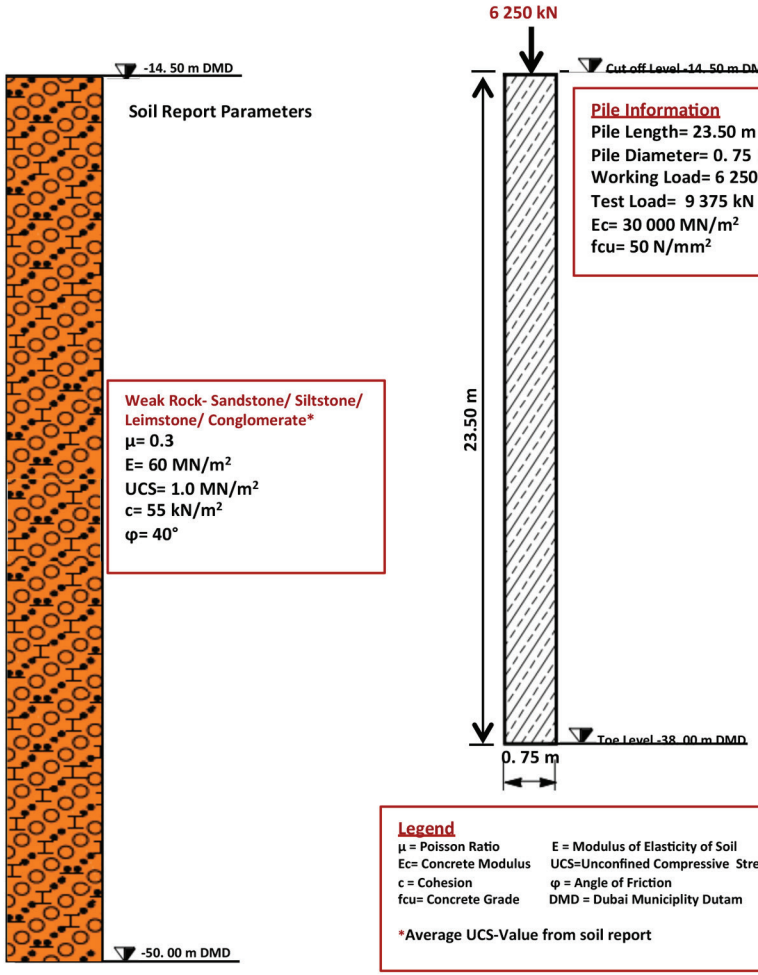

Weak Rock- Sandstone/ Siltstone/ Leimstone/ Conglomerate*
μ= 0.3
E= 60 MN/m²
UCS= 1.0 MN/m²
c= 55 kN/m²
φ= 40°

Pile Information
Pile Length= 23.50 m
Pile Diameter= 0. 75 m
Working Load= 6 250 kN
Test Load= 9 375 kN
Ec= 30 000 MN/m²
fcu= 50 N/mm²

Legend

μ = Poisson Ratio	E = Modulus of Elasticity of Soil
Ec= Concrete Modulus	UCS=Unconfined Compressive Strength
c = Cohesion	φ = Angle of Friction
fcu= Concrete Grade	DMD = Dubai Municiplity Dutam

*Average UCS-Value from soil report

Modelling by using Soil Report Parameters

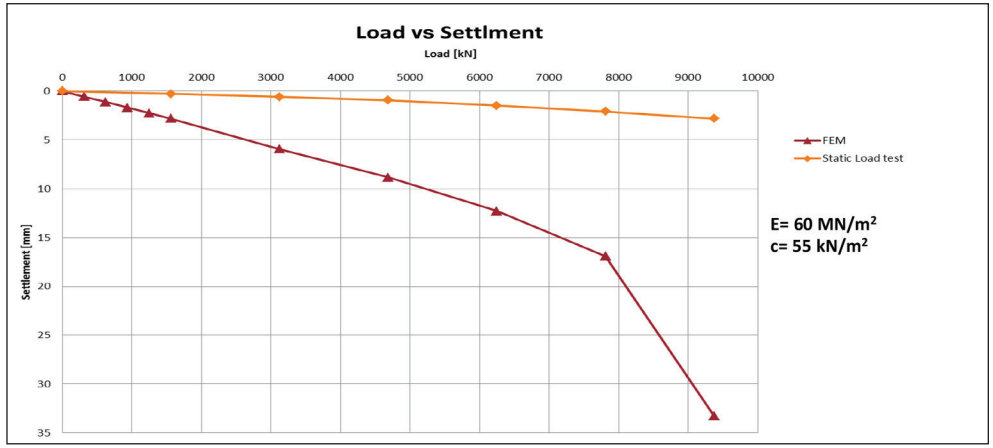

E= 60 MN/m²
c= 55 kN/m²

Back-Analysis of Soil Properties from Load Test

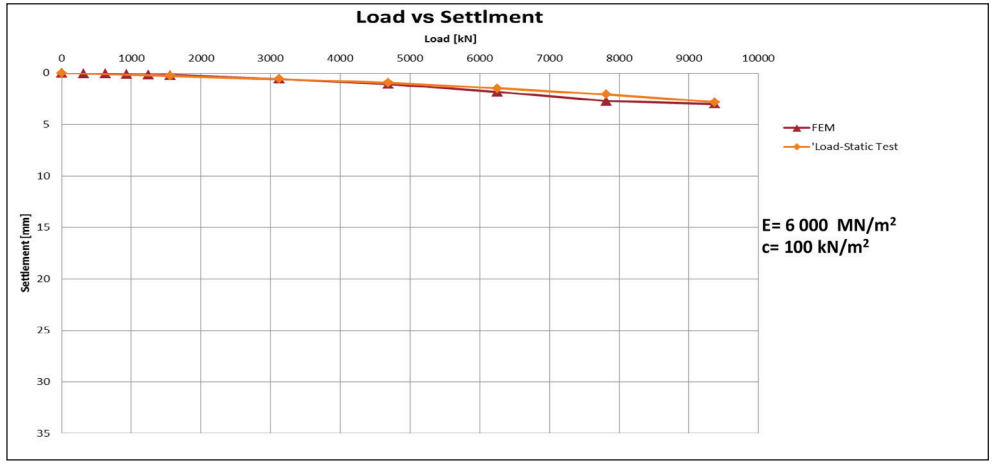

E= 6 000 MN/m²
c= 100 kN/m²

Pile Summary Sheet
P46

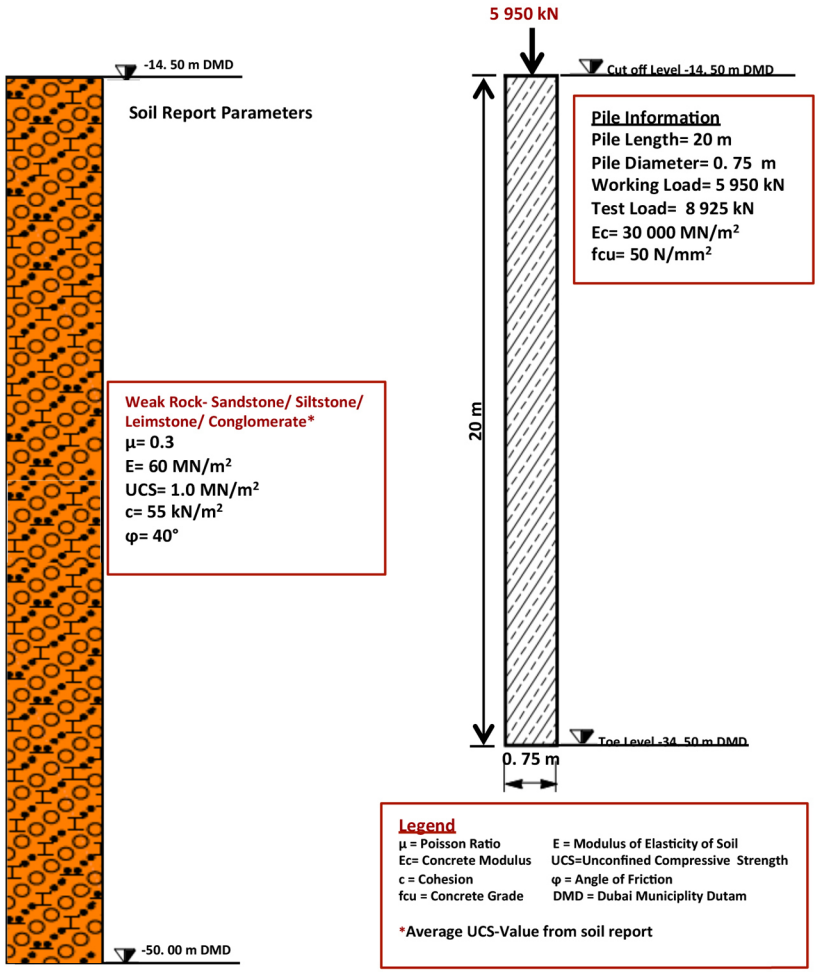

Pile Information
Pile Length= 20 m
Pile Diameter= 0. 75 m
Working Load= 5 950 kN
Test Load= 8 925 kN
Ec= 30 000 MN/m²
fcu= 50 N/mm²

Legend

μ = Poisson Ratio	E = Modulus of Elasticity of Soil
Ec= Concrete Modulus	UCS=Unconfined Compressive Strength
c = Cohesion	φ = Angle of Friction
fcu = Concrete Grade	DMD = Dubai Municiplity Dutam

*Average UCS-Value from soil report

Modelling by using Soil Report Parameters

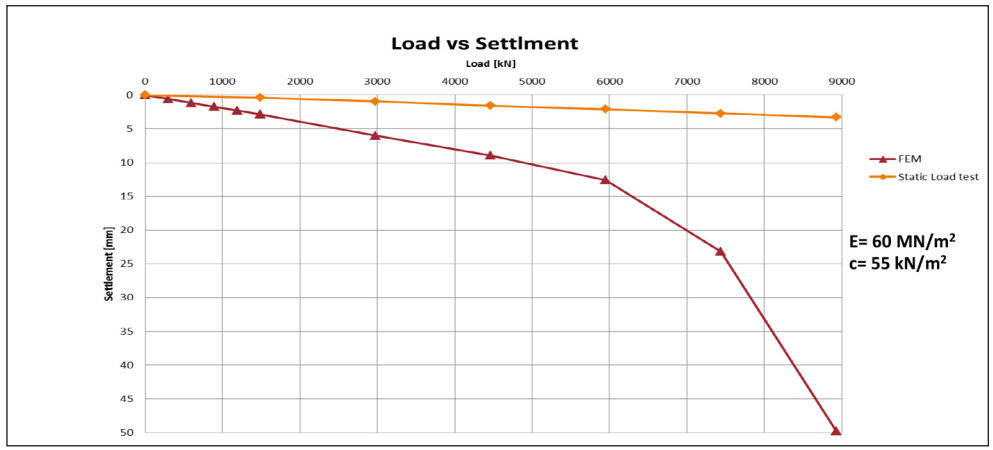

Back-Analysis of Soil Properties from Load Test

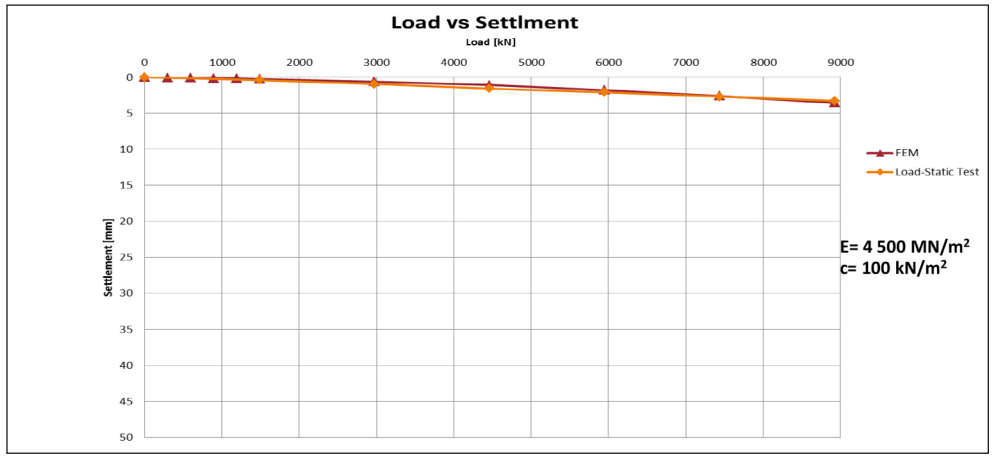

Pile Summary Sheet
P47

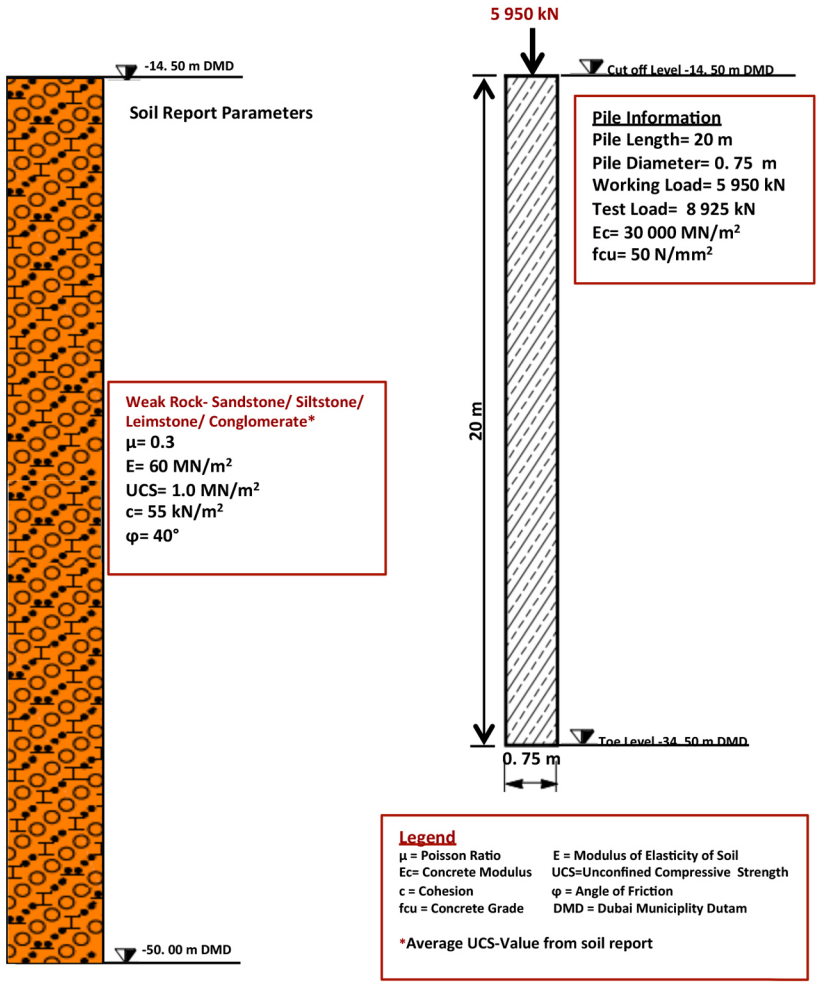

Pile Information
Pile Length= 20 m
Pile Diameter= 0. 75 m
Working Load= 5 950 kN
Test Load= 8 925 kN
Ec= 30 000 MN/m²
fcu= 50 N/mm²

Legend

μ = Poisson Ratio	E = Modulus of Elasticity of Soil
Ec= Concrete Modulus	UCS=Unconfined Compressive Strength
c = Cohesion	φ = Angle of Friction
fcu = Concrete Grade	DMD = Dubai Municiplity Dutam

*Average UCS-Value from soil report

Modelling by using Soil Report Parameters

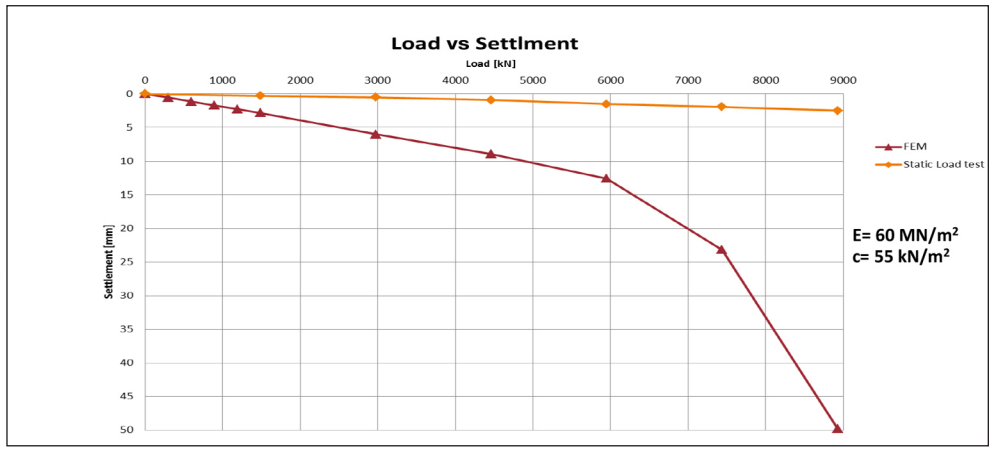

Back-Analysis of Soil Properties from Load Test

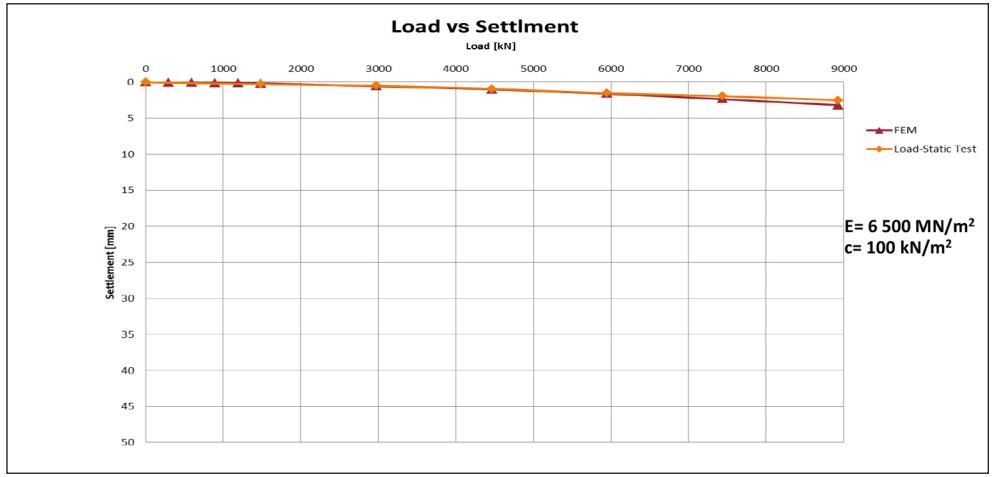

Pile Summary Sheet
P48

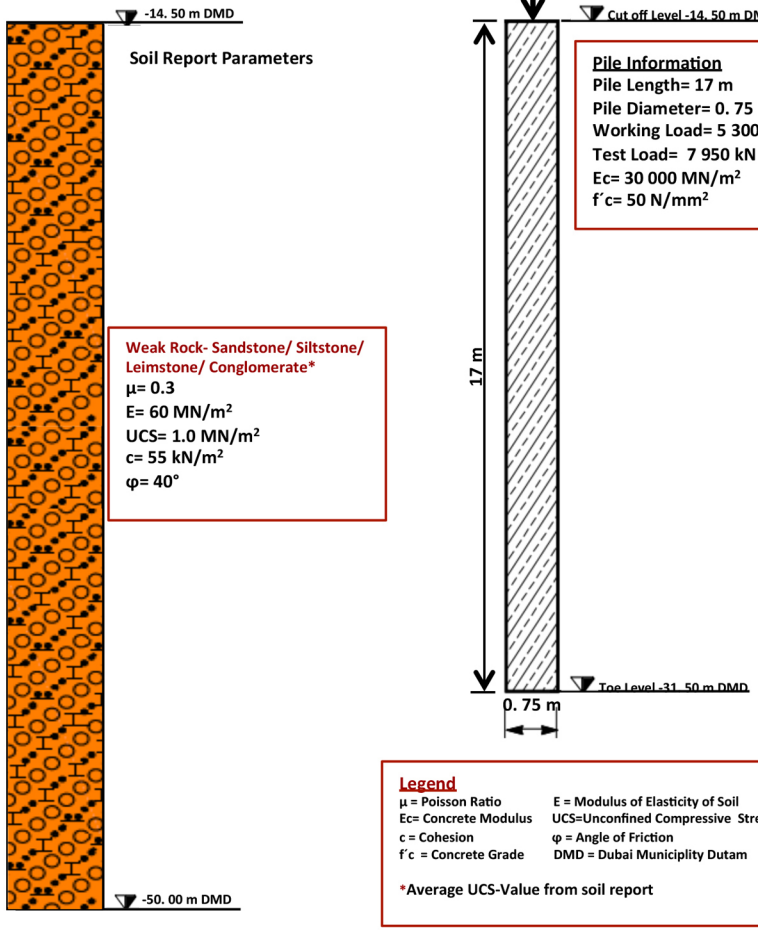

Pile Information
Pile Length= 17 m
Pile Diameter= 0. 75 m
Working Load= 5 300 kN
Test Load= 7 950 kN
Ec= 30 000 MN/m²
f´c= 50 N/mm²

Legend

μ = Poisson Ratio	E = Modulus of Elasticity of Soil
Ec= Concrete Modulus	UCS=Unconfined Compressive Strength
c = Cohesion	φ = Angle of Friction
f´c = Concrete Grade	DMD = Dubai Municiplity Dutam

*Average UCS-Value from soil report

Modelling by using Soil Report Parameters

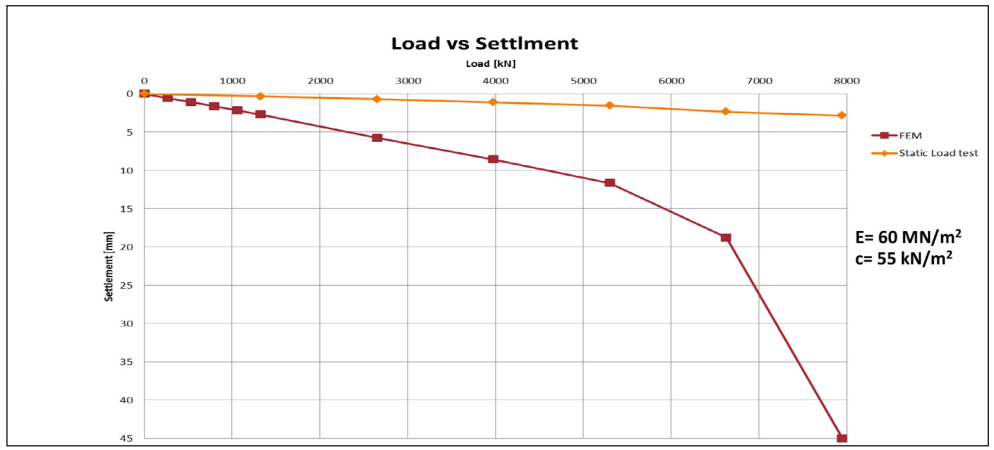

Back-Analysis of Soil Properties from Load Test

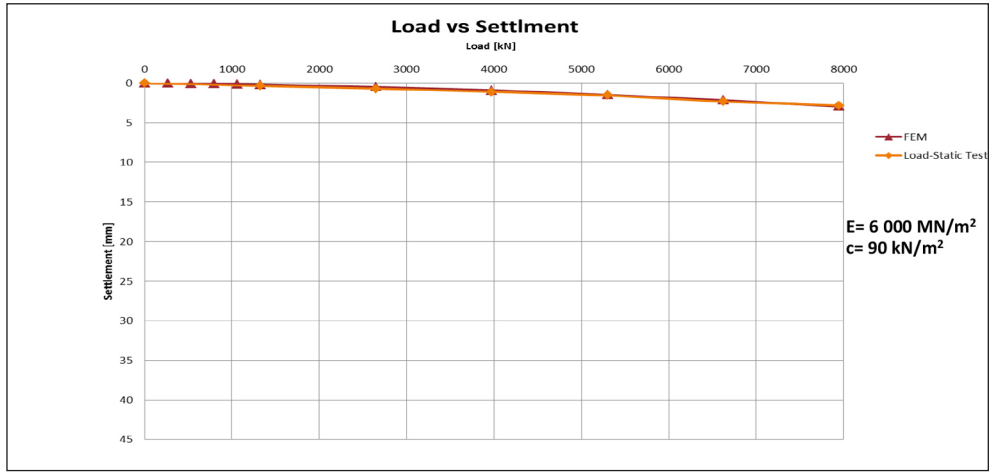

Pile Summary Sheet
P49

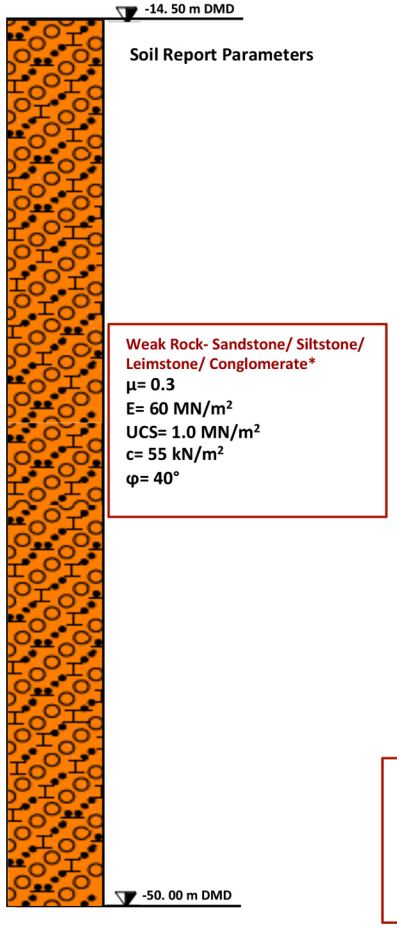

Weak Rock- Sandstone/ Siltstone/ Leimstone/ Conglomerate*
μ= 0.3
E= 60 MN/m²
UCS= 1.0 MN/m²
c= 55 kN/m²
φ= 40°

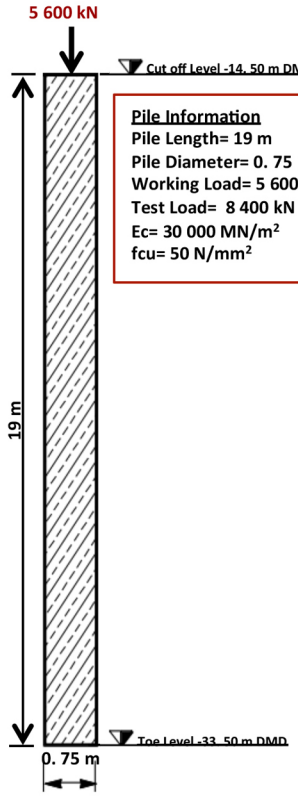

Pile Information
Pile Length= 19 m
Pile Diameter= 0. 75 m
Working Load= 5 600 kN
Test Load= 8 400 kN
Ec= 30 000 MN/m²
fcu= 50 N/mm²

Legend

μ = Poisson Ratio	E = Modulus of Elasticity of Soil
Ec= Concrete Modulus	UCS=Unconfined Compressive Strength
c = Cohesion	φ = Angle of Friction
fcu = Concrete Grade	DMD = Dubai Municiplity Dutam

*Average UCS-Value from soil report

Modelling by using Soil Report Parameters

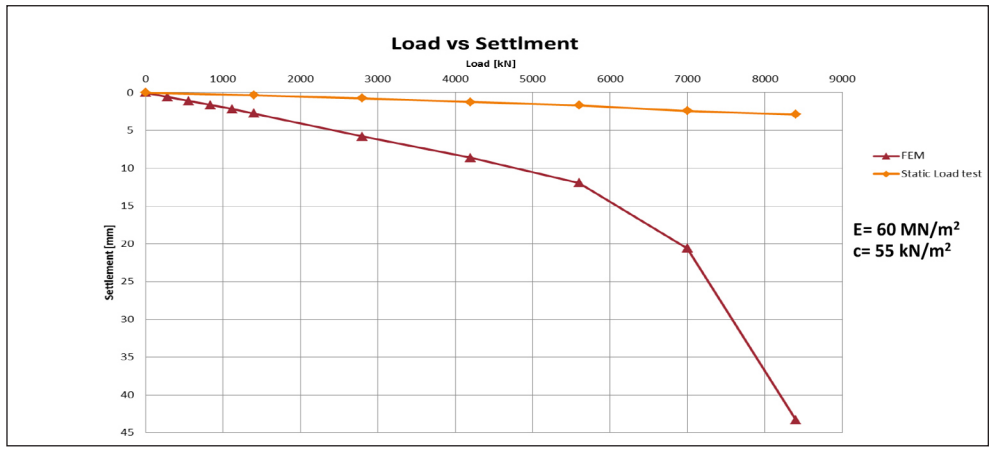

E= 60 MN/m²
c= 55 kN/m²

Back-Analysis of Soil Properties from Load Test

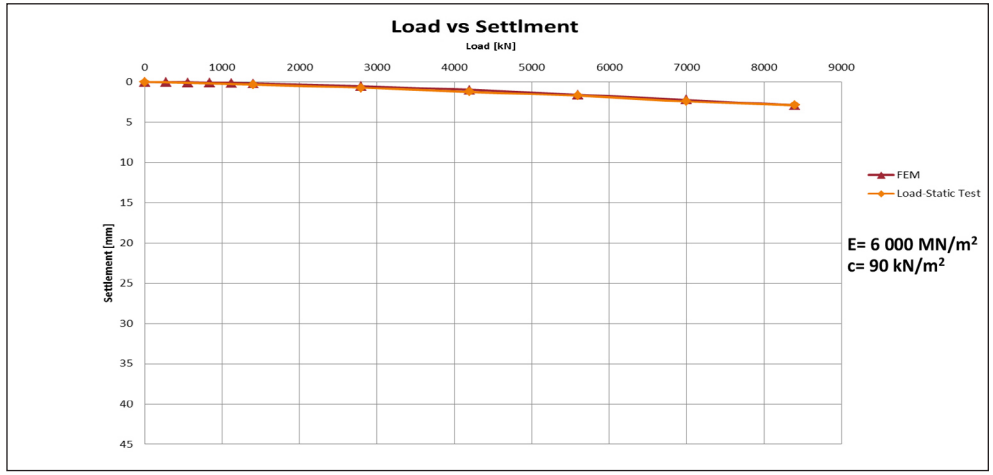

E= 6 000 MN/m²
c= 90 kN/m²

Pile Summary Sheet
P50

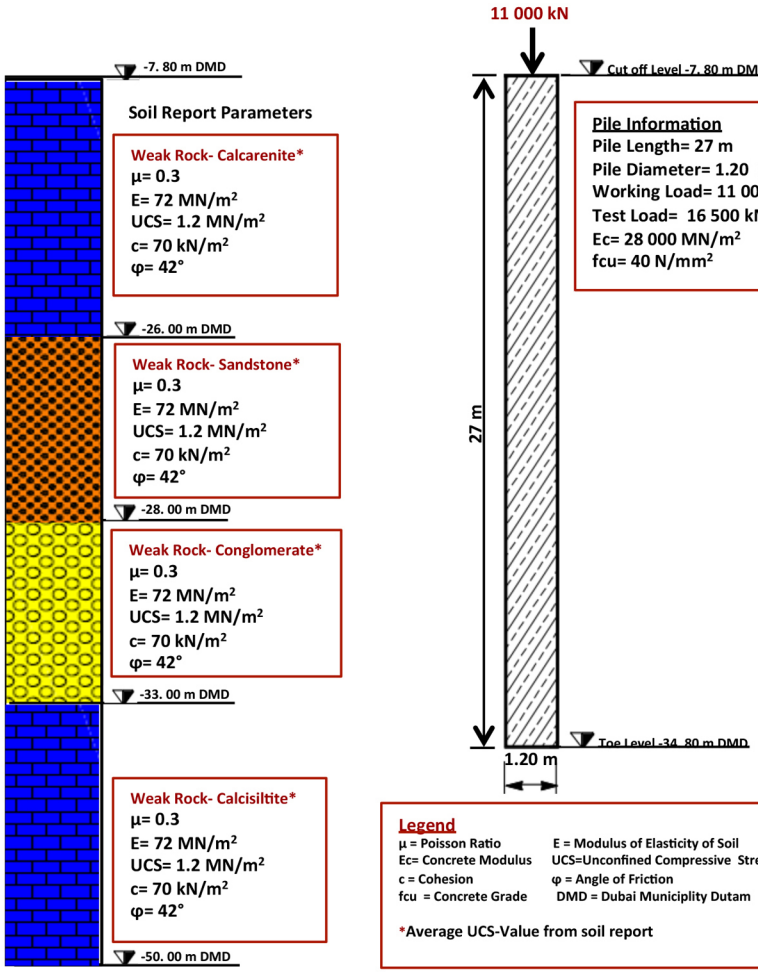

Pile Information
Pile Length= 27 m
Pile Diameter= 1.20 m
Working Load= 11 000 kN
Test Load= 16 500 kN
Ec= 28 000 MN/m²
fcu= 40 N/mm²

Legend

μ = Poisson Ratio	E = Modulus of Elasticity of Soil
Ec= Concrete Modulus	UCS=Unconfined Compressive Strength
c = Cohesion	φ = Angle of Friction
fcu = Concrete Grade	DMD = Dubai Municiplity Dutam

*Average UCS-Value from soil report

Modelling by using Soil Report Parameters

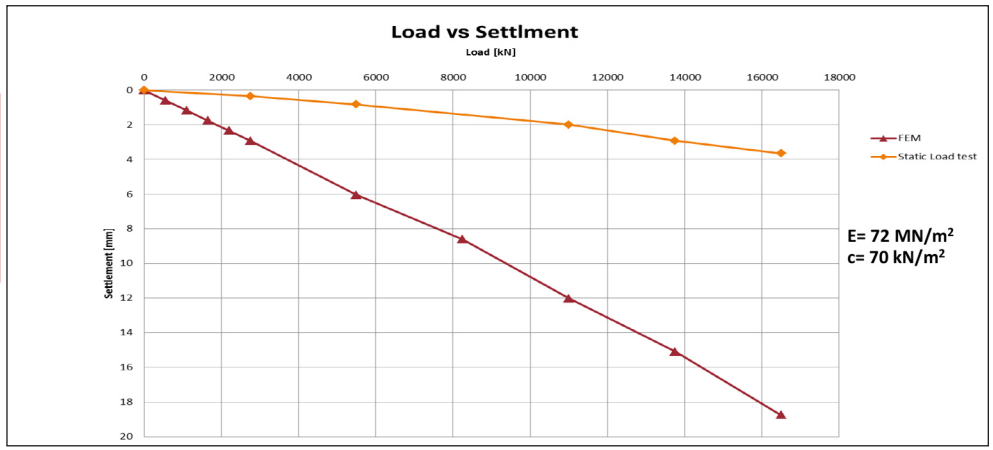

Back-Analysis of Soil Properties from Load Test

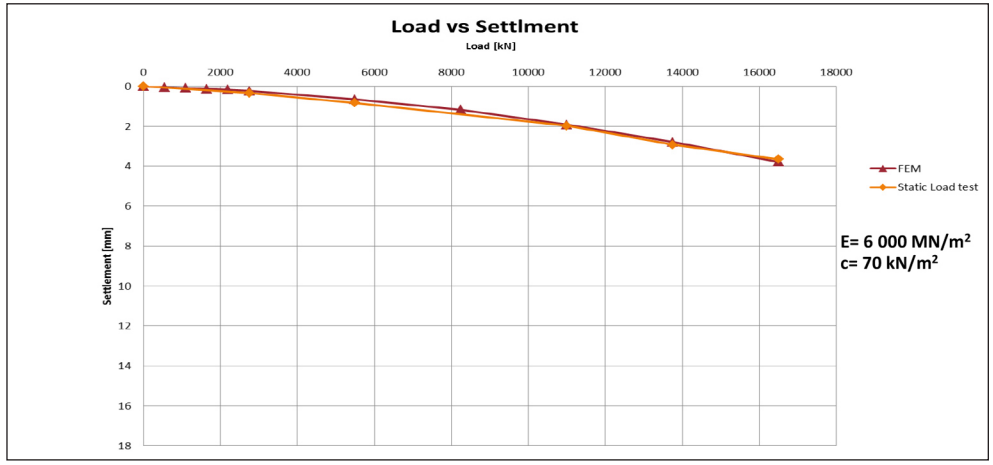

Pile Summary Sheet
P51

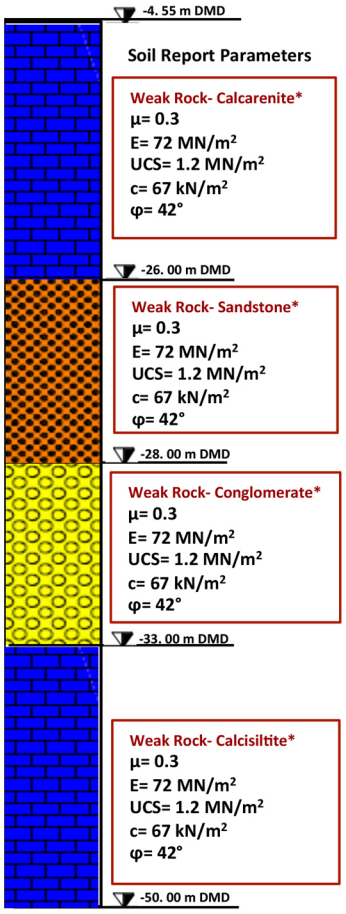

Soil Report Parameters

Weak Rock- Calcarenite*
μ= 0.3
E= 72 MN/m²
UCS= 1.2 MN/m²
c= 67 kN/m²
φ= 42°

Weak Rock- Sandstone*
μ= 0.3
E= 72 MN/m²
UCS= 1.2 MN/m²
c= 67 kN/m²
φ= 42°

Weak Rock- Conglomerate*
μ= 0.3
E= 72 MN/m²
UCS= 1.2 MN/m²
c= 67 kN/m²
φ= 42°

Weak Rock- Calcisiltite*
μ= 0.3
E= 72 MN/m²
UCS= 1.2 MN/m²
c= 67 kN/m²
φ= 42°

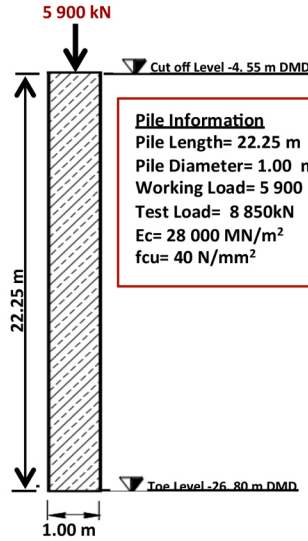

Pile Information
Pile Length= 22.25 m
Pile Diameter= 1.00 m
Working Load= 5 900 kN
Test Load= 8 850kN
Ec= 28 000 MN/m²
fcu= 40 N/mm²

Legend
μ = Poisson Ratio
E = Modulus of Elasticity of Soil
Ec= Concrete Modulus
UCS=Unconfined Compressive Strength
c = Cohesion
φ = Angle of Friction
fcu = Concrete Grade
DMD = Dubai Municiplity Dutam

*Average UCS-Value from soil report

Modelling by using Soil Report Parameters

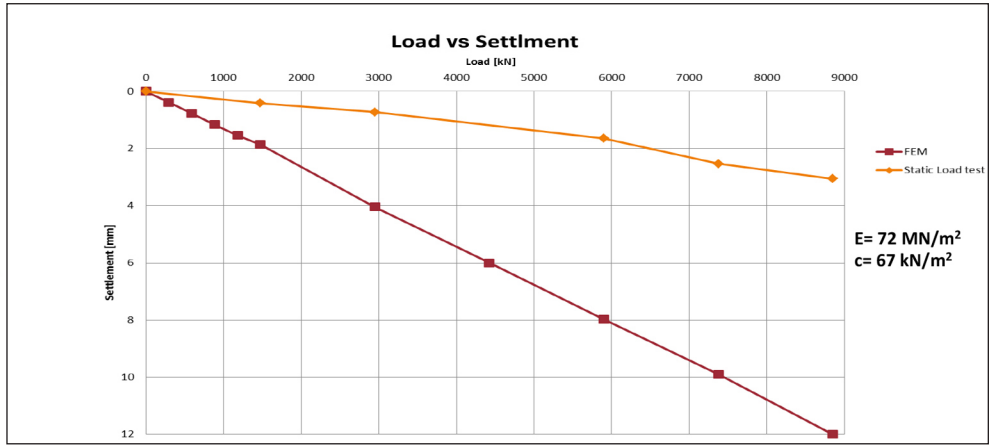

Back-Analysis of Soil Properties from Load Test

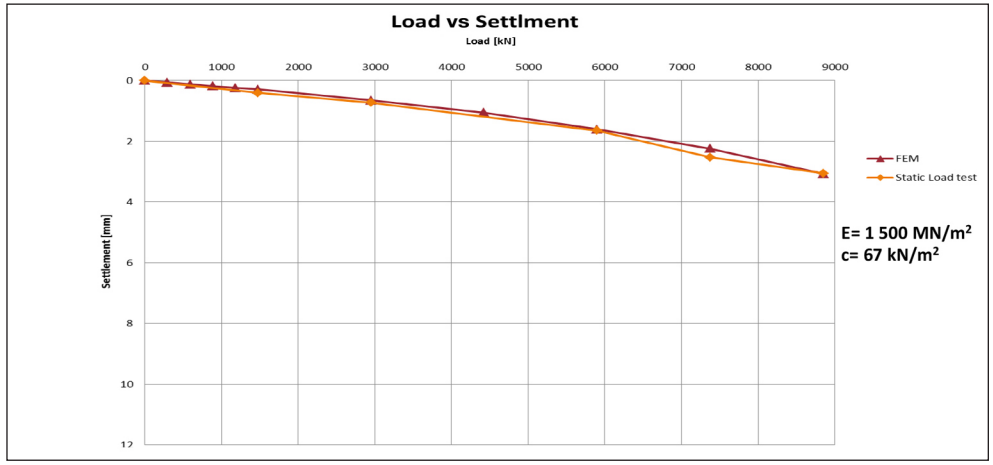

Pile Summary Sheet
P52

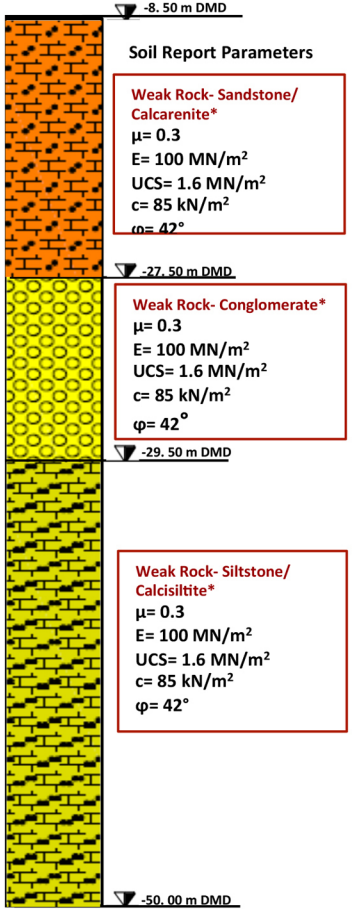

Soil Report Parameters

Weak Rock- Sandstone/ Calcarenite*
μ= 0.3
E= 100 MN/m²
UCS= 1.6 MN/m²
c= 85 kN/m²
φ= 42°

Weak Rock- Conglomerate*
μ= 0.3
E= 100 MN/m²
UCS= 1.6 MN/m²
c= 85 kN/m²
φ= 42°

Weak Rock- Siltstone/ Calcisiltite*
μ= 0.3
E= 100 MN/m²
UCS= 1.6 MN/m²
c= 85 kN/m²
φ= 42°

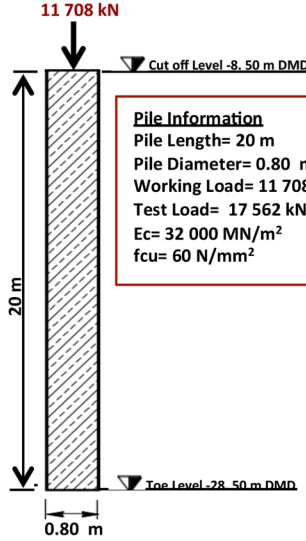

Pile Information
Pile Length= 20 m
Pile Diameter= 0.80 m
Working Load= 11 708 kN
Test Load= 17 562 kN
Ec= 32 000 MN/m²
fcu= 60 N/mm²

Legend

μ = Poisson Ratio	E = Modulus of Elasticity of Soil
Ec= Concrete Modulus	UCS=Unconfined Compressive Strength
c = Cohesion	φ = Angle of Friction
fcu = Concrete Grade	DMD = Dubai Municiplity Dutam

*Average UCS-Value from soil report

Modelling by using Soil Report Parameters

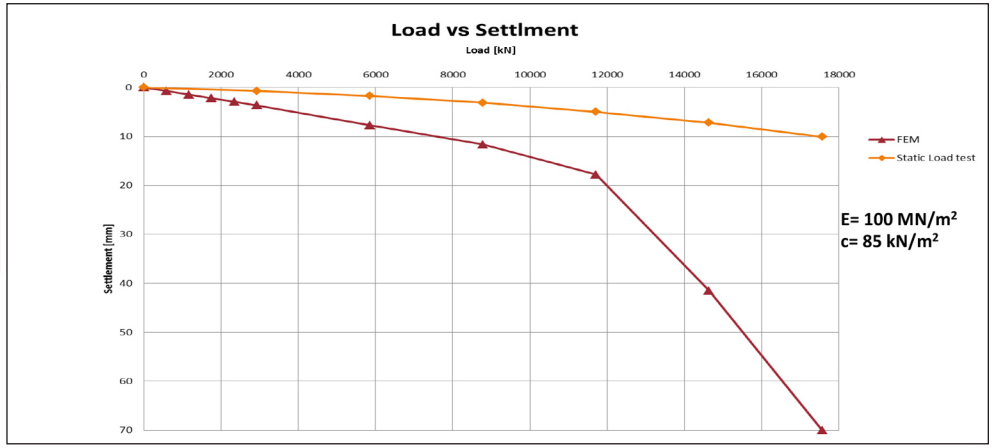

Back-Analysis of Soil Properties from Load Test

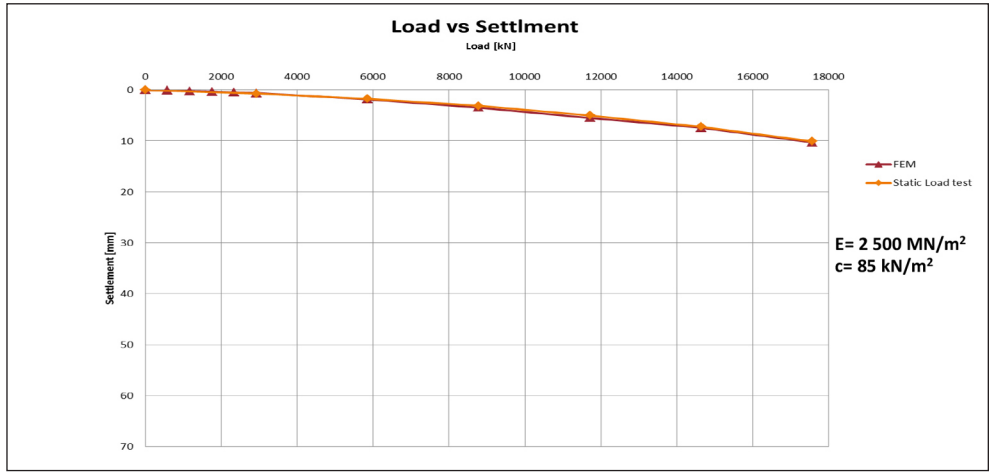

Pile Summary Sheet
P53

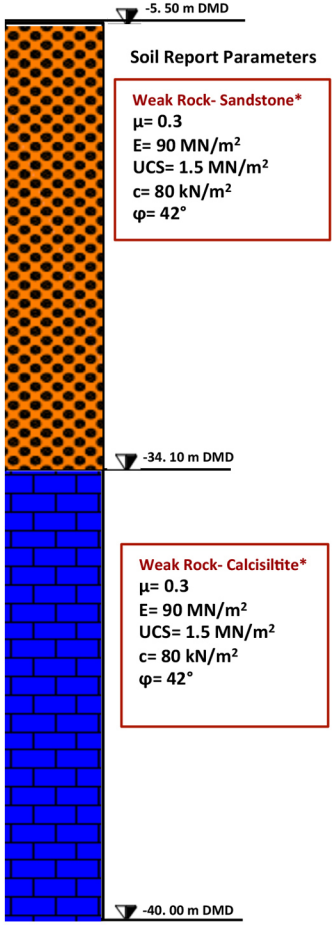

Soil Report Parameters

Weak Rock- Sandstone*
μ= 0.3
E= 90 MN/m²
UCS= 1.5 MN/m²
c= 80 kN/m²
φ= 42°

Weak Rock- Calcisiltite*
μ= 0.3
E= 90 MN/m²
UCS= 1.5 MN/m²
c= 80 kN/m²
φ= 42°

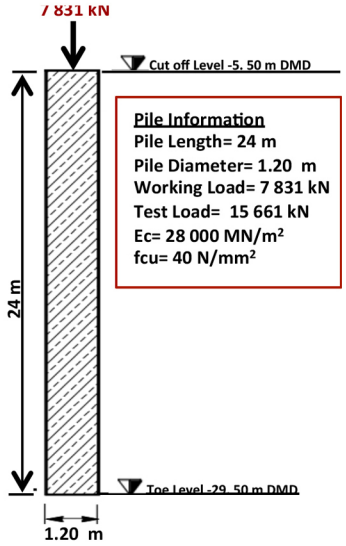

Pile Information
Pile Length= 24 m
Pile Diameter= 1.20 m
Working Load= 7 831 kN
Test Load= 15 661 kN
Ec= 28 000 MN/m²
fcu= 40 N/mm²

Legend

μ = Poisson Ratio	E = Modulus of Elasticity of Soil
Ec= Concrete Modulus	UCS=Unconfined Compressive Strength
c = Cohesion	φ = Angle of Friction
fcu = Concrete Grade	DMD = Dubai Municiplity Dutam

*Average UCS-Value from soil report

Modelling by using Soil Report Parameters

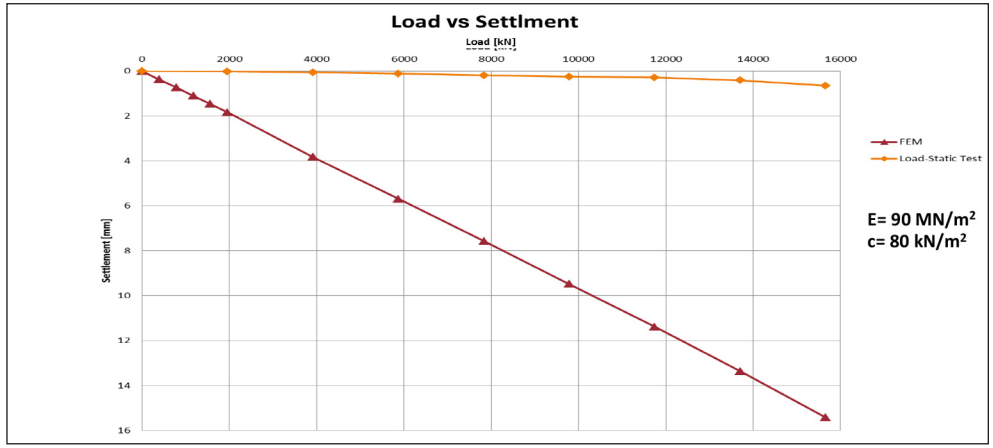

E= 90 MN/m²
c= 80 kN/m²

Back-Analysis of Soil Properties from Load Test

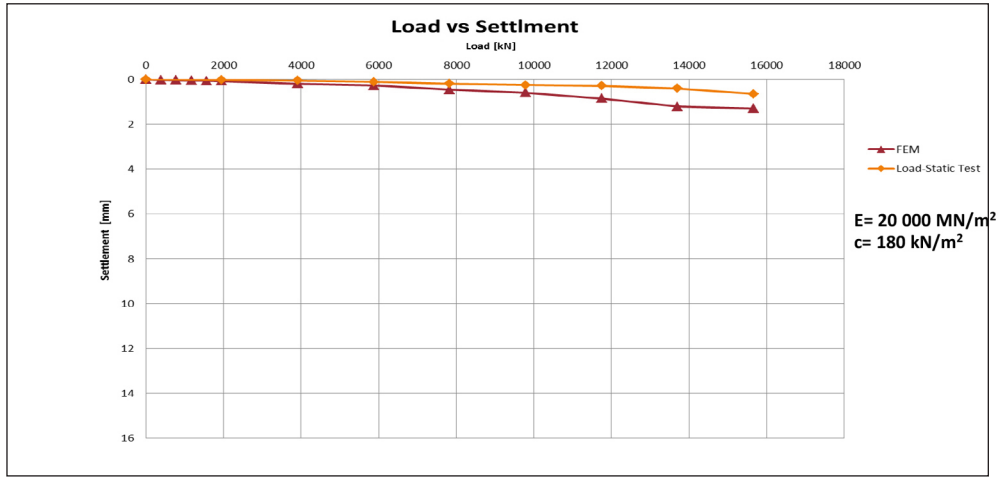

E= 20 000 MN/m²
c= 180 kN/m²

Pile Summary Sheet
P54

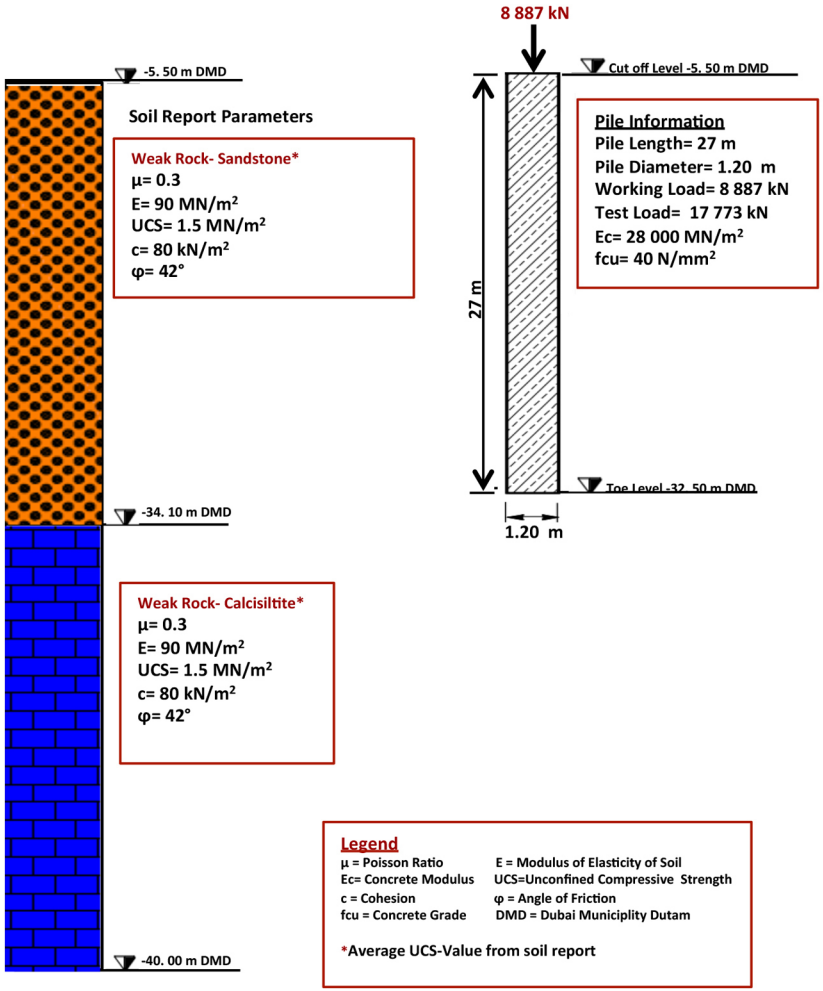

Soil Report Parameters

Weak Rock- Sandstone*
μ= 0.3
E= 90 MN/m²
UCS= 1.5 MN/m²
c= 80 kN/m²
φ= 42°

Weak Rock- Calcisiltite*
μ= 0.3
E= 90 MN/m²
UCS= 1.5 MN/m²
c= 80 kN/m²
φ= 42°

Pile Information
Pile Length= 27 m
Pile Diameter= 1.20 m
Working Load= 8 887 kN
Test Load= 17 773 kN
Ec= 28 000 MN/m²
fcu= 40 N/mm²

Legend
μ = Poisson Ratio
E = Modulus of Elasticity of Soil
Ec= Concrete Modulus
UCS=Unconfined Compressive Strength
c = Cohesion
φ = Angle of Friction
fcu = Concrete Grade
DMD = Dubai Municiplity Dutam

*Average UCS-Value from soil report

Modelling by using Soil Report Parameters

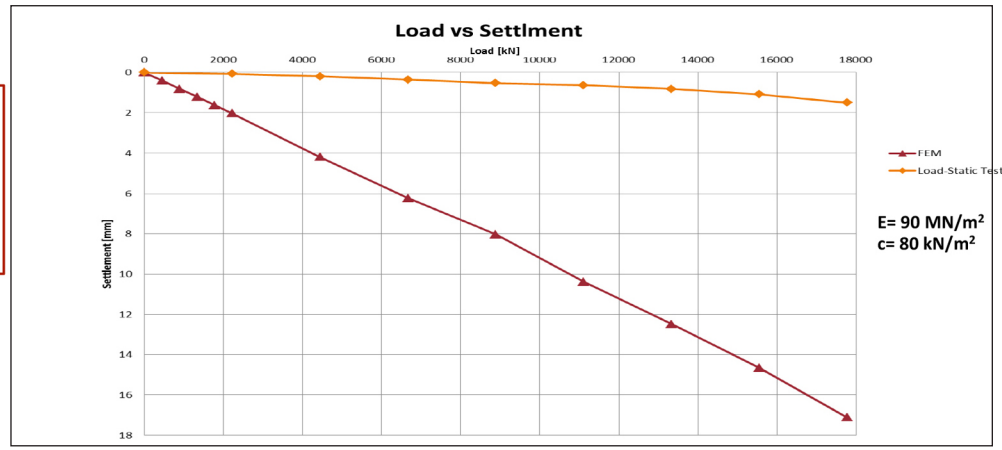

E= 90 MN/m²
c= 80 kN/m²

Back-Analysis of Soil Properties from Load Test

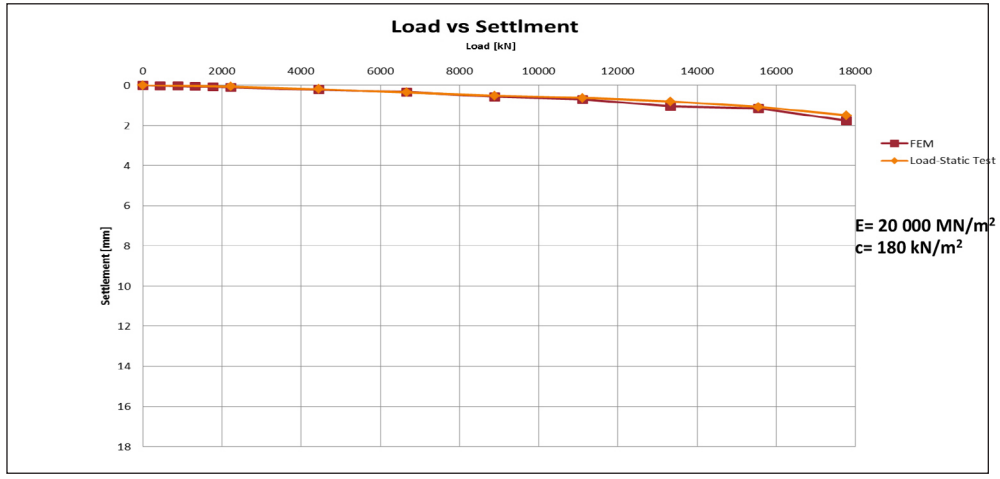

E= 20 000 MN/m²
c= 180 kN/m²

Pile Summary Sheet
P55

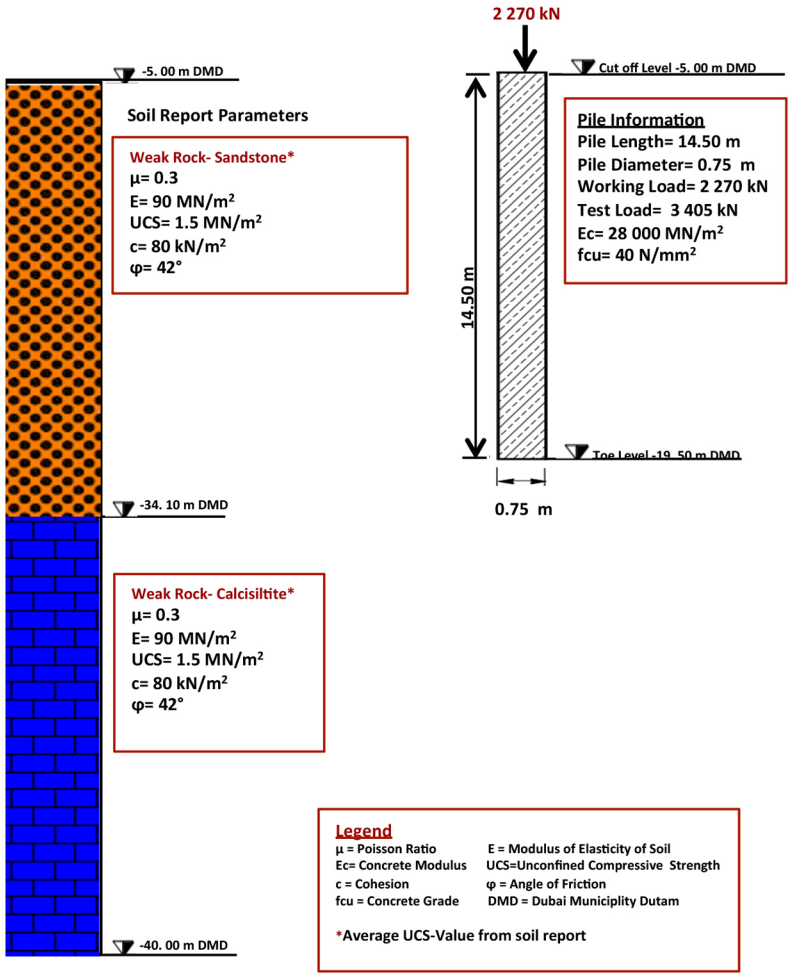

Soil Report Parameters

Weak Rock- Sandstone*
μ= 0.3
E= 90 MN/m²
UCS= 1.5 MN/m²
c= 80 kN/m²
φ= 42°

Pile Information
Pile Length= 14.50 m
Pile Diameter= 0.75 m
Working Load= 2 270 kN
Test Load= 3 405 kN
Ec= 28 000 MN/m²
fcu= 40 N/mm²

Weak Rock- Calcisiltite*
μ= 0.3
E= 90 MN/m²
UCS= 1.5 MN/m²
c= 80 kN/m²
φ= 42°

Legend

μ = Poisson Ratio	E = Modulus of Elasticity of Soil
Ec= Concrete Modulus	UCS=Unconfined Compressive Strength
c = Cohesion	φ = Angle of Friction
fcu = Concrete Grade	DMD = Dubai Municiplity Dutam

*Average UCS-Value from soil report

Modelling by using Soil Report Parameters

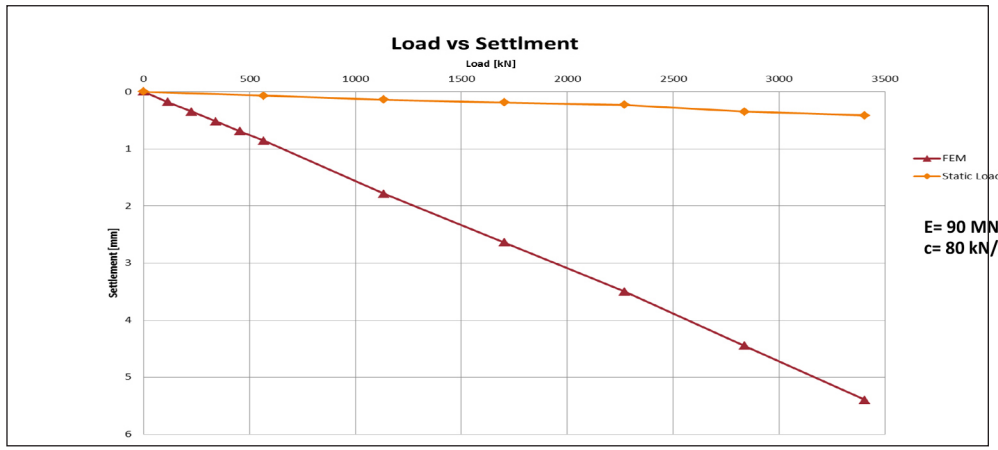

E= 90 MN/m²
c= 80 kN/m²

Back-Analysis of Soil Properties from Load Test

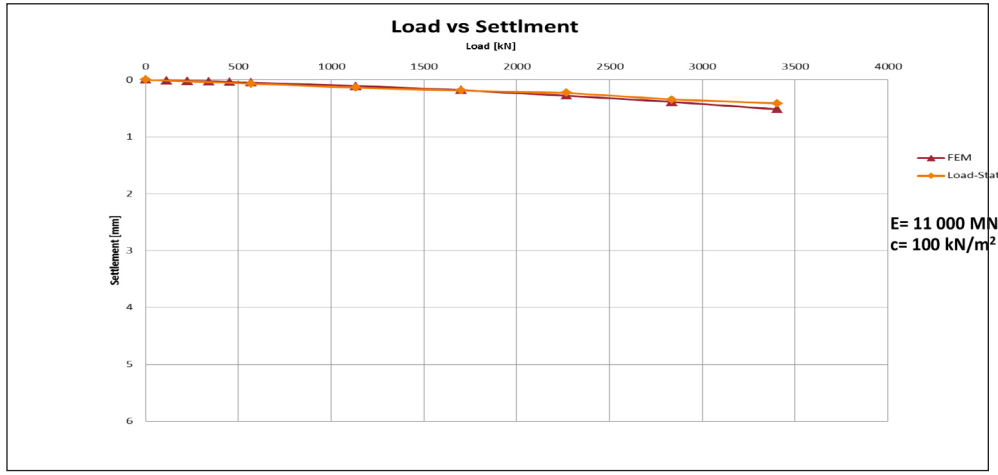

E= 11 000 MN/m²
c= 100 kN/m²

Pile Summary Sheet
P56

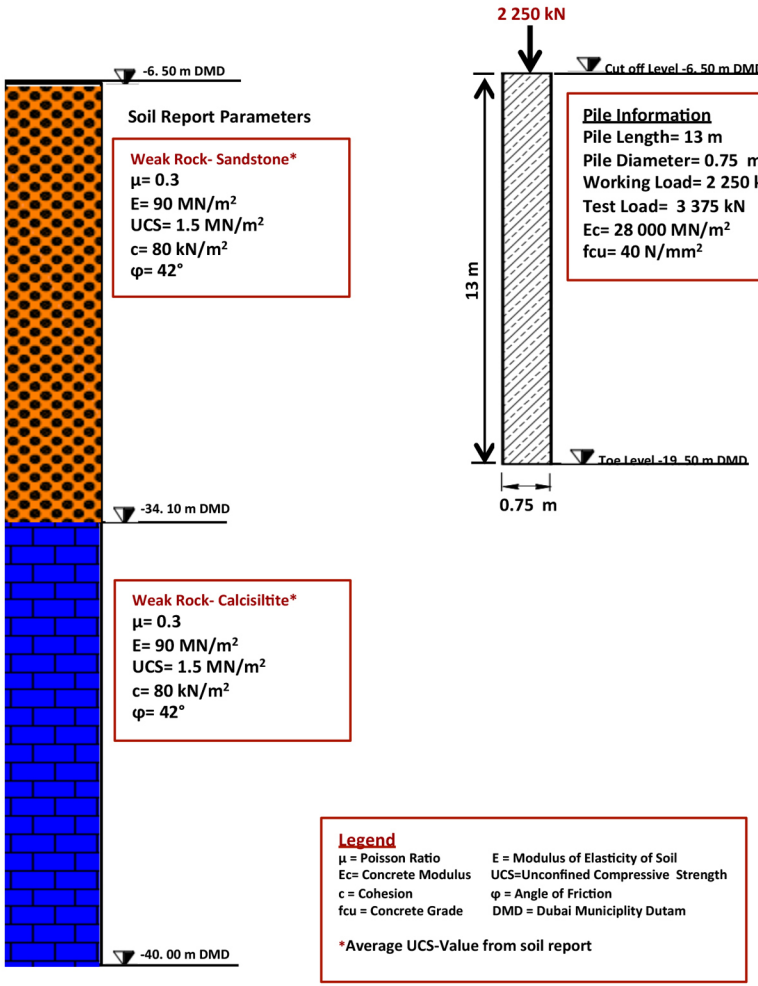

Pile Information
Pile Length= 13 m
Pile Diameter= 0.75 m
Working Load= 2 250 kN
Test Load= 3 375 kN
Ec= 28 000 MN/m²
fcu= 40 N/mm²

Legend

μ = Poisson Ratio	E = Modulus of Elasticity of Soil
Ec= Concrete Modulus	UCS=Unconfined Compressive Strength
c = Cohesion	φ = Angle of Friction
fcu = Concrete Grade	DMD = Dubai Municiplity Dutam

*Average UCS-Value from soil report

Modelling by using Soil Report Parameters

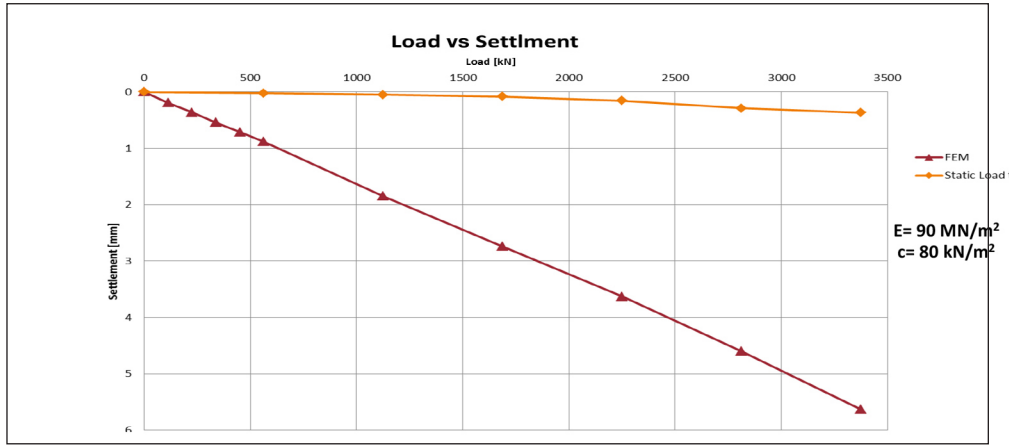

Back-Analysis of Soil Properties from Load Test

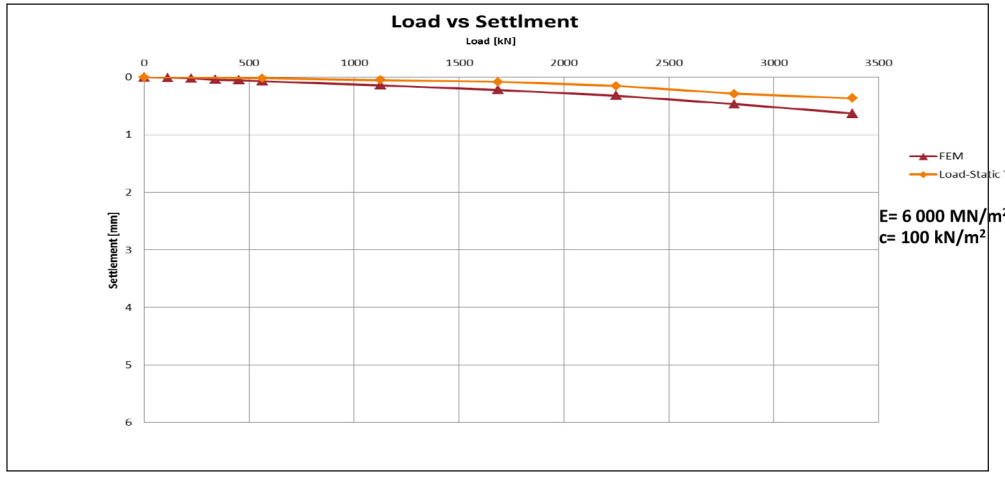

Pile Summary Sheet
P57

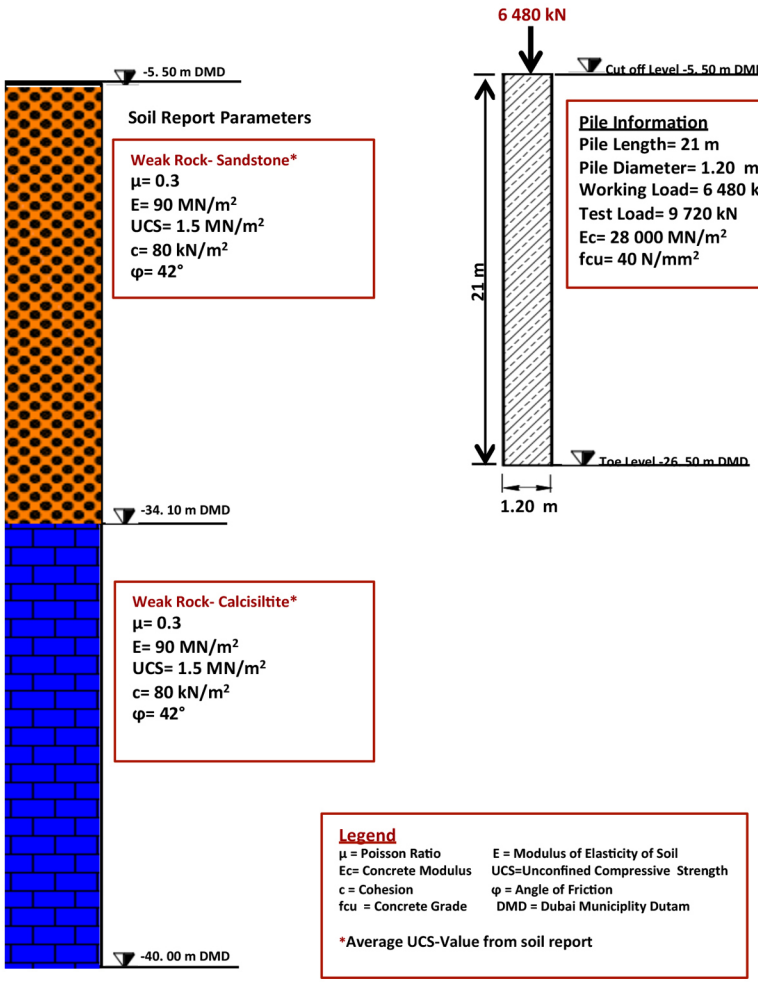

Modelling by using Soil Report Parameters

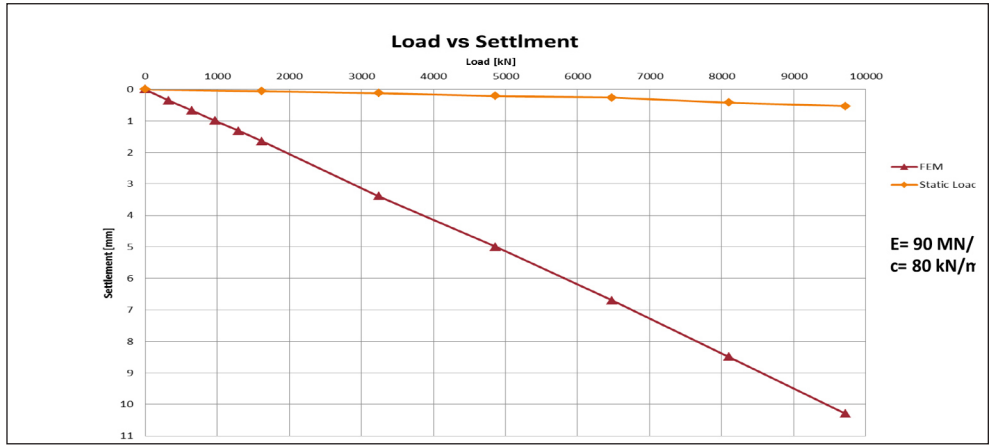

Back-Analysis of Soil Properties from Load Test

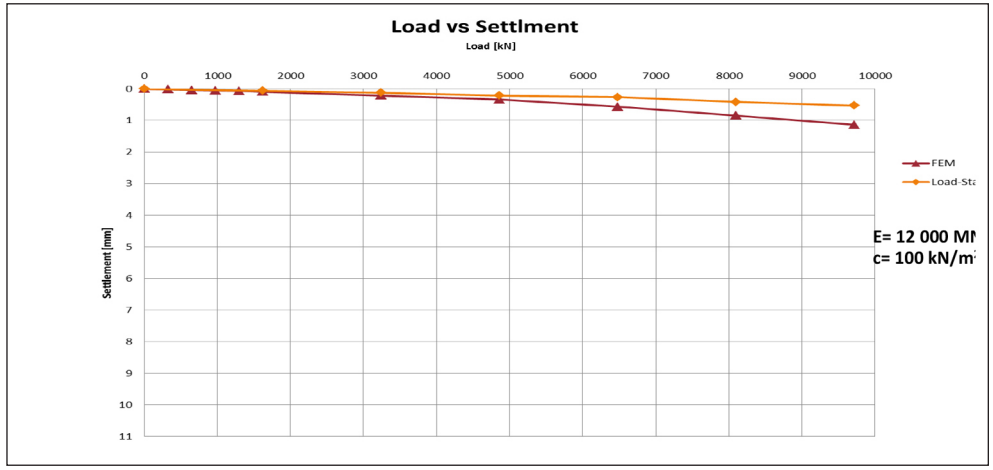

Pile Summary Sheet
P58

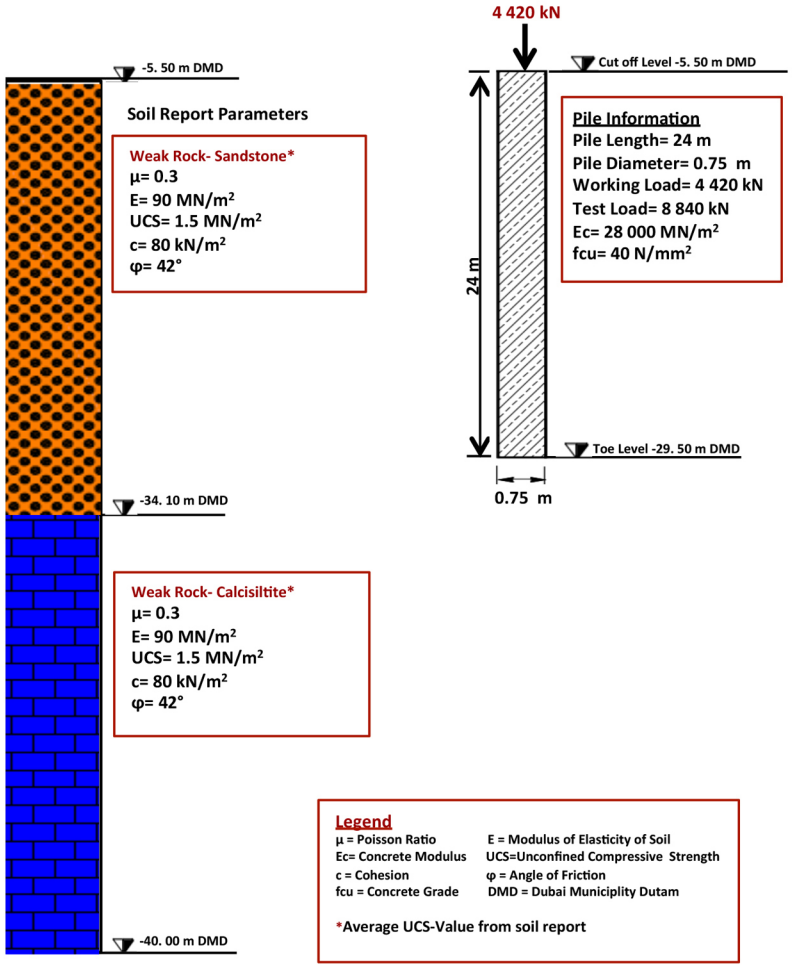

Legend

μ = Poisson Ratio	E = Modulus of Elasticity of Soil
Ec= Concrete Modulus	UCS=Unconfined Compressive Strength
c = Cohesion	φ = Angle of Friction
fcu = Concrete Grade	DMD = Dubai Municiplity Dutam

*Average UCS-Value from soil report

Modelling by using Soil Report Parameters

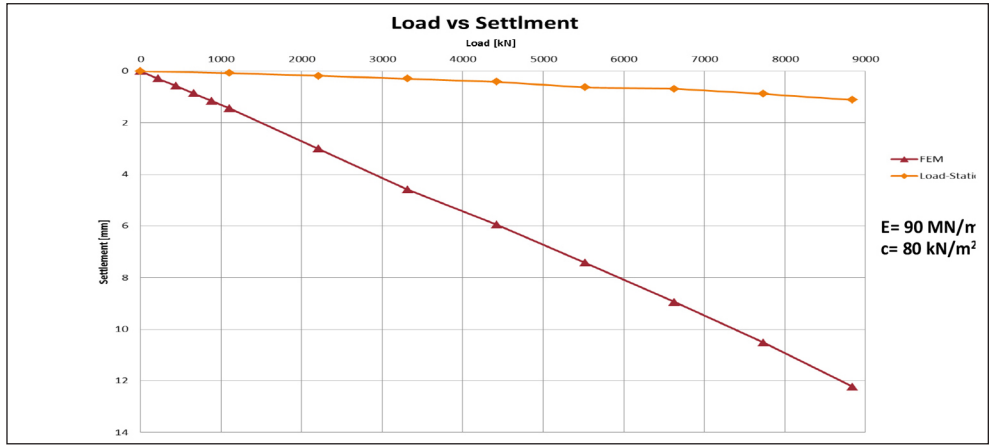

Back-Analysis of Soil Properties from Load Test

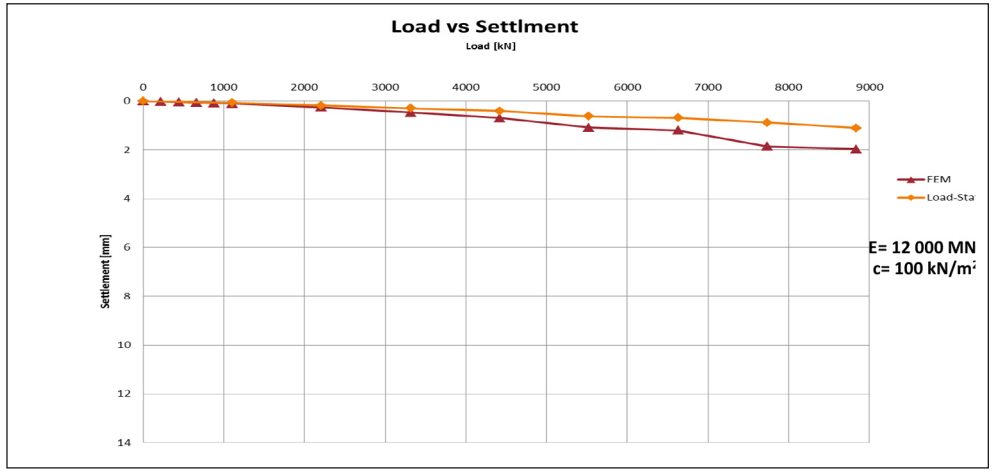

Pile Summary Sheet
P59

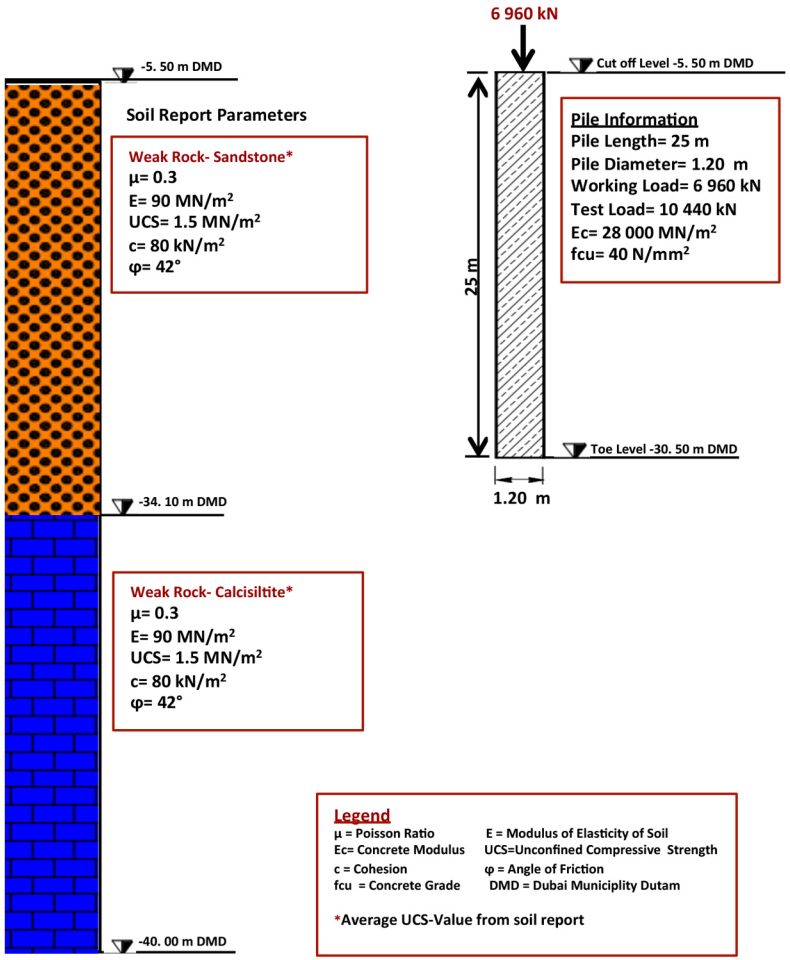

Legend

μ = Poisson Ratio — E = Modulus of Elasticity of Soil
Ec= Concrete Modulus — UCS=Unconfined Compressive Strength
c = Cohesion — φ = Angle of Friction
fcu = Concrete Grade — DMD = Dubai Municiplity Dutam

*Average UCS-Value from soil report

Modelling by using Soil Report Parameters

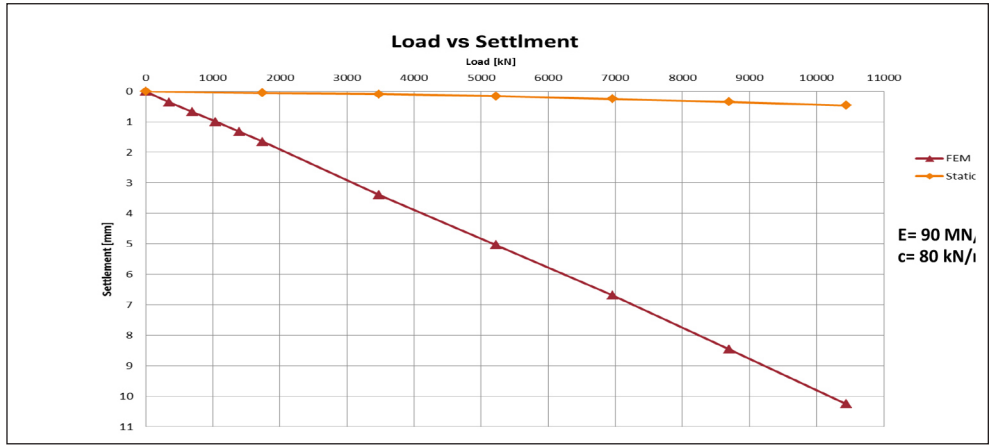

Back-Analysis of Soil Properties from Load Test

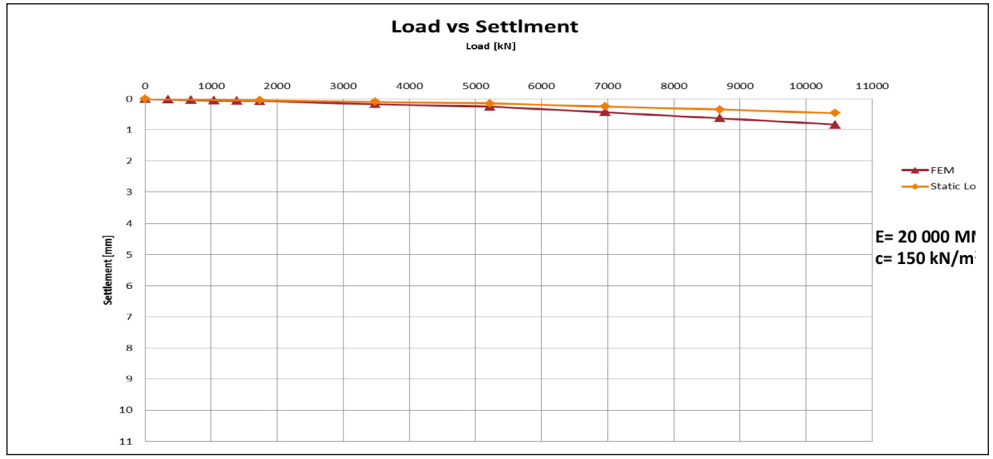

Pile Summary Sheet
P60

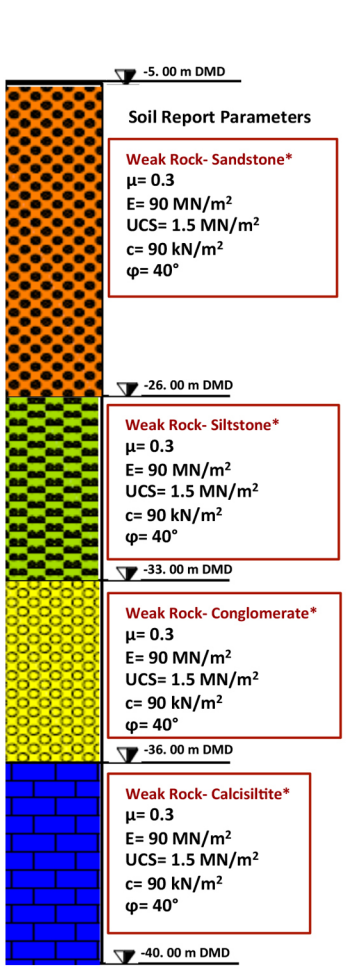

Soil Report Parameters

Weak Rock- Sandstone*
μ= 0.3
E= 90 MN/m²
UCS= 1.5 MN/m²
c= 90 kN/m²
φ= 40°

Weak Rock- Siltstone*
μ= 0.3
E= 90 MN/m²
UCS= 1.5 MN/m²
c= 90 kN/m²
φ= 40°

Weak Rock- Conglomerate*
μ= 0.3
E= 90 MN/m²
UCS= 1.5 MN/m²
c= 90 kN/m²
φ= 40°

Weak Rock- Calcisiltite*
μ= 0.3
E= 90 MN/m²
UCS= 1.5 MN/m²
c= 90 kN/m²
φ= 40°

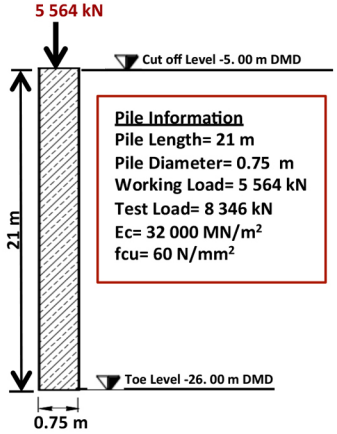

Pile Information
Pile Length= 21 m
Pile Diameter= 0.75 m
Working Load= 5 564 kN
Test Load= 8 346 kN
Ec= 32 000 MN/m²
fcu= 60 N/mm²

Legend

μ = Poisson Ratio	E = Modulus of Elasticity of Soil
Ec= Concrete Modulus	UCS=Unconfined Compressive Strength
c = Cohesion	φ = Angle of Friction
fcu = Concrete Grade	DMD = Dubai Municiplity Dutam

*Average UCS-Value from soil report

Modelling by using Soil Report Parameters

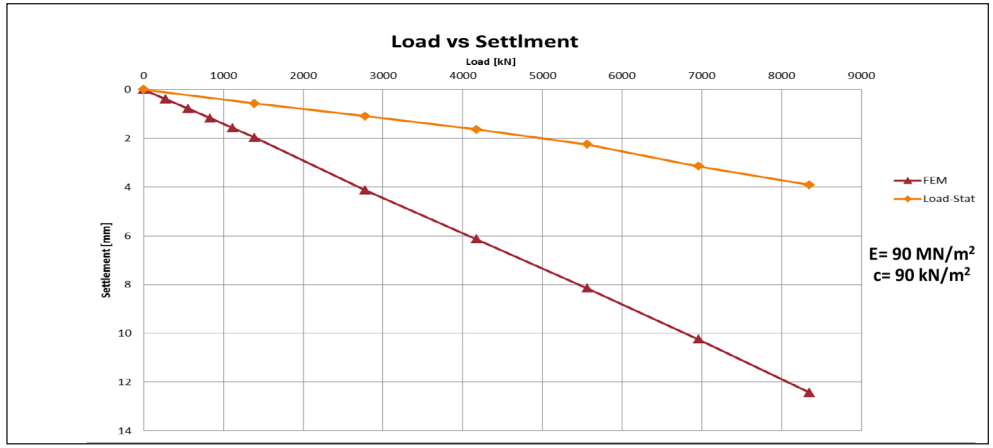

Back-Analysis of Soil Properties from Load Test

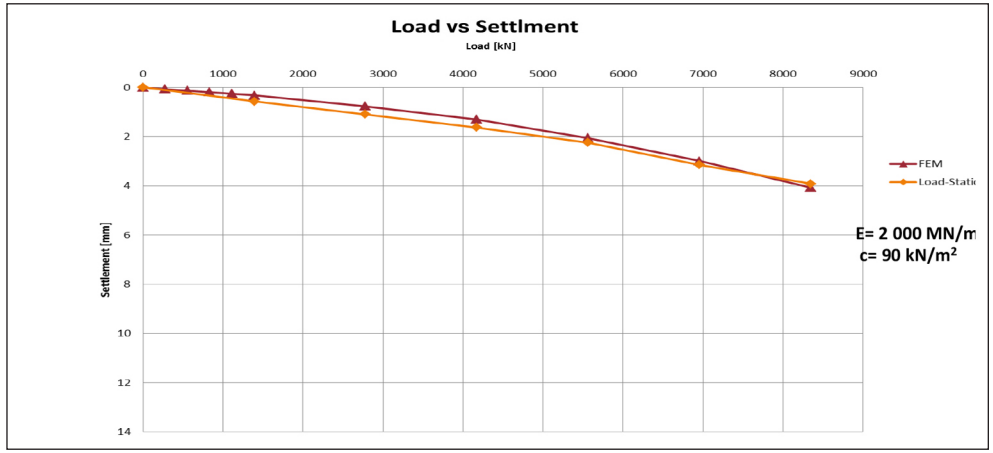

Pile Summary Sheet
P61

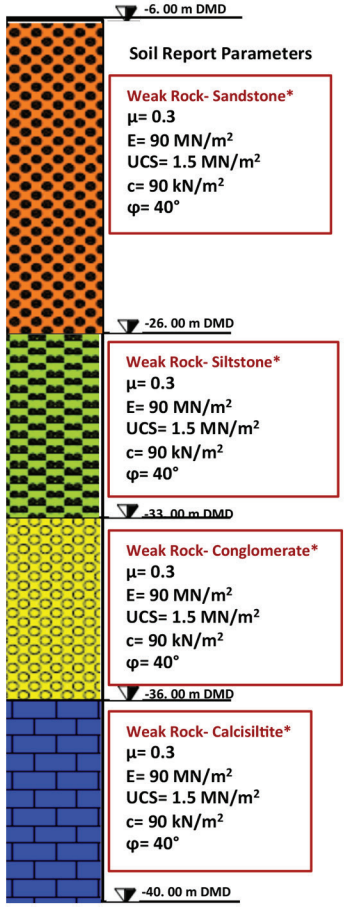

Soil Report Parameters

Weak Rock- Sandstone*
μ= 0.3
E= 90 MN/m²
UCS= 1.5 MN/m²
c= 90 kN/m²
φ= 40°

Weak Rock- Siltstone*
μ= 0.3
E= 90 MN/m²
UCS= 1.5 MN/m²
c= 90 kN/m²
φ= 40°

Weak Rock- Conglomerate*
μ= 0.3
E= 90 MN/m²
UCS= 1.5 MN/m²
c= 90 kN/m²
φ= 40°

Weak Rock- Calcisiltite*
μ= 0.3
E= 90 MN/m²
UCS= 1.5 MN/m²
c= 90 kN/m²
φ= 40°

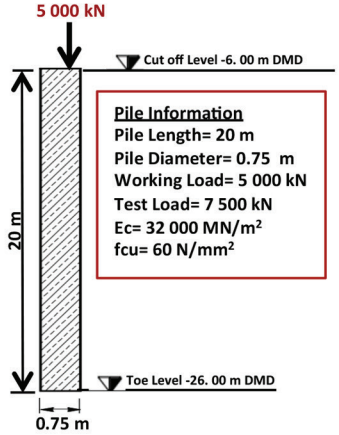

Pile Information
Pile Length= 20 m
Pile Diameter= 0.75 m
Working Load= 5 000 kN
Test Load= 7 500 kN
Ec= 32 000 MN/m²
fcu= 60 N/mm²

Legend

μ = Poisson Ratio	E = Modulus of Elasticity of Soil
Ec= Concrete Modulus	UCS=Unconfined Compressive Strength
c = Cohesion	φ = Angle of Friction
fcu = Concrete Grade	DMD = Dubai Municiplity Dutam

*Average UCS-Value from soil report

Modelling by using Soil Report Parameters

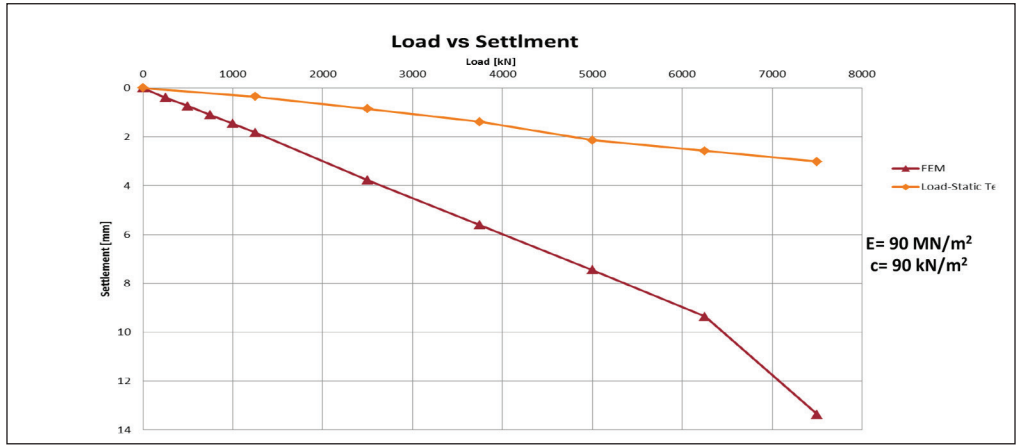

Back-Analysis of Soil Properties from Load Test

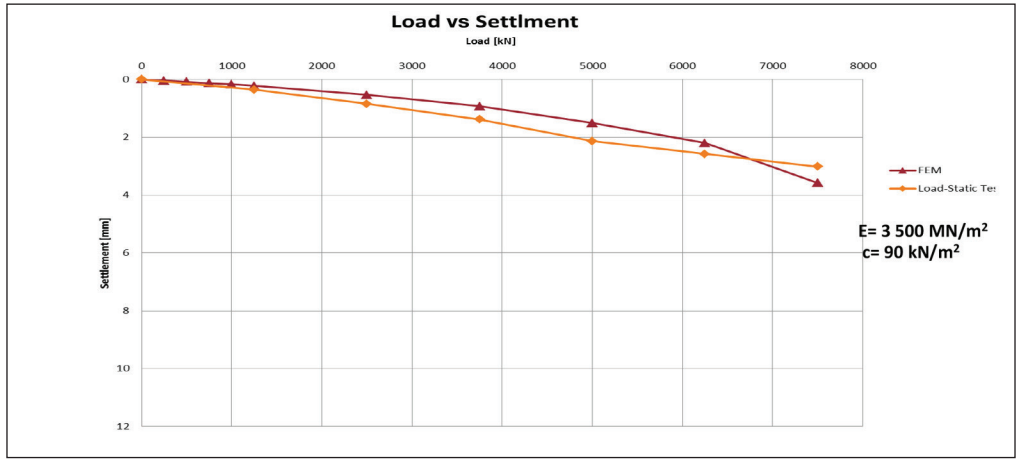

Pile Summary Sheet
P62

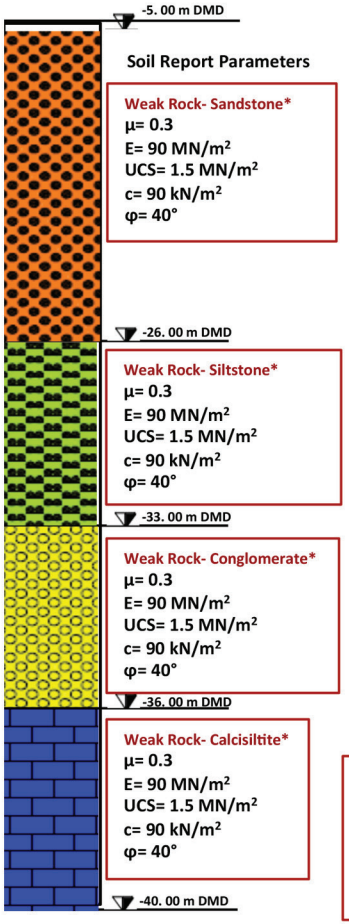

Soil Report Parameters

Weak Rock- Sandstone*
μ= 0.3
E= 90 MN/m²
UCS= 1.5 MN/m²
c= 90 kN/m²
φ= 40°

Weak Rock- Siltstone*
μ= 0.3
E= 90 MN/m²
UCS= 1.5 MN/m²
c= 90 kN/m²
φ= 40°

Weak Rock- Conglomerate*
μ= 0.3
E= 90 MN/m²
UCS= 1.5 MN/m²
c= 90 kN/m²
φ= 40°

Weak Rock- Calcisiltite*
μ= 0.3
E= 90 MN/m²
UCS= 1.5 MN/m²
c= 90 kN/m²
φ= 40°

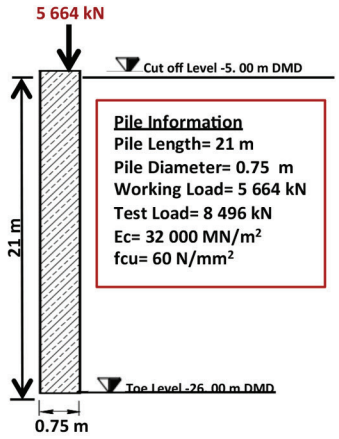

Pile Information
Pile Length= 21 m
Pile Diameter= 0.75 m
Working Load= 5 664 kN
Test Load= 8 496 kN
Ec= 32 000 MN/m²
fcu= 60 N/mm²

Legend

μ = Poisson Ratio	E = Modulus of Elasticity of Soil
Ec= Concrete Modulus	UCS=Unconfined Compressive Strength
c = Cohesion	φ = Angle of Friction
fcu = Concrete Grade	DMD = Dubai Municiplity Dutam

*Average UCS-Value from soil report

Modelling by using Soil Report Parameters

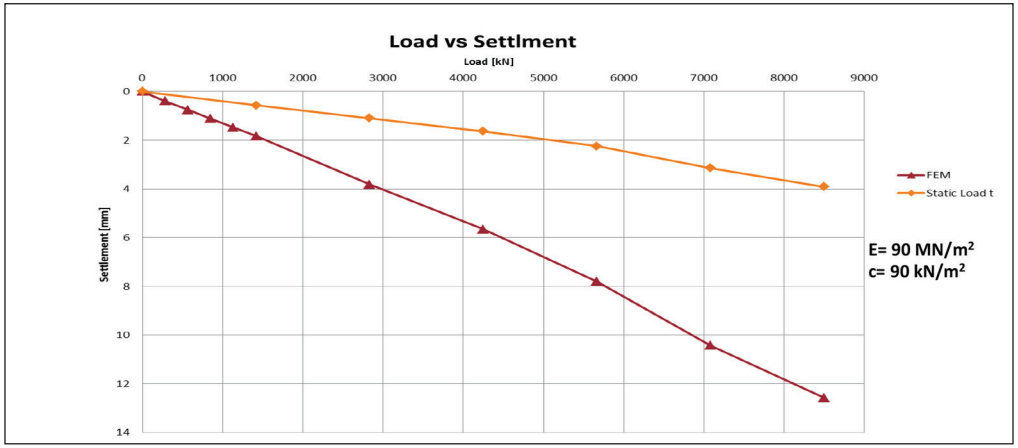

Back-Analysis of Soil Properties from Load Test

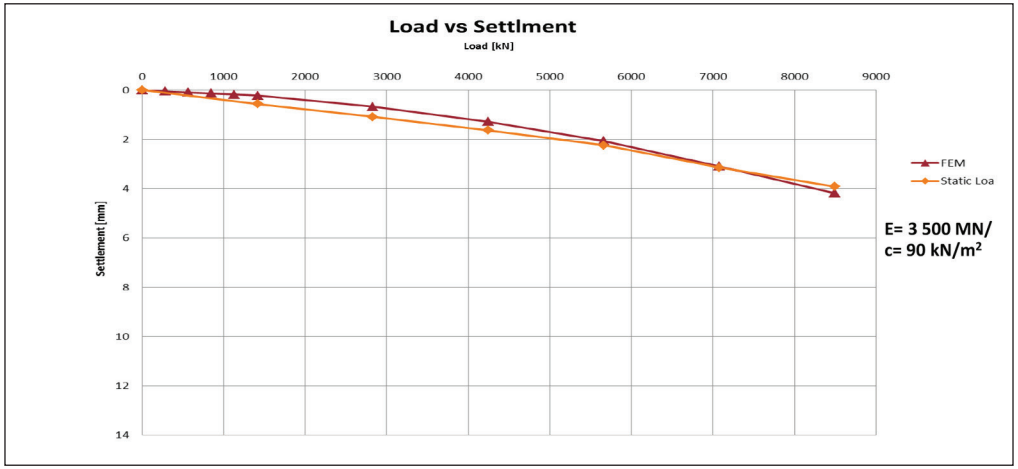

Pile Summary Sheet
P63

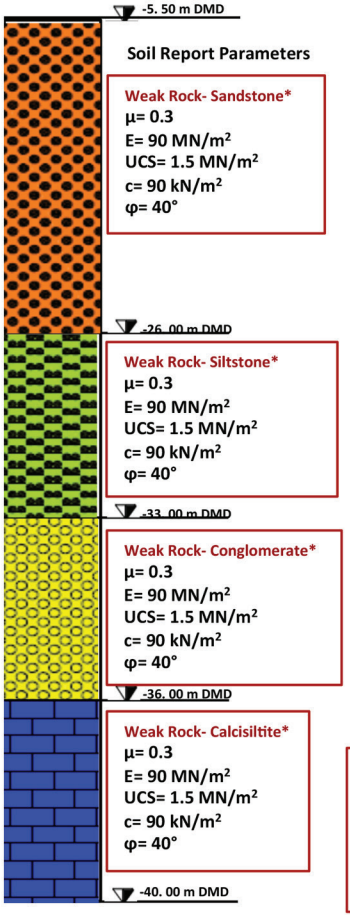

Soil Report Parameters

Weak Rock- Sandstone*
μ= 0.3
E= 90 MN/m²
UCS= 1.5 MN/m²
c= 90 kN/m²
φ= 40°

Weak Rock- Siltstone*
μ= 0.3
E= 90 MN/m²
UCS= 1.5 MN/m²
c= 90 kN/m²
φ= 40°

Weak Rock- Conglomerate*
μ= 0.3
E= 90 MN/m²
UCS= 1.5 MN/m²
c= 90 kN/m²
φ= 40°

Weak Rock- Calcisiltite*
μ= 0.3
E= 90 MN/m²
UCS= 1.5 MN/m²
c= 90 kN/m²
φ= 40°

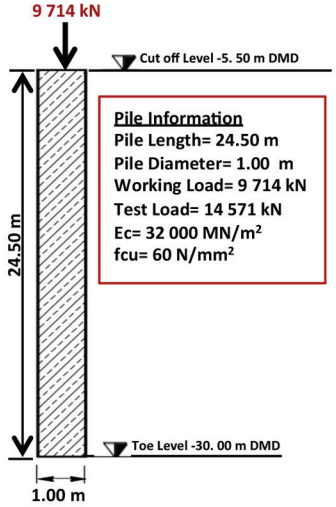

Pile Information
Pile Length= 24.50 m
Pile Diameter= 1.00 m
Working Load= 9 714 kN
Test Load= 14 571 kN
Ec= 32 000 MN/m²
fcu= 60 N/mm²

Legend

μ = Poisson Ratio	E = Modulus of Elasticity of Soil
Ec= Concrete Modulus	UCS=Unconfined Compressive Strength
c = Cohesion	φ = Angle of Friction
fcu = Concrete Grade	DMD = Dubai Municiplity Dutam

*Average UCS-Value from soil report

Modelling by using Soil Report Parameters

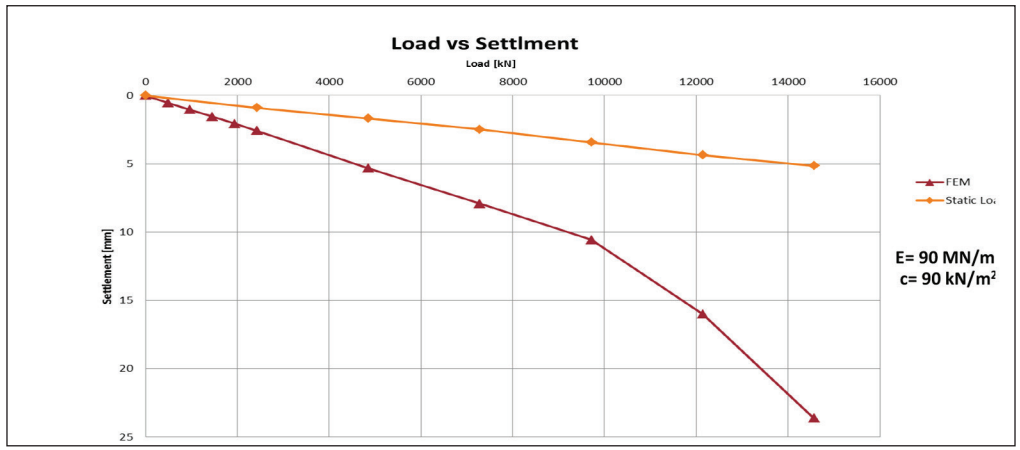

Back-Analysis of Soil Properties from Load Test

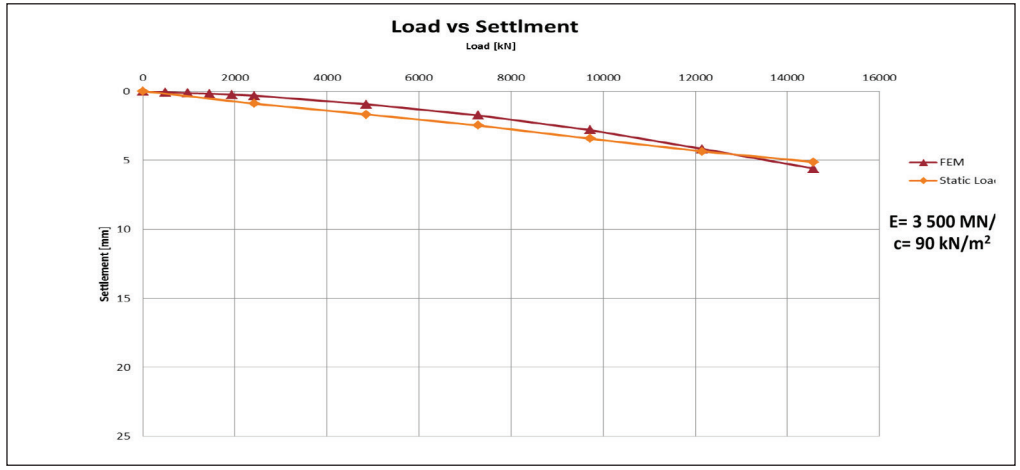

Pile Summary Sheet
P64

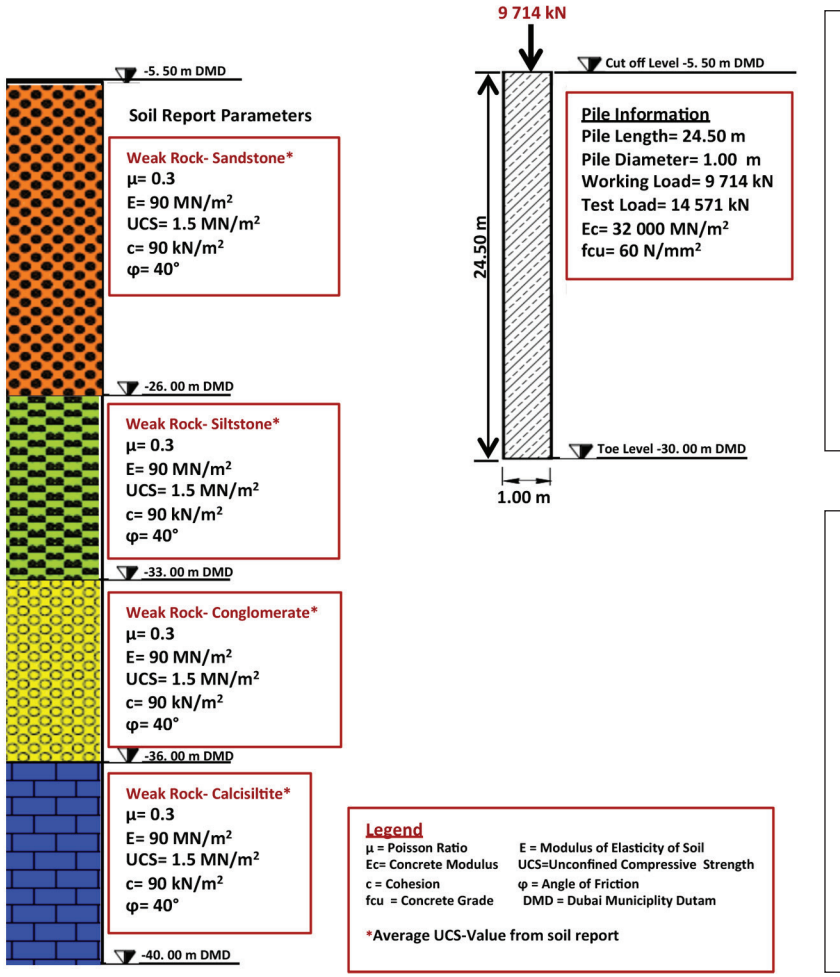

Pile Information
Pile Length= 24.50 m
Pile Diameter= 1.00 m
Working Load= 9 714 kN
Test Load= 14 571 kN
Ec= 32 000 MN/m²
fcu= 60 N/mm²

Legend
μ = Poisson Ratio
E = Modulus of Elasticity of Soil
Ec= Concrete Modulus
UCS=Unconfined Compressive Strength
c = Cohesion
φ = Angle of Friction
fcu = Concrete Grade
DMD = Dubai Municiplity Dutam

*Average UCS-Value from soil report

Modelling by using Soil Report Parameters

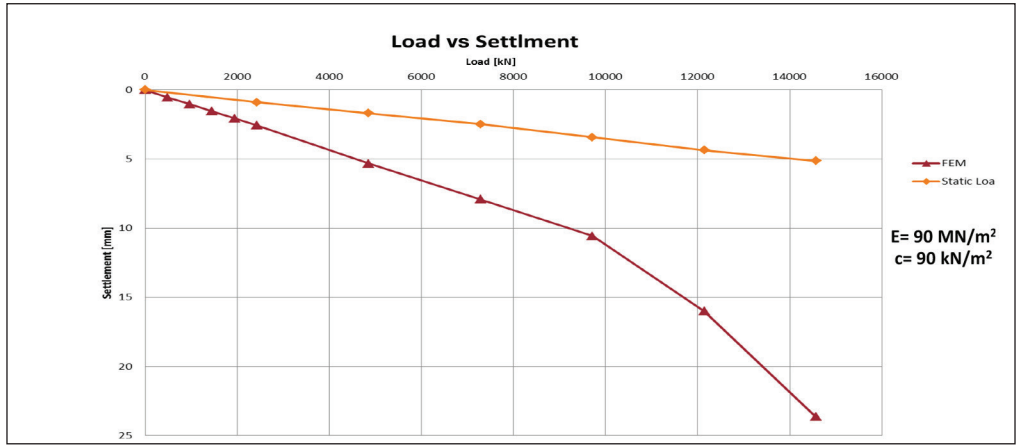

Back-Analysis of Soil Properties from Load Test

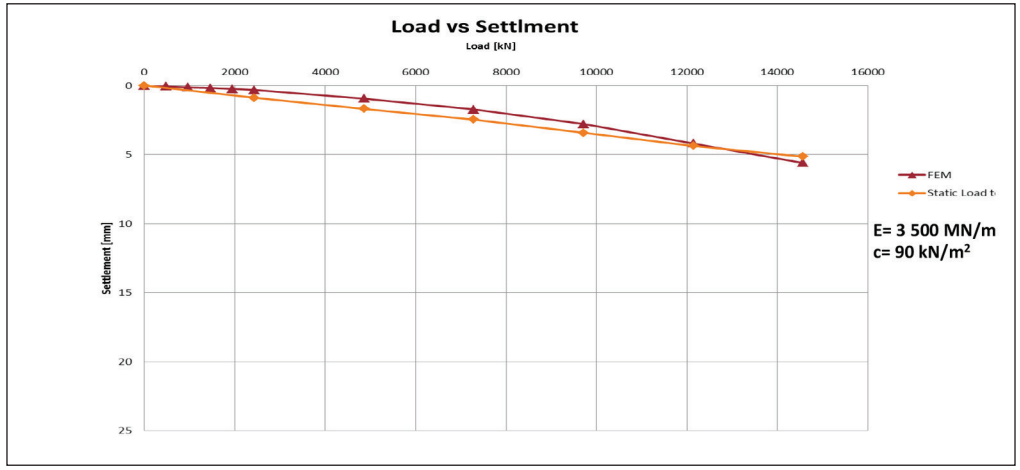

Pile Summary Sheet
P65

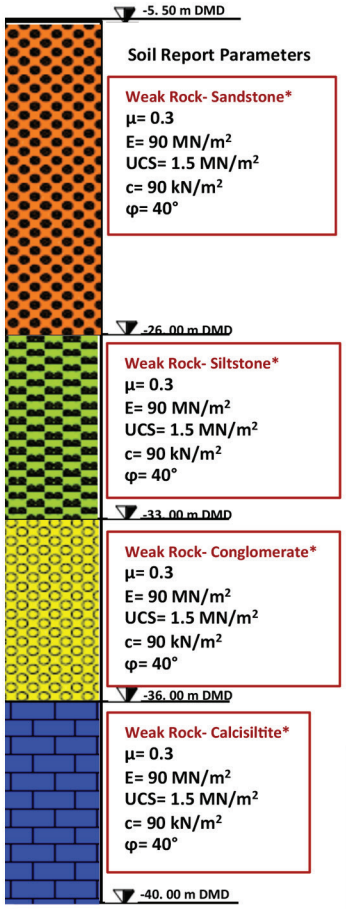

Soil Report Parameters

Weak Rock- Sandstone*
μ= 0.3
E= 90 MN/m²
UCS= 1.5 MN/m²
c= 90 kN/m²
φ= 40°

Weak Rock- Siltstone*
μ= 0.3
E= 90 MN/m²
UCS= 1.5 MN/m²
c= 90 kN/m²
φ= 40°

Weak Rock- Conglomerate*
μ= 0.3
E= 90 MN/m²
UCS= 1.5 MN/m²
c= 90 kN/m²
φ= 40°

Weak Rock- Calcisiltite*
μ= 0.3
E= 90 MN/m²
UCS= 1.5 MN/m²
c= 90 kN/m²
φ= 40°

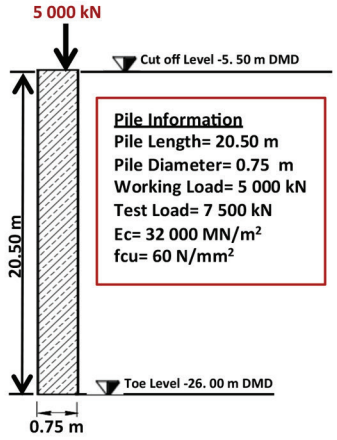

Pile Information
Pile Length= 20.50 m
Pile Diameter= 0.75 m
Working Load= 5 000 kN
Test Load= 7 500 kN
Ec= 32 000 MN/m²
fcu= 60 N/mm²

Legend

μ = Poisson Ratio	E = Modulus of Elasticity of Soil
Ec= Concrete Modulus	UCS=Unconfined Compressive Strength
c = Cohesion	φ = Angle of Friction
fcu = Concrete Grade	DMD = Dubai Municiplity Dutam

*Average UCS-Value from soil report

Modelling by using Soil Report Parameters

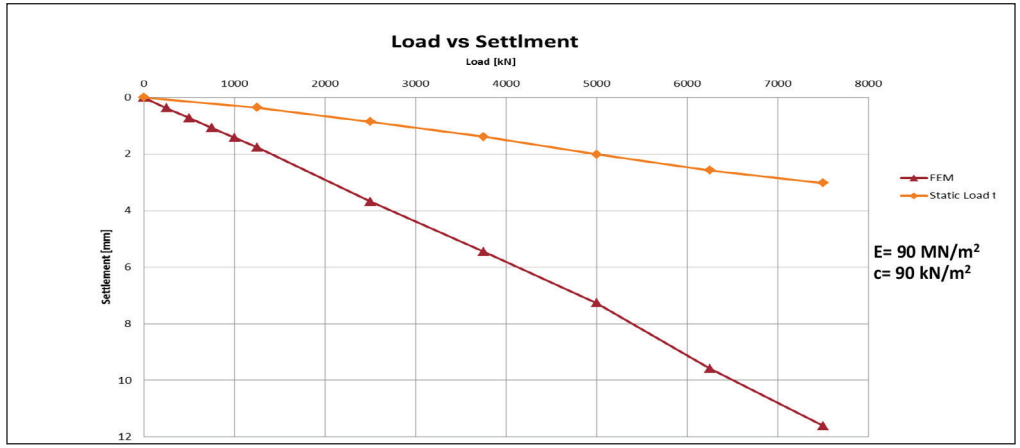

Back-Analysis of Soil Properties from Load Test

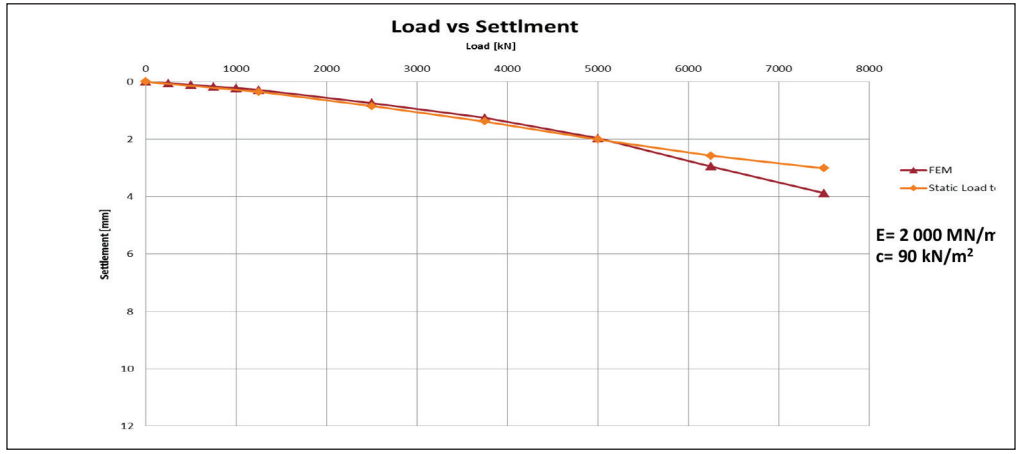

Pile Summary Sheet
P66

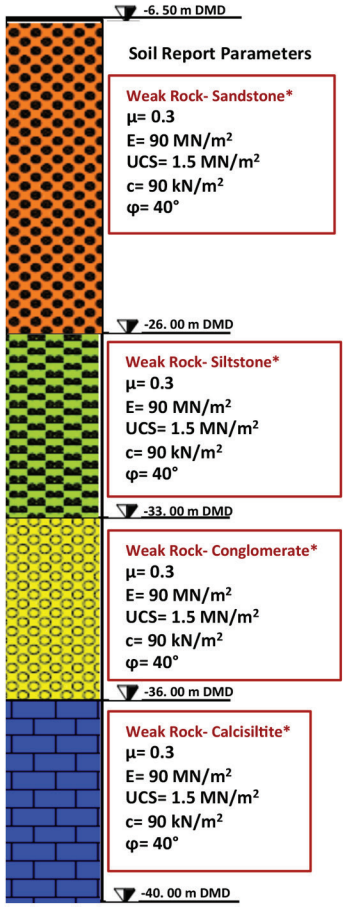

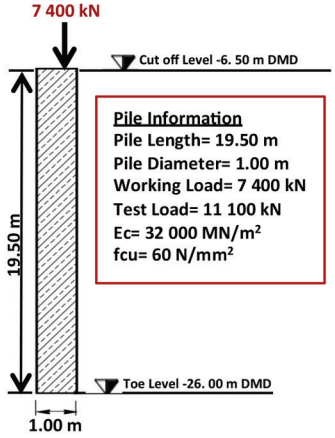

Pile Information
Pile Length= 19.50 m
Pile Diameter= 1.00 m
Working Load= 7 400 kN
Test Load= 11 100 kN
Ec= 32 000 MN/m²
fcu= 60 N/mm²

Legend

μ = Poisson Ratio	E = Modulus of Elasticity of Soil
Ec= Concrete Modulus	UCS=Unconfined Compressive Strength
c = Cohesion	φ = Angle of Friction
fcu = Concrete Grade	DMD = Dubai Municiplity Dutam

*Average UCS-Value from soil report

Modelling by using Soil Report Parameters

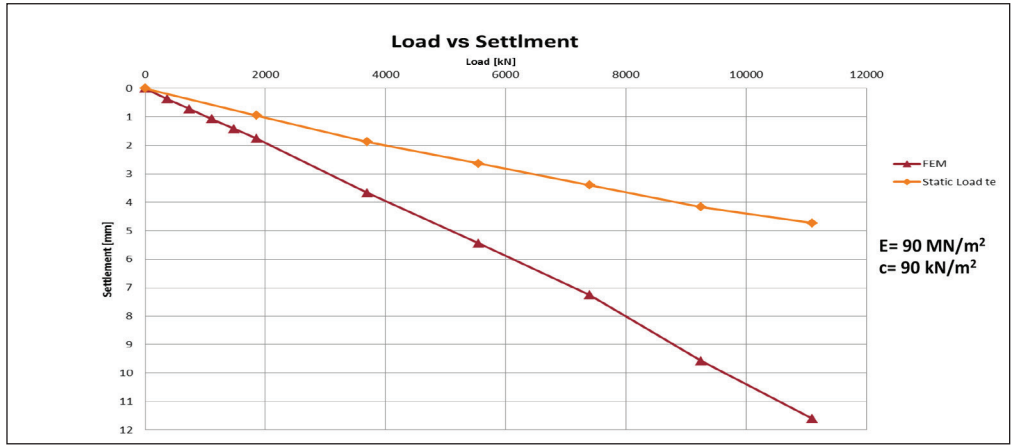

Back-Analysis of Soil Properties from Load Test

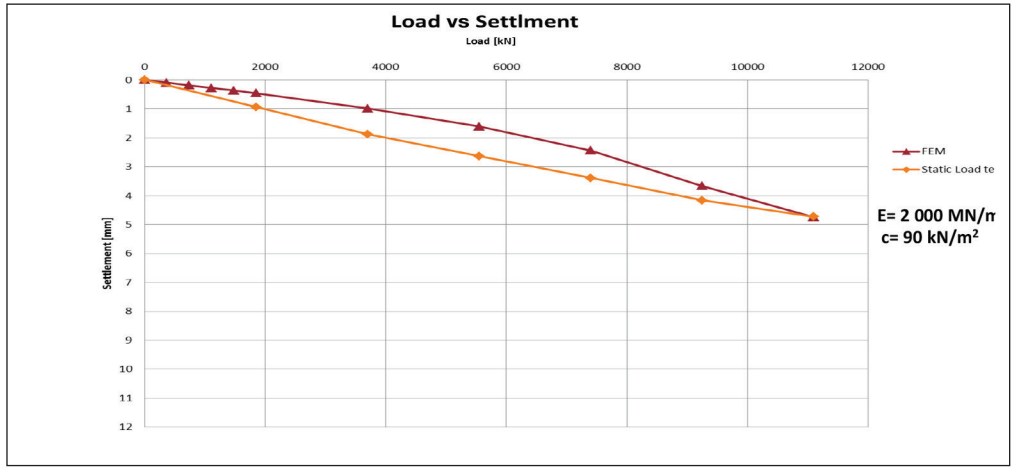

Pile Summary Sheet
P67

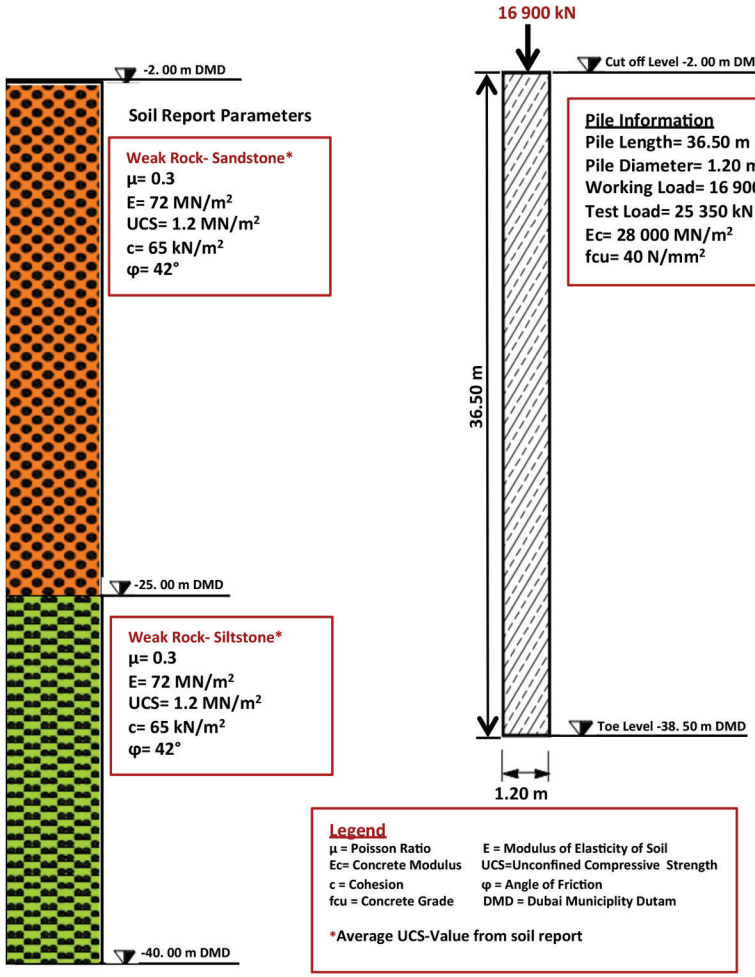

Modelling by using Soil Report Parameters

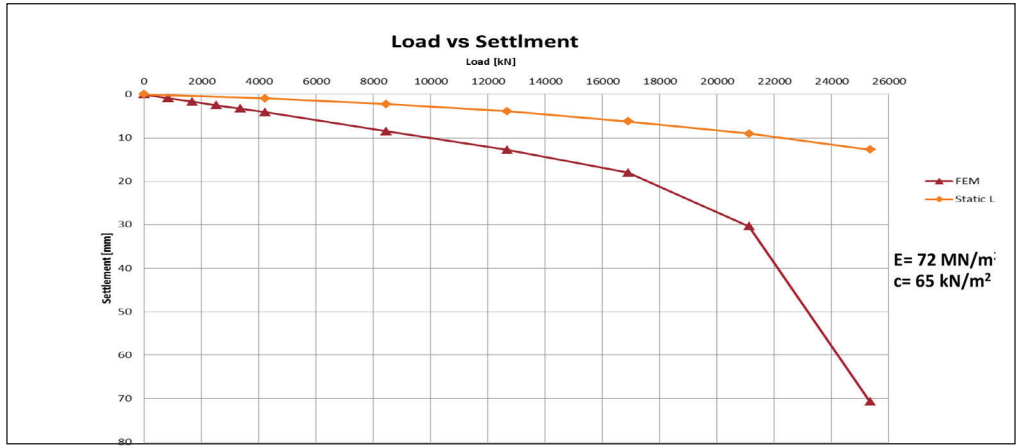

Back-Analysis of Soil Properties from Load Test

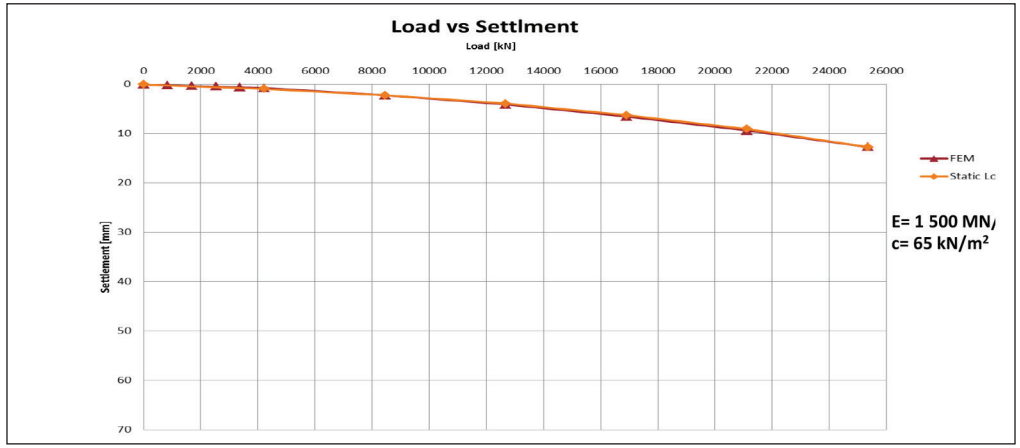

Pile Summary Sheet
P68

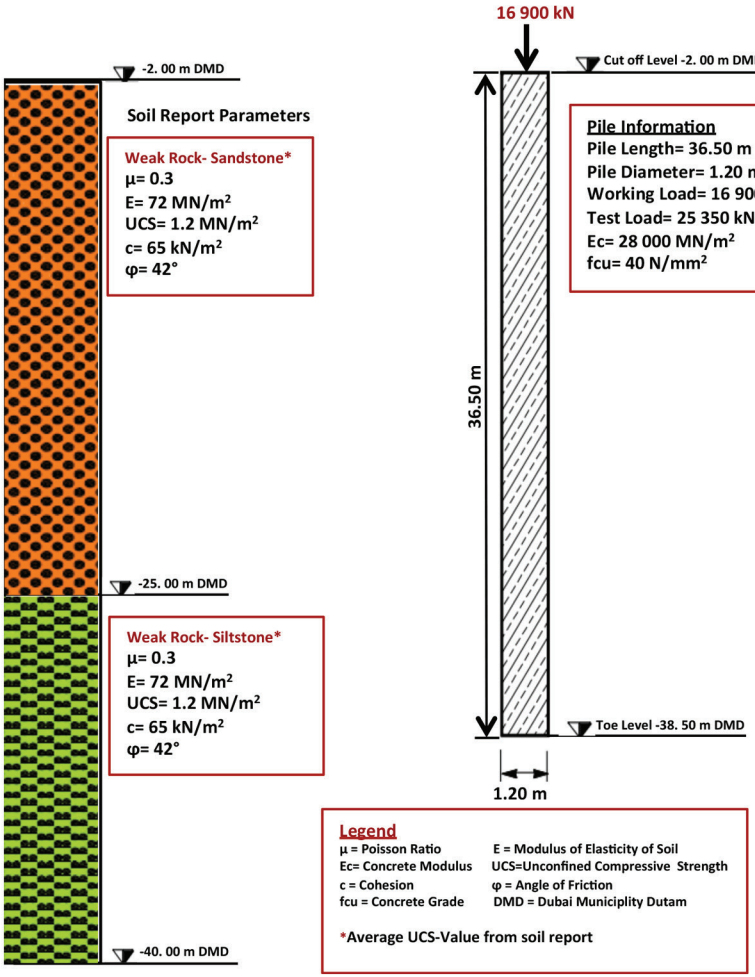

Legend

μ = Poisson Ratio — E = Modulus of Elasticity of Soil
Ec= Concrete Modulus — UCS=Unconfined Compressive Strength
c = Cohesion — φ = Angle of Friction
fcu = Concrete Grade — DMD = Dubai Municiplity Dutam

*Average UCS-Value from soil report

Modelling by using Soil Report Parameters

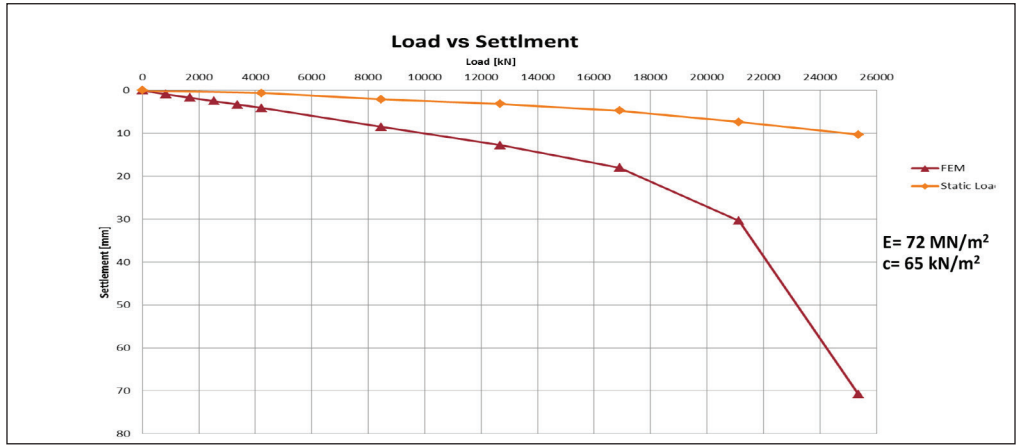

Back-Analysis of Soil Properties from Load Test

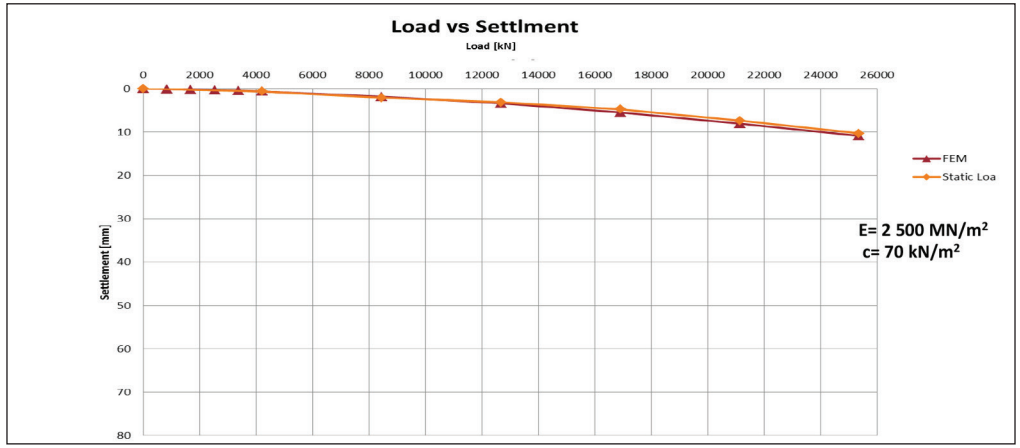

Pile Summary Sheet
P69

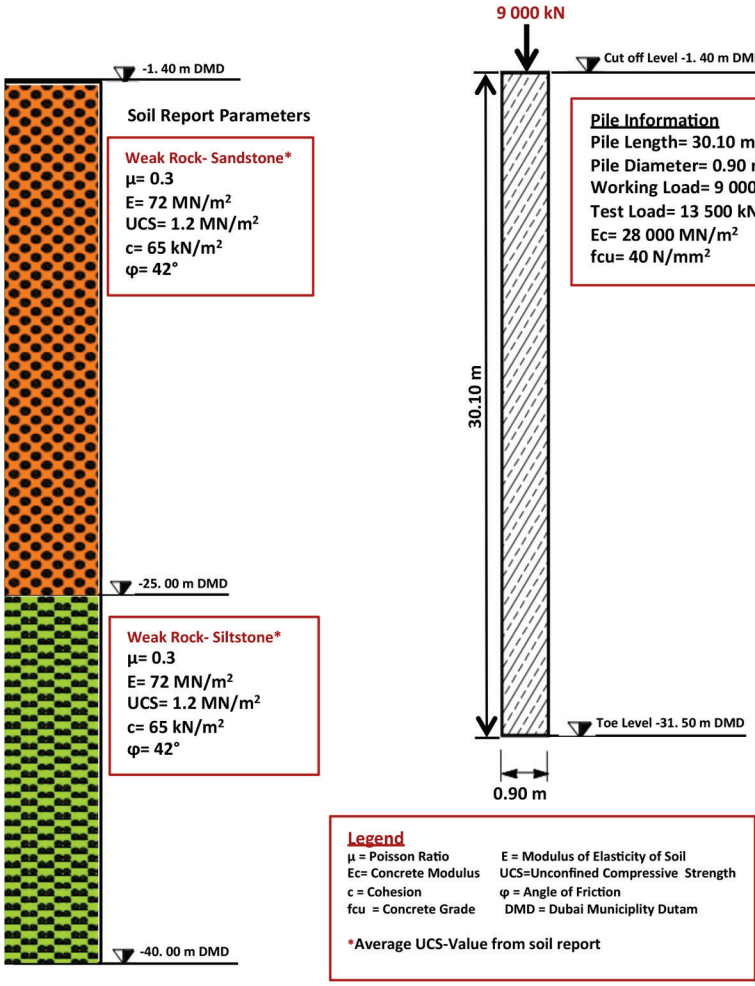

Pile Information
Pile Length= 30.10 m
Pile Diameter= 0.90 m
Working Load= 9 000 kN
Test Load= 13 500 kN
Ec= 28 000 MN/m²
fcu= 40 N/mm²

Legend

μ = Poisson Ratio	E = Modulus of Elasticity of Soil
Ec= Concrete Modulus	UCS=Unconfined Compressive Strength
c = Cohesion	φ = Angle of Friction
fcu = Concrete Grade	DMD = Dubai Municiplity Dutam

*Average UCS-Value from soil report

Modelling by using Soil Report Parameters

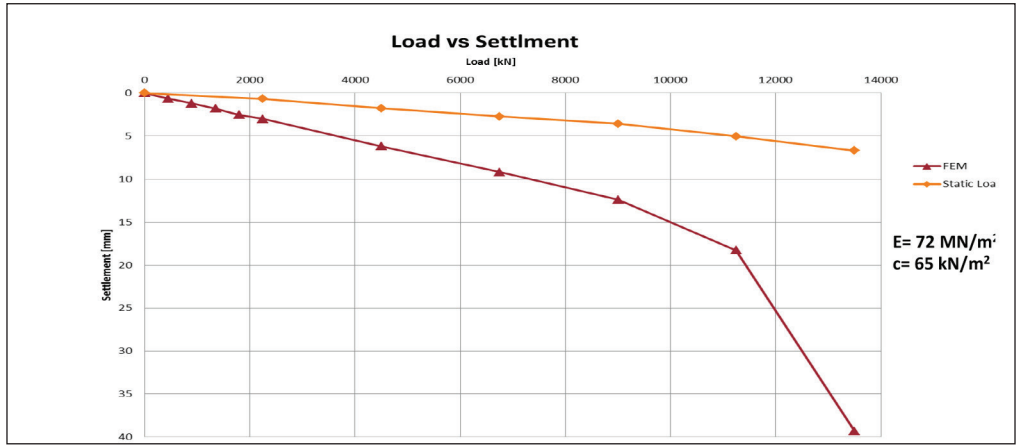

Back-Analysis of Soil Properties from Load Test

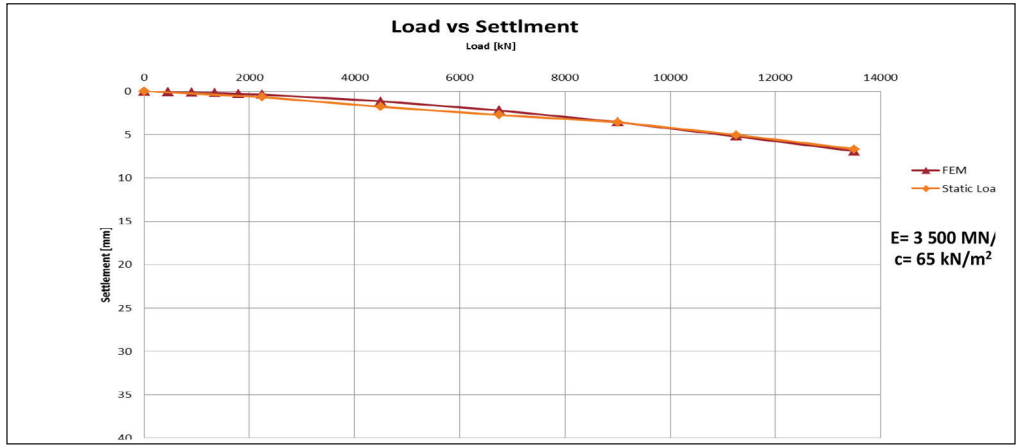

Pile Summary Sheet
P70

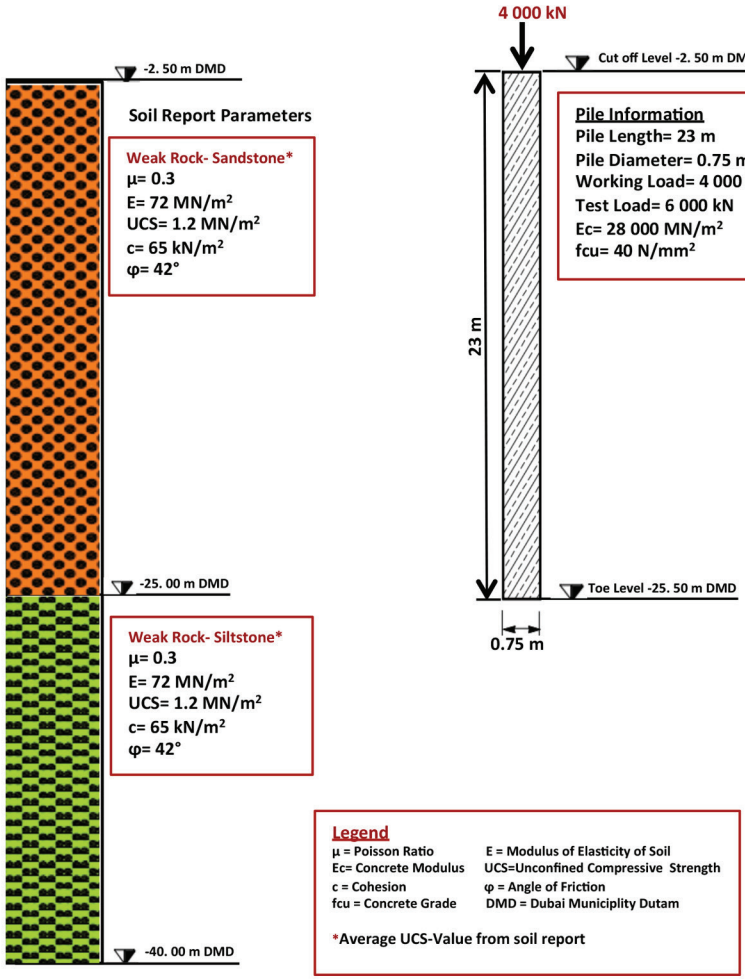

Pile Information
Pile Length= 23 m
Pile Diameter= 0.75 m
Working Load= 4 000 kN
Test Load= 6 000 kN
Ec= 28 000 MN/m²
fcu= 40 N/mm²

Legend

μ = Poisson Ratio	E = Modulus of Elasticity of Soil
Ec= Concrete Modulus	UCS=Unconfined Compressive Strength
c = Cohesion	φ = Angle of Friction
fcu = Concrete Grade	DMD = Dubai Municiplity Dutam

*Average UCS-Value from soil report

Modelling by using Soil Report Parameters

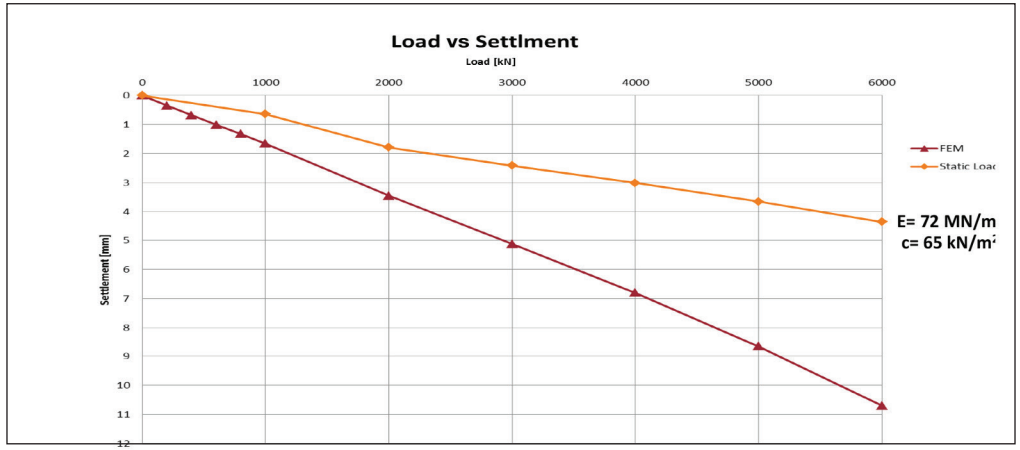

Back-Analysis of Soil Properties from Load Test

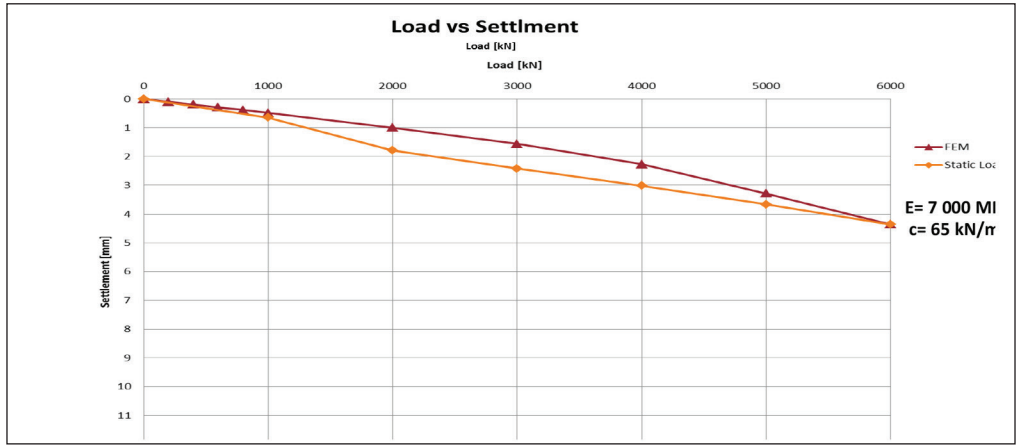

Pile Summary Sheet
P71

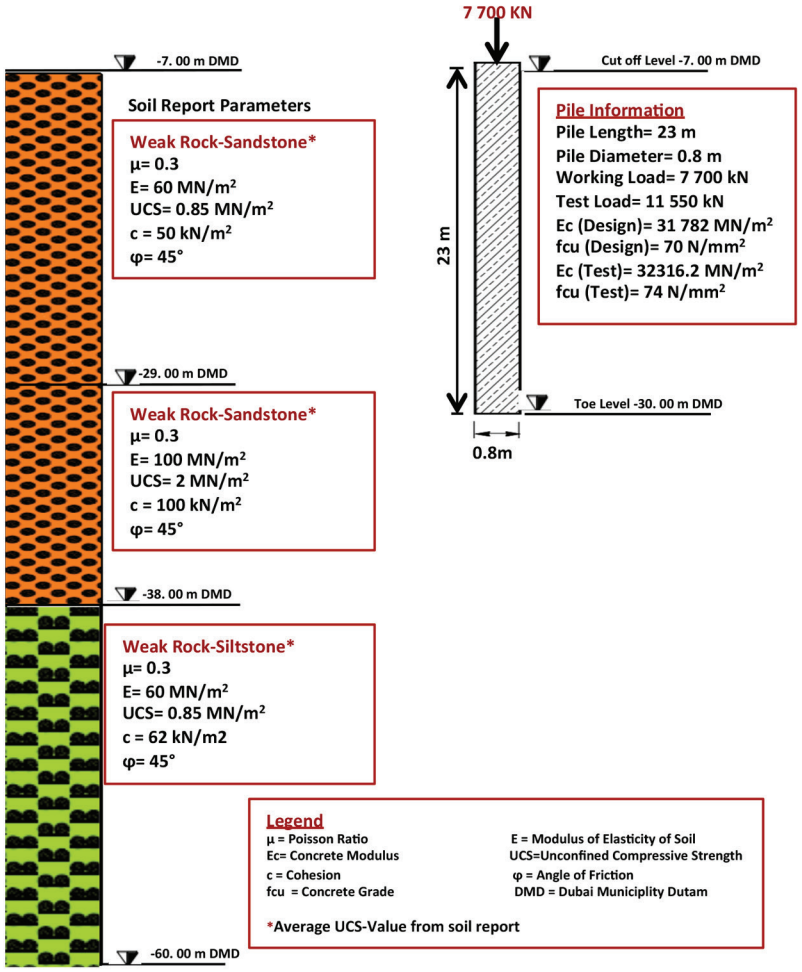

Soil Report Parameters

Weak Rock-Sandstone*
μ= 0.3
E= 60 MN/m²
UCS= 0.85 MN/m²
c = 50 kN/m²
φ= 45°

Weak Rock-Sandstone*
μ= 0.3
E= 100 MN/m²
UCS= 2 MN/m²
c = 100 kN/m²
φ= 45°

Weak Rock-Siltstone*
μ= 0.3
E= 60 MN/m²
UCS= 0.85 MN/m²
c = 62 kN/m2
φ= 45°

Pile Information
Pile Length= 23 m
Pile Diameter= 0.8 m
Working Load= 7 700 kN
Test Load= 11 550 kN
Ec (Design)= 31 782 MN/m²
fcu (Design)= 70 N/mm²
Ec (Test)= 32316.2 MN/m²
fcu (Test)= 74 N/mm²

Legend
μ = Poisson Ratio
E = Modulus of Elasticity of Soil
Ec= Concrete Modulus
UCS=Unconfined Compressive Strength
c = Cohesion
φ = Angle of Friction
fcu = Concrete Grade
DMD = Dubai Municiplity Datum

*Average UCS-Value from soil report

Modelling by using Soil Report Parameters

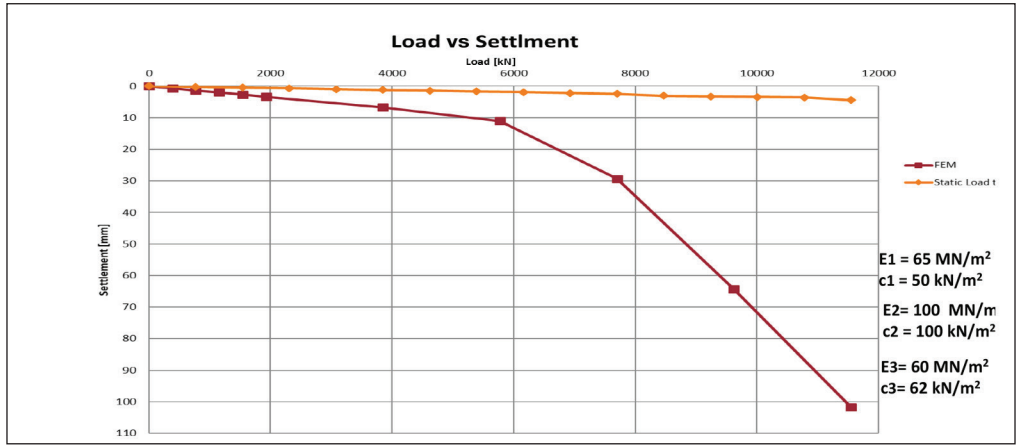

Back-Analysis of Soil Properties from Load Test

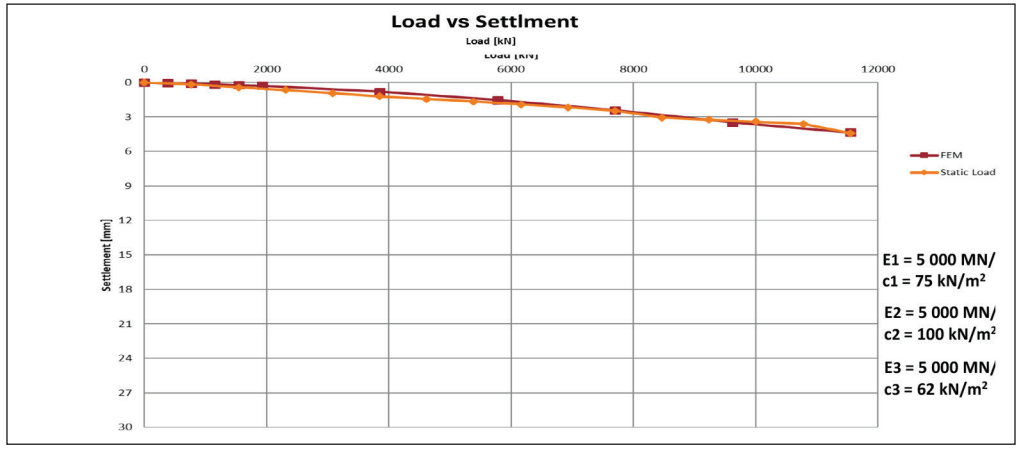

Pile Summary Sheet
P72

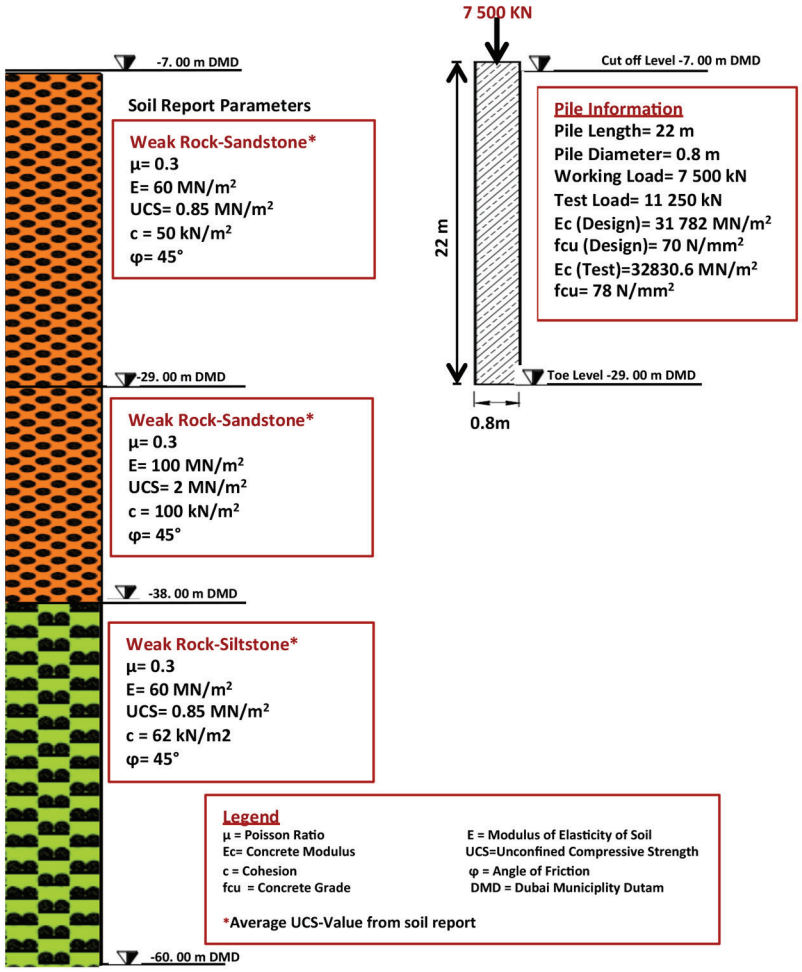

Soil Report Parameters

Weak Rock-Sandstone*
μ= 0.3
E= 60 MN/m²
UCS= 0.85 MN/m²
c = 50 kN/m²
φ= 45°

Weak Rock-Sandstone*
μ= 0.3
E= 100 MN/m²
UCS= 2 MN/m²
c = 100 kN/m²
φ= 45°

Weak Rock-Siltstone*
μ= 0.3
E= 60 MN/m²
UCS= 0.85 MN/m²
c = 62 kN/m2
φ= 45°

Pile Information
Pile Length= 22 m
Pile Diameter= 0.8 m
Working Load= 7 500 kN
Test Load= 11 250 kN
Ec (Design)= 31 782 MN/m²
fcu (Design)= 70 N/mm²
Ec (Test)=32830.6 MN/m²
fcu= 78 N/mm²

Legend
μ = Poisson Ratio
E = Modulus of Elasticity of Soil
Ec= Concrete Modulus
UCS=Unconfined Compressive Strength
c = Cohesion
φ = Angle of Friction
fcu = Concrete Grade
DMD = Dubai Municiplity Dutam

*Average UCS-Value from soil report

Modelling by using Soil Report Parameters

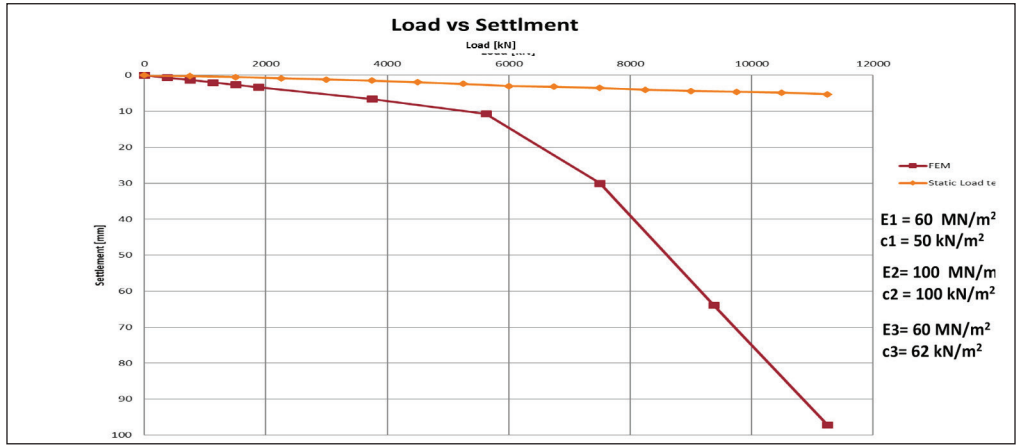

Back-Analysis of Soil Properties from Load Test

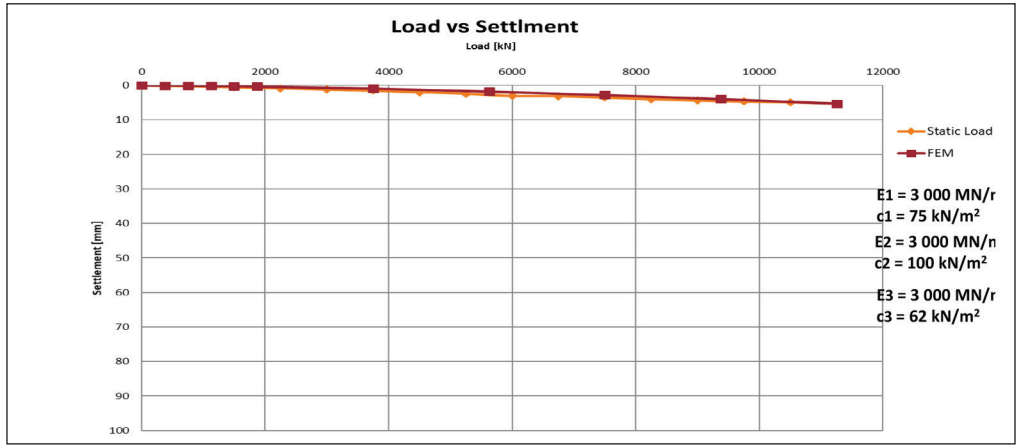

Pile Summary Sheet
P73

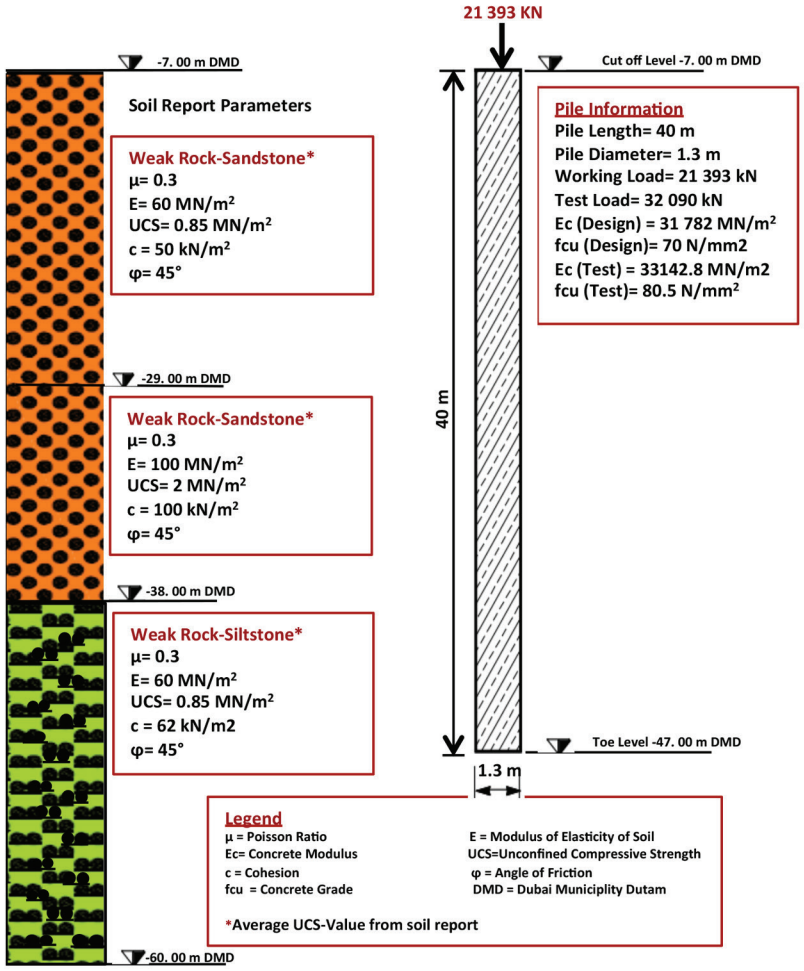

Modelling by using Soil Report Parameters

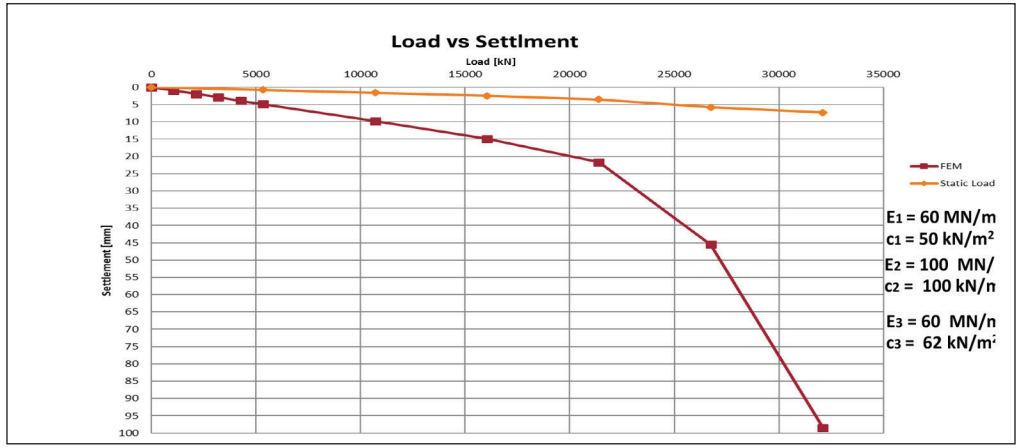

Back-Analysis of Soil Properties from Load Test

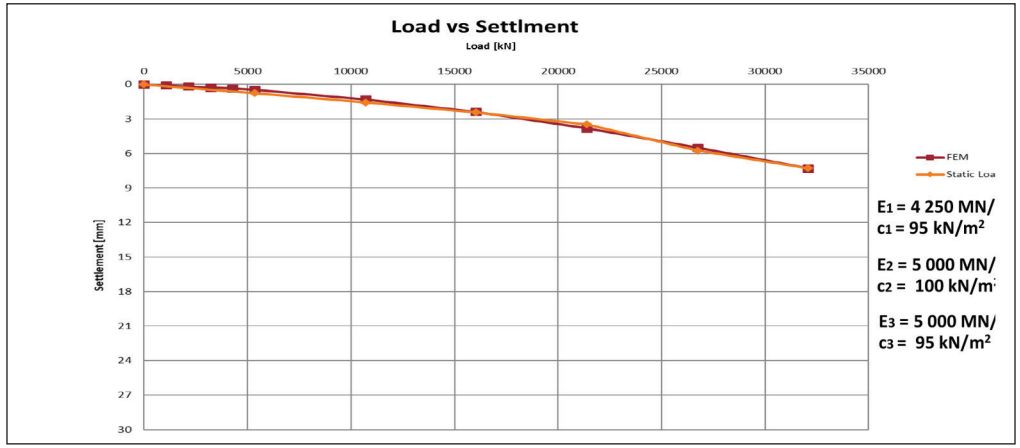

Pile Summary Sheet
P74

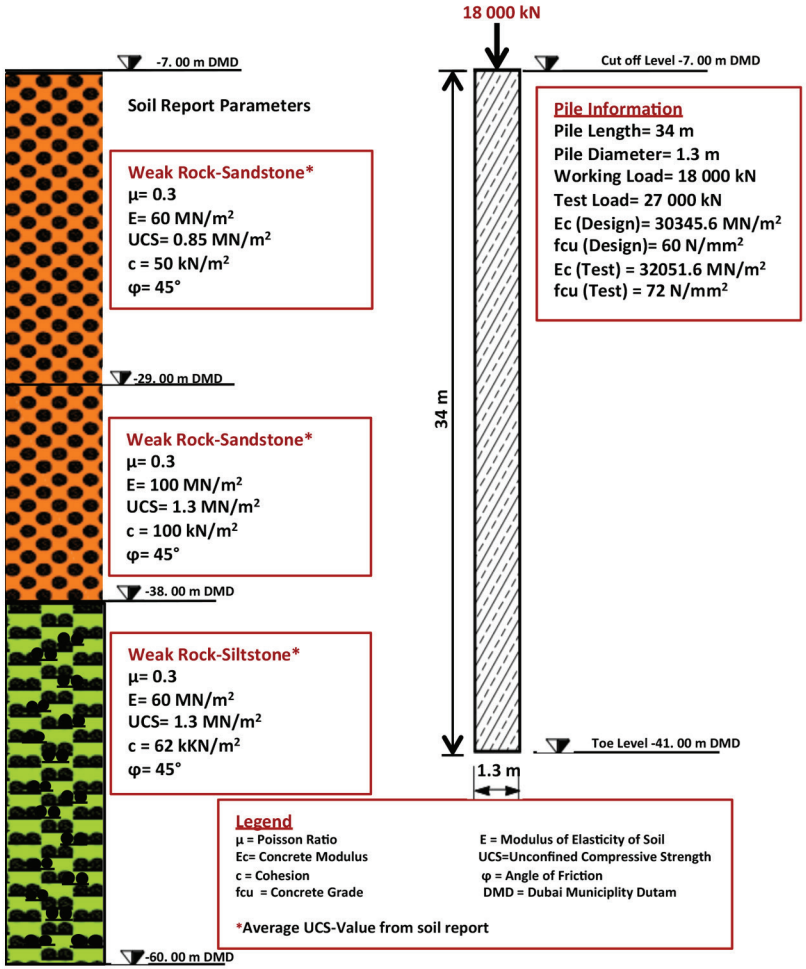

Pile Information
Pile Length= 34 m
Pile Diameter= 1.3 m
Working Load= 18 000 kN
Test Load= 27 000 kN
Ec (Design)= 30345.6 MN/m²
fcu (Design)= 60 N/mm²
Ec (Test) = 32051.6 MN/m²
fcu (Test) = 72 N/mm²

Modelling by using Soil Report Parameters

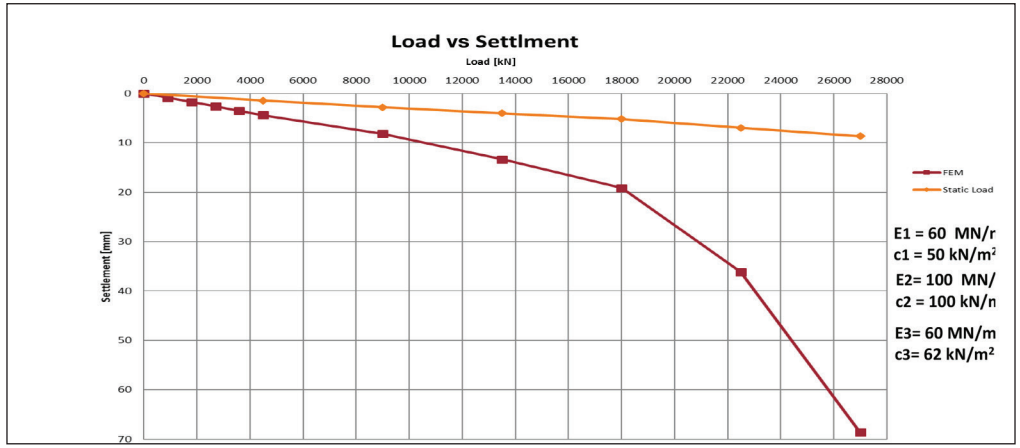

Back-Analysis of Soil Properties from Load Test

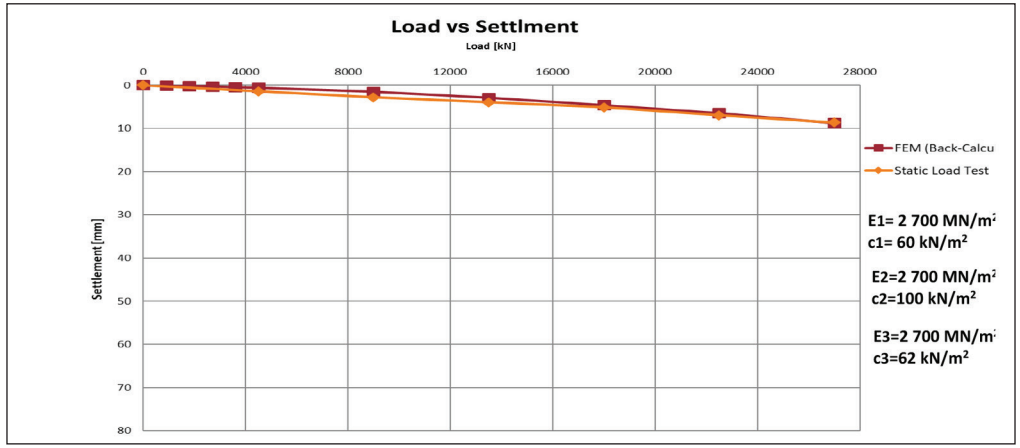

Pile Summary Sheet
P75

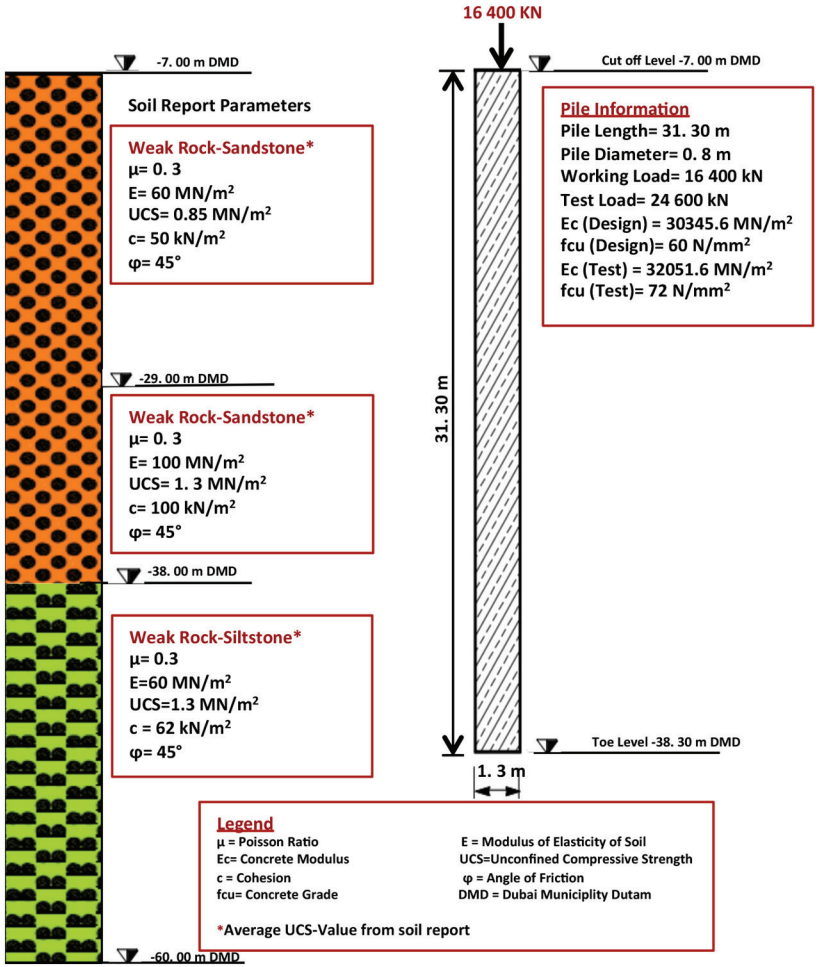

Modelling by using Soil Report Parameters

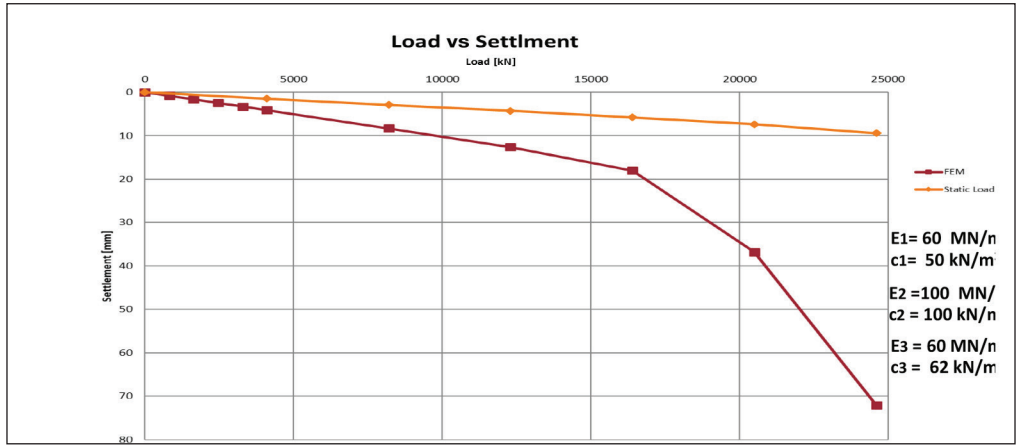

Back-Analysis of Soil Properties from Load Test

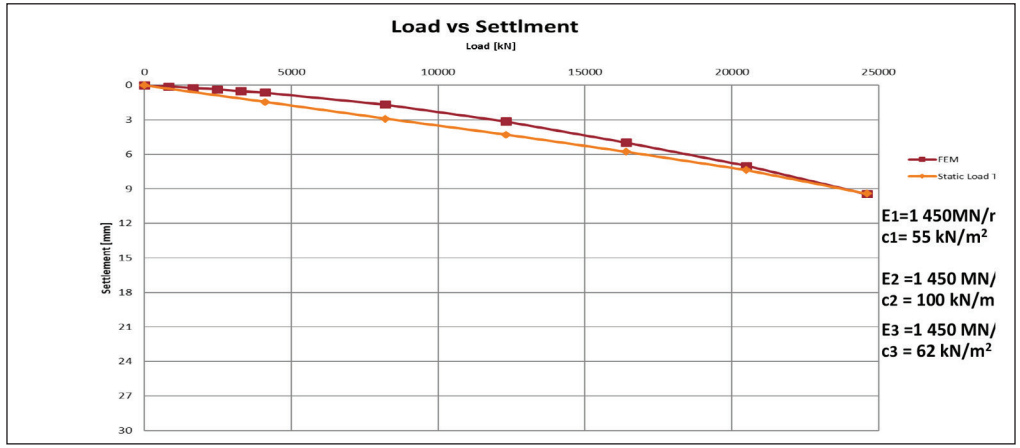

Pile Summary Sheet
P76

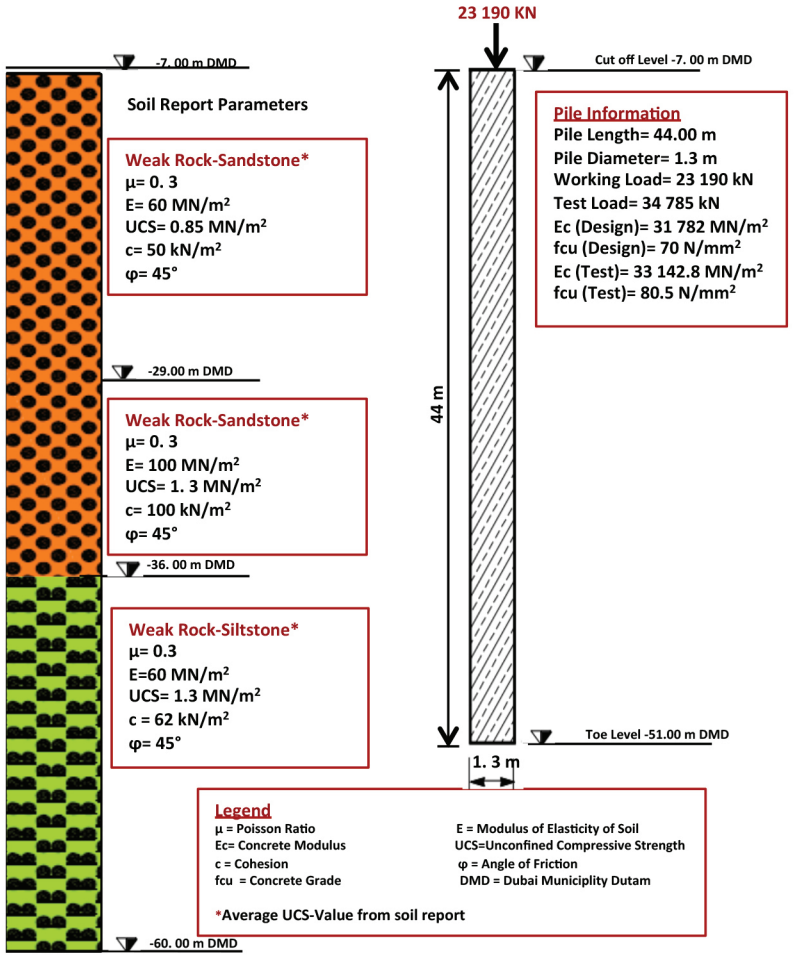

Modelling by using Soil Report Parameters

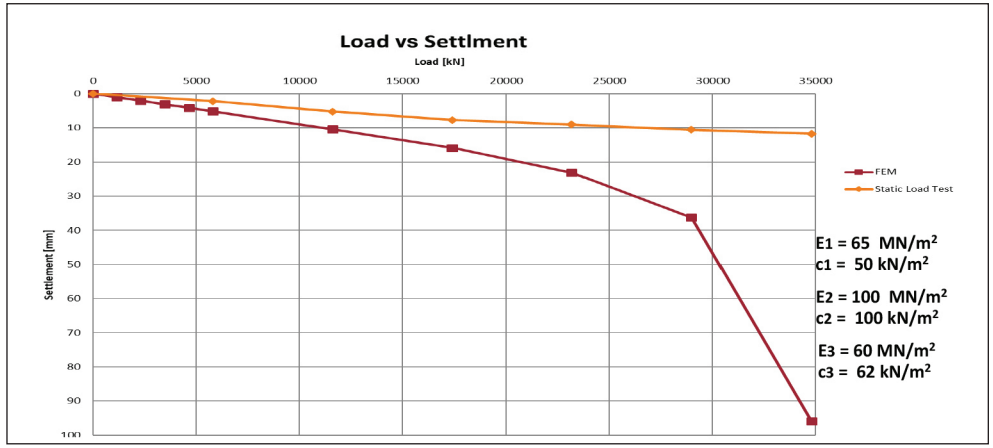

Back-Analysis of Soil Properties from Load Test

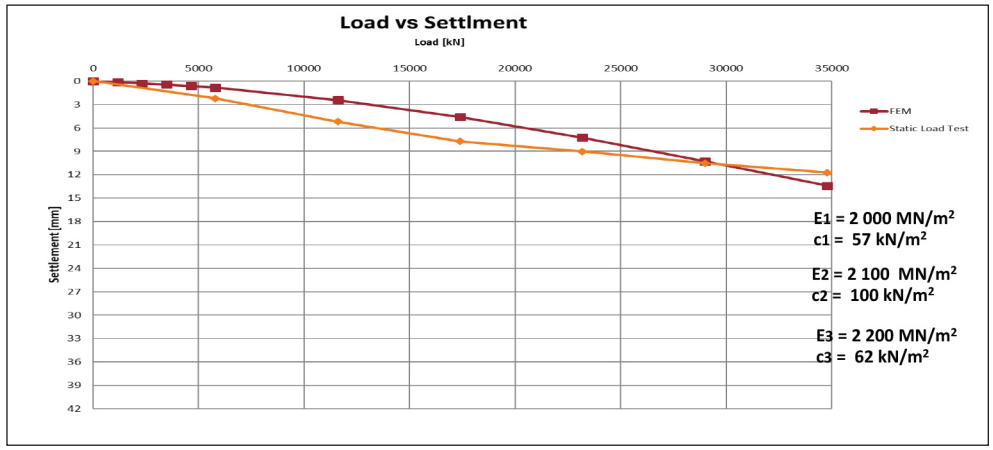

Pile Summary Sheet
P77

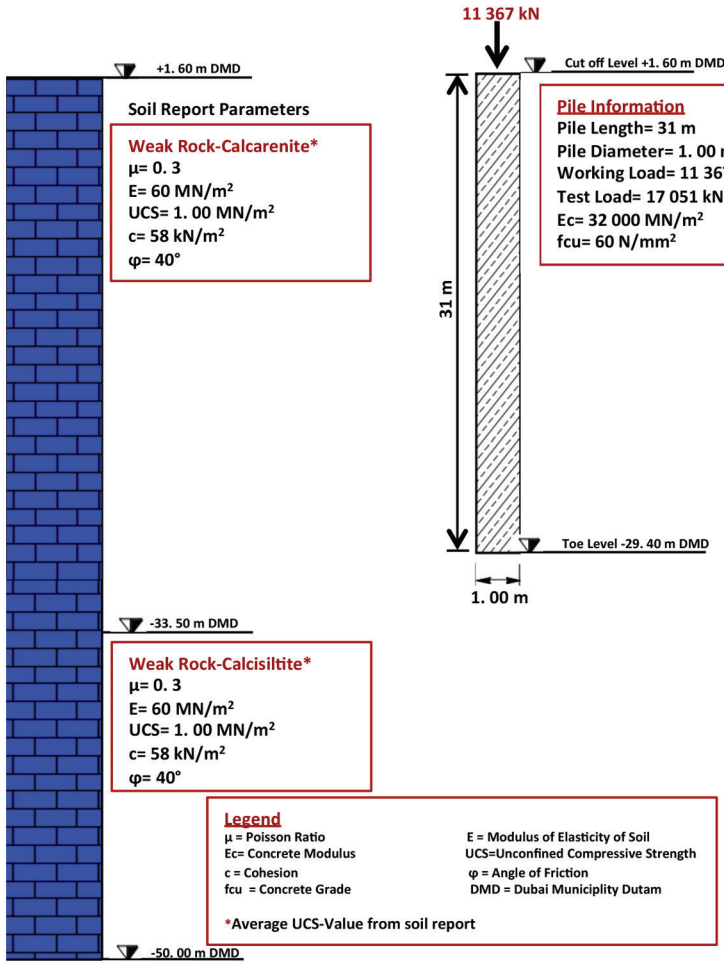

Modelling by using Soil Report Parameters

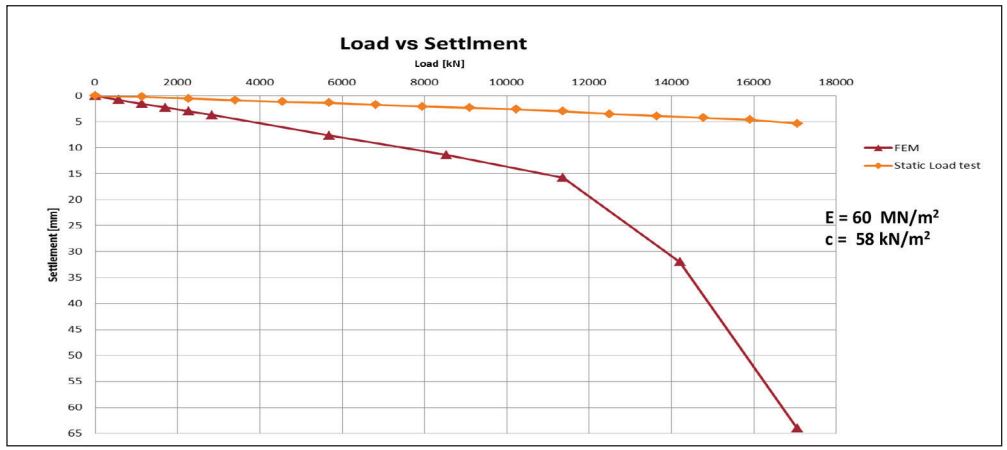

Back-Analysis of Soil Properties from Load Test

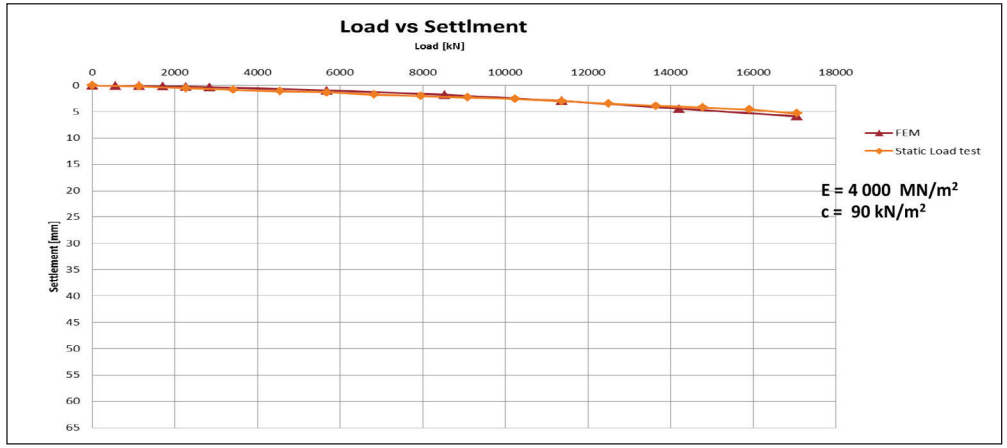

Pile Summary Sheet
P78

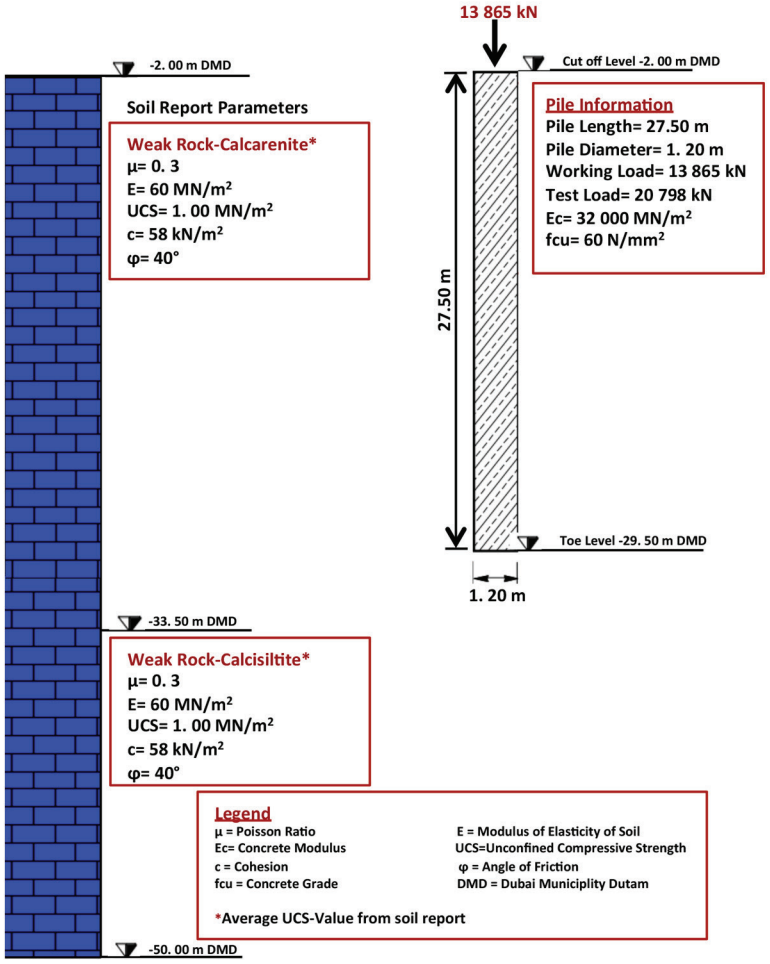

Modelling by using Soil Report Parameters

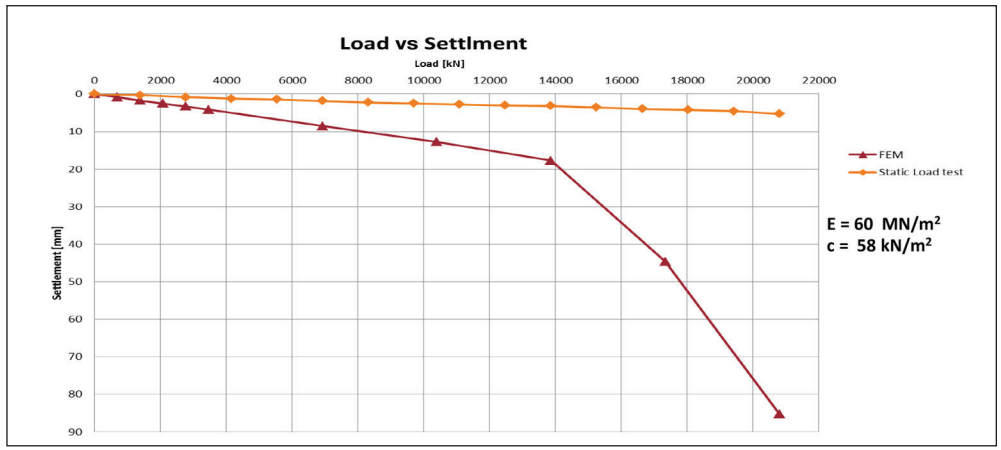

Back-Analysis of Soil Properties from Load Test

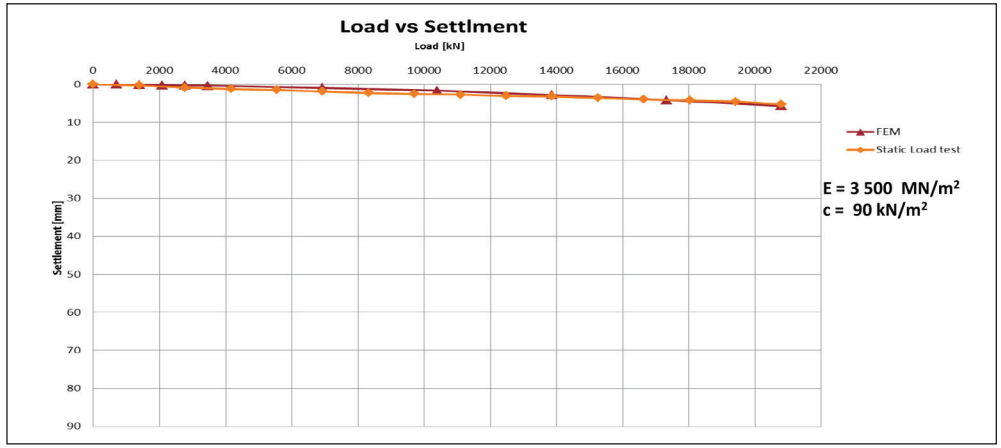

Pile Summary Sheet
P79

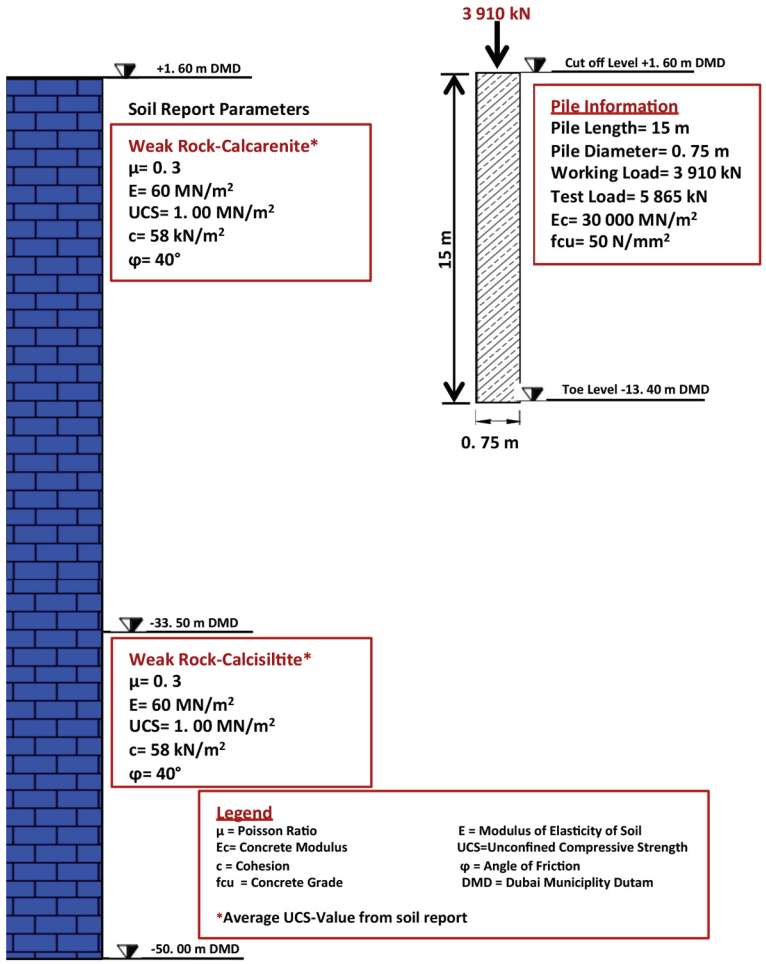

Soil Report Parameters

Weak Rock-Calcarenite*
μ= 0. 3
E= 60 MN/m²
UCS= 1. 00 MN/m²
c= 58 kN/m²
φ= 40°

Pile Information
Pile Length= 15 m
Pile Diameter= 0. 75 m
Working Load= 3 910 kN
Test Load= 5 865 kN
Ec= 30 000 MN/m²
fcu= 50 N/mm²

Weak Rock-Calcisiltite*
μ= 0. 3
E= 60 MN/m²
UCS= 1. 00 MN/m²
c= 58 kN/m²
φ= 40°

Legend

μ = Poisson Ratio	E = Modulus of Elasticity of Soil
Ec= Concrete Modulus	UCS=Unconfined Compressive Strength
c = Cohesion	φ = Angle of Friction
fcu = Concrete Grade	DMD = Dubai Municiplity Dutam

*Average UCS-Value from soil report

Modelling by using Soil Report Parameters

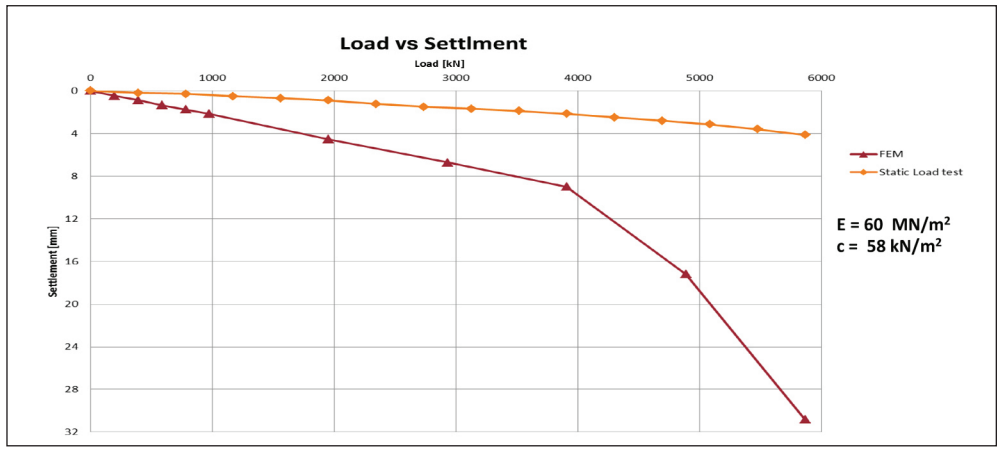

Back-Analysis of Soil Properties from Load Test

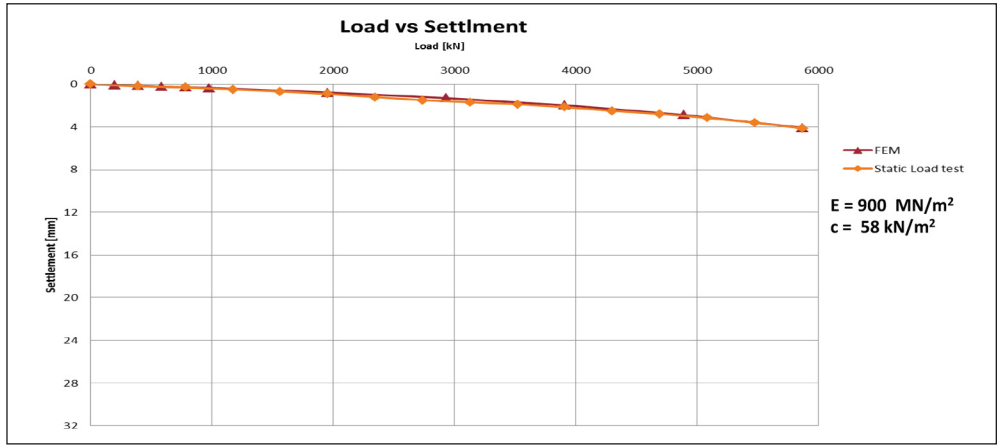

Pile Summary Sheet
P80

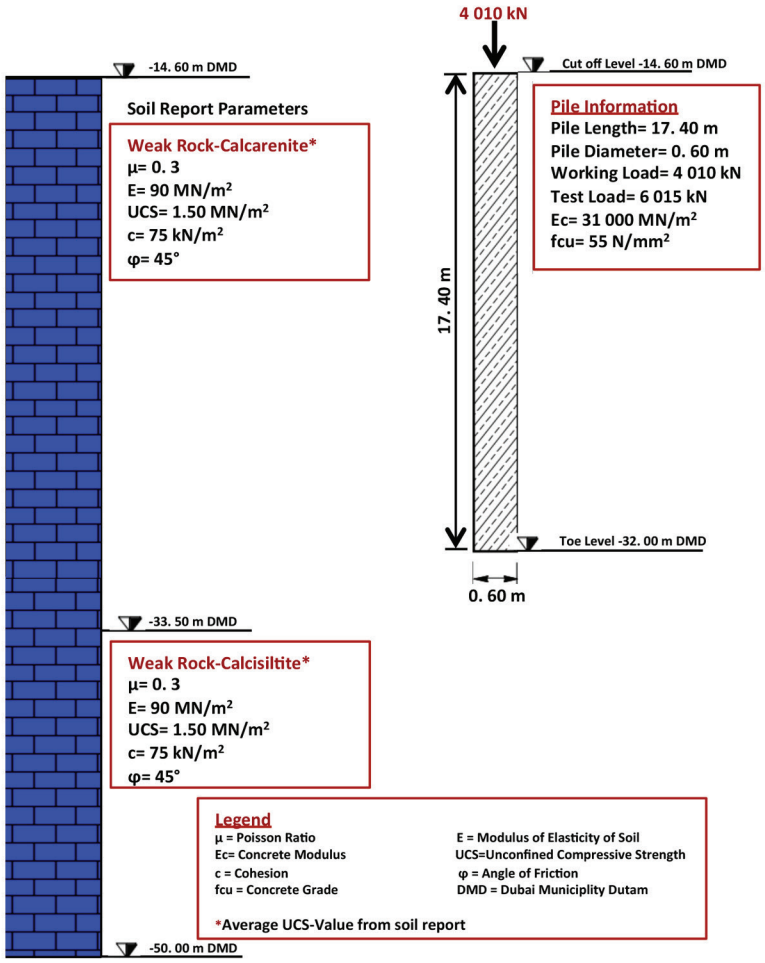

Modelling by using Soil Report Parameters

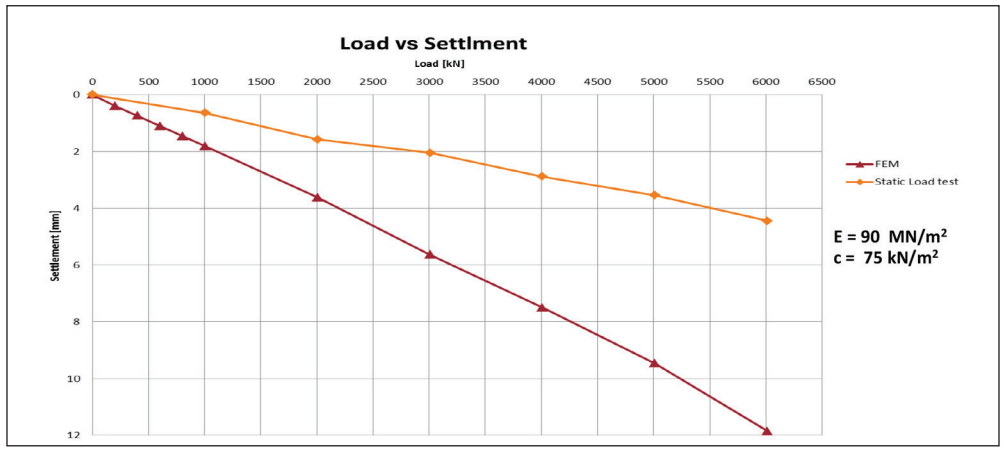

Back-Analysis of Soil Properties from Load Test

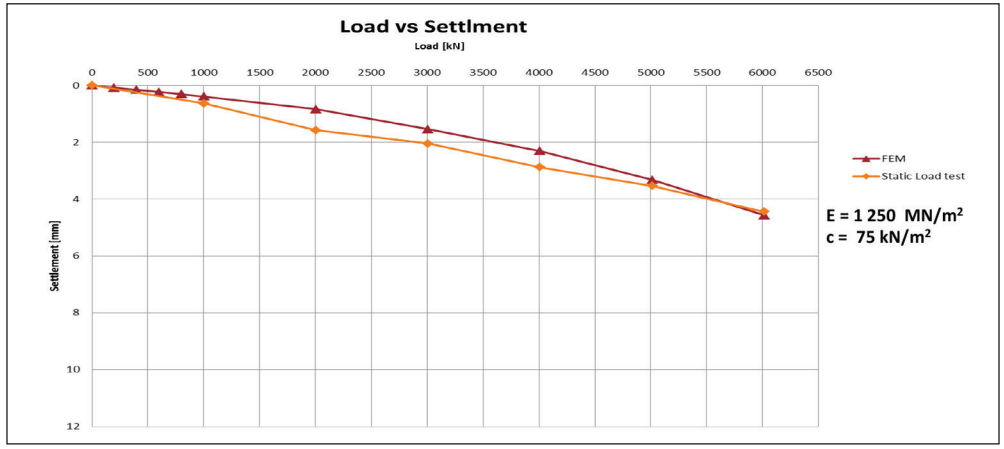

Pile Summary Sheet
P81

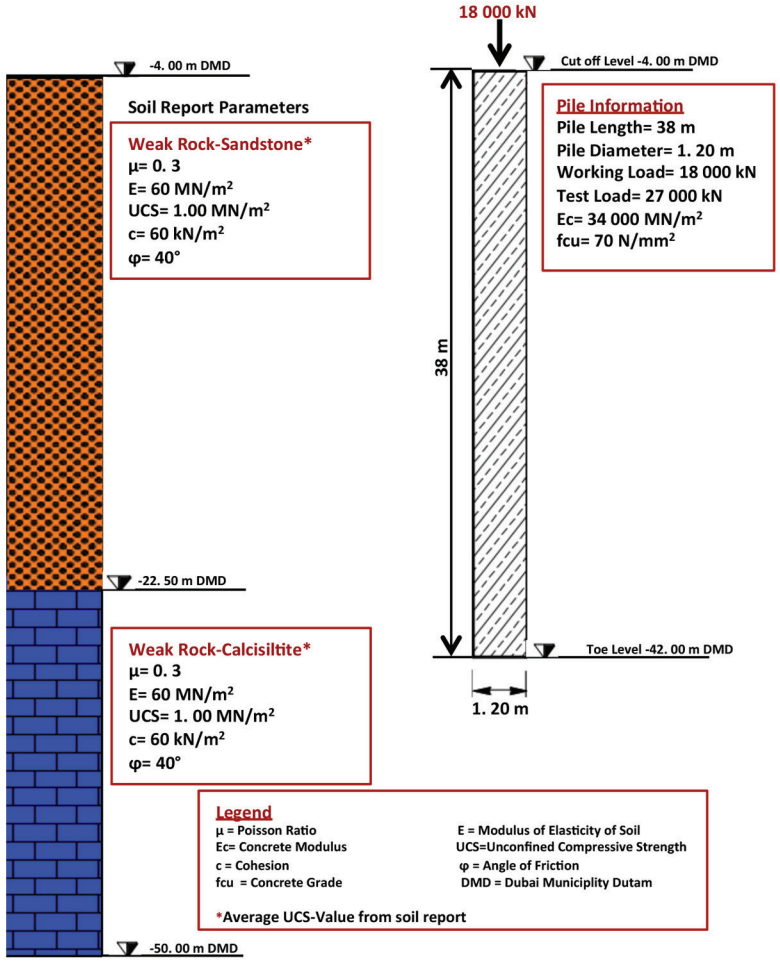

Modelling by using Soil Report Parameters

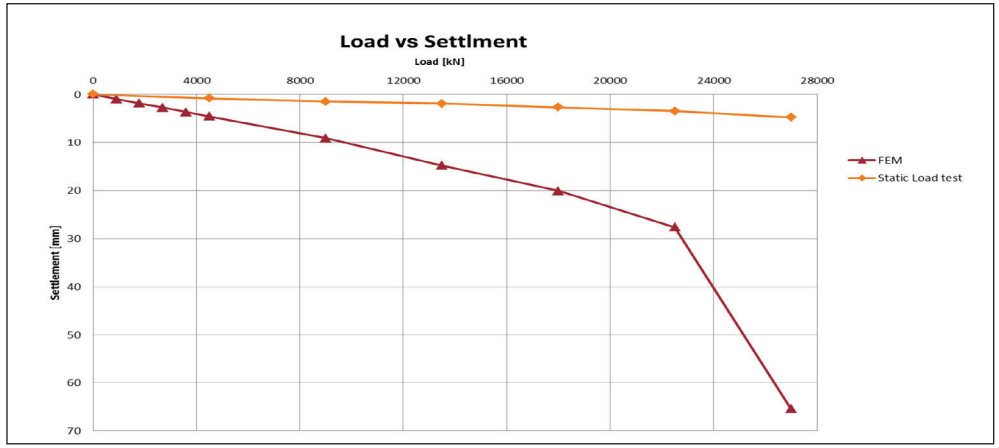

Back-Analysis of Soil Properties from Load Test

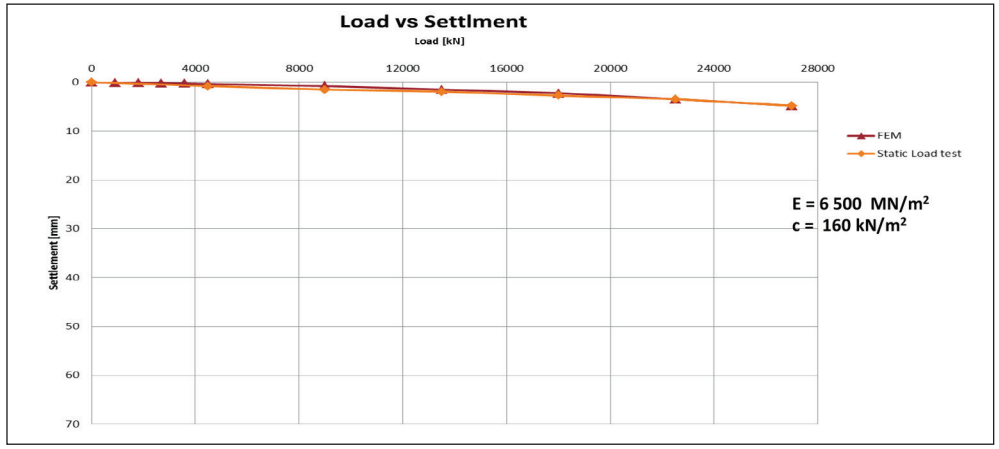

Pile Summary Sheet
P82

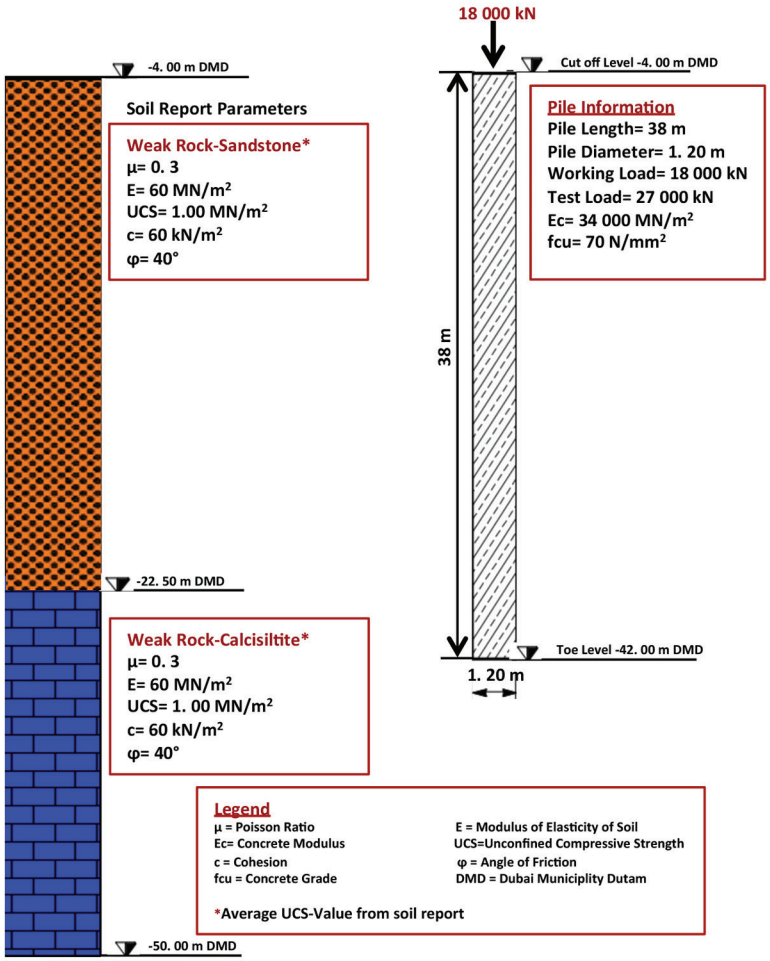

Modelling by using Soil Report Parameters

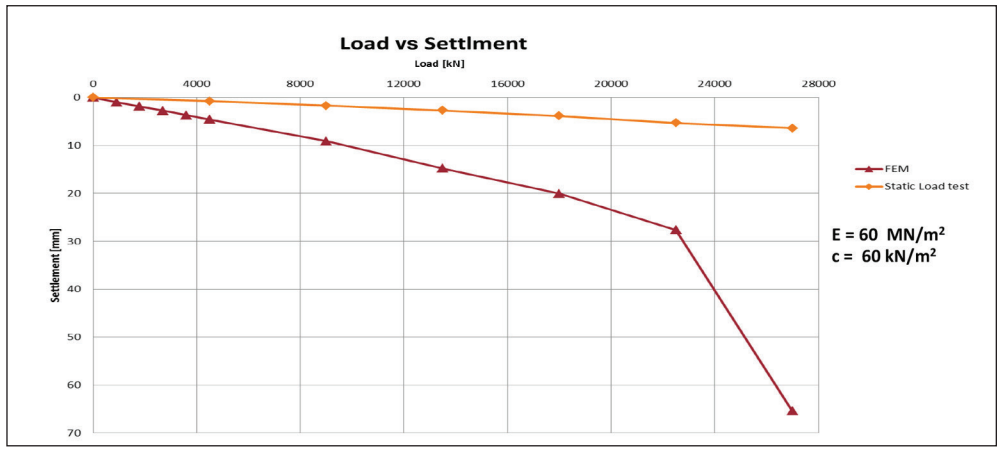

Back-Analysis of Soil Properties from Load Test

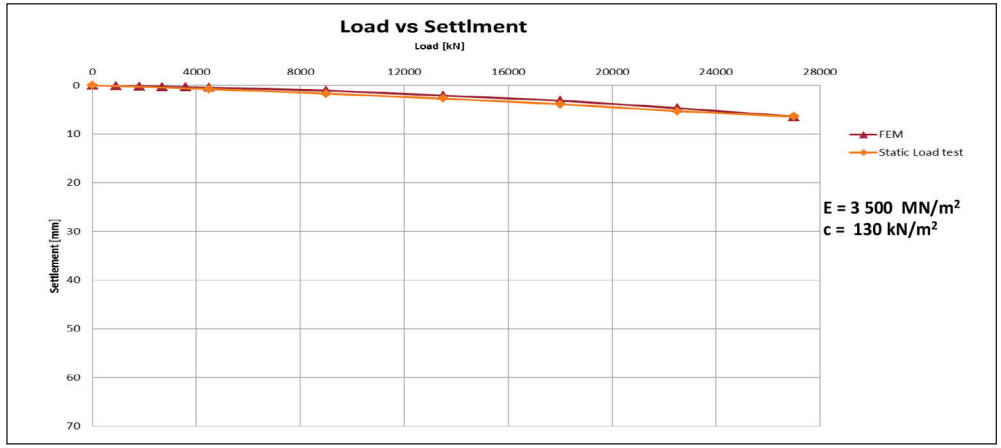

Pile Summary Sheet
P83

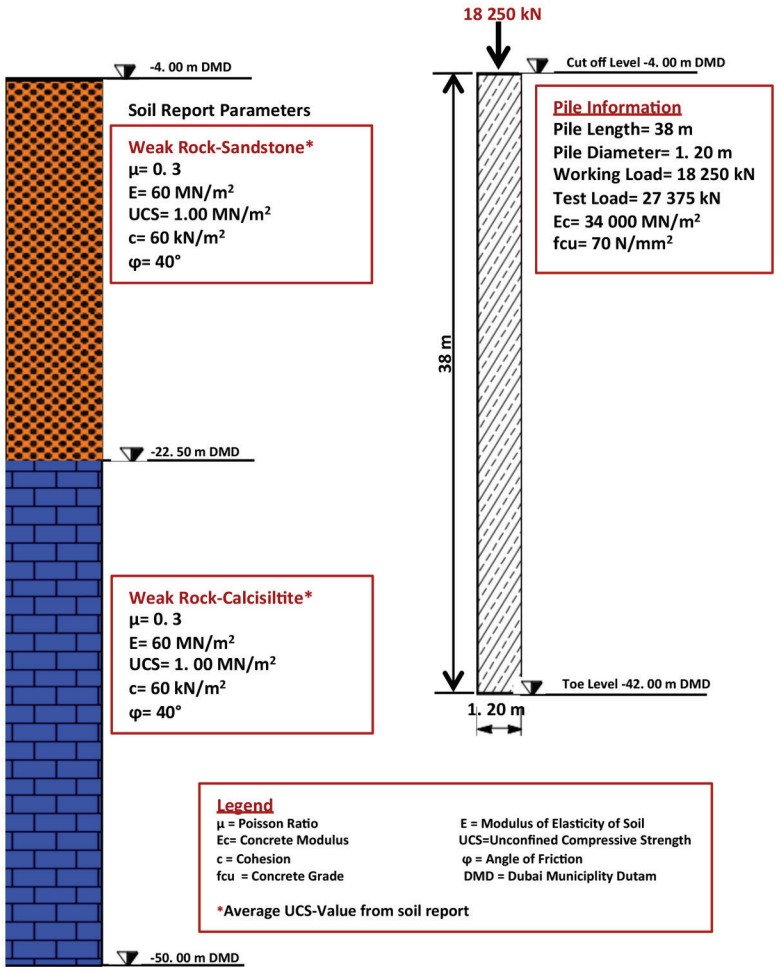

Modelling by using Soil Report Parameters

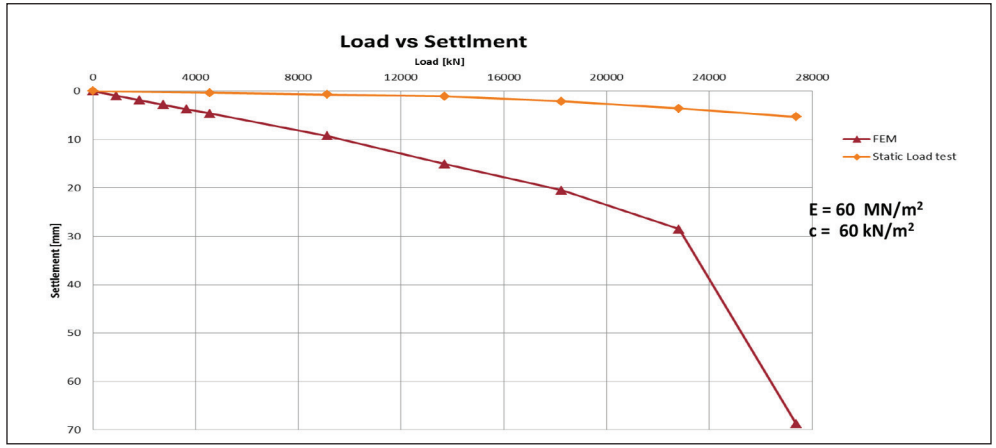

Back-Analysis of Soil Properties from Load Test

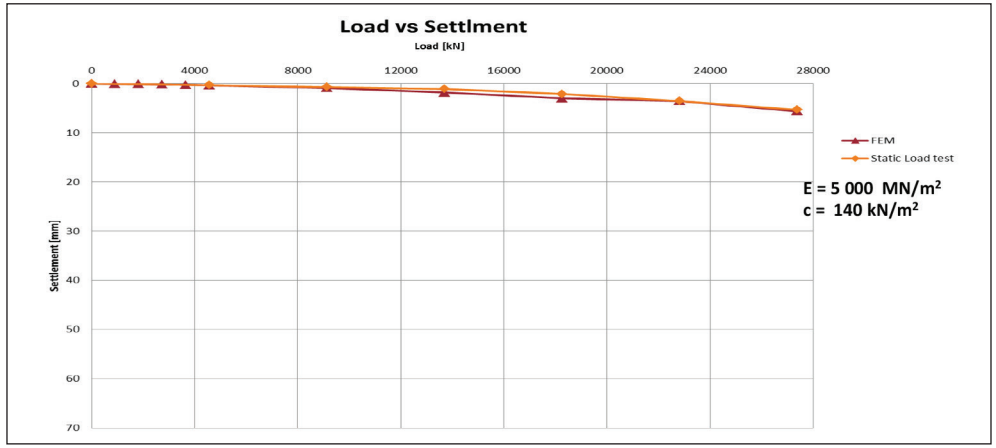

Pile Summary Sheet
P84

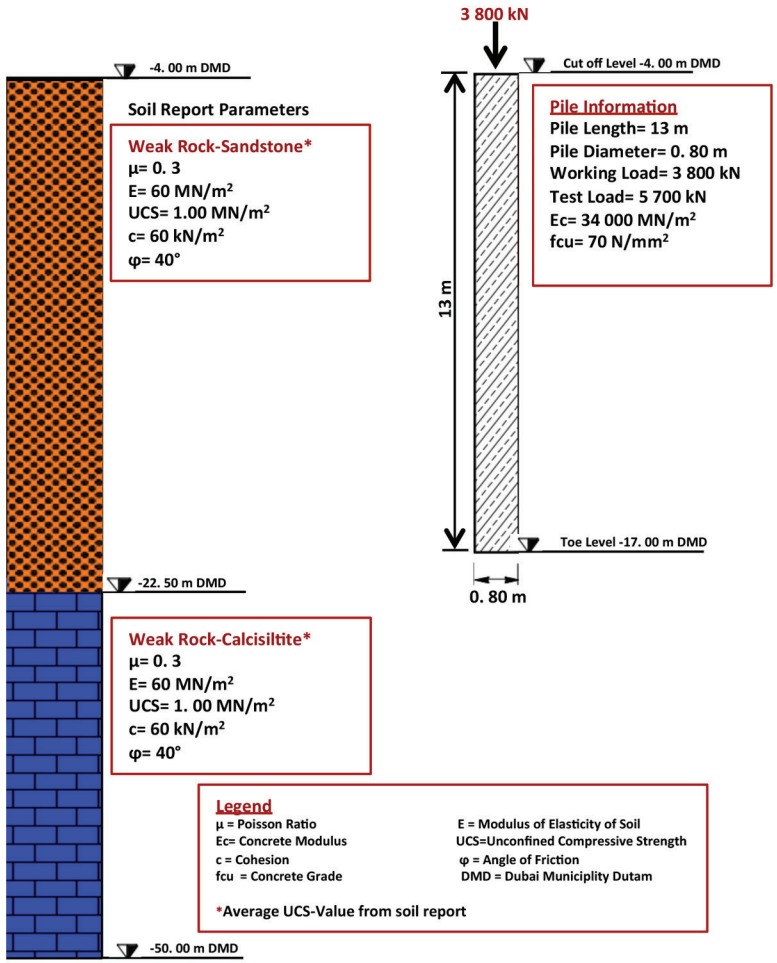

Modelling by using Soil Report Parameters

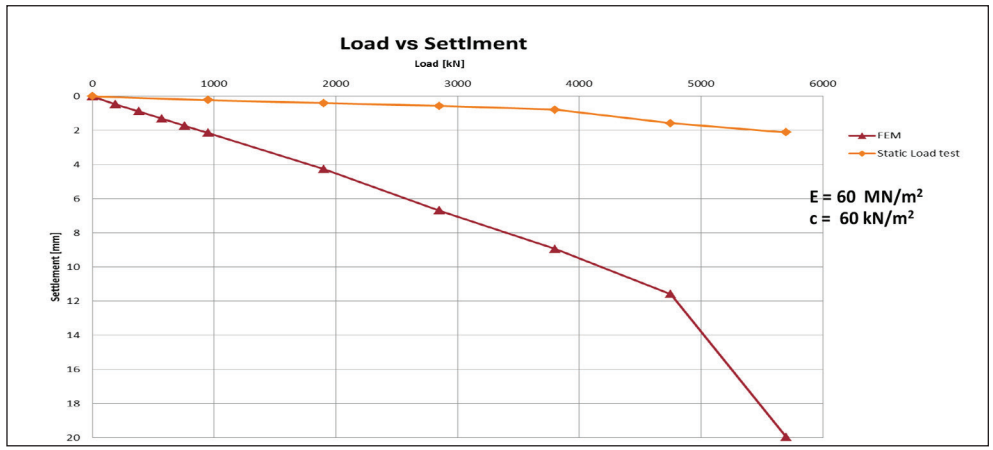

Back-Analysis of Soil Properties from Load Test

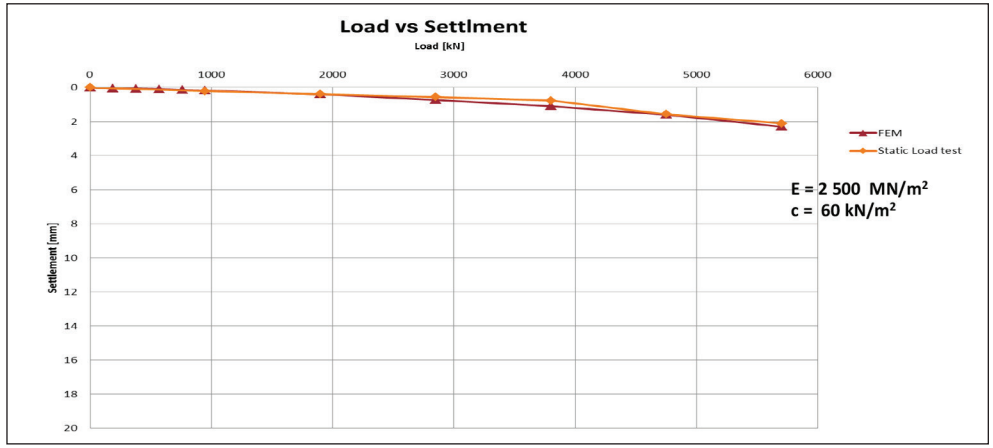

Pile Summary Sheet
P85

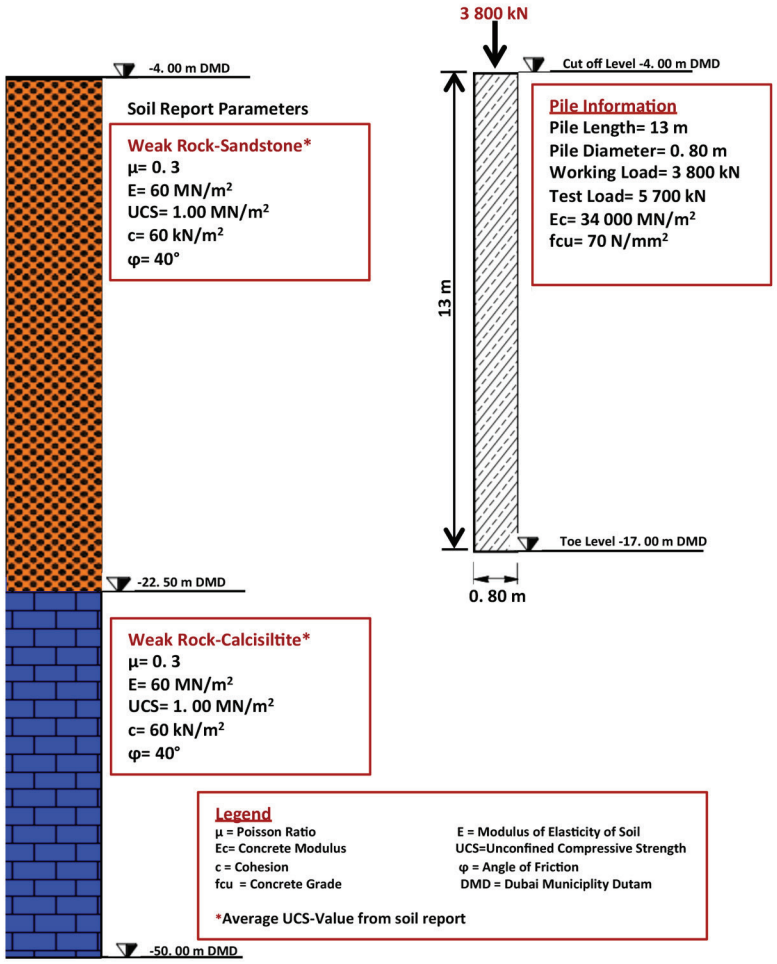

Soil Report Parameters

Weak Rock-Sandstone*
μ= 0. 3
E= 60 MN/m²
UCS= 1.00 MN/m²
c= 60 kN/m²
φ= 40°

Pile Information
Pile Length= 13 m
Pile Diameter= 0. 80 m
Working Load= 3 800 kN
Test Load= 5 700 kN
Ec= 34 000 MN/m²
fcu= 70 N/mm²

Weak Rock-Calcisiltite*
μ= 0. 3
E= 60 MN/m²
UCS= 1. 00 MN/m²
c= 60 kN/m²
φ= 40°

Legend

μ = Poisson Ratio	E = Modulus of Elasticity of Soil
Ec= Concrete Modulus	UCS=Unconfined Compressive Strength
c = Cohesion	φ = Angle of Friction
fcu = Concrete Grade	DMD = Dubai Municiplity Dutam

*Average UCS-Value from soil report

Modelling by using Soil Report Parameters

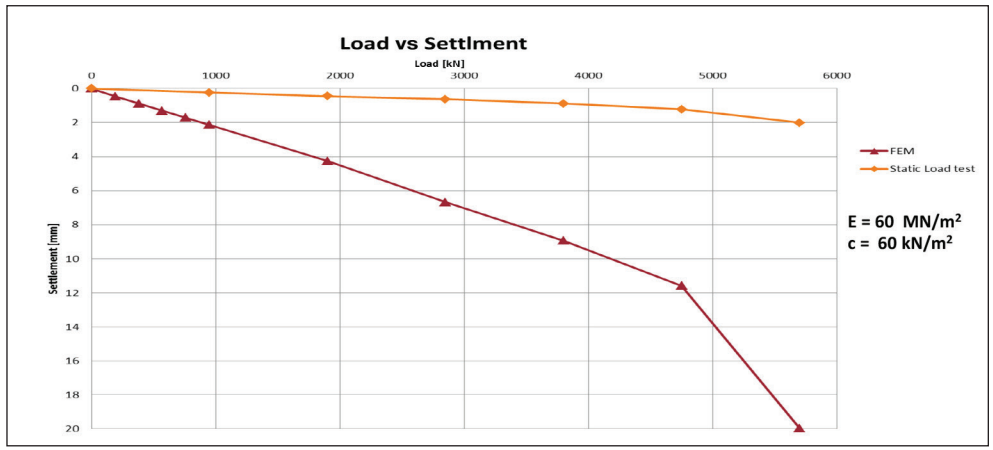

Back-Analysis of Soil Properties from Load Test

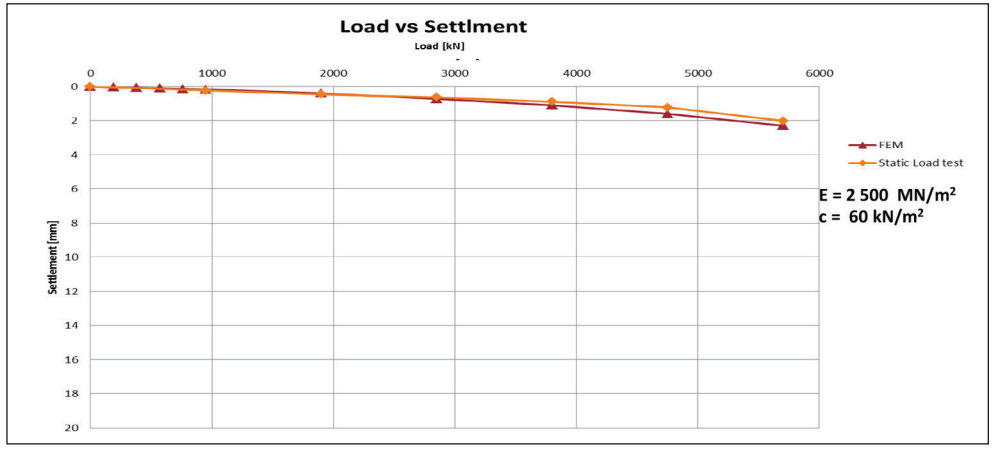

Pile Summary Sheet
P86

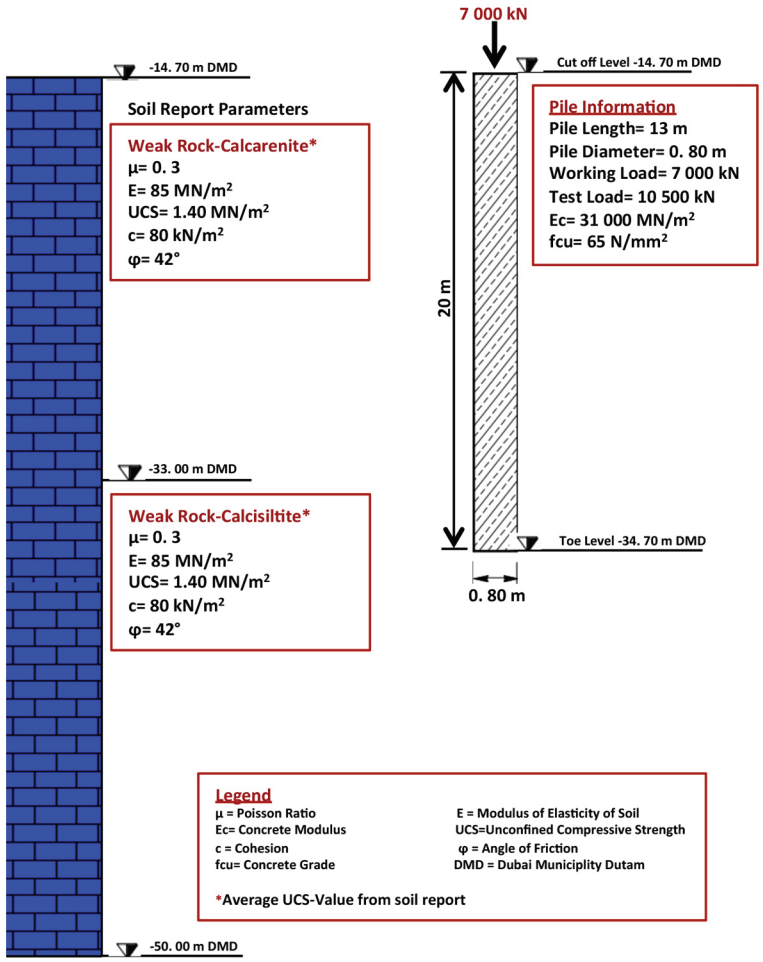

Soil Report Parameters

Weak Rock-Calcarenite*
μ= 0. 3
E= 85 MN/m²
UCS= 1.40 MN/m²
c= 80 kN/m²
φ= 42°

Weak Rock-Calcisiltite*
μ= 0. 3
E= 85 MN/m²
UCS= 1.40 MN/m²
c= 80 kN/m²
φ= 42°

Pile Information
Pile Length= 13 m
Pile Diameter= 0. 80 m
Working Load= 7 000 kN
Test Load= 10 500 kN
Ec= 31 000 MN/m²
fcu= 65 N/mm²

Legend

μ = Poisson Ratio	E = Modulus of Elasticity of Soil
Ec= Concrete Modulus	UCS=Unconfined Compressive Strength
c = Cohesion	φ = Angle of Friction
fcu= Concrete Grade	DMD = Dubai Municiplity Dutam

*Average UCS-Value from soil report

Modelling by using Soil Report Parameters

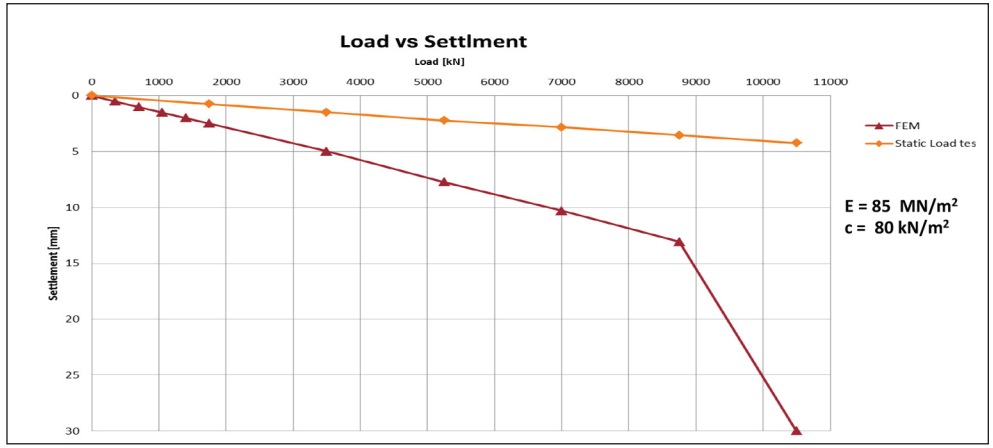

Back-Analysis of Soil Properties from Load Test

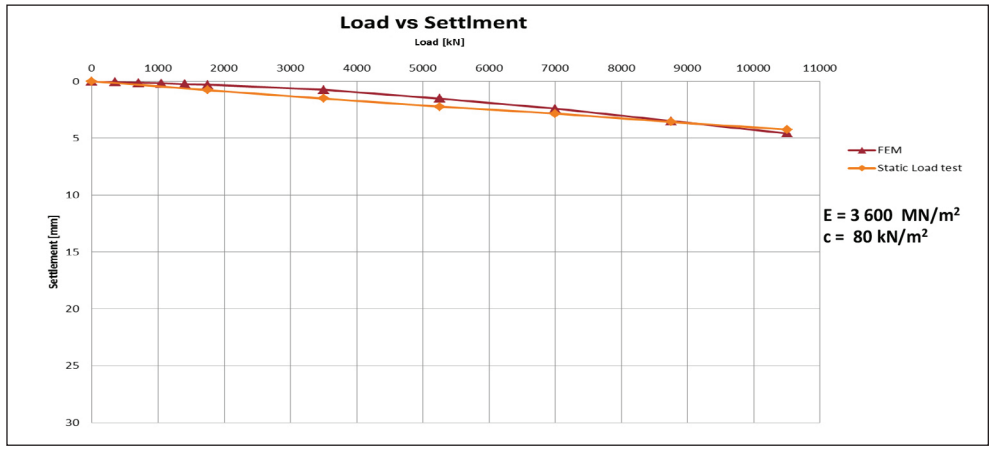

Pile Summary Sheet
P87

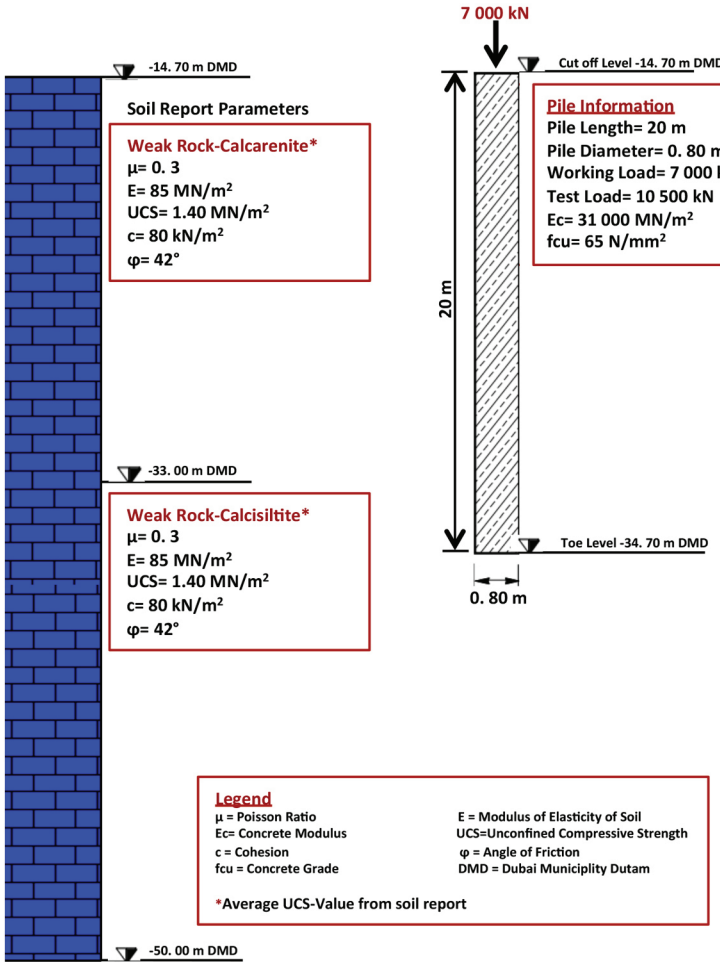

Soil Report Parameters

Weak Rock-Calcarenite*
- μ= 0. 3
- E= 85 MN/m²
- UCS= 1.40 MN/m²
- c= 80 kN/m²
- φ= 42°

Weak Rock-Calcisiltite*
- μ= 0. 3
- E= 85 MN/m²
- UCS= 1.40 MN/m²
- c= 80 kN/m²
- φ= 42°

Pile Information
- Pile Length= 20 m
- Pile Diameter= 0. 80 m
- Working Load= 7 000 kN
- Test Load= 10 500 kN
- Ec= 31 000 MN/m²
- fcu= 65 N/mm²

Legend

μ = Poisson Ratio	E = Modulus of Elasticity of Soil
Ec= Concrete Modulus	UCS=Unconfined Compressive Strength
c = Cohesion	φ = Angle of Friction
fcu = Concrete Grade	DMD = Dubai Municiplity Dutam

*Average UCS-Value from soil report

Modelling by using Soil Report Parameters

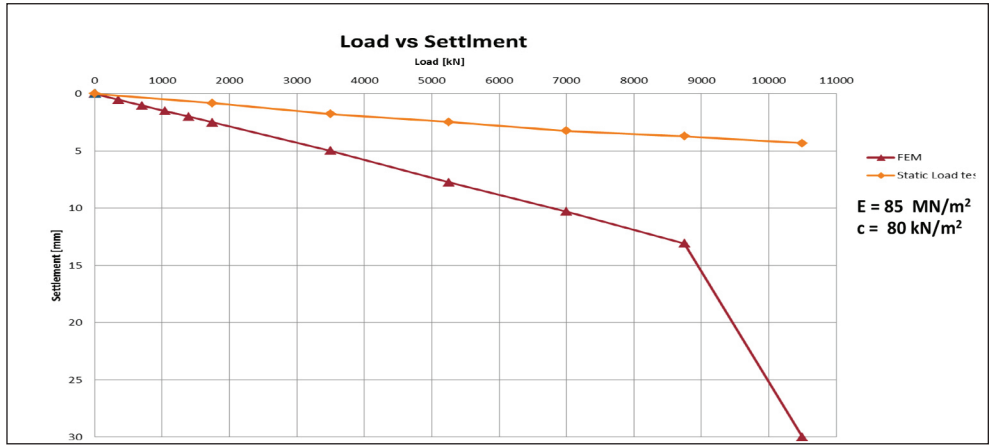

Back-Analysis of Soil Properties from Load Test

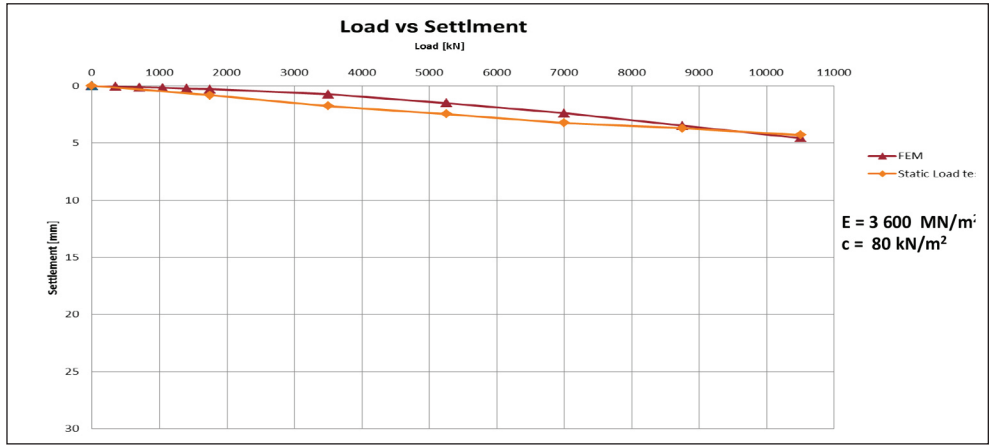

Pile Summary Sheet
P88

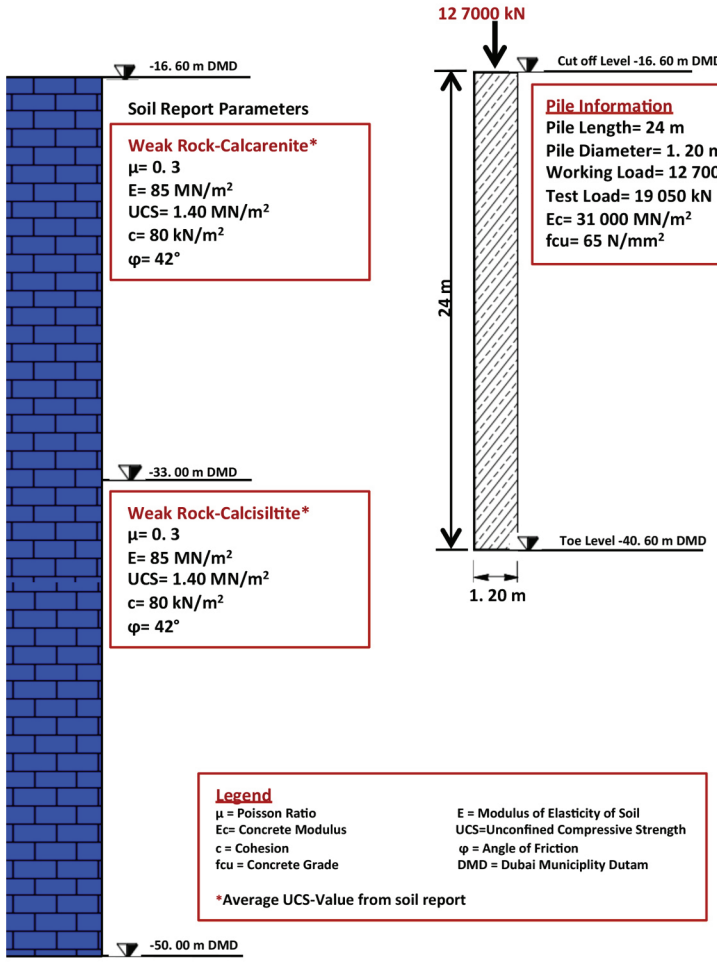

Modelling by using Soil Report Parameters

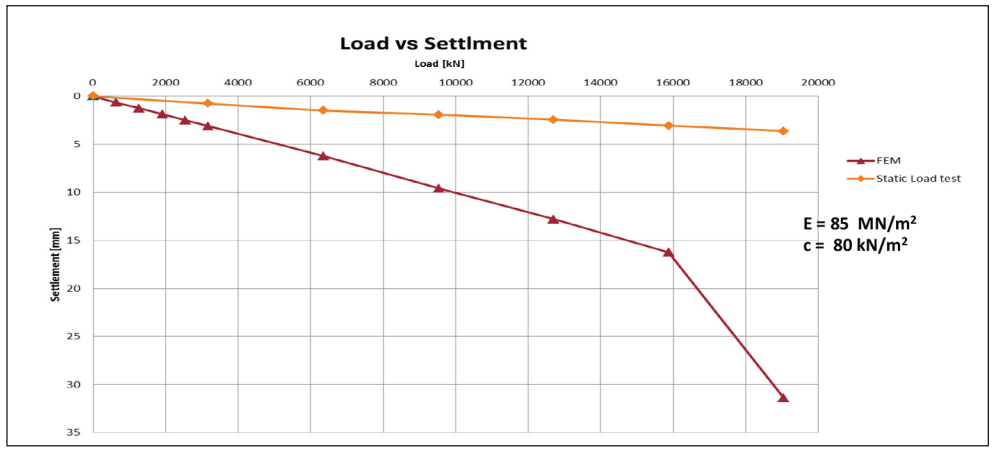

Back-Analysis of Soil Properties from Load Test

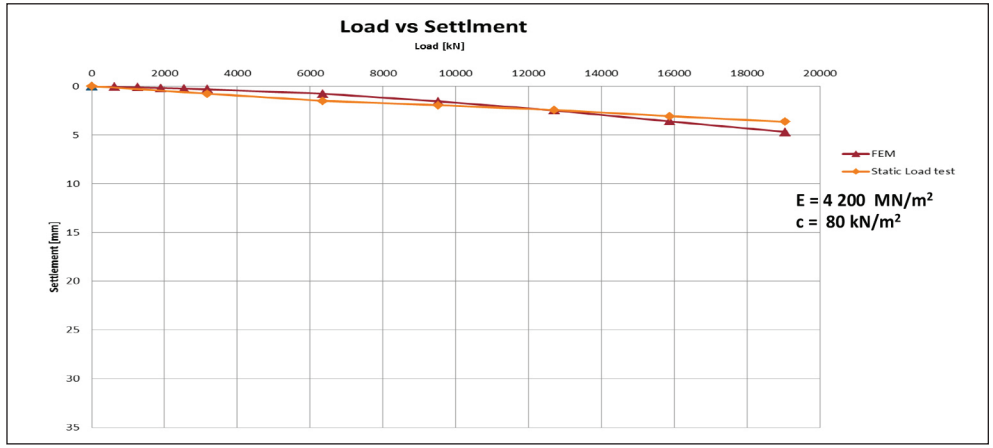

Pile Summary Sheet
P89

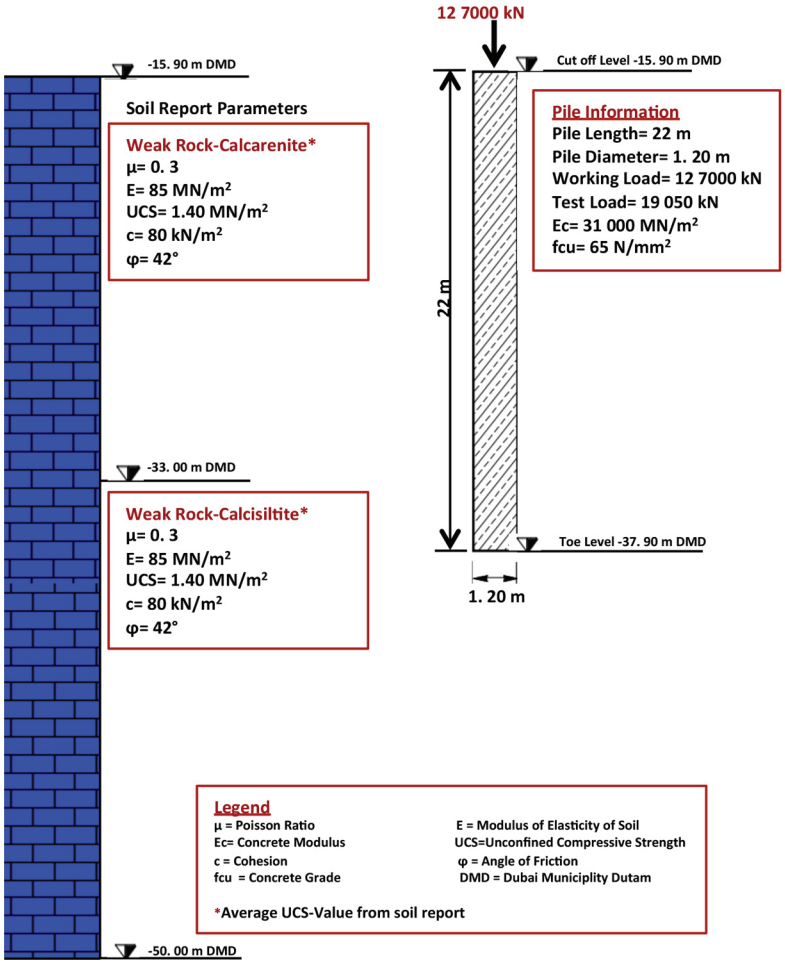

Modelling by using Soil Report Parameters

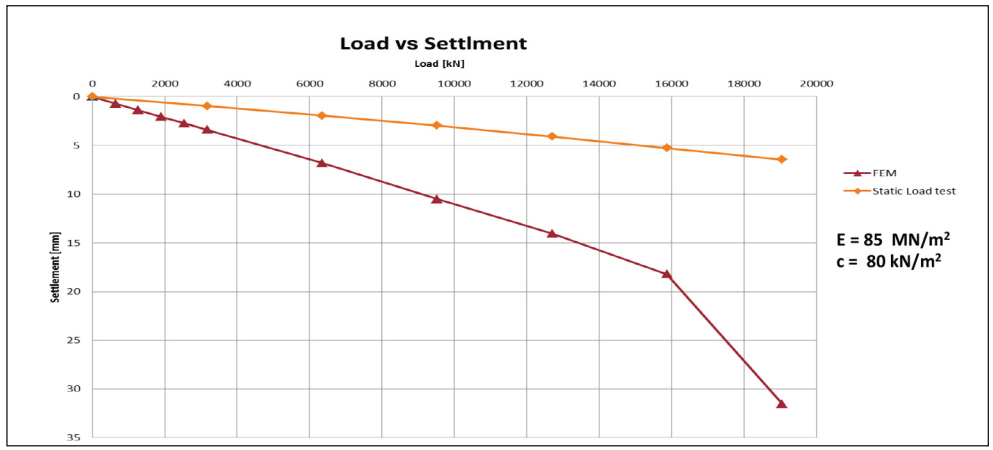

Back-Analysis of Soil Properties from Load Test

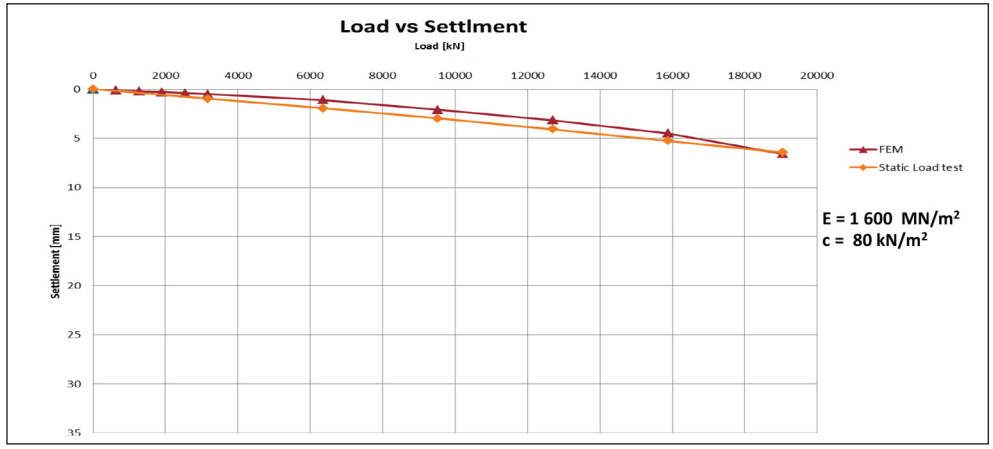

Pile Summary Sheet
P90

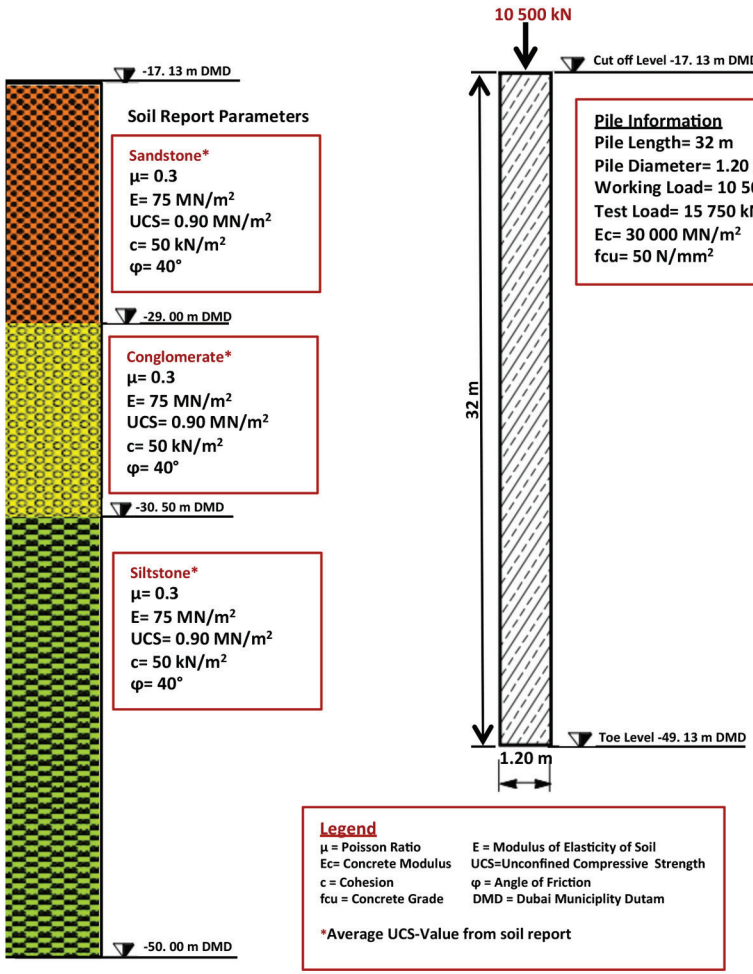

Pile Information
Pile Length= 32 m
Pile Diameter= 1.20 m
Working Load= 10 500 kN
Test Load= 15 750 kN
Ec= 30 000 MN/m²
fcu= 50 N/mm²

Legend

μ = Poisson Ratio	E = Modulus of Elasticity of Soil
Ec= Concrete Modulus	UCS=Unconfined Compressive Strength
c = Cohesion	φ = Angle of Friction
fcu = Concrete Grade	DMD = Dubai Municiplity Dutam

*Average UCS-Value from soil report

Modelling by using Soil Report Parameters

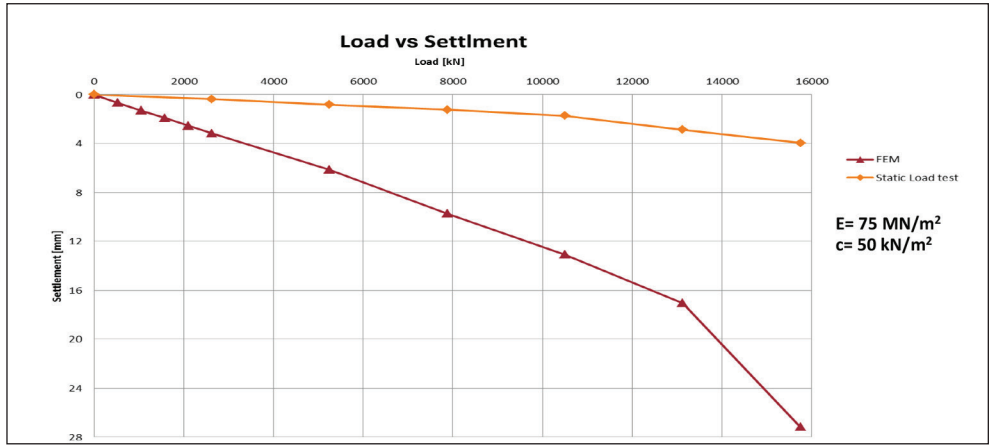

Back-Analysis of Soil Properties from Load Test

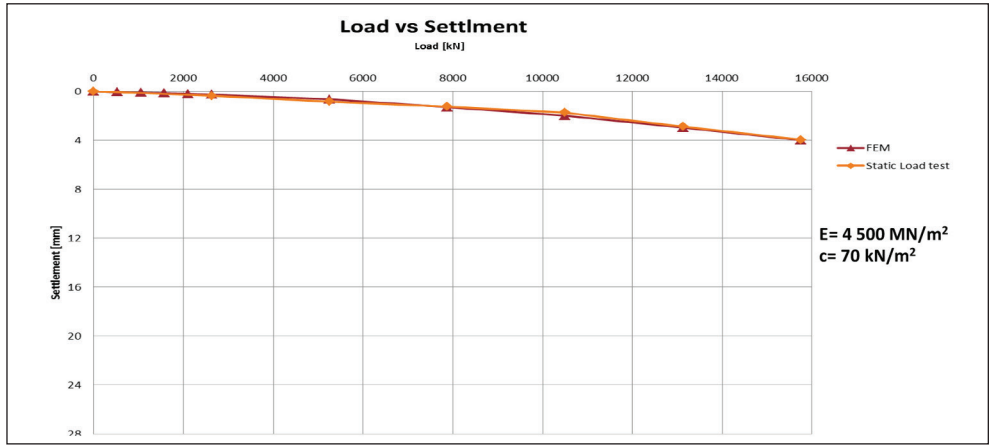

Pile Summary Sheet
P91

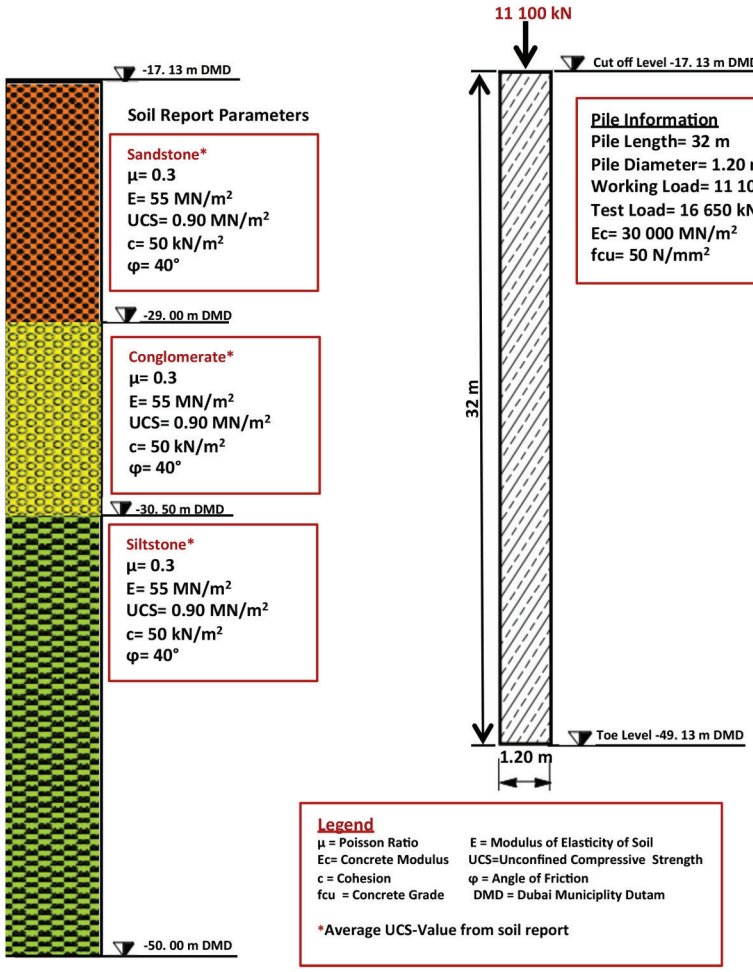

Modelling by using Soil Report Parameters

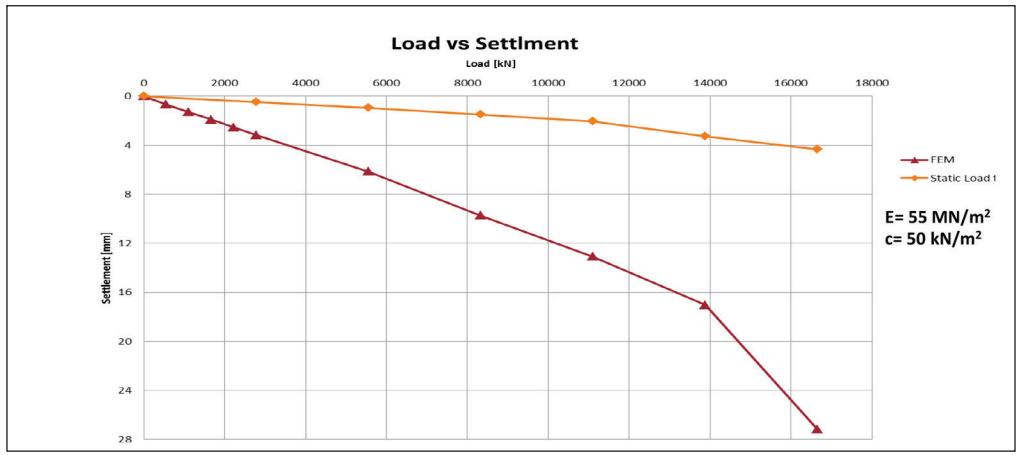

Back-Analysis of Soil Properties from Load Test

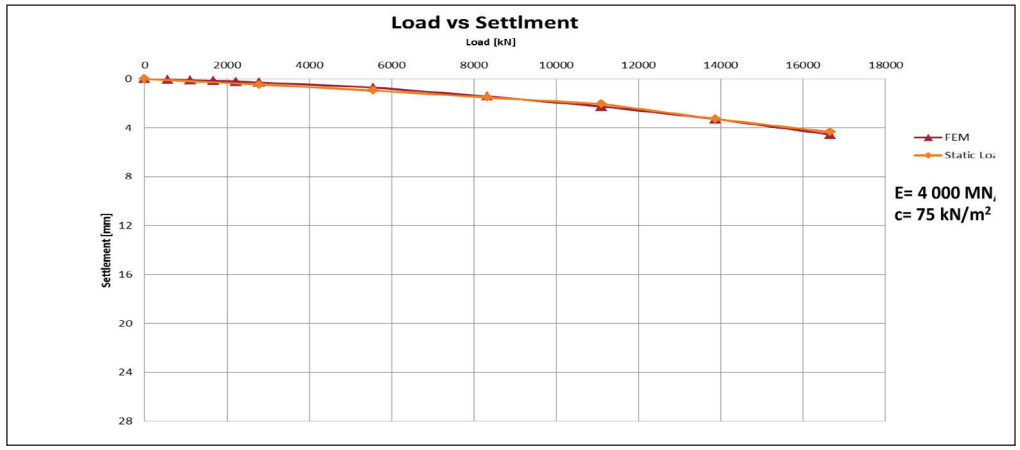

Pile Summary Sheet
P92

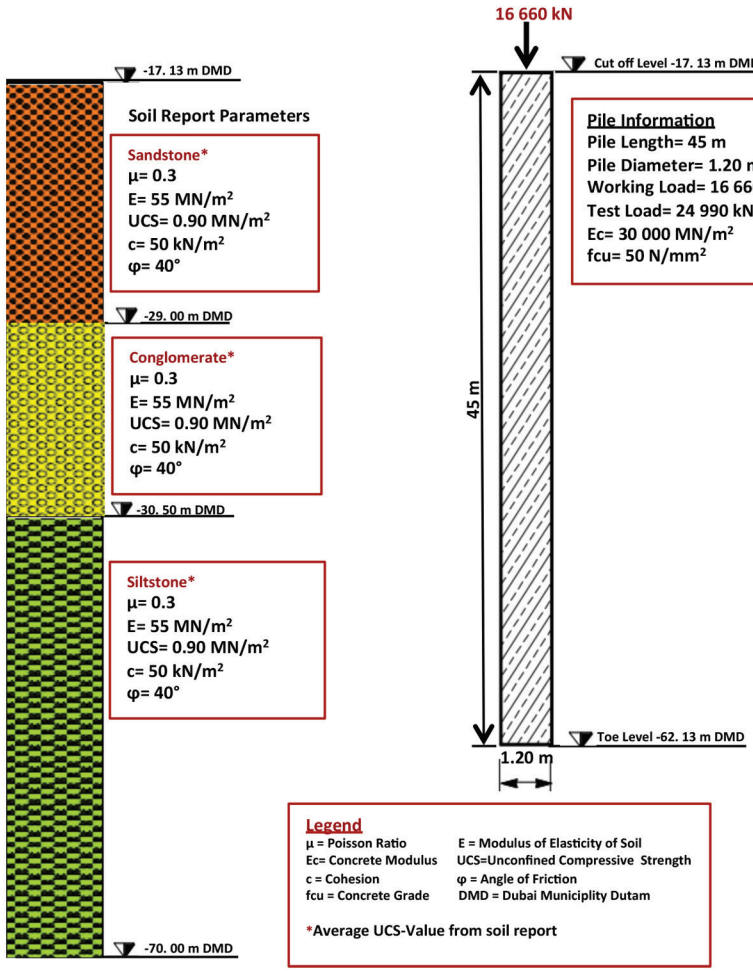

Modelling by using Soil Report Parameters

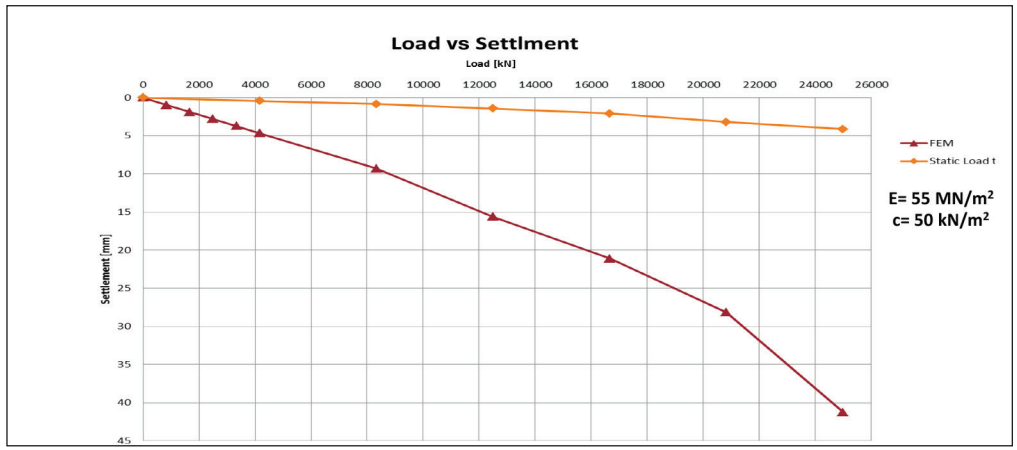

Back-Analysis of Soil Properties from Load Test

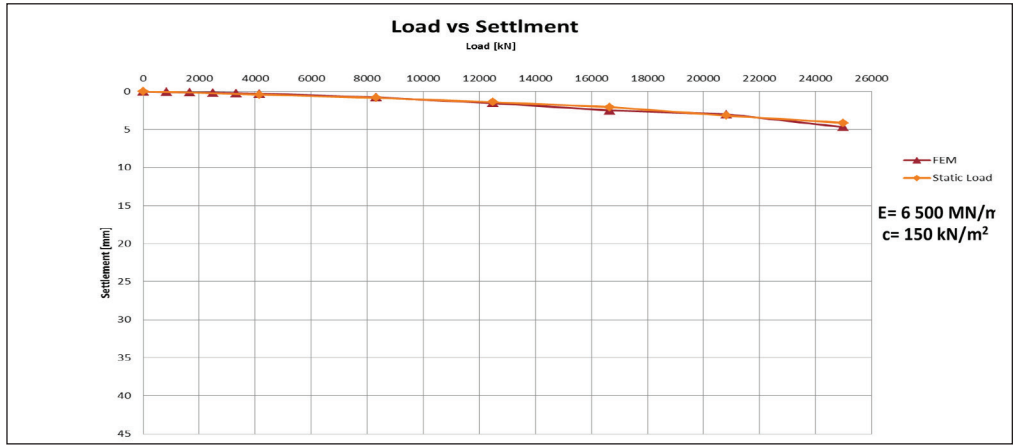

Pile Summary Sheet
P93

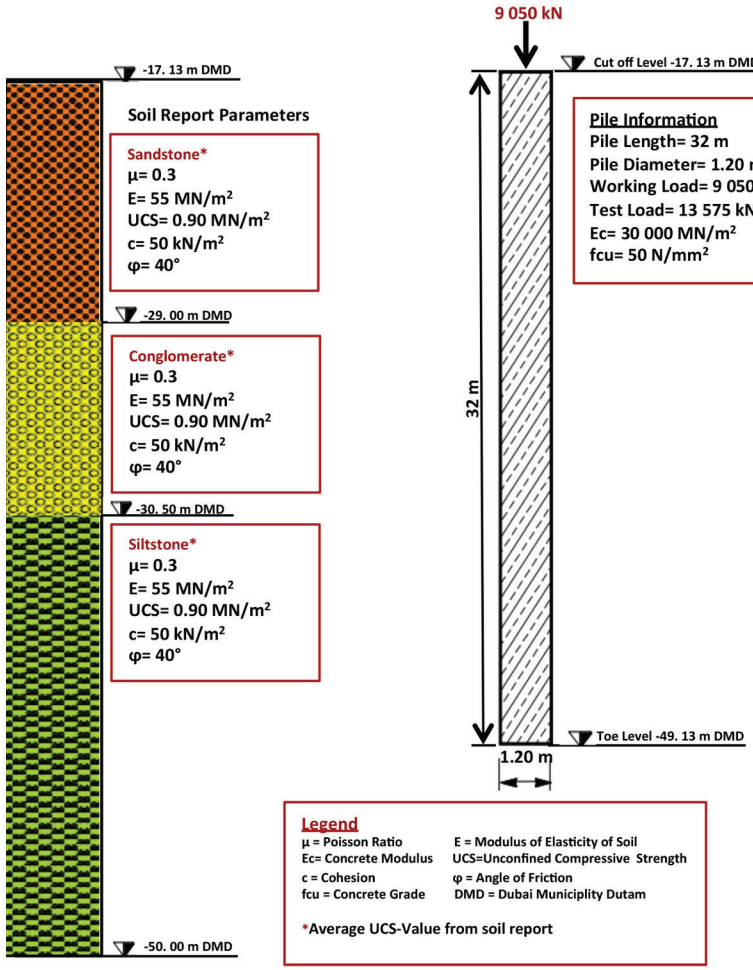

Modelling by using Soil Report Parameters

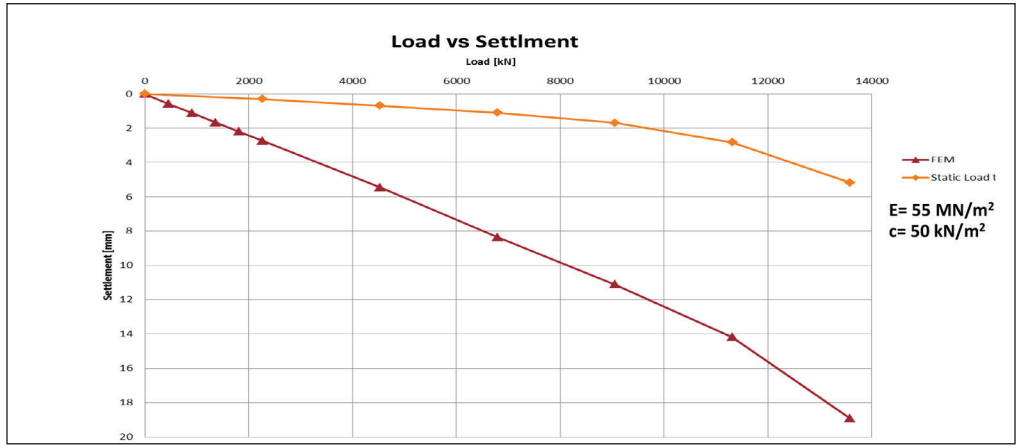

Back-Analysis of Soil Properties from Load Test

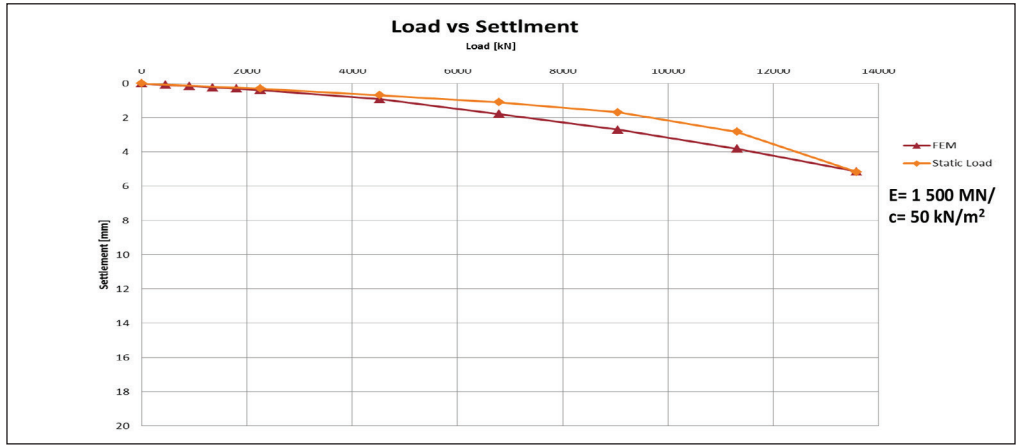

Pile Summary Sheet
P94

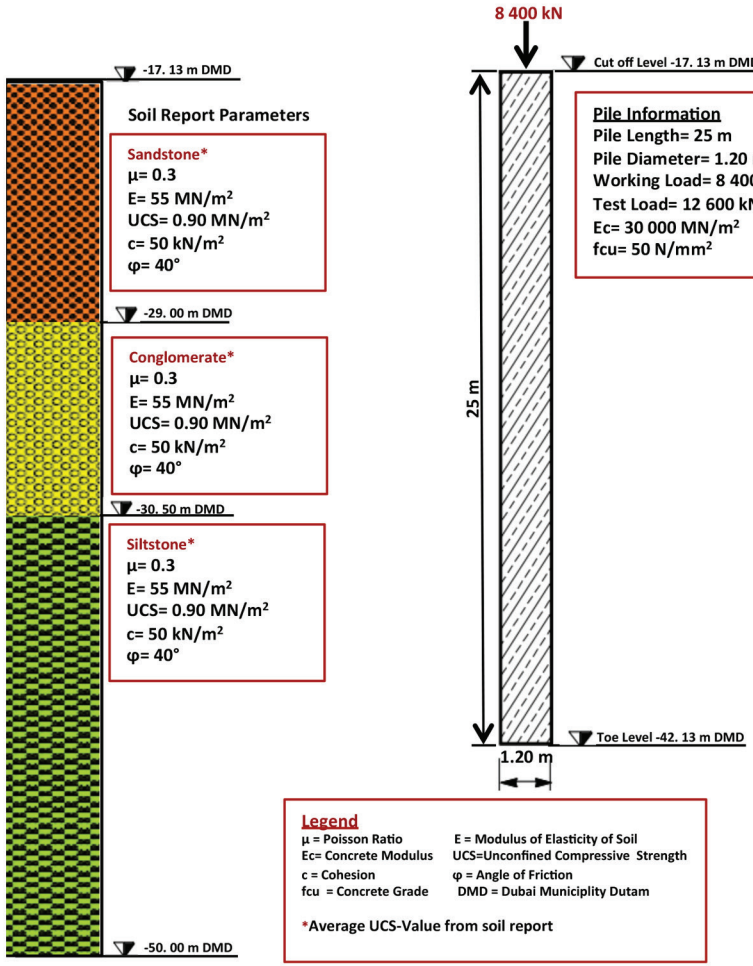

Modelling by using Soil Report Parameters

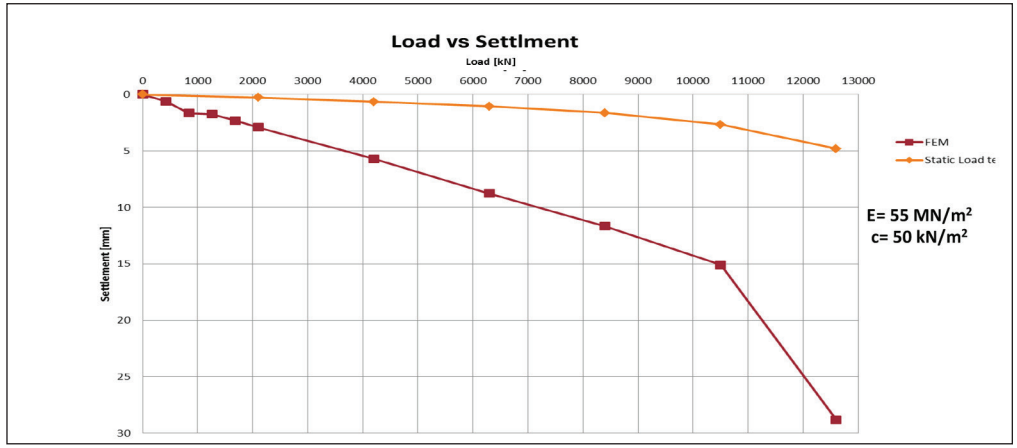

Back-Analysis of Soil Properties from Load Test

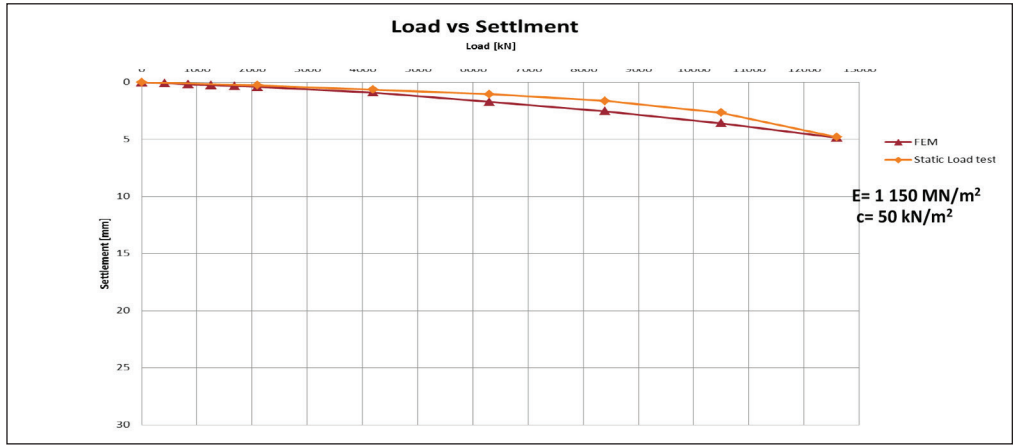

Pile Summary Sheet
P95

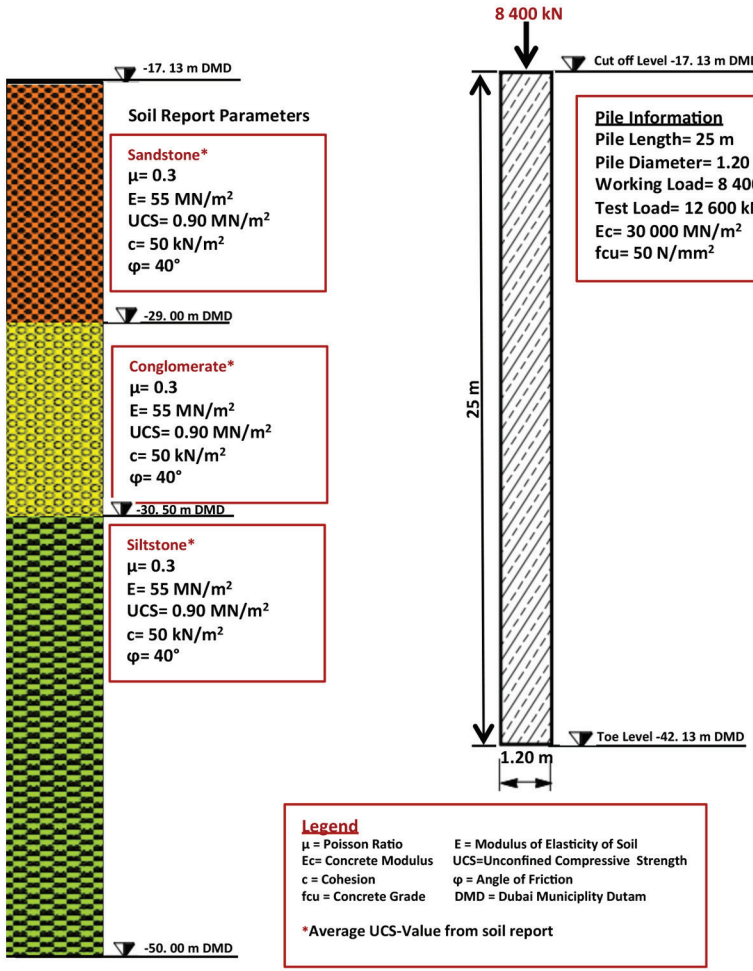

Pile Information
Pile Length= 25 m
Pile Diameter= 1.20 m
Working Load= 8 400 kN
Test Load= 12 600 kN
Ec= 30 000 MN/m²
fcu= 50 N/mm²

Legend

μ = Poisson Ratio	E = Modulus of Elasticity of Soil
Ec= Concrete Modulus	UCS=Unconfined Compressive Strength
c = Cohesion	φ = Angle of Friction
fcu = Concrete Grade	DMD = Dubai Municiplity Dutam

*Average UCS-Value from soil report

Modelling by using Soil Report Parameters

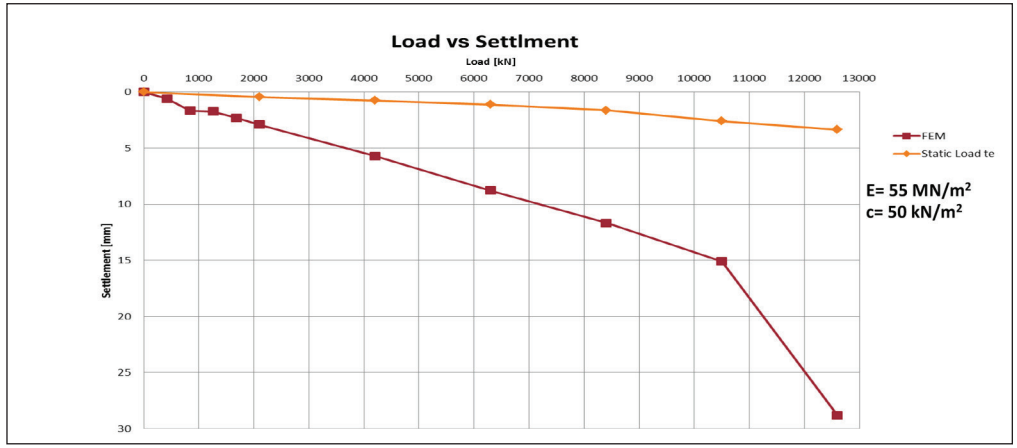

Back-Analysis of Soil Properties from Load Test

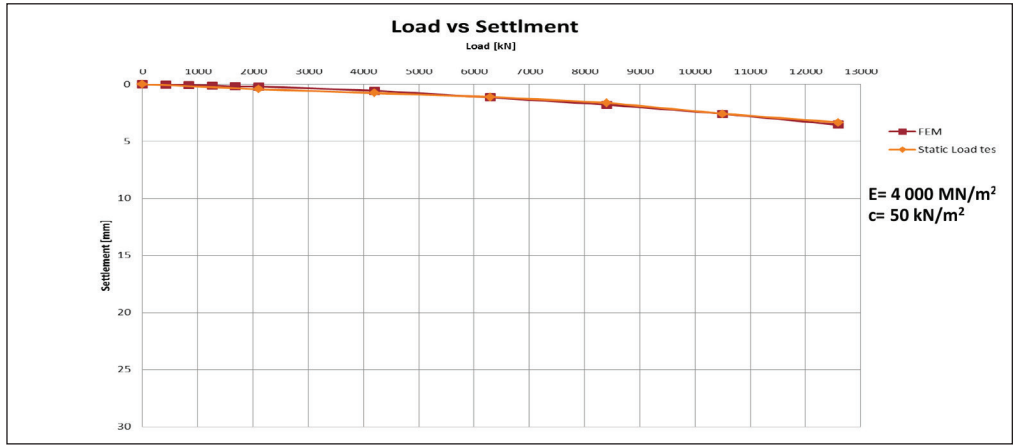

Pile Summary Sheet
P96

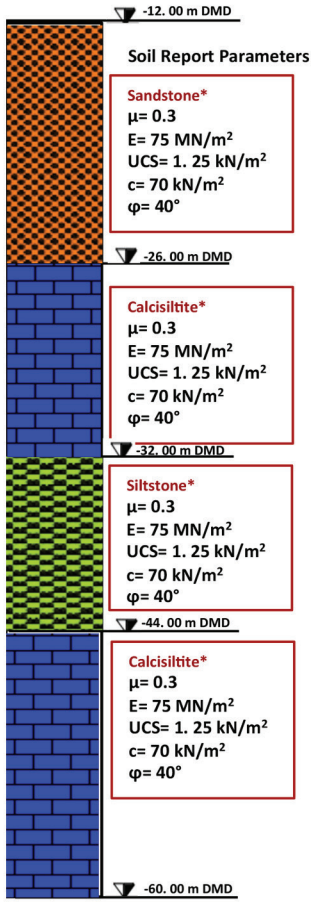

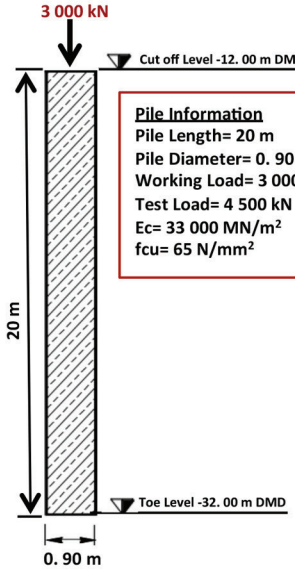

Pile Information
Pile Length= 20 m
Pile Diameter= 0. 90 m
Working Load= 3 000 kN
Test Load= 4 500 kN
Ec= 33 000 MN/m²
fcu= 65 N/mm²

Legend

μ = Poisson Ratio — E = Modulus of Elasticity of Soil
Ec= Concrete Modulus — UCS=Unconfined Compressive Strength
c = Cohesion — φ = Angle of Friction
fcu = Concrete Grade — DMD = Dubai Municiplity Dutam

*Average UCS-Value from soil report

Modelling by using Soil Report Parameters

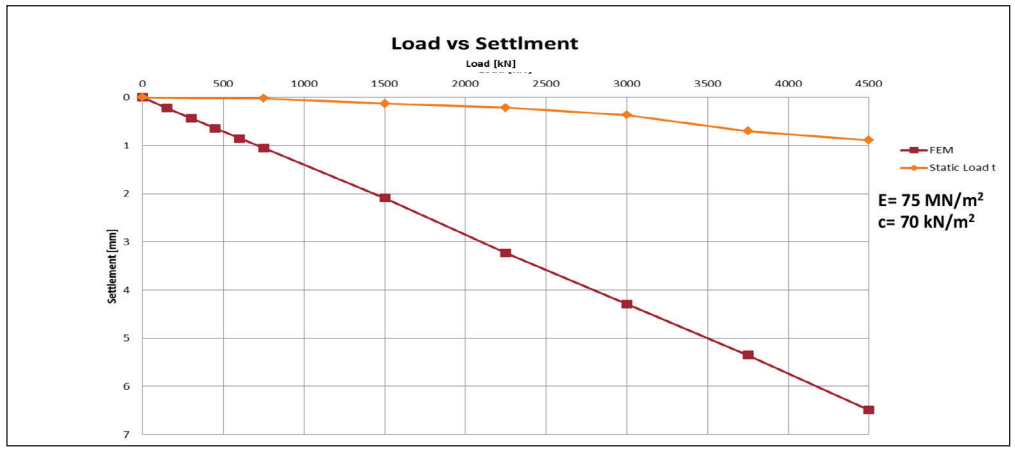

Back-Analysis of Soil Properties from Load Test

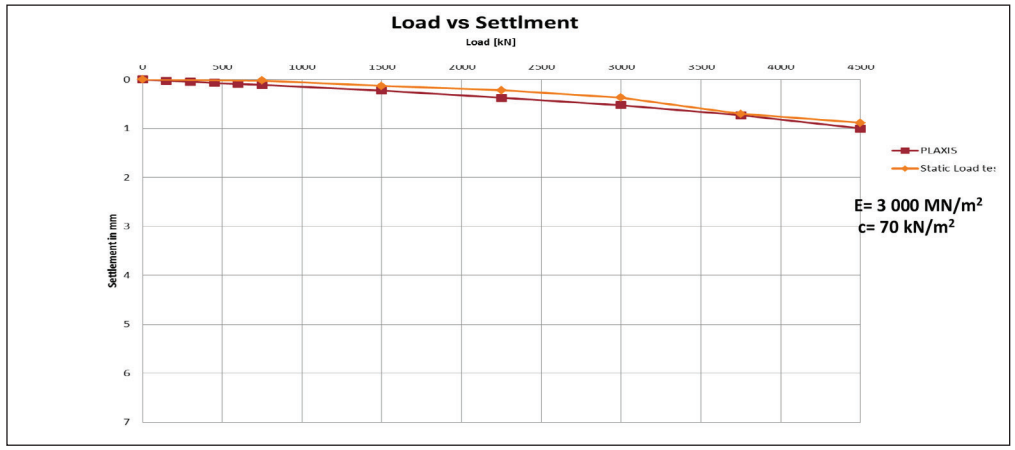

Pile Summary Sheet
P97

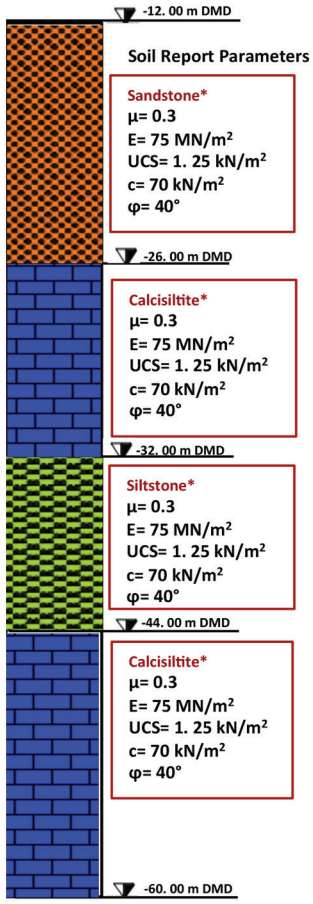

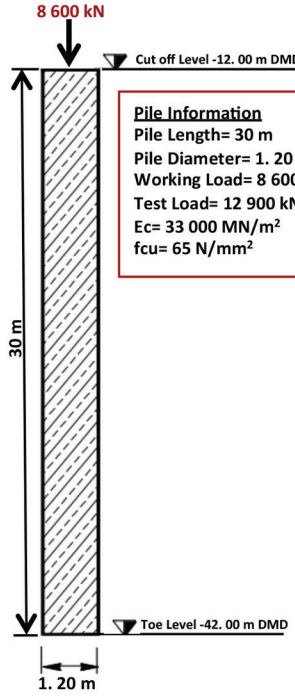

Pile Information
Pile Length= 30 m
Pile Diameter= 1. 20 m
Working Load= 8 600 kN
Test Load= 12 900 kN
Ec= 33 000 MN/m²
fcu= 65 N/mm²

Legend

μ = Poisson Ratio	E = Modulus of Elasticity of Soil
Ec= Concrete Modulus	UCS=Unconfined Compressive Strength
c = Cohesion	φ = Angle of Friction
fcu = Concrete Grade	DMD = Dubai Municiplity Dutam

*Average UCS-Value from soil report

Modelling by using Soil Report Parameters

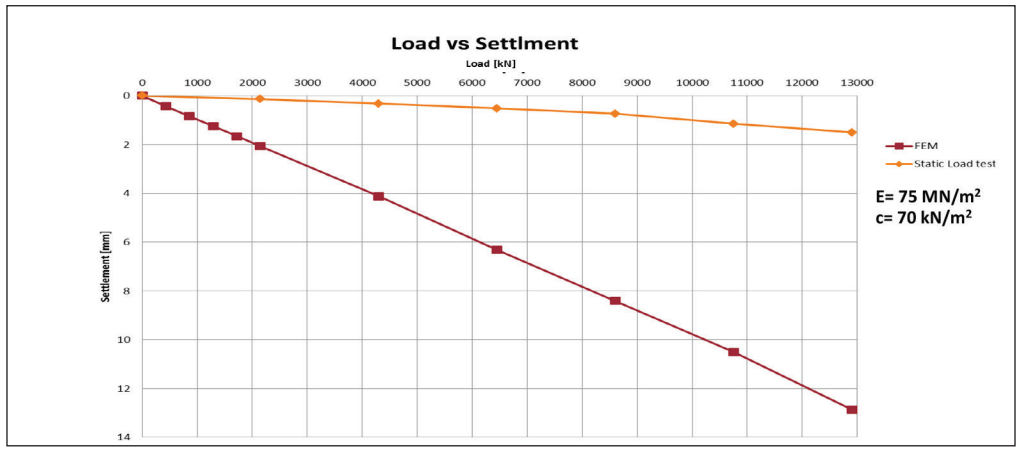

Back-Analysis of Soil Properties from Load Test

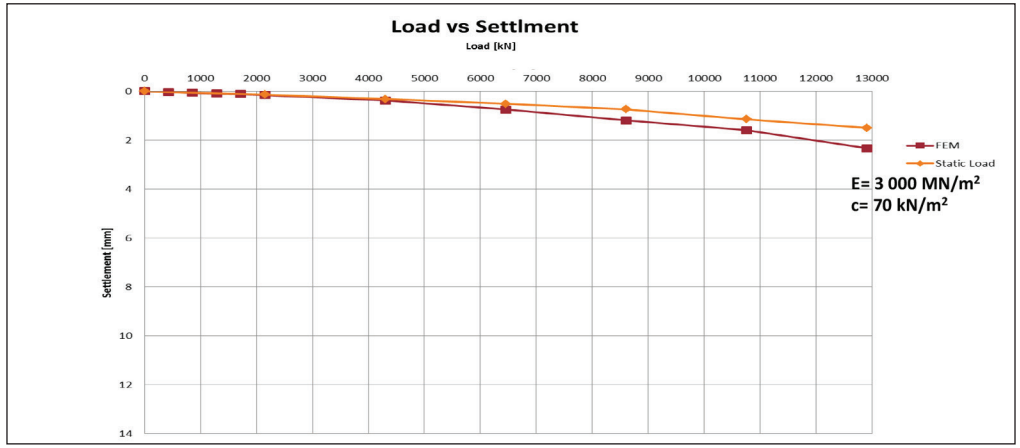

Pile Summary Sheet
P98

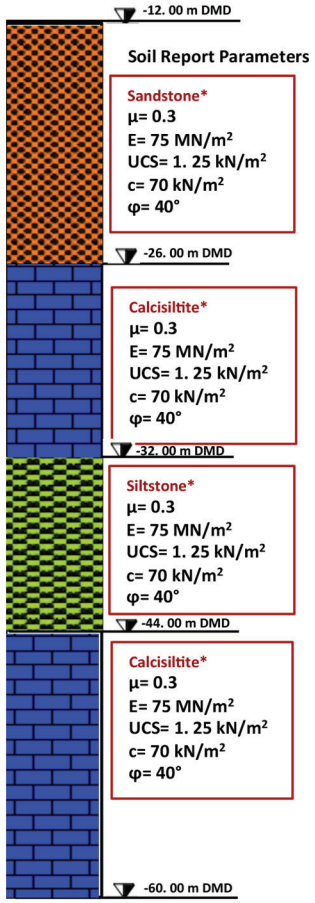

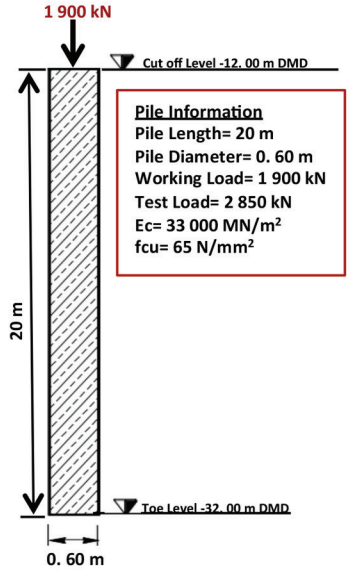

Pile Information
Pile Length= 20 m
Pile Diameter= 0. 60 m
Working Load= 1 900 kN
Test Load= 2 850 kN
Ec= 33 000 MN/m²
fcu= 65 N/mm²

Legend

μ = Poisson Ratio	E = Modulus of Elasticity of Soil
Ec= Concrete Modulus	UCS=Unconfined Compressive Strength
c = Cohesion	φ = Angle of Friction
f´c = Concrete Grade	DMD = Dubai Municiplity Dutam

*Average UCS-Value from soil report

Modelling by using Soil Report Parameters

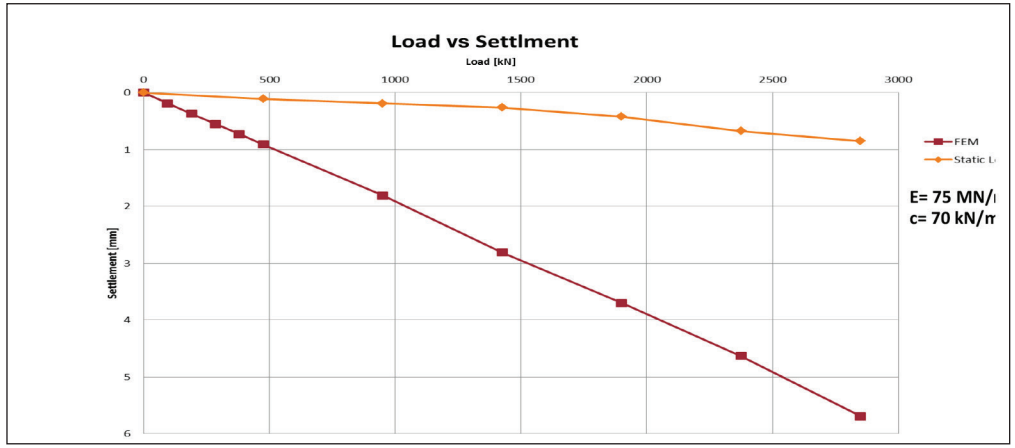

Back-Analysis of Soil Properties from Load Test

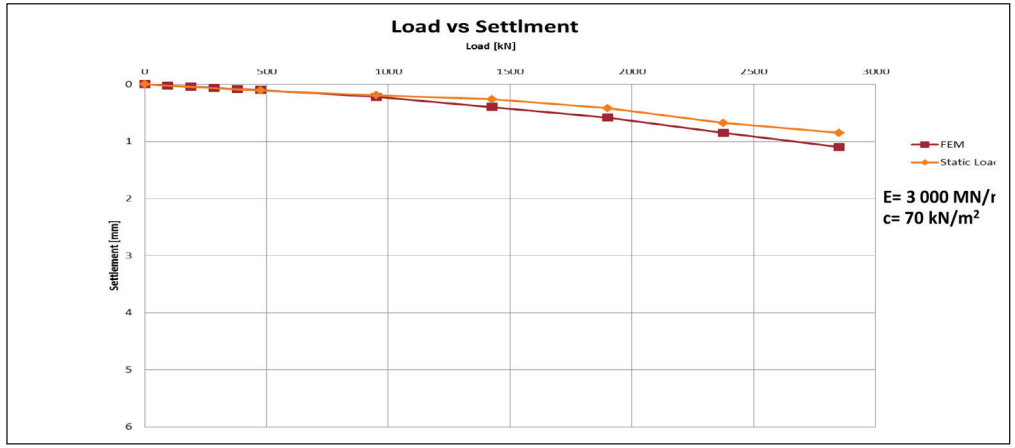

Pile Summary Sheet
P99

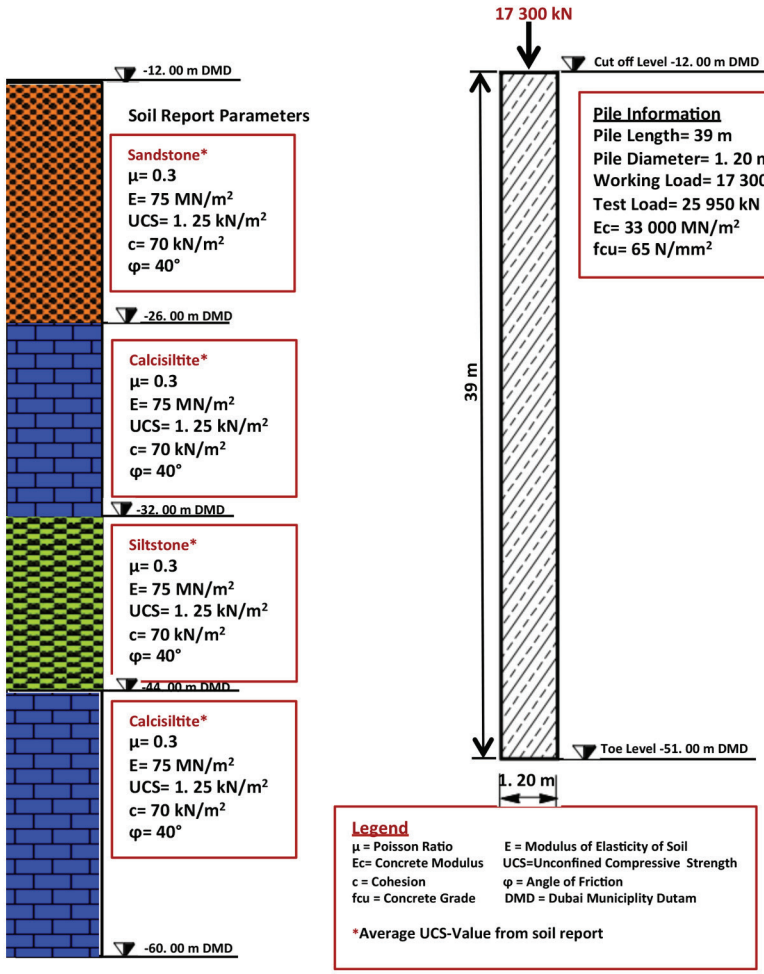

Pile Information
Pile Length= 39 m
Pile Diameter= 1. 20 m
Working Load= 17 300 kN
Test Load= 25 950 kN
Ec= 33 000 MN/m²
fcu= 65 N/mm²

Legend

μ = Poisson Ratio	E = Modulus of Elasticity of Soil
Ec= Concrete Modulus	UCS=Unconfined Compressive Strength
c = Cohesion	φ = Angle of Friction
fcu = Concrete Grade	DMD = Dubai Municiplity Dutam

*Average UCS-Value from soil report

Modelling by using Soil Report Parameters

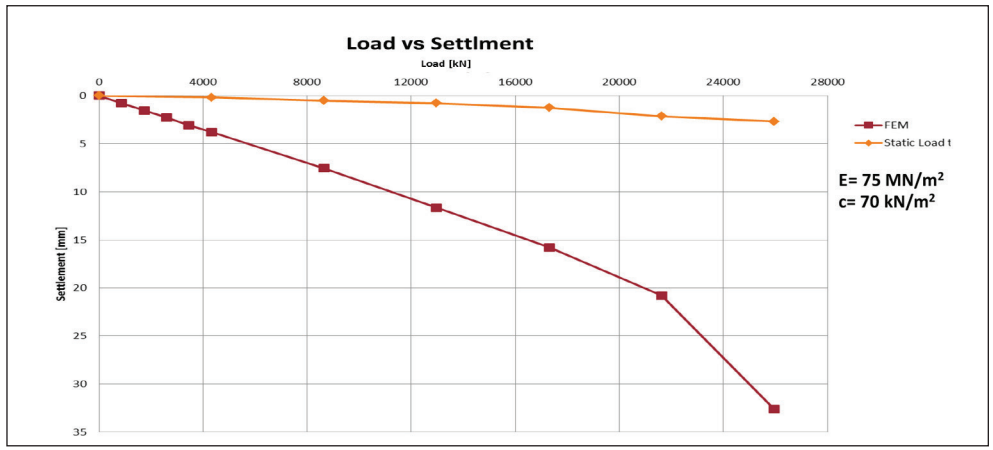

Back-Analysis of Soil Properties from Load Test

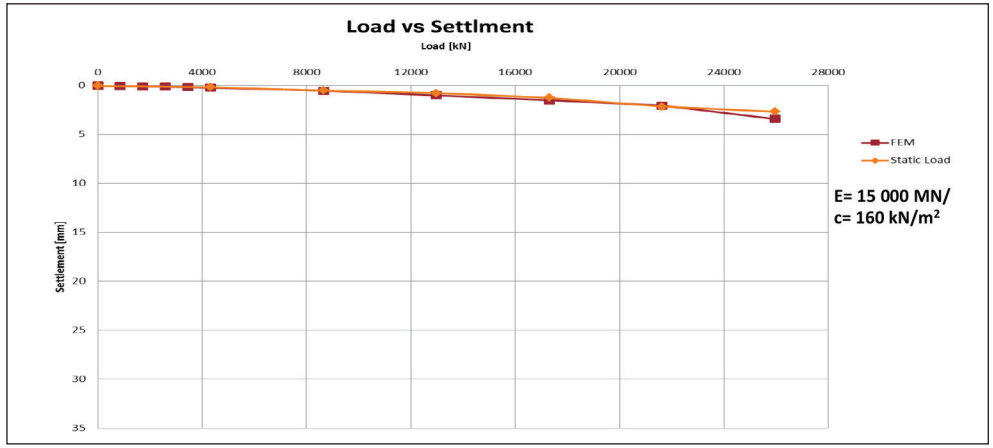

Pile Summary Sheet
P101

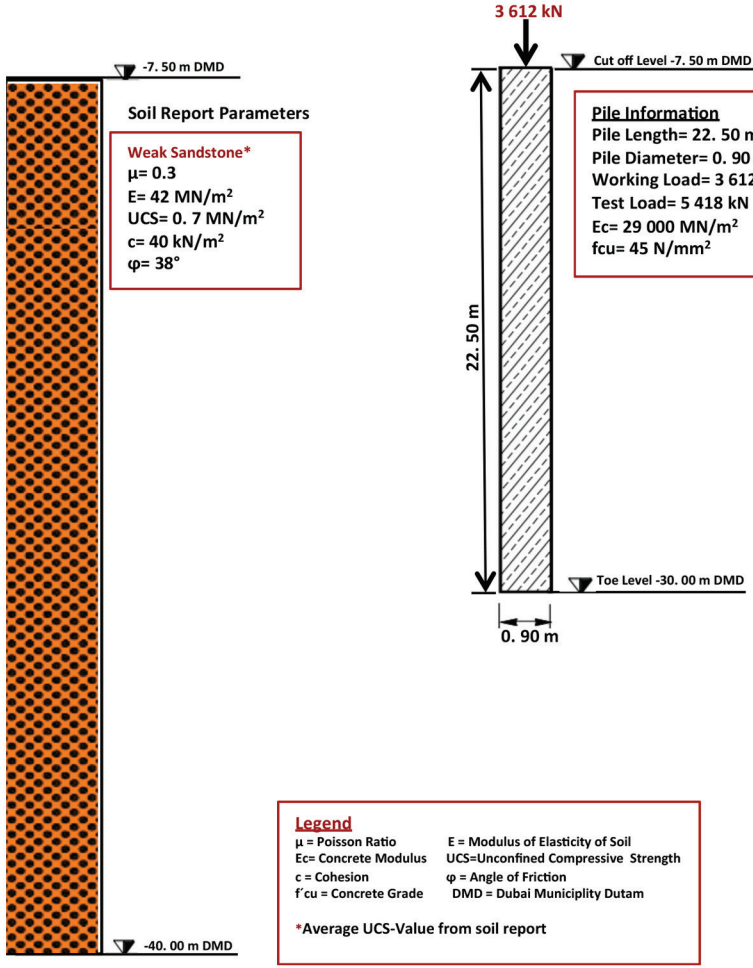

Legend

μ = Poisson Ratio — E = Modulus of Elasticity of Soil
Ec= Concrete Modulus — UCS=Unconfined Compressive Strength
c = Cohesion — φ = Angle of Friction
f´cu = Concrete Grade — DMD = Dubai Municiplity Dutam

*Average UCS-Value from soil report

Modelling by using Soil Report Parameters

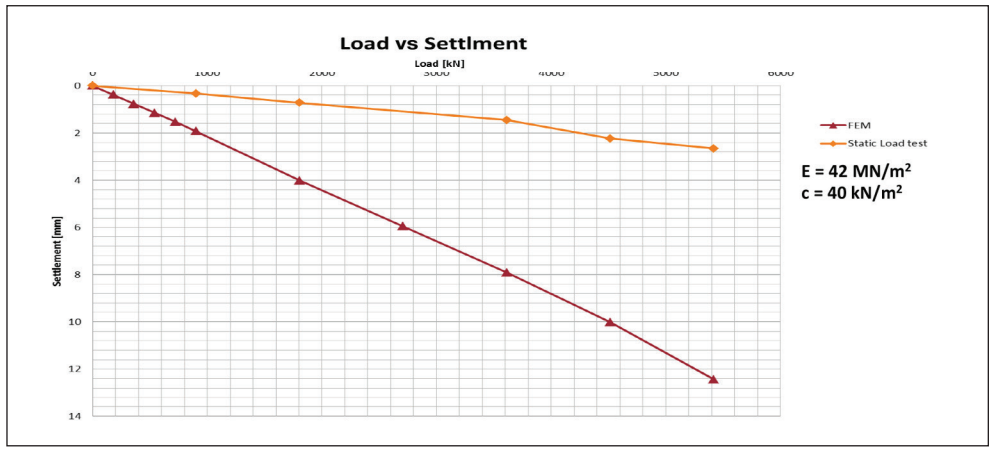

Back-Analysis of Soil Properties from Load Test

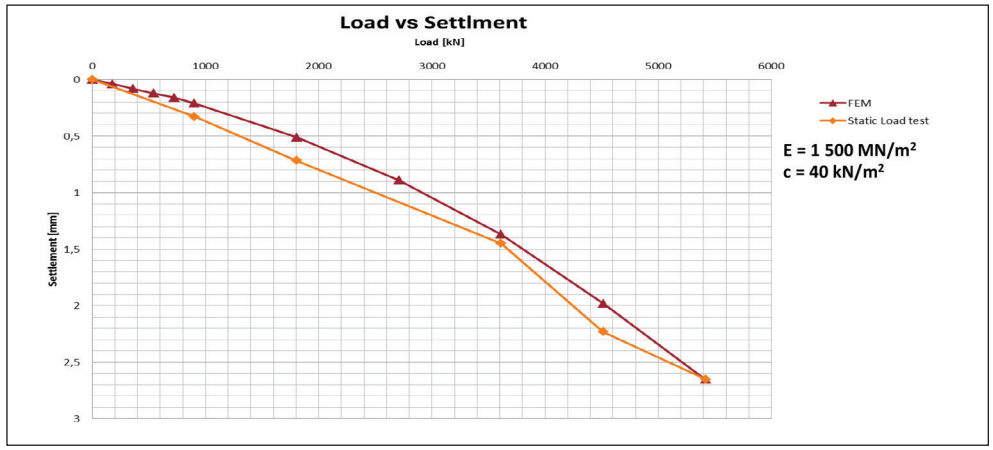

Pile Summary Sheet
P102

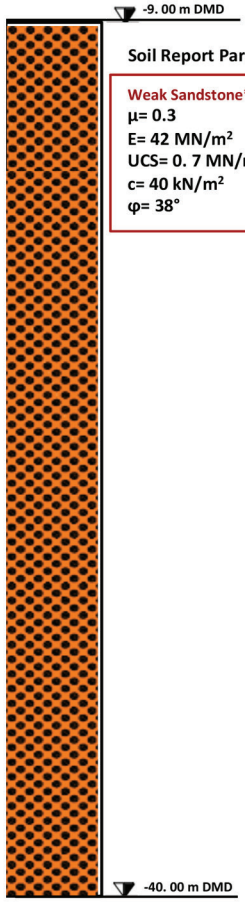

Soil Report Parameters

Weak Sandstone*
μ= 0.3
E= 42 MN/m²
UCS= 0. 7 MN/m²
c= 40 kN/m²
φ= 38°

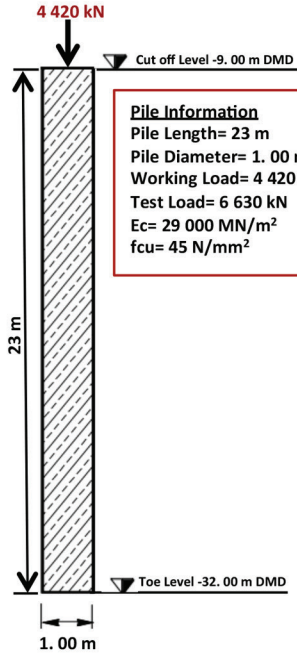

Pile Information
Pile Length= 23 m
Pile Diameter= 1. 00 m
Working Load= 4 420 kN
Test Load= 6 630 kN
Ec= 29 000 MN/m²
fcu= 45 N/mm²

Legend

μ = Poisson Ratio	E = Modulus of Elasticity of Soil
Ec= Concrete Modulus	UCS=Unconfined Compressive Strength
c = Cohesion	φ = Angle of Friction
fcu = Concrete Grade	DMD = Dubai Municiplity Dutam

*Average UCS-Value from soil report

Modelling by using Soil Report Parameters

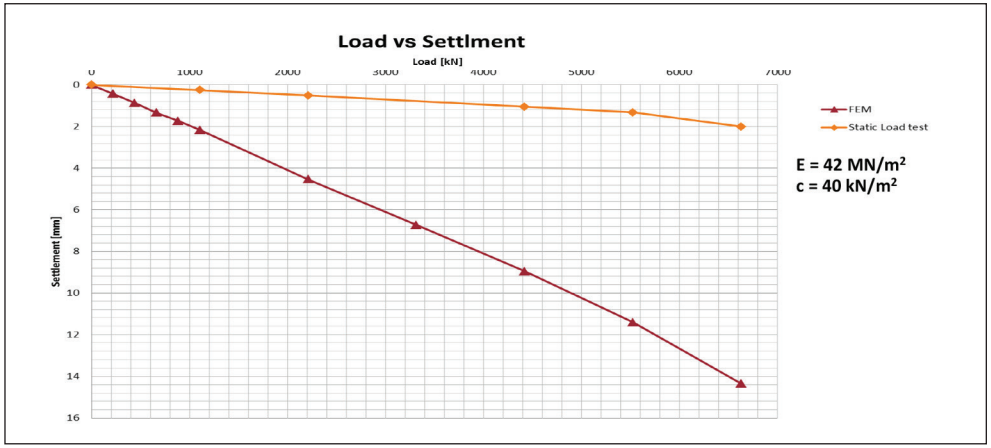

Back-Analysis of Soil Properties from Load Test

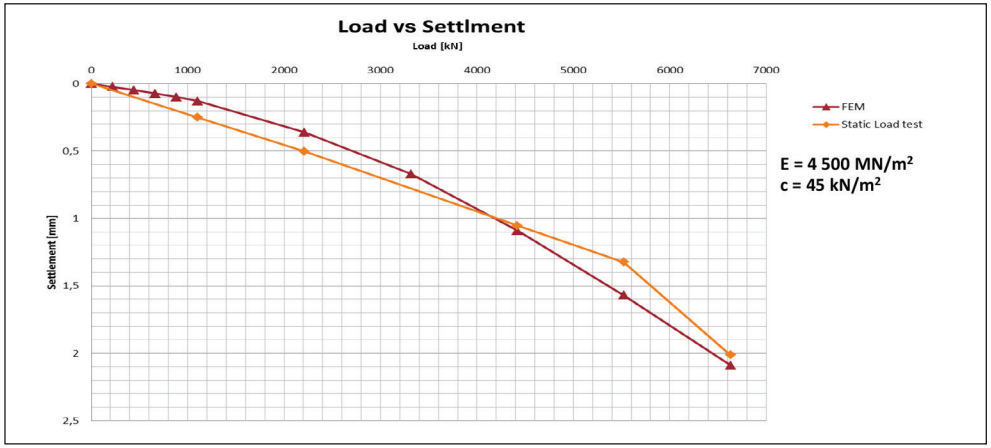

Pile Summary Sheet
P103

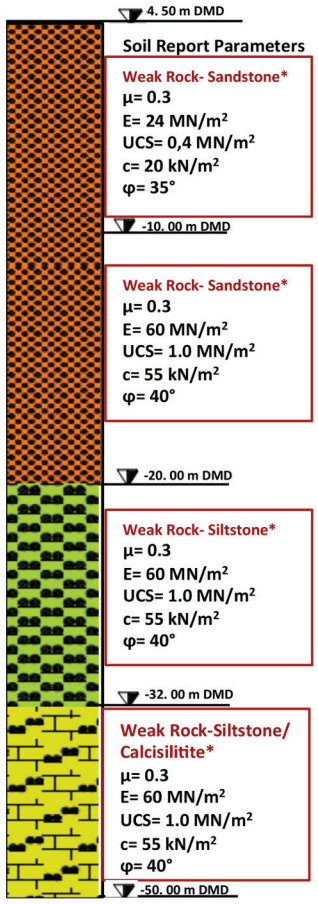

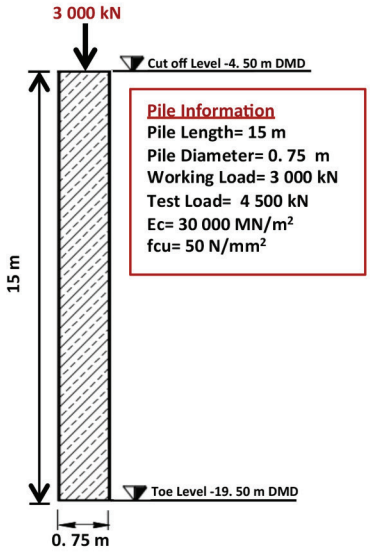

Pile Information
Pile Length= 15 m
Pile Diameter= 0. 75 m
Working Load= 3 000 kN
Test Load= 4 500 kN
Ec= 30 000 MN/m²
fcu= 50 N/mm²

Legend
μ = Poisson Ratio
E = Modulus of Elasticity of Soil
Ec= Concrete Modulus
UCS=Unconfined Compressive Strength
c = Cohesion
φ = Angle of Friction
fcu = Concrete Grade
DMD = Dubai Municiplity Dutam

*Average UCS-Value from soil report

Modelling by using Soil Report Parameters

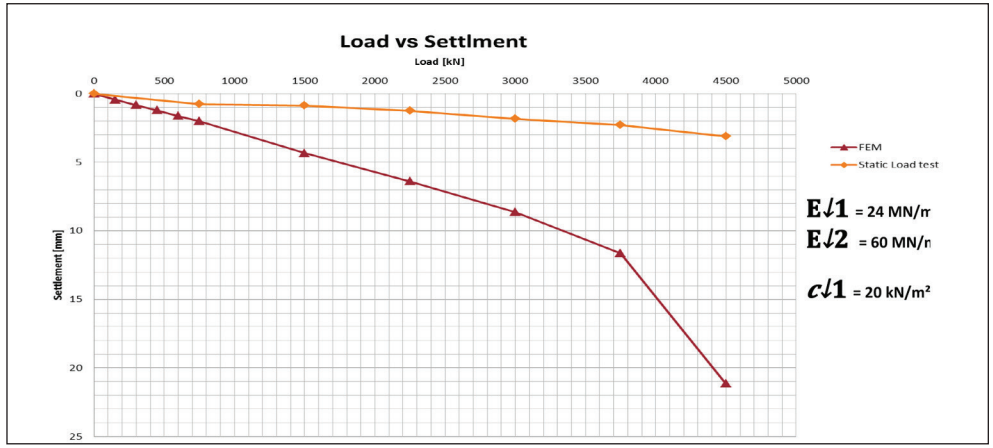

Back-Analysis of Soil Properties from Load Test

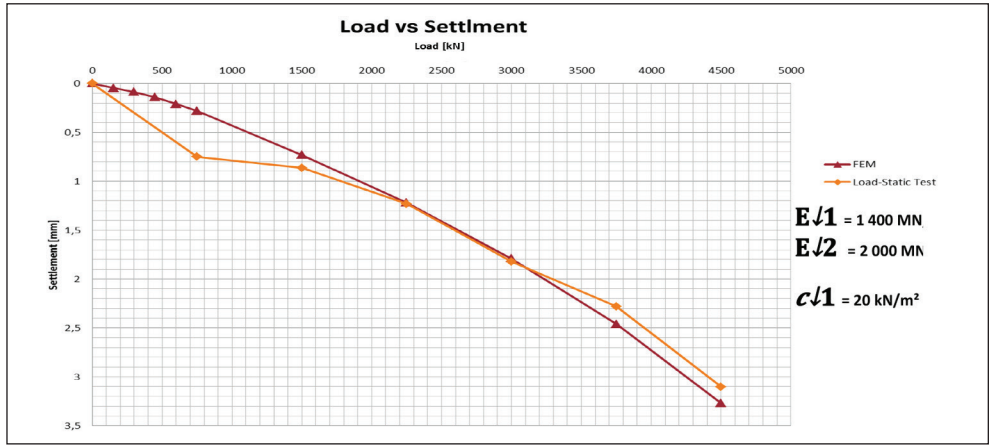

Pile Summary Sheet
P104

Soil Report Parameters

Silty Sand*
μ= 0.3
E= 24 MN/m²
UCS= 0,4 MN/m²
c= 20 kN/m²
φ= 30°

Weak Rock- Sandstone*
μ= 0.3
E= 60 MN/m²
UCS= 1.0 MN/m²
c= 55 kN/m²
φ= 40°

Weak Rock- Siltstone*
μ= 0.3
E= 60 MN/m²
UCS= 1.0 MN/m²
c= 55 kN/m²
φ= 40°

Weak Rock-Siltstone/ Calcisilitite*
μ= 0.3
E= 60 MN/m²
UCS= 1.0 MN/m²
c= 55 kN/m²
φ= 40°

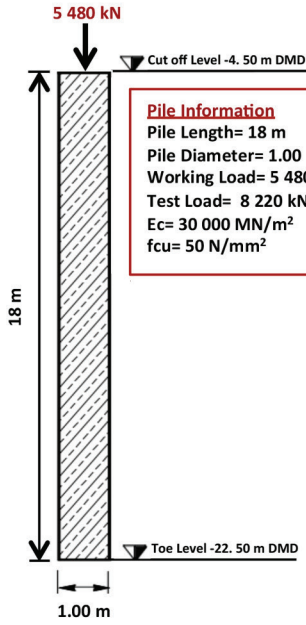

Pile Information
Pile Length= 18 m
Pile Diameter= 1.00 m
Working Load= 5 480 kN
Test Load= 8 220 kN
Ec= 30 000 MN/m²
fcu= 50 N/mm²

Legend

μ = Poisson Ratio	E = Modulus of Elasticity of Soil
Ec= Concrete Modulus	UCS=Unconfined Compressive Strength
c = Cohesion	φ = Angle of Friction
fcu = Concrete Grade	DMD = Dubai Municiplity Dutam

*Average UCS-Value from soil report

Modelling by using Soil Report Parameters

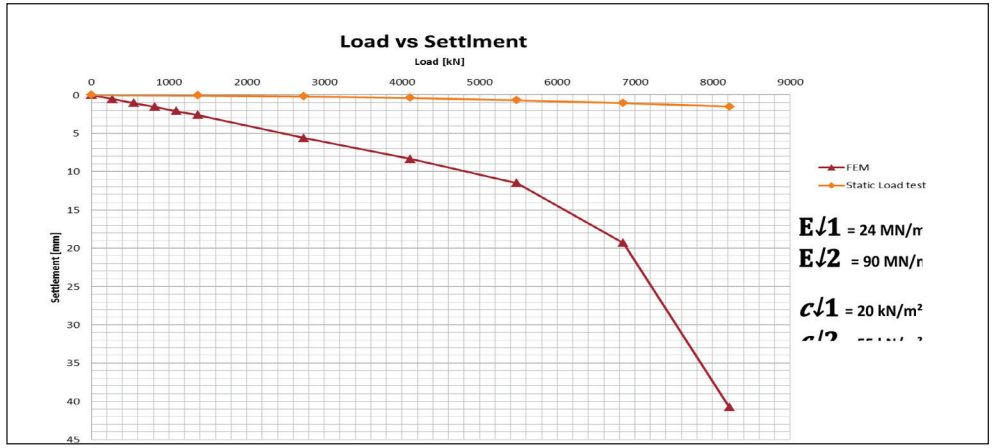

Back-Analysis of Soil Properties from Load Test

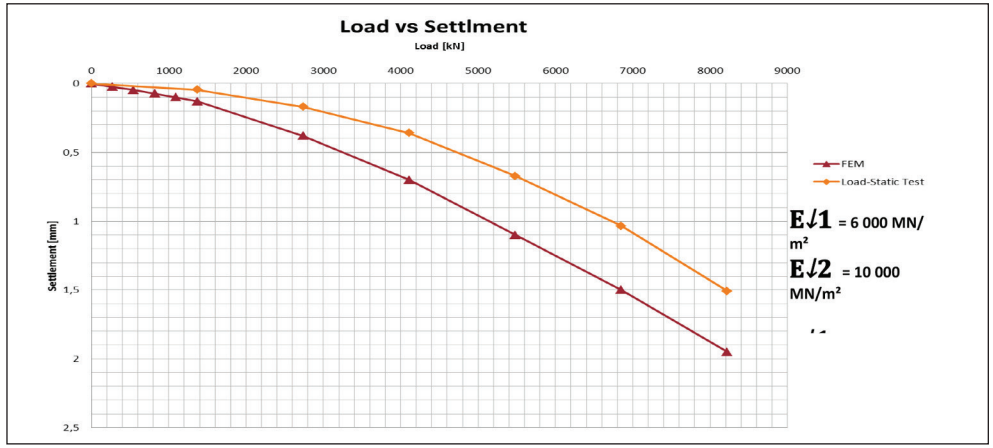

Pile Summary Sheet
P105

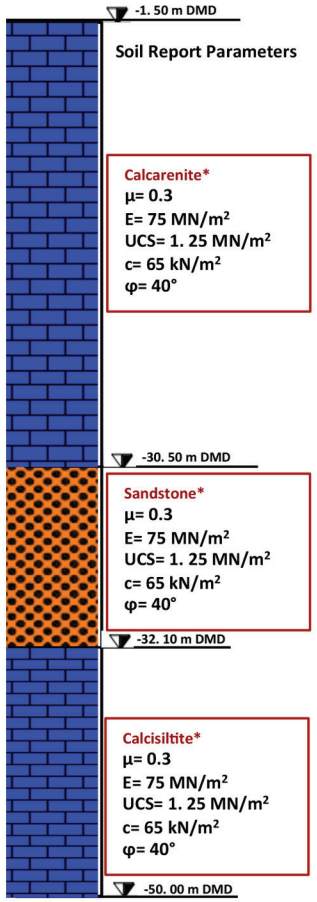

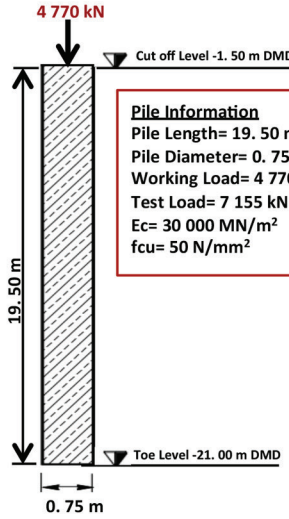

Pile Information
Pile Length= 19. 50 m
Pile Diameter= 0. 75 m
Working Load= 4 770 kN
Test Load= 7 155 kN
Ec= 30 000 MN/m²
fcu= 50 N/mm²

Legend

μ = Poisson Ratio	E = Modulus of Elasticity of Soil
Ec= Concrete Modulus	UCS=Unconfined Compressive Strength
c = Cohesion	φ = Angle of Friction
fcu = Concrete Grade	DMD = Dubai Municiplity Dutam

*Average UCS-Value from soil report

Modelling by using Soil Report Parameters

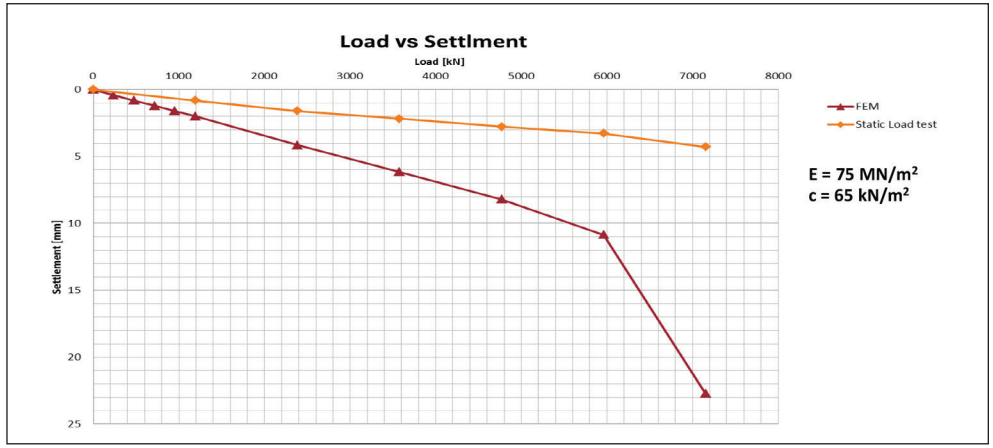

E = 75 MN/m²
c = 65 kN/m²

Back-Analysis of Soil Properties from Load Test

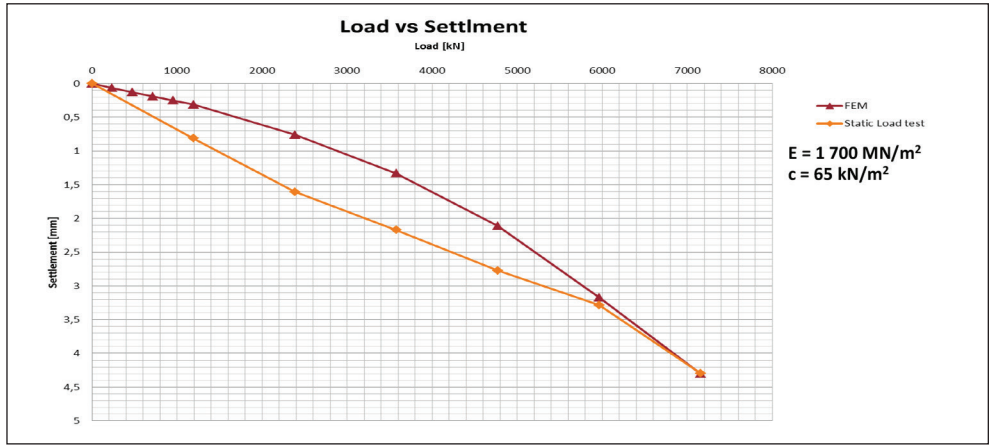

E = 1 700 MN/m²
c = 65 kN/m²

Pile Summary Sheet
P100

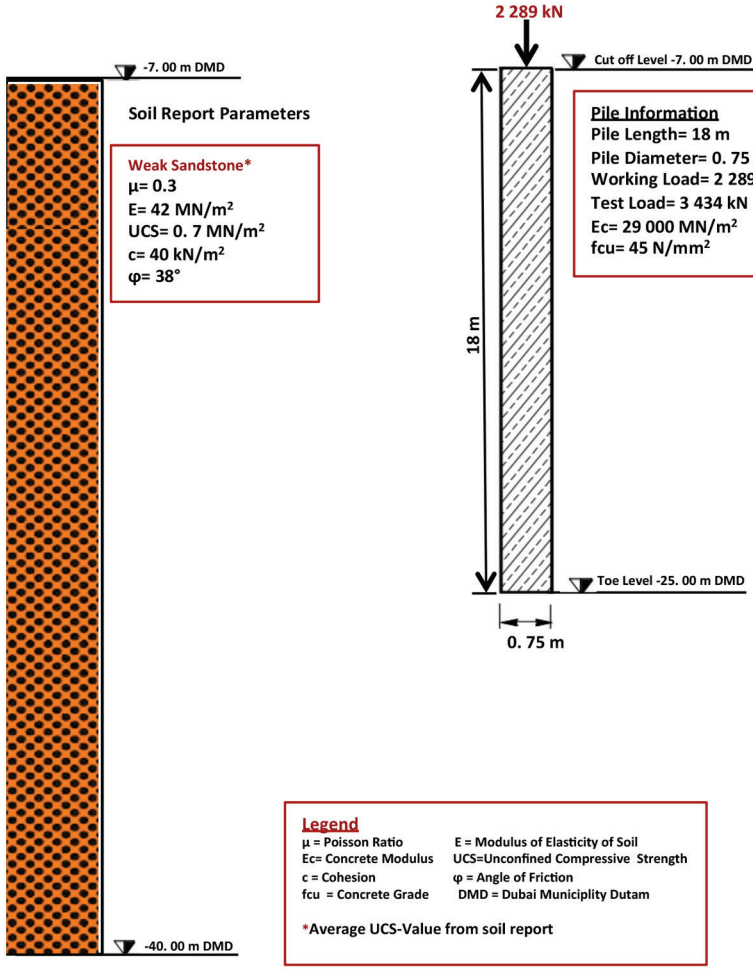

Legend

μ = Poisson Ratio — E = Modulus of Elasticity of Soil
Ec= Concrete Modulus — UCS=Unconfined Compressive Strength
c = Cohesion — φ = Angle of Friction
fcu = Concrete Grade — DMD = Dubai Municiplity Dutam

*Average UCS-Value from soil report

Modelling by using Soil Report Parameters

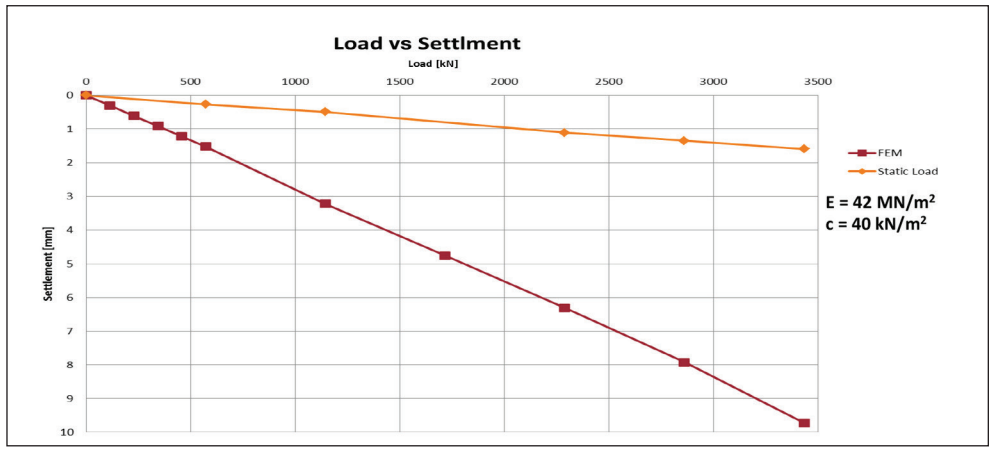

Back-Analysis of Soil Properties from Load Test

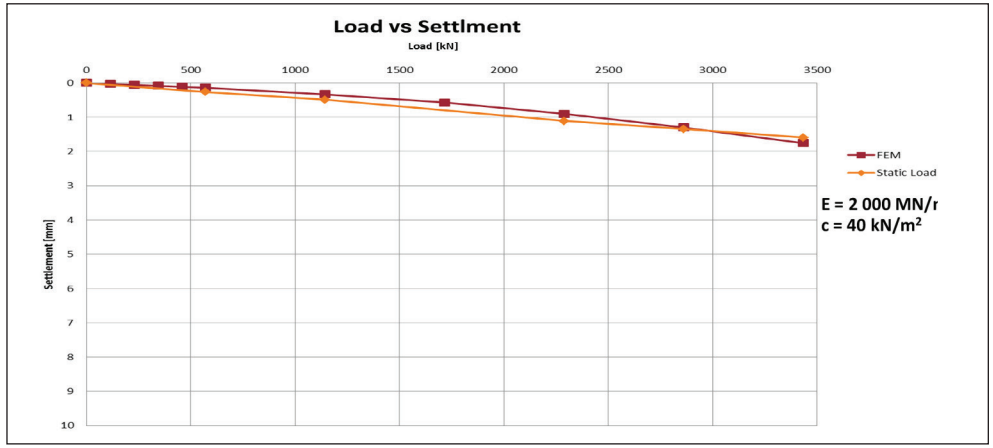

Pile Summary Sheet
P106

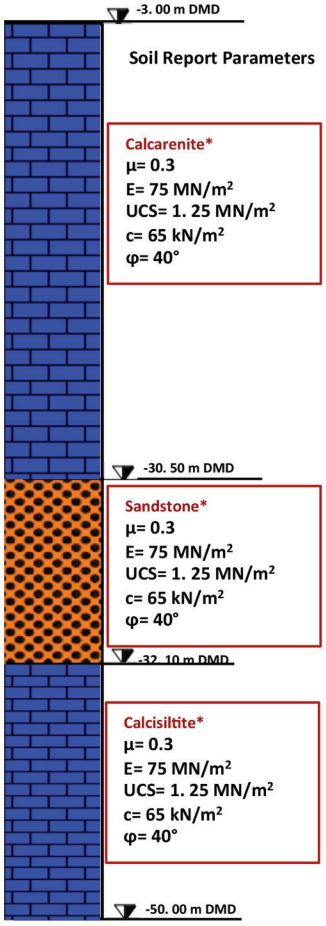

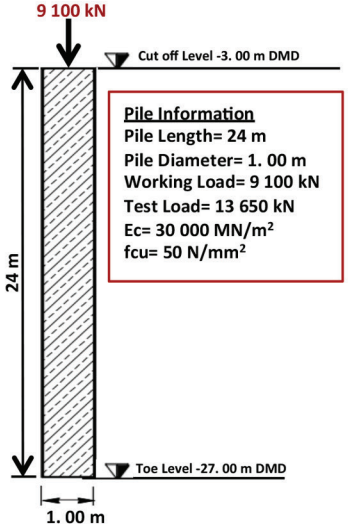

Pile Information
Pile Length= 24 m
Pile Diameter= 1. 00 m
Working Load= 9 100 kN
Test Load= 13 650 kN
Ec= 30 000 MN/m²
fcu= 50 N/mm²

Legend

μ = Poisson Ratio	E = Modulus of Elasticity of Soil
Ec= Concrete Modulus	UCS=Unconfined Compressive Strength
c = Cohesion	φ = Angle of Friction
f´c = Concrete Grade	DMD = Dubai Municiplity Datum

*Average UCS-Value from soil report

Modelling by using Soil Report Parameters

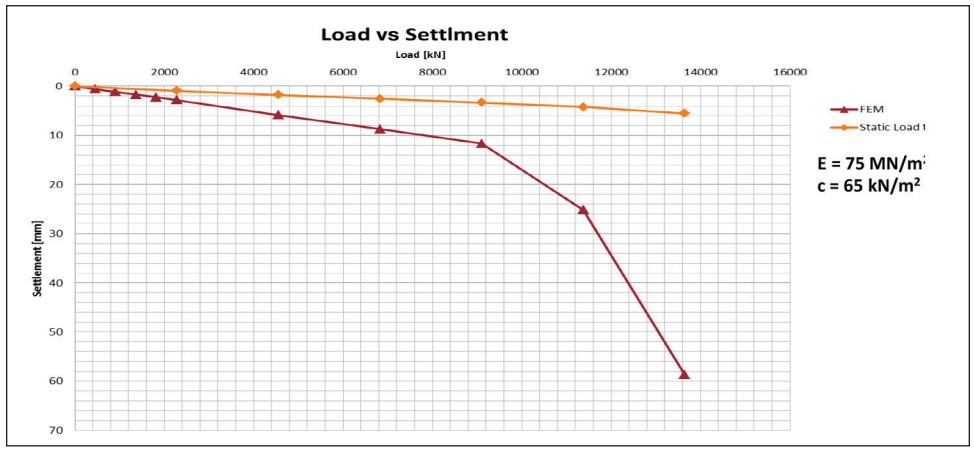

Back-Analysis of Soil Properties from Load Test

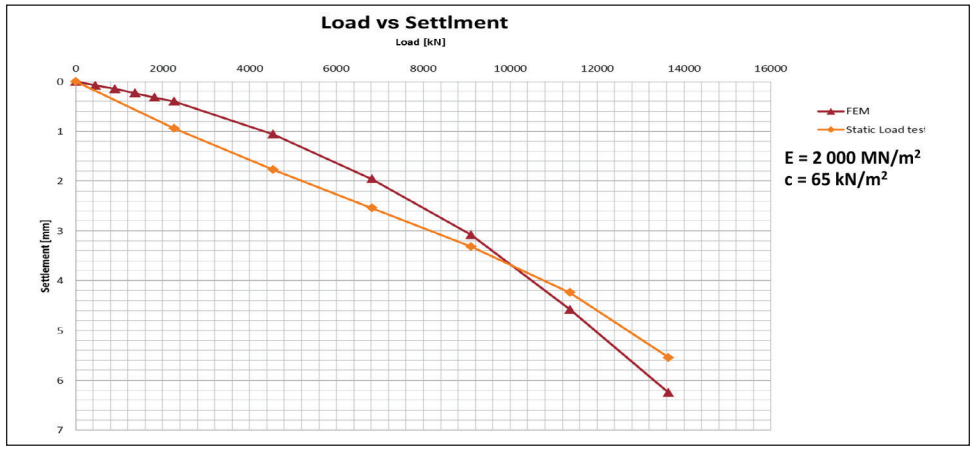

Pile Summary Sheet
P107

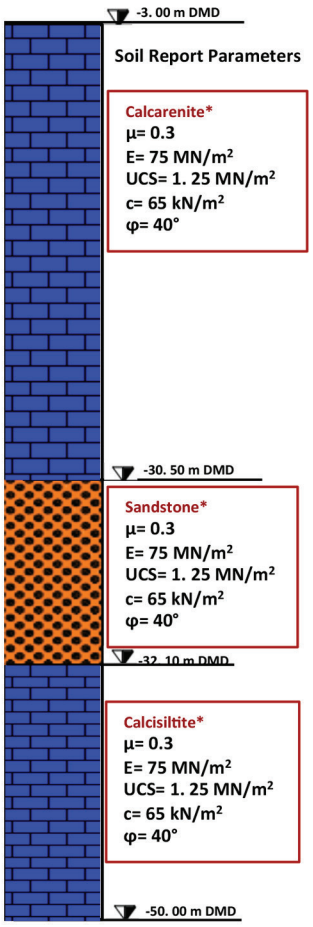

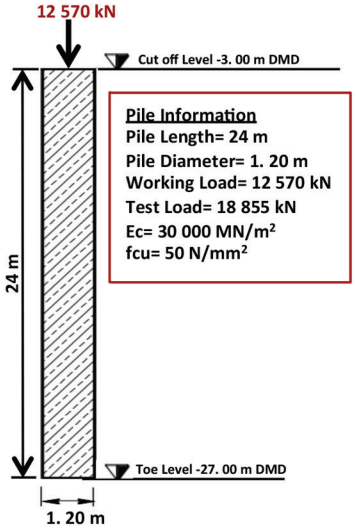

Pile Information
Pile Length= 24 m
Pile Diameter= 1. 20 m
Working Load= 12 570 kN
Test Load= 18 855 kN
Ec= 30 000 MN/m²
fcu= 50 N/mm²

Legend

μ = Poisson Ratio	E = Modulus of Elasticity of Soil
Ec= Concrete Modulus	UCS=Unconfined Compressive Strength
c = Cohesion	φ = Angle of Friction
f´c = Concrete Grade	DMD = Dubai Municiplity Dutam

*Average UCS-Value from soil report

Modelling by using Soil Report Parameters

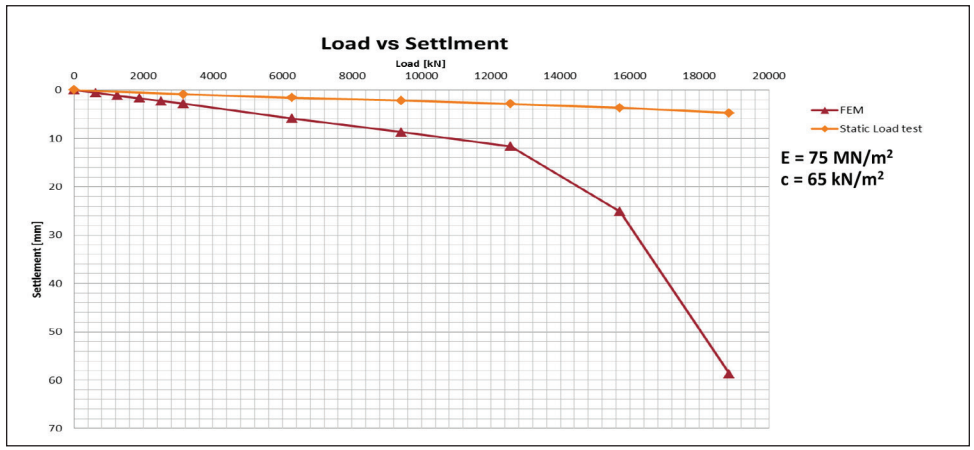

Back-Analysis of Soil Properties from Load Test

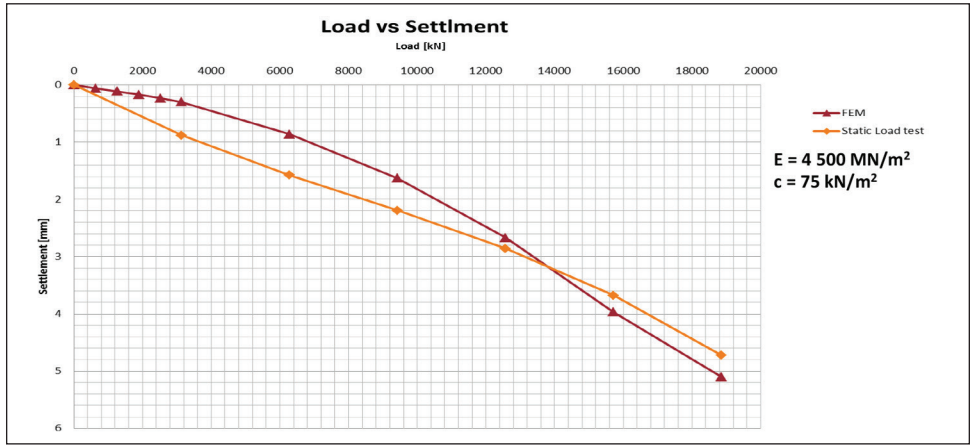

Pile Summary Sheet
P108

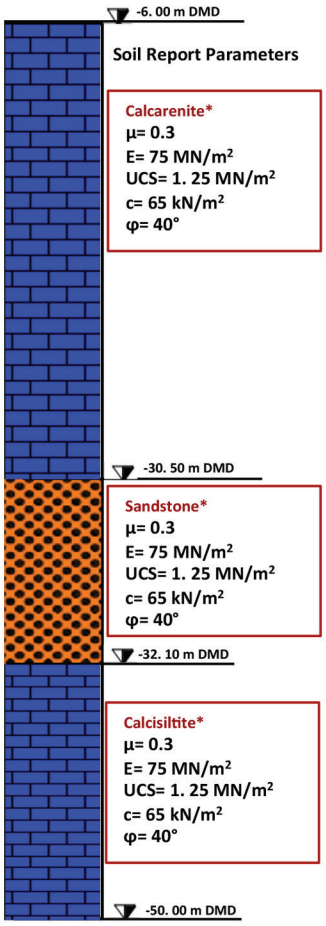

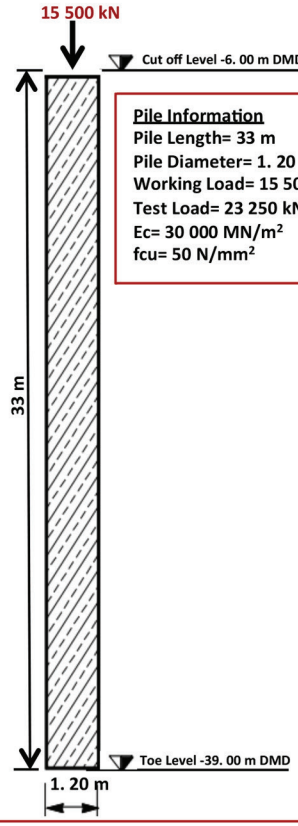

Pile Information
Pile Length= 33 m
Pile Diameter= 1. 20 m
Working Load= 15 500 kN
Test Load= 23 250 kN
Ec= 30 000 MN/m²
fcu= 50 N/mm²

Legend

μ = Poisson Ratio	E = Modulus of Elasticity of Soil
Ec= Concrete Modulus	UCS=Unconfined Compressive Strength
c = Cohesion	φ = Angle of Friction
fcu = Concrete Grade	DMD = Dubai Municiplity Dutam

*Average UCS-Value from soil report

Modelling by using Soil Report Parameters

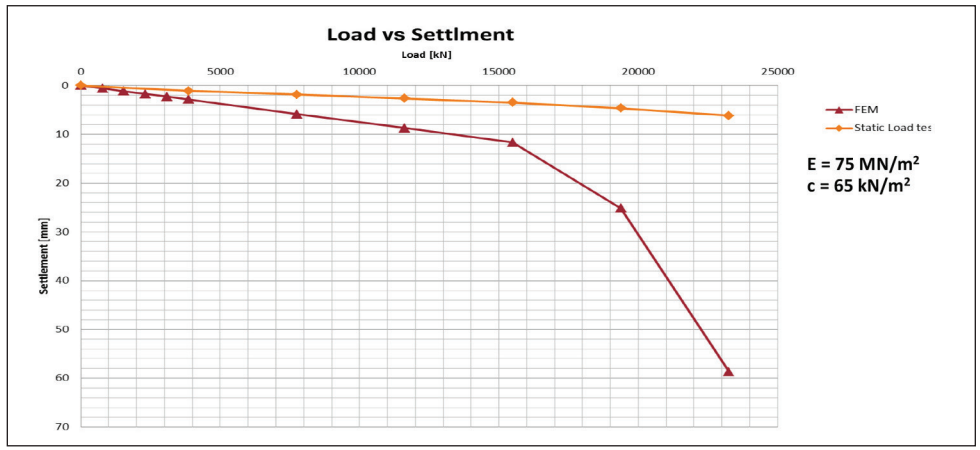

Back-Analysis of Soil Properties from Load Test

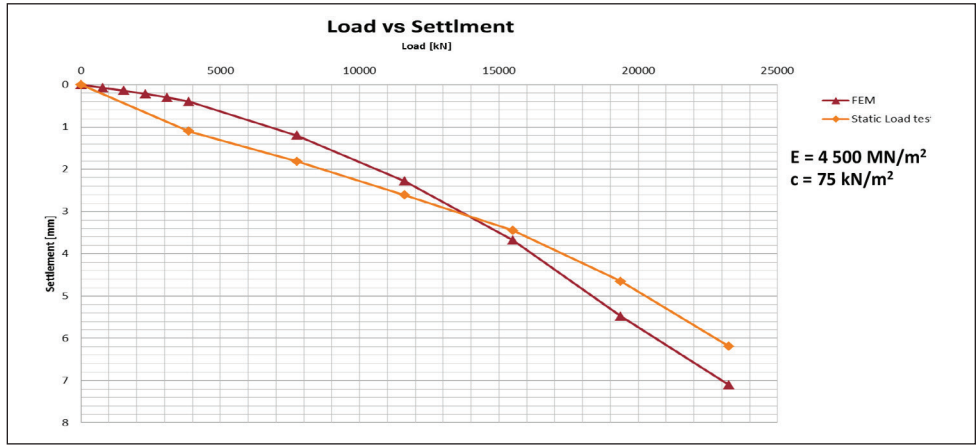

Pile Summary Sheet
P109

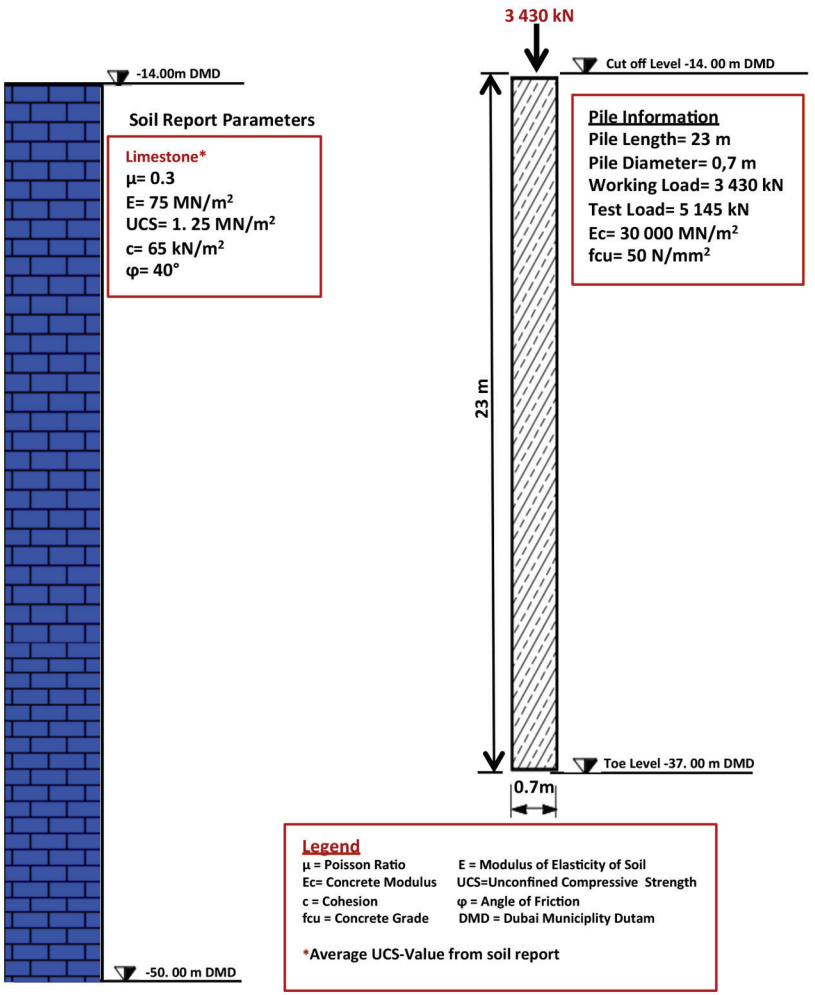

Modelling by using Soil Report Parameters

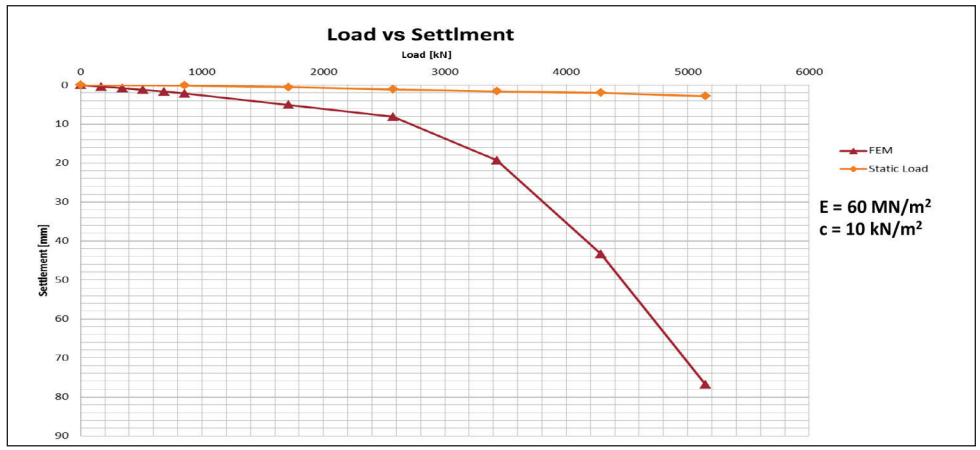

Back-Analysis of Soil Properties from Load Test

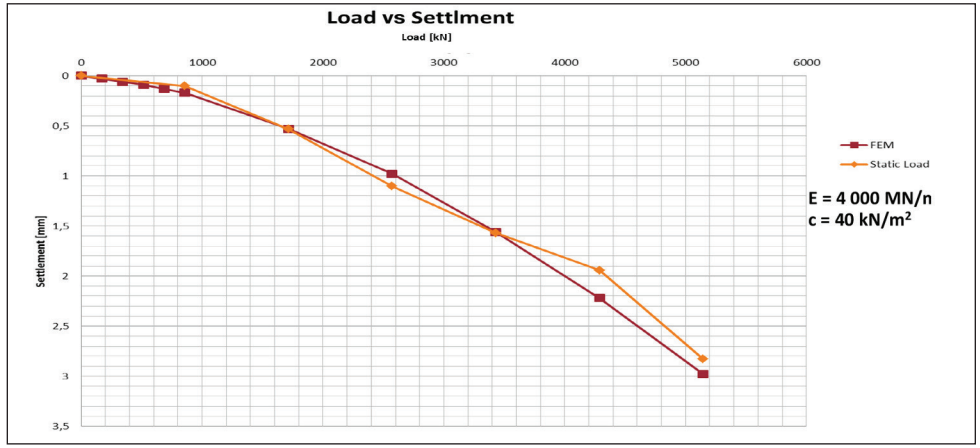

Pile Summary Sheet
P110

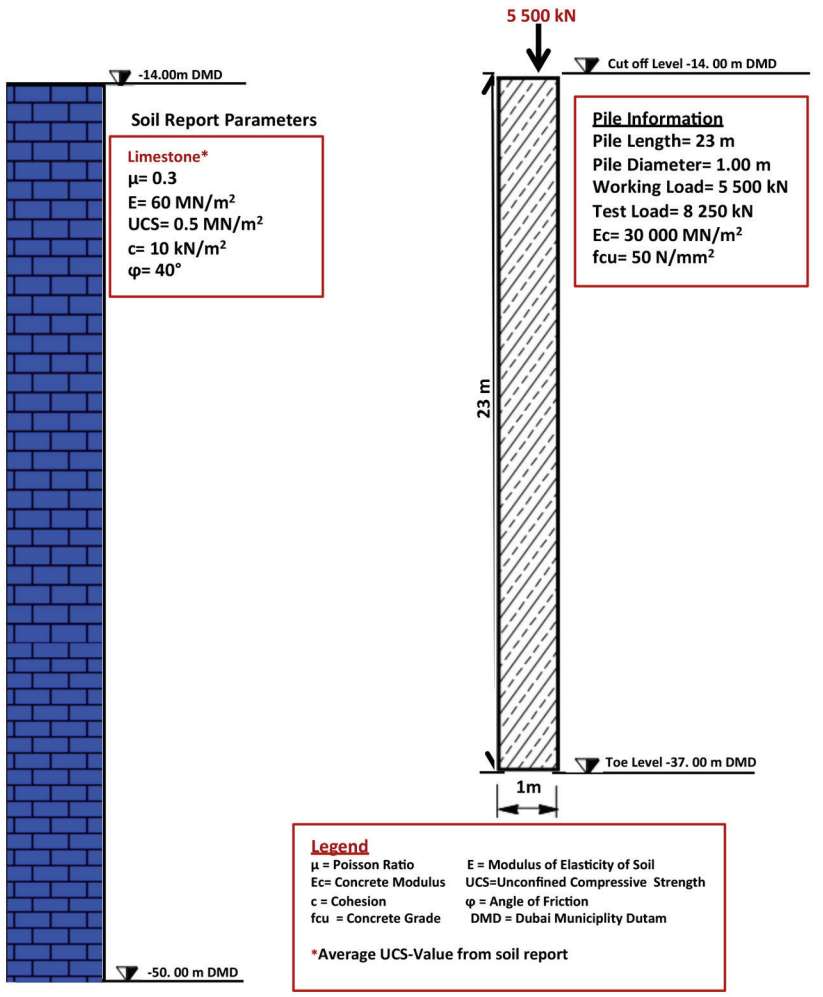

Modelling by using Soil Report Parameters

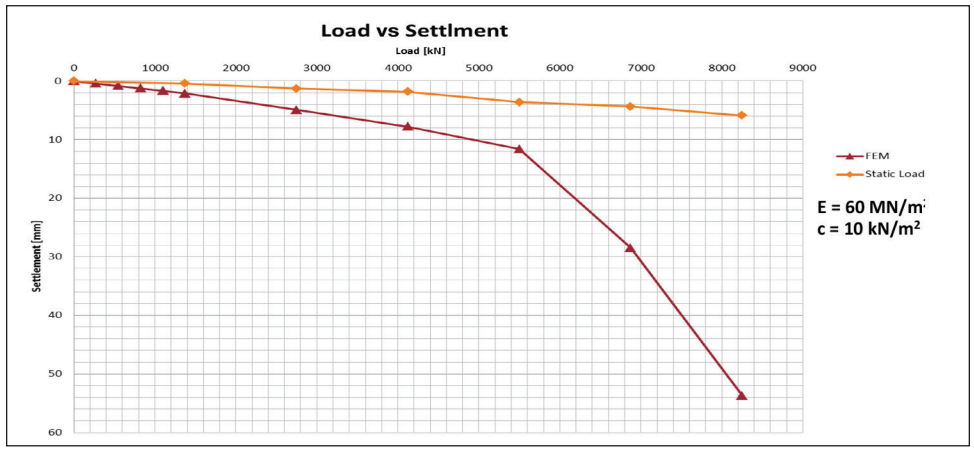

Back-Analysis of Soil Properties from Load Test

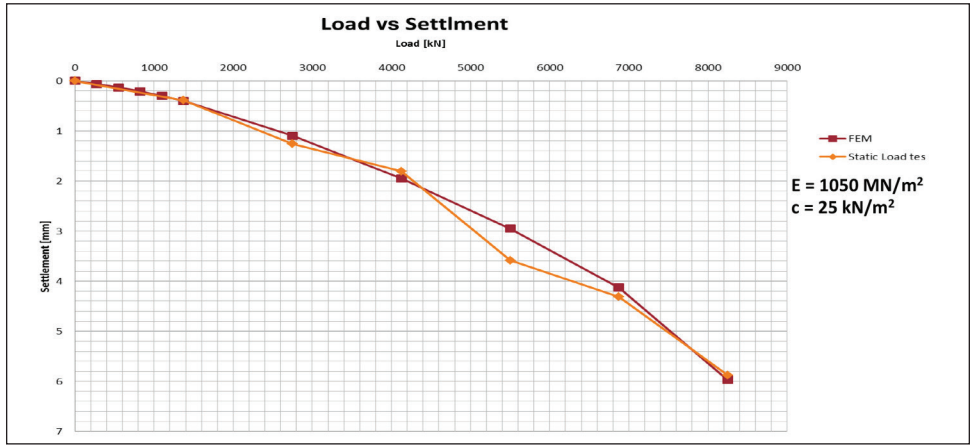

Pile Summary Sheet
P111

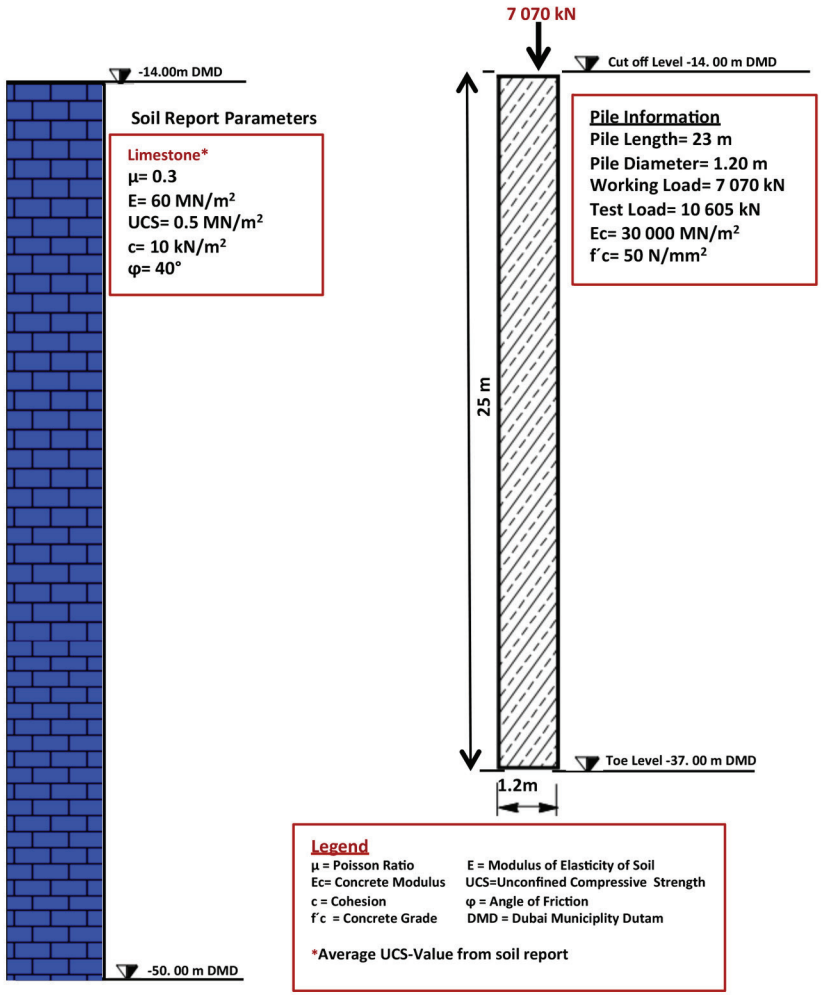

Modelling by using Soil Report Parameters

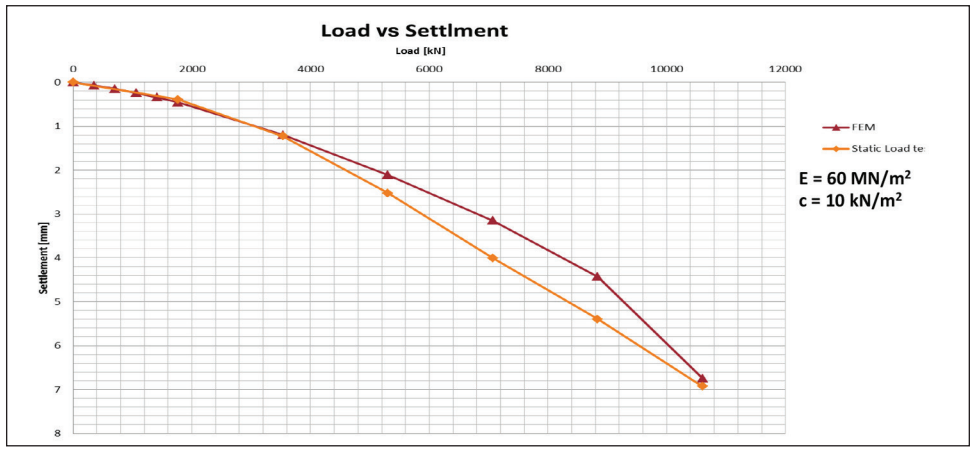

Back-Analysis of Soil Properties from Load Test

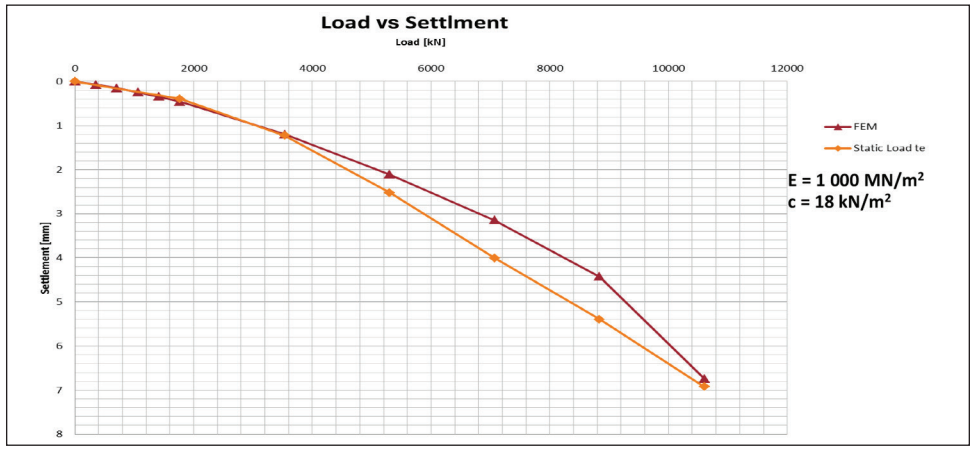

Pile Summary Sheet
P112

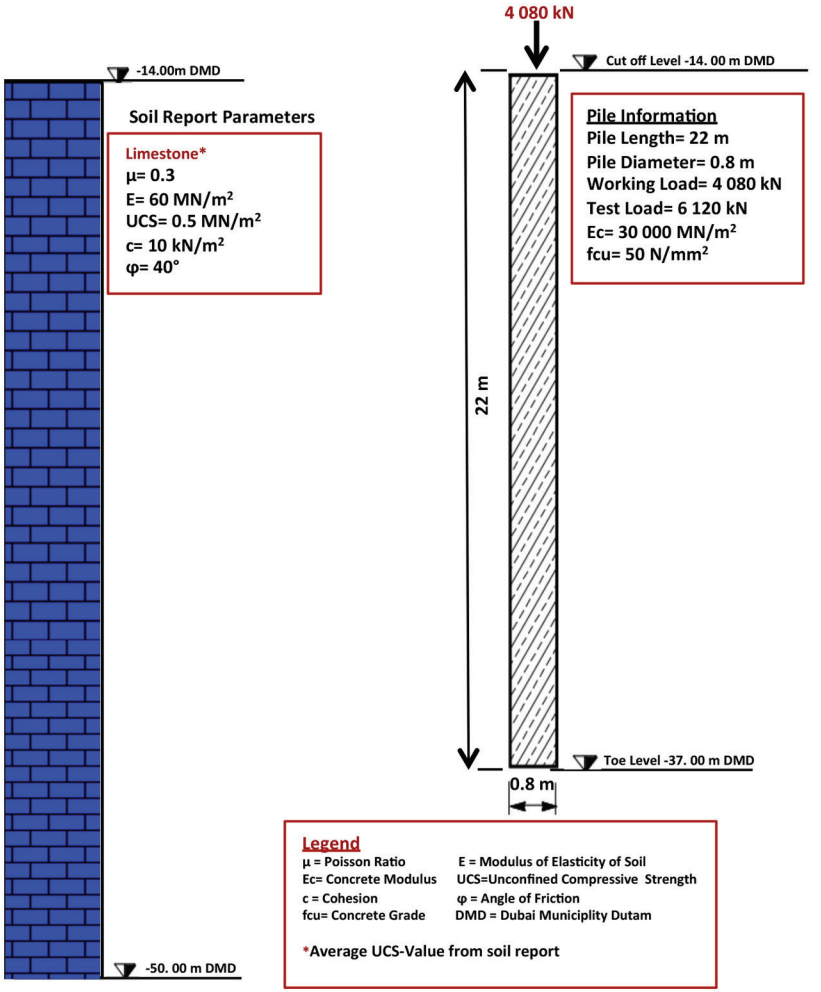

Modelling by using Soil Report Parameters

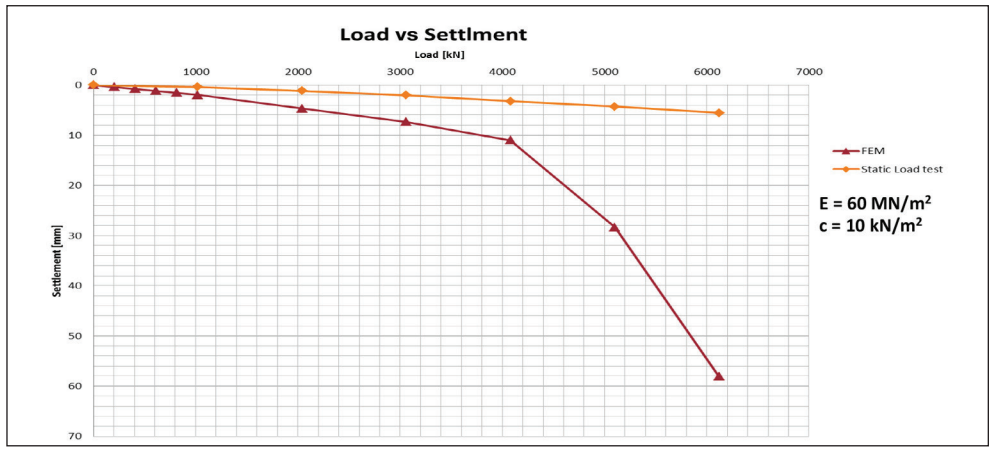

Back-Analysis of Soil Properties from Load Test

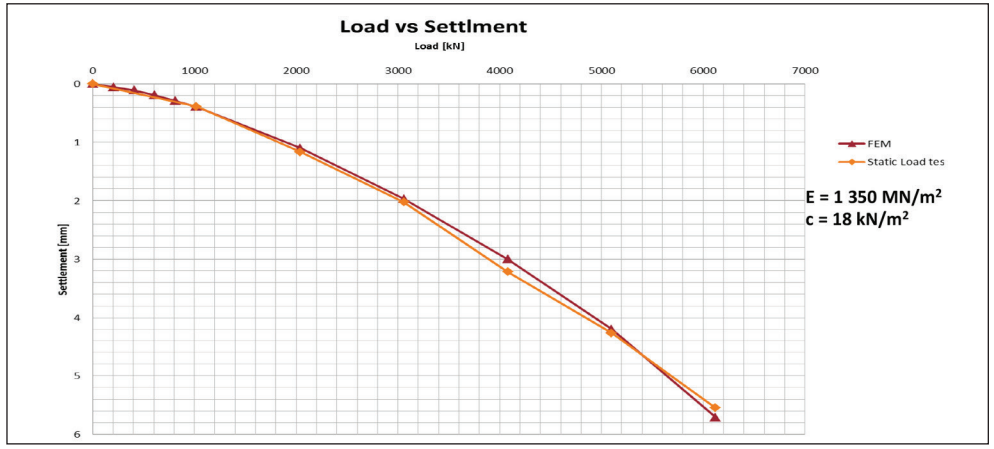

Pile Summary Sheet
P113

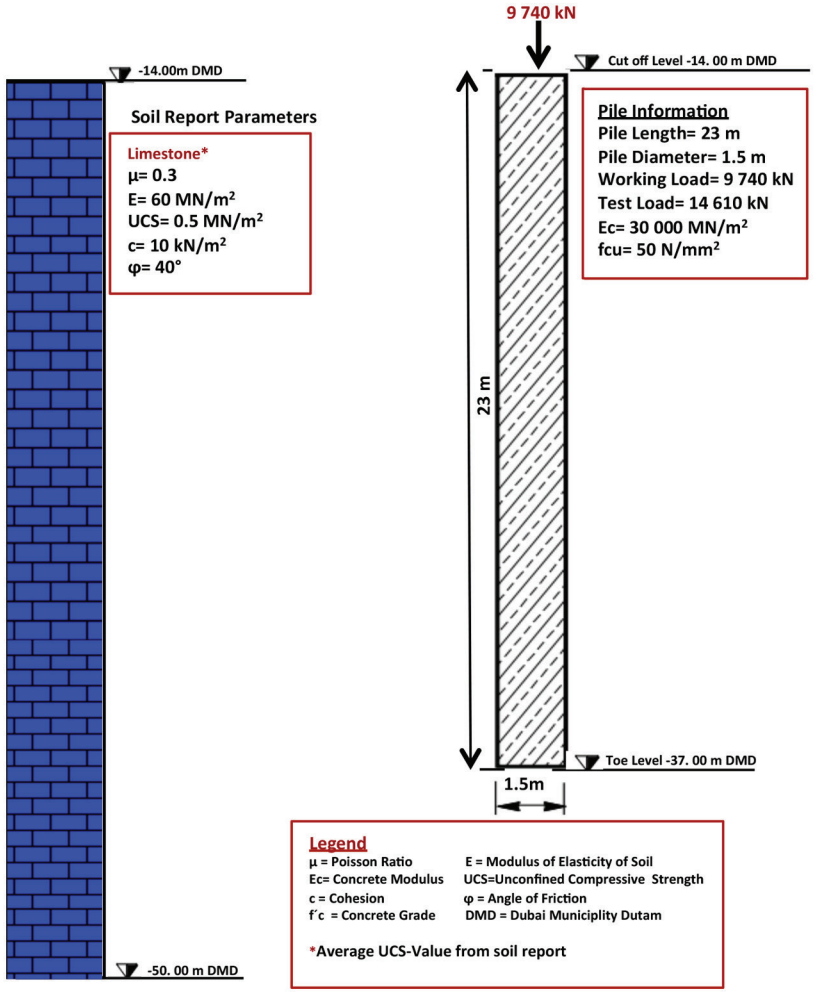

Soil Report Parameters

Limestone*
- μ= 0.3
- E= 60 MN/m²
- UCS= 0.5 MN/m²
- c= 10 kN/m²
- φ= 40°

Pile Information
- Pile Length= 23 m
- Pile Diameter= 1.5 m
- Working Load= 9 740 kN
- Test Load= 14 610 kN
- Ec= 30 000 MN/m²
- fcu= 50 N/mm²

Legend

μ = Poisson Ratio	E = Modulus of Elasticity of Soil
Ec= Concrete Modulus	UCS=Unconfined Compressive Strength
c = Cohesion	φ = Angle of Friction
f´c = Concrete Grade	DMD = Dubai Municiplity Dutam

*Average UCS-Value from soil report

Modelling by using Soil Report Parameters

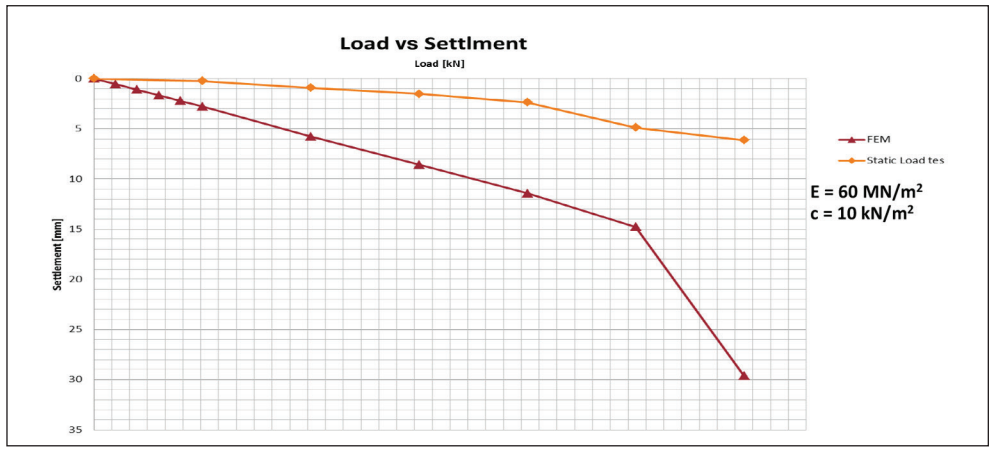

Back-Analysis of Soil Properties from Load Test

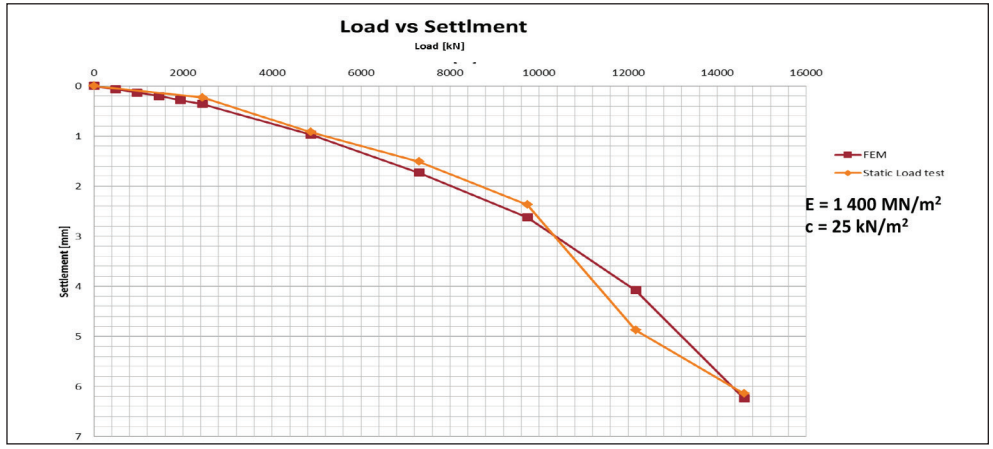

Pile Summary Sheet
P114

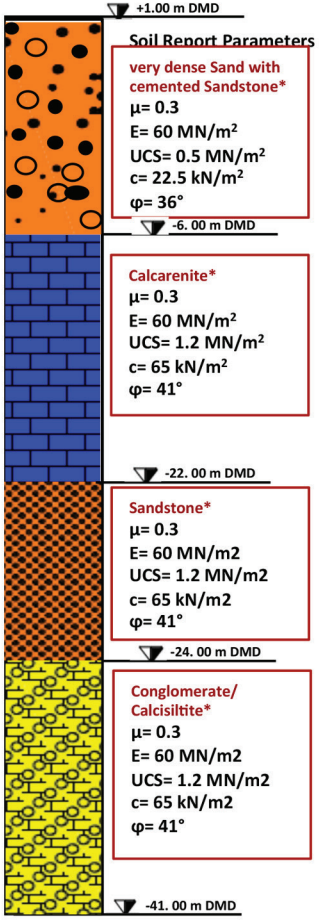

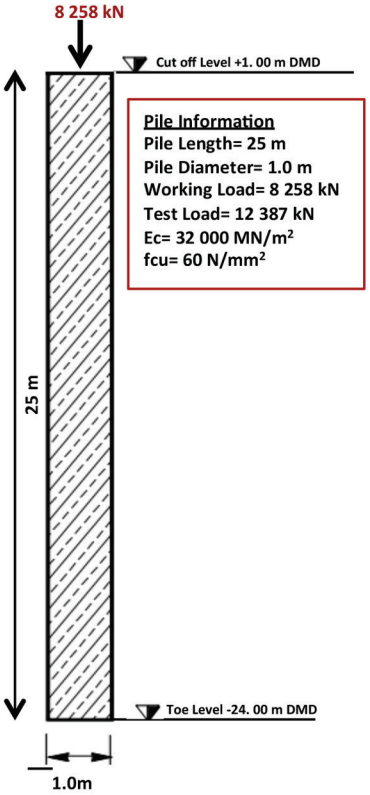

Pile Information
Pile Length= 25 m
Pile Diameter= 1.0 m
Working Load= 8 258 kN
Test Load= 12 387 kN
Ec= 32 000 MN/m²
fcu= 60 N/mm²

Legend

μ = Poisson Ratio	E = Modulus of Elasticity of Soil
Ec= Concrete Modulus	UCS=Unconfined Compressive Strength
c = Cohesion	φ = Angle of Friction
fcu = Concrete Grade	DMD = Dubai Municiplity Dutam

*Average UCS-Value from soil report

Modelling by using Soil Report Parameters

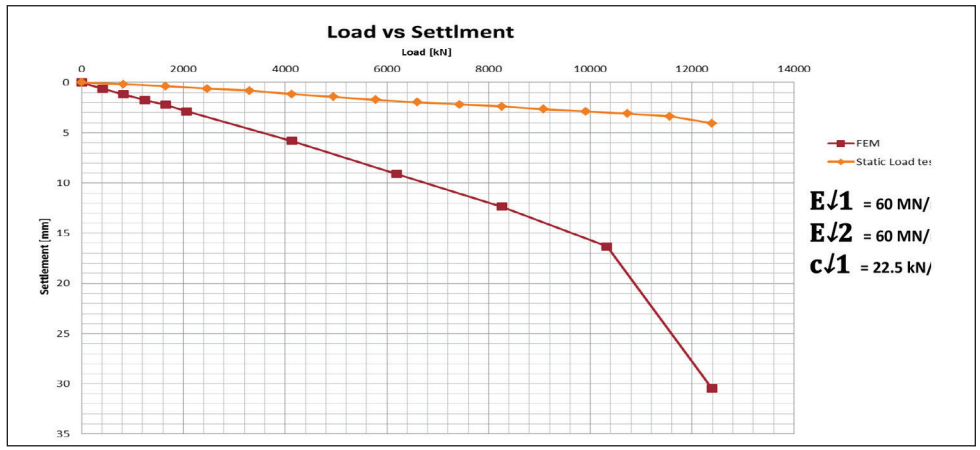

Back-Analysis of Soil Properties from Load Test

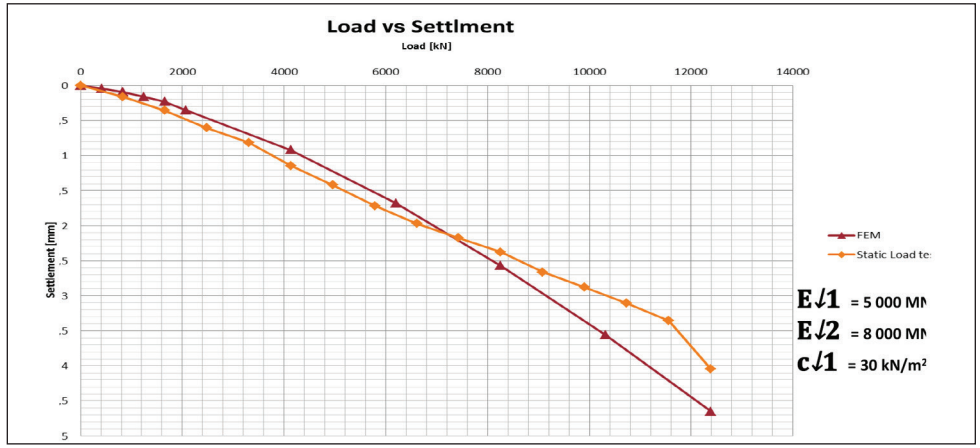

Pile Summary Sheet
P115

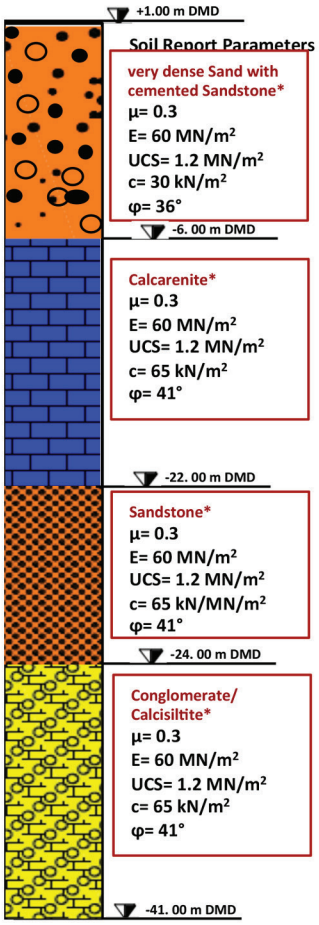

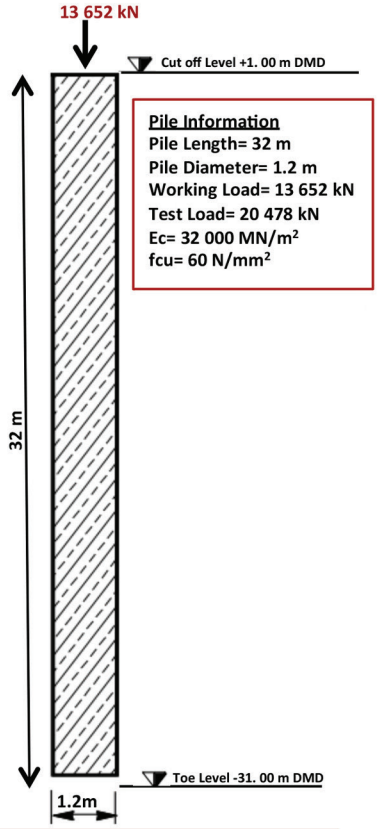

Pile Information
Pile Length= 32 m
Pile Diameter= 1.2 m
Working Load= 13 652 kN
Test Load= 20 478 kN
Ec= 32 000 MN/m²
fcu= 60 N/mm²

Legend

μ = Poisson Ratio	E = Modulus of Elasticity of Soil
Ec= Concrete Modulus	UCS=Unconfined Compressive Strength
c = Cohesion	φ = Angle of Friction
fcu = Concrete Grade	DMD = Dubai Municiplity Dutam

*Average UCS-Value from soil report

Modelling by using Soil Report Parameters

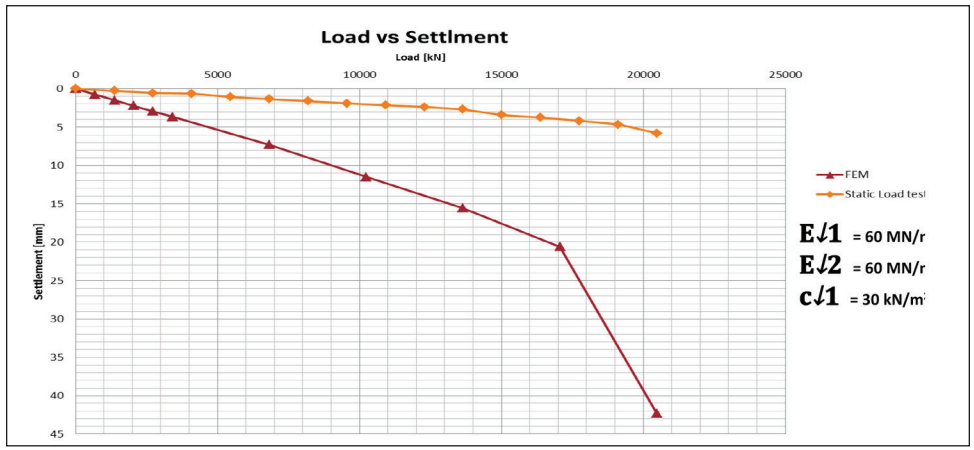

Back-Analysis of Soil Properties from Load Test

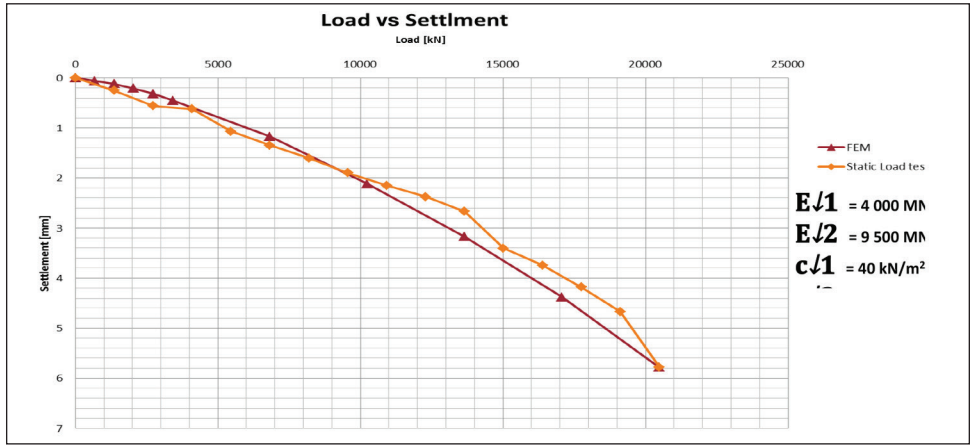

Pile Summary Sheet
P116

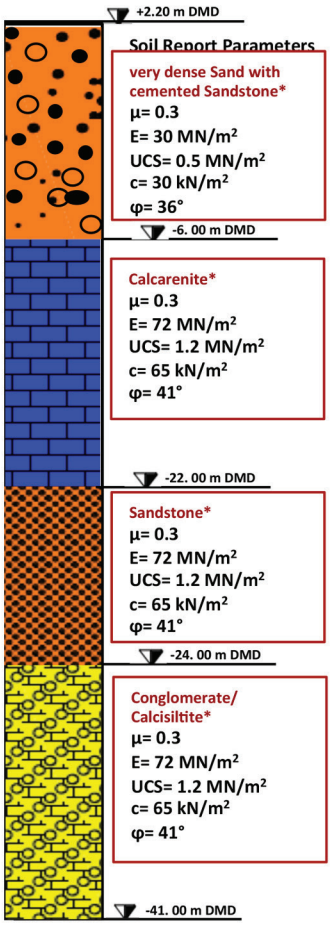

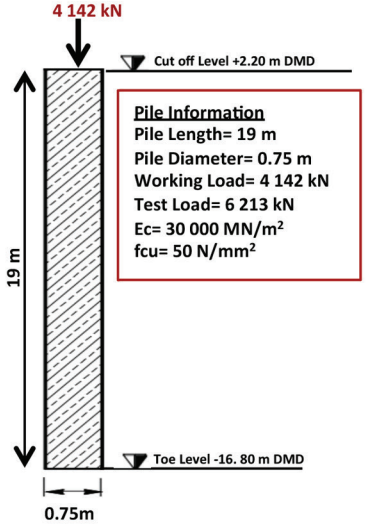

Pile Information
Pile Length= 19 m
Pile Diameter= 0.75 m
Working Load= 4 142 kN
Test Load= 6 213 kN
Ec= 30 000 MN/m²
fcu= 50 N/mm²

Legend

μ = Poisson Ratio	E = Modulus of Elasticity of Soil
Ec= Concrete Modulus	UCS=Unconfined Compressive Strength
c = Cohesion	φ = Angle of Friction
fcu = Concrete Grade	DMD = Dubai Municiplity Dutam

*Average UCS-Value from soil report

Modelling by using Soil Report Parameters

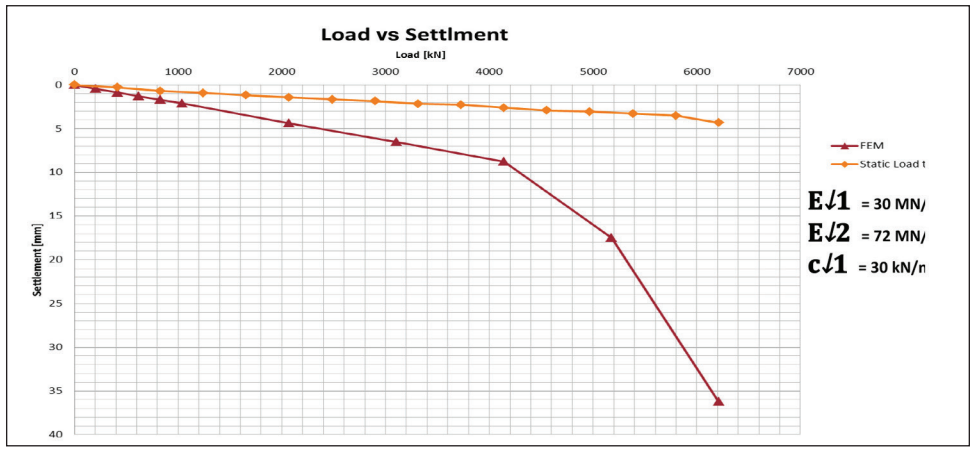

Back-Analysis of Soil Properties from Load Test

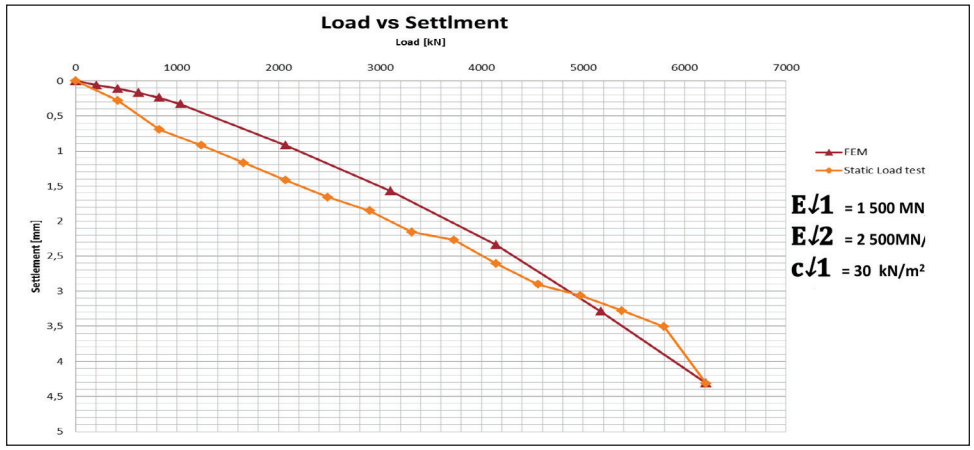

Appendix 2 Projects boreholes summary

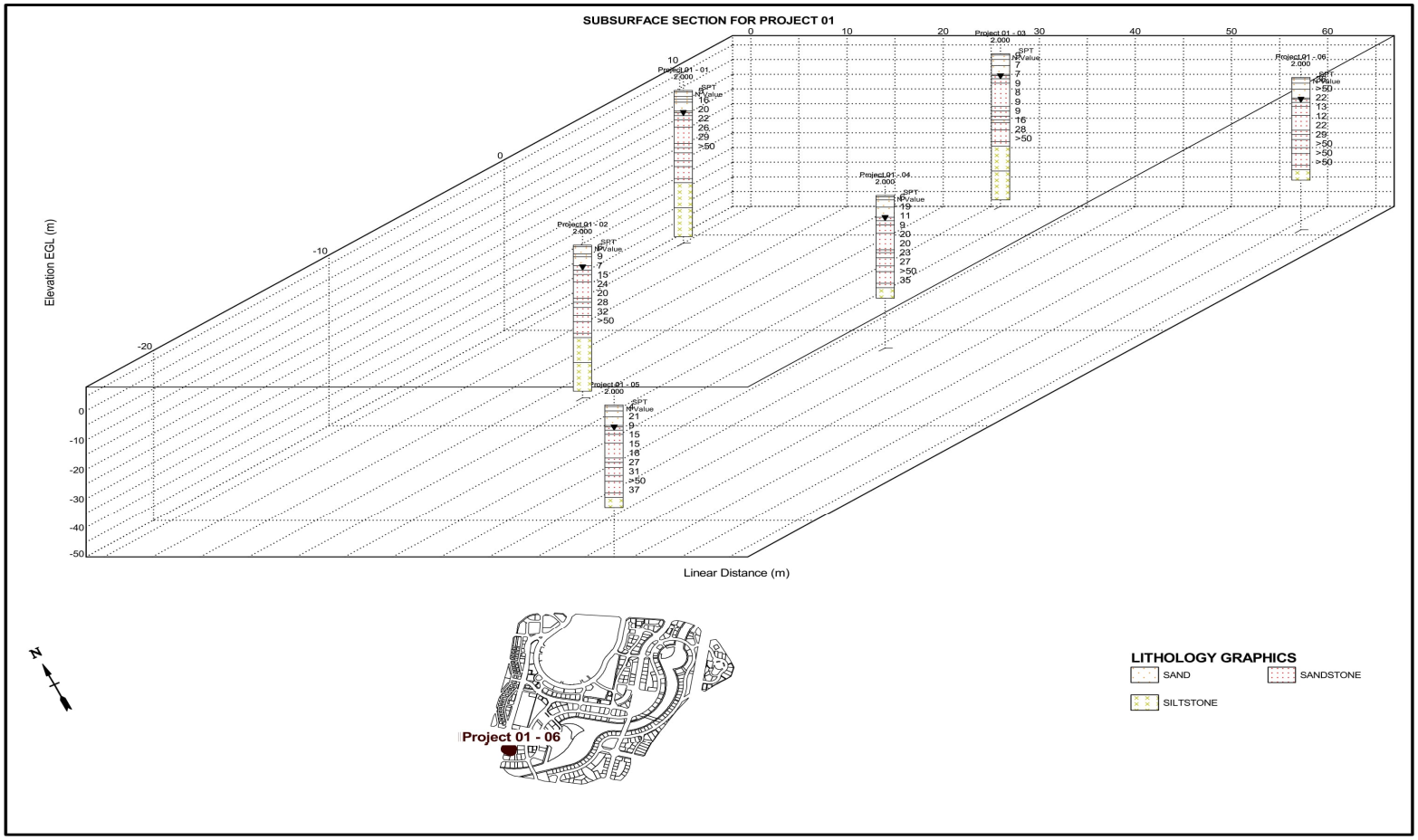
SUBSURFACE SECTION FOR PROJECT 01
Elevation EGL (m)
Linear Distance (m)
Project 01 - 01
Project 01 - 02
Project 01 - 03
Project 01 - 04
Project 01 - 05
Project 01 - 06
SPT N Value
LITHOLOGY GRAPHICS
SAND
SANDSTONE
SILTSTONE
N

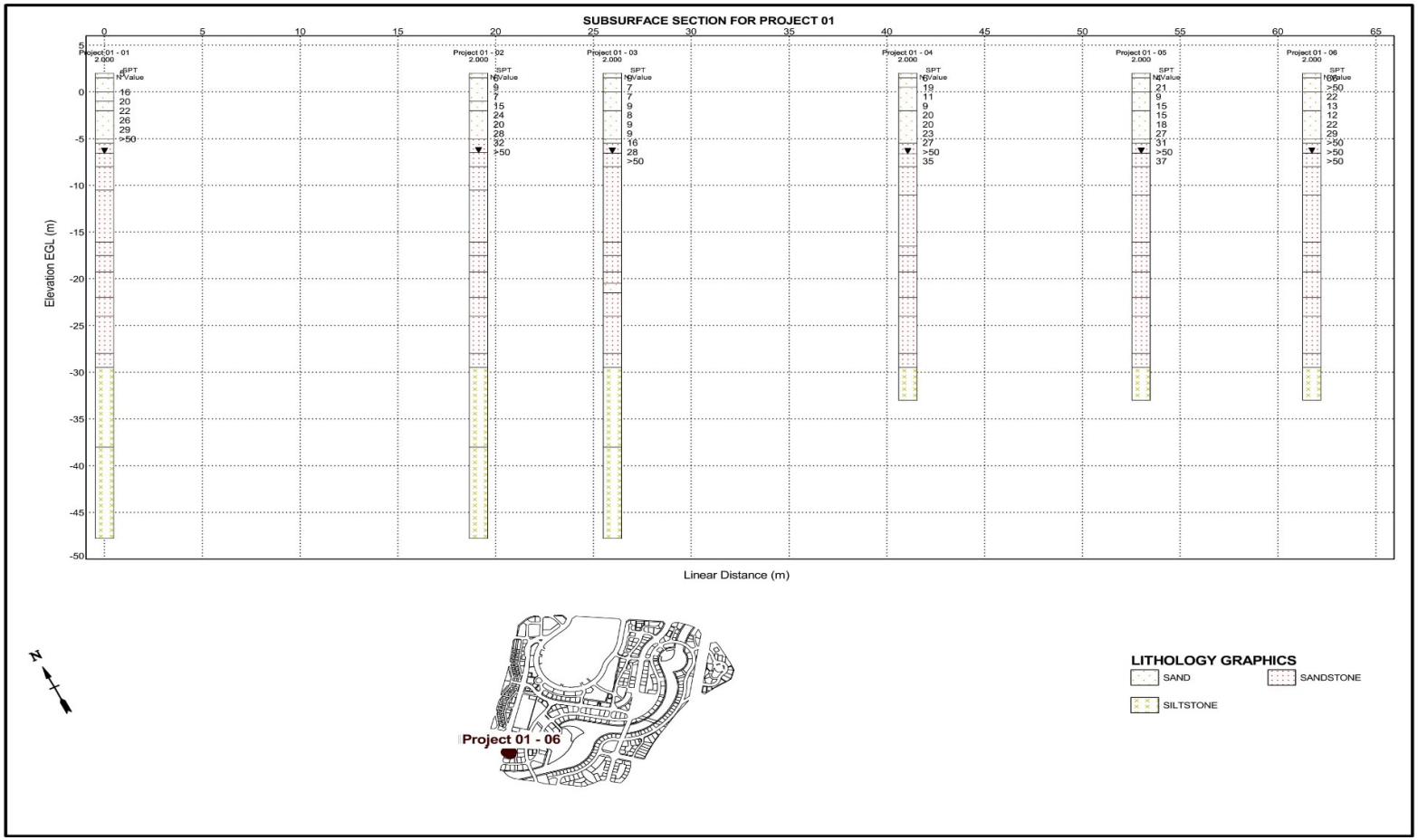
SUBSURFACE SECTION FOR PROJECT 01
Elevation EGL (m)
Linear Distance (m)
Project 01 - 01
Project 01 - 02
Project 01 - 03
Project 01 - 04
Project 01 - 05
Project 01 - 06
SPT N-Value
16 20 22 26 29 >50
9 7 15 24 20 28 32 >50
7 7 9 8 9 9 16 28 >50
19 11 9 20 20 23 27 >50 35
21 9 15 15 18 27 31 >50 37
>50 22 13 12 22 29 >50 >50 >50
N
Project 01 - 06
LITHOLOGY GRAPHICS
SAND
SANDSTONE
SILTSTONE

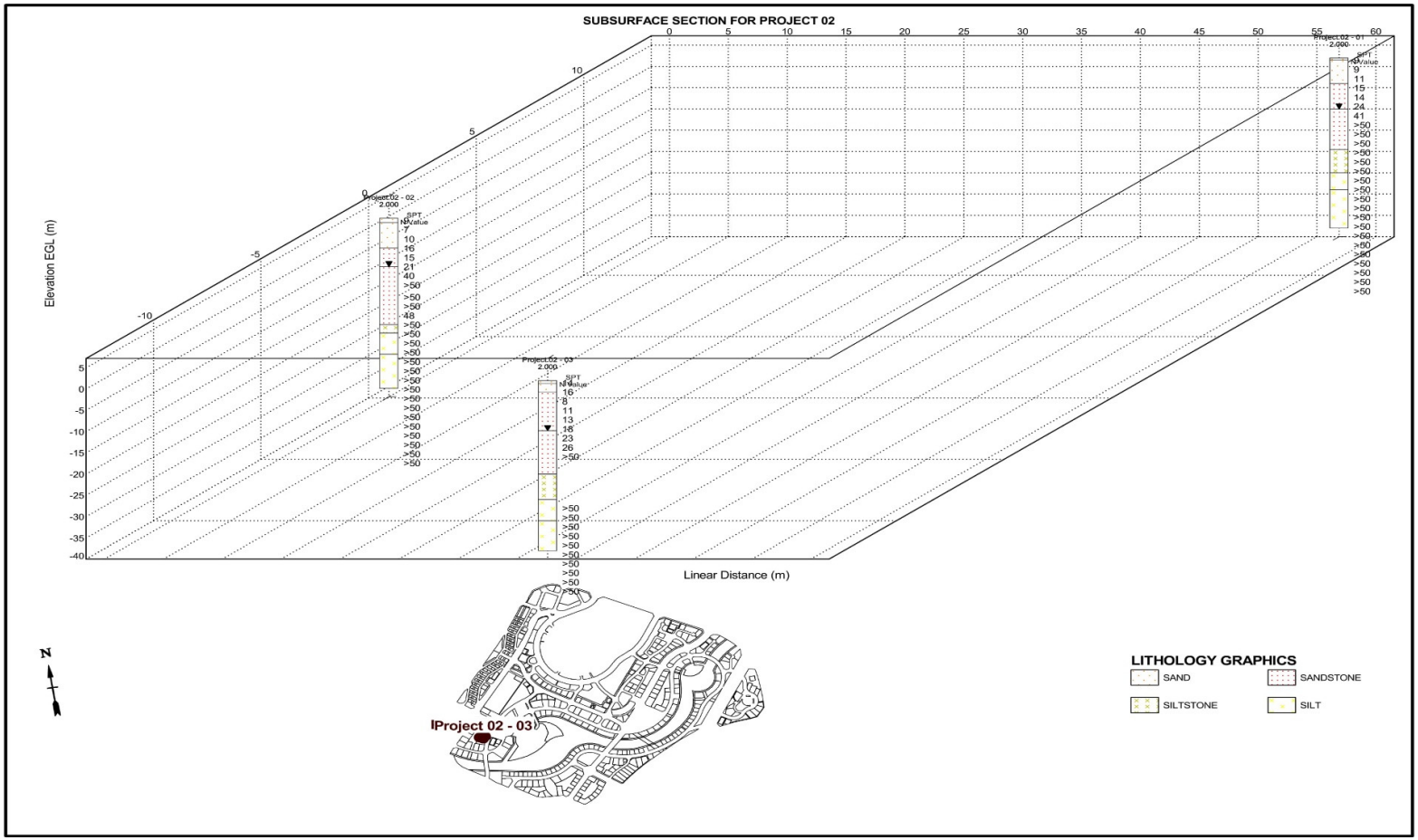
SUBSURFACE SECTION FOR PROJECT 02
Elevation EGL (m)
Linear Distance (m)
Project 02 - 03
LITHOLOGY GRAPHICS
SAND
SANDSTONE
SILTSTONE
SILT
N

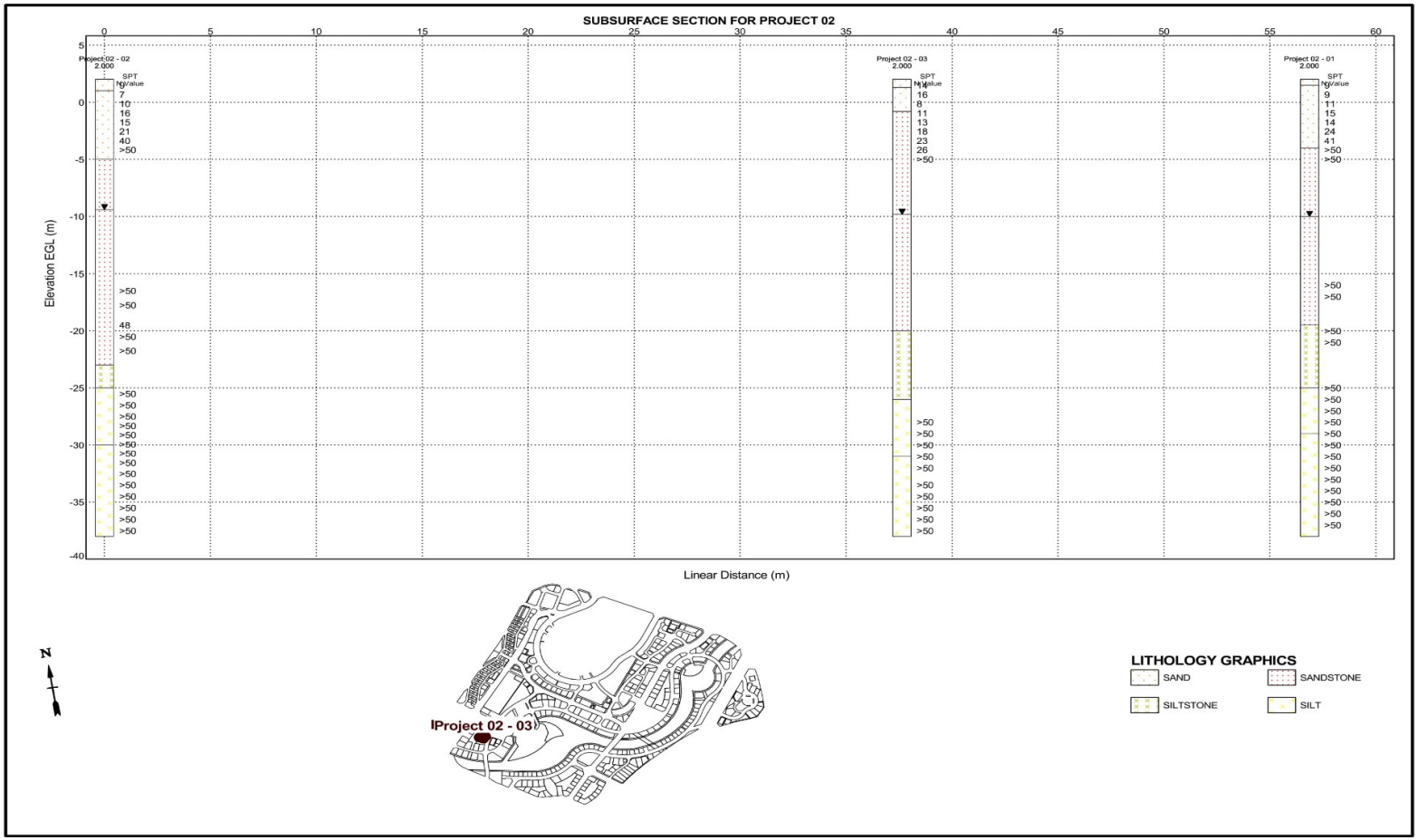
SUBSURFACE SECTION FOR PROJECT 02
Elevation EGL (m)
Linear Distance (m)
Project 02 - 02
Project 02 - 03
Project 02 - 01
SPT N-value
Project 02 - 03
N
LITHOLOGY GRAPHICS
SAND
SANDSTONE
SILTSTONE
SILT

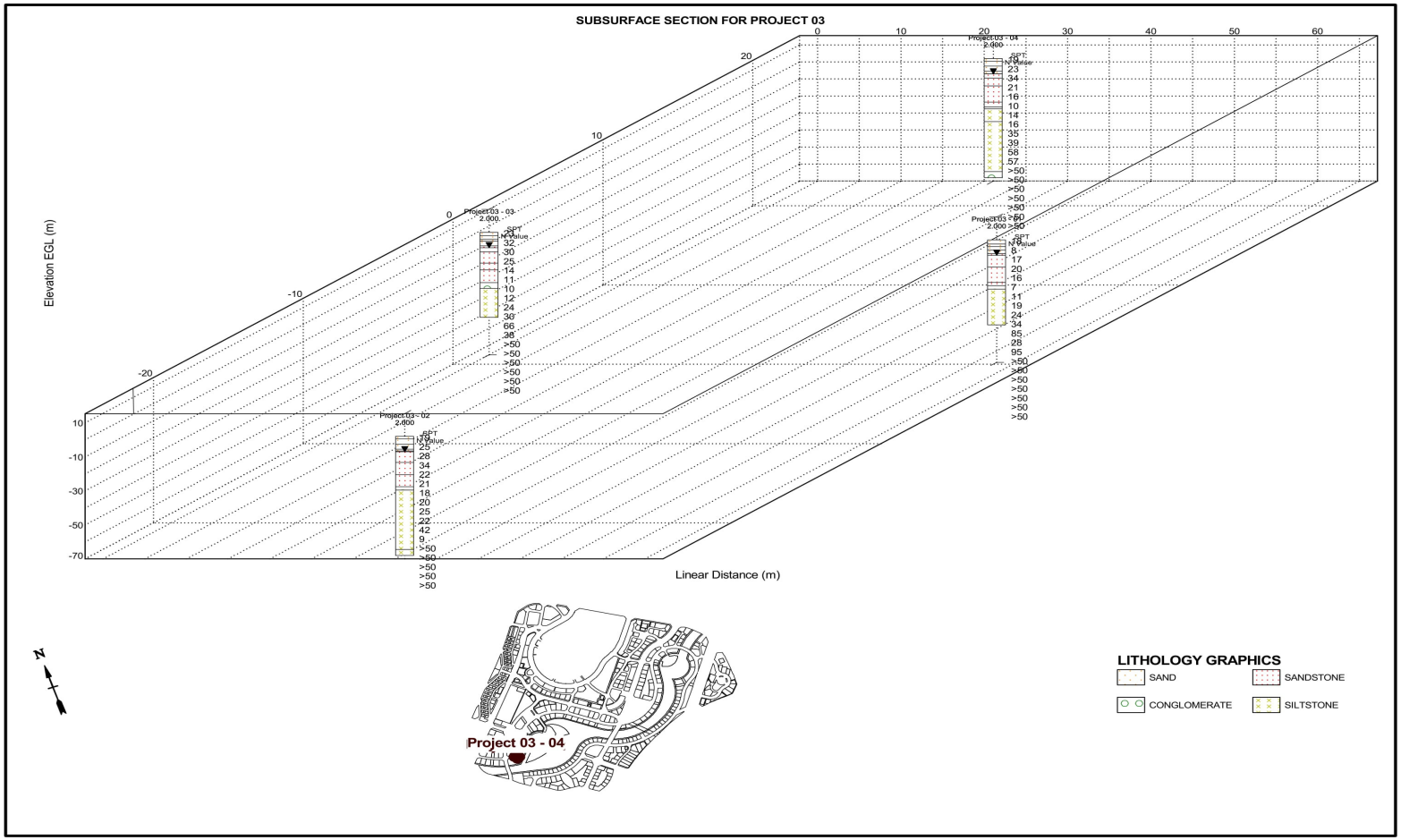
SUBSURFACE SECTION FOR PROJECT 03
Elevation EGL (m)
Linear Distance (m)
Project 03 - 04
Project 03 - 03
Project 03 - 02
Project 03 - 01
SPT N Value
LITHOLOGY GRAPHICS
SAND
SANDSTONE
CONGLOMERATE
SILTSTONE
N

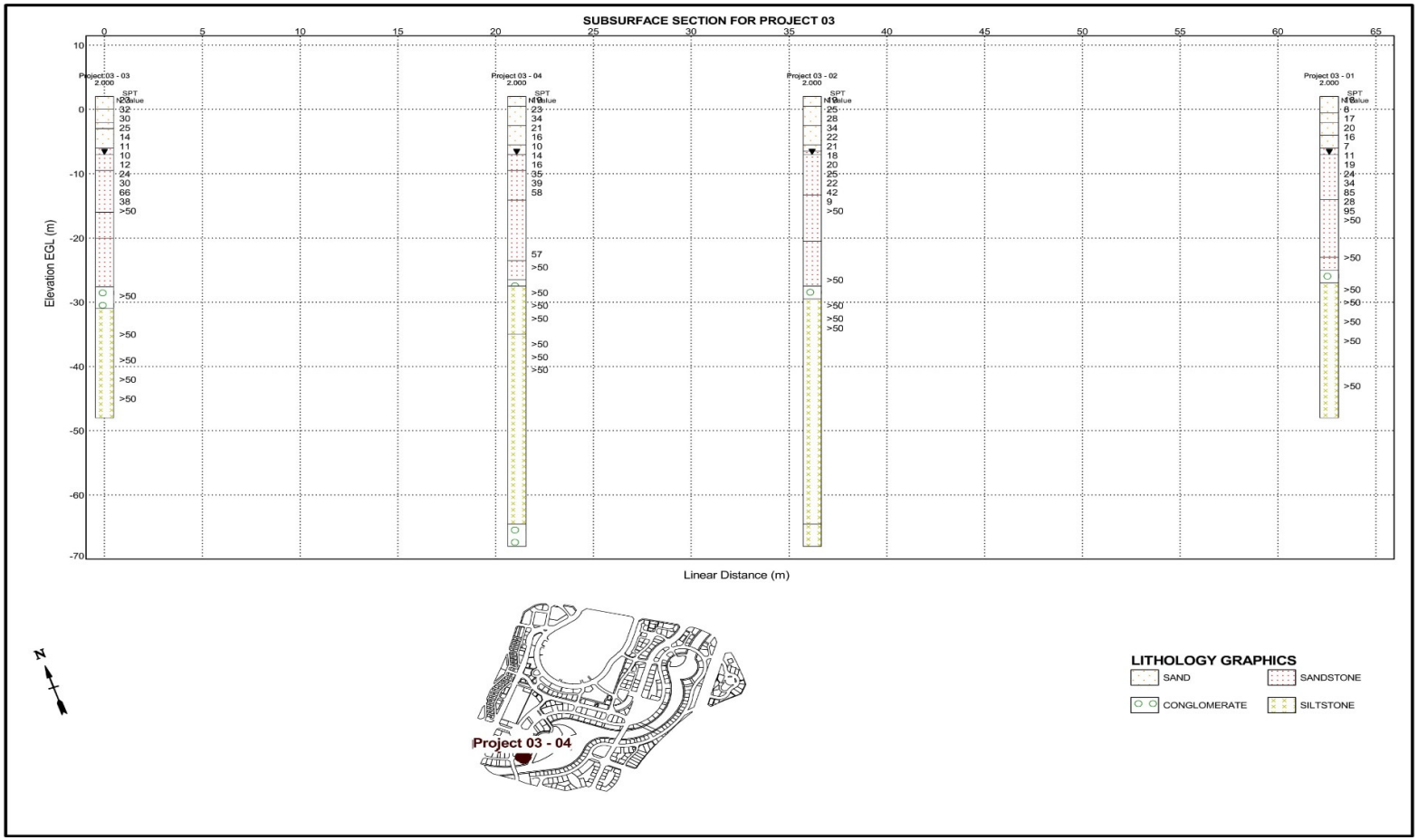
SUBSURFACE SECTION FOR PROJECT 03
Elevation EGL (m)
Linear Distance (m)
Project 03 - 03
Project 03 - 04
Project 03 - 02
Project 03 - 01
SPT N Value
Project 03 - 04
LITHOLOGY GRAPHICS
SAND
SANDSTONE
CONGLOMERATE
SILTSTONE
N

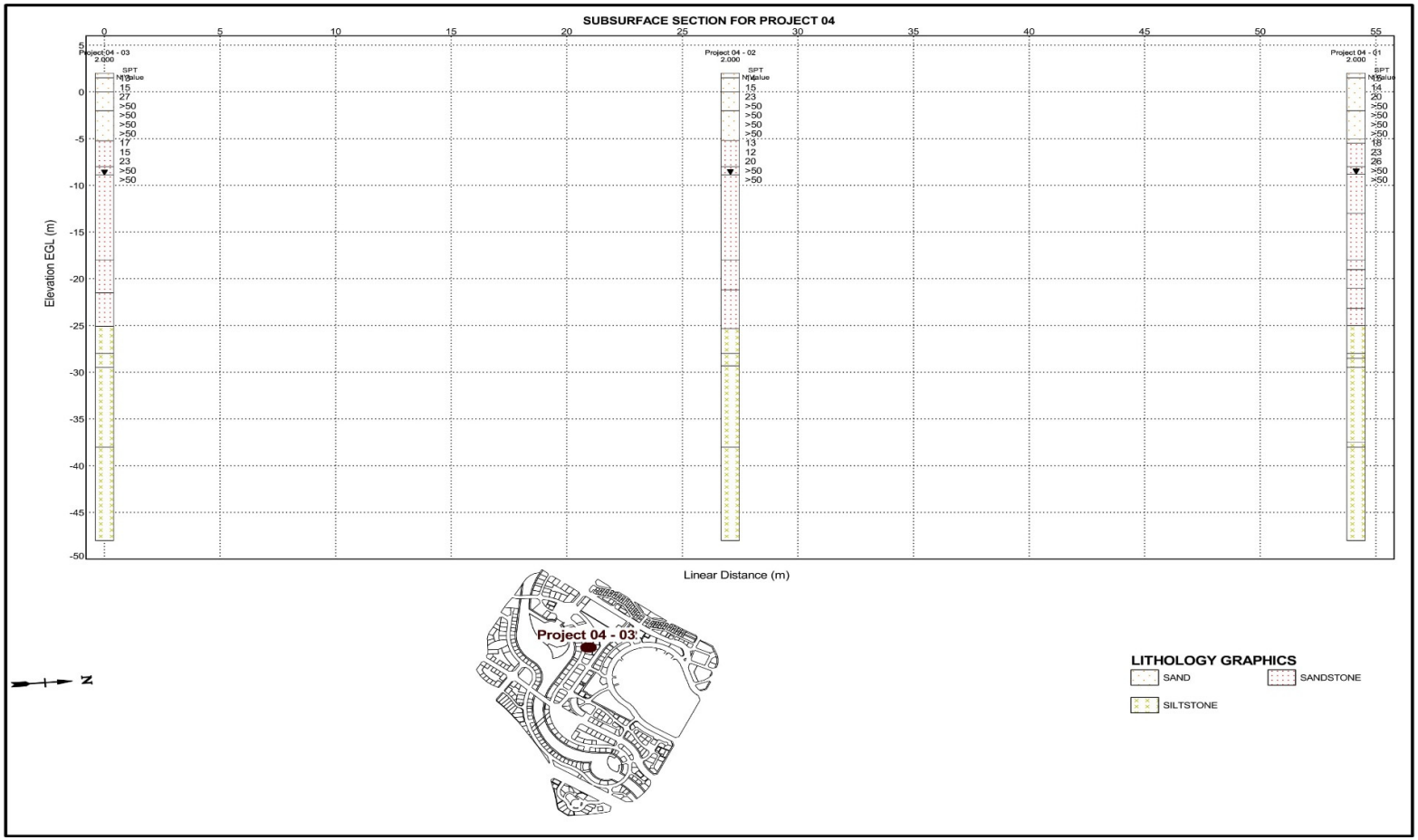
SUBSURFACE SECTION FOR PROJECT 04
Elevation EGL (m)
Linear Distance (m)
Project 04 - 03
Project 04 - 02
Project 04 - 01
SPT N Value
Project 04 - 03
Project 04 - 03
N
LITHOLOGY GRAPHICS
SAND
SANDSTONE
SILTSTONE

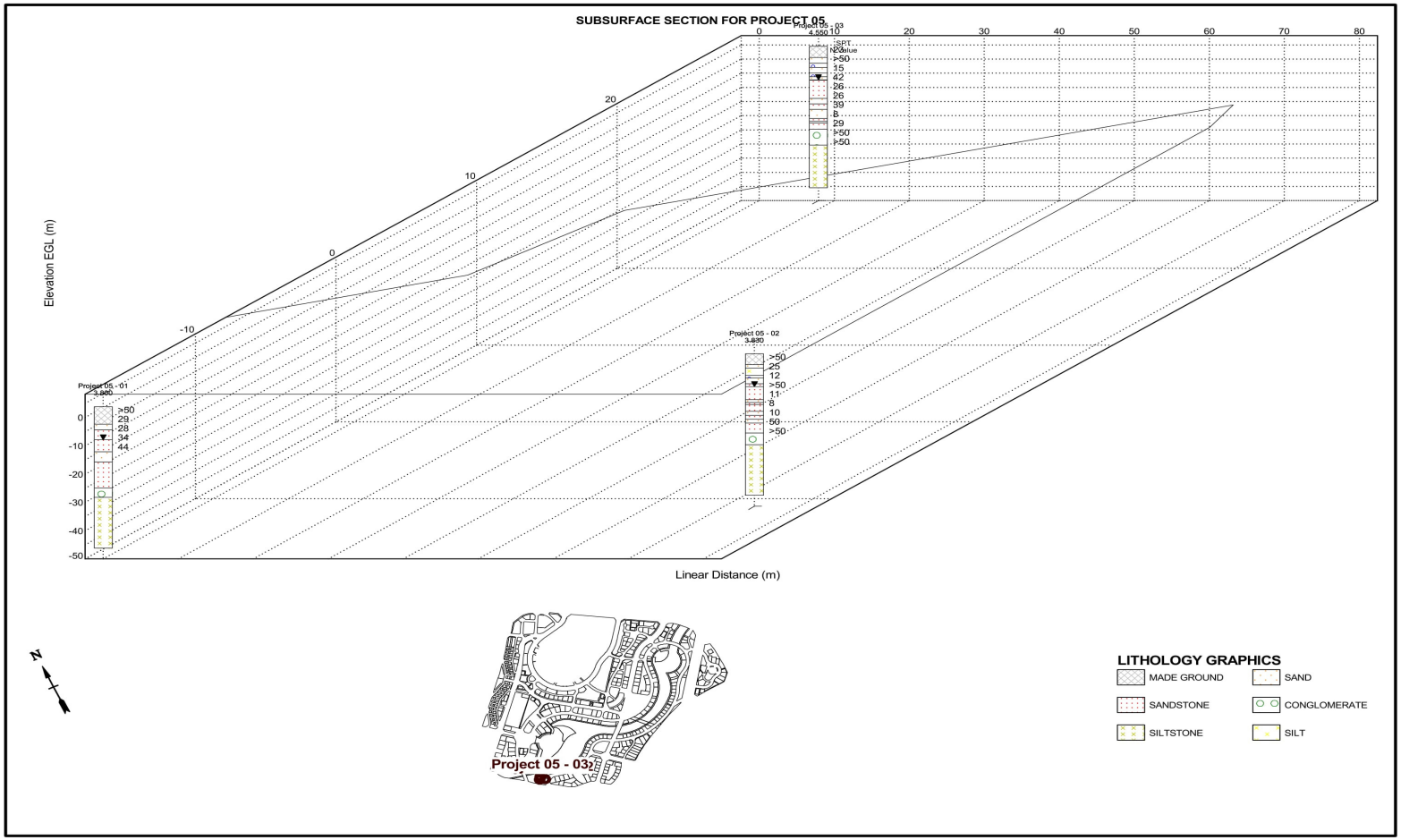
SUBSURFACE SECTION FOR PROJECT 05
Elevation EGL (m)
Linear Distance (m)
Project 05 - 01
3.800
Project 05 - 02
3.830
Project 05 - 03
4.920
SPT
N-Value
LITHOLOGY GRAPHICS
MADE GROUND
SAND
SANDSTONE
CONGLOMERATE
SILTSTONE
SILT
Project 05 - 03

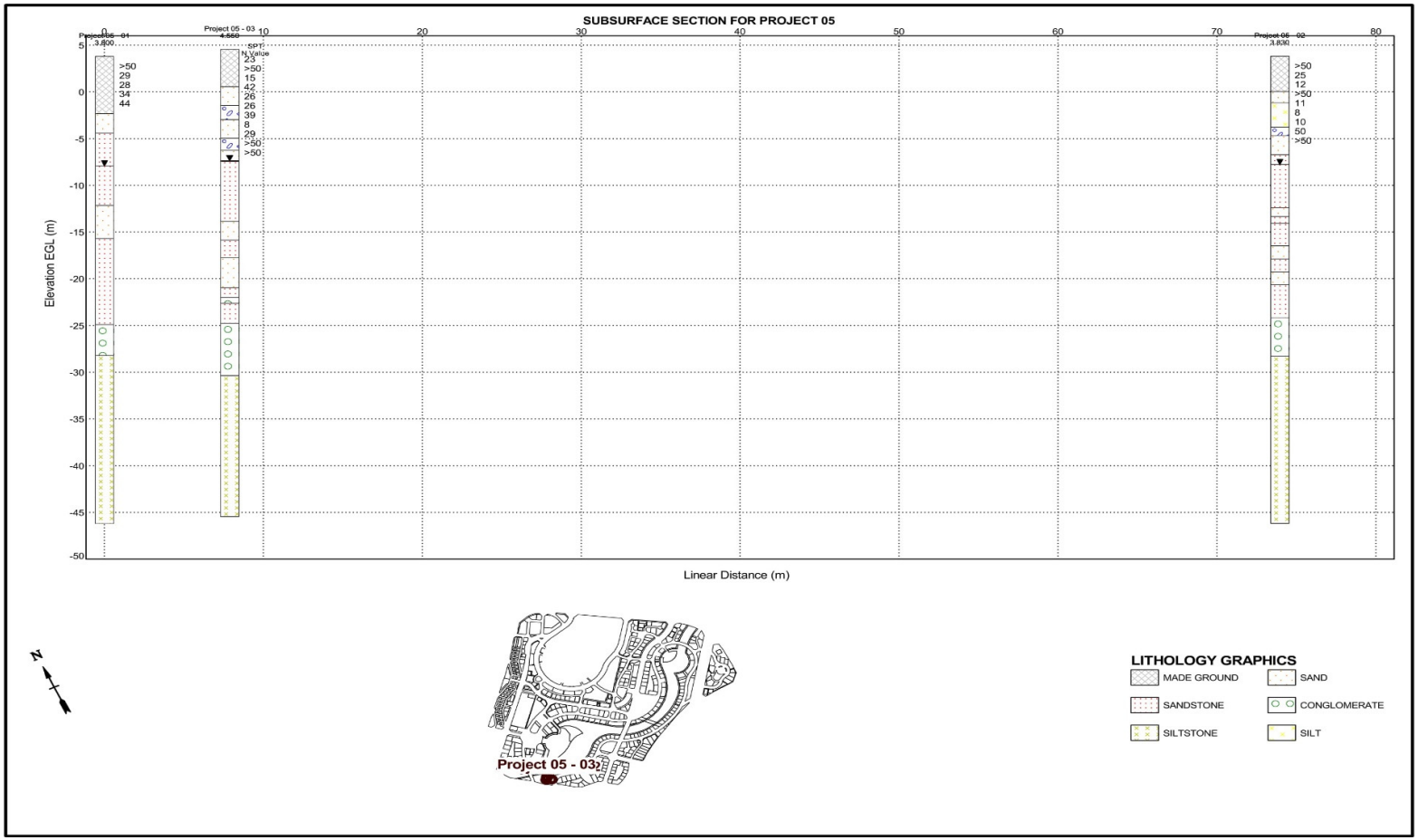
SUBSURFACE SECTION FOR PROJECT 05
Project 05 - 01
-3.800
Project 05 - 03
-4.550
SPT
N Value
Project 05 - 02
-3.830
>50
29
28
34
44
23
>50
15
42
26
26
39
8
29
>50
>50
>50
25
12
>50
11
8
10
50
>50
Elevation EGL (m)
Linear Distance (m)
N
Project 05 - 03
LITHOLOGY GRAPHICS
MADE GROUND
SAND
SANDSTONE
CONGLOMERATE
SILTSTONE
SILT

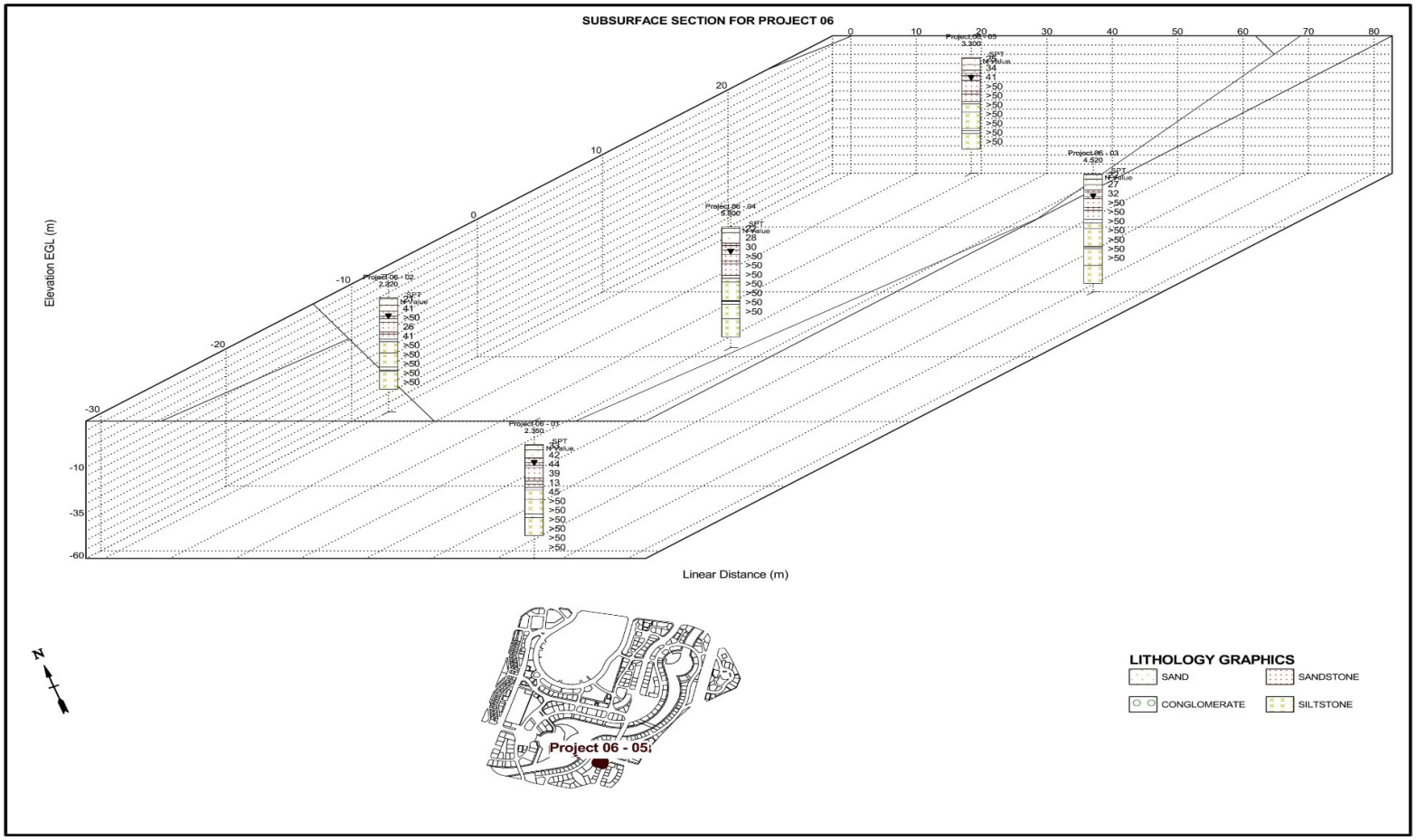
SUBSURFACE SECTION FOR PROJECT 06
Elevation EGL (m)
Linear Distance (m)
Project 06 - 01
Project 06 - 02
Project 06 - 03
Project 06 - 04
Project 06 - 05
SPT N-Value
LITHOLOGY GRAPHICS
SAND
SANDSTONE
CONGLOMERATE
SILTSTONE
N
Project 06 - 05

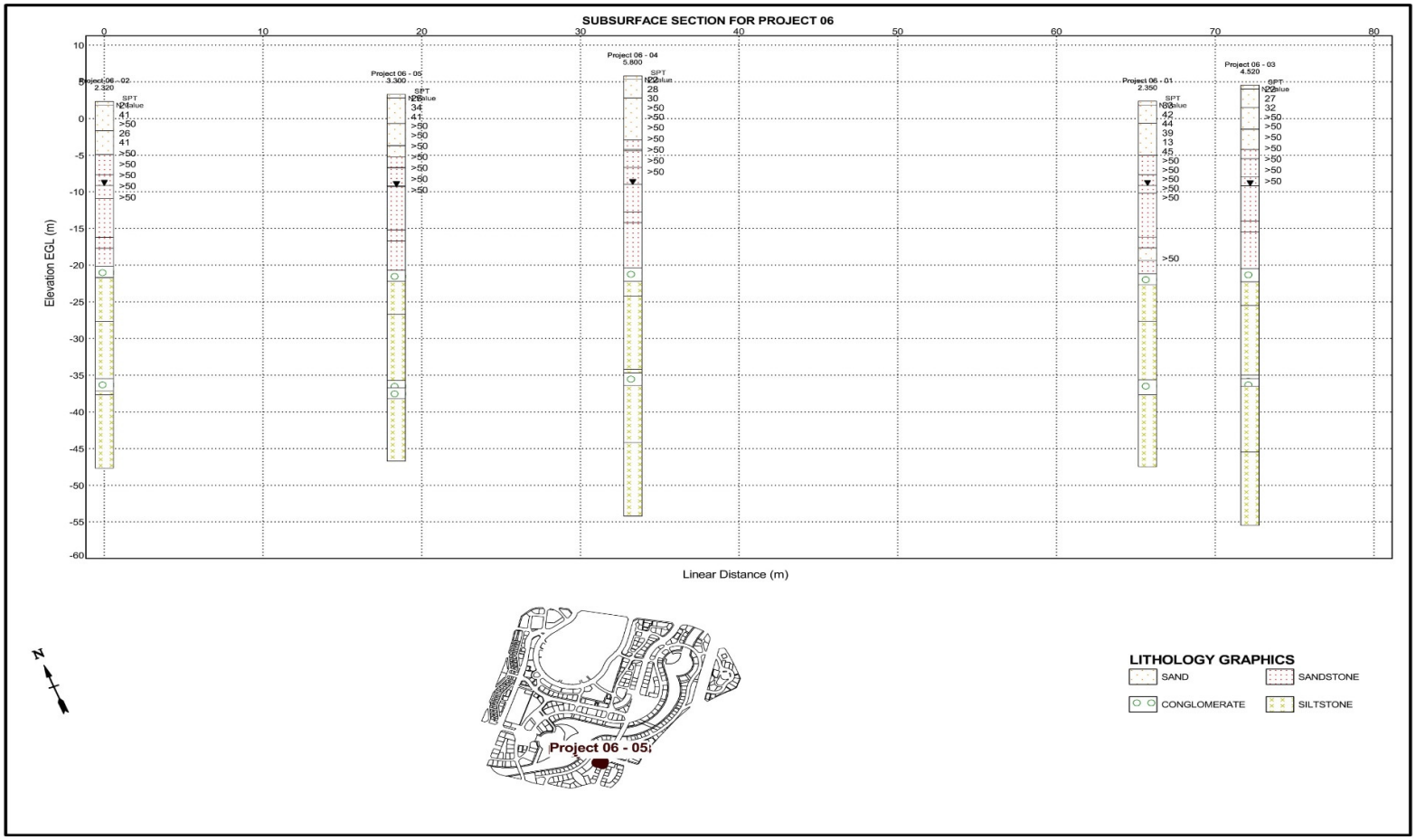
SUBSURFACE SECTION FOR PROJECT 06
Elevation EGL (m)
Linear Distance (m)
Project 06 - 02
2.320
Project 06 - 05
3.300
Project 06 - 04
5.800
Project 06 - 01
2.350
Project 06 - 03
4.520
SPT
N Value
Project 06 - 05
N
LITHOLOGY GRAPHICS
SAND
SANDSTONE
CONGLOMERATE
SILTSTONE

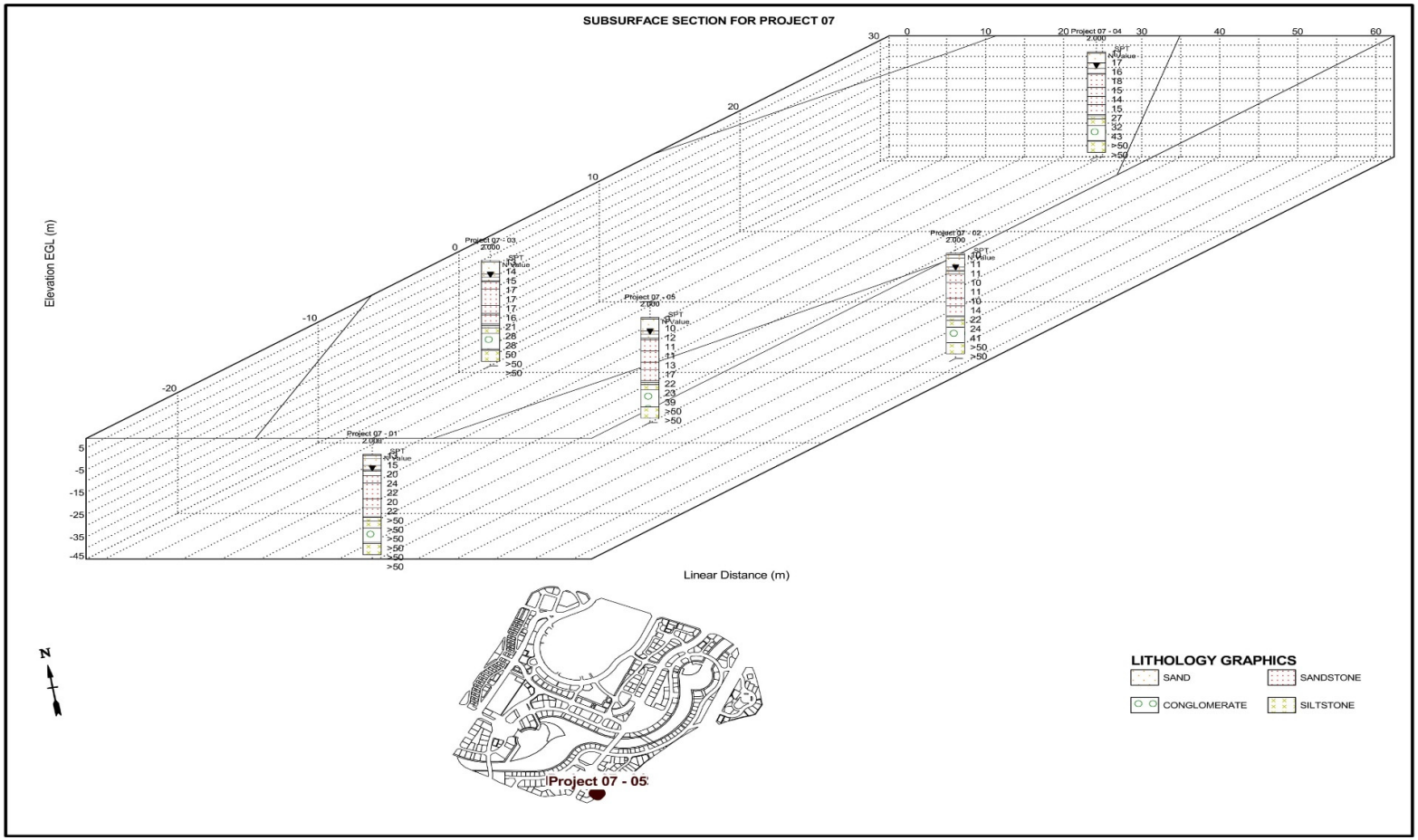
SUBSURFACE SECTION FOR PROJECT 07
Elevation EGL (m)
Linear Distance (m)
Project 07 - 01
Project 07 - 02
Project 07 - 03
Project 07 - 04
Project 07 - 05
SPT NValue
N
LITHOLOGY GRAPHICS
SAND
SANDSTONE
CONGLOMERATE
SILTSTONE
Project 07 - 05

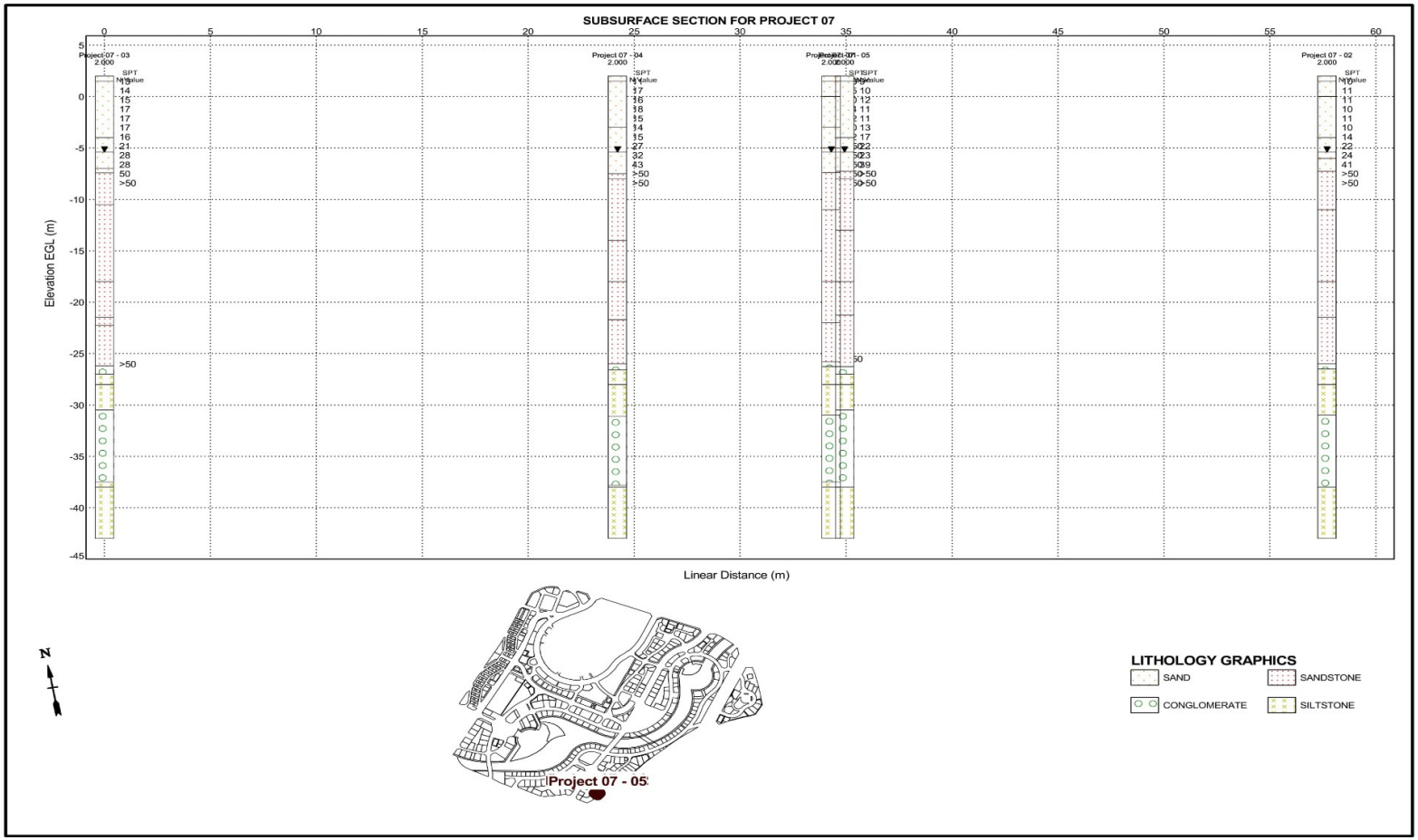
SUBSURFACE SECTION FOR PROJECT 07
Elevation EGL (m)
Linear Distance (m)
Project 07 - 03
Project 07 - 04
Project 07 - 05
Project 07 - 02
SPT N Value
LITHOLOGY GRAPHICS
SAND
SANDSTONE
CONGLOMERATE
SILTSTONE
N
Project 07 - 05

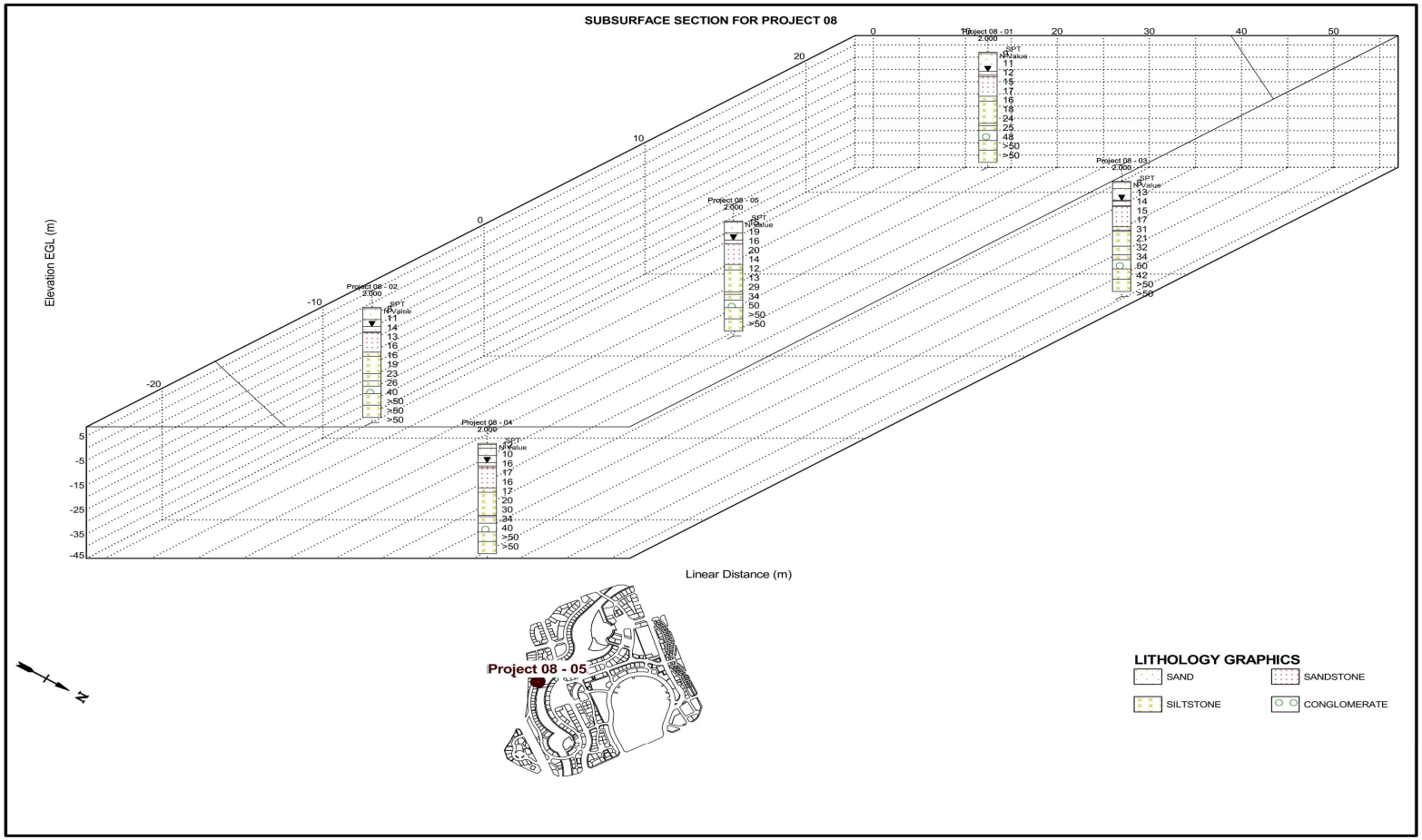
SUBSURFACE SECTION FOR PROJECT 08
Elevation EGL (m)
Linear Distance (m)
Project 08 - 01
Project 08 - 02
Project 08 - 03
Project 08 - 04
Project 08 - 05
SPT N-Value
LITHOLOGY GRAPHICS
SAND
SANDSTONE
SILTSTONE
CONGLOMERATE
N

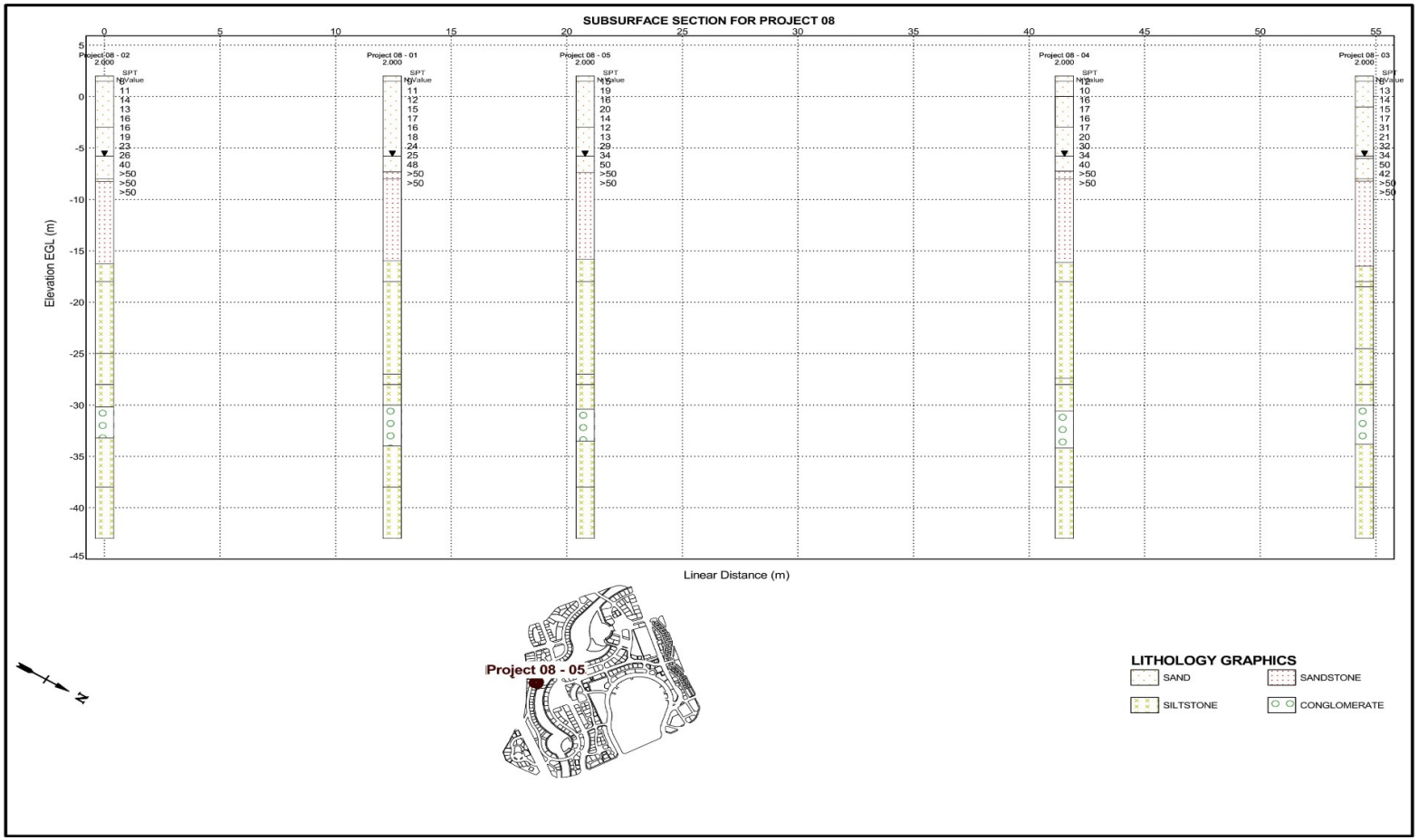
SUBSURFACE SECTION FOR PROJECT 08
Project 08 - 02
2.000
Project 08 - 01
2.000
Project 08 - 05
2.000
Project 08 - 04
2.000
Project 08 - 03
2.000
SPT
N-Value
Elevation EGL (m)
Linear Distance (m)
Project 08 - 05
N
LITHOLOGY GRAPHICS
SAND
SANDSTONE
SILTSTONE
CONGLOMERATE

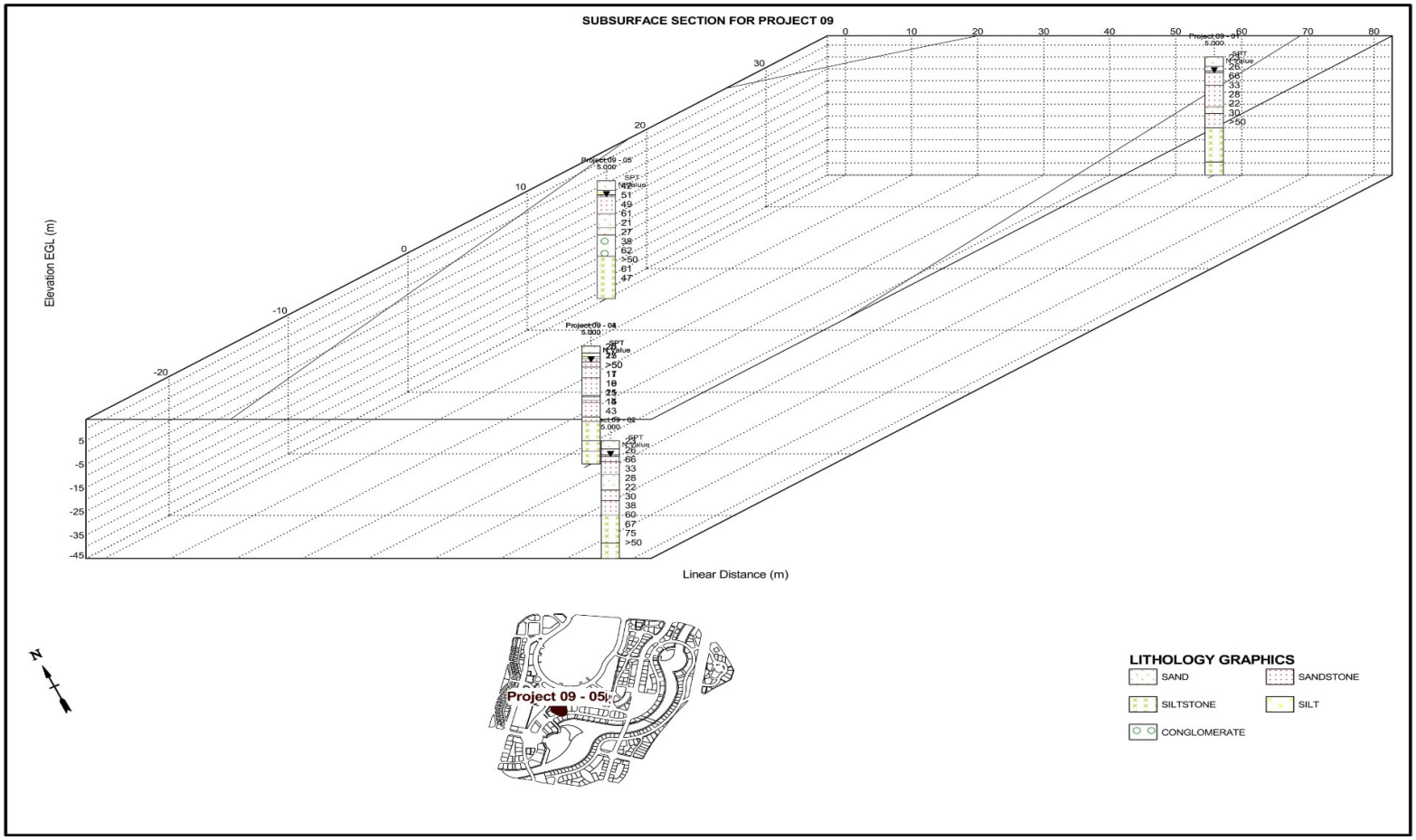
SUBSURFACE SECTION FOR PROJECT 09
Elevation EGL (m)
Linear Distance (m)
Project 09 - 05
LITHOLOGY GRAPHICS
SAND
SANDSTONE
SILTSTONE
SILT
CONGLOMERATE

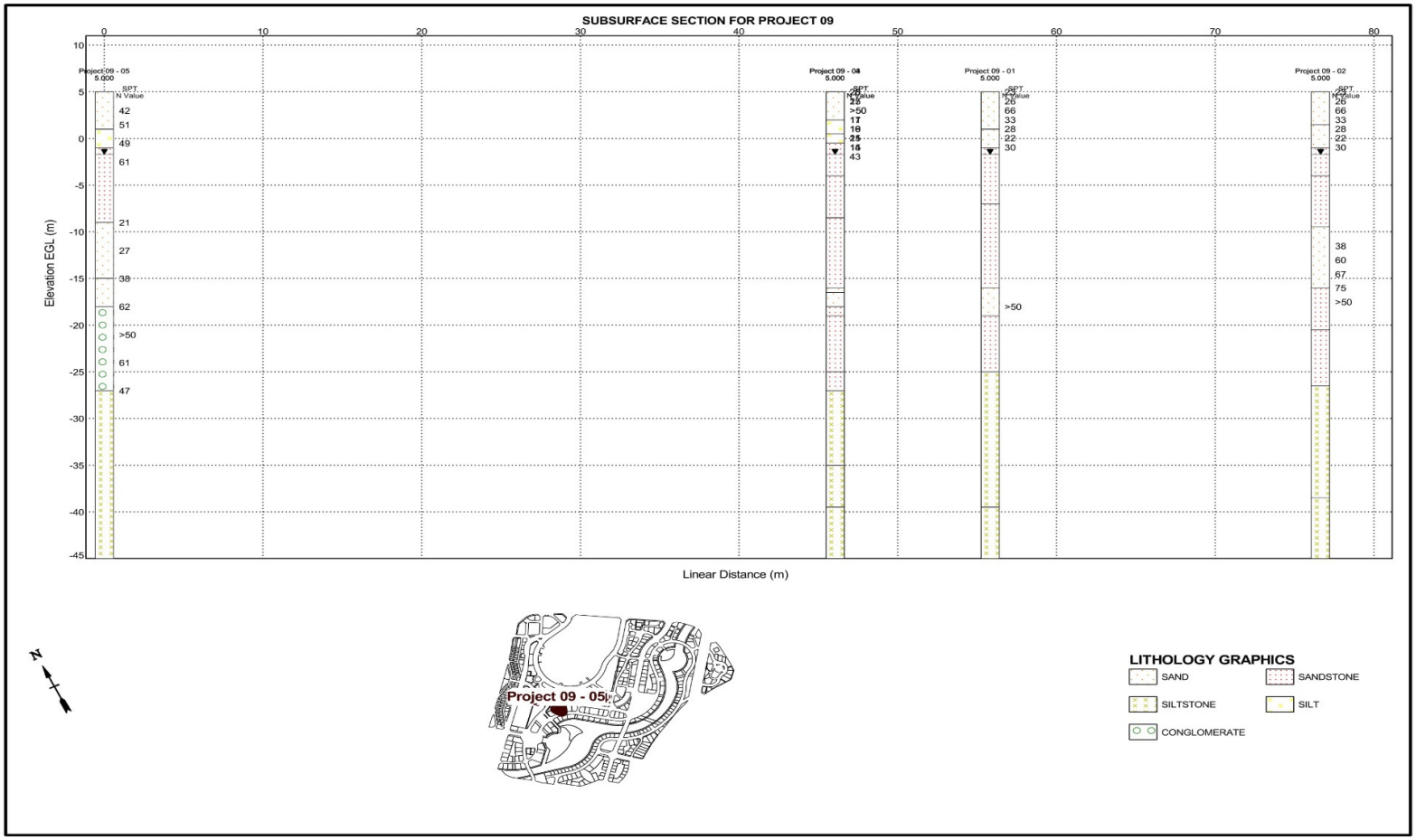
SUBSURFACE SECTION FOR PROJECT 09
Elevation EGL (m)
Linear Distance (m)
Project 09 - 05
Project 09 - 04
Project 09 - 01
Project 09 - 02
SPT N Value
42
51
49
61
21
27
38
62
>50
61
47
>50
17
18
25
15
43
26
66
33
28
22
30
38
60
67
75
>50
N
Project 09 - 05
LITHOLOGY GRAPHICS
SAND
SANDSTONE
SILTSTONE
SILT
CONGLOMERATE

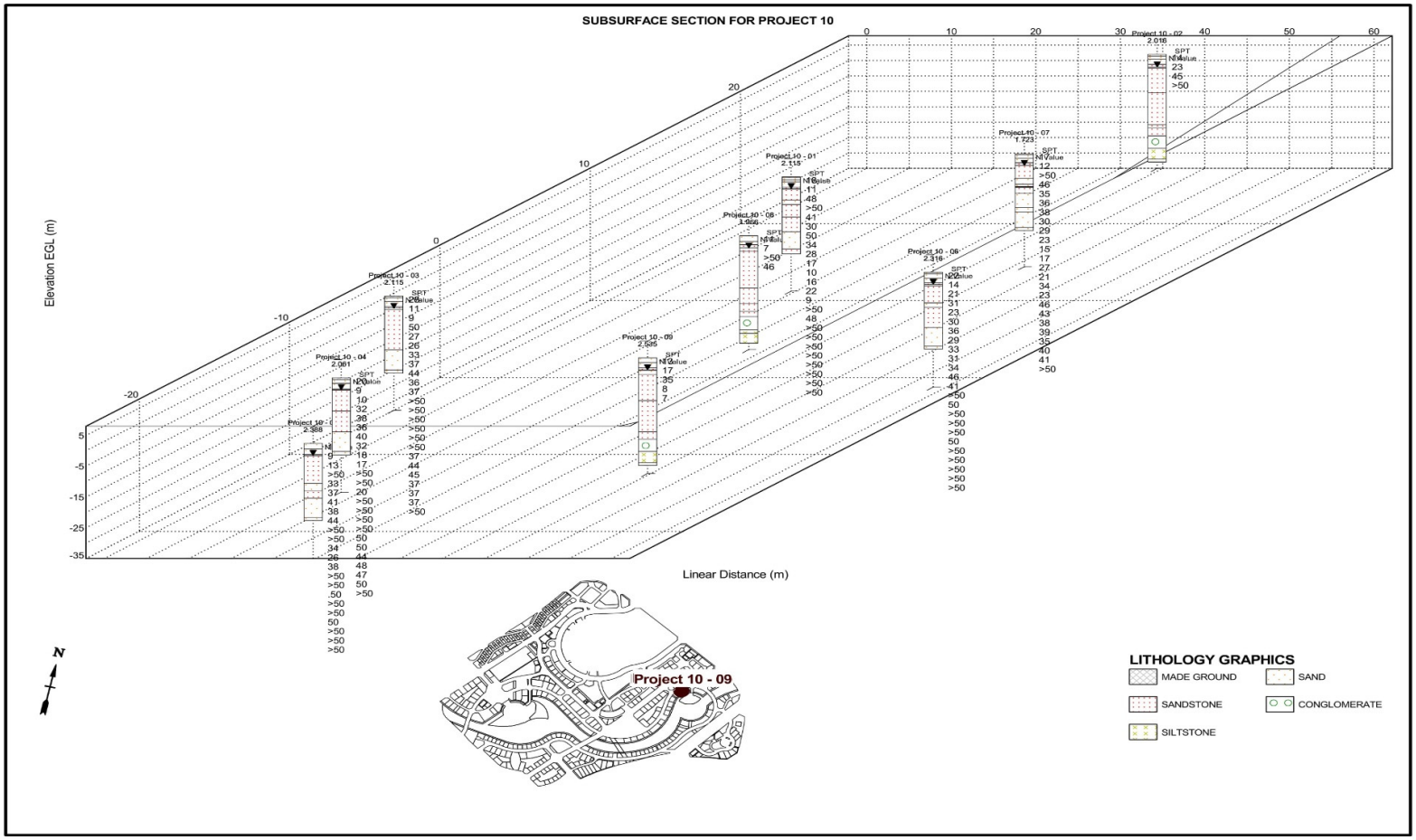
SUBSURFACE SECTION FOR PROJECT 10
Elevation EGL (m)
Linear Distance (m)
Project 10 - 09
LITHOLOGY GRAPHICS
MADE GROUND
SAND
SANDSTONE
CONGLOMERATE
SILTSTONE
N

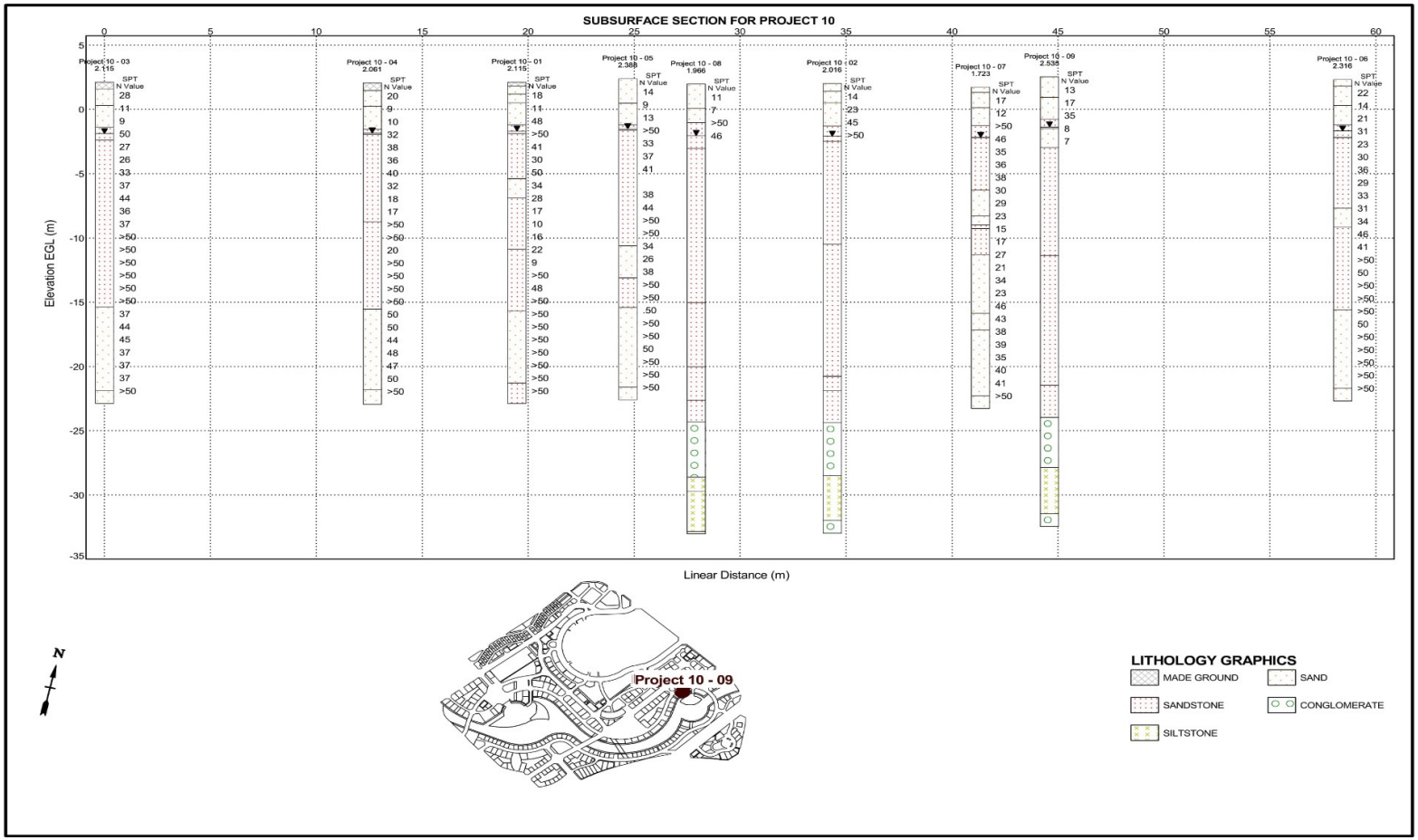
SUBSURFACE SECTION FOR PROJECT 10
Elevation EGL (m)
Linear Distance (m)
Project 10 - 03
2.115
Project 10 - 04
2.061
Project 10 - 01
2.115
Project 10 - 05
2.388
Project 10 - 08
1.966
Project 10 - 02
2.016
Project 10 - 07
1.723
Project 10 - 09
2.535
Project 10 - 06
2.316
SPT N Value
Project 10 - 09
N
LITHOLOGY GRAPHICS
MADE GROUND
SAND
SANDSTONE
CONGLOMERATE
SILTSTONE

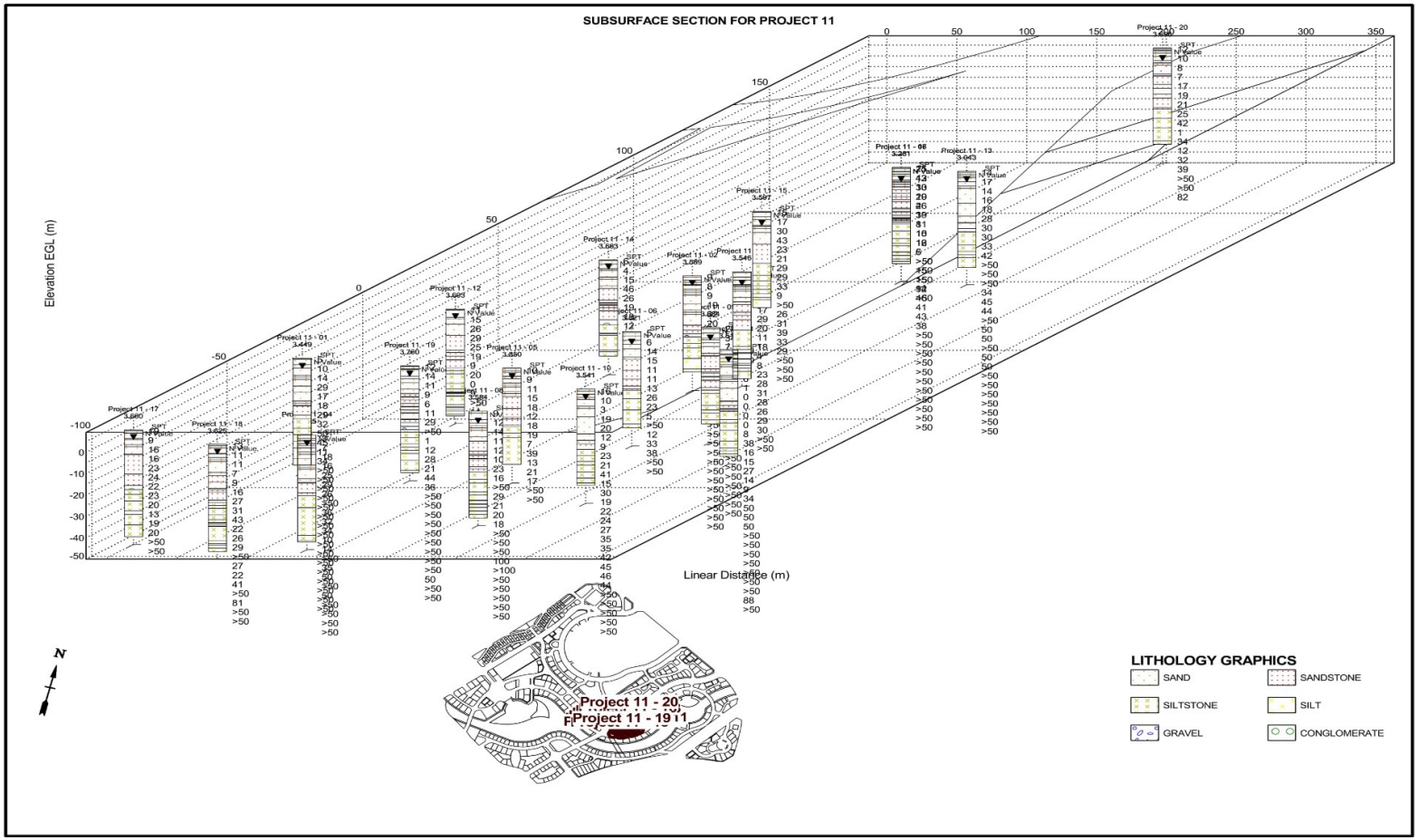
SUBSURFACE SECTION FOR PROJECT 11
Elevation EGL (m)
Linear Distance (m)
N
Project 11 - 20
Project 11 - 19
LITHOLOGY GRAPHICS
SAND
SANDSTONE
SILTSTONE
SILT
GRAVEL
CONGLOMERATE

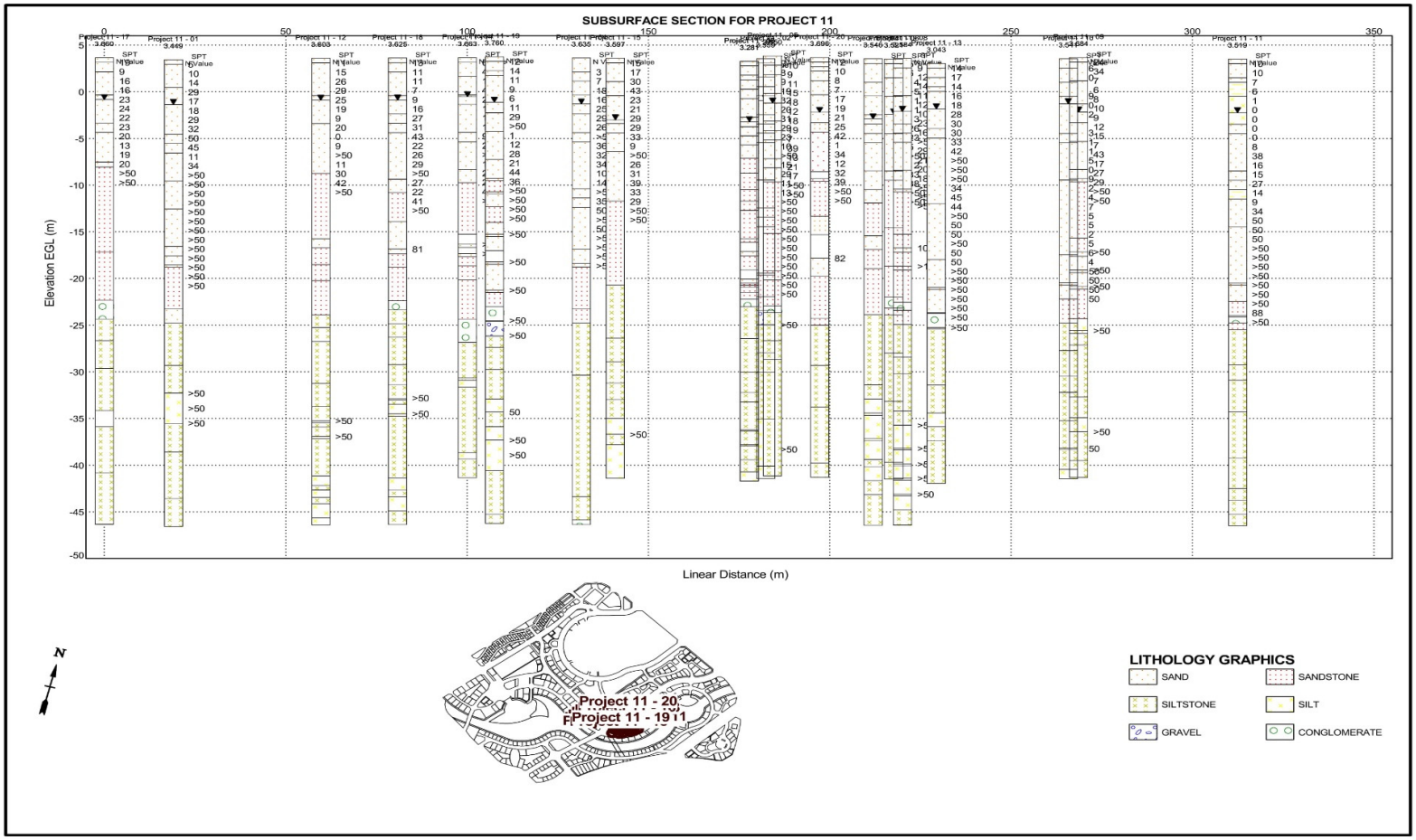
SUBSURFACE SECTION FOR PROJECT 11
Elevation EGL (m)
Linear Distance (m)
Project 11 - 20
Project 11 - 19
N
LITHOLOGY GRAPHICS
SAND
SANDSTONE
SILTSTONE
SILT
GRAVEL
CONGLOMERATE

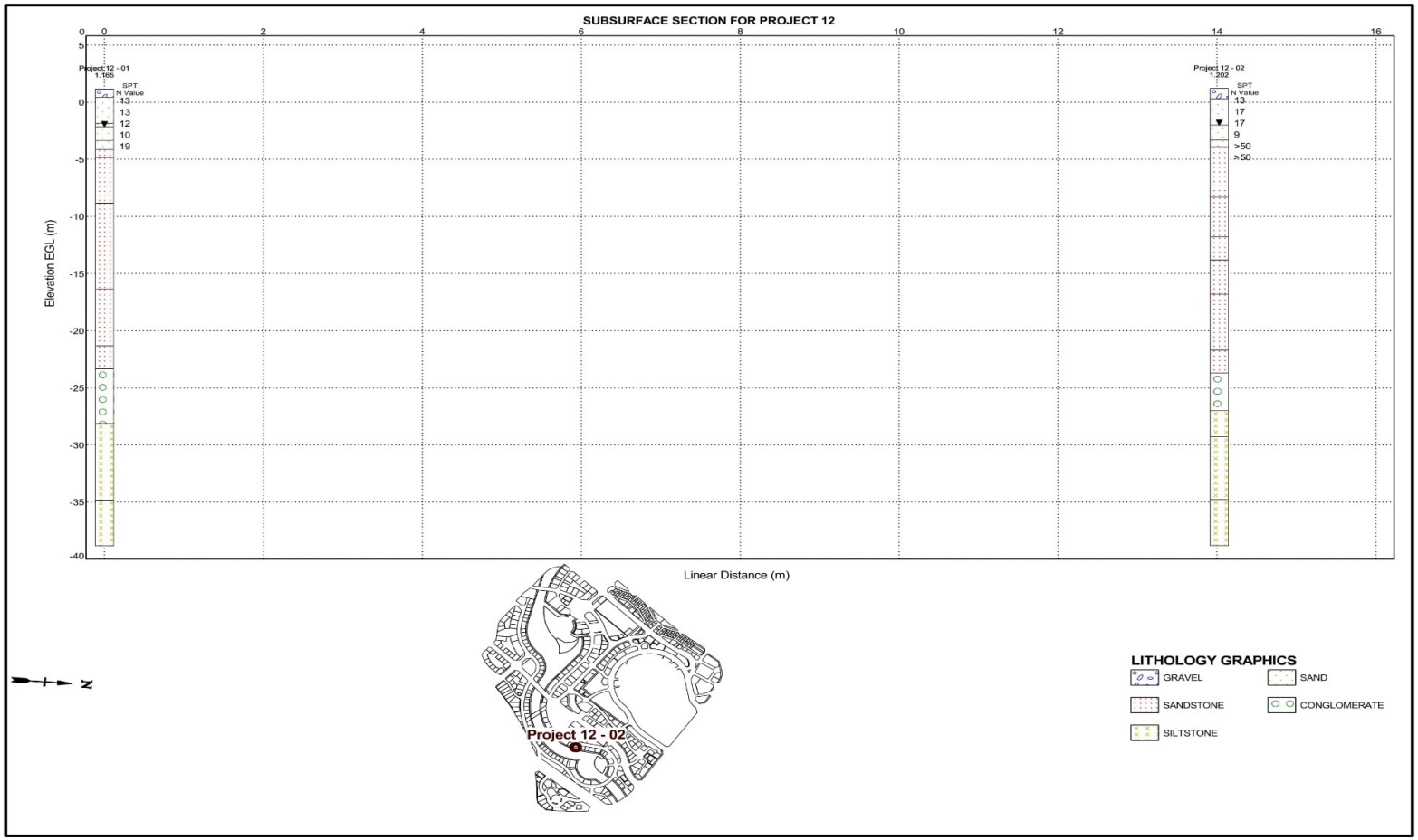
SUBSURFACE SECTION FOR PROJECT 12
Project 12 - 01
1.165
SPT
N Value
13
13
12
10
19
Project 12 - 02
1.202
SPT
N Value
13
17
17
9
>50
>50
Elevation EGL (m)
Linear Distance (m)
Project 12 - 02
N
LITHOLOGY GRAPHICS
GRAVEL
SAND
SANDSTONE
CONGLOMERATE
SILTSTONE

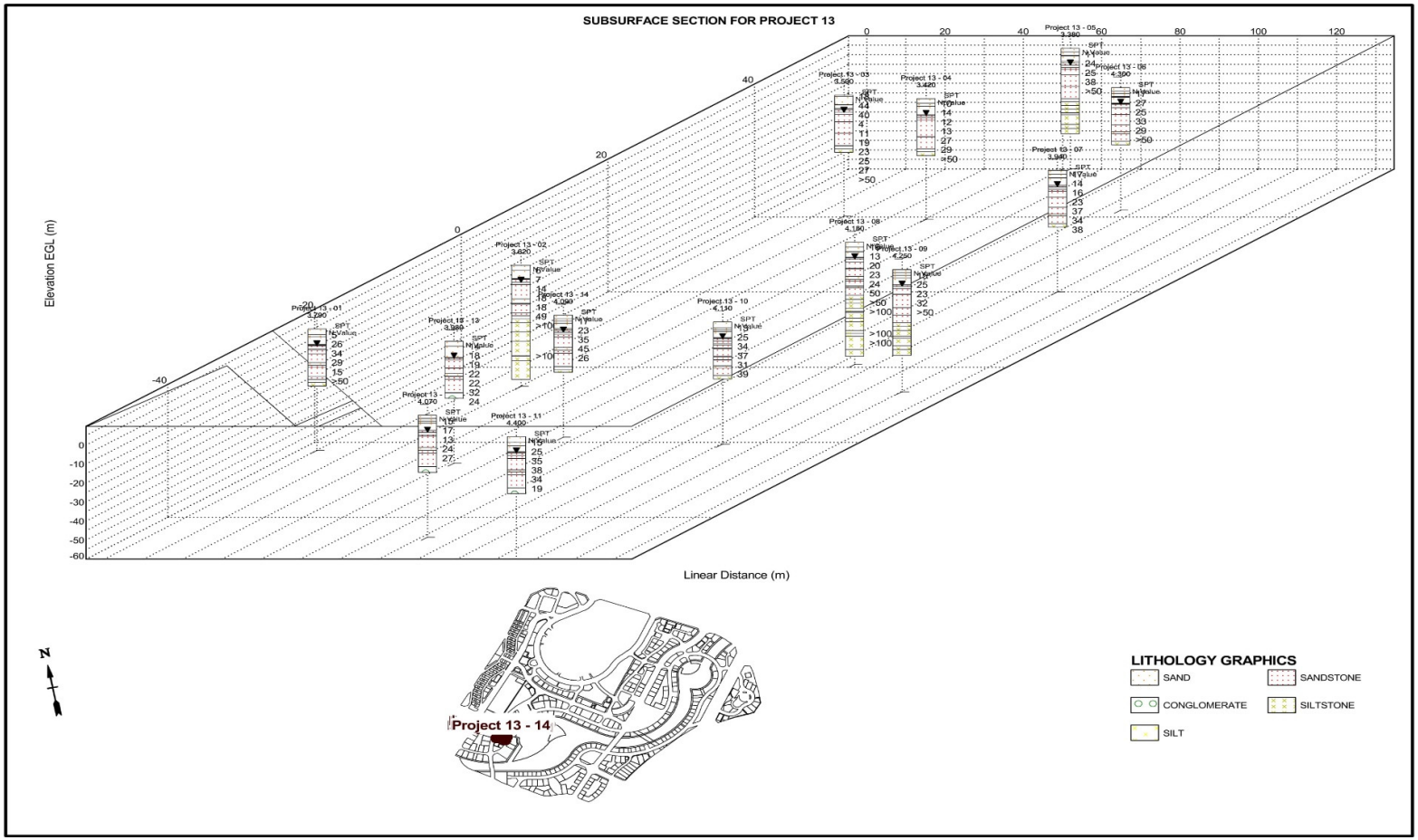
SUBSURFACE SECTION FOR PROJECT 13
Elevation EGL (m)
Linear Distance (m)
Project 13 - 14
LITHOLOGY GRAPHICS
SAND
SANDSTONE
CONGLOMERATE
SILTSTONE
SILT

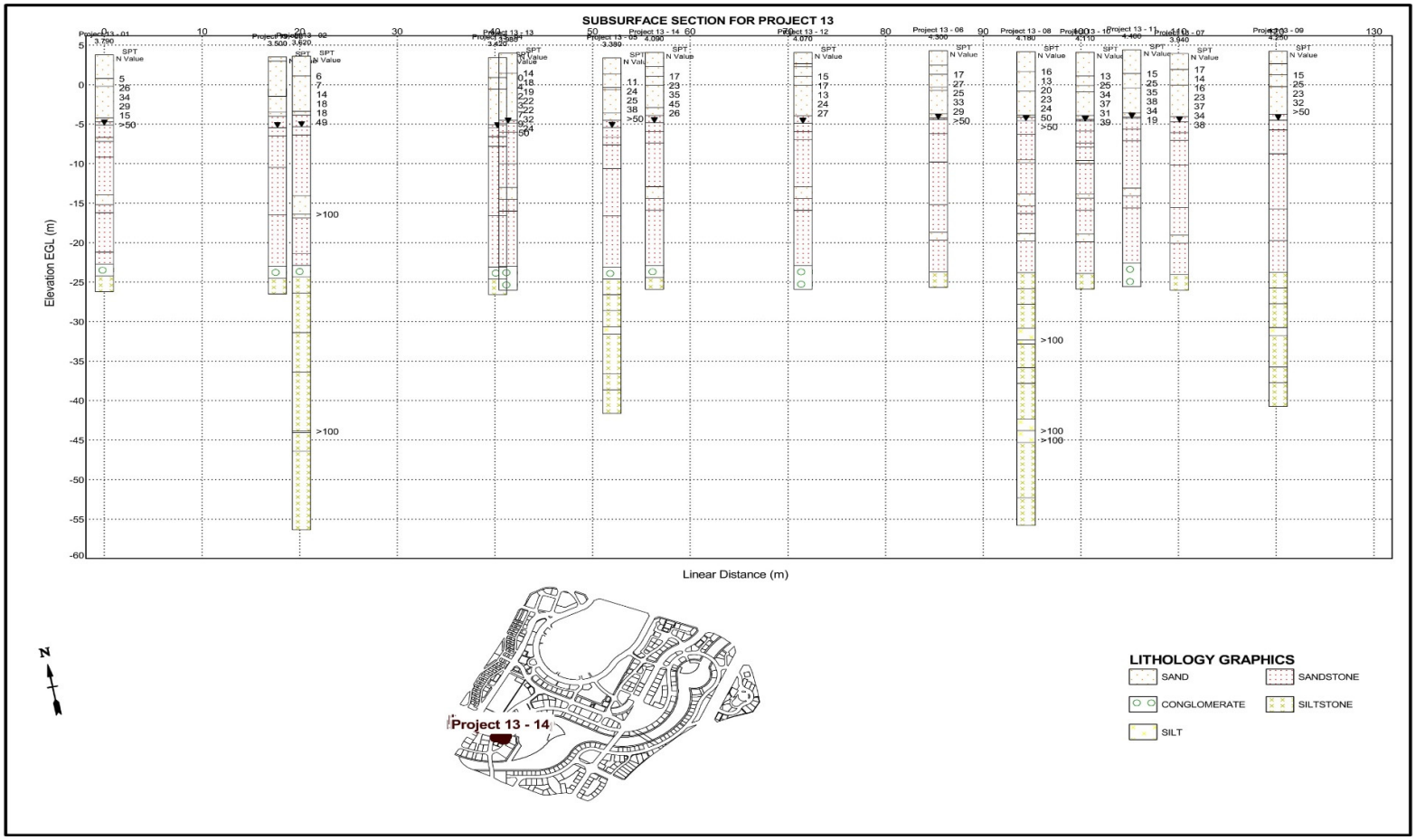
SUBSURFACE SECTION FOR PROJECT 13
Elevation EGL (m)
Linear Distance (m)
Project 13 - 14
LITHOLOGY GRAPHICS
SAND
SANDSTONE
CONGLOMERATE
SILTSTONE
SILT

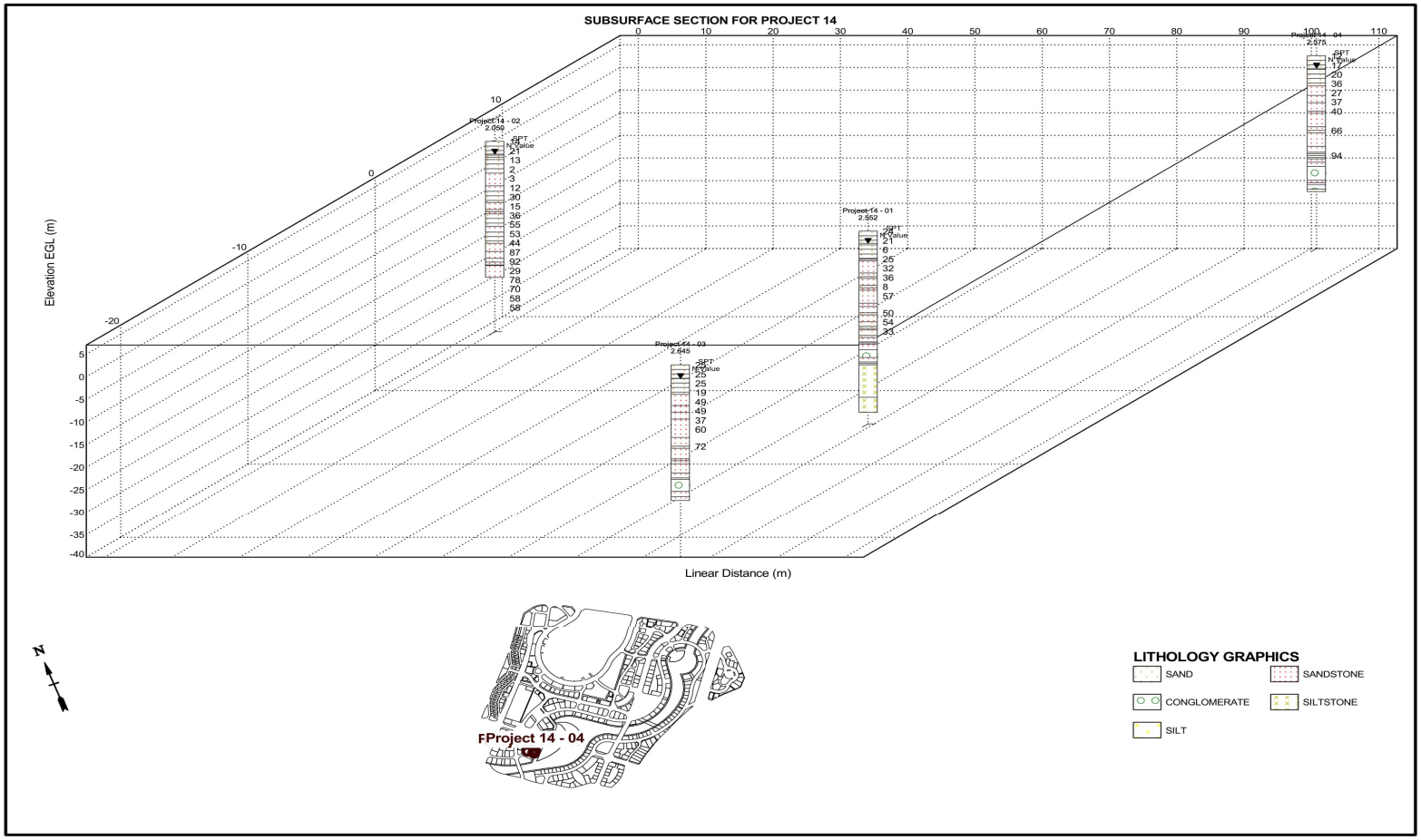
SUBSURFACE SECTION FOR PROJECT 14
Elevation EGL (m)
Linear Distance (m)
Project 14 - 02
2.050
Project 14 - 01
2.552
Project 14 - 03
2.645
Project 14 - 04
2.575
SPT N Value
FProject 14 - 04
N
LITHOLOGY GRAPHICS
SAND
SANDSTONE
CONGLOMERATE
SILTSTONE
SILT

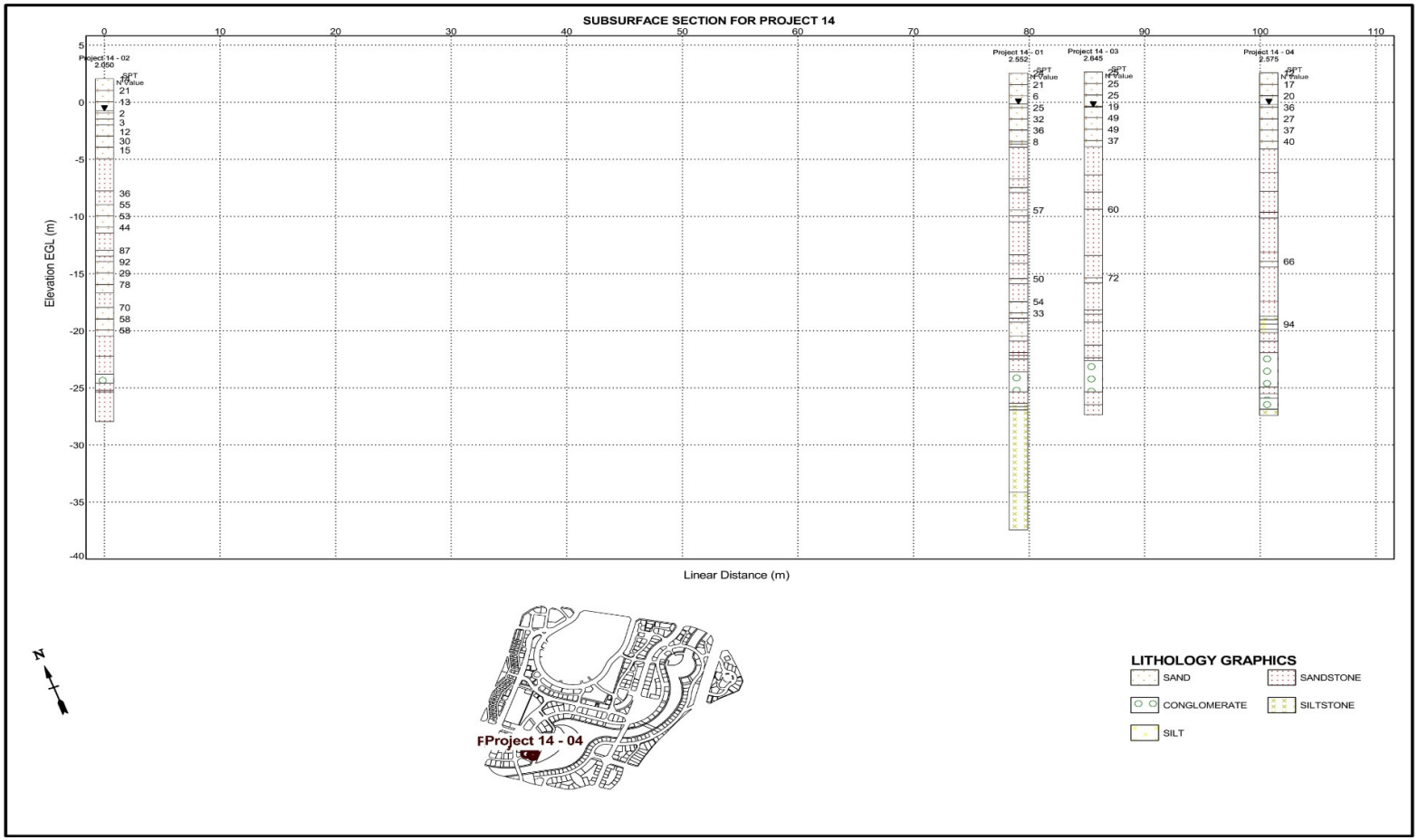
SUBSURFACE SECTION FOR PROJECT 14
Elevation EGL (m)
Linear Distance (m)
Project 14 - 02
2.050
Project 14 - 01
2.552
Project 14 - 03
2.645
Project 14 - 04
2.575
SPT
N-Value
LITHOLOGY GRAPHICS
SAND
SANDSTONE
CONGLOMERATE
SILTSTONE
SILT
N
Project 14 - 04

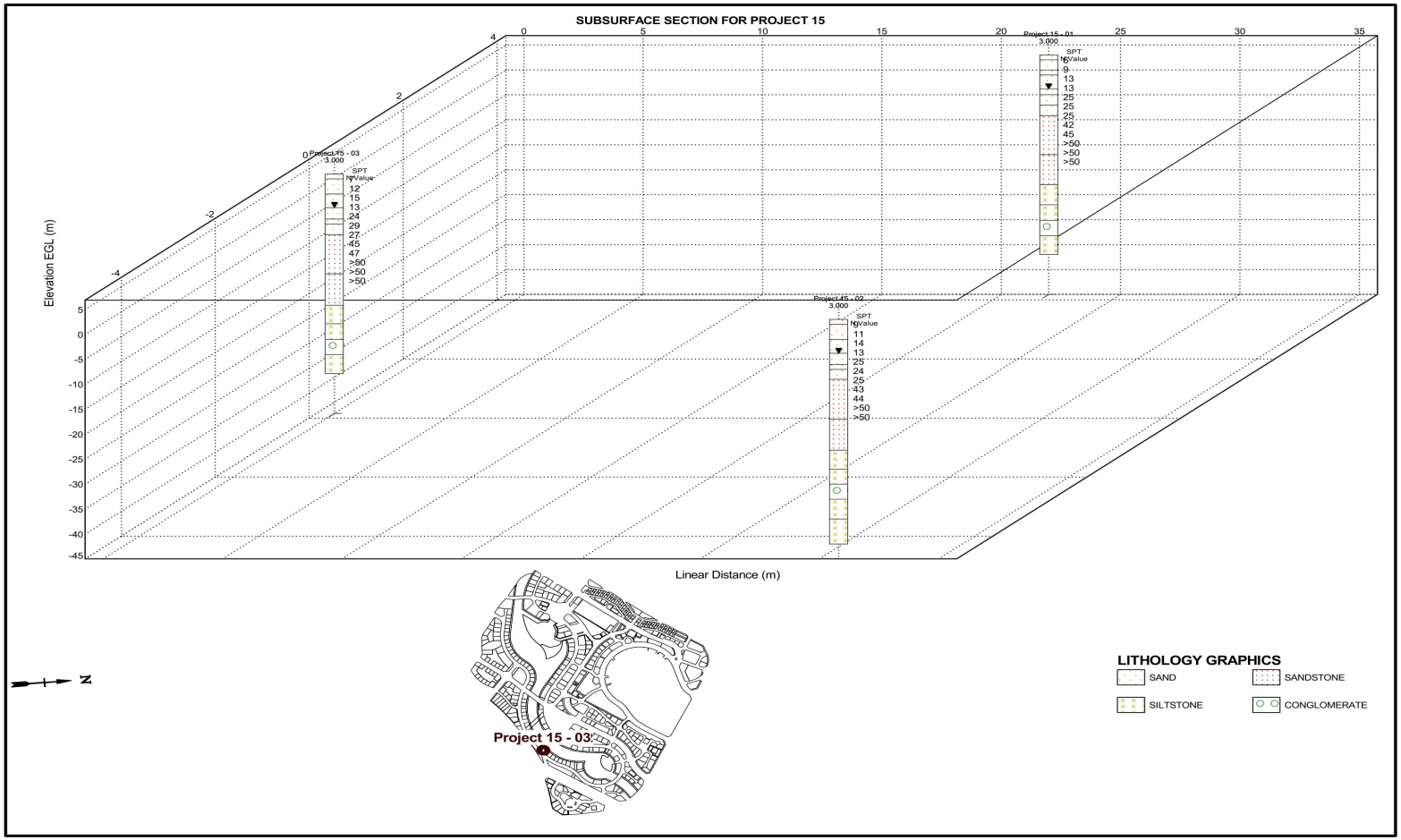
SUBSURFACE SECTION FOR PROJECT 15
Elevation EGL (m)
Linear Distance (m)
Project 15 - 03
3.000
SPT
N Value
12
15
13
24
29
27
45
47
>50
>50
>50
Project 15 - 01
3.000
SPT
N Value
9
13
13
25
25
25
42
45
>50
>50
>50
Project 15 - 02
3.000
SPT
N Value
11
14
13
25
24
25
43
44
>50
>50
Project 15 - 03
N
LITHOLOGY GRAPHICS
SAND
SANDSTONE
SILTSTONE
CONGLOMERATE

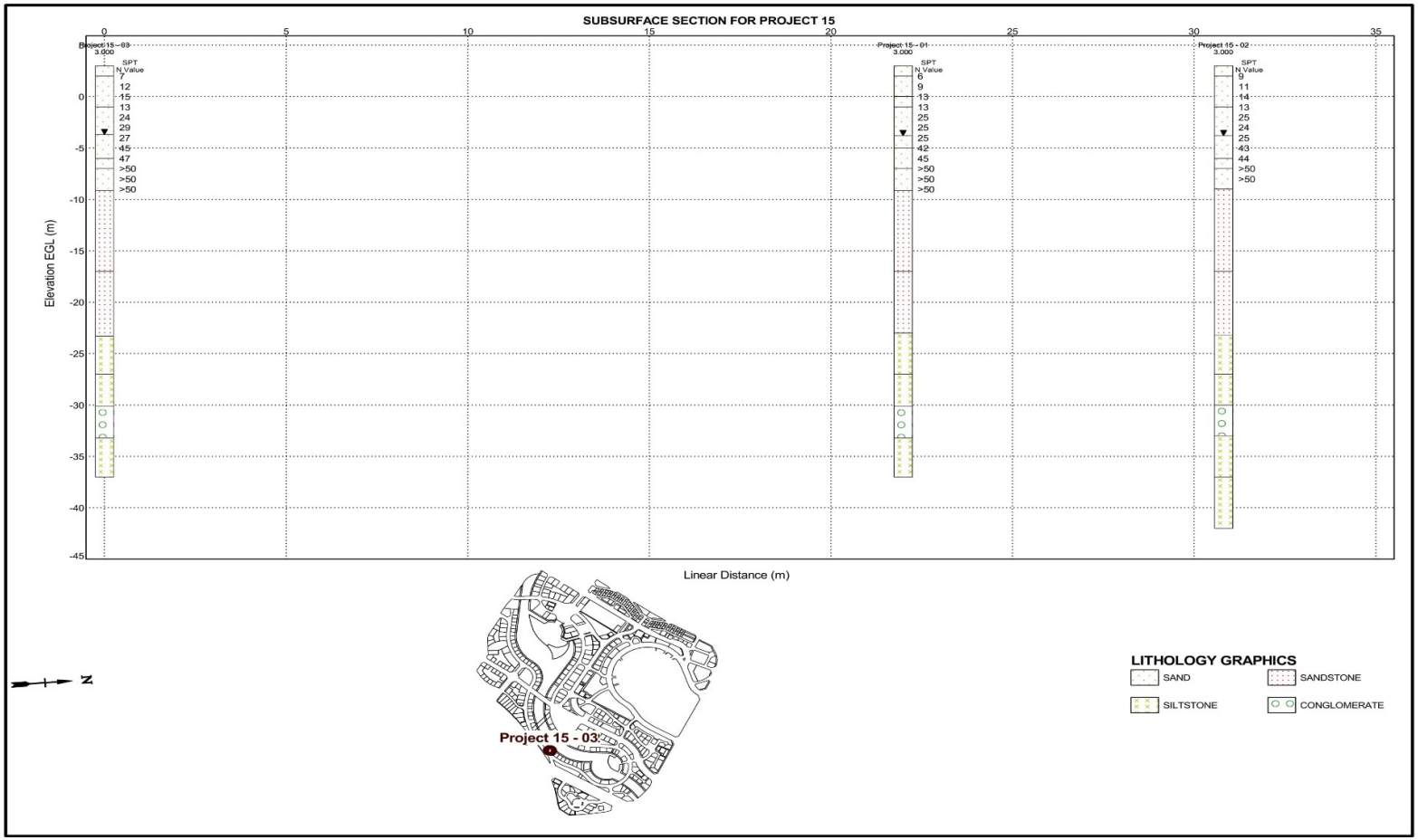
SUBSURFACE SECTION FOR PROJECT 15
Project 15 - 03
3.000
SPT N Value
7
12
15
13
24
29
27
45
47
>50
>50
>50
Project 15 - 01
3.000
SPT N Value
6
9
13
13
25
25
25
42
45
>50
>50
>50
Project 15 - 02
3.000
SPT N Value
9
11
14
13
25
24
25
43
44
>50
>50
Elevation EGL (m)
Linear Distance (m)
N
Project 15 - 03
LITHOLOGY GRAPHICS
SAND
SANDSTONE
SILTSTONE
CONGLOMERATE

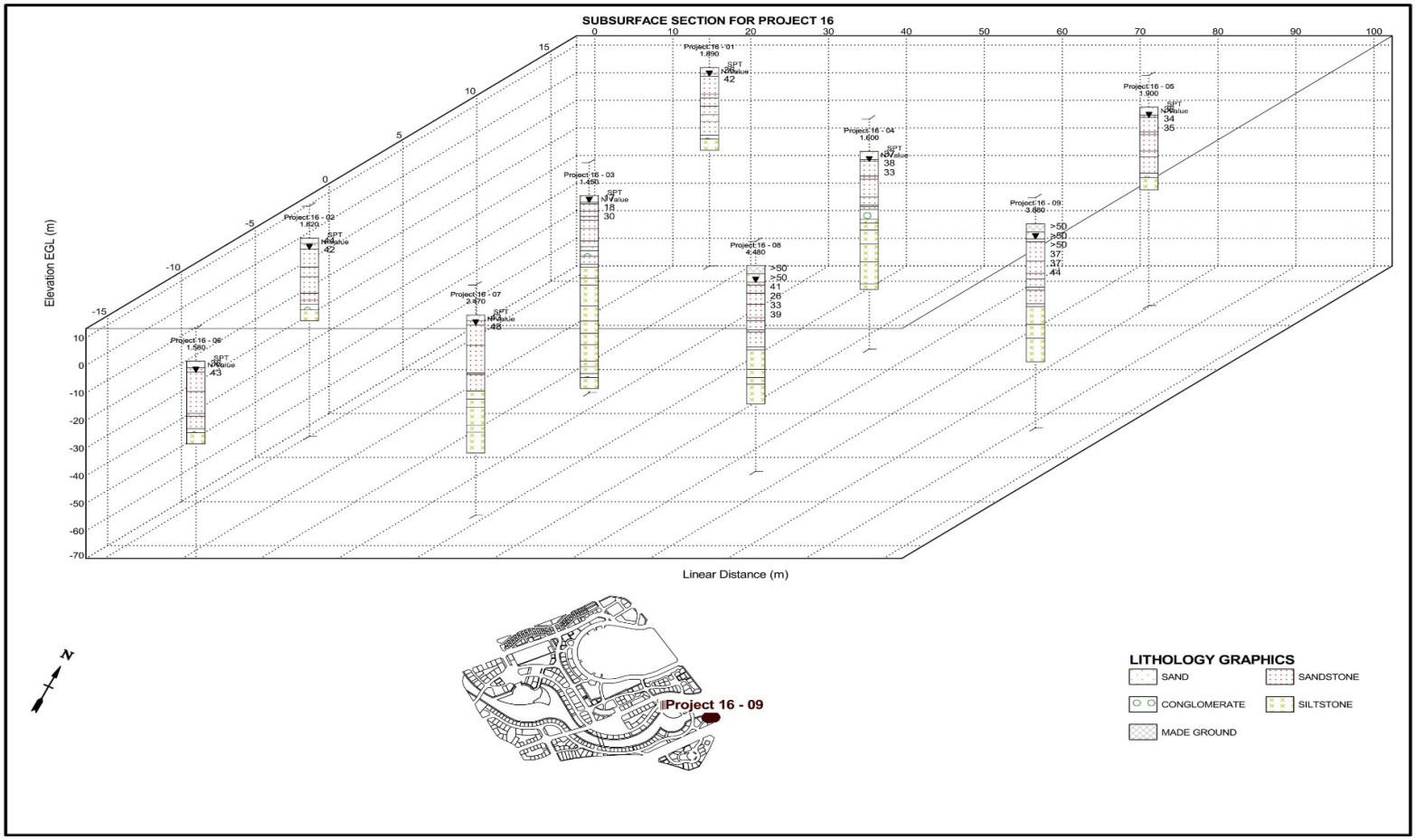
SUBSURFACE SECTION FOR PROJECT 16
Elevation EGL (m)
Linear Distance (m)
Project 16 - 01
1.890
SPT N-Value
42
Project 16 - 02
1.820
SPT N-Value
42
Project 16 - 03
1.450
SPT N-Value
18
30
Project 16 - 04
1.600
SPT N-Value
38
33
Project 16 - 05
1.900
SPT N-Value
34
35
Project 16 - 06
1.580
SPT N-Value
43
Project 16 - 07
2.470
SPT N-Value
48
Project 16 - 08
4.480
>50
>50
41
26
33
39
Project 16 - 09
3.880
>50
>50
>50
37
37
44
N
Project 16 - 09
LITHOLOGY GRAPHICS
SAND
SANDSTONE
CONGLOMERATE
SILTSTONE
MADE GROUND

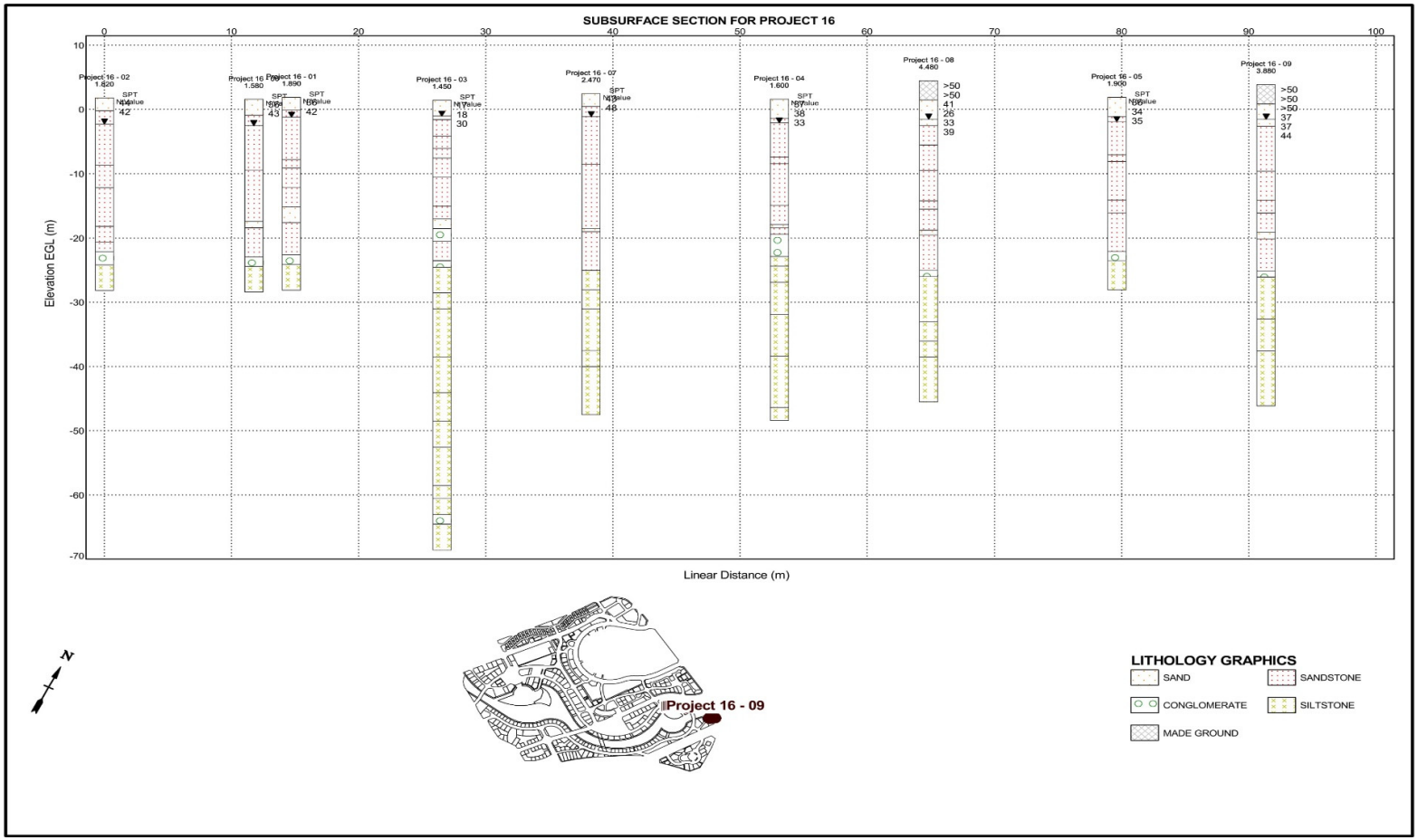
SUBSURFACE SECTION FOR PROJECT 16
Elevation EGL (m)
Linear Distance (m)
Project 16 - 02
1.620
SPT N Value
42
Project 16 - 08
4.480
>50
>50
41
26
33
39
Project 16 - 09
3.880
>50
>50
>50
37
37
44
Project 16 - 05
1.950
34
35
Project 16 - 03
1.450
18
30
Project 16 - 07
2.470
48
Project 16 - 04
1.600
38
33
Project 16 - 09
N
LITHOLOGY GRAPHICS
SAND
SANDSTONE
CONGLOMERATE
SILTSTONE
MADE GROUND

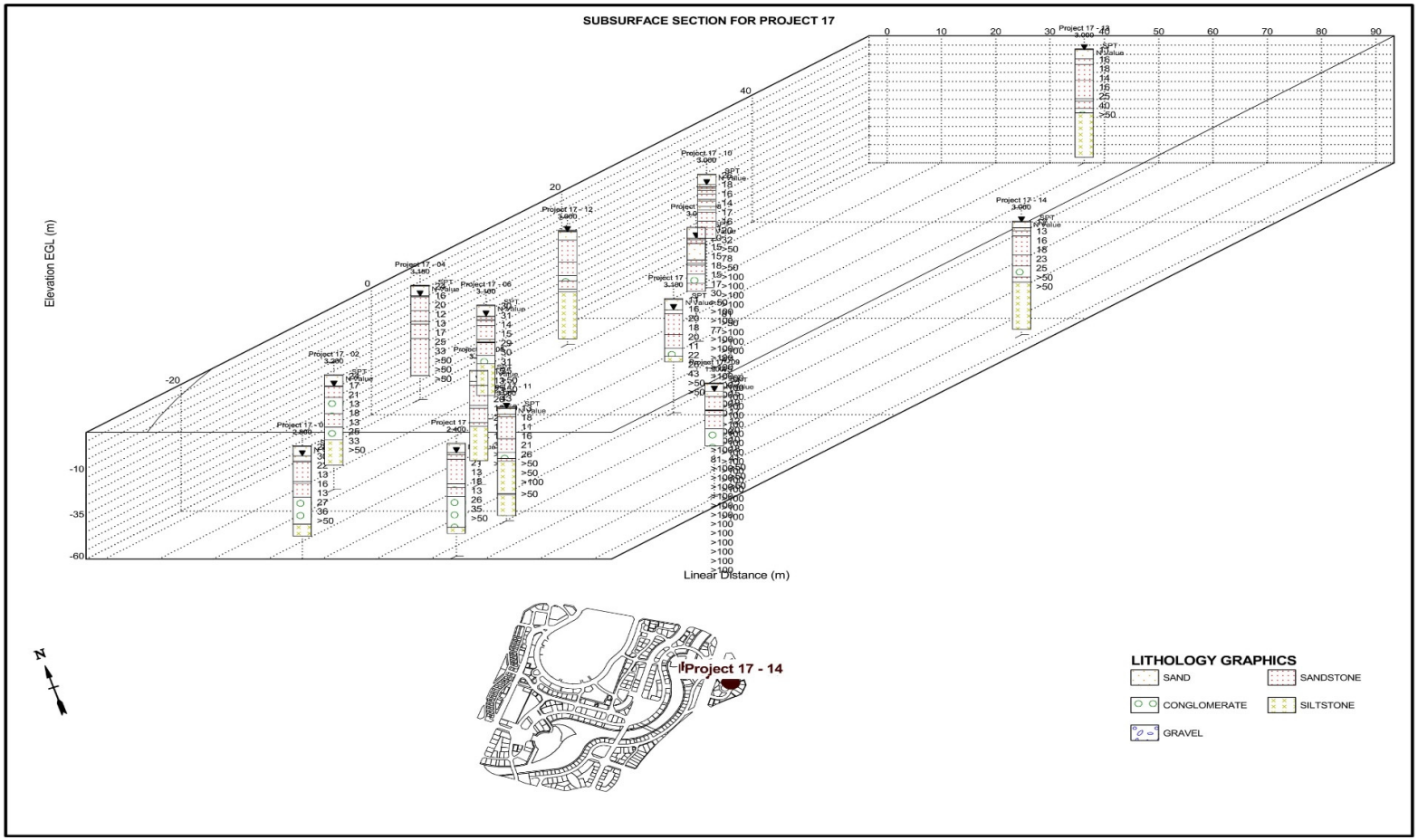
SUBSURFACE SECTION FOR PROJECT 17
Elevation EGL (m)
Linear Distance (m)
Project 17 - 14
LITHOLOGY GRAPHICS
SAND
SANDSTONE
CONGLOMERATE
SILTSTONE
GRAVEL

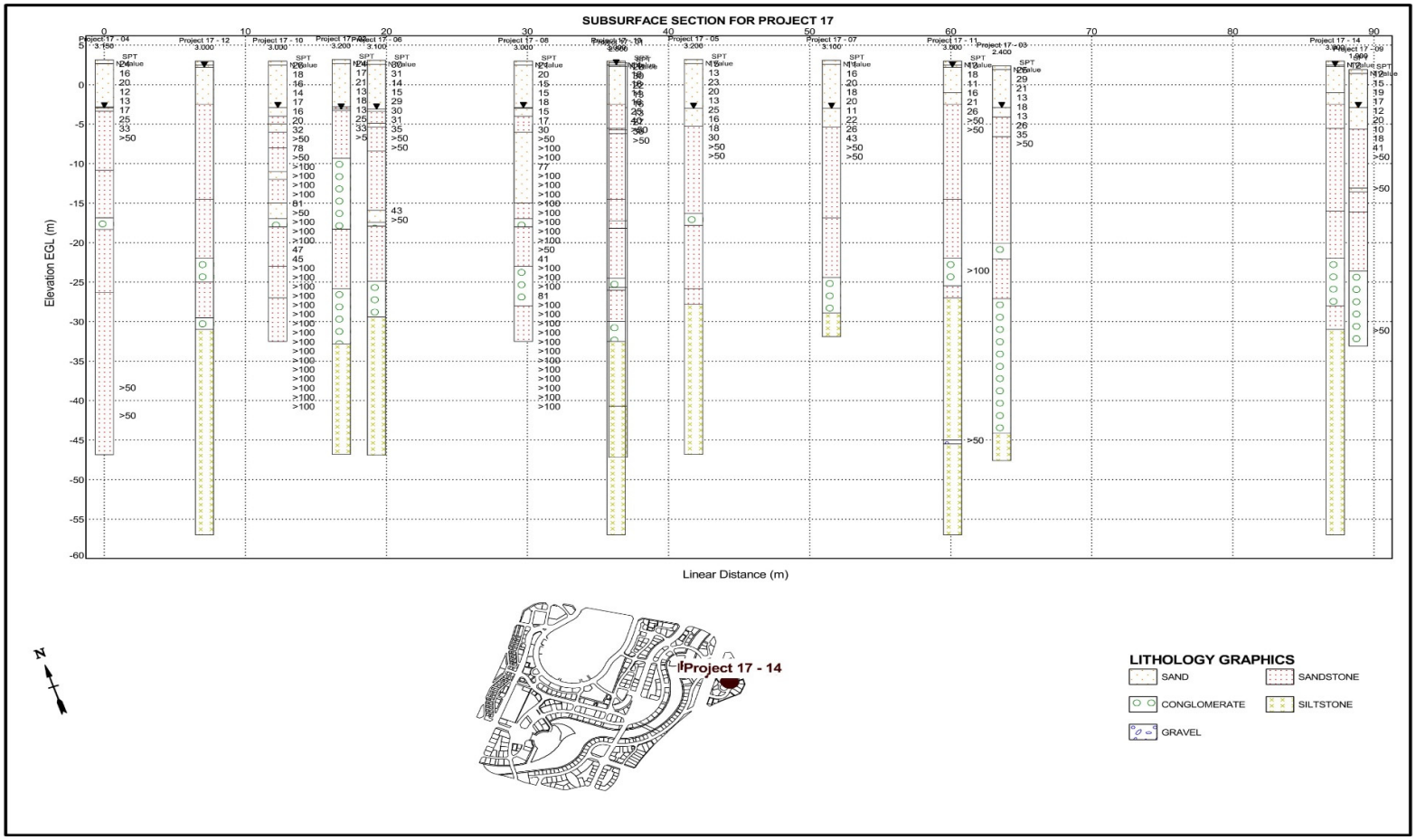
SUBSURFACE SECTION FOR PROJECT 17
Elevation EGL (m)
Linear Distance (m)
Project 17 - 14
LITHOLOGY GRAPHICS
SAND
SANDSTONE
CONGLOMERATE
SILTSTONE
GRAVEL

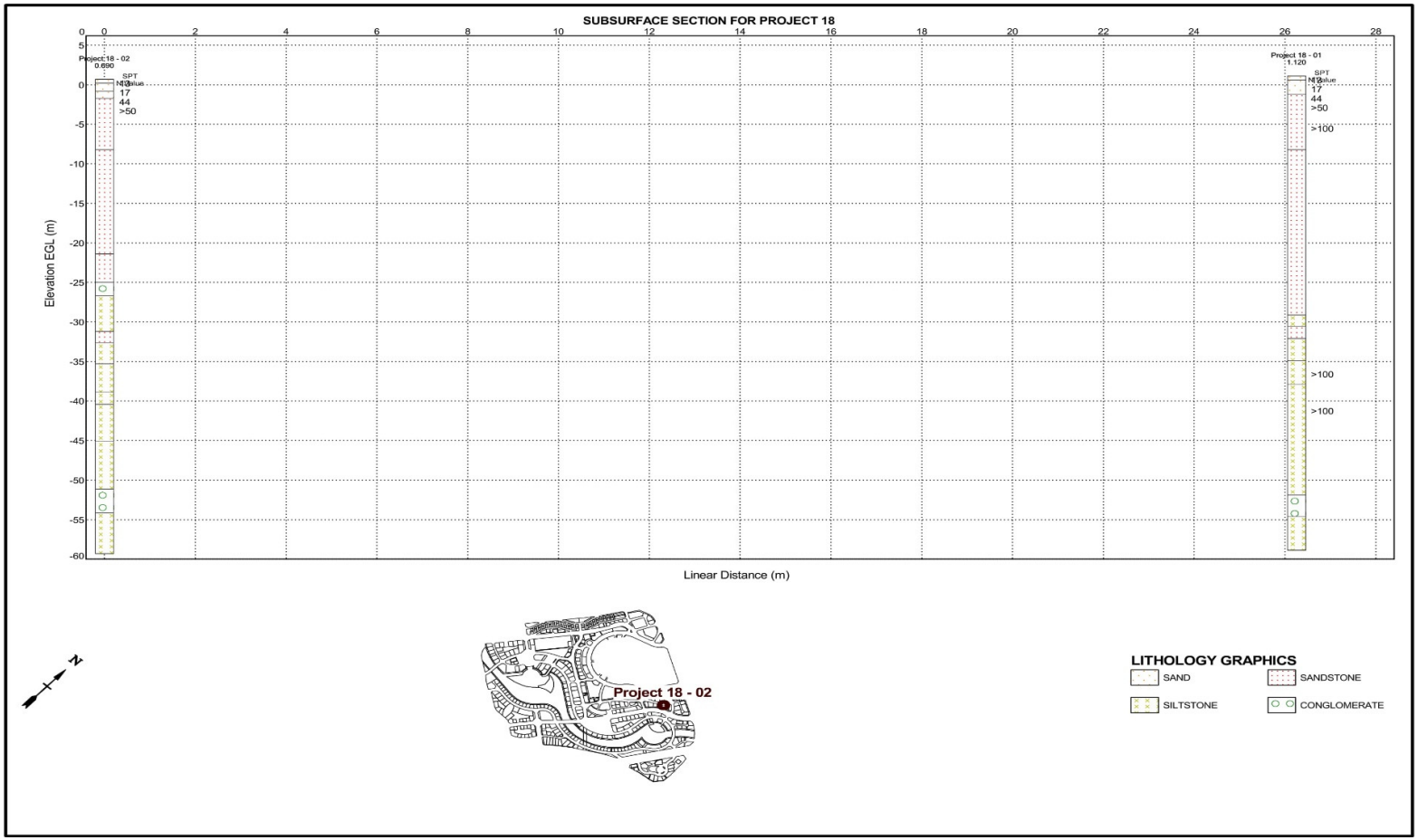
SUBSURFACE SECTION FOR PROJECT 18
Project 18 - 02
0.690
SPT
N Value
17
44
>50
Project 18 - 01
1.120
SPT
N Value
17
44
>50
>100
>100
>100
Elevation EGL (m)
Linear Distance (m)
Project 18 - 02
N
LITHOLOGY GRAPHICS
SAND
SANDSTONE
SILTSTONE
CONGLOMERATE

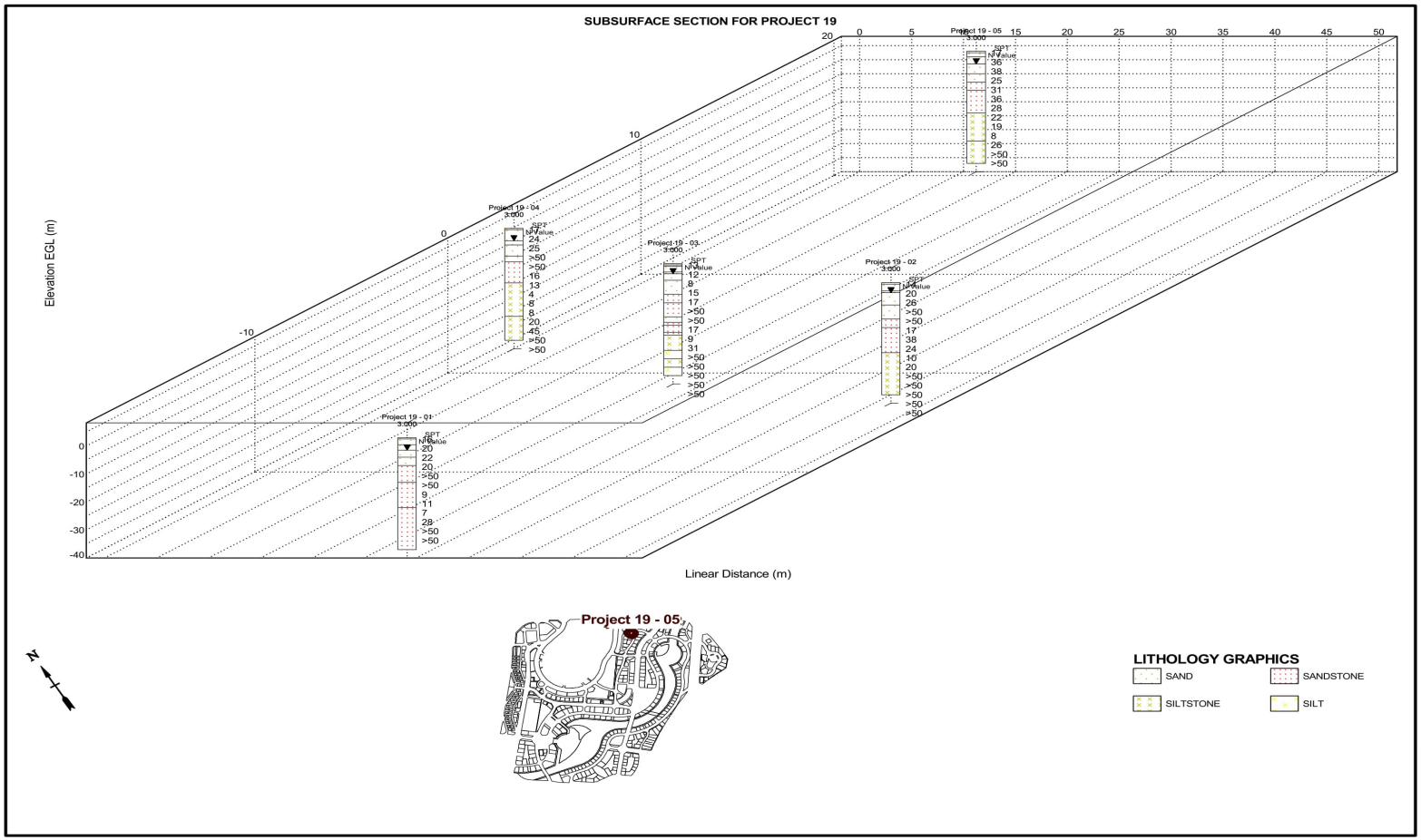
SUBSURFACE SECTION FOR PROJECT 19
Elevation EGL (m)
Linear Distance (m)
Project 19 - 01
Project 19 - 02
Project 19 - 03
Project 19 - 04
Project 19 - 05
SPT N Value
Project 19 - 05
N
LITHOLOGY GRAPHICS
SAND
SANDSTONE
SILTSTONE
SILT

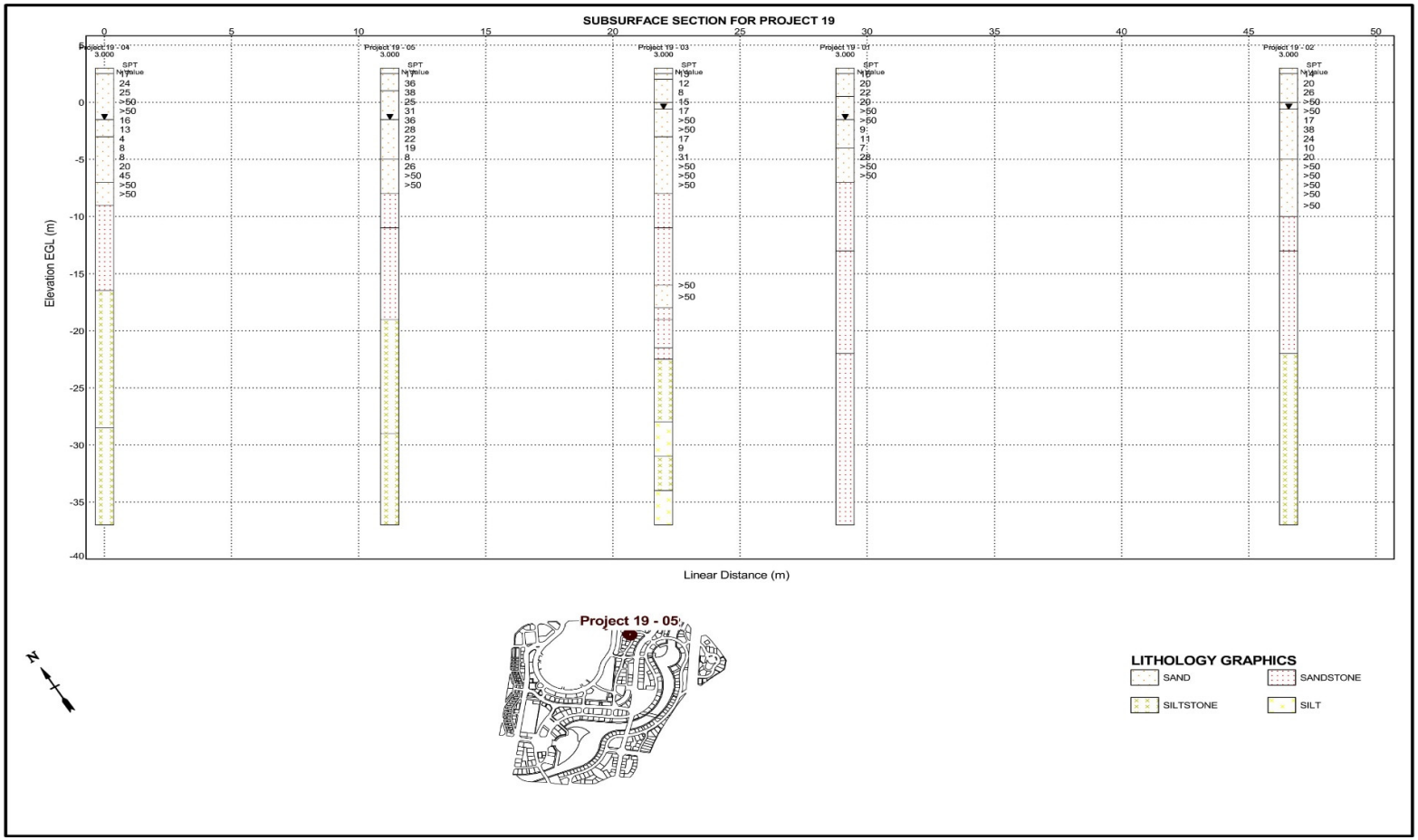
SUBSURFACE SECTION FOR PROJECT 19
Elevation EGL (m)
Linear Distance (m)
Project 19 - 04
Project 19 - 05
Project 19 - 03
Project 19 - 01
Project 19 - 02
SPT N value
Project 19 - 05
N
LITHOLOGY GRAPHICS
SAND
SANDSTONE
SILTSTONE
SILT

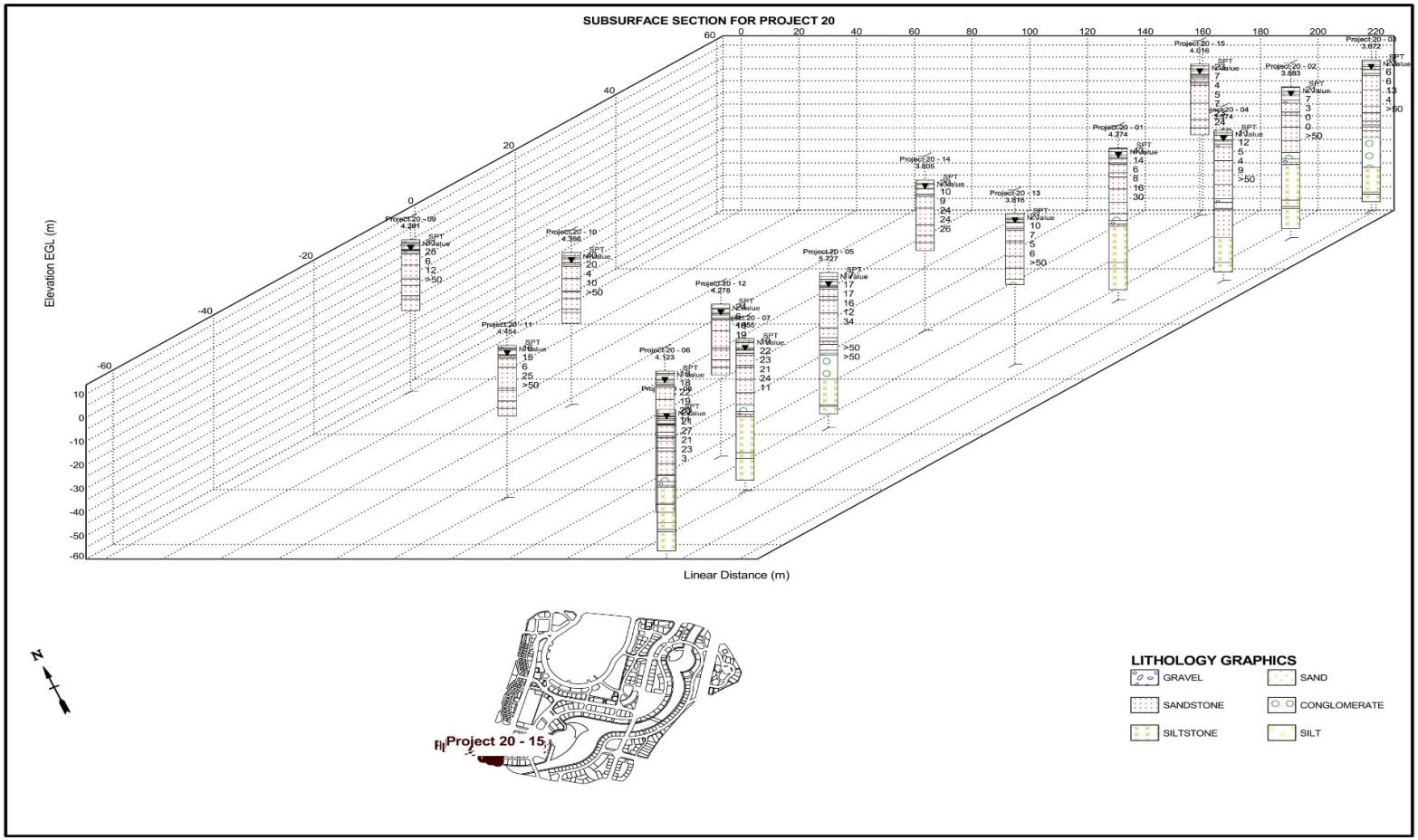
SUBSURFACE SECTION FOR PROJECT 20
Elevation EGL (m)
Linear Distance (m)
Project 20 - 15
LITHOLOGY GRAPHICS
GRAVEL
SAND
SANDSTONE
CONGLOMERATE
SILTSTONE
SILT

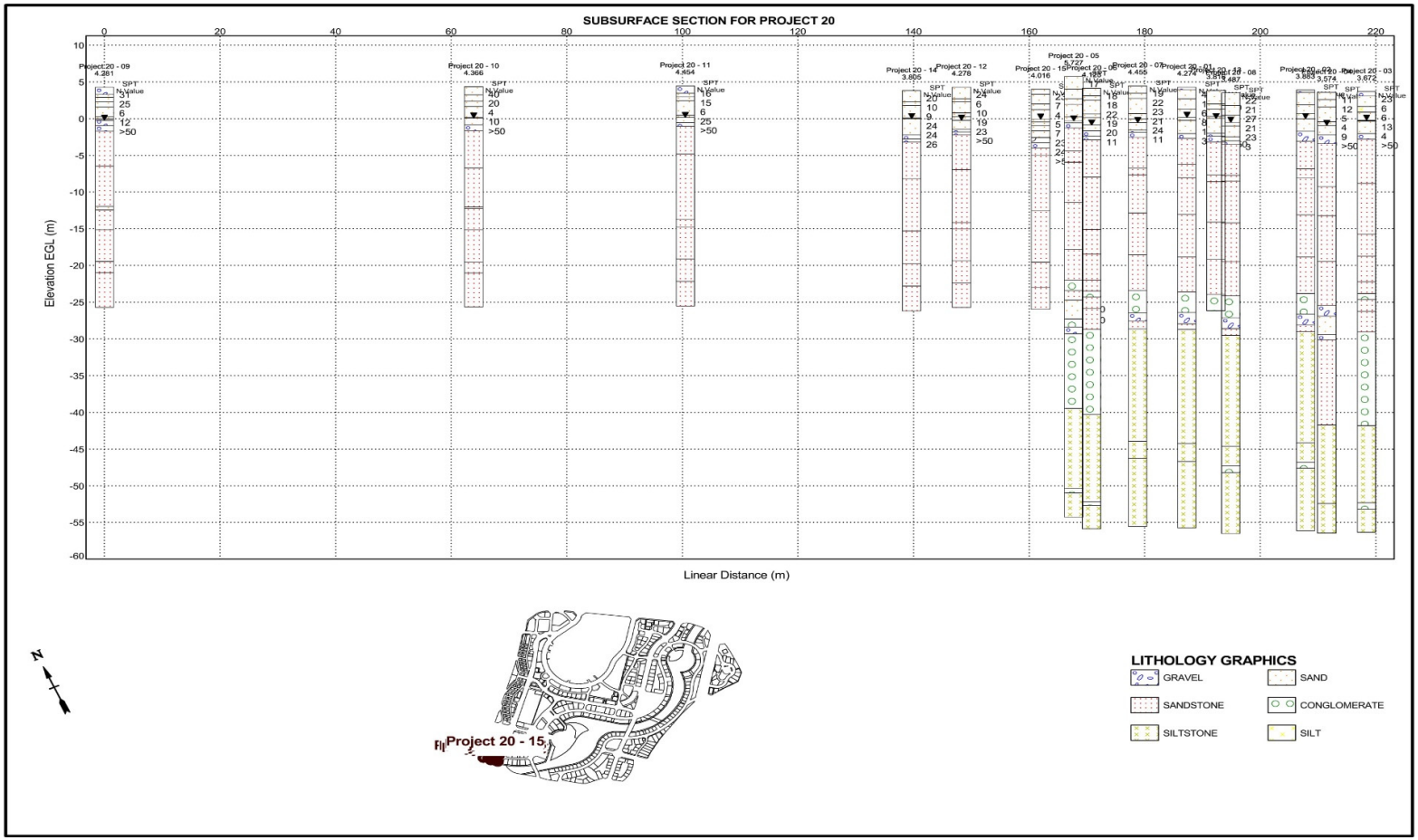
SUBSURFACE SECTION FOR PROJECT 20
Elevation EGL (m)
Linear Distance (m)
Project 20 - 09
Project 20 - 10
Project 20 - 11
Project 20 - 14
Project 20 - 12
Project 20 - 15
Project 20 - 05
Project 20 - 06
Project 20 - 07
Project 20 - 01
Project 20 - 08
Project 20 - 02
Project 20 - 03
SPT N Value
LITHOLOGY GRAPHICS
GRAVEL
SAND
SANDSTONE
CONGLOMERATE
SILTSTONE
SILT
N
Project 20 - 15

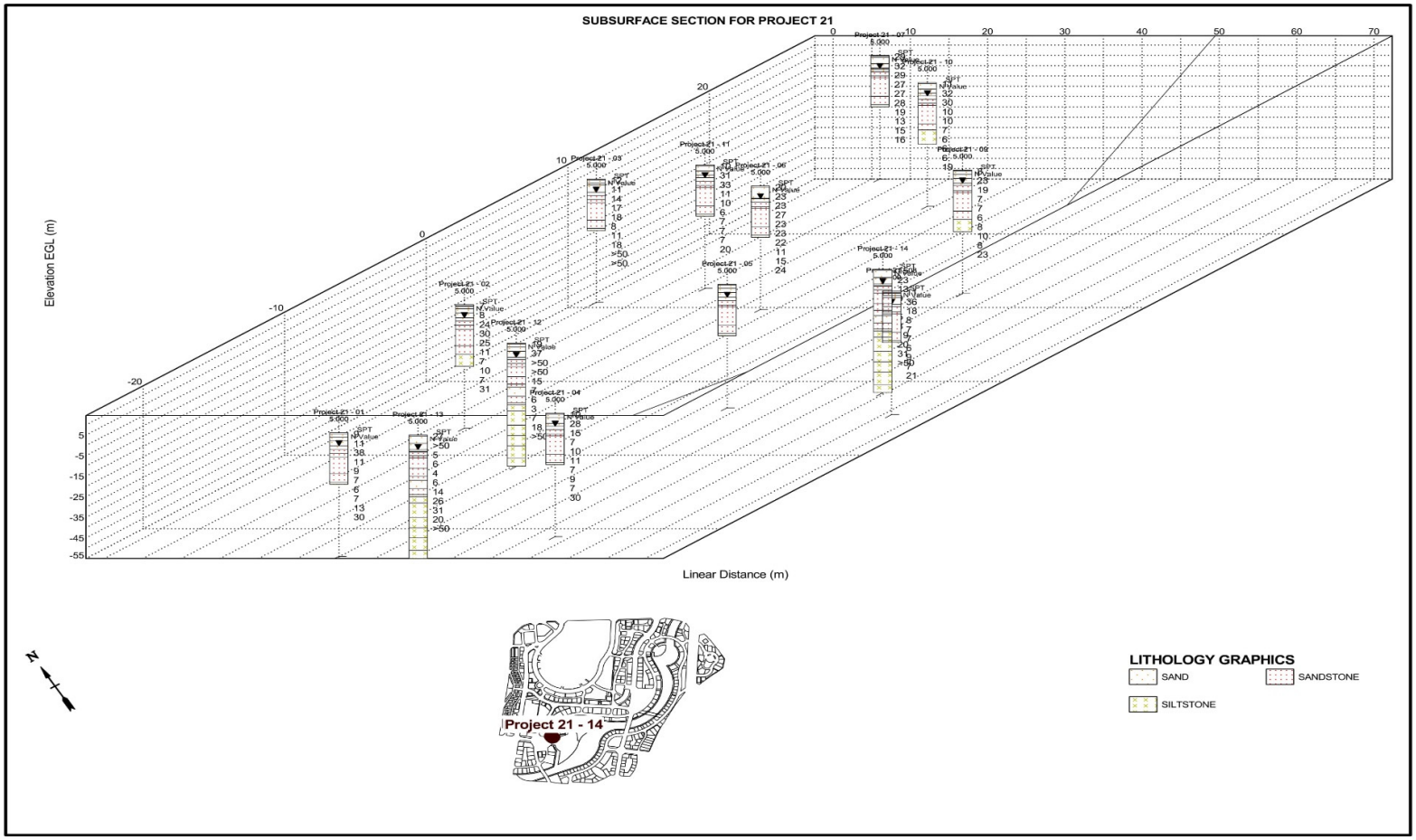
SUBSURFACE SECTION FOR PROJECT 21
Elevation EGL (m)
Linear Distance (m)
Project 21 - 14
LITHOLOGY GRAPHICS
SAND
SANDSTONE
SILTSTONE

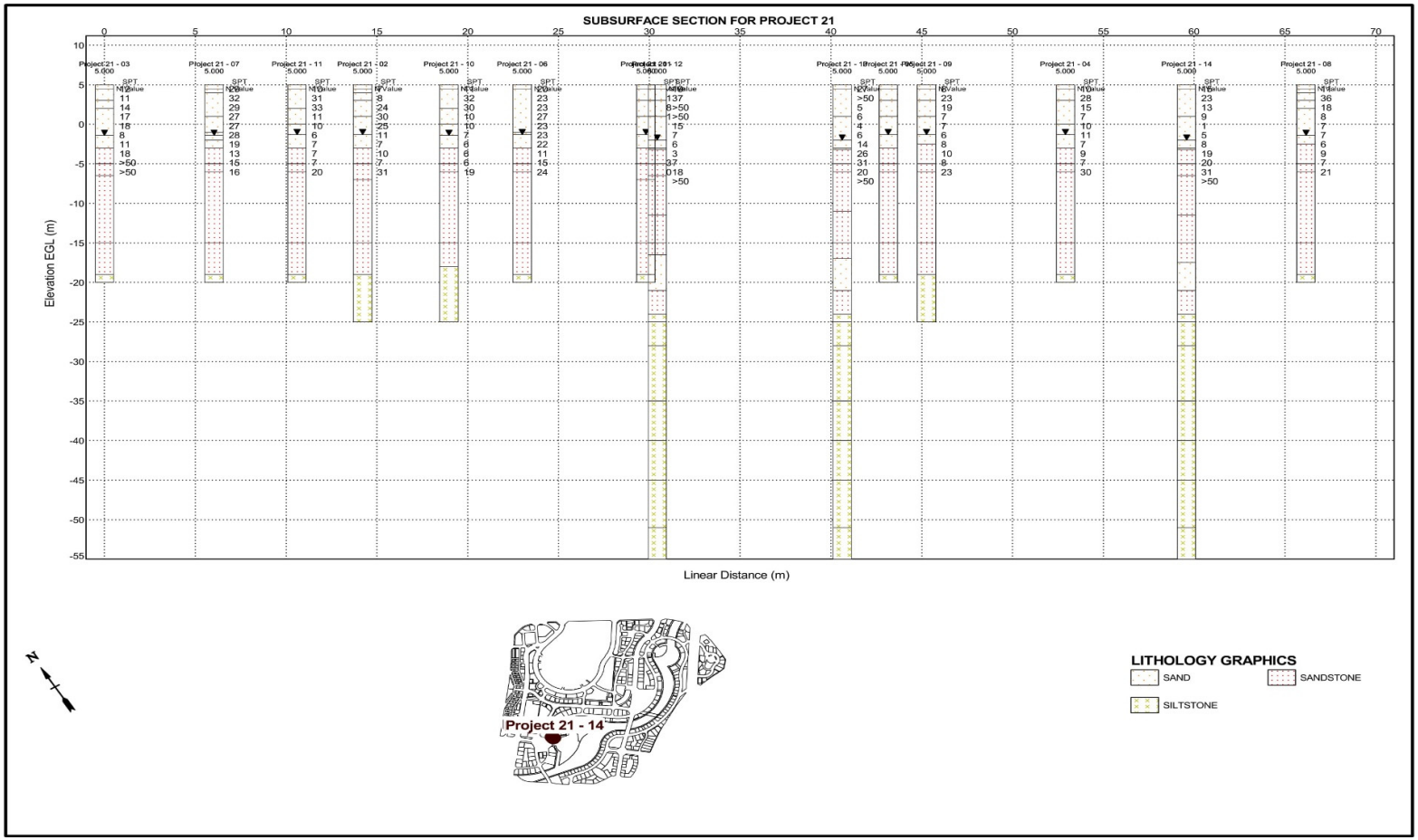
SUBSURFACE SECTION FOR PROJECT 21
Elevation EGL (m)
Linear Distance (m)
Project 21 - 03
Project 21 - 07
Project 21 - 11
Project 21 - 02
Project 21 - 10
Project 21 - 06
Project 21 - 12
Project 21 - 09
Project 21 - 04
Project 21 - 14
Project 21 - 08
SPT N-Value
Project 21 - 14
N
LITHOLOGY GRAPHICS
SAND
SANDSTONE
SILTSTONE

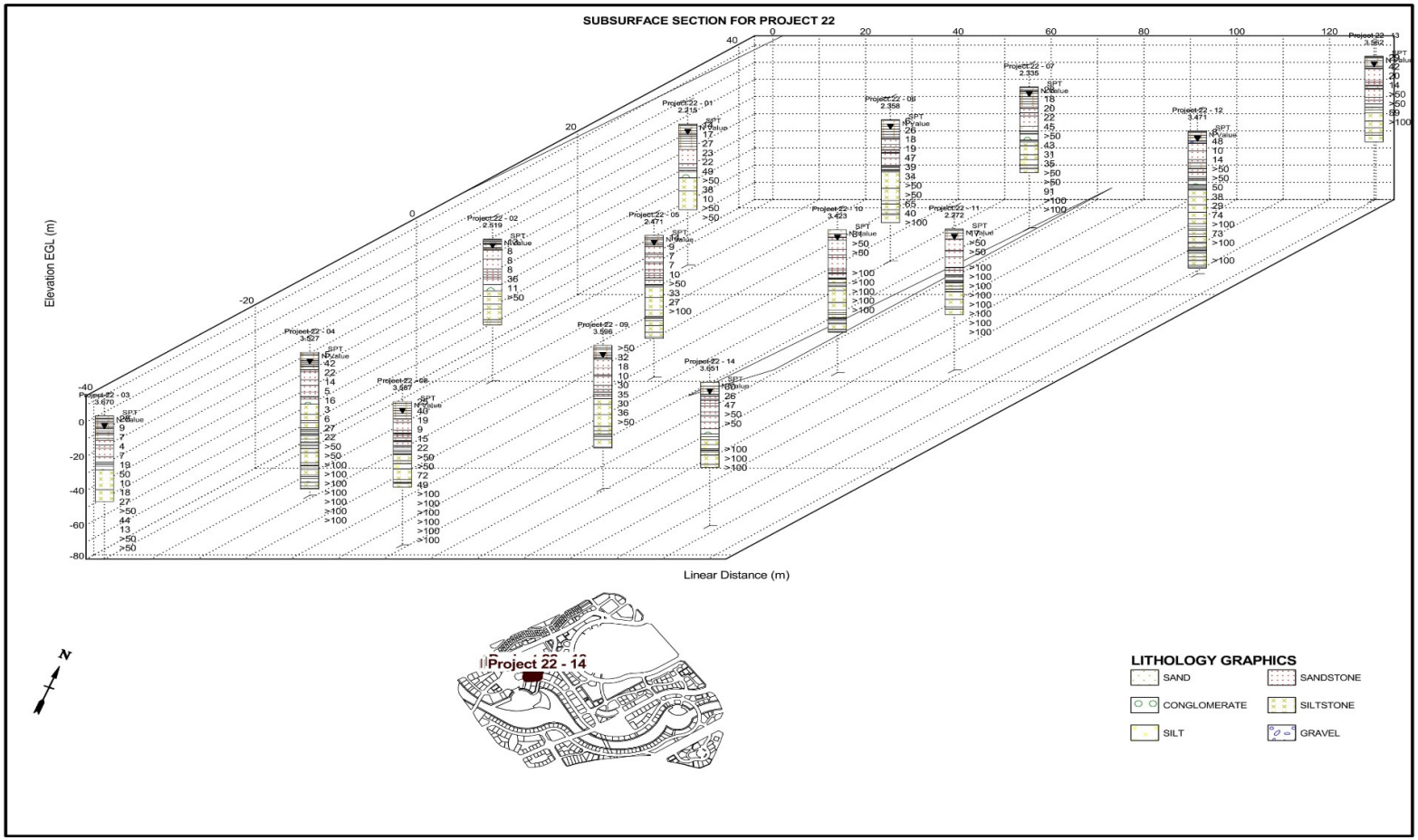
SUBSURFACE SECTION FOR PROJECT 22
Elevation EGL (m)
Linear Distance (m)
Project 22 - 14
LITHOLOGY GRAPHICS
SAND
SANDSTONE
CONGLOMERATE
SILTSTONE
SILT
GRAVEL

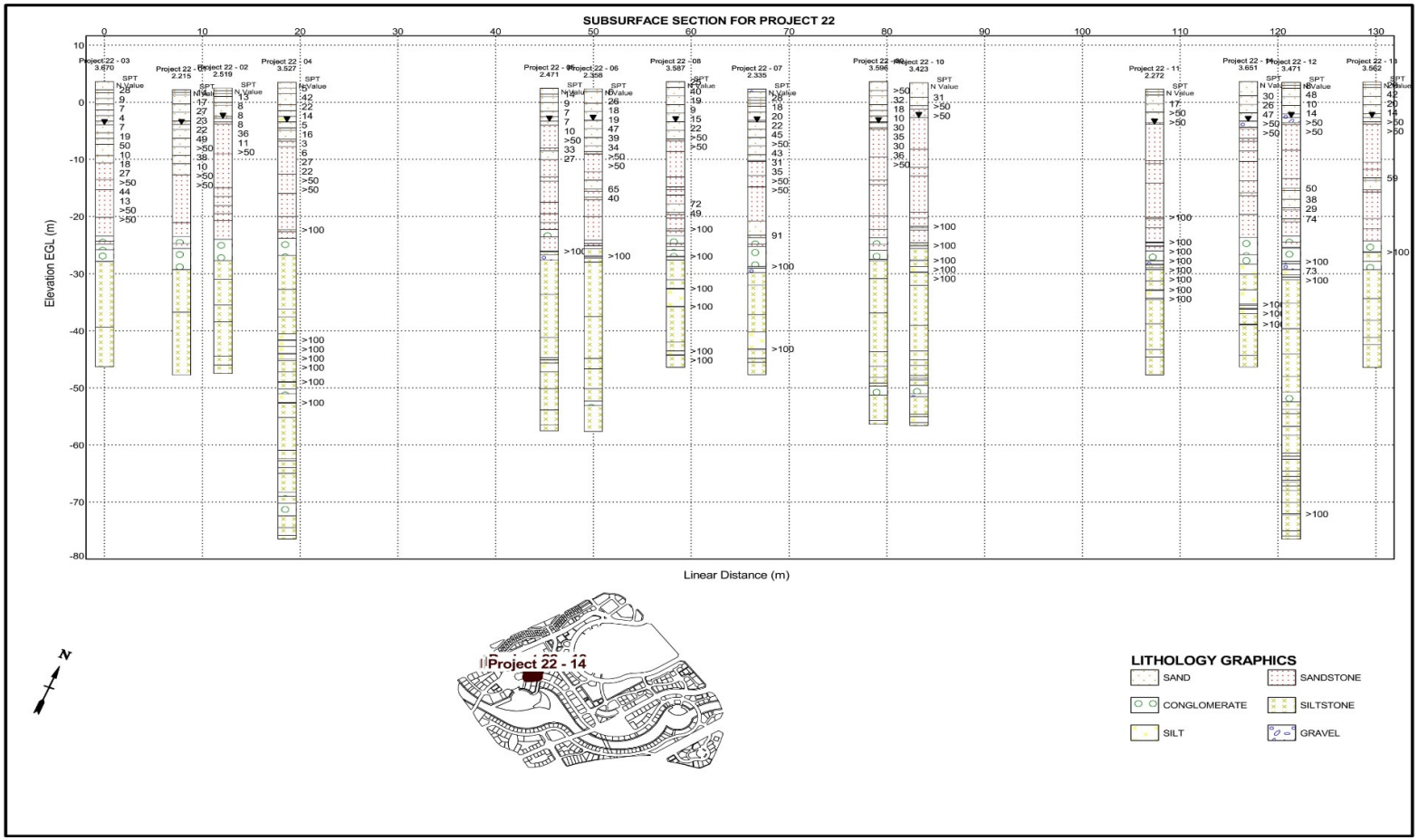
SUBSURFACE SECTION FOR PROJECT 22
Elevation EGL (m)
Linear Distance (m)
Project 22 - 14
LITHOLOGY GRAPHICS
SAND
SANDSTONE
CONGLOMERATE
SILTSTONE
SILT
GRAVEL

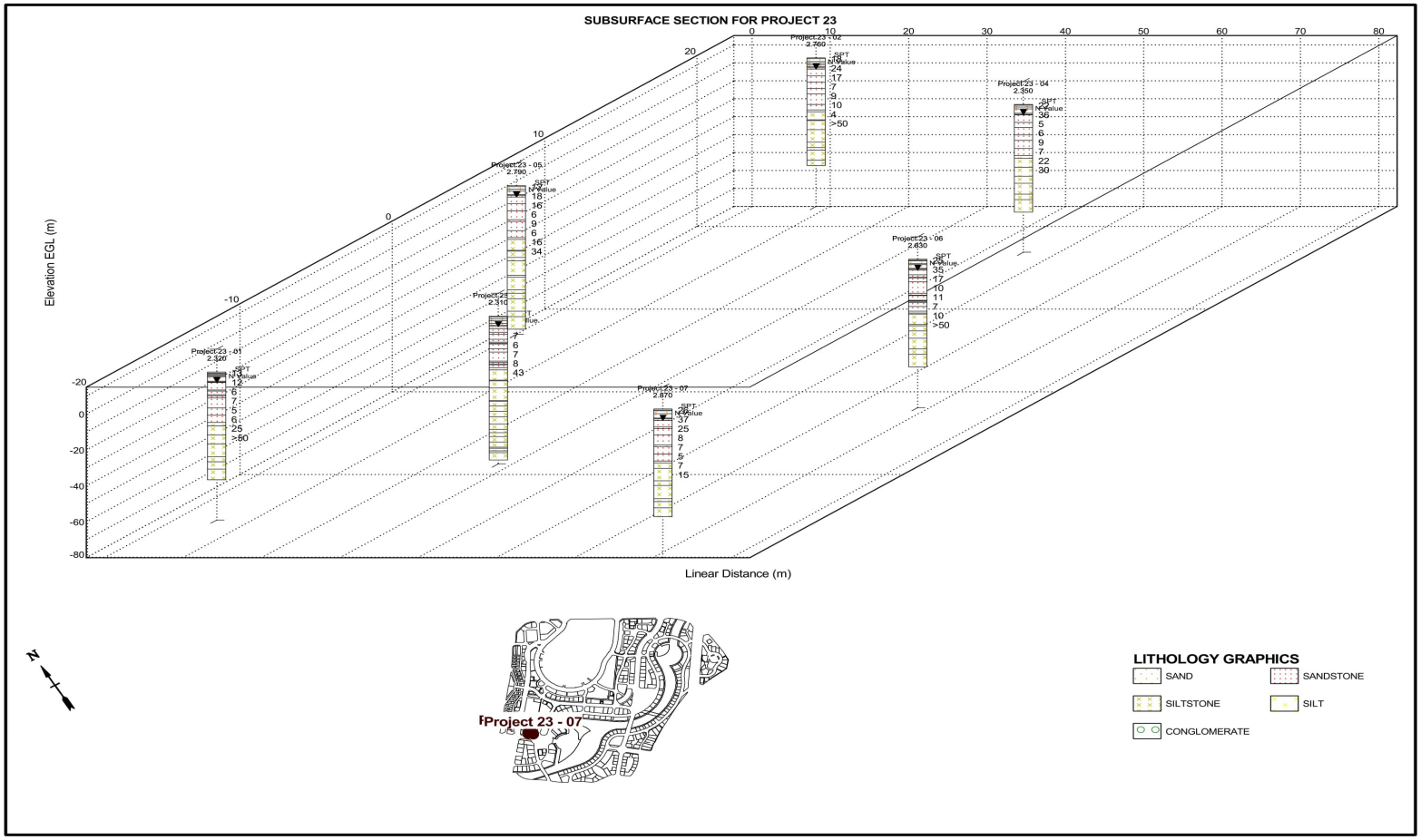
SUBSURFACE SECTION FOR PROJECT 23
Elevation EGL (m)
Linear Distance (m)
Project 23 - 01
Project 23 - 04
Project 23 - 05
Project 23 - 06
Project 23 - 07
LITHOLOGY GRAPHICS
SAND
SANDSTONE
SILTSTONE
SILT
CONGLOMERATE

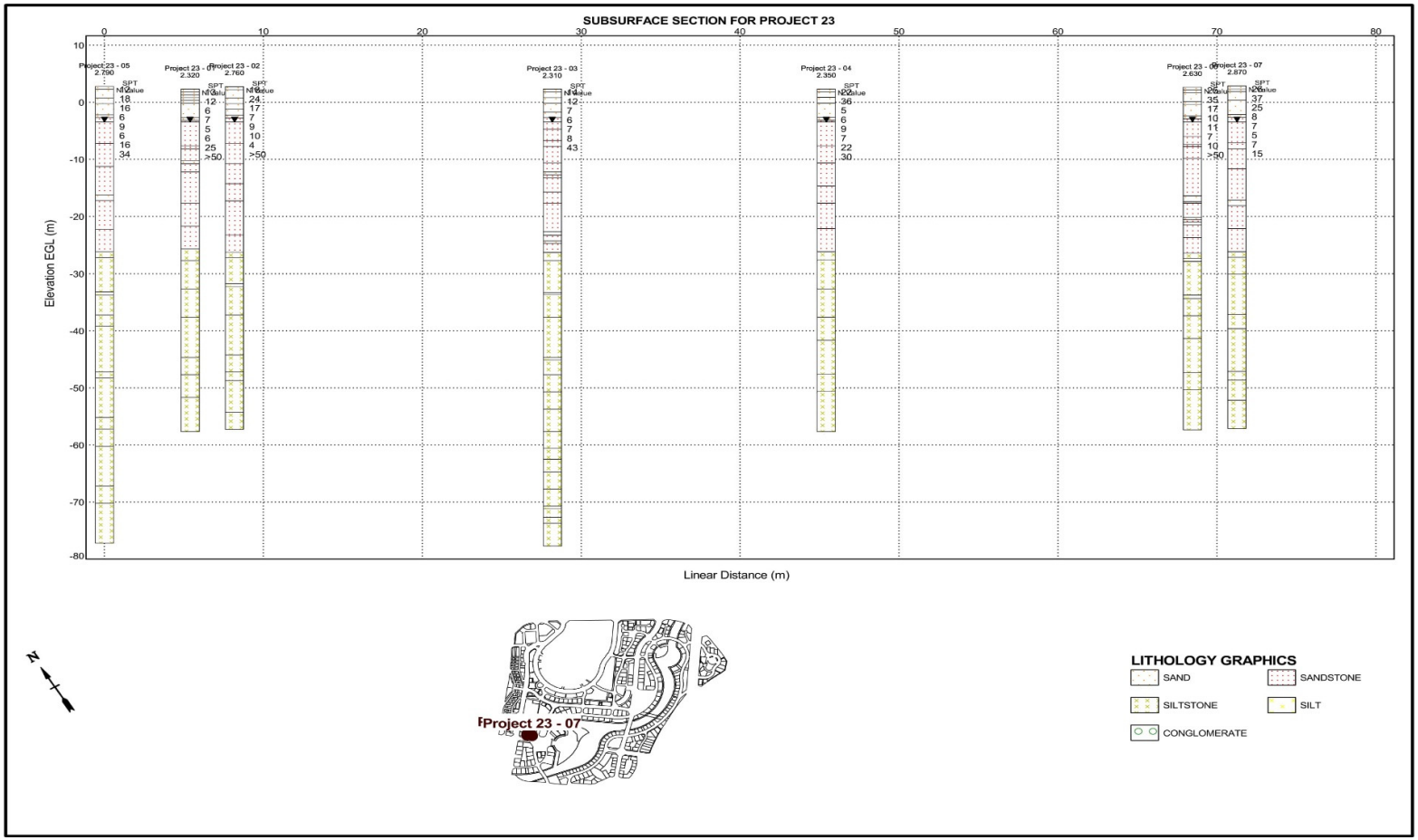
SUBSURFACE SECTION FOR PROJECT 23
Elevation EGL (m)
Linear Distance (m)
Project 23 - 05
Project 23 - 01
Project 23 - 02
Project 23 - 03
Project 23 - 04
Project 23 - 06
Project 23 - 07
SPT N Value
Project 23 - 07
LITHOLOGY GRAPHICS
SAND
SANDSTONE
SILTSTONE
SILT
CONGLOMERATE

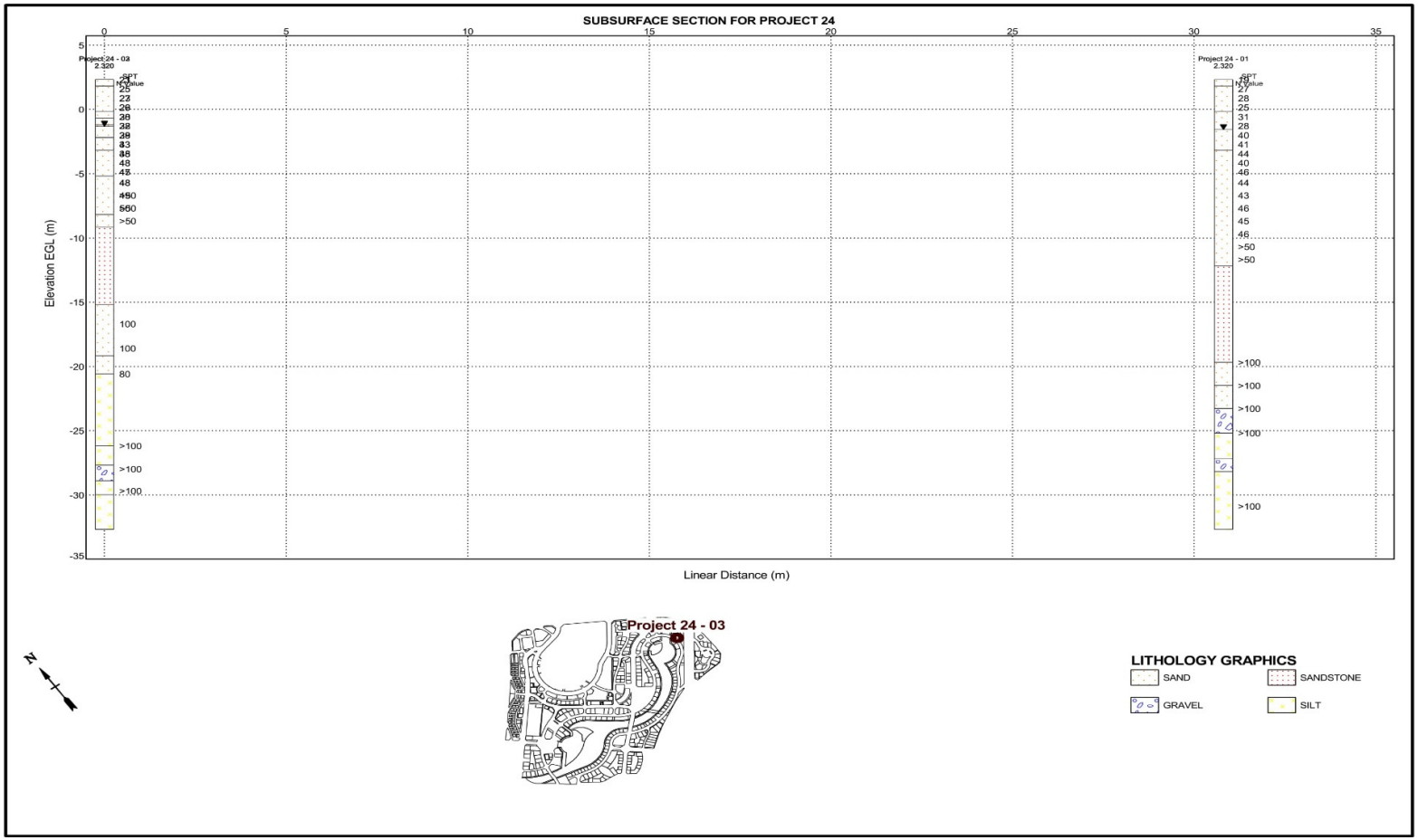
SUBSURFACE SECTION FOR PROJECT 24
Elevation EGL (m)
Linear Distance (m)
Project 24 - 03
Project 24 - 01
SPT N Value
LITHOLOGY GRAPHICS
SAND
SANDSTONE
GRAVEL
SILT

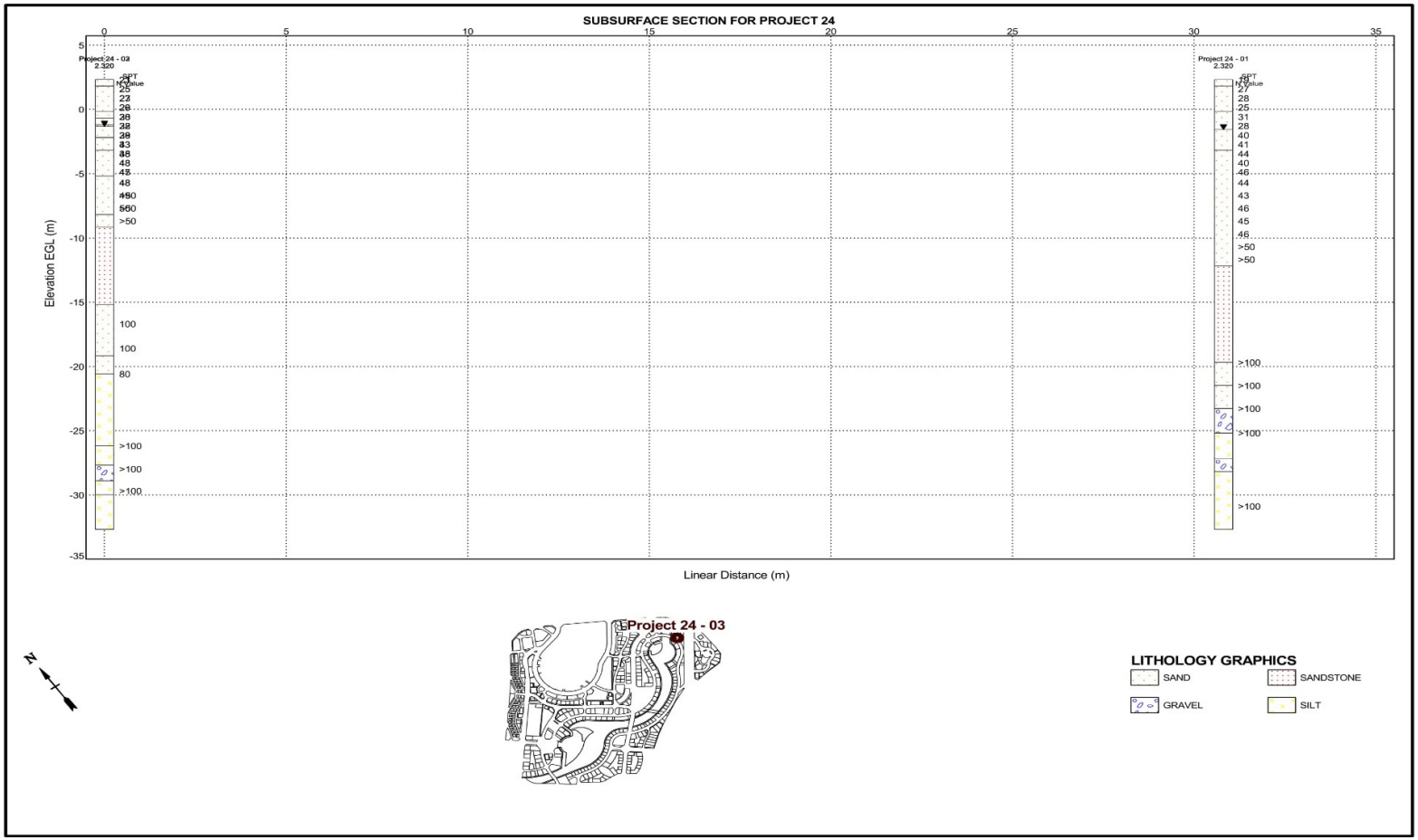
SUBSURFACE SECTION FOR PROJECT 24
Elevation EGL (m)
Linear Distance (m)
Project 24 - 03
Project 24 - 01
SPT N Value
LITHOLOGY GRAPHICS
SAND
SANDSTONE
GRAVEL
SILT
N

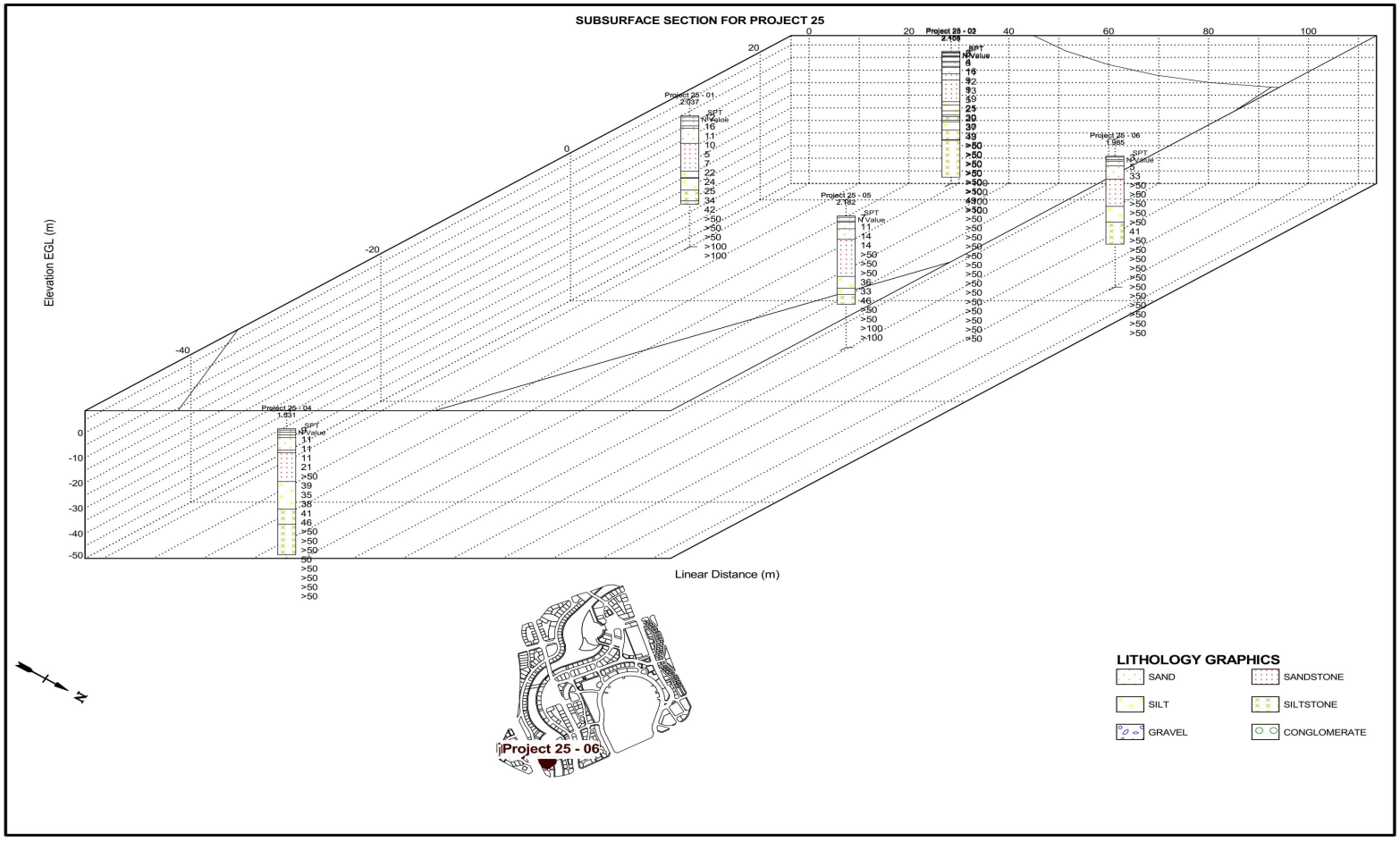
SUBSURFACE SECTION FOR PROJECT 25
Elevation EGL (m)
Linear Distance (m)
Project 25 - 01
Project 25 - 02
Project 25 - 03
Project 25 - 04
Project 25 - 05
Project 25 - 06
SPT N Value
LITHOLOGY GRAPHICS
SAND
SANDSTONE
SILT
SILTSTONE
GRAVEL
CONGLOMERATE
N

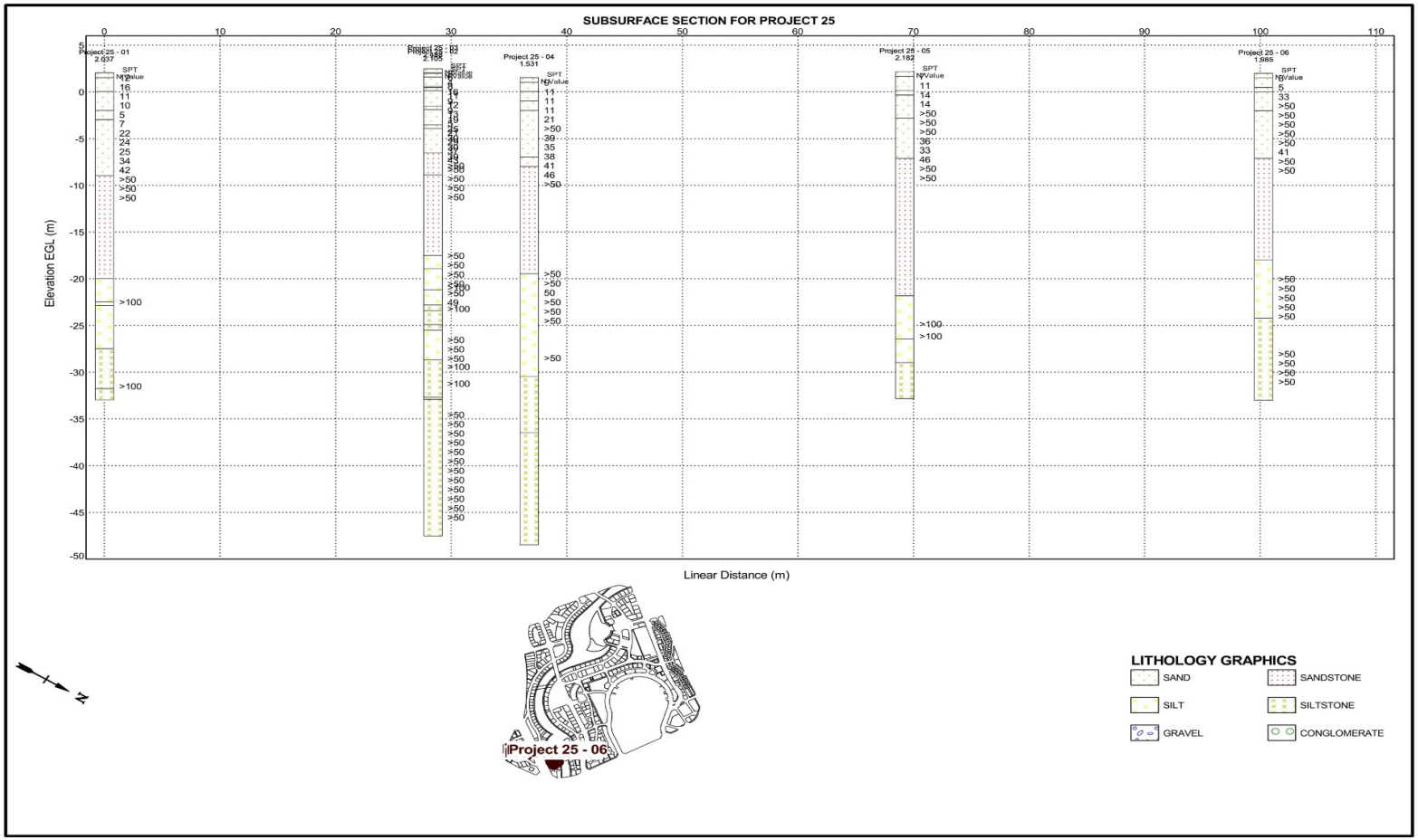
SUBSURFACE SECTION FOR PROJECT 25
Elevation EGL (m)
Linear Distance (m)
Project 25 - 01
Project 25 - 04
Project 25 - 05
Project 25 - 06
Project 25 - 06
LITHOLOGY GRAPHICS
SAND
SANDSTONE
SILT
SILTSTONE
GRAVEL
CONGLOMERATE

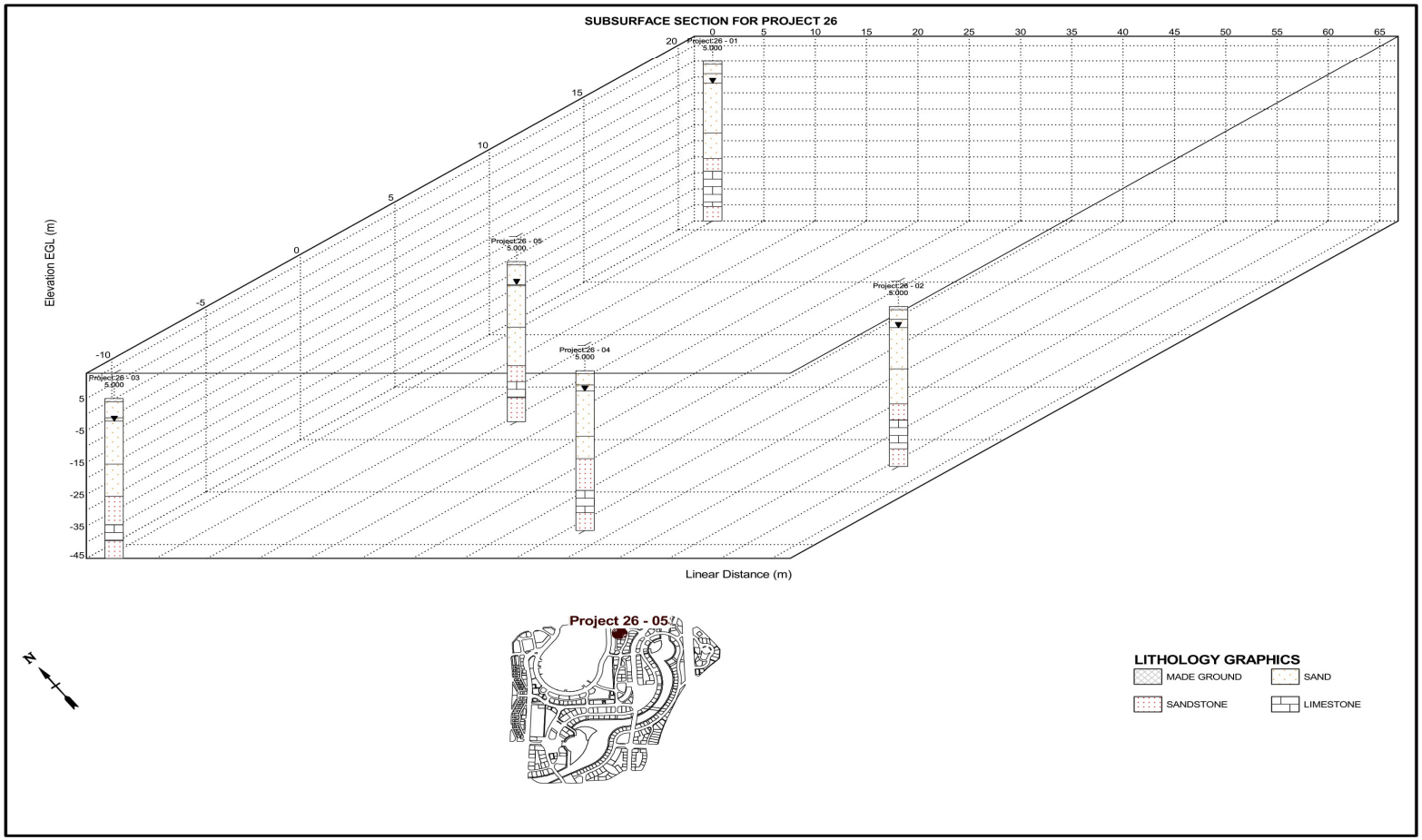
SUBSURFACE SECTION FOR PROJECT 26
Elevation EGL (m)
Linear Distance (m)
Project:26 - 01
S.000
Project:26 - 05
S.000
Project:26 - 02
S.000
Project:26 - 04
S.000
Project:26 - 03
S.000
Project 26 - 05
N
LITHOLOGY GRAPHICS
MADE GROUND
SAND
SANDSTONE
LIMESTONE

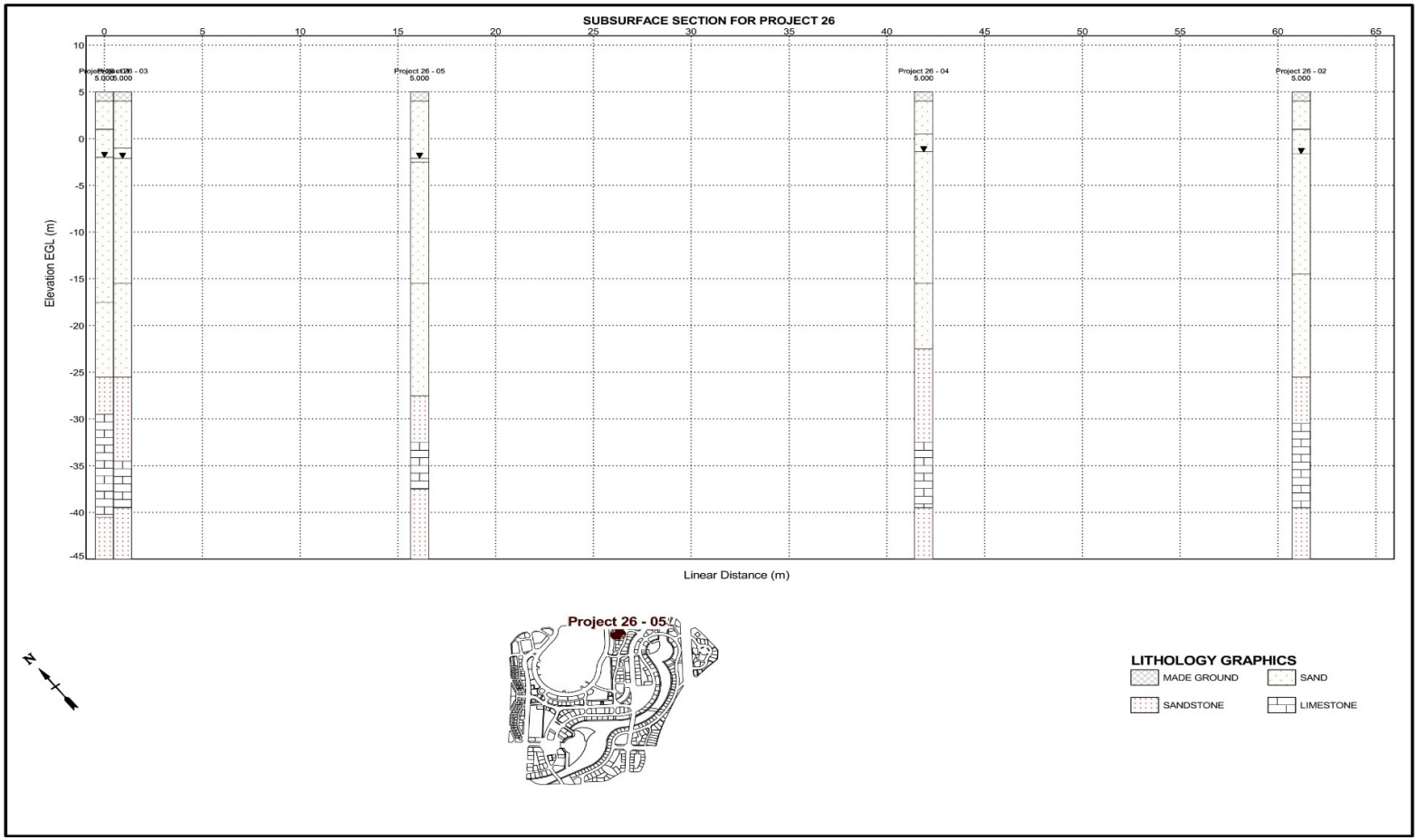
SUBSURFACE SECTION FOR PROJECT 26
Elevation EGL (m)
Linear Distance (m)
Project 26 - 03
5.000
Project 26 - 05
5.000
Project 26 - 04
5.000
Project 26 - 02
5.000
Project 26 - 05
N
LITHOLOGY GRAPHICS
MADE GROUND
SAND
SANDSTONE
LIMESTONE

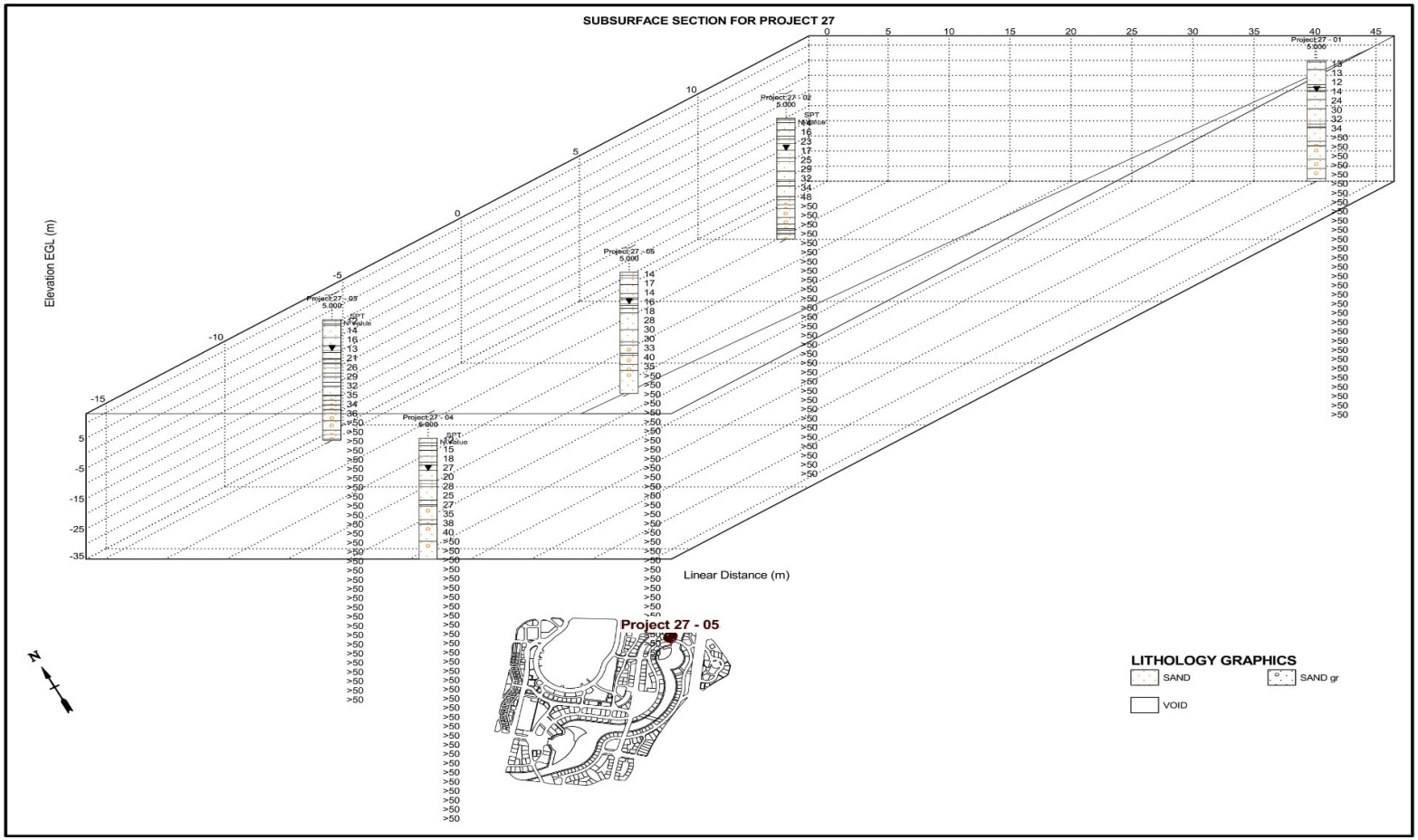
SUBSURFACE SECTION FOR PROJECT 27
Elevation EGL (m)
Linear Distance (m)
Project 27 - 05
LITHOLOGY GRAPHICS
SAND
SAND gr
VOID

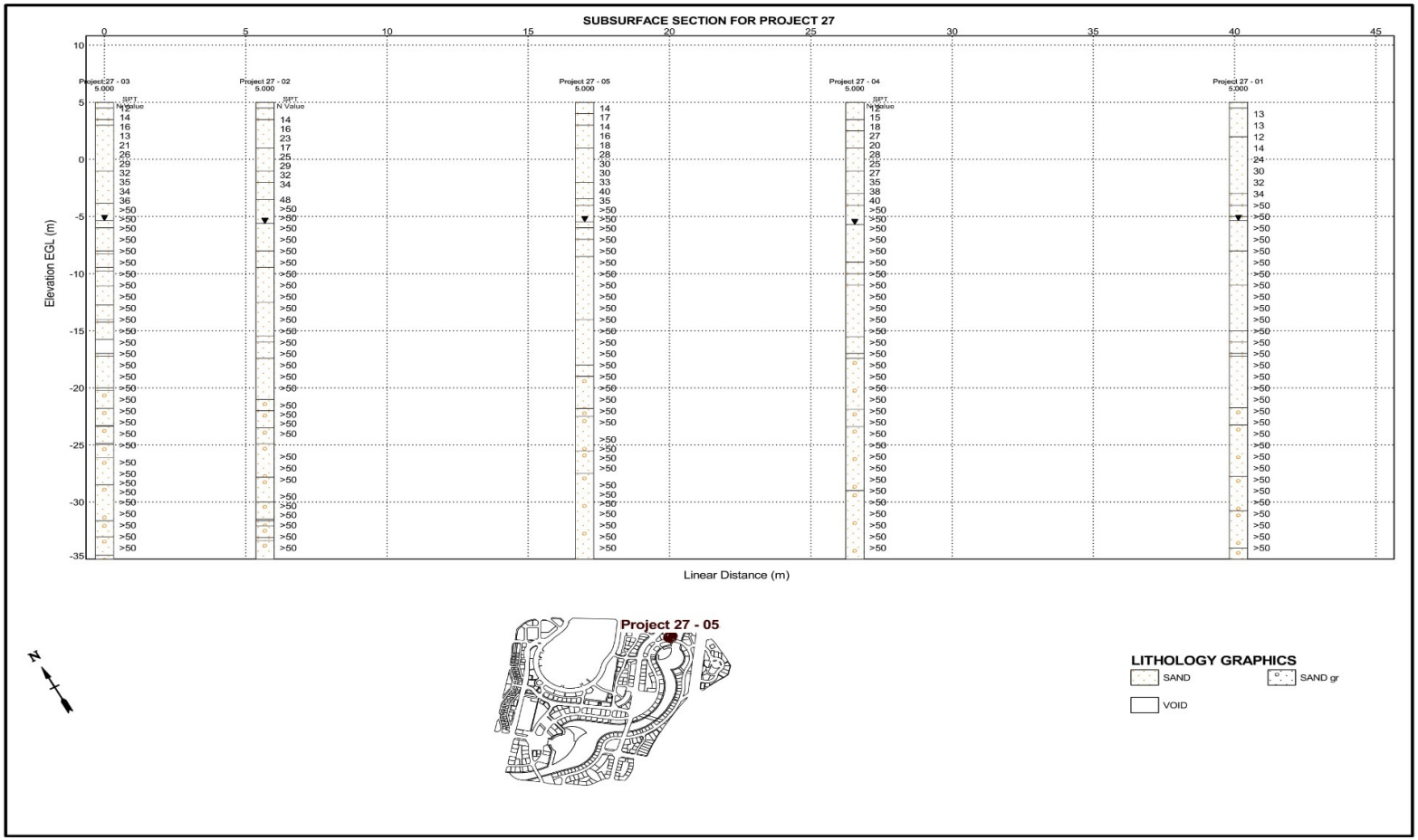
SUBSURFACE SECTION FOR PROJECT 27
Project 27 - 03
5.000
Project 27 - 02
5.000
Project 27 - 05
5.000
Project 27 - 04
5.000
Project 27 - 01
5.000
SPT
N Value
Elevation EGL (m)
Linear Distance (m)
Project 27 - 05
N
LITHOLOGY GRAPHICS
SAND
SAND gr
VOID

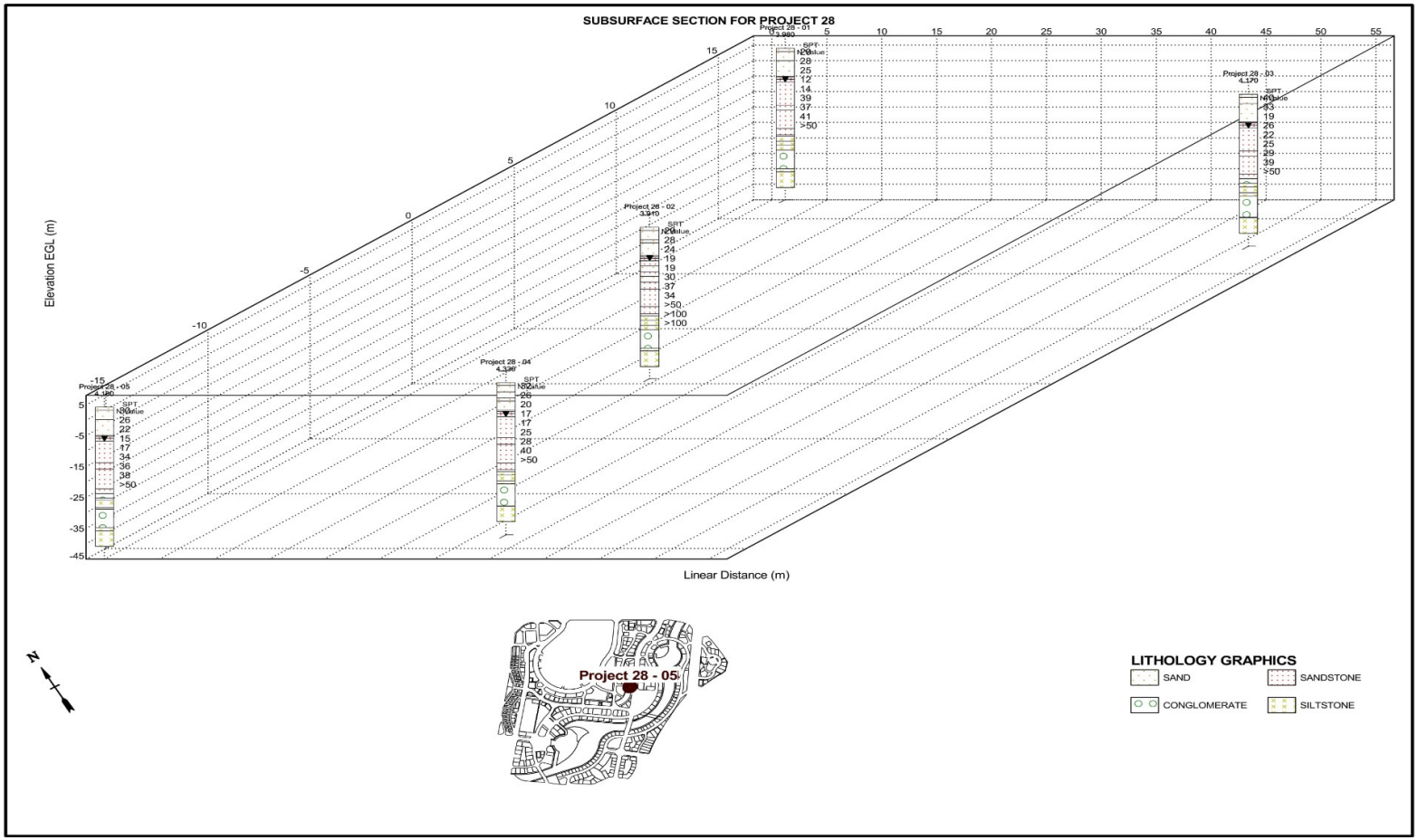
SUBSURFACE SECTION FOR PROJECT 28
Elevation EGL (m)
Linear Distance (m)
Project 28 - 01
Project 28 - 02
Project 28 - 03
Project 28 - 04
Project 28 - 05
SPT N60 Value
LITHOLOGY GRAPHICS
SAND
SANDSTONE
CONGLOMERATE
SILTSTONE
N

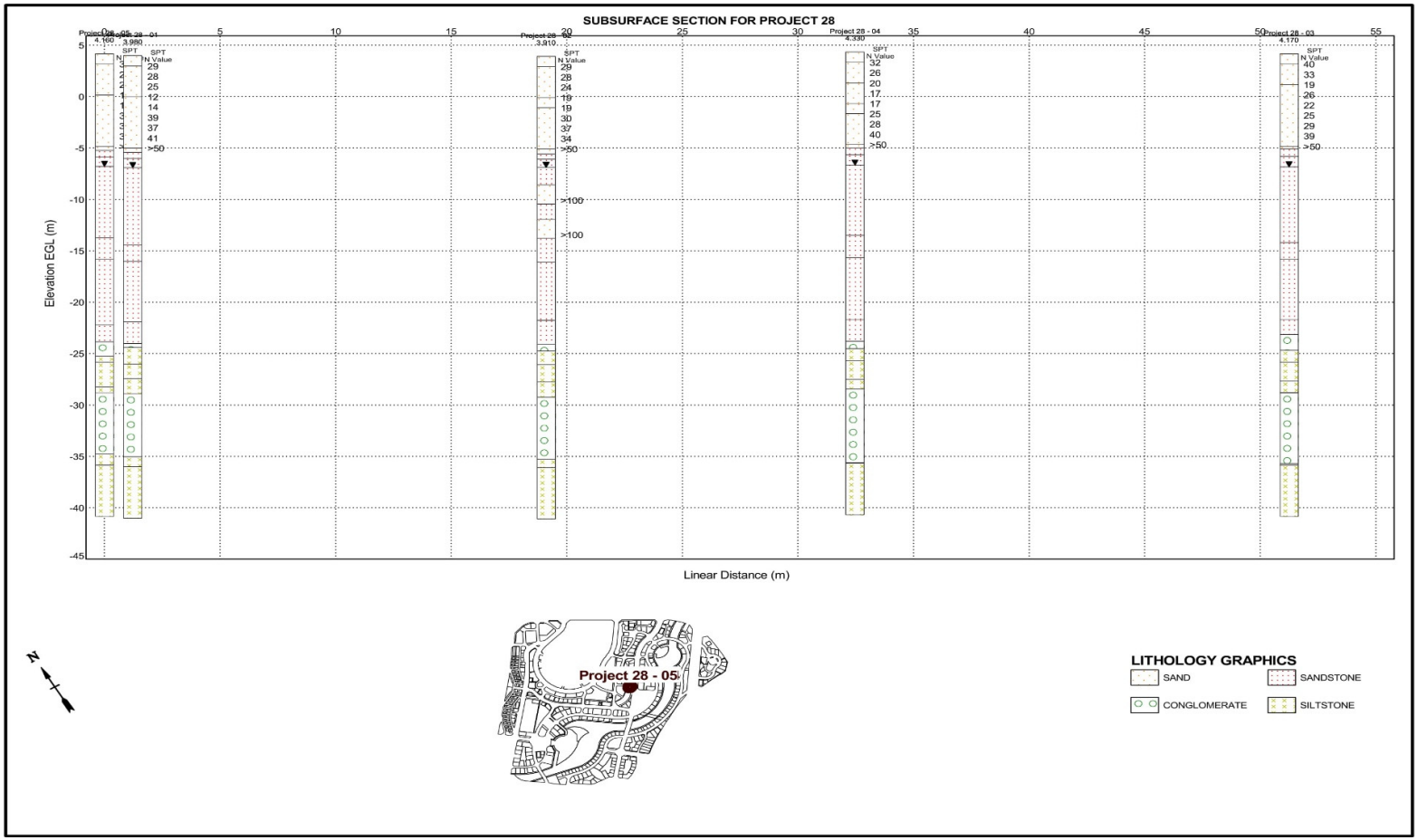
SUBSURFACE SECTION FOR PROJECT 28
Elevation EGL (m)
Linear Distance (m)
Project 28 - 05
4.160
Project 28 - 01
3.980
Project 28 - 02
3.910
Project 28 - 04
4.330
Project 28 - 03
4.170
SPT N Value
29 28 25 12 14 39 37 41 >50
29 28 24 19 19 30 37 34 >50 >100 >100
32 26 20 17 17 25 28 40 >50
40 33 19 26 22 25 29 39 >50
Project 28 - 05
LITHOLOGY GRAPHICS
SAND
SANDSTONE
CONGLOMERATE
SILTSTONE

Appendix 3 Case study project static load test results

Load %		Pile P75		Pile P74	
		Load (kN)	Average settlement (mm)	Load (kN)	Average settlement (mm)
Zero to working load	0	0	0	0	0
	25	4100	-1.45	4500	-1.41
	50	8200	-2.92	9000	-2.81
	75	12300	-4.3	13500	-3.98
	100	16400	-5.77	18000	-5.14
Working load to zero	75	18450	-5.12	13500	-4.96
	50	8200	-4.21	9000	-3.79
	25	4100	-2.8	4500	-1.56
	0	0	-0.4	0	-0.28
Zero to test load	100	16400	-6.1	18000	-5.59
	125	20500	-7.36	22500	-6.91
	150	24600	-9.41	27000	-8.39
Test load to zero	125	20500	-8.81	22500	-8.3
	100	16400	-8.01	18000	-7.38
	75	12300	-7.08	13500	-6.15
	50	8200	-5.89	9000	-4.63
	25	4100	-3.26	4500	-2.29
	0	0	-0.92	0	-0.78

Load %		Pile P73		Pile P76	
		Load (kN)	Average Settlement (mm)	Load (kN)	Average Settlement (mm)
Zero to Working Load	0	0	0	0	0
	25	5348.25	-0.76	5797.5	-2.22
	50	10696.5	-1.57	11595	-5.31
	75	16044.75	-2.44	17392.5	-7.75
	100	21393	-3.48	23190	-9.18
Working Load to Zero	75	16044.75	-3.48	17392.5	-9.08
	50	10696.5	-3.01	11595	-7.74
	25	5348.25	-2.18	5797.5	-5.3
	0	0	-0.58	0	-0.48
Zero to Test Load	0	0	-.58	0	-0.48
	100	21393	-4.63	23190	-9.39
	125	26741.25	-5.76	28987.5	-10.52
	150	32089.5	-7.03	34785	-11.72
Test Load to Zero	125	26741.25	-7.03	28987.5	-11.64
	100	21393	-6.63	23190	-10.52
	75	16044.75	-5.8	17392.5	-9.31
	50	10696.5	-4.75	11595	-7.74
	25	5348.25	-2.64	5797.5	-5.28
	0	0	-0.84	0	-0.89

Load %		Pile P72		Pile P71	
		Load (kN)	Average settlement(mm)	Load (kN)	Average settlement(mm)
Zero to test load	0	0	0	0	0
	10	750	-0.27	770	-0.16
	20	1500	-0.53	1540	-0.41
	30	2250	-0.86	2310	-0.65
	40	3000	-1.17	3080	-0.93
	50	3750	-1.49	3850	-1.2
	60	4500	-1.96	4620	-1.43
	70	5250	-2.38	5390	-1.65
	80	6000	-2.83	6160	-1.92
	90	6750	-3.16	6930	-2.18
	100	7500	-3.51	7700	-2.55
Test load to zero	100	7500	-3.51	7700	-2.55
	90	6750	-3.46	6930	-2.45
	80	6000	-3.34	6160	-2.33
	70	5250	-3.02	5390	-2.2
	60	4500	-2.94	4620	-2.01
	50	3750	-2.65	3850	-1.78
	40	3000	-2.22	3080	-1.53
	30	2250	-1.77	2310	-1.25
	20	1500	-1.07	1540	-0.98
	10	750	-0.86	770	-0.64
	0	0	-0.63	0	-0.33
Zero to test load	0	0	-.63	0	-0.33
	10	750	-0.83	770	-0.63
	20	1500	-1.06	1540	-0.98
	30	2250	-1.38	2310	-1.29
	40	3000	-1.68	3080	-1.59
	50	3750	-2	3850	-1.86
	60	4500	-2.35	4620	-2.13
	70	5250	-2.72	5390	-2.33
	80	6000	-3.03	6160	-2.51
	90	6750	-3.35	6930	-2.69
	100	7500	-3.7	7700	-2.86
	110	8250	-4.02	8470	-3.06
	120	9000	-4.35	9240	-3.24
	130	9750	-4.63	10010	-3.42
	140	10500	-4.86	10780	-3.6
	150	11250	-5.29	11550	-4.18
Test load to zero	150	11250	-5.29	11550	-4.18
	140	10500	-5.25	10780	-4.35
	130	9750	-5.22	10010	-4.26
	120	9000	-5.09	9240	-4.14
	110	8250	-4.94	8470	-4.03
	100	7500	-4.75	7700	-3.86
	90	6750	-4.51	6930	-3.71
	80	6000	-4.21	6160	-3.51
	70	5250	-3.82	5390	-3.35
	60	4500	-3.38	4620	-3.14
	50	3750	-2.86	3850	-2.88
	40	3000	-2.35	3080	-2.59
	30	2250	-1.84	2310	-2.27
	20	1500	-1.33	1540	-1.94
	10	750	-1.04	770	-1.5
	0	0	-0.84	0	-0.81